frontiers | Research Topics

Clinical therapy of brain tumors

Edited by
Bo yuan Huang, Gerardo Caruso, Fusheng Liu,
Jun Yang and Hongbo Zhang

Published in
Frontiers in Neurology
Frontiers in Oncology

ISSN 1664-8714
ISBN 978-2-8325-6430-1
DOI 10.3389/978-2-8325-6430-1

About Frontiers

Frontiers is more than just an open access publisher of scholarly articles: it is a pioneering approach to the world of academia, radically improving the way scholarly research is managed. The grand vision of Frontiers is a world where all people have an equal opportunity to seek, share and generate knowledge. Frontiers provides immediate and permanent online open access to all its publications, but this alone is not enough to realize our grand goals.

Frontiers journal series

The Frontiers journal series is a multi-tier and interdisciplinary set of open-access, online journals, promising a paradigm shift from the current review, selection and dissemination processes in academic publishing. All Frontiers journals are driven by researchers for researchers; therefore, they constitute a service to the scholarly community. At the same time, the *Frontiers journal series* operates on a revolutionary invention, the tiered publishing system, initially addressing specific communities of scholars, and gradually climbing up to broader public understanding, thus serving the interests of the lay society, too.

Dedication to quality

Each Frontiers article is a landmark of the highest quality, thanks to genuinely collaborative interactions between authors and review editors, who include some of the world's best academicians. Research must be certified by peers before entering a stream of knowledge that may eventually reach the public - and shape society; therefore, Frontiers only applies the most rigorous and unbiased reviews. Frontiers revolutionizes research publishing by freely delivering the most outstanding research, evaluated with no bias from both the academic and social point of view. By applying the most advanced information technologies, Frontiers is catapulting scholarly publishing into a new generation.

What are Frontiers Research Topics?

Frontiers Research Topics are very popular trademarks of the *Frontiers journals series*: they are collections of at least ten articles, all centered on a particular subject. With their unique mix of varied contributions from Original Research to Review Articles, Frontiers Research Topics unify the most influential researchers, the latest key findings and historical advances in a hot research area.

Find out more on how to host your own Frontiers Research Topic or contribute to one as an author by contacting the Frontiers editorial office: frontiersin.org/about/contact

Clinical therapy of brain tumors

Topic editors

Bo yuan Huang — Capital Medical University, China
Gerardo Caruso — University Hospital of Policlinico G. Martino, Italy
Fusheng Liu — Capital Medical University, China
Jun Yang — Capital Medical University, China
Hongbo Zhang — Second Affiliated Hospital of Nanchang University, China

Citation

Huang, B. y., Caruso, G., Liu, F., Yang, J., Zhang, H., eds. (2025). *Clinical therapy of brain tumors*. Lausanne: Frontiers Media SA. doi: 10.3389/978-2-8325-6430-1

Table of contents

frontiers | Frontiers in Neurology

TYPE Editorial
PUBLISHED 23 May 2025
DOI 10.3389/fneur.2025.1610463

OPEN ACCESS

EDITED AND REVIEWED BY
David D. Eisenstat,
Royal Children's Hospital, Australia

*CORRESPONDENCE
Boyuan Huang
✉ 525111209@qq.com

†These authors have contributed equally to this work

RECEIVED 12 April 2025
ACCEPTED 12 May 2025
PUBLISHED 23 May 2025

CITATION
Huang B, Zhao H, Yang J, Liu F, Caruso G, Zhang H and Chen L (2025) Editorial: Clinical therapy of brain tumors.
Front. Neurol. 16:1610463.
doi: 10.3389/fneur.2025.1610463

Editorial: Clinical therapy of brain tumors

Boyuan Huang[1]*, Huijun Zhao[1], Jun Yang[2], Fusheng Liu[2], Gerardo Caruso[3], Hongbo Zhang[4†] and Lin Chen[1†]

[1]Second Department of Neurosurgery, Capital Medical University Electric Power Teaching Hospital/State GridBeijing Electric Power Hospital, Beijing, China, [2]Beijing Tiantan Hospital, Capital Medical University, Beijing, China, [3]University Hospital of Policlinico G. Martino, Messina, Italy, [4]Second Affiliated Hospital of Nanchang University, Nanchang, China

KEYWORDS

brain tumor treatment, radiotherapy, chemotherapy, immunotherapy, neurosurgery

Editorial on the Research Topic
Clinical Therapy of Brain Tumors

Brain tumors are devastating diseases, accounting for a significant proportion of cancer-related mortality and morbidity in both adults and children. Over the past few years, treatment for brain tumors have witnessed dramatic progress. This is largely due to advances in surgical skills, more rational and personalized radiotherapy and chemotherapy, and continually updated immunotherapies that modulate the immune microenvironment or specifically target tumor cells. This editorial summarizes significant findings on surgery, radiotherapy, chemotherapy, immunotherapy and other treatment published in the Research Topic, Clinical Therapy of Brain Tumors, Frontiers in Neurology, emphasizing their impact on advancing the understanding and treatment of brain tumors. The current Research Topic includes 17 papers, among which 7 were considered as Original Research, with 3 Reviews and 7 case reports.

1 Surgical treatment for brain tumors

Prior to surgery, various imaging techniques can provide information about the nature of the tumor, including its location, blood supply, metabolic status, and key surrounding functional areas. Furthermore, magnetoencephalography (MEG) and guided transcranial magnetic stimulation (nTMS) have emerged as new tools for the localization of important areas of function. It was found that the application of nTMS could improve surgical total resection rates for low-grade gliomas (LGGs) by approximately 16% and increase median progression-free survival (PFS) from 15.4 months to 22.4 months (1, 2). Moreover, application of intraoperative assistive technology such as intraoperative navigation, intraoperative magnetic resonance imaging, intraoperative ultrasound and intraoperative fluorescence, which can assist the operator in effectively localizing lesion and extent of the tumor, can also increase the success of the operation. In addition, intraoperative electrophysiological monitoring techniques and intraoperative awakening technique can help the surgeon localize the important functional areas of the brain, which play a significant role in protecting the function of the important functional areas of the patient. Duan et al. highlighted that with proper management of the sagittal sinus and protection of the associated veins, the surgical treatment strategy for the "radical"

resection of parasagittal sinus meningioma is effective, safe and simple to perform. He et al. reviewed the clinical characteristics and treatment outcomes of 14 patients with polymorphic low-grade neuroepithelial tumor of the young and highlighted that stereoelectroencephalography was pivotal for cases with unclear lateralization, aiding in identifying the link between the tumor and seizures. They suggested that following established epilepsy surgery protocols for brain tumor management, early intervention and extended resection can improve the rate of postoperative seizure freedom. Gui et al. reported a rare case of neurocytoma originating from cranial nerve V.

2 Radiotherapy for brain tumors

Radiotherapy is primarily used to treat malignant neoplasms, including gliomas and brain metastases, benign neoplasms that are not amenable to complete resection, such as meningiomas, as well as neoplasms that appear sensitive to radiotherapy, such as germ cell tumors. In recent years, with the development in science and technology, a multitude of novel techniques have been employed in radiotherapy, such as proton radiotherapy and heavy ion radiotherapy (HIRT), which has led to significant improvement in patient prognoses. Compared with conventional radiotherapy, proton radiotherapy, with more precise dose distribution, is able to further protect the surrounding normal tissues without loss of clinical efficacy (3). Although the current evidence for proton radiotherapy in brain tumors is limited, it still shows good prospects for application (4). In the current Research Topic, Palenzuela et al. studied acute toxicity of chemotherapy in central nervous system germ cell tumor patients according to age. Li et al. found that adjuvant beam radiation therapy could enhance overall survival (OS) in younger primary single intracranial atypical meningioma patients.

3 Systemic therapy for brain tumors

Systemic anti-tumor agents broadly include traditional cytotoxic chemotherapeutic agents, molecularly targeted agents and immunotherapeutic agents, mainly for high grade gliomas, brain metastases, lymphomas, etc. The molecularly targeted agents includes IDH1/2 mutant inhibitors, BRAF/MEK inhibitors, NTRK fusion inhibitors, MET kinase inhibitors, antiangiogenic drugs, etc. Vorasidenib, an oral IDH1/2 mutant inhibitor, was shown in a phase III study to significantly increase progression-free survival (PFS) in patients with grade 2 IDH-mutated oligodendroglioma or astrocytoma (5). In the Research Topic, Bao et al. made a retrospective study of chemotherapy strategies for adults with IDH-wildtype glioblastoma (GBM). In addition, National Comprehensive Cancer Network Guidelines (NCCN) recommended that patients with NTRK-compatible gliomas should be treated with NTRK fusion inhibitors, such as larotrectinib and entrectinib (6, 7). Although it can increase PFS of patients, bevacizumab, the first antiangiogenic drug approved by the FDA and recommended by NCCN to treat recurrent GBM, still failed in prolonging OS (8). Currently, the most promising immunotherapeutic agents against brain tumors are only immune checkpoint inhibitors, such as PD-1/PD-L1 antibodies (Pembrolizumab, Nivolumab). Although failed in phase III clinical trial against recurrent GBM (9), anti-PD-1 immunotherapy still showed efficiency in increasing GBM patient OS as neoadjuvant systemic therapy (10).

Other forms of immunotherapy, including tumor vaccine therapy, chimeric antigen receptor T (CAR-T) cell therapy and oncolytic virus therapy, have also shown promise in the treatment of brain tumors. A dendritic cell vaccine called DCVax-L showed obvious efficacy in clinical trials against primary GBM, with a median OS of 23.1 months (11). G47Δ, based on human herpes simplex virus, had markedly improved 1-year survival rate to 84.2%, and median OS to 20.2 months for residual or recurrent GBM patients (12). In 2021, G47Δwas approved for marketing in Japan for the treatment of residual or recurrent GBM. According to these above results, the Society for Immunotherapy Of Cancer (SITC) published a consensus statement that immunotherapy can be used as a salvage treatment option for gliomas patients after conventional treatment, which required further optimization of combination therapy (13). In the current Research Topics, Chen et al. performed a literature review about the immune microenvironment and immunotherapy for chordoma. In addition, Pu et al. unveiled substantial involvement of MAP2K3 in gliomas, indicating the potential of the enzyme to serve as a prognostic biomarker related to immunity. Through the regulation of the infiltration of immune cells, MAP2K3 can affect the prognosis of patients with glioma. Shen et al. performed a multivariate Cox proportional hazards regression analyses to identify independent prognostic variables for GBM patients with synchronous metastasis (SM). They found that radiotherapy, chemotherapy, and surgery constitute an effective treatment regimen for patients with SM. Luo et al. performed a literature review in which they summarized the latest advancements in understanding the molecular mechanisms that regulate regulated cell death in glioma and explore the interconnections between different cell death processes. Palenzuela et al. compared the tolerance of chemotherapy across age-groups within the SIOP-CNS-GCT-II trial.

4 Tumor treating fields for brain tumors

Tumor treating fields (TTF) is a new type of therapy applying physics that works by delivering low-intensity, medium-frequency alternating electric fields through a patch applied to the scalp. The fundamental mechanism by which TTF exerts its therapeutic effect involves anti-tumor cell mitosis, suppression of DNA damage repair, disruption of tumor cell migration, and potentiation of anti-tumor immune responses (14). The versatility of this therapeutic modality renders it a promising candidate for concurrent utilization with chemotherapy, radiotherapy, anti-angiogenic therapy, and immunotherapy (15). The results from a prospective, single-arm, phase I clinical trial demonstrated that the combination of TTFields and chemotherapy may offer survival benefits for recurrent GBM patients (16). Moreover, TTF in combination with TMZ and pembrolizumab adjuvant therapy could improved the median OS of primary GBM patients to 24.8 months, with a two-year OS rate of 52.4% (17), which

supported the safety and efficiency of TTF in combination with chemotherapy and immunotherapy, and thus requires further exploration. Currently, TTF has been recommended by the NCCN for combined administration with TMZ for primary GBM patients after surgery or radiotherapy, or alone for recurrent GBM patients (15).

5 Conclusion

Recent advancements in surgical assistive technologies have led to significant progress in the field of neurosurgery. These technologies play a crucial role in protecting vital neurological functions, enabling neurosurgeons to more accurately determine the margin between tumor and normal brain tissue. Additionally, these technologies have also contributed to increasing the extent of brain tumor resection and, consequently, enhancing the prognosis for brain tumor patients. Radiotherapy constitutes a critical localized treatment modality for gliomas, playing a pivotal role in the management of inoperable cases and/or for local disease control. Continuous advancements in novel radiotherapy techniques have led to enhanced control of brain tumors while concurrently reducing adverse effects. Drug therapy, immunotherapy and TTF, emerged as critical tools in the control of brain tumors, have also demonstrated efficacy in the management of brain tumors. Consequently, the future holds more promising significant advancements in the treatment of brain tumors, which will further improve patient outcomes.

Author contributions

BH: Writing – original draft, Writing – review & editing. HZhao: Data curation, Writing – review & editing. JY: Writing – review & editing, Investigation, Project administration. FL: Investigation, Conceptualization, Data curation, Writing – review & editing. GC: Writing – review & editing, Software, Validation, Visualization. HZhan: Software, Writing – review & editing, Investigation. LC: Software, Writing – review & editing, Conceptualization, Supervision.

Funding

The author(s) declare that financial support was received for the research and/or publication of this article. This program was funded by the Science and Technology Project of the Genertec Guozhong Healthcare Group administered by BH.

Conflict of interest

The authors declare that the research was conducted in the absence of any commercial or financial relationships that could be construed as a potential conflict of interest.

The author(s) declared that they were an editorial board member of Frontiers, at the time of submission. This had no impact on the peer review process and the final decision.

Publisher's note

References

1. Frey D, Schilt S, Strack V, Zdunczyk A, Rösler J, Niraula B, et al. Navigated transcranial magnetic stimulation improves the treatment outcome in patients with brain tumors in motor eloquent locations. *Neuro Oncol.* (2014) 16:1365–72. doi: 10.1093/neuonc/nou110

2. Picht T, Frey D, Thieme S, Kliesch S, Vajkoczy P. Presurgical navigated TMS motor cortex mapping improves outcome in glioblastoma surgery: a controlled observational study. *J Neurooncol.* (2016) 126:535–43. doi: 10.1007/s11060-015-1993-9

3. Goff KM, Zheng C, Alonso-Basanta M. Proton radiotherapy for glioma and glioblastoma. *Chin Clin Oncol.* (2022) 11:46. doi: 10.21037/cco-22-92

4. Qiu X, Gao J, Hu J, Yang J, Hu W, Huang Q, et al. Proton radiotherapy in the treatment of IDH-mutant diffuse gliomas: an early experience from shanghai proton and heavy ion center. *J Neurooncol.* (2023) 162:503–14. doi: 10.1007/s11060-022-04202-5

5. Mellinghoff IK, van den Bent MJ, Blumenthal DT, Touat M, Peters KB, Clarke J, et al. Vorasidenib in IDH1- or IDH2-Mutant Low-Grade Glioma. *N Engl J Med.* (2023) 389:589–601. doi: 10.1056/NEJMoa2304194

6. Marcus L, Donoghue M, Aungst S, Myers CE, Helms WS, Shen G, et al. FDA approval summary: entrectinib for the treatment of NTRK gene fusion solid tumors. *Clin Cancer Res.* (2021) 27:928–32. doi: 10.1158/1078-0432.CCR-20-2771

7. Hong DS, DuBois SG, Kummar S, Farago AF, Albert CM, Rohrberg KS, et al. Larotrectinib in patients with TRK fusion-positive solid tumours: a pooled analysis of three phase 1/2 clinical trials. *Lancet Oncol.* (2020) 21:531–40. doi: 10.1016/S1470-2045(19)30856-3

8. Wick W, Gorlia T, Bendszus M, Taphoorn M, Sahm F, Harting I, et al. Lomustine and bevacizumab in progressive glioblastoma. *N Engl J Med.* (2017) 377:1954–63. doi: 10.1056/NEJMoa1707358

9. Reardon DA, Brandes AA, Omuro A, Mulholland P, Lim M, Wick A, et al. Effect of nivolumab vs bevacizumab in patients with recurrent glioblastoma: the CheckMate 143 phase 3 randomized clinical trial. *JAMA Oncol.* (2020) 6:1003–10. doi: 10.1001/jamaoncol.2020.1024

10. Cloughesy TF, Mochizuki AY, Orpilla JR, Hugo W, Lee AH, Davidson TB, et al. Neoadjuvant anti-PD-1 immunotherapy promotes a survival benefit with intratumoral and systemic immune responses in recurrent glioblastoma. *Nat Med.* (2019) 25:477–86. doi: 10.1038/s41591-018-0337-7

11. Liau LM, Ashkan K, Brem S, Campian JL, Trusheim JE, Iwamoto FM, et al. Association of autologous tumor lysate-loaded dendritic cell vaccination with extension of survival among patients with newly diagnosed and recurrent glioblastoma: a phase 3 prospective externally controlled cohort trial. *JAMA Oncol.* (2023) 9:112–21. doi: 10.1001/jamaoncol.2022.5370

12. Todo T, Ito H, Ino Y, Ohtsu H, Ota Y, Shibahara J, et al. Intratumoral oncolytic herpes virus G47Δ for residual or recurrent glioblastoma: a phase 2 trial. *Nat Med.* (2022) 28:1630–9. doi: 10.1038/s41591-022-01897-x

13. Sampson JH, Gunn MD, Fecci PE, Ashley DM. Brain immunology and immunotherapy in brain tumours. *Nat Rev Cancer.* (2020) 20:12–25. doi: 10.1038/s41568-019-0224-7

14. Nabors B, Portnow J, Hattangadi-Gluth J, Horbinski C, NCCN CNS. tumor guidelines update for (2023). *Neuro Oncol.* (2023) 25:2114–6. doi: 10.1093/neuonc/noad169

15. Vergote I, Macarulla T, Hirsch FR, Hagemann C, Miller DS. Tumor Treating Fields (TTFields) Therapy Concomitant with Taxanes for Cancer Treatment. *Cancers (Basel)*. (2023) 15:636. doi: 10.3390/cancers15030636

16. Guo C, Yang Q, He Z, Duan H, Liu R, Mu Y. Tumor-treating fields combined with second-line chemotherapy reached pro-gression free survival of 833 months in Chinese recurrent glioblastoma. *Neuro Oncol.* (2023) 25:ii117. doi: 10.1093/neuonc/noad137.395

17. Tran DD, Ghiaseddin AP, Chen D, Le SB. Final analysis of 2-THE-TOP: a phase 2 study of TTFields (Op-tune) plus pembrolizumab plus maintenance temozolomide (TMZ) in patients with newly diagnosed glioblastoma. *J Clin Oncol.* (2023) 41:2024. doi: 10.1200/JCO.2023.41.16_suppl.2024

frontiers | Frontiers in Neurology

TYPE Case Report
PUBLISHED 14 February 2024
DOI 10.3389/fneur.2024.1349044

OPEN ACCESS

EDITED BY
Bo Yuan Huang,
Capital Medical University, China

REVIEWED BY
Felix Mircea Brehar,
Carol Davila University of Medicine and Pharmacy, Romania
Diogo Goulart Corrêa,
Rio de Janeiro State University, Brazil

*CORRESPONDENCE
Jun Yang
8020223@zju.edu.cn
Huiqing Zhang
8021026@zju.edu.cn

†These authors share first authorship

‡These authors have contributed equally to this work

RECEIVED 04 December 2023
ACCEPTED 29 January 2024
PUBLISHED 14 February 2024

CITATION
Yang T, Hu J, Li L, Xu H, Zhang C, Huang Z, Yang J and Zhang H (2024) The imaging dynamic changes in the malignant transformation of an epidermoid cyst: a case report and literature review.
Front. Neurol. 15:1349044.
doi: 10.3389/fneur.2024.1349044

The imaging dynamic changes in the malignant transformation of an epidermoid cyst: a case report and literature review

Tian Yang[1†], Jibo Hu[1†], Lele Li[2], Houyun Xu[1], Caijuan Zhang[1], Zhilan Huang[1], Jun Yang[1*‡] and Huiqing Zhang[1*‡]

[1]Department of Radiology, The Fourth Affiliated Hospital of School of Medicine, and International School of Medicine, International Institutes of Medicine, Zhejiang University, Yiwu, China, [2]Department of Clinical Laboratory, The Fourth Affiliated Hospital of School of Medicine, and International School of Medicine, International Institutes of Medicine, Zhejiang University, Yiwu, China

Malignant transformation of epidermoid cysts is a rare complication. Most of the previously reported cases have involved postoperative malignant transformations. We present a case of malignant transformation of a nonpostoperative epidermoid tumor into squamous cell carcinoma (SCC) that occurred in a 61-year-old Chinese woman. The patient's initial cranial MRI scan showed an epidermoid cyst with marginal enhancement in the pre-pontine cistern, and the lesion gradually enlarged after 10 months. A craniotomy was performed using to remove part of the tumor via the right retrosigmoid approach, and postoperative pathology confirmed that the transformation of the epidermoid cyst was malignant. Our case study suggests that the possibility of malignant transformation of epidermoid cyst should not be ignored on the basis of enhanced imaging features, regardless of whether they are nodular, annular, or patchy, as is the case for inflammation. Strict follow-up is required for early detection of malignant transformation to prompt correspondingly early clinical treatment.

KEYWORDS

epidermoid cysts, malignant transformation, squamous cell carcinoma, pre-pontine cistern, follow-up

Introduction

An intracranial epidermoid cyst is a rare developmental benign tumor whose malignant transformation is very rare and has been poorly reported. Most of the reported cases involved postoperative malignant transformation, and cases without surgical treatment for malignant transformation are even rarer. In this paper, we report a case in which malignant transformation of an epidermoid cyst was confirmed by pathology and describe its dynamic imaging manifestations within 2 years to improve the clinical understanding of the malignant transformation of a cranial epidermoid cyst.

Case report

A 61-year-old female patient was admitted to the Department of Neurosurgery, the Fourth Affiliated Hospital of Zhejiang University School of Medicine, due to restricted right eye abduction. The patient had progressive worsening of symptoms for 8 months, accompanied by

blurred vision and double vision. She had no history of tumors or brain disorders, and no family members had any related medical history. Laboratory tests did not reveal abnormalities, such as tumor markers or thrombotic markers. On December 28, 2021, a cranial MRI scan revealed a nodular abnormal signal in the pre-pontine cistern with unclear borders and irregular morphology, which was consistent with the imaging findings of epidermoid cysts (Figures 1A–E). However, a patchy enhancement lesion was shown in the adjacent pons, and the clinician thought that this feature might due to inflammation in the pons adjacent to the epidermoid cyst and could not rule out the possibility of a tumor (Figures 1F–I). The lesion extends from the optic chiasm to the beginning of the right abducens nerve, the lesion is in close proximity to the right trigeminal nerve, abducens nerve, and optic chiasm nerve (Figures 1C,J–L). The patient and their families refused surgery because of the high risk of surgery. Doctors recommended treatment with methylprednisolone sodium succinate to improve symptoms of abducens nerve irritation and instructed the patient regarding the need for close follow-up. However, the patient did not pay enough attention to the treatment and stopped treatment independently after 8 days.

On July 6, 2022, the patient underwent another MRI scan, which showed that the right pontine edge enhancement lesion was larger than it was on December 28, 2021, and that cystic lesions had appeared (Figure 2). The lesion at the right margin of the pons exhibited annular enhancement and extended into the brachium pontis. On October 10, 2022, the patient underwent another cranial computerized tomography (CT), a magnetic resonance enhancement scan, and magnetic resonance spectroscopy (MRS) due to worsening symptoms. The results showed that the lesion was further expanded than it was on July 6, 2022 (Figures 3A–D). A cystic solid lesion was revealed in the immediate vicinity of the right pontine border, the right brachium pontis, and the right cerebellar hemisphere. The boundaries of the cystic-solid lesions were unclear, and the solid component was markedly enhanced. The lesions were in close proximity to the right abducens nerve, some lesions invaded the brainstem, and the meninges adjacent to the brainstem were thickened (Figure 3E). CT of the brain showed an area of low-density lesions with speckled calcifications (Figure 3F). The area of the lesion located in the pontine and right brachium pontis showed an elevated Cho peak, a decreased NAA peak, and a Lac peak (Figure 3G). At the same time, the patient underwent a comprehensive examination, and no obvious tumor signs were found outside the brain.

On October 13, 2022, the doctor performed a craniotomy to remove part of the tumor via the right retrosigmoid approach. Histopathological examination of tissue taken from the anterior pre-pontine cistern showed features consistent with epidermoid cysts (Figure 4A). Histopathological results of tissue taken from the brainstem showed invasion by carcinoma (Figure 4B); immunohistochemistry (IHC) confirmed that CK (AE1/AE3) was

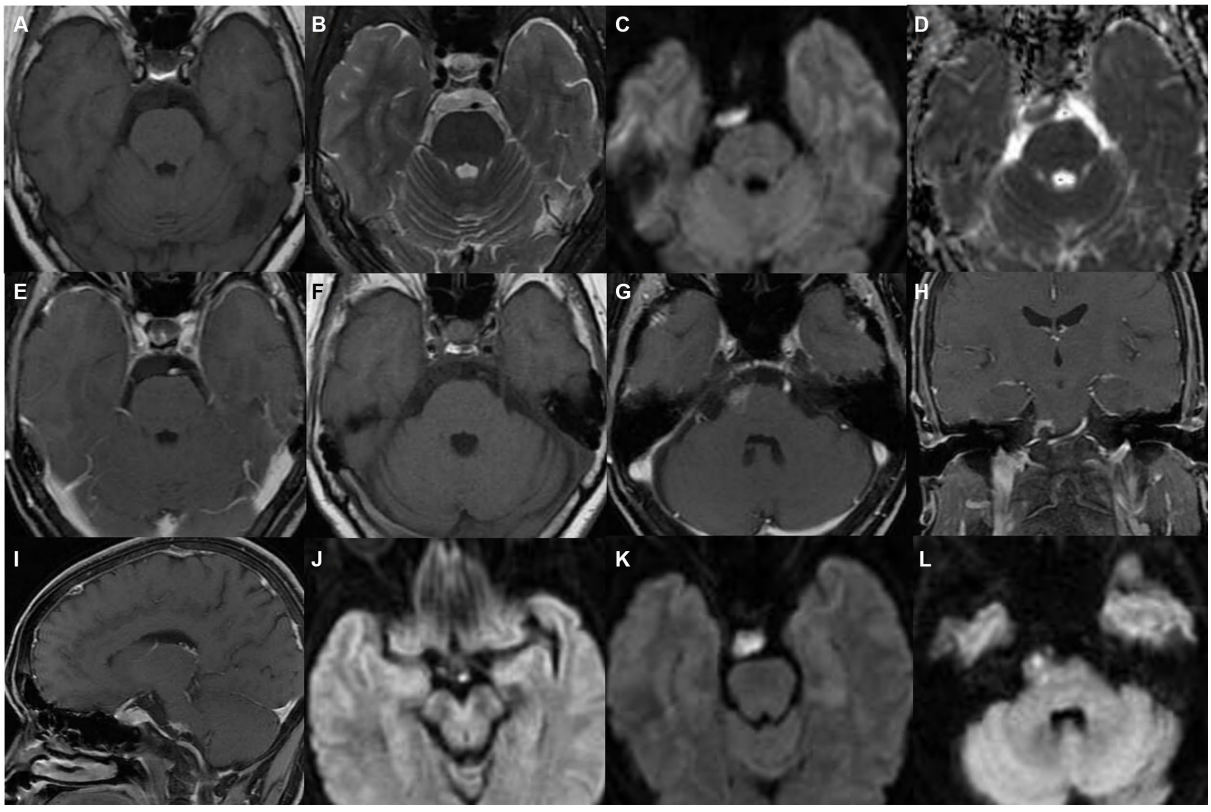

FIGURE 1
MRI in December 2021. **(A–E)** The nodule in the pre-pontine cistern showed a low-intensity signal on T1-weighted imaging, a high-intensity signal on T2-weighted imaging, a high-intensity signal on diffusion-weighted imaging (DWI), a low-intensity signal on an apparent diffusion coefficient plot (ADC), and no enhancement on contrast-enhanced T1-weighted imaging; **(F–I)** the lesion is adjacent to the right edge of the pons and shows patch-like enhancement, the boundary is not clear; **(C,J–L)** the lesion extends from the optic chiasm to the beginning of the right abducens nerve, the lesion is in close proximity to the right trigeminal nerve, abducens nerve, and optic chiasm nerve.

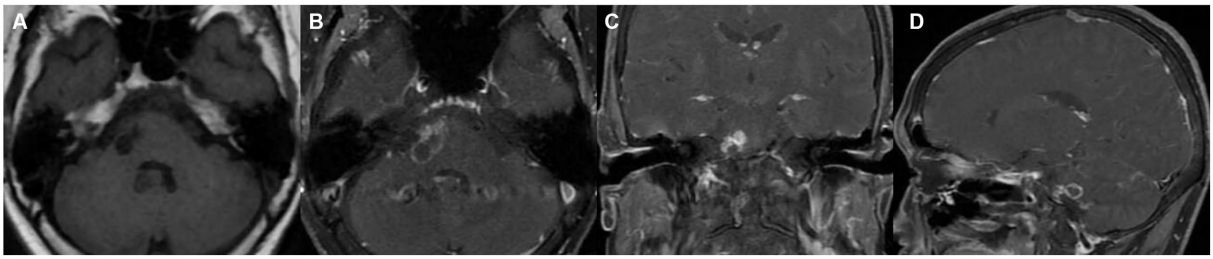

FIGURE 2
Imaging taken in July 2022. **(A)** Cystic lesions are visible on the right side of the pons on T1-weighted imaging; **(B–D)** contrast-enhanced scan image showing that the lesion had a ring shape and nodular enhancement features, and the lesion invaded the brachium pontis and was considered to be a neoplastic lesion.

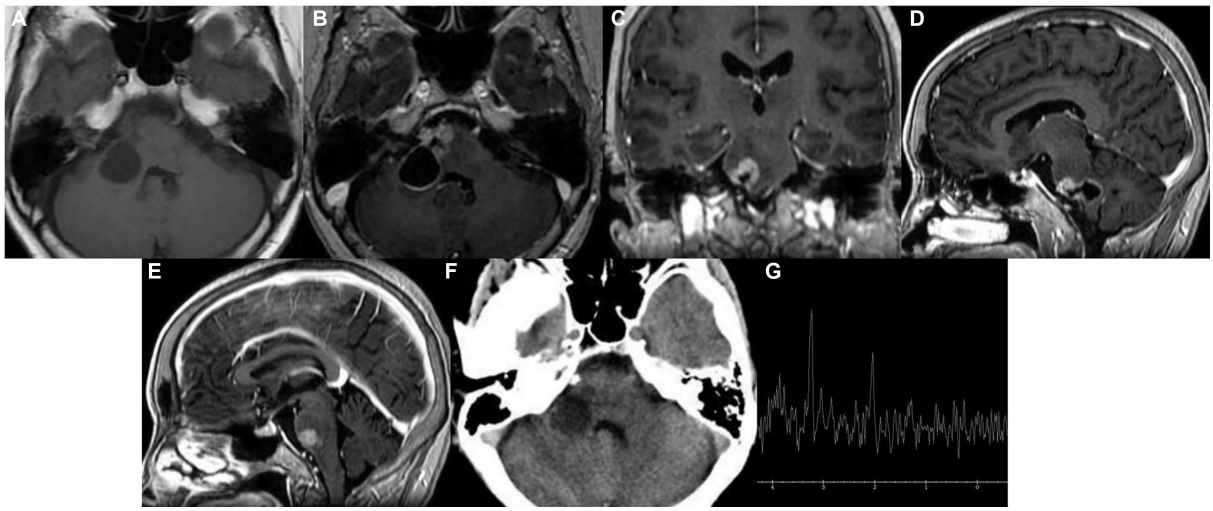

FIGURE 3
Imaging examination in October 2022. **(A–D)** A cystic solid shadow was observed in the right pons, brachium pontis, and right cerebellar hemisphere; **(E)** the adjacent meninges were slightly thickened; **(F)** speckled calcification appeared in the low-density lesion area; and **(G)** single-voxel 1H + MR spectroscopy (MRS).

positive (Figure 4C), GATA3 (Figure 4D) was positive, vimentin was focally expressed (Figure 4E), GFAP, S-100, IDH-1, Oligo-2, TTF-1, PAX8, CK20, and CDX-2 were negative, and the Ki-67 proliferation index was 20% (Figure 4F).

On October 18, 2022, the patient underwent the first cranial MRI enhancement examination (Figure 5A) after surgery, and the patient underwent radiation therapy in another hospital for 1 month. On January 6, 2023 (Figure 5B), magnetic resonance enhancement revealed that the unresected cystic solid lesions in the brainstem were slightly smaller than on October 18, 2022. On February 25, 2023, the lesions (Figure 5C) were slightly larger than before, with diffuse meningeal metastases (Figure 5D). Ventriculoperitoneal shunt was performed on April 6, 2023, and six cycles of bevacizumab (avastin) combined with nab-paclitaxel combined with carboplatin chemotherapy were performed from April 24, 2023 to September 22, 2023. During this period, on July 6, 2023 (Figure 5E), MRI showed that the condition of cranial metastases has improved compared to before. On October 06, 2023, the cranial metastases (Figure 5F) progressed than it was on July 6, 2023, and chemotherapy was performed with temozolomide. The patient was hospitalized on October 31, 2023 due to terminal tumor and lung infection, and unfortunately passed away on November 11, 2023 due to worsening of his condition.

Discussion

During normal embryonic development, there is no epithelial tissue in the human brain. Therefore, the vast majority of intracranial squamous cell carcinomas (SCCs) are secondary to distant metastasis of primary malignancies, such as head and neck cancer and lung cancer. Since 1912, when Ens first proposed the malignant transformation of epidermoid cysts, corresponding studies have been performed, most of which involved postoperative malignant transformations, which occurred only rarely. Cases of malignant transformation without surgical treatment, as reported here, are even rarer.

At present, the reported malignant transformation of epidermoid cysts mostly occurs in middle-aged female patients, with an average age of 54 years (1–3). The most common location is the cerebellopontine angle, accounting for approximately 61.5%

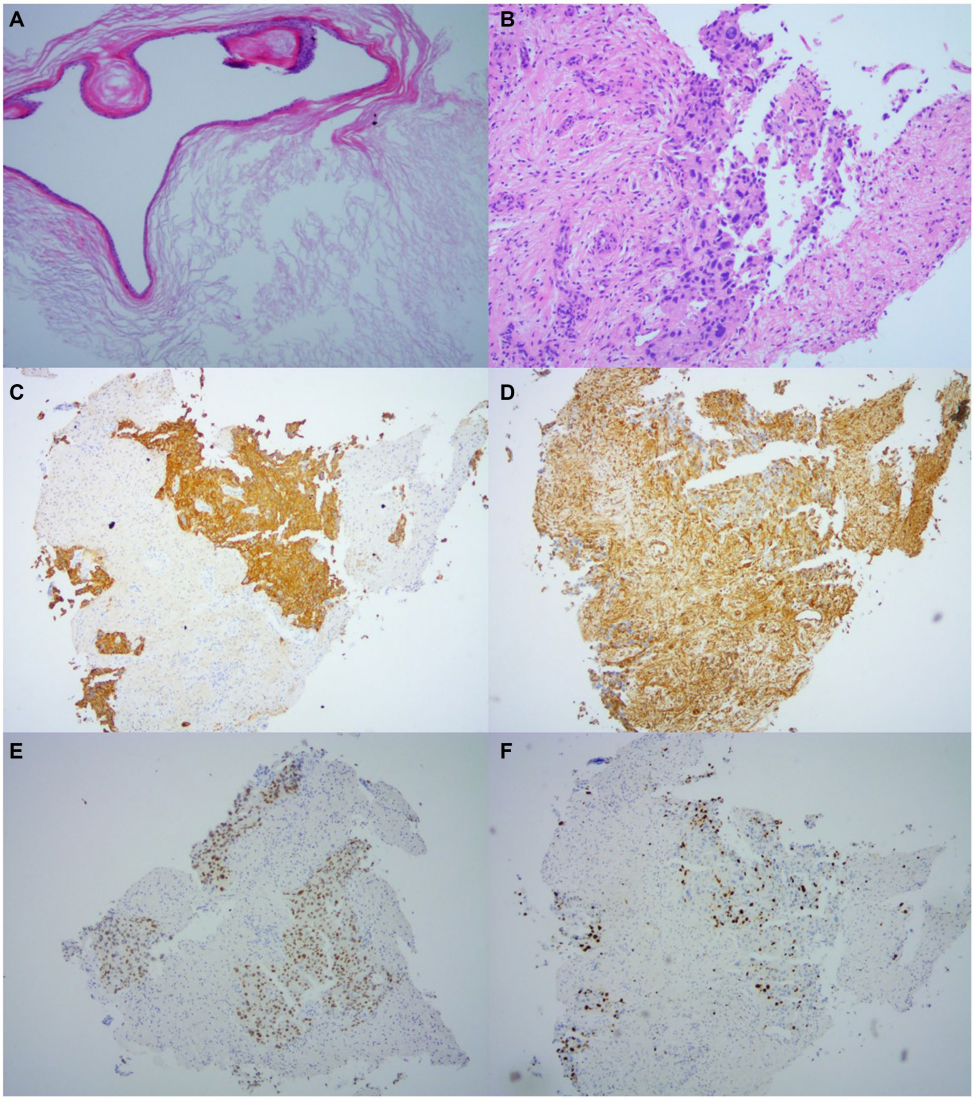

FIGURE 4
Histopathology. **(A)** Histopathology taken from the anterior pre-pontine cistern shows lamellar keratoses with a stratified squamous epithelium lined with a sac wall, consistent with the characteristics of an epidermoid cyst (HE × 100). **(B)** Histopathology taken from within the brainstem shows carcinoma invasion (HE × 100). **(C–F)** IHC results were taken from brainstem lesions: CK (AE1/AE3) was positive **(C)**, GATA3 **(D)** was positive, Vimentin was focal-expressing **(E)**, and Ki-67 proliferation index was 20%.

of cases. The average postoperative malignant transformation time is 82.7 months, and the prognosis is poor (1). It has been reported that patients who have undergone surgery alone have survived the shortest time to die within 1 month, and it is very rare to survive for more than 5 years (4). The lesion in a 61-year-old woman described in this article originated from the pre-pontine cistern, developed diffuse meningeal metastases only 4 months after surgery, and unfortunately led to the patient passing away 13 months after surgery. However, the mechanism of malignant transformation in epidermoid cysts is unclear, and studies have suggested that chronic inflammation caused by epidermoid cyst rupture or surgical foreign body presence and incomplete surgical resection may be the main factors involved (5). Several studies have suggested that when squamous metaplasia or *p53* mutation is observed in pathological specimens of epidermoid cysts, vigilance is needed for malignant transformation (1). This novel study reported the malignant transformation of an epidermoid cyst in the pineal region in which gene sequencing revealed a low mutational burden (l Mut/Mb), microsatellite stability, and loss of *CDKN* 2A/B, *MTAP* (exons 2–8), and *PTEN* (exons 6–9) (6). IHC of malignant transformation of epidermoid cysts is positive for CK and EMA (7–9). In this case, IHC revealed CK and GATA3 expression, which was similar to what was previously reported.

Epidermoid cysts are slow-growing, benign lesions that are usually asymptomatic for many years. Epidermoid cysts are variable and exhibit multiple outcomes as the disease progresses, such as resolution, hemorrhage, and malignant transformation (10–12); however, when symptoms and signs develop rapidly, enhancement of lesion margins and nodular enhancement suggest the possibility of malignant transformation of epidermoid cysts (13). Patchy enhancement of adjacent tissues of epidermoid cysts has been reported to indicate chemical meningitis, but malignant

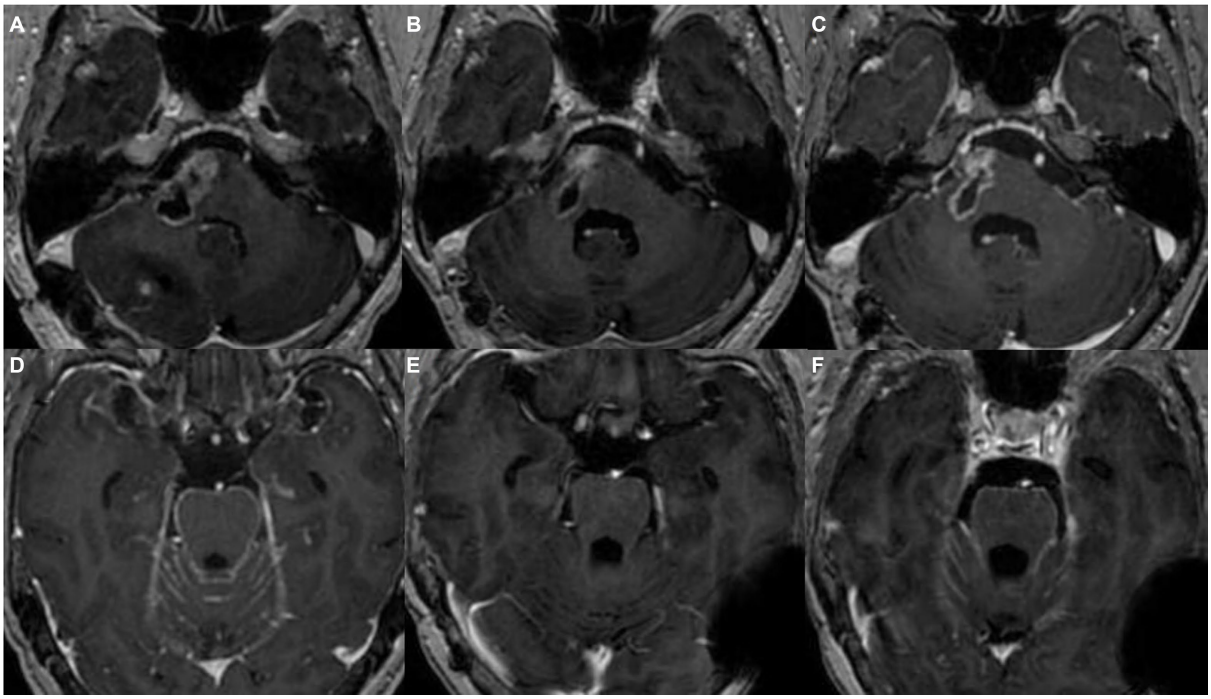

FIGURE 5
MRI-enhanced image of postoperative lesions. **(A)** The image of some unresected lesions in the brainstem area before postoperative radiotherapy; **(B)** unresected cystic solid lesions in the brainstem on January 6, 2023; **(C)** the image of brainstem lesions on February 25, 2023; **(D)** diffuse meningeal metastases on February 25, 2023; **(E)** diffuse meningeal metastases on July 6, 2023; and **(F)** diffuse meningeal metastases on October 06, 2023.

transformation should not be ruled out (14). To rule out malignant transformation, it is necessary to observe the patient's signs, morphology, and progression of the lesion, such as whether there is prominent rapid tumor growth, tissue edema, and nodular enhancement in adjacent or cystic lesions. The initial imaging results of the patient we reported showed patchy enhancement of the lesion adjacent to the pons, and the initial diagnosis was chemical inflammation around the epidermoid cyst. After 7 months of follow-up, the patient's symptoms progressively worsened, the lesion was obviously enlarged with necrosis, the adjacent brain tissue was invaded, and edema bands had formed around the lesion. MRS showed an increase in the Cho peak. The nonsignificant decrease in NAA peak intensity may have been due to the inclusion of normal tissue at the time of selection of the region of interest. Nodular leptomeningeal enhancement is an early imaging sign of leptomeningeal metastasis after malignant transformation of epidermoid cysts (14). Similarly, the last MRI of this patient before surgery showed lesion invasion of the brainstem and thickening of the meninges near the brainstem, which indicated leptomeningeal invasion. Diffuse meningeal metastases developed 4 months postoperatively and subsequently progressively worsened.

Imaging findings of epidermoid cyst malignancy are not specific and often present with enhancement features of the lesion, with or without cerebral edema. It has been suggested (15) that enhancement of epidermoid cyst margins or nodular enhancement is usually a sign of malignant transformation, and patchy enhancement of lesion margins is often thought to be chemical meningitis due to cyst rupture, but atypical for malignant transformation. It has also been suggested (10) that almost all cases have worsening of signs and different degrees of enhancement of lesions before malignant transformation, so atypical enhancement methods need to be combined with patients' signs to make the best diagnosis.

The most important differentiating factor of intracranial epidermoid cyst malignancy on imaging is metastasis; therefore, when a single intracranial lesion is present, a comprehensive examination should also be performed to rule out the diagnosis of extracranial metastases. In this case, after comprehensive inspection to rule out metastatic tumors, malignant transformation of the epidermoid cyst was diagnosed according to the pathological results, which were consistent with the criteria of Hamlat et al. (16). The history of early disease progression was unknown because the patient did not undergo relevant tests before starting to experience symptoms or within 8 months of symptom onset. This case is the first cases diagnosed in our hospital; moreover, there are no other case data for comparison, and it is still necessary to summarize the characteristics of similar cases.

Conclusion

Although epidermoid cysts are mostly benign and malignant transformation is rare, it does occur. Patients with epidermoid cysts should be followed up, either surgically or conservatively. In addition, if there are nodal, annular or patchy imaging enhancement features, such as is in inflammation, the possibility of malignant transformation of epidermoid cysts cannot be ignored, and close follow-up is required for early detection of malignant transformation to prompt correspondingly early clinical treatment.

Data availability statement

The original contributions presented in the study are included in the article/supplementary material; further inquiries can be directed to the corresponding authors.

Ethics statement

The studies involving humans were approved by Human Research Ethics Committee of the Fourth Affiliated Hospital of Zhejiang University School of Medicine. The studies were conducted in accordance with the local legislation and institutional requirements. Written informed consent for participation was not required from the participants or the participants' legal guardians/next of kin in accordance with the national legislation and institutional requirements. Written informed consent was obtained from the individual(s) for the publication of any potentially identifiable images or data included in this article.

Author contributions

TY: Funding acquisition, Writing – original draft, Writing – review & editing. JH: Writing – original draft, Writing – review & editing. LL: Funding acquisition, Writing – review & editing. HX: Writing – review & editing. CZ: Writing – review & editing. ZH: Writing – review & editing. JY: Funding acquisition, Resources, Writing – review & editing. HZ: Resources, Writing – review & editing.

Funding

The author(s) declare financial support was received for the research, authorship, and/or publication of this article. This study was supported by the Jinhua City Major Scientific and Technological Research Foundation of China [no. 2021-3-012] and Scientific Research Projects of Zhejiang Provincial Department of Education (no. Y202353877 and Y202353450).

Conflict of interest

The authors declare that the research was conducted in the absence of any commercial or financial relationships that could be construed as a potential conflict of interest.

Publisher's note

References

1. Sakamoto H, Akimoto J, Tsutsumi M, Ken KM, Ichimasu N, Kohno M. Radiopathological characteristics of malignant transformation of an epidermoid cyst in the cerebellopontine angle: a case report. *Surg Neurol Int*. (2022) 13:135. doi: 10.25259/SNI_1226_2021

2. Lakhdar F, Hakkou EM, Gana R, Maaqili RM, Bellakhdar F. Malignant transformation six months after removal of intracranial epidermoid cyst: A case report. *Case Rep Neurol Med*. (2011) 2011:525289. doi: 10.1155/2011/525289

3. Tamura K, Aoyagi M, Wakimoto H, Tamaki M, Yamamoto K, Yamamoto M, et al. Malignant transformation eight years after removal of a benign epidermoid cyst: a case report. *J Neuro-Oncol*. (2006) 79:67–72. doi: 10.1007/s11060-005-9117-6

4. Tognetti F, Lanzino G, Manetto V, Calbucci F. Intracranial squamous cell carcinoma arising in remnant of extirpated epidermoid cyst. *Br J Neurosurg*. (1991) 5:303–5. doi: 10.3109/02688699109005191

5. Mliyh L, Di Perri D, Onofrj V. Intracranial squamous cell carcinoma of the cerebello-pontine angle mimicking a cystic acoustic schwannoma. A case report with discussion of differential diagnosis and review of literature. *Radiol Case Rep*. (2023) 18:753–6. doi: 10.1016/j.radcr.2022.11.048

6. Gerges MM, Godil SS, Rumalla K, Liechty B, Pisapia DJ, Magge RS, et al. Genomic profile of a primary squamous cell carcinoma arising from malignant transformation of a pineal epidermoid cyst. *Acta Neurochir*. (2019) 161:1829–34. doi: 10.1007/s00701-019-03983-5

7. Monaco R, Boscaino A, Di Blasi A, D'Antonio A, Profeta G, De Falco R, et al. Intraepithelial carcinoma arising in an endodermal cyst of the posterior fossa. *Neuropathology*. (2003) 23:219–24. doi: 10.1046/j.1440-1789.2003.00497.x

8. Hatem O, Bedou G, Bertrand JL, Camo J, Bousquet C. Intracranial primary epidermoid carcinoma. *Neurochirurgie*. (2002) 48:109–12.

9. Asahi T, Kurimoto M, Endo S, Monma F, Ohi M, Takami M. Malignant transformation of cerebello-pontine angle epidermoid. *J Clin Neurosci*. (2001) 8:572–4. doi: 10.1054/jocn.2000.0856

10. Kaneko T, Fujinaga Y, Ichinohe F, Ogiwara T, Horiuchi T. Spontaneous regression of radiologically diagnosed epidermoid cyst originating from the cerebellopontine angle. *World Neurosurg*. (2020) 144:238–43. doi: 10.1016/j.wneu.2020.09.008

11. Jamjoom DZ, Alamer A, Tampieri D. Correlation of radiological features of white epidermoid cysts with histopathological findings. *Sci Rep*. (2022) 12:2314. doi: 10.1038/s41598-022-06167-x

12. Zuo P, Sun T, Wang Y, Geng Y, Zhang P, Wu Z, et al. Primary squamous cell carcinomas arising in intracranial epidermoid cysts: a series of nine cases and systematic review. *Front Oncol*. (2021) 11:750899. doi: 10.3389/fonc.2021.750899

13. Fereydonyan N, Taheri M, Kazemi F. Cerebellar squamous cell carcinoma due to malignant transformation of cerebellopontine angle epidermoid cyst. *Prague Med Rep*. (2019) 120:95–102. doi: 10.14712/23362936.2019.14

14. Demuth S, Lasry DE, Obaid S, Letourneau-Guillon L, Chasse M, Belanger K, et al. Pseudo-chemical meningitis and the malignant transformation of an epidermoid cyst. *Can J Neurol Sci*. (2019) 46:642–4. doi: 10.1017/cjn.2019.235

15. Kodama H, Maeda M, Hirokawa Y, Suzuki H, Hori K, Taki W, et al. MRI findings of malignant transformation of epidermoid cyst: case report. *J Neuro-Oncol*. (2007) 82:171–4. doi: 10.1007/s11060-006-9255-5

16. Hamlat A, Hua ZF, Saikali S, Laurent JF, Gedouin D, Ben-Hassel M, et al. Malignant transformation of intra-cranial epithelial cysts: systematic article review. *J Neuro-Oncol*. (2005) 74:187–94. doi: 10.1007/s11060-004-5175-4

frontiers | Frontiers in Neurology

TYPE Case Report
PUBLISHED 28 February 2024
DOI 10.3389/fneur.2024.1351674

OPEN ACCESS

EDITED BY
Bo yuan Huang,
Capital Medical University, China

REVIEWED BY
Felix Mircea Brehar,
Carol Davila University of Medicine and Pharmacy, Romania
S. Ottavio Tomasi,
Paracelsus Medical University, Austria

*CORRESPONDENCE
Jun Cao
caojun13651611423@126.com

†These authors have contributed equally to this work and share first authorship

RECEIVED 06 December 2023
ACCEPTED 16 February 2024
PUBLISHED 28 February 2024

CITATION
Zhang D, Liu H, Zhang M and Cao J (2024) Adult supratentorial extraventricular anaplastic ependymoma with cerebrospinal fluid dissemination metastases: a case report. *Front. Neurol.* 15:1351674. doi: 10.3389/fneur.2024.1351674

Adult supratentorial extraventricular anaplastic ependymoma with cerebrospinal fluid dissemination metastases: a case report

Daojin Zhang†, Hongbing Liu†, Maosong Zhang† and Jun Cao*

Department of Neurosurgery, The First Affiliated Hospital of Wannan Medical College (Yijishan Hospital of Wannan Medical College), Wuhu, China

Background: Ependymomas mostly locate in the infratentorial region and often occur in children. Anaplastic ependymomas account for 45–47% of supratentorial and 15–17% of infratentorial ependymomas, also known as malignant ependymomas. Adult supratentorial extraventricular anaplastic ependymoma (SEAE) is rare in clinical practice, and only a few cases have been reported so far, and there is no clinical study with large sample size. We report a case of adult supratentorial extraventricular anaplastic ependymoma in the occipital lobe with cerebrospinal fluid dissemination metastases.

Case description: A 58-year-old female patient presented with unexplained pain in multiple parts of the body for the past half a year, mainly manifested as pain in the head, abdomen and chest. On August, 2022, Head MRI of the patient showed abnormal signal shadow in the left occipital lobe, which was considered a malignant lesion. The patient underwent tumor resection under general anesthesia on September 3, 2022. Postoperative pathological examination showed anaplastic ependymoma. The postoperative follow-up head MRI showed multiple cerebrospinal fluid dissemination metastases in the brain.

Conclusion: Adult SEAE is a rare tumor with high malignancy and have a tendency to disseminate into the CSF, resulting in drop metastases. Immunohistochemistry is very important for the diagnosis of SEAE. It is recommended to administer adjuvant chemotherapy or radiation therapy appropriately after surgery, based on the tumor being completely resected as much as possible.

KEYWORDS

supratentorial extraventricular, anaplastic ependymoma, dissemination metastases, operation, pathology

Introduction

Ependymoma refers to central nervous system tumor originating from the ependymal cell of the ventricle and the central canal of spinal cord, or ependymal cell nest in the white matter of the brain. It often occurs in children and accounts for only 2–9% of adult neuroepithelial cell tumors (1). In 2021, World Health Organization (WHO) revised the classification of ependymoma to supratentorial ependymoma, posterior fossa ependymoma, spinal ependymoma, and subependymoma (2). As a WHO grade III tumor, supratentorial

extraventricular anaplastic ependymoma has the characteristics of high recurrence rate, low survival rate and rare occurrence. At present, there are only a few case reports of supratentorial extraventricular anaplastic ependymoma, and there is no clinical study with large sample size. In this study, the clinical manifestations, imaging features, pathological features, treatment methods and prognosis of a patient with supratentorial extraventricular anaplastic ependymoma with cerebrospinal fluid dissemination metastases were analyzed and the results were reported as follows.

Case presentation

A 58-year-old female patient presented with unexplained pain in the head, abdomen and chest in the past 6 months, and has been checked many times in the hospital without special abnormalities was found. Before admission, she experienced symptoms of nausea, vomiting, and fatigue, and has lost 10 kg of weight in the past 2 months. On August, 2022, PET-CT of the patient showed a hypermetabolic mass in the left occipital lobe and left basal ganglia, which was considered to be malignant. Visual examination upon admission revealed that the patient had contralateral hemianopsia in both eyes. After admission, the head CT showed a slightly high-density mass in the left occipital lobe, hippocampus, and corpus callosum. T2-weighted image of head MRI showed hyperintensity of the lesion with surrounding edema. Axial T1-enhanced image of head MRI showed patchy mild enhancement of the lesion, part of the lesion encompassed the posterior part of the left lateral ventricle (Figure 1).

On September, 2022, the patient underwent microsurgical resection of the space-occupying lesion in the left occipital lobe under general anesthesia. During the operation, the lesion can be seen to be dark red in color, with rich blood supply, infiltrative growth and soft texture. The lesion tissue and part of the occipital lobe were resected along the edema zone of the tumor. The size of the excised lesion is approximately 5.5 cm × 5.0 cm × 4.0 cm. Due to the extensive infiltration of the patient's tumor, in order to preserve the patient's neurological function and ensure life safety, the tumor was not completely removed during surgery.

The pathological diagnosis was anaplastic ependymoma (Figure 2). However, the patient's consciousness gradually deteriorated and seizures occurred after operation. She was transferred to the neurosurgical intensive care unit and underwent tracheostomy 7 days after operation. After treatment, the patient regained clear consciousness, and had V-grade muscle strength in both limbs. One month after surgery, focal radiation therapy (59.40 Gy in 1.8 Gy daily fractions) and chemotherapy (temozolomide) were administered. Eight months after operation, the patient developed frequent epileptic seizures, and head MRI showed multiple cerebrospinal fluid dissemination metastases in the brain (Figure 3). The patient's family decided to give up treatment, and the patient died 9 months after operation.

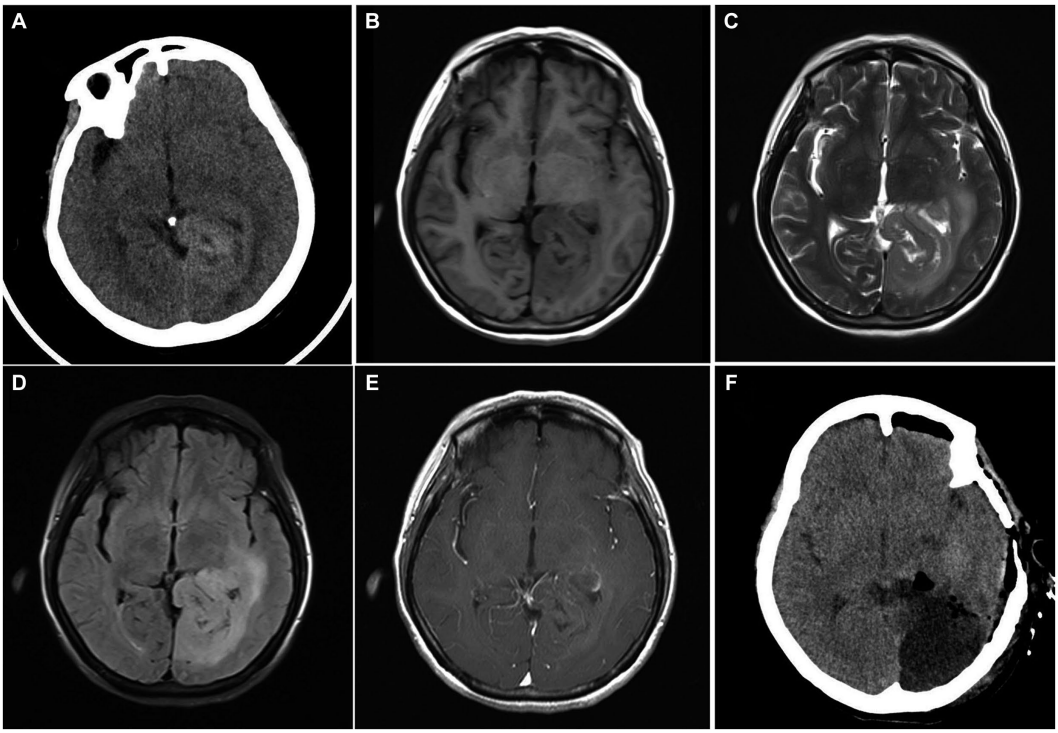

FIGURE 1
(A) Head CT on admission showed a slightly high-density mass in the left occipital lobe. **(B)** The lesion was hypointense on T1-weighted image. **(C)** T2-weighted image of head MRI showed hyperintensity of the lesion with surrounding edema. **(D)** T2-FLAIR image showed mixed signals with ill-defined borders. **(E)** Axial T1-enhanced image showed patchy mild enhancement of the lesion, part of the lesion encompassed the posterior part of the left lateral ventricle. **(F)** The head CT at 4 h after operation showed that the tumor was largely removed, and there was no obvious bleeding in the operation area.

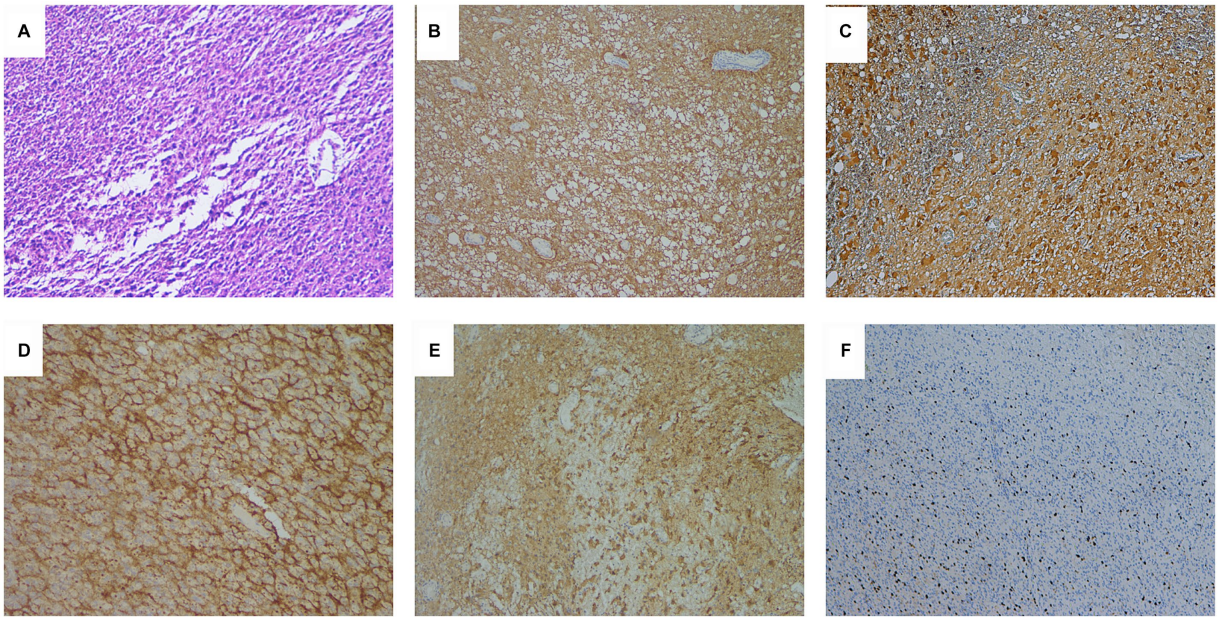

FIGURE 2
(A) Hematoxylin–eosin staining showed poorly differentiated tumor cells with hyperchromatic nuclei and proliferation of vascular endothelial cells (×100). **(B)** Immunohistochemical results showed diffuse cytoplasmic glial fibrillary acidic protein (GFAP) immunoreactivity (×100), **(C)** diffuse cytoplasmic and nuclear S100 immunoreactivity (×100), and **(D)** diffuse perinuclear epithelial membrane antigen (EMA) immunoreactivity suggestive of ependymal differentiation (×200). **(E)** Diffuse cytoplasmic and nuclear AE1/AE3 immunoreactivity (×100). **(F)** Ki-67 proliferation index was approximately 20% (×100).

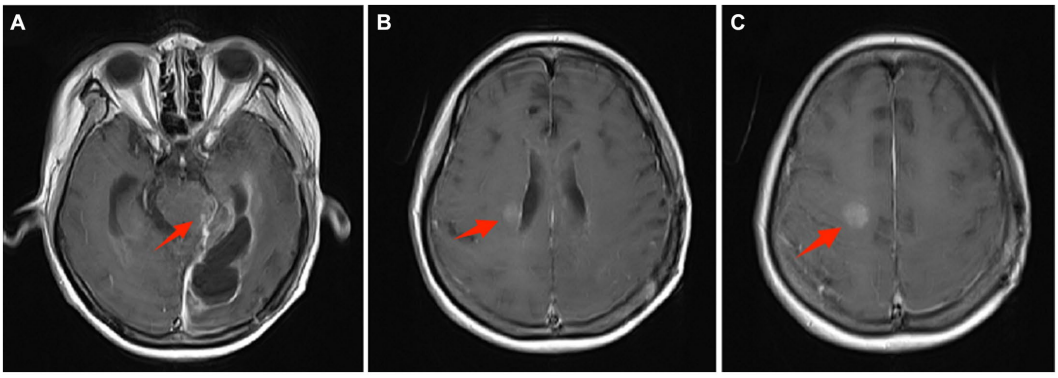

FIGURE 3
Eight months after operation, head MRI showed multiple cerebrospinal fluid dissemination metastases in the brain. **(A)** On enhanced magnetic resonance imaging, the arrow points to the tumor metastasis at the brainstem. **(B)** The arrow points to the metastatic tumor near the right ventricle. **(C)** The arrow points to a metastatic tumor in front of the right central sulcus.

Discussion

Supratentorial anaplastic ependymoma is a rare and highly malignant tumor, most of which occurs in the ventricle, but a small part of which can occur in the brain parenchyma and has no obvious correlation with the ventricle. Adult supratentorial extraventricular anaplastic ependymoma (SEAE) is rare in clinical practice, and only a few cases have been reported so far (Table 1). SEAE grows rapidly, mainly characterized by headache, vomiting, lethargy, anorexia, diplopia and other intracranial hypertension symptoms, and may be accompanied by epileptic seizures. Specific symptoms also depend on the location of the tumor, such as the tumor located in the frontal lobe, which can cause memory loss and mental abnormalities, and the tumor located in the occipital lobe, which can cause visual field changes (14). This patient presented with multiple unexplained pain throughout the body and visual field changes, which we speculated was related to the tumor invasion of the occipital lobe, the splenium of the corpus callosum and the hippocampus.

The pathological features of anaplastic ependymoma were high tumor cell density, diverse cell morphology, poor cell differentiation, obvious nuclear atypia, more mitoses, and loss of the arrangement structure of ependymal epithelial cells (10). Compared with ependymoma, the perivascular pseudorosette structures of anaplastic ependymoma were significantly reduced, and vascular endothelial cell

TABLE 1 Cases of supratentorial extraventricular anaplastic ependymoma in the literature.

Report	Age (years)	Sex	Location	Therapy	CSF dissemination metastases	Overall survival
Takeshima et al., 2002 (3)	70	Female	Right frontal lobe	Surgery	Not find	>14 months
Kojima et al., 2003 (4)	56	Female	Left temporal lobe	Surgery + radiotherapy	Not find	Unknown
Moritani et al., 2003 (5)	50	Female	Right temporal lobe	Surgery + chemotherapy	Not find	20 months
Miyazawa et al., 2007 (6)	33	Male	Left angular gyrus	Surgery + radiotherapy + chemotherapy	Not find	>6 months
Niazi et al., 2009 (7)	36	Female	Right frontal lobe	Surgery + radiotherapy	Not find	>29 months
	18	Male	Right frontal lobe			14 months
Davis et al., 2011 (8)	22	Female	Frontotemporal	Surgery + radiotherapy	Not find	>54 months
Romero et al., 2012 (9)	23	Male	Frontal lobe	Surgery + radiotherapy	Not find	Unknown
Iwamoto et al., 2014 (10)	61	Male	Right temporal lobe	Surgery + radiotherapy +chemotherapy	Dissemination metastases in spine	>12 months
Han et al., 2014 (11)	23	Male	Left occipital lobe	Surgery + radiotherapy	Dissemination metastases in spine	>48 months
Khilji et al., 2014 (12)	2	Male	Superolateral to the Right lateral ventricle	Surgery + radiotherapy	Not find	Unknown
Pachella et al., 2015 (13)	21	Male	Light temporoparietal	Surgery + radiotherapy + chemotherapy	Not find	Unknown
Lavrador et al., 2018 (14)	69	Female	Right frontoparietal	Surgery + chemotherapy	Not find	18 months
Kharosekar et al., 2018 (15)	11	Female	Right frontoparietal	Surgery + radiotherapy	Not find	Unknown
Seo et al., 2019 (16)	42	Male	Right frontal lobe	Surgery + radiotherapy	Not find	>12 months
Falcón et al., 2023 (17)	19	Male	Right frontal lobe	Surgery + radiotherapy	Not find	Unknown
This study	58	Female	Left occipital lobe	Surgery + radiotherapy + chemotherapy	Dissemination metastases in brain	9 months

proliferation and pseudopalisade necrosis were common. Immunohistochemistry is very important for the diagnosis of anaplastic ependymoma. GFAP, S-100 and vimentin are positive in anaplastic ependymoma, and AE1/AE3 and EMA staining can also be positive (11).

Anaplastic ependymoma also have a tendency to disseminate into the cerebrospinal fluid (CSF), resulting in drop metastases (11). According to the 16 reported cases of supratentorial extraventricular anaplastic ependymoma so far, 3 of them reported cerebrospinal fluid dissemination and metastasis, with an incidence rate of 18.8% (Table 1). In the present case, dissemination and drop metastases occurred without recurrence at the primary site after adjuvant local field radiotherapy were identified.

The standard treatment for anaplastic ependymal tumors is total resection as far as possible, and adjuvant therapy such as appropriate local radiotherapy and chemotherapy after surgery (14). However, opinions on adjuvant therapy are divergent. For SEAE patients with high Ki-67 positive rate, some studies suggest that if the benefits of postoperative radiotherapy exceed the risk of recurrence of natural therapy in non-children and patients without obvious contraindications, appropriate radiotherapy can be given according to clinical practice (12). Therefore, the patient in this study was treated with appropriate extended resection of the lesion combined with local radiotherapy and chemotherapy.

According to previous literature, the factors that lead to poor prognosis of patients with anaplastic ependymoma include young age, incomplete tumor resection, tissue differentiation insufficiency, and tumor location above the tentorium and outside the ventricle. Among them, age and whether the tumor is completely resected are the most important factors (17). Ependymomas recur more frequently in the initial location after local failure. Kharosekar et al. (15) believed that if the tumor was completely located in the cortex, the patient might have a better prognosis. And, Saito et al. (16) reported that anaplastic ependymomas can disseminate within the central nervous system without local failure.

Conclusion

Adult SEAE is a rare tumor with high malignancy and variable clinical features. SEAE also have a tendency to disseminate into the CSF, resulting in drop metastases. Immunohistochemistry is helpful for the diagnosis of SEAE. The treatment of adult SEAE has not been completely unified. It is recommended that on the basis of surgical treatment, appropriate adjuvant chemotherapy or radiotherapy should be given according to the specific conditions after surgery.

Data availability statement

The datasets presented in this article are not readily available because of ethical and privacy restrictions. Requests to access the datasets should be directed to the corresponding author.

Ethics statement

The studies involving humans were approved by the First Affiliated Hospital of Wannan Medical College (Yijishan Hospital of Wannan Medical College). The studies were conducted in accordance with the local legislation and institutional requirements. Written informed consent for participation in this study was provided by the participants' legal guardians/next of kin. Written informed consent was obtained from the individual(s) for the publication of any potentially identifiable images or data included in this article.

Author contributions

DZ: Resources, Validation, Writing – original draft. HL: Data curation, Formal analysis, Software, Supervision, Writing – original draft. MZ: Methodology, Project administration, Software, Supervision, Validation, Writing – original draft. JC: Conceptualization, Formal analysis, Funding acquisition, Supervision, Validation, Visualization, Writing – review & editing.

Funding

The author(s) declare financial support was received for the research, authorship, and/or publication of this article. This work was supported by the "Peak" Training Program for Scientific Research of Yijishan Hospital (grant number PF2019003).

Conflict of interest

The authors declare that the research was conducted in the absence of any commercial or financial relationships that could be construed as a potential conflict of interest.

Publisher's note

References

1. Rudà R, Bruno F, Pellerino A, Soffietti R. Ependymoma: evaluation and management updates. *Curr Oncol Rep*. (2022) 24:985–93. doi: 10.1007/s11912-022-01260-w

2. Gritsch S, Batchelor TT, Gonzalez Castro LN. Diagnostic, therapeutic, and prognostic implications of the 2021 World Health Organization classification of tumors of the central nervous system. *Cancer*. (2022) 128:47–58. doi: 10.1002/cncr.33918

3. Takeshima H, Kawahara T, Uchida H, Hirano H, Nakazato Y, Kuratsu J. Brain surface ependymoma with repeated episodes of intratumoral hemorrhage--case report. *Neurol Med Chir (Tokyo)*. (2002) 42:166–9. doi: 10.2176/nmc.42.166

4. Kojima A, Yamaguchi N, Okui S, Kamiya M, Hirato J, Nakazato Y. Parenchymal anaplastic ependymoma with intratumoral hemorrhage: a case report. *Brain Tumor Pathol*. (2003) 20:85–8. doi: 10.1007/BF02483452

5. Moritani S, Kushima R, Bamba M, Kobayashi TK, Oka H, Fujimoto M, et al. Highly anaplastic extraventricular ependymoma arising in an adult, mimicking metastatic adenocarcinoma with heavy stromal inflammation and emperiporesis. *Pathol Int*. (2003) 53:539–46. doi: 10.1046/j.1440-1827.2003.01517.x

6. Miyazawa T, Hirose T, Nakanishi K, Uozumi Y, Tsuzuki N, Shima K. Supratentorial ectopic cortical ependymoma occurring with intratumoral hemorrhage. *Brain Tumor Pathol*. (2007) 24:35–40. doi: 10.1007/s10014-007-0215-3

7. Niazi TN, Jensen EM, Jensen RL. WHO Grade II and III supratentorial hemispheric ependymomas in adults: case series and review of treatment options. *J Neuro-Oncol*. (2009) 91:323–8. doi: 10.1007/s11060-008-9717-z

8. Davis MJ, Hasan F, Weinreb I, Wallace MC, Kiehl TR. Extraventricular anaplastic ependymoma with metastasis to scalp and neck. *J Neuro-Oncol*. (2011) 104:599–604. doi: 10.1007/s11060-010-0525-x

9. Romero FR, Zanini MA, Ducati LG, Vital RB, de Lima Neto NM, Gabarra RC. Purely cortical anaplastic ependymoma. *Case Rep Oncol Med*. (2012) 2012:541431. doi: 10.1155/2012/541431

10. Iwamoto N, Murai Y, Yamamoto Y, Adachi K, Teramoto A. Supratentorial extraventricular anaplastic ependymoma in an adult with repeated intratumoral hemorrhage. *Brain Tumor Pathol*. (2014) 31:138–43. doi: 10.1007/s10014-013-0146-0

11. Han MH, Park KS, Park SH, Hwang JH. Supratentorial extraventricular anaplastic ependymoma presenting with repeated intratumoral hemorrhage. *Brain Tumor Res Treat*. (2014) 2:81–6. doi: 10.14791/btrt.2014.2.2.81

12. Khilji MF, Hamid RS, Qureshi A. Supratentorial extraventricular anaplastic ependymoma in a child. *BMJ Case Rep*. (2014) 2014:bcr2014203750. doi: 10.1136/bcr-2014-203750

13. Pachella LA, Kamiya-Matsuoka C, Lee EL, Olar A, Yung WK. Supratentorial extraventricular anaplastic ependymoma with extracranial metastasis. *J Clin Neurosci*. (2015) 22:605–7. doi: 10.1016/j.jocn.2014.09.006

14. Lavrador JP, Oliveira E, Teixeira JC, Lopes JP, Pimentel J, Carvalho MH. Adult supratentorial extraventricular anaplastic ependymoma: therapeutic approach and clinical review. *Asian J Neurosurg*. (2018) 13:105–9. doi: 10.4103/1793-5482.181121

15. Kharosekar H, Bhide A, Velho V, Bijwe S. Pediatric isolated cortical (ectopic) anaplastic ependymoma. *Asian J Neurosurg*. (2018) 13:144–6. doi: 10.4103/1793-5482.181133

16. Seo SW, Kang HJ, Lee MS, Suh SJ, Lee YS, Lee JH, et al. A case of recurrent supratentorial extraventricular anaplastic ependymoma in adult. *Brain Tumor Res Treat*. (2019) 7:44–7. doi: 10.14791/btrt.2019.7.e26

17. Falcón JE, Velázquez JA, García R, Téllez I, Rodríguez MA. Surgical treatment of a supratentorial extraventricular ependymoma: a case report. *Cureus*. (2023) 15:e40196. doi: 10.7759/cureus.40196

frontiers | Frontiers in Neurology

TYPE Original Research
PUBLISHED 15 March 2024
DOI 10.3389/fneur.2024.1360741

OPEN ACCESS

EDITED BY
Bo yuan Huang,
Capital Medical University, China

REVIEWED BY
Sukwoo Hong,
Toranomon Hospital, Japan
Muhammet Enes Gurses,
University of Miami, United States

*CORRESPONDENCE
Xianzhen Chen
✉ chenxianzheny@126.com
Yajun Xue
✉ xue_yj@163.com

†These authors have contributed equally to this work and share first authorship

RECEIVED 24 December 2023
ACCEPTED 04 March 2024
PUBLISHED 15 March 2024

CITATION
Li C, Qin J, Xue F, Shen Z, Lin Q, Xue Y and Chen X (2024) Rethinking the effects of adjuvant beam radiation therapy on overall survival in atypical meningioma patients: age considerations.
Front. Neurol. 15:1360741.
doi: 10.3389/fneur.2024.1360741

Rethinking the effects of adjuvant beam radiation therapy on overall survival in atypical meningioma patients: age considerations

Chao Li[1†], Jiajun Qin[1†], Fei Xue[1†], Zhaoli Shen[1], Qi Lin[1], Yajun Xue[2*] and Xianzhen Chen[1*]

[1]Department of Neurosurgery, Shanghai Tenth People's Hospital, School of Medicine, Tongji University, Shanghai, China, [2]Department of Neurosurgery, Shanghai General Hospital, Shanghai Jiao Tong University School of Medicine, Shanghai, China

Background: This study aimed to investigate the effects of adjuvant beam radiation therapy (ABRT) on overall survival (OS) in patients with primary single intracranial atypical meningioma (AM), with a focus on age-related outcomes.

Methods: We conducted a retrospective study using data from SEER database. Our cohort consisted of patients diagnosed with a primary single intracranial AM tumor and had undergone surgery. The primary endpoint was OS. For survival analysis, univariable and multivariable Cox regression analysis were performed. A multivariable additive Cox model was used to assess the functional relationship between age and OS in patients with or without ABRT.

Results: Of the 2,759 patients included, 1,650 underwent gross total resection and 833 received ABRT. Multivariable Cox analysis indicated that ABRT did not significantly influence OS across the entire cohort. According to the multivariable generalized additive Cox model, the relative risk of all-cause mortality increased with advancing age in both ABRT-yes and ABRT-no group. ABRT-yes had a lower relative risk than ABRT-no when age ≤ 55 years old while a higher relative risk when age > 55 years old. Subsequent multivariable Cox analysis showed that ABRT was associated with a significant lower risk for all-cause mortality in patients with age ≤ 55 years old while a significant higher risk in patients with age > 55 years old.

Conclusion: Our study found that ABRT enhanced OS in younger primary single intracranial AM patients. But we also revealed a negative correlation between OS and ABRT in older patients.

KEYWORDS

atypical meningioma, gross total resection, radiation therapy, overall survival, age

Introduction

Meningiomas are the most common primary tumors of the central nervous system, accounting for 40.0%, and are predominantly located in the cranial region (1). Atypical meningioma (AM) is the predominant subtype of WHO II meningiomas which accounts for 18.3% of total meningiomas (2). Surgery and adjuvant radiotherapy are two main treatment therapies for AM patients according to the 2016 and 2021 European Association of

Neuro-Oncology (EANO) guidelines (3, 4). Surgery, aiming for Simpson I resection, stands as the primary treatment given that the extent of resection has been identified as an independent prognostic risk factor, supporting by abundant evidence (5–9). However, the efficacy of adjuvant beam radiation therapy (ABRT) for the treatment of AM patients remains an area of contention (4, 10). Conflicting results regarding ABRT's effectiveness have been reported for AM patients. Some studies found ABRT was independently associated with worse overall survival (OS) and/or progression free survival (PFS) in AM patients (11–15), while some studies argued ABRT's protective role against mortality and/or recurrence (9, 16–20). There are also studies that have found ABRT did not significantly influence the prognosis (21–25). The effect of ABRT in AM patients still needs to be elucidated.

Age is a recognized risk factor for the occurrence of meningiomas. Meningiomas mostly occur in old individuals and the incidence rate increase obviously with age, rarely occurring in children (1). Interestingly, the gender distribution of patients shifts with age, showing an initial rise in the female to male ratio that eventually declines in older populations (26). A previous study showed that tumor gene expression and chromosome abnormalities were associated with patient gender (27). Some studies also found that younger and older meningioma patients had different tumor pathology characteristics (28–32). Additionally, age could potentially influence the effect of radiation therapy. As some tumors' clinical and biology behavior can change with age (33), and as aging process is associated with a decrease function of various organ systems, potentially heightening the risk of radiation-related side effects (34–37). The influence of age on the effect of radiation therapy with respect to prognosis has been discussed across various tumor types and many studies have elucidated that age might modulate the impact of radiation therapy, leading to prognosis variations among different age groups. Some studies reported that radiation therapy significantly decreased adverse outcomes in younger tumor patients, but increasing adverse outcomes in older patients (37–39). While some studies reported the opposed results (40–42). Considering impaired neurocognitive function and comorbidities might lead to radiation-induced toxicity, radiation therapy for old brain tumor patients is challenging (43).

The Surveillance, Epidemiology and End Results (SEER) database is a public database, which covers approximately 28% of population of United States. SEER database record demographic, oncology, treatment, and survival data. Surgery and radiation therapy information is released as part of the first course of treatment.[1] And a lot of studies employed SEER data to discuss the efficacies of surgery type and adjuvant radiotherapy in a variety of tumor types (44–46). Some research studies have also assessed the role of ABRT in AM patients utilizing SEER or other database (6, 8, 25, 47). However, there are limited research studies which focus on the influence of age on the radiation therapy efficacy in AM patients who have undergone surgery. Hence, the aim of this study was to investigate impact of ABRT on OS in primary single intracranial AM patients with a focus on age, drawing upon a vast pool of carefully selected cases from SEER database.

Materials and methods

Ethics statement

The SEER database is publicly accessible, and we have obtained the access. Since all patients in this study were from this database, this study did not require the procedure, participate, or publish consent of patients, nor the approval of the ethics committee.

Patient selection

This research adhered to the Strengthening the Reporting of Observational Studies in Epidemiology (STROBE) guidelines. Patients diagnosed with primary single intracranial AM who had undergone surgery were selected from a dataset containing 17 registries [Nov 2021 Sub (2000–2019)] in the SEER database. The inclusion criteria were: (1) Diagnosis of AM; (2) Primary site should be intracranial; and (3) Microscopic confirmation for each case. The exclusion criteria were: (1) History of tumors; (2) Clinical information was missing or unclear; (3) Surgery was not performed; (4) Chemotherapy was administered; (5) Age < 18 years old; and (6) Follow-up time ≤ 3 months. Details of the inclusion and exclusion criteria are presented in Supplementary Note 1. Meningioma sizes larger than 150 mm were rare and more likely to be coding errors, so the limit was set at 150 mm, in line with previous research (48). The research query can be found in Supplementary Note 2. The flow diagram is shown in Figure 1.

Variables

Demographic, oncological, treatment, and survival information were obtained for analysis. Demographic information included age, gender, race, and marital status. Oncological information such as year of diagnosis, tumor size, primary site, and laterality were recorded. Treatment information included surgery and ABRT (yes or no). Regarding surgery information, entries recorded as "55" and "30" under "Surg Prim Site (1998+)" were classified as gross total resection (GTR), while codes "20," "21," and "40" constituted subtotal resection (STR). Patients with "RX Summ--Surg/Rad Seq" recorded as "Radiation after surgery" and "Radiation recode" recorded as "Beam radiation" were identified as having undergone ABRT. The endpoint was OS, with a maximum follow-up period of 60 months.

Statistical analysis

The comparison of categorical variables between different groups was performed using Chi-square test or, when appropriate, Fisher's exact test. The comparison of continuous variables was performed by Student's t-test or Mann–Whitney U test where appropriate, as our previous study described (49). For OS analysis, Kaplan–Meier method was used to estimate OS rate. Univariable Cox regression analysis was performed and variables with p values less than 0.1 in univariable

1 https://seer.cancer.gov/

Abbreviations: ABRT, adjuvant beam radiation therapy; AM, atypical meningioma; OS, overall survival; GTR, gross total resection; STR, subtotal resection; SEER, Surveillance, Epidemiology and End Results; HR, hazard ratio.

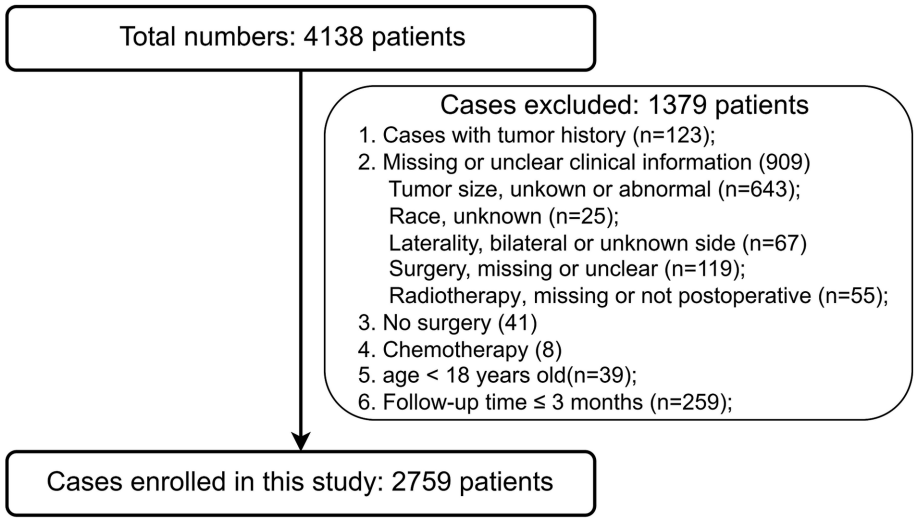

FIGURE 1
The flow diagram of patient selection.

analysis were included in the multivariable Cox regression analysis. Hazard ratio (HR) and 95% confidence interval were calculated. A multivariable additive Cox proportional hazard model was used to assess the functional relationship between age and OS in patients with or without ABRT. The relative risk was calculated and then visualized with smooth spline curve. The abscissa value at the intersection point of the curves for the ABRT-yes group and the ABRT-no group was used as the cut-off value for age. The effect of ABRT was assessed using multivariable Cox regression analysis, and the interaction was inspected using likelihood ratio test in different age groups.

A p-value of less than 0.05 was considered statistically significant. All statistical analyses were performed using R-4.2.0 (R Foundation for Statistical Computing, Vienna, Austria) and Empower Stats 4.1 (X&Y solutions, Inc. Boston, Massachusetts).

Results

Patient characteristics

From the 4,138 patients who initially met the inclusion criteria (Figure 1), 1,379 were excluded, leaving 2,759 for study. All the patients were diagnosed by histology. The characteristics of the patients are shown in Table 1. The mean age was 58.5 ± 14.9 years old. Major patients were females (57.8%; female to male ratio = 1.37). Most patients were white race (73.5%). The mean tumor size was 49.0 ± 16.8 mm. Most tumor sites were identified as cerebral meninges, with only 0.7% being recorded as the brain. Cases of left laterality and right laterality were similar. And most patients (58.5%) were married. As for treatment, 1,650 (59.8%) patients underwent GTR and 1,109 (40.2%) patients underwent STR. Most patients (1926, 69.8%) did not received ABRT and 833 (30.2%) patients received it. There are some variables that are different between ABRT-yes and ABRT-no group, including age ($p = 0.003$), year of diagnosis ($p < 0.001$), tumor size ($p = 0.001$), laterality ($p = 0.039$), marital status ($p = 0.040$), and surgery type ($p < 0.001$). Patients received ABRT was younger and had a large tumor size. Notably, there was an observed increase in the ratio of ABRT-yes to ABRT-no trend over the years. Importantly, ABRT-yes group had a higher proportion (48.1% vs. 36.8%) of patients who received STR.

Univariable and multivariable Cox analysis for OS in the entire cohort

The maximum follow-up time was established at 60 months, during which 349 (12.7%) patients experienced all-cause mortality. The estimated 3-year OS rate was 90.3 ± 0.6%, the estimated 5-year OS rate was 82.8 ± 0.9%.

The univariable and multivariable Cox analysis results were shown in Table 2. Univariable Cox analysis showed that age (HR 1.06 [1.05, 1.07], $p < 0.001$), male gender (HR 1.26 [1.02, 1.56], $p = 0.029$), black race (HR 1.47 [1.12, 1.93], $p = 0.005$), tumor size (HR 1.01 [1.01, 1.02], $p < 0.001$), marital status (HR 3.76 [2.85, 4.97], $p < 0.001$ for 'Widowed'; HR 1.83 [1.19, 2.80], $p = 0.006$ for 'Other'), and STR (HR 1.41 [1.15, 1.75], $p = 0.001$) had a significant HR for OS. These variables and ABRT were enrolled in the multivariable analysis. Older age (HR 1.06 [1.05, 1.07], $p < 0.001$), male gender (HR 1.32 [1.05, 1.65], $p = 0.016$), black race (HR 1.47 [1.11, 1.95], $p = 0.005$), larger tumor size (1.01 [1.01, 1.02], $p < 0.001$), and STR (1.43 [1.16, 1.77], $p < 0.001$) were independent risk factors for OS. Interestingly, some marital status also had a significant impact for prognosis, such as widowed (2.08 [1.52, 2.84], $p < 0.001$) and single (1.78 [1.33, 2.39], $p < 0.001$). However, ABRT did not show a significant HR in the multivariable analysis in the overall population (1.21 [0.96, 1.54], $p = 0.115$).

Association between age and risk of all-cause mortality in different ABRT groups

Multivariable additive Cox proportional model was used to assess the functional relationship between age and the risk of all-cause mortality

TABLE 1 Baseline characteristics of atypical meningioma patients.

	All	ABRT		*p*
		No	Yes	
Subjects, n (%)	2,759	1,926	833	
Age, years	58.5 ± 14.9	59.0 ± 15.3	57.3 ± 13.7	0.003
Gender				0.765
Female, n (%)	1,595 (57.8%)	1,117 (58.0%)	478 (57.4%)	
Male, n (%)	1,164 (42.2%)	809 (42.0%)	355 (42.6%)	
Race				0.448
White	2028 (73.5%)	1,410 (73.2%)	618 (74.2%)	
Black	388 (14.1%)	281 (14.6%)	107 (12.8%)	
Others	343 (12.4%)	235 (12.2%)	108 (13.0%)	
Year of diagnosis				<0.001
2004–2008	527 (19.1%)	410 (21.3%)	117 (14.0%)	
2009–2016	1,445 (52.4%)	985 (51.1%)	460 (55.2%)	
2017–2019	787 (28.5%)	531 (27.6%)	256 (30.7%)	
Tumor size, mm	49.0 ± 16.8	48.3 ± 16.7	50.7 ± 16.7	0.001
Primary site				0.170
Cerebral meninges	2,740 (99.3%)	1,910 (99.2%)	830 (99.6%)	
Brain	19 (0.7%)	16 (0.8%)	3 (0.4%)	
Laterality				0.039
Left	1,346 (48.8%)	932 (48.4%)	414 (49.7%)	
Right	1,276 (46.2%)	885 (46.0%)	391 (46.9%)	
Paired site	137 (5.0%)	109 (5.7%)	28 (3.4%)	
Marital status				0.040
Married	1,615 (58.5%)	1,101 (57.2%)	514 (61.7%)	
Divorced	235 (8.5%)	173 (9.0%)	62 (7.4%)	
Widowed	217 (7.9%)	167 (8.7%)	50 (6.0%)	
Single	548 (19.9%)	379 (19.7%)	169 (20.3%)	
Other	144 (5.2%)	106 (5.5%)	38 (4.6%)	
Surgery type				<0.001
GTR	1,650 (59.8%)	1,218 (63.2%)	432 (51.9%)	
STR	1,109 (40.2%)	708 (36.8%)	401 (48.1%)	

ABRT, adjuvant beam radiation therapy; GTR, gross total resection; STR, subtotal resection.

in patients with and without ABRT, respectively. The model was adjusted with variables which showed significant HR in the multivariable Cox analysis, including gender, race, marital status, tumor size, and surgery type. The HR was calculated at different ages and the results was shown in Figure 2. As we can see, the relative risk for OS increased with age in both ABRT-yes and ABRT-no group. But when age ≤ 55 years old, ABRT-yes had a lower relative risk for OS than ABRT-no. And when age > 55 years old, ABRT-yes was associated with a higher risk for OS.

Effect of ABRT for OS in different age groups

The HR of ABRT for OS was calculated with different Cox model adjusted by different variables. As we can see in Table 3, the crude model was adjusted with no variable, the Adjust model I was adjusted with demographic variables, including gender, race, age, and marital status. The Adjust model II was adjusted with demographic, tumor, and treatment variables, including gender, race, age, marital status, tumor size, laterality, primary site, and surgery type. In the crude model, although the HR of ABRT in patients with age ≤ 55 years old was small (0.51 [0.26, 1.02]), the *p* value (0.058) did not meet the level of statistical significance. The HR of ABRT in patients with age > 55 years old was 1.20 [0.94, 1.53] ($p = 0.152$) in the crude model. And in Adjust model I, the HR of ABRT was 0.49 [0.25, 0.97] ($p = 0.042$) and 1.59 [1.23, 2.06] ($p < 0.001$) in patients with age ≤ 55 years old and > 55 years old, respectively. In Adjust model II, the HR of ABRT was 0.49 [0.25, 0.99] ($p = 0.045$) and 1.52 [1.17, 1.98] ($p = 0.002$) in patients with age ≤ 55 years old and > 55 years old, respectively. These results from multivariable adjusted models showed

TABLE 2 Univariable and multivariable Cox analysis of atypical meningioma patients.

	Univariable analysis		Multivariable analysis*	
	HR (95% CI)	*p*	HR (95% CI)	*p*
Age, years	1.06 (1.05, 1.07)	<0.001	1.06 (1.05, 1.07)	<0.001
Gender				
Female	Ref		Ref	
Male	1.26 (1.02, 1.56)	0.029	1.32 (1.05, 1.65)	0.016
Race				
White	Ref		Ref	
Black	1.47 (1.12, 1.93)	0.005	1.47 (1.11, 1.95)	0.005
Others	0.69 (0.47, 1.01)	0.057	0.72 (0.49, 1.05)	0.091
Year of diagnosis				
2004–2008	Ref			
2009–2016	0.97 (0.76, 1.24)	0.792		
2017–2019	1.21 (0.82, 1.80)	0.337		
Tumor size, mm	1.01 (1.01, 1.02)	<0.001	1.01 (1.01, 1.02)	<0.001
Primary site				
Cerebral meninges	Ref			
Brian	0.73 (0.18, 2.92)	0.653		
Laterality				
Left	Ref			
Right	1.17 (0.94, 1.45)	0.149		
Paired site	1.03 (0.60, 1.74)	0.923		
Marital status				
Married	Ref		Ref	
Divorced	1.02 (0.67, 1.55)	0.936	1.04 (0.68, 1.59)	0.866
Widowed	3.76 (2.85, 4.97)	<0.001	2.08 (1.52, 2.84)	<0.001
Single	1.33 (1.00, 1.76)	0.051	1.78 (1.33, 2.39)	<0.001
Other	1.83 (1.19, 2.80)	0.006	1.87 (1.21, 2.88)	0.005
Surgery type				
GTR	Ref		Ref	
STR	1.41 (1.15, 1.75)	0.001	1.43 (1.16, 1.77)	<0.001
ABRT				
No	Ref		Ref	
Yes	1.02 (0.81, 1.29)	0.855	1.21 (0.96, 1.54)	0.115

*ABRT and variables with $p < 0.1$ in univariable analysis were enrolled in the multivariable analysis. GTR, gross total resection; STR, subtotal resection; ABRT, adjuvant beam radiation therapy; HR, hazard ratio; 95% CI, 95% confidence interval.

that ABRT associated with a lower risk of all-cause death in patients with age ≤ 55 years old while a higher risk of death in patients with age > 55 years old. And a significant interaction was observed between age group and ABRT across all three models ($p = 0.015$, 0.001, and 0.001 for Crude model, Adjust model I, and Adjust model II, respectively).

Discussion

Our study aimed to investigate the effect of ABRT for OS in primary single intracranial AM patients, with a focus on the age. Our results demonstrated that in younger patients (age ≤ 55 years old) ABRT associated with a lower risk of all-cause mortality while in older patients (age > 55 years old) ABRT associated with a higher risk of death.

Given the small number of AM patients at individual centers, various studies have also used public database to investigate the efficacy of different treatment methods in AM patients. But the results of these studies are not consistent. In 2012, Stessin et al. (50) used SEER database to explore the effect of ABRT in nonbenign meningioma patients. They included both WHO II and III cases, enrolling and analyzing 657 patients together. After multivariable analysis, they found that ABRT did not appear as a significant

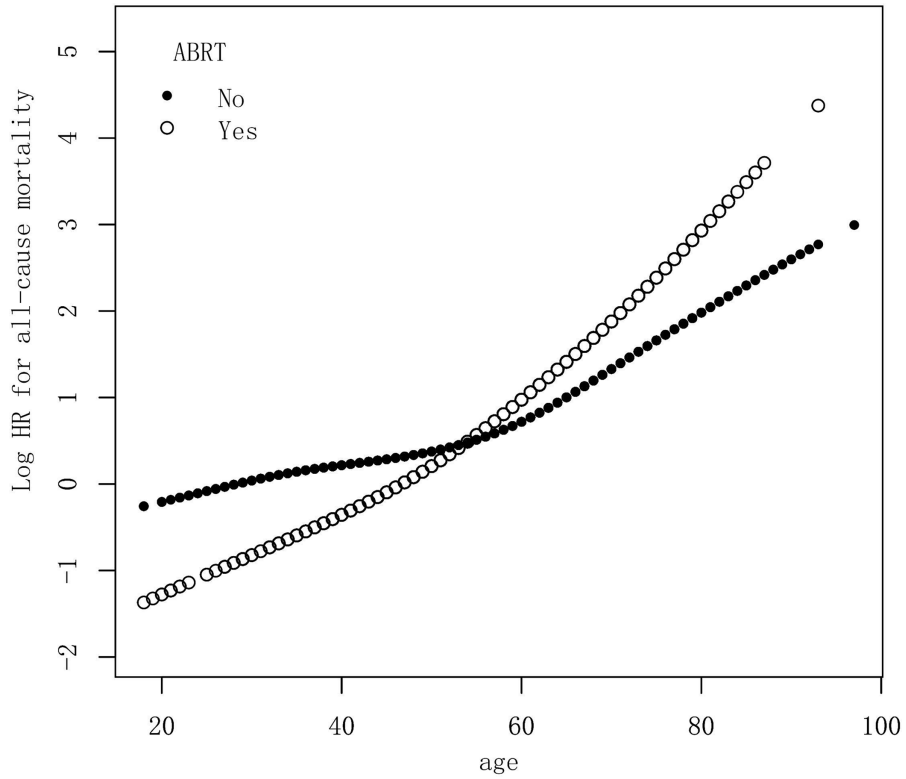

FIGURE 2
Multivariable additive Cox proportional hazard model demonstrated the relationship between age and the risk of all-cause mortality in patients with or without ABRT. The model was adjusted with variables, including gender, race, marital status, tumor size, and surgery type. HR, hazard ratio; ABRT, adjuvant beam radiation therapy.

TABLE 3 Effect of adjuvant beam radiation therapy for overall survival in different age groups.

	Crude model		Adjust model I		Adjust model II	
	HR (95% CI)	*p*	HR (95% CI)	*p*	HR (95% CI)	*p*
Age ≤ 55 years old	0.51 (0.26, 1.02)	0.058	0.49 (0.25, 0.97)	0.042	0.49 (0.25, 0.99)	0.045
Age > 55 years old	1.20 (0.94, 1.53)	0.152	1.59 (1.23, 2.06)	<0.001	1.52 (1.17, 1.98)	0.002
P for interaction		0.015		0.001		0.001

The Hazard ratios (HR) of adjuvant beam radiation therapy (ABRT) intervention were calculated with Cox proportional hazards model in different age groups. Interaction analyses were conducted for ABRT and age group on overall survival in different models.
Crude model: adjust for none.
Adjust model I: adjust for demographic variables including: gender, race, age, and marital status.
Adjust model II: adjust for demographic, tumor, and treatment variables including: gender, race, age, marital status, tumor size, laterality, primary site, and surgery type.

prognostic factor. In 2015, Aizer et al. (6) also utilized the SEER database, enrolling 575 AM patients. The authors found ABRT did not affect OS. In 2018, Rydzewski et al. (5) enrolled 3,529 AM patients from the National Cancer Data Base and identified ABRT as a significant factor in enhancing OS in multivariable analysis. In 2019, Zeng et al. (8) also used SEER database and enrolled 1,014 AM patients, founding that ABRT did not significantly influence OS across the cohort.

When we used the SEER database, we enrolled a large number of AM patients (covering overing 2,700 cases), second only to Rydzewski et al.'s study (5), as far as we know. And we carefully selected patients and made the cohort homogeneous, consisting only of patients with primary single intracranial AM, and excluding patients with multiple meningiomas or spinal meningiomas. Given that AM is not a malignancy tumor and is associated with lower mortality compared to malignant tumors, such as glioblastoma (51), lung cancer (52), cervical cancer (53), and gastric cancer (54), the inclusion of these malignant tumors could introduce bias into the survival analysis of AM. So, patients with tumor history were also excluded. Additionally, to eliminate the impact of perioperative mortality, we included only patients with follow-up time exceeding 3 months. Strict inclusion and exclusion criteria can make our results more reliable.

The increased risk of all-cause mortality in older AM patients receiving ABRT can be attributed to two primary factors. Firstly, ABRT may not offer benefits to older AM patients, possibly due to heightened radiation toxicity in this age group. Studies have reported that elderly patients were more susceptible to brain atrophy and

dementia induced by radiation than younger patients (55, 56). As a result, younger AM patients may benefit from ABRT with a good tolerance of radiation toxicity, while older patients may be less tolerable and thus experience worse outcomes from ABRT. Secondly, the increased mortality observed in older patients receiving ABRT could be due to the patients' inherently worse oncological characteristics, such as a more aggressive pathological phenotype or larger postoperative residuals. This may suggest that treatment for tumors with ABRT in older patients was insufficient.

Despite observing an increased risk of all-cause mortality in older AM patients, we cannot conclusively state that ABRT will cause the deterioration of OS in older AM patients since the burden of proof needs to be high. The efficacy of ABRT in moderating AM prognosis remains to be validated through robust prospective research, such as the ROAM/EORTC-1308 trial (57).

Anyway, our observations underscore the need for refined treatment approaches for older AM patients. And it is gratifying to note that we observed ABRT noticeably improved OS in younger AM patients. This insight suggests that younger patients with AM might be more suitable candidates for ABRT, potentially guiding clinicians toward more aggressive treatment approaches in this demographic.

Future research should investigate the biological and pathological variances in AM tumors between younger and older patients. Biomarkers that can predict response to ABRT should also be identified. The 2021 EANO guidelines advocate for ABRT in WHO II meningioma patients, particularly patients without GTR. Our findings also revealed that patients receiving ABRT had a significantly higher proportion of STR (see Table 1). The impact of ABRT on patients with different extent of resection (GTR or STR) should also be explored in the future.

There are several limitations in this study. Firstly, the details of ABRT, including dose, time, fractionation, etc., are unavailable from SEER database. Secondly, the details of pathology information for tumors are also not available, such as Ki-67 index. Thirdly, we employed the additive Cox proportional hazard model to calculate the relative risk and visualized it using smooth spline curve, with the age cut-off value (55 years old) determined by the intersection point. Although the additive Cox proportional hazard model is commonly utilized to build smooth spline curves and identify cut-off values (58–64), several considerations must be considered. For instance, the inclusion of smoothing parameters might complicate the interpretation of the results and cause the overfitting. Moreover, the cut-off value was chose based on the statistical criteria alone, its medical and biological significance needs to be clarified. Lastly, PFS information and cause-specific death data are not available for AM patients in the SEER database. Nevertheless, our study's results based on OS also warrant attention since OS is the gold standard primary endpoint in the tumor studies of clinical investigations (65, 66).

Conclusion

In conclusion, our study found that ABRT improved OS in younger primary single intracranial AM patients. We also revealed a negative correlation between OS and ABRT in older patients. This observation might stem from the long-term toxicity of radiation therapy for older patients. And it also might be attributed to the more invasive nature of tumors or larger postoperative residuals in this age group treated with ABRT, rendering the treatment insufficient. Our results call for a careful examination of both possibilities and further research is needed explore the optimal treatment strategies for AM patients, especially for elderly patients.

Data availability statement

The data analyzed in this study was obtained from the National Institutes of Health (NIH), National Cancer Institute (NCI), Surveillance, Epidemiology, and End Results (SEER) database, the following licenses/restrictions apply: to request access to the Research Plus Data, users must login with an eRA Commons account that is associated with an institutional email address (.edu, .gov, .org, or work email address) for user authentication. Users with access only to the Research Data are not eligible to request specialized databases and cannot upgrade to Research Plus without an eRA Commons account or an HHS PIV card. Requests to access these datasets should be directed to SEER, https://seerdataaccess.cancer.gov/seer-data-access.

Ethics statement

Ethical approval was not required for the studies involving humans because the SEER database is publicly accessible, and we have obtained the access. Since all patients in this study are from this database, this study does not require the approval of the ethics committee. The studies were conducted in accordance with the local legislation and institutional requirements. Written informed consent for participation was not required from the participants or the participants' legal guardians/next of kin in accordance with the national legislation and institutional requirements because the patient data from SEER are strictly de-identified.

Author contributions

CL: Formal analysis, Methodology, Writing – original draft. JQ: Methodology, Writing – original draft. FX: Methodology, Writing – original draft. ZS: Methodology, Writing – review & editing. QL: Methodology, Writing – review & editing. YX: Conceptualization, Supervision, Writing – review & editing. XC: Conceptualization, Supervision, Writing – review & editing.

Funding

The author(s) declare financial support was received for the research, authorship, and/or publication of this article. This research was funded by the Program of Shanghai Municipal Commission of Health (No. 201940126), Program of Shanghai Tenth People's Hospital

(No. 2023YJXYSB008), and Program of Science and Technology Commission of Shanghai Municipality (No. 23141901100).

Acknowledgments

The authors wish to thank Jingfang Tang (Shanghai Putuo Center for Disease Control and Prevention) for her help with data analysis.

Conflict of interest

The authors declare that the research was conducted in the absence of any commercial or financial relationships that could be construed as a potential conflict of interest.

Publisher's note

Supplementary material

The Supplementary material for this article can be found online at: https://www.frontiersin.org/articles/10.3389/fneur.2024.1360741/full#supplementary-material

References

1. Ostrom QT, Price M, Neff C, Cioffi G, Waite KA, Kruchko C, et al. CBTRUS statistical report: primary brain and other central nervous system tumors diagnosed in the United States in 2015-2019. *Neuro Oncology*. (2022) 24:v1–v95. doi: 10.1093/neuonc/noac202

2. Ren L, Hua L, Deng J, Cheng H, Wang D, Chen J, et al. Favorable long-term outcomes of chordoid meningioma compared with the other WHO grade 2 meningioma subtypes. *Neurosurgery*. (2022) 92:745–55. doi: 10.1227/neu.0000000000002272

3. Goldbrunner R, Minniti G, Preusser M, Jenkinson MD, Sallabanda K, Houdart E, et al. EANO guidelines for the diagnosis and treatment of meningiomas [review]. *Lancet Oncol*. (2016) 17:E383–91. doi: 10.1016/s1470-2045(16)30321-7

4. Goldbrunner R, Stavrinou P, Jenkinson MD, Sahm F, Mawrin C, Weber DC, et al. EANO guideline on the diagnosis and management of meningiomas. *Neuro-Oncology*. (2021) 23:1821–34. doi: 10.1093/neuonc/noab150

5. Rydzewski NR, Lesniak MS, Chandler JP, Kalapurakal JA, Pollom E, Tate MC, et al. Gross total resection and adjuvant radiotherapy most significant predictors of improved survival in patients with atypical meningioma. *Cancer*. (2018) 124:734–42. doi: 10.1002/cncr.31088

6. Aizer AA, Bi WL, Kandola MS, Lee EQ, Nayak L, Rinne ML, et al. Extent of resection and overall survival for patients with atypical and malignant meningioma. *Cancer*. (2015) 121:4376–81. doi: 10.1002/cncr.29639

7. Li D, Jiang P, Xu S, Li C, Xi S, Zhang J, et al. Survival impacts of extent of resection and adjuvant radiotherapy for the modern management of high-grade meningiomas. *J Neuro Oncol*. (2019) 145:125–34. doi: 10.1007/s11060-019-03278-w

8. Zeng Q, Shi F, Guo Z. Effectiveness of postoperative radiotherapy on atypical meningioma patients: a population-based study. *Front Oncol*. (2019) 9:34. doi: 10.3389/fonc.2019.00034

9. Li H, Zhang YS, Zhang GB, Zhang GJ, Wang B, Li D, et al. Treatment protocol, long-term follow-up, and predictors of mortality in 302 cases of atypical meningioma. *World Neurosurg*. (2019) 122:e1275–84. doi: 10.1016/j.wneu.2018.11.032

10. Preusser M, Brastianos PK, Mawrin C. Advances in meningioma genetics: novel therapeutic opportunities. *Nat Rev Neurol*. (2018) 14:106–15. doi: 10.1038/nrneurol.2017.168

11. Yoon H, Mehta MP, Perumal K, Helenowski IB, Chappell RJ, Akture E, et al. Atypical meningioma: randomized trials are required to resolve contradictory retrospective results regarding the role of adjuvant radiotherapy. *J Cancer Res Ther*. (2015) 11:59–66. doi: 10.4103/0973-1482.148708

12. Champeaux C, Dunn L. World Health Organization grade II meningioma: a 10-year retrospective study for recurrence and prognostic factor assessment. *World Neurosurg*. (2016) 89:180–6. doi: 10.1016/j.wneu.2016.01.055

13. Champeaux C, Wilson E, Shieff C, Khan AA, Thorne L. WHO grade II meningioma: a retrospective study for outcome and prognostic factor assessment. *J Neuro Oncol*. (2016) 129:337–45. doi: 10.1007/s11060-016-2181-2

14. Champeaux C, Houston D, Dunn L. Atypical meningioma. A study on recurrence and disease-specific survival. *Neurochirurgie*. (2017) 63:273–81. doi: 10.1016/j.neuchi.2017.03.004

15. Garcia-Segura ME, Erickson AW, Jairath R, Munoz DG, Das S. Necrosis and brain invasion predict radio-resistance and tumor recurrence in atypical meningioma: a retrospective cohort study. *Neurosurgery*. (2020) 88:E42–8. doi: 10.1093/neuros/nyaa348

16. Dohm A, McTyre ER, Chan MD, Fan C, Isom S, Bourland JD, et al. Early or late radiotherapy following gross or subtotal resection for atypical meningiomas: clinical outcomes and local control. *J Clin Neurosci*. (2017) 46:90–8. doi: 10.1016/j.jocn.2017.08.023

17. Unterberger A, Ng E, Pradhan A, Kondajji A, Kulinich D, Duong C, et al. Adjuvant radiotherapy for atypical meningiomas is associated with improved progression free survival. *J Neurol Sci*. (2021) 428:117590. doi: 10.1016/j.jns.2021.117590

18. Hemmati SM, Ghadjar P, Grün A, Badakhshi H, Zschaeck S, Senger C, et al. Adjuvant radiotherapy improves progression-free survival in intracranial atypical meningioma. *Radiat Oncol*. (2019) 14:160. doi: 10.1186/s13014-019-1368-z

19. Chen WC, Magill ST, Wu A, Vasudevan HN, Morin O, Aghi MK, et al. Histopathological features predictive of local control of atypical meningioma after surgery and adjuvant radiotherapy. *J Neurosurg*. (2018) 130:1–8. doi: 10.3171/2017.9.Jns171609

20. Song D, Xu D, Han H, Gao Q, Zhang M, Wang F, et al. Postoperative adjuvant radiotherapy in atypical meningioma patients: a meta-analysis study. *Front Oncol*. (2021) 11:787962. doi: 10.3389/fonc.2021.787962

21. Rebchuk AD, Alam A, Hounjet CD, Chaharyn BM, Gooderham PA, Yip S, et al. Survival and recurrence outcomes following adjuvant radiotherapy for grade 2 intracranial meningiomas: 13-year experience in a tertiary-care center. *World Neurosurg*. (2022) 161:e748–56. doi: 10.1016/j.wneu.2022.02.088

22. Jenkinson MD, Waqar M, Farah JO, Farrell M, Barbagallo GM, McManus R, et al. Early adjuvant radiotherapy in the treatment of atypical meningioma. *J Clin Neurosci*. (2016) 28:87–92. doi: 10.1016/j.jocn.2015.09.021

23. Keric N, Kalasauskas D, Freyschlag CF, Gempt J, Misch M, Poplawski A, et al. Impact of postoperative radiotherapy on recurrence of primary intracranial atypical meningiomas. *J Neuro Oncol*. (2020) 146:347–55. doi: 10.1007/s11060-019-03382-x

24. Zhu H, Bi WL, Aizer A, Hua L, Tian M, Den J, et al. Efficacy of adjuvant radiotherapy for atypical and anaplastic meningioma. *Cancer Med*. (2019) 8:13–20. doi: 10.1002/cam4.1531

25. Zhang GJ, Liu XY, You C. Clinical factors and outcomes of atypical meningioma: a population-based study. *Front Oncol*. (2021) 11:676683. doi: 10.3389/fonc.2021.676683

26. Wiemels J, Wrensch M, Claus EB. Epidemiology and etiology of meningioma. *J Neuro Oncol*. (2010) 99:307–14. doi: 10.1007/s11060-010-0386-3

27. Tabernero MD, Espinosa AB, Maillo A, Rebelo O, Vera JF, Sayagues JM, et al. Patient gender is associated with distinct patterns of chromosomal abnormalities and sex chromosome linked gene-expression profiles in meningiomas. *Oncologist*. (2007) 12:1225–36. doi: 10.1634/theoncologist.12-10-1225

28. Maiuri F, De Caro ML, de Divitiis O, Vergara P, Mariniello G. Spinal meningiomas: age-related features. *Clin Neurol Neurosurg*. (2011) 113:34–8. doi: 10.1016/j.clineuro.2010.08.017

29. Sano K, Wakai S, Ochiai C, Takakura K. Characteristics of intracranial meningiomas in childhood. *Childs Brain*. (1981) 8:98–106. doi: 10.1159/000119971

30. Zhao X, Zhao D, Wu Y, Gao W, Cui H, Wang Y, et al. Meningioma in the elderly: characteristics, prognostic factors, and surgical strategy. *J Clin Neurosci*. (2018) 56:143–9. doi: 10.1016/j.jocn.2018.06.011

31. Park JS, Sade B, Oya S, Kim CG, Lee JH. The influence of age on the histological grading of meningiomas. *Neurosurg Rev*. (2014) 37:425–9. doi: 10.1007/s10143-014-0537-7

32. Pant I, Chaturvedi S, Sarma P, Singh G. Histopathological mapping of meningiomas: a 10-year retrospective analysis. *Indian J Neurosurgery*. (2021) 10:203–9. doi: 10.1055/s-0040-1718990

33. Khan SA, Morris M, Idrees K, Gimbel MI, Rosenberg S, Zeng Z, et al. Colorectal cancer in the very young: a comparative study of tumor markers, pathology and survival in early onset and adult onset patients. *J Pediatr Surg*. (2016) 51:1812–7. doi: 10.1016/j.jpedsurg.2016.07.015

34. Hoffe S, Balducci L. Cancer and age: general considerations. *Clin Geriatr Med*. (2012) 28:1–18. doi: 10.1016/j.cger.2011.09.001

35. Hernández L, Terradas M, Camps J, Martín M, Tusell L, Genescà A. Aging and radiation: bad companions. *Aging Cell*. (2015) 14:153–61. doi: 10.1111/acel.12306

36. Wang K, Tepper JE. Radiation therapy-associated toxicity: Etiology, management, and prevention. *CA Cancer J Clin*. (2021) 71:437–54. doi: 10.3322/caac.21689

37. Zhang T, Bi N, Zhou Z, Chen D, Feng Q, Liang J, et al. The impact of age on the survival outcomes and risk of radiation pneumonitis in patients with unresectable locally advanced non-small cell lung cancer receiving chemoradiotherapy. *J Thorac Dis*. (2020) 12:4347–56. doi: 10.21037/jtd-20-2137

38. Yan W, Christos P, Nori D, Chao KS, Ravi A. Is there a cause-specific survival benefit of postmastectomy radiation therapy in women younger than age 50 with T3N0 invasive breast cancer? A SEER database analysis: outcomes by receptor status/race/age: analysis using the NCI surveillance, epidemiology, and end results (SEER) database. *Am J Clin Oncol*. (2013) 36:552–7. doi: 10.1097/COC.0b013e31825d529b

39. Valero J, Peleteiro P, Henríquez I, Conde A, Piquer T, Lozano A, et al. Age, gleason score, and PSA are important prognostic factors for survival in metastatic castration-resistant prostate cancer. Results of the uroncor group (uro-oncological tumors) of the Spanish Society of Radiation Oncology (SEOR). *Clin Transl Oncol*. (2020) 22:1378–89. doi: 10.1007/s12094-019-02274-w

40. Li Y, Liu H, Zhou Y, Zhou Z, Liu W, Zhao L, et al. The survival effect of radiotherapy on stage II/III rectal cancer in different age groups: formulating radiotherapy decision-making based on age. *Front Oncol*. (2021) 11:695640. doi: 10.3389/fonc.2021.783564

41. Xiao G, Cao Y, Qiu X, Wang W, Wang Y. Influence of gender and age on the survival of patients with nasopharyngeal carcinoma. *BMC Cancer*. (2013) 13:226. doi: 10.1186/1471-2407-13-226

42. He MT, Lu XX, Gou ZC. Effects of postmastectomy radiotherapy on survival in different age groups for patients with T3N0M0 breast cancer. *Breast*. (2021) 60:247–54. doi: 10.1016/j.breast.2021.11.006

43. Minniti G, Filippi AR, Osti MF, Ricardi U. Radiation therapy for older patients with brain tumors. *Radiat Oncol*. (2017) 12:101. doi: 10.1186/s13014-017-0841-9

44. Lee CM, Szabo A, Shrieve DC, Macdonald OK, Gaffney DK. Frequency and effect of adjuvant radiation therapy among women with stage I endometrial adenocarcinoma. *JAMA*. (2006) 295:389–97. doi: 10.1001/jama.295.4.389

45. Fernandes AT, Shinohara ET, Guo M, Mitra N, Wilson LD, Rengan R, et al. The role of radiation therapy in malignant thymoma: a surveillance, epidemiology, and end results database analysis. *J Thorac Oncol*. (2010) 5:1454–60. doi: 10.1097/JTO.0b013e3181e8f345

46. Mell LK, Carmona R, Gulaya S, Lu T, Wu J, Saenz CC, et al. Cause-specific effects of radiotherapy and lymphadenectomy in stage I-II endometrial cancer: a population-based study. *J Natl Cancer Inst*. (2013) 105:1656–66. doi: 10.1093/jnci/djt279

47. Wang C, Kaprealian TB, Suh JH, Kubicky CD, Ciporen JN, Chen Y, et al. Overall survival benefit associated with adjuvant radiotherapy in WHO grade II meningioma. *Neuro-Oncology*. (2017) 19:1263–70. doi: 10.1093/neuonc/nox007

48. Moreau JT, Hankinson TC, Baillet S, Dudley RWR. Individual-patient prediction of meningioma malignancy and survival using the surveillance, epidemiology, and end results database. *NPJ Digit Med*. (2020) 3:12. doi: 10.1038/s41746-020-0219-5

49. Lu GH, Gong SG, Li C, Zhao QH, Jiang R, Luo CJ, et al. Prognostic value of gamma-glutamyltransferase in male patients with idiopathic pulmonary arterial hypertension. *Front Cardiovasc Med*. (2020) 7:580908. doi: 10.3389/fcvm.2020.580908

50. Stessin AM, Schwartz A, Judanin G, Pannullo SC, Boockvar JA, Schwartz TH, et al. Does adjuvant external-beam radiotherapy improve outcomes for nonbenign meningiomas? A surveillance, epidemiology, and end results (SEER)-based analysis. *J Neurosurg*. (2012) 117:669–75. doi: 10.3171/2012.7.JNS111439

51. Brown NF, Ottaviani D, Tazare J, Gregson J, Kitchen N, Brandner S, et al. Survival outcomes and prognostic factors in glioblastoma. *Cancers*. (2022) 14:3161. doi: 10.3390/cancers14133161

52. Ganti AK, Klein AB, Cotarla I, Seal B, Chou E. Update of incidence, prevalence, survival, and initial treatment in patients with non-small cell lung cancer in the US. *JAMA Oncol*. (2021) 7:1824–32. doi: 10.1001/jamaoncol.2021.4932

53. Cohen CM, Wentzensen N, Castle PE, Schiffman M, Zuna R, Arend RC, et al. Racial and ethnic disparities in cervical cancer incidence, survival, and mortality by histologic subtype. *J Clin Oncol*. (2023) 41:1059–68. doi: 10.1200/JCO.22.01424

54. Li H, Zhang H, Zhang H, Wang Y, Wang X, Hou H. Survival of gastric cancer in China from 2000 to 2022: a nationwide systematic review of hospital-based studies. *J Glob Health*. (2022) 12:11014. doi: 10.7189/jogh.12.11014

55. Asai A, Matsutani M, Matsuda T, Tanaka Y, Funada N. Radiation-induced brain atrophy. *Gan No Rinsho*. (1989) 35:1325–9. jpn.

56. Stylopoulos LA, George AE, de Leon MJ, Miller JD, Foo SH, Hiesiger E, et al. Longitudinal CT study of parenchymal brain changes in glioma survivors. *AJNR Am J Neuroradiol*. (1988) 9:517–22.

57. Jenkinson MD, Javadpour M, Haylock BJ, Young B, Gillard H, Vinten J, et al. The ROAM/EORTC-1308 trial: radiation versus observation following surgical resection of atypical meningioma: study protocol for a randomised controlled trial. *Trials*. (2015) 16:519. doi: 10.1186/s13063-015-1040-3

58. Klein JP, Moeschberger ML. *Survival analysis: techniques for censored and truncated data*. New York. 2nd: Springer (2003).

59. Perperoglou A, Sauerbrei W, Abrahamowicz M, Schmid M. A review of spline function procedures in R. *BMC Med Res Methodol*. (2019) 19:46. doi: 10.1186/s12874-019-0666-3

60. Wood SN, Pya N, Säfken B. Smoothing parameter and model selection for general smooth models. *J Am Stat Assoc*. (2016) 111:1548–63. doi: 10.1080/01621459.2016.1180986

61. Ji X, Wang Y, Hu Z, Ma Y, Man S, Li K, et al. Effectiveness of subcutaneous tumor necrosis factor inhibitors in patients with ankylosing spondylitis: a real-world prospective observational cohort study in China. *Front Pharmacol*. (2019) 10:1476. doi: 10.3389/fphar.2019.01476

62. Wang S, Zhou Z, Fan F, Qi L, Jia J, Sun P, et al. Joint effect of non-invasive central systolic blood pressure and peripheral systolic blood pressure on incident hypertension in a Chinese community-based population. *Sci Rep*. (2018) 8:3229. doi: 10.1038/s41598-018-21023-7

63. Yu Y, Li M, Huang X, Zhou W, Wang T, Zhu L, et al. A U-shaped association between the LDL-cholesterol to HDL-cholesterol ratio and all-cause mortality in elderly hypertensive patients: a prospective cohort study. *Lipids Health Dis*. (2020) 19:238. doi: 10.1186/s12944-020-01413-5

64. Zhou S, Jiang W, Wang H, Wei N, Yu Q. Predictive value of pretreatment albumin-to-alkaline phosphatase ratio for overall survival for patients with advanced non-small cell lung cancer. *Cancer Med*. (2020) 9:6268–80. doi: 10.1002/cam4.3244

65. Driscoll JJ, Rixe O. Overall survival: still the gold standard: why overall survival remains the definitive end point in cancer clinical trials. *Cancer J*. (2009) 15:401–5. doi: 10.1097/PPO.0b013e3181bdc2e0

66. Mailankody S, Prasad V. Overall survival vs disease-specific survival-reply. *JAMA Oncol*. (2018) 4:586–7. doi: 10.1001/jamaoncol.2017.3865

frontiers | Frontiers in Neurology

TYPE Original Research
PUBLISHED 08 April 2024
DOI 10.3389/fneur.2024.1364917

OPEN ACCESS

EDITED BY
Bo yuan Huang,
Capital Medical University, China

REVIEWED BY
Yingxi Wu,
Air Force Medical University, China
Hao Teng,
Shengjing Hospital of China Medical University, China

*CORRESPONDENCE
Qijiang Xiong
✉ xqj_neurosurgery@163.com

RECEIVED 03 January 2024
ACCEPTED 27 March 2024
PUBLISHED 08 April 2024

CITATION
Duan Z, Zhou C, Yan X, Du W, Xia X, Shi H, Su H, Zhang Y, He X and Xiong Q (2024) Efficacy and safety of a "radical" surgical strategy in the treatment of parasagittal sinus meningioma.
Front. Neurol. 15:1364917.
doi: 10.3389/fneur.2024.1364917

Efficacy and safety of a "radical" surgical strategy in the treatment of parasagittal sinus meningioma

Zihao Duan, Changlong Zhou, Xiaoxiao Yan, Wei Du, Xiaohui Xia, Hui Shi, Hai Su, Yi Zhang, Xuenong He and Qijiang Xiong*

Department of Neurosurgery, the Affiliated Yongchuan Hospital of Chongqing Medical University, Chongqing, China

Background: No standardized criteria for surgical resection of parasagittal sinus meningiomas (PSM) have been established, and different surgical strategies have been proposed. The aim of the present study was to investigate the efficacy and safety of a "radical" surgical strategy in the treatment of PSM.

Methods: The clinical histories, radiological findings, pathologic features, and surgical records of 53 patients with PSM admitted by the same surgical team using the "radical" surgical strategy were retrospectively analyzed between 2018 and 2023.

Results: Among the 53 PSM cases, 16 (30.2%) had a patent sinus proper, 28 (52.8%) had partial obstruction of the sinus proper, and 9 (17.0%) had complete obstruction of the sinus proper before the operation. During operation, Simpson grade I resection was performed in 34 (64.2%) cases and Simpson grade II in 19 (35.8%) cases. Postoperative pathologic examination suggested tumors of WHO grade I in 47 (88.7%) cases, WHO grade II in 4 (7.5%) cases, and WHO grade III in 2 (3.8%) cases. Postoperative complications primarily included a small amount of delayed intracerebral hemorrhage in 3 (5.7%) cases, exacerbation of cerebral edema in 3 (5.7%) cases, exacerbation of motor and sensory deficits in 4 (7.5%) cases, and intracranial infection in 2 (3.8%) cases. There were no cases of death or new-onset neurological dysfunction. Dizziness and headache symptoms improved to varying degrees, and a seizure-free status was achieved postoperatively. Excluding one case lost to follow-up, the average follow-up period was 33 months, and there were no cases of recurrence.

Conclusion: A "radical" strategy for the surgical management of PSM is effective, safe, and simple to perform, provided that the sagittal sinus is properly managed and its associated veins are protected.

KEYWORDS

sagittal sinus, meningioma, surgical strategy, microsurgery, parasagittal sinus meningioma

1 Introduction

Parasagittal sinus meningioma (PSM) was first described by Cushing and Eisenhardt (1) as a tumor that occupies the parasagittal angle of the sagittal sinus, with no brain tissue between the tumor and the sagittal sinus. PSMs may also partially or completely invade the sagittal sinus. PSM accounts for 20%–30% (2) of all meningiomas and 25% of the meningiomas seen in our department

during the same period. Although meningiomas grow slowly and are generally well-defined, PSMs tend to invade the superior sagittal sinus to varying degrees and are adjacent to many cortical veins and major functional areas. This greatly increases the difficulty of complete surgical resection, making radical resection of PSMs without complications and recurrence a major challenge for neurosurgeons.

Given these difficulties and risks, no consensus on the surgical management of PSM currently exists. A literature review showed that surgical strategies can be broadly categorized as "radical" (3–8) or "cautious" (2, 9–11). "Radical" resection strategies typically consist of resecting the tumor inside and outside the sagittal sinus, followed by ligation and division, suture repair, or reconstruction of the sagittal sinus, to enhance the likelihood of achieving surgical cure. "Cautious" resection strategies typically focus on intraoperative protection of the venous sinuses and only involve resection of the tumor outside the sinus without operating on the part inside the sinus, followed by observation, radiotherapy, or re-operation; however, there is an increased risk of tumor residue and recurrence.

In this study, we adopted a "radical" surgical strategy for 53 patients with PSM at our center and achieved satisfactory results. We summarize and detail the surgical techniques and perioperative management of PSM with different degrees of sinus invasion.

2 Materials and methods

A total of 53 cases of PSM treated by the same surgical team using a "radical" surgery strategy at the Department of Neurosurgery of Yongchuan Hospital, Chongqing Medical University were collected between 2018 and 2023. MRI (plain + enhanced + MRV) and CT were performed at the time of admission; some patients also underwent CTV or DSA. The lesions were on the right side of the sinus in 31 (58.5%) cases and on the left side in 22 (41.5%) cases. The maximum size was 7.7 × 6.5 × 6.7 cm, the minimum size was 1.6 × 1.4 × 1.0 cm, and the mean size was 4.0 × 3.6 × 4.0 cm. There were 23 (43.4%) cases accompanied with peritumoral brain edema, of which 7 (13.2%) cases were severe. PSM was broadly classified into three types based on the degree of sinus invasion. Type I (patent) tumors adhere to or invade only the outer layer of the sagittal sinus wall and do not affect the sinus proper; this is comparable to Sindou type I. Type II (partial obstruction) tumors have broken through the outer layer of the sagittal sinus wall and are pushing or growing into the sinus proper, resulting in partial obstruction of the sinus cavity; this includes Sindou types II-IV. Type III (complete obstruction) tumors involve two or all walls of the sagittal sinus with complete obstruction of the sinus proper and includes Sindou types V and VI. General characteristics and preoperative clinical symptoms concerning 53 patients with PSM are summarized in Tables 1, 2, respectively.

The study was approved by the Medical Research Ethics Committee of Yongchuan Hospital, Chongqing Medical University (no. 2023-KLS-65).

TABLE 1 General characteristics of the 53 patients with PSM.

Parameter	Frequency (%)
Number of patients	53
Age (years, mean ± SD)	53.4 ± 14.1
Primary: Recurrent	53:0
Sex (male: female)	22:31(1:1.4)
Mean tumor size	4.0 × 3.6 × 4.0 cm
Tumor site	
Anterior 1/3 of SSS*	12(22.6%)
Middle 1/3 of SSS	25(47.2%)
Posterior 1/3 of SSS	11(20.8%)
Confluence of sinuses	5(9.4%)
Extent of SSS invasion	
Type I* (patent)	16(30.2%)
Type II* (partial obstruction)	28(52.8%)
Type III* (complete obstruction)	9(17.0%)
WHO pathological grade	
I	47(88.7%)
II	4(7.5%)
III	2(3.8%)

*SSS, superior sagittal sinus; type I equivalent to Sindou type I, type II equivalent to Sindou types II–IV, type III equivalent to Sindou types V–VI.

2.1 "Radical" surgical strategy

2.1.1 Management of sinuses and associated veins with tumor involvement

For type I, the outer layer of the sinus wall was resected while keeping the sinus proper intact, and a gelatin sponge or muscle paste was used to cover the defect and immobilize it with "bio-protein gel" (Figures 1A,B). For type II, if the tumor grew into the lateral recess and only compressed the sinus cavity, the lateral recesses were cut open, the tumor was resected, and the roof of the sinus and the lateral wall were then closed with sutures (Figures 1C,D). If the tumor had grown into the sinus proper and invaded the one or both two sinus walls, the sinus wall and the tumor inside the sinus were resected, and sinus repair or sinus reconstruction was performed using autologous dura mater, the temporal fascia, or artificial meninges (Figures 1E,F). For type III, the sinus was ligated proximally and distally, and the sinus and the tumor inside the sinus were resected (Figures 1G,H). Patch repair for reconstruction of the sinus cavity could also be considered if poor venous compensation is observed.

2.1.2 Management of tumors involving the skull

If the tumor only caused local hyperplasia or destruction of the inner table of the skull, the skull was ground with a bur to remove the diseased bone and completely cauterized using an electric knife. If the tumor had caused serious changes in the skull, then that part of the skull was removed, and a titanium mesh or other material was used to repair the cranial defect.

2.1.3 Management of tumors near the arachnoid, pia mater, or brain tissue

Tissues were resected together in cases of tumor involvement.

2.1.4 Management of the tumor base

The dura of the tumor base, which includes 2 cm of normal dura outside the tumor, was resected.

TABLE 2 Preoperative clinical symptoms.

Site / Symptom	Anterior 1/3 of SSS	Middle 1/3 of SSS	Posterior 1/3 of SSS	Confluence of sinuses	Total
Dizziness, headache	9(75.0%)	14(56.0%)	7(63.6%)	5(100.0%)	35(66.0%)
Cognitive dysfunction	4(33.3%)	6(25.0%)			10(18.9%)
Numbness (lower and/or upper limbs)		7(28.0%)			7(13.2%)
Fatigue (lower and/or upper limbs)		8(32.0%)			8(15.1%)
Generalized seizures	3(25.0%)	2(8.0%)			5(9.4%)
Focal seizures		4(16.0%)	1(9.1%)		5(9.4%)
Decreased vision	3(25.0%)	2(8.0%)	2(18.2%)	3(60.0%)	10(18.9%)
Asymptomatic	1(8.3%)	5	2		8

2.2 Postoperative observation and evaluation

Postoperatively, the patient was admitted to the neurosurgical intensive care unit for management for 1–3 days, and cranial CT was performed immediately after resuscitation and respirator weaning. The first MRI (plain + enhanced + MRV) examination was completed within 3 days postoperative. Surgical outcomes were assessed clinically and by imaging.

2.3 Follow-up

Radiological follow-up and clinical evaluation were performed at 3, 6, and 12 months postoperative and annually thereafter. The follow-up interval was shortened for patients who underwent sinus wall resection with patch reconstruction.

3 Results

Based on the Simpson grade of meningioma resection (12), all 53 cases in the cohort underwent complete resection under microscopy and MRI confirmation within 3 days postoperative. Simpson grade I resection was achieved in 34 (64.2%) cases, and Simpson grade II resection was achieved in 19 (35.8%) cases. Among the patients presenting with preoperative symptoms of cognitive dysfunction, limb numbness or fatigue, and vision loss, 33 (62.3%) patients demonstrated postoperative improvement, while 20 (37.7%) patients continued to experience persistent symptoms (Table 3). Postoperative dizziness and headache symptoms improved to varying degrees, and a seizure-free status was achieved. The outer layer of the sinus wall was resected in 14 (26.4%) patients (a representative case is illustrated in Figure 2) and electrocoagulation only occurred in 2 (3.8%) patients. The sinus wall was directly sutured in 13 (24.5%) patients, all exhibiting mild stenosis (Figure 3). Patch reconstruction was performed in 20 (37.7%) patients, with sinus patency confirmed using MRV in all cases (Figure 4). Sinus ligation and division were performed in 4 (7.6%) patients (Figure 5).

There were no cases of perioperative death. There were 3 (5.7%) cases of small late-onset intracerebral hemorrhage after heparin anticoagulant therapy, which did not increase after heparin was discontinued; 3 (5.7%) cases of postoperative exacerbation of cerebral edema and symptoms of cranial hypertension, which gradually improved with dehydration, protein, and hormones; 4 (7.5%) cases of postoperative exacerbation of limb numbness and paralysis, which recovered in 1 month in conjunction with rehabilitation therapy; and 2 (3.8%) cases of intracranial infections, which recovered after antibiotic treatment. There were no definitive cases of air embolism and MRV-confirmed venous sinus thrombosis. Pathologic findings suggested tumors of WHO grade I in 47 (88.7%) cases, WHO grade II in 4 (7.5%) cases, and WHO grade III in 2 (3.8%) cases.

Excluding one patient lost to follow-up, 52 patients were followed up through June 2023 for a total ranging from 6 to 63 months (mean follow-up 33 months). There were no cases of recurrence.

4 Discussion

In a seminal paper published in 1957, Simpson et al. (12) introduced a classification system consisting of five levels for meningioma resection and provided detailed definitions for each level, elucidating the relationship between the extent of tumor resection and its recurrence. This correlation has since formed the theoretical foundation underlying the aggressive surgical treatment strategy for meningiomas. However, parasagittal sinus meningiomas are often located in critical intracranial areas, and surgical procedures are prone to damage important cortical areas, the superior sagittal sinus, and its important collateral draining veins, which are often accompanied by various degrees of complications, such as limb paralysis, severe cerebral edema, and even death.

To mitigate these risks, researchers have adopted a surgical strategy of "conservative resection," but a large body of evidence suggests that meningioma recurrence is strongly correlated with the degree of resection. Conservative resection of PSM is associated with an increased recurrence rate (3, 5, 6), emphasizing the importance of radical resection. Management of the tumor invading the sinus and the associated veins is essential for achieving radical resection of PSM. Sindou et al. (3) found that repair and reconstruction of the sinus after radical tumor resection or restoration of sinus circulation by a bypass resulted in a recurrence

rate of only 4%. Zhang et al. (8) reported a recurrence rate of 0% and a postoperative complication rate of 7.2% after radical tumor resection and sinus reconstruction with a simplified surgical strategy. All complications were treated aggressively, and all patients recovered uneventfully.

Our team has formulated a "radical surgery strategy" for PSMs based on "Simpson Grade I Resection Criteria" for meningiomas, especially the corresponding sinus management strategy according to the degree of sinus invasion of PSMs, which is easy to implement during surgery, does not significantly increase surgical risk and postoperative complications, and has shown remarkable therapeutic results. To improve the surgical management of PSMs, we believe that the following issues should be considered.

4.1 Assessment, identification, and protection of the sagittal sinus, tributary veins, and collateral veins

Protection of the venous circulation is known to be critical to surgical success for PSMs. Preoperative prognosis combined with intraoperative reality or intraoperative evaluation, utilizing techniques such as indocyanine (ICG) (13) video angiography, is required. First, a detailed preoperative evaluation of the cerebral veins based on DSA, CTV, or MRV imaging was performed. In particular, MRV is increasingly becoming the preferred option for visualization of intracranial veins because it is non-invasive and radiation-free. However, preoperative imaging of the sinus does not

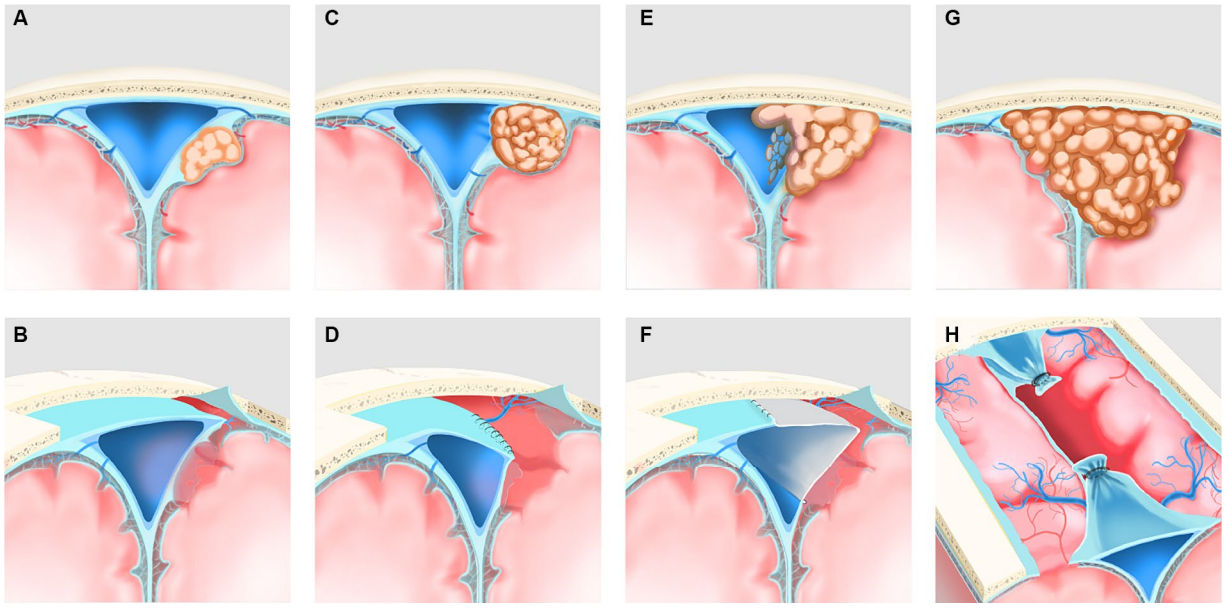

FIGURE 1
Reclassification of PSM and its corresponding surgical methodologies was illustrated. **(A)** Type I (patent) preoperatively, the tumor invaded the outer layer of the ipsilateral sagittal sinus wall only and did not affect the sinus proper. **(B)** Postoperatively, the extra-sinus tumor and the outer layer of the sinus wall, which was involved owing to the tumor, were resected. **(C)** Type II (partial obstruction) preoperatively; the tumor grew into the lateral recess and only pushed the sinus cavity, resulting in mild obstruction of the sinus proper. **(D)** Postoperatively, the lateral recess was cut open, the extra- and intra-sinus tumor was resected, and the roof of the sinus and the ipsilateral wall were then closed with sutures. **(E)** Type II (partial obstruction) preoperatively, the tumor grew into the sinus cavity and invade the one or both of the two sinus walls with more severe obstruction of the sinus proper. **(F)** Postoperatively, the sinus wall involved owing to the tumor, and the extra- and intra-sinus tumor were resected, and sinus repair or sinus reconstruction was performed using a patch. **(G)** Type III (complete obstruction)preoperatively, the tumor involved two or all walls of the sagittal sinus with complete obstruction of the sinus proper. **(H)** Postoperatively, the sinus involved owing to the tumor was ligated proximally and distally, and the sinus and the extra- and intra-sinus tumor were resected.

TABLE 3 **Surgical outcomes.**

Extent of SSS invasion	Cases	Grade of resection		Neurological function	
		Simpson I	Simpson II*	Improvement	Same as preoperative
Type I (patent)	16	14	2	11	5
Type II (partial obstruction)	28	16	12	19	9
Type III (complete obstruction)	9	4	5	3	6

*Simpson grade II resection is defined as electrocoagulation only with complete or partial preservation of the sinus wall to avoid affecting the collateral veins.

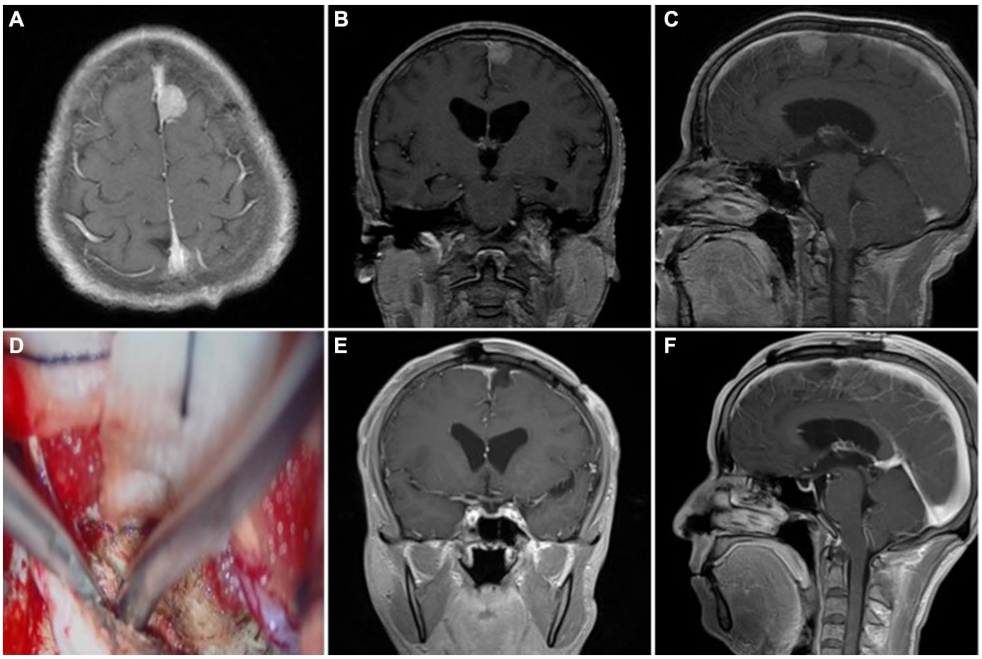

FIGURE 2
Representative case 1, type I (patent sinus). **(A–C)** Preoperative enhanced MRI images. **(D)** Intraoperative resection of the outer layer of the sinus wall. **(E,F)** Postoperative enhanced MRI images.

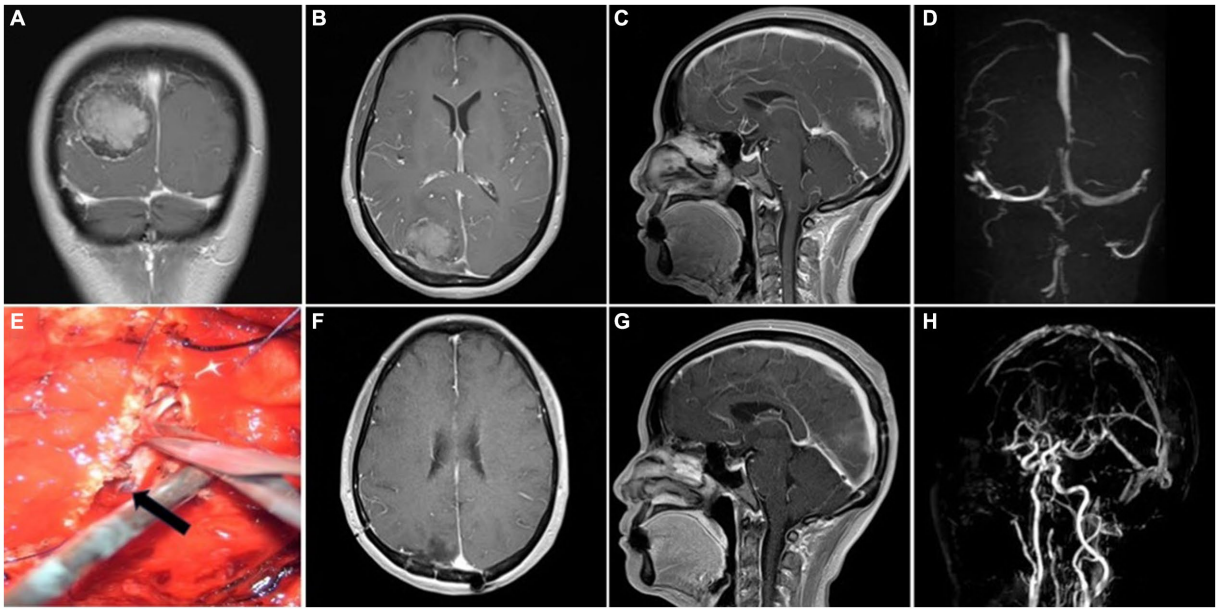

FIGURE 3
Representative case 2, type II (partial sinus obstruction). **(A–C)** Preoperative enhanced MRI images. **(D)** Preoperative MRV images. **(E)** Intraoperative suture repair of the sinus wall. The arrow shows the intact inner layer compressed by tumor. **(F,G)** Postoperative enhanced MRI images. **(H)** Postoperative MRV images.

always match the actual condition of the sinus, so intraoperative biopsy or opening of the sinus wall is recommended for exploration to determine whether the sinus is completely obstructed. Furthermore, it is not recommended to perform direct ligation and resection of the superior sagittal sinus without assessing whether the local drainage vein is well compensated, even if preoperative imaging indicates type III. When preoperative symptoms of venous hypertension are under consideration, along with imaging indicating a scarcity of side drainage veins around the tumor, characterized by small venous vessel diameters and a singular

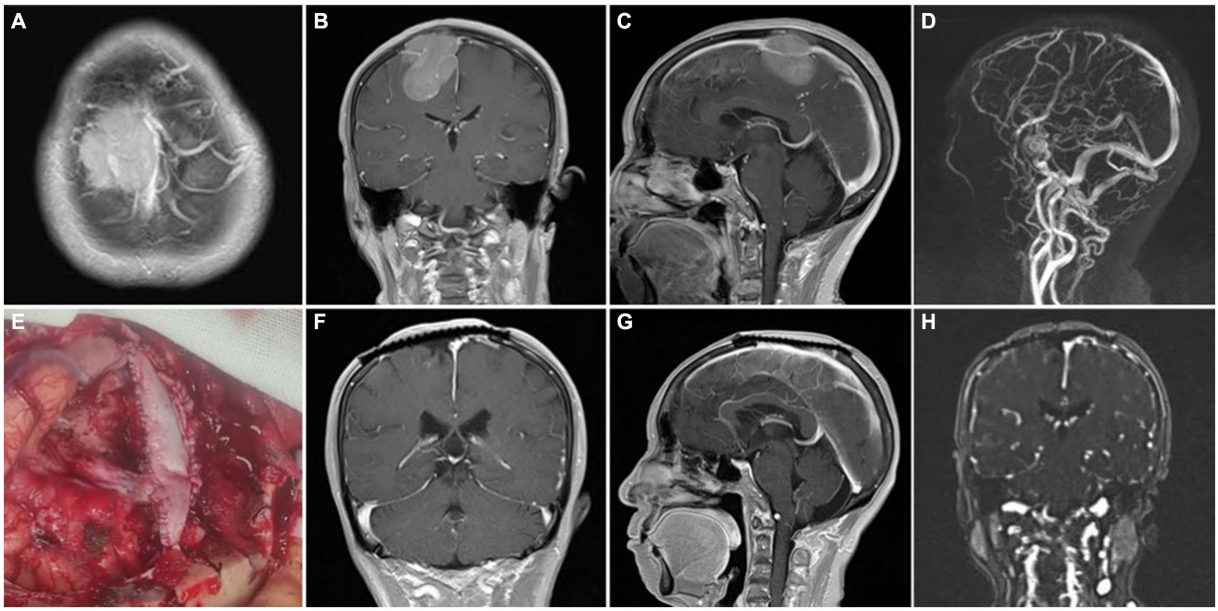

FIGURE 4
Representative case 3, type III (complete sinus obstruction). **(A–C)** Preoperative enhanced MRI images. **(D)** Preoperative MRV images. **(E)** Intraoperative patch reconstruction of the sinus wall. **(F,G)** Postoperative enhanced MRI images with concurrent titanium mesh repair of the cranial defect. **(H)** Postoperative MRV images.

drainage pattern, or when peritumoral brain edema (PTBE) coincides with poor brain-tumor interface-related edema (PIRE) (14, 15), there is a likelihood of insufficient local compensatory drainage veins. Hence, reconstruction of the sinus cavity warrants consideration (Figure 4). Conversely, we believe excision of the sinus without reconstruction is safe (Figure 5). Increased tumor size is accompanied by compression of the cerebral cortex and cortical bridging veins, which usually exhibit pathological changes upon compression by the tumor, resulting in poor venous return. The collateral venous circulation will gradually develop and play an important role in venous return. Destruction of veins during the procedure may lead to several adverse consequences, such as cerebral infarction or hemorrhage, seizures or neurological deficits, and even death in severe cases. Therefore, protecting the peritumoral veins is critical to the success of the procedure (16, 17). Intraoperatively, it is necessary to open the dura mater from above the tumor to avoid damaging the cortical veins at the tumor margins and to fully decompress the tumor. Then, the margins of the tumor are isolated after a decrease in peritumoral venous tension and relaxation of the tumor-brain interface. Finally, tumor veins must be accurately identified, and all preservable normal veins must be protected.

4.2 Control of bleeding after opening the sinus wall, as well as prevention and monitoring of air embolism

In our experience, the sinus wall is opened from the proximal to the distal end, and a single gelatin sponge was applied immediately afterward to stop proximal hemorrhage; gelatin sponge fragments should not be used to prevent leaving residue in the sinus. In addition, the tumor is resected from the proximal to the distal end, and the sinus wall is sutured or repaired while gradually advancing until the tumor is resected and the sinus is reconstructed. The risk of air embolism varies among case reports and is affected by surgical position. Air embolism was diagnosed in only one of the 100 patients (1%) reported by Alvernia and Sindou (18), although most patients were in a semi-sitting position. The management of air embolism is primarily focused on prevention, with particular emphasis placed on ensuring that the operative area is positioned below the level of the heart when incising the sinus wall. After the proximal sinus wall was opened, the surgical assistant immediately closed the defect with a gelatin sponge and resected the tumor toward its distal end while ensuring that the proximal end remained closed. When the reconstruction was completed, the last of the residual tumor in the distal sinus was resected, and blood flowed from the distal end, confirming adequate perfusion of the reconstructed sinus segment and overflowing from the distal end (terminal pinhole). Then, the sinus was closed by tightening the suture. Currently, no effective monitoring procedures are available for early identification of air embolism. Indicators of air embolism can appear on transesophageal ultrasound or various anesthesia monitoring systems but with a clear time lag.

4.3 Prevention and treatment of venous sinus thrombosis

Although most meningiomas are benign tumors, they are strongly associated with systemic thromboembolic states. The intrinsic biological activity of meningiomas exerts local and

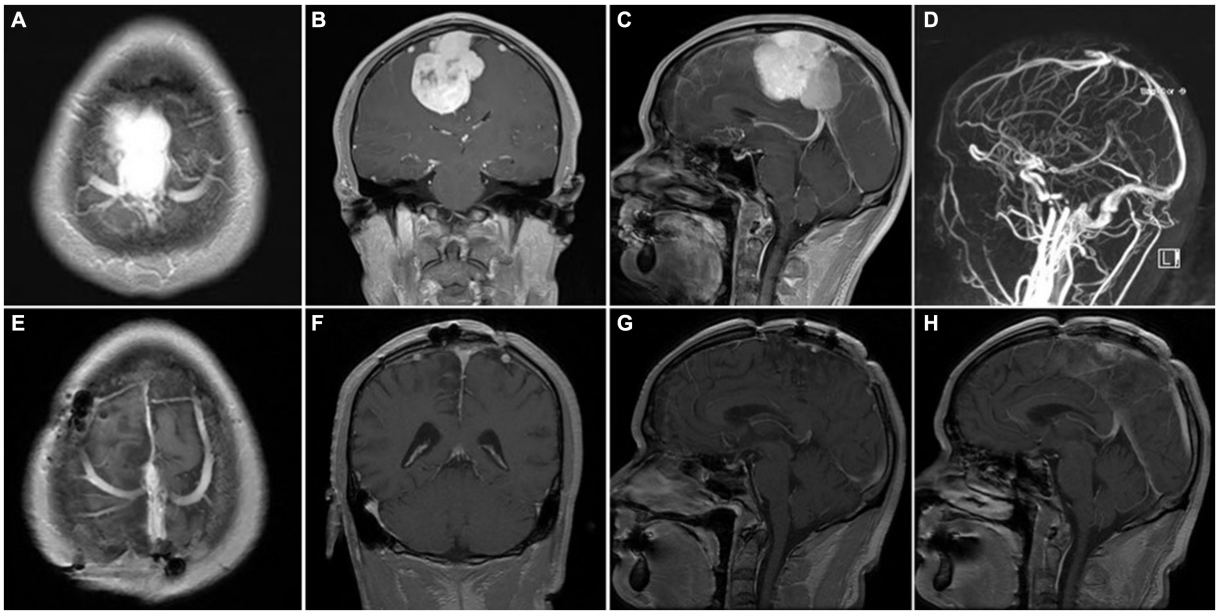

FIGURE 5
Representative case 4, type III (complete sinus obstruction). **(A–C)** preoperative enhanced MRI images. **(D)** preoperative MRV images. **(E–H)** Postoperative enhanced MRI images. Intraoperative sinus ligation and division without sinus reconstruction.

systemic hormonal and hematologic effects that play a major role in venous sinus thrombosis. In particular, parasagittal sinus meningiomas are more prone to promote local thrombosis because of their complex connections with vascular structures (4). In addition, excessive intraoperative manipulation of the venous sinus and sacrifice of peritumoral veins can promote thrombosis in the injured vessels. Currently, the preferred imaging modality for diagnosing venous sinus thrombosis is MRV, which is highly sensitive, non-invasive, and free of radiation, making it favored by many physicians and patients (19). The need for anticoagulants in the management of venous sinus thrombosis has been underscored by many researchers in the literature. Sindou et al. (3) concluded that anticoagulant therapy is required for at least 3 months after radical resection, a strategy that does not increase the rate of bleeding complications. A review of 34 studies on the interventional management of venous sinus thrombosis by Medel et al. (20) concluded that systemic anticoagulant therapy is a rational initial strategy for the treatment of venous sinus thrombosis, even in the presence of cerebral hemorrhage. A retrospective study of patients with cerebellopontine angle tumors by Moore et al. (21) found that five of the 43 patients developed thrombosis of the transverse and sigmoid sinuses after tumor resection. All patients with thrombosis were treated with intravenous heparin without any complications, allowing us to conclude that initiating anticoagulant therapy early in the postoperative period is safe and effective and prevents the progression of venous sinus thrombosis. Similar to other researchers, we hypothesized that patients undergoing patch repair or venous sinus reconstruction may have a higher incidence of venous sinus thrombosis due to the surgical procedure simultaneously compromising the original support of dural structures at the three corners of the sagittal sinus, rendering the sinus cavities more vulnerable to factors such as blood pressure, blood volume, blood viscosity, intracranial pressure, and cerebral edema. Therefore, meticulous management of these aforementioned factors is imperative during the postoperative period. We routinely implemented low molecular weight heparin anticoagulant therapy after the initial CT re-examination to rule out intracranial hemorrhage, during which the patient was closely observed for neurological symptoms and gastrointestinal, oral, and skin mucosal bleeding. In addition, coagulation function, thromboelastography, coagulation index, and other indicators were monitored with detailed follow-up. Following discharge, appropriate oral antiplatelet or anticoagulant medications were administered for 3–6 months post-operation. In the present cohort, anticoagulant therapy was applied in 20 cases of patch reconstruction and 13 cases of sinus wall suturing. There were no cases of hemorrhage other than only 3 cases of small delayed intracerebral hemorrhage in the edematous area outside the tumor, and there were no cases of venous sinus thrombosis.

4.4 Innovations of this study

This study has several innovations compared with other studies. The "radical" surgical strategy for PSMs is described in detail, and all the technical details of this surgical strategy, including the management of tumors with different types of sinus involvement, the method of sinus reconstruction, and the control of intraoperative hemorrhage are described in detail so that our treatment model is clear and easy to understand. Additionally, the details of the venous reconstruction technique are relatively simple and do not require complicated operations, such as the use of autologous saphenous vein

bypass, making the approach to venous sinus reconstruction easier to implement.

4.5 Limitations

The follow-up period of this study was limited, so the long-term effectiveness of our "radical" surgical strategy must be confirmed with a longer follow-up period. Given that our surgical approach was as aggressive as that reported by Sindou et al. (3), we predict that the long-term recurrence rate of our procedure will be comparable to theirs, at approximately 4%. At the same time, we recognize that our sample size is relatively small compared to other studies, which may affect our judgment of the long-term effects of surgical strategies. Therefore, the sample size should be increased in future studies to facilitate a more in-depth, comprehensive, and accurate investigation of the long-term efficacy and safety of this surgical strategy.

5 Conclusion

A "radical" surgical strategy for increasing the degree of parasagittal sinus meningioma resection and reducing the rates of residual tumor and recurrence is effective, safe, and simple to perform, provided that the sagittal sinus is properly managed and its associated veins are protected.

Data availability statement

The original contributions presented in the study are included in the article/supplementary material, further inquiries can be directed to the corresponding author.

Ethics statement

The studies involving humans were approved by Medical Research Ethics Committee of Yongchuan Hospital, Chongqing Medical University. The studies were conducted in accordance with the local legislation and institutional requirements. The participants provided their written informed consent to participate in this study. Written informed consent was obtained from the individual(s) for the publication of any potentially identifiable images or data included in this article.

Author contributions

ZD: Data curation, Formal analysis, Investigation, Methodology, Software, Validation, Writing – original draft, Writing – review & editing. CZ: Conceptualization, Funding acquisition, Resources, Supervision, Writing – review & editing. XY: Writing – review & editing. WD: Investigation, Writing – review & editing. XX: Methodology, Writing – review & editing, Formal analysis. HSh: Methodology, Writing – review & editing. HSu: Conceptualization, Writing – review & editing. YZ: Conceptualization, Writing – review & editing. XH: Conceptualization, Writing – review & editing. QX: Conceptualization, Methodology, Writing – review & editing, Formal analysis, Investigation, Project administration, Supervision, Validation, Writing – original draft.

Funding

The author(s) declare financial support was received for the research, authorship, and/or publication of this article. This work was supported by the Natural Science Foundation of Chongqing, China (no. cstc2021jcyj-msxm X0552) and the Natural Science Foundation of Yongchuan, Chongqing, China (no. 2023yc-jckx20051).

Acknowledgments

The authors would like to thank Editage (www.editage.cn) for English language editing.

Conflict of interest

The authors declare that the research was conducted in the absence of any commercial or financial relationships that could be construed as a potential conflict of interest.

Publisher's note

References

1. Cushing H, Eisenhardt L. Meningiomas: their classification, regional behaviour, life history, and surgical end results. *JAMA*. (1939) 112:175. doi: 10.1001/jama.1939.02800020081030

2. Mathiesen T. Parasagittal meningiomas. *Handb Clin Neurol*. (2020) 170:93–100. doi: 10.1016/B978-0-12-822198-3.00031-8

3. Sindou MP, Alvernia JE. Results of attempted radical tumor removal and venous repair in 100 consecutive meningiomas involving the major dural sinuses. *J Neurosurg*. (2006) 105:514–25. doi: 10.3171/jns.2006.105.4.514

4. Raza SM, Gallia GL, Brem H, Weingart JD, Long DM, Olivi A. Perioperative and long-term outcomes from the management of parasagittal meningiomas invading the superior sagittal sinus. *Neurosurgery*. (2010) 67:885–93. doi: 10.1227/NEU.0b013e3181ef2a18

5. Sindou M. Meningiomas involving major dural sinuses: should we attempt at radical removal and venous repair? *World Neurosurg*. (2014) 81:46–7. doi: 10.1016/j.wneu.2013.07.119

6. Wang S, Ying J, Wei L, Li S, Jing J. Guidance value of intracranial venous circulation evaluation to parasagittal meningioma operation. *Int J Clin Exp Med*. (2015) 8:13508–15.

7. Sindou M. Meningiomas invading the sagittal or transverse sinuses, resection with venous reconstruction. *J Clin Neurosci*. (2001) 8:8–11. doi: 10.1054/jocn.2001.0868

8. Zhang N, Yang T, Hameed F, Zhang X, Yao Y, Li D, et al. Can safe and radical resection of all types of parasagittal meningiomas be achievable? -the introduction of a simplified surgical strategy. *Neurol Res*. (2021) 43:259–66. doi: 10.1080/01616412.2020.1847530

9. Gatterbauer B, Gevsek S, Höftberger R, Lütgendorf-Caucig C, Ertl A, Mallouhi A, et al. Multimodal treatment of parasagittal meningiomas: a single-center experience. *J Neurosurg*. (2017) 127:1249–56. doi: 10.3171/2016.9.JNS161859

10. Munich SA, Eddelman D, Byrne RW. Retrospective review of a venous sparing approach to resection of parasagittal meningiomas. *J Clin Neurosci*. (2019) 64:194–200. doi: 10.1016/j.jocn.2019.02.013

11. Tomasello F, Conti A, Cardali S, Angileri FF. Venous preservation-guided resection: a changing paradigm in parasagittal meningioma surgery. *J Neurosurg*. (2013) 119:74–81. doi: 10.3171/2012.11.JNS112011

12. Simpson D. The recurrence of intracranial meningiomas after surgical treatment. *J Neurol Neurosurg Psychiatry*. (1957) 20:22–39. doi: 10.1136/jnnp.20.1.22

13. Marchese E, Della Pepa GM, la Rocca G, Albanese A, Ius T, Simboli GA, et al. Application of indocyanine green video angiography in vascular neurosurgery. *J Neurosurg Sci*. (2019) 63:656–60. doi: 10.23736/S0390-5616.19.04753-2

14. Wang X, Wang MY, Qian K, Chen L, Zhang FC. Classification and protection of Peritumoral draining veins of parasagittal and Falcine Meningiomas. *World Neurosurg*. (2018) 117:e362–70. doi: 10.1016/j.wneu.2018.06.037

15. Yin T, Zhang J, Zhang H, Zhao Q, Wei L, Wang S. Poor brain-tumor Interface-related edema generation and cerebral venous decompensation in parasagittal Meningiomas. *World Neurosurg*. (2018) 115:e544–51. doi: 10.1016/j.wneu.2018.04.092

16. Magill ST, Theodosopoulos PV, McDermott MW. Resection of falx and parasagittal meningioma: complication avoidance. *J Neuro-Oncol*. (2016) 130:253–62. doi: 10.1007/s11060-016-2283-x

17. Cai Q, Wang S, Wang J, Tian Q, Huang T, Qin H, et al. Classification of Peritumoral veins in convexity and parasagittal Meningiomas and its significance in preventing cerebral venous infarction. *World Neurosurg*. (2021) 149:e261–8. doi: 10.1016/j.wneu.2021.02.041

18. Alvernia JE, Sindou M. Parasagittal meningiomas In: JH Lee, editor. *Meningiomas: Diagnosis, treatment, and outcome*. London: Springer (2009). 309–17.

19. Benjamin CG, Sen RD, Golfinos JG, Sen C, Roland JT, McMenomey S, et al. Postoperative cerebral venous sinus thrombosis in the setting of surgery adjacent to the major dural venous sinuses. *J Neurosurg*. (2018) 1:1–7.

20. Medel R, Monteith SJ, Crowley RW, Dumont AS. A review of therapeutic strategies for the management of cerebral venous sinus thrombosis. *Neurosurg Focus*. (2009) 27:E6. doi: 10.3171/2009.8.FOCUS09154

21. Moore J, Thomas P, Cousins V, Rosenfeld JV. Diagnosis and Management of Dural Sinus Thrombosis following resection of cerebellopontine angle tumors. *J Neurol Surg B Skull Base*. (2014) 75:402–8. doi: 10.1055/s-0034-1376421

frontiers | Frontiers in Oncology

TYPE Case Report
PUBLISHED 07 May 2024
DOI 10.3389/fonc.2024.1359093

OPEN ACCESS

EDITED BY
Gerardo Caruso,
University Hospital of Policlinico G. Martino, Italy

REVIEWED BY
Byram Ozer,
NCI Neuro-Oncology Branch, United States
Nicholas Gottardo,
Perth Children's Hospital, Australia

*CORRESPONDENCE
Barbara Castelli
Barbara.castelli@meyer.it

RECEIVED 20 December 2023
ACCEPTED 21 March 2024
PUBLISHED 07 May 2024

CITATION
Castelli B, Tellini M, Guidi M, Di Nicola M, Giunti L, Buccoliero AM, Censullo ML, Iacono A, Desideri I, Genitori L, Sardi I and Fonte C (2024) Case report: complete long-lasting response to multimodal third line treatment with neurosurgical resection, carmustine wafer implantation and dabrafenib plus trametinib in a *BRAFV600E* mutated high-grade glioma.
Front. Oncol. 14:1359093.
doi: 10.3389/fonc.2024.1359093

Case report: complete long-lasting response to multimodal third line treatment with neurosurgical resection, carmustine wafer implantation and dabrafenib plus trametinib in a *BRAFV600E* mutated high-grade glioma

Barbara Castelli[1*], Marco Tellini[1], Melina Guidi[1], Marco Di Nicola[1], Laura Giunti[1], Anna Maria Buccoliero[2], Maria Luigia Censullo[1], Alessandro Iacono[3], Isacco Desideri[4], Lorenzo Genitori[5], Iacopo Sardi[1] and Carla Fonte[1]

[1]Neuro-oncology Department, Meyer Children's Hospital IRCCS, Florence, Italy, [2]Pathology Department, Meyer Children's Hospital IRCCS, Florence, Italy, [3]Radiology Department, Meyer Children's Hospital IRCCS, Florence, Italy, [4]Radiotherapy Department, Careggi Hospital, Florence, Italy, [5]Neurosurgery Department, Meyer Children's Hospital IRCCS, Florence, Italy

Dabrafenib plus trametinib is a promising new therapy for patients affected by *BRAFV600E*-mutant glioma, with high overall response and manageable toxicity. We described a complete and long-lasting response in a case of recurrent anaplastic pleomorphic xanthoastrocytoma CNS WHO-grade 3 *BRAFV600E* mutated. Due to very poor prognosis, there are a few described cases of high-grade glioma (HGG) patients treated with the combined target therapy as third-line treatment. The emergence of optimized sequencing strategies and targeted agents, including multimodal and systemic therapy with dabrafenib plus trametinib, will continue to broaden personalized therapy in HGG improving patient outcomes.

KEYWORDS

high-grade glioma, MEK inhibitors, target therapy, dabrafenib, trametinib, pleomorphic xanthoastrocytoma, BRAFV600E, BRAF inhibitors

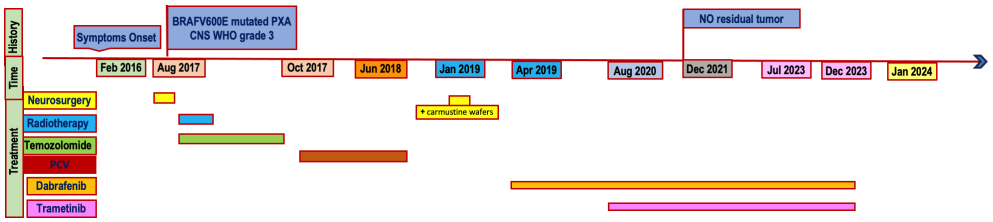

GRAPHICAL ABSTRACT
Timeline.

1 Introduction

High-grade gliomas (HGGs), tumors of neuroepithelial origin (1), represent the most common primary intracranial tumor in adults (2, 3). Differently, low- grade gliomas (LGGs) predominate in children (4, 5).

HGGs display a dismal prognosis despite surgical and chemo radiotherapeutic advances (1) and standard of care is commonly not curative. Throughout the understanding of molecular basis of tumors and recent insights, survival outcomes modestly increased, however, remaining limited and challenging. Therefore, worldwide researches are moving towards new frontiers and ongoing trials are investigating novel targeted agents (1). In the last years, important advances in the field of molecular biology and pathology have been accomplished (6).

MAPK (mitogen-activated protein kinase) pathway, implicated in carcinogenesis, has been found altered in most glial tumors (7, 8), promoting cellular overgrowth and overcoming metabolic stress (9). The pathway includes a small G protein (RAS) and three protein kinases in a downstream signaling pathway (respectively RAF – composed of A-RAF, B-RAF and RAF-1 or C-RAF kinases, MEK – composed of MEK1 and MEK2, ERK – composed of ERK1 and ERK2) (10, 11). ERK (extracellular signal-regulated kinase) is a MAPK that functions as the major effector of the RAS oncoprotein, translocating to the nucleus to activate transcription factors (10). Driving oncogenic mutations should develop upstream of the MAPK pathway (11).

Most *BRAF* variants are missense mutations at amino acid position 600, resulting in an exchange of valine for glutamate (referred to as *BRAFV600E*) (12). Activating *BRAFV600E* kinase mutations occur in ~7% of human malignancies (13). Initially described in melanoma, colon and papillary thyroid carcinoma, these alterations have also been observed in primary nervous system tumors (14). High mutation frequencies have been detected in pleomorphic xanthoastrocytomas (PXA), gangliogliomas and extra-cerebellar pilocytic astrocytomas (14), but the mutation has also been found in others HGGs (12), in particular in epithelioid glioblastoma (15).

The BRAF inhibitors vemurafenib, dabrafenib and encorafenib selectively target BRAF kinase, interfering with MAPK signaling pathway (16). Selumetinib and trametinib are MEK inhibitors (MEKi) (7). The combination of BRAF and MEK inhibitor have been approved in various cancers by the US Food and Drugs Administration (FDA) (17) and the European Medicines Agency (EMA). It is known that the blockage of two downstream pathway components with dual BRAF/MEK inhibition may improve tumor control and patient survival (18).

Recently, MEK inhibitors and BRAF inhibitors have been successfully used in pediatric LGG patients (19), with a relatively well-tolerated side effect profile (1). Few data are available on their efficacy in relapsing refractory HGGs.

Herein we report a case of complete long-lasting response to combined dabrafenib/trametinib as third-line therapy in a patient with frontal HGG.

2 Case report

In February 2016, a 21-year-old white female presented her first seizure episode. In August 2016 she was admitted to Anna Meyer Children's Hospital IRCCS in Florence for recurrent episodes. Imaging revealed a left frontal lesion (Figure 1). A partial resection was performed. The histological examination diagnosed anaplastic PXA *BRAFV600E* mutated CNS WHO-grade 3. The lesion was composed of pleomorphic, xanthomatous and oligodendrocyte-like cells. Perivascular lymphocytic cuffing and numerous granular bodies were present. Mitoses (more than 5 X 10 HPF) and necrosis were seen (Figure 2). At immunohistochemistry GFAP, CD34 and *BRAF* p.V600E resulted positive; rare cells expressed synaptophysin. Molecular study confirmed *BRAF* p.V600E mutation (c. 1799T>A) whereas FISH analysis documented homozygous deletion of *CDKN2A*.

From October 2016 to December 2016 a volumetric modulated radiotherapy course was delivered for a total dose of 59,4 Gy in 33 fractions with concomitant and adjuvant temozolomide therapy (Stupp regimen). However, O6-methylguanine-DNA methyltransferase (MGMT) promoter was not methylated. Brain MRI at the end of radiotherapy revealed residual disease (Figure 3A).

In October 2017 (14 months after first surgical resection), a brain MRI showed progressive disease next to the resected area (first progression, Figure 3B), therefore six courses of chemotherapy with procarbazine, lomustine and vincristine (PCV) were administered (the last in June 2018) with disease control.

In January 2019 (7 months after the end of second line treatment) a cranial MRI showed progression of disease (second progression, Figure 3C) and another neurosurgical partial resection with carmustine wafers implantation was performed. The histological analysis confirmed the previous diagnosis. Considering the residual

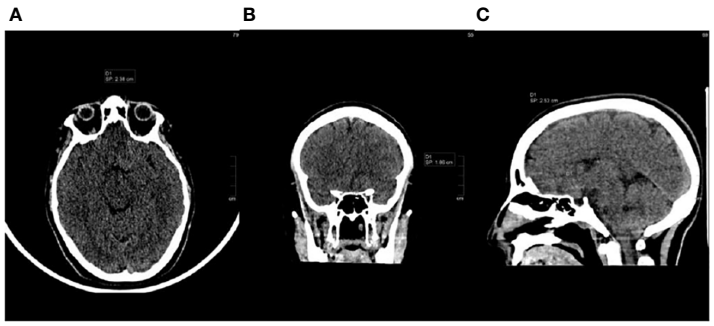

FIGURE 1
Brain CT scan at diagnosis, August 2016 [**(A)**: axial, **(B)**: coronal, **(C)**: sagittal].

disease, in April 2019 the 24-year-old female patient with *BRAF* mutated anaplastic PXA started third-line therapy with dabrafenib. In August 2019 she suffered from Herpes Zoster reactivation, leading to temporary target drug suspension. The well-known tumor residue was less evident on the subsequent MRIs performed every three/four months. Given the literature data of the most effectiveness with better tolerability and the reduced possibility of resistance (13, 20–22), in August 2020 the patient started combination treatment with dabrafenib plus trametinib. Temporary interruption was required for pyrexia and in September 2020 for the occurrence of erythema nodosum grade 3 Common Terminology Criteria for Adverse Events (CTCAE) v.4. Dabrafenib and trametinib were then continued at a reduced dose (25%-50% reduction). The combined therapy was overall well tolerated. Since December 2021 the residual tumor has not been longer visible (Figure 3D). MRI evaluation, performed on July 27^{th,}2023, showed no recurrence of the disease, three years after BRAF/MEK inhibitor combination treatment beginning. In December 2023, considering the optimal response and the reported toxicity, the dual target treatment was interrupted. Last MRI, performed on January 29th, 2024 (one month after drug cessation, 5 years after second progression) revealed persistent complete response (Figure 3E).

3 Discussion and conclusion

PXA is a tumor with a wide range of morphology (19). Two WHO grades (CNS WHO 2 or 3) are assigned, based on a mitotic count of more than 5 mitoses per 10 microscopic high power fields (19). Grade 3 includes the anaplastic variant (23). Anaplastic PXA is associated with poorer clinical outcomes compared with PXA CNS WHO 2 (24).

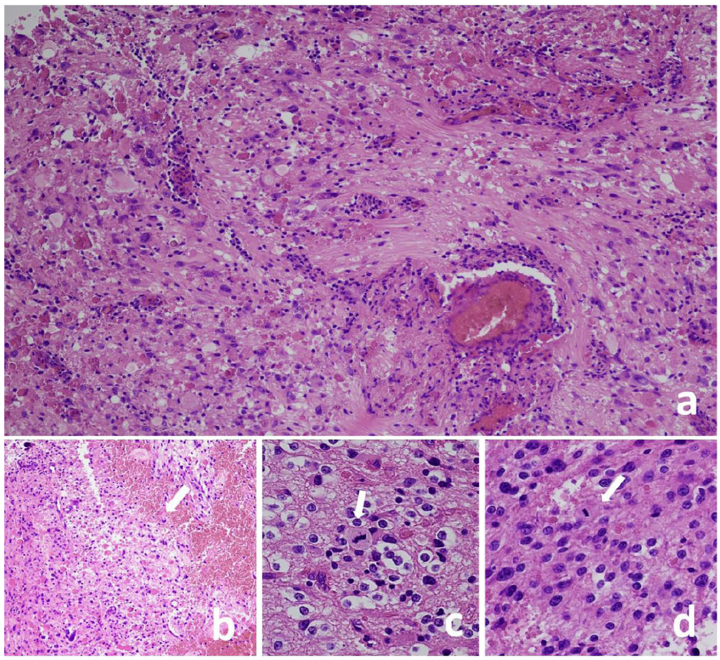

FIGURE 2
Pleomorphic xanthoastrocytoma, CNS WHO grade 3, lesion composed of pleomorphic cells **(A)** and oligodendrocyte-like cells **(C)**. Perivascular lymphocyte cuffing and granular bodies are present **(A)** as well as necrosis [**(B)**, arrow] and mitoses [**(C, D)**, arrows]. Hematoxylin and eosin stain **(A-D)**; Original magnification: a-b 10 X, c 40 X, d 20 X.

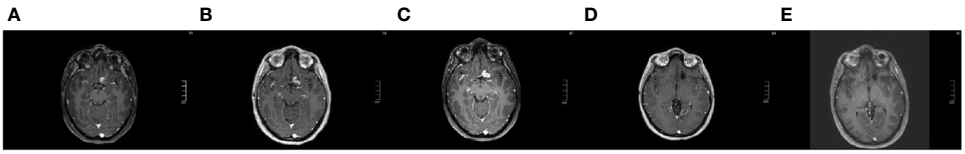

FIGURE 3
Axial T1 contrast-enhanced brain MRI [**(A)**: after first line therapy, January 2017; **(B)**: at first progression, October 2017; **(C)**: at second progression, presurgical, December 2018; **(D)**: complete response during target therapy, December 2021; **(E)**: persistence complete response one month after target therapy interruption, January 2024].

Anaplastic variant of PXA shows histological characteristics as well as clinical course comparable with Grade 3 astrocytoma (25). Gross total resection should be the goal of initial treatment and it remains unclear whether adjuvant radiation and chemotherapy are able to prevent progression or dissemination (24). Early disease recurrence in anaplastic PXA is associated with fatal outcomes (25). *BRAFV600E* mutation can be detected in up to 70% of these tumors, combined with *CDKN2A* homozygous deletion in greater than 90% (19). Considering the emerging molecular landscape and the frequent failure of conventional therapies, novel therapeutic strategies are under investigation in the treatment of HGGs.

Targeted therapies, including mutant BRAF inhibitors (dabrafenib) and MEK inhibitors (trametinib), have yet shown promising results in other cancers refractory to conventional chemotherapy (26). The safety and effectiveness of MEKi treatment have also been established in improving symptomatology and quality of life in patients affected by plexiform neurofibromas in Neurofibromatosis Type I (7). Considering brain tumors, MAPK inhibitors have shown encouraging results in LGG showing alterations of this pathway. Dabrafenib demonstrated meaningful clinical activity and acceptable tolerability in patients with *BRAFV600*-mutant LGG (27). Trametinib was an active and feasible treatment for progressive pediatric MAPK-aberrant LGGs, leading to disease control (28). Recently, the Food and Drug Administration (FDA) approved dabrafenib in combination with trametinib for the treatment of pediatric *BRAFV600E* LGG (29). Instead, data are still limited on their efficacy in *BRAFV600E* mutated HGGs. In 2014 Robinson et al. described the first known case of complete response in a *BRAFV600E*-mutated HGG to vemurafenib (BRAF inhibitor) therapy (20). In 2022 Arbour et al. reported an 18-year-old female with a grade 3 PXA treated upfront with dabrafenib and trametinib and conducted a systematic literature review of patients with HGG and *BRAFV600E* mutations treated with BRAF inhibitors (30).

In a phase 2 Rare Oncology Agnostic Research (ROAR) basket trial (NCT02034110) Dabrafenib plus trametinib showed clinically meaningful activity in patients with BRAFV600E mutation-positive recurrent or refractory HGG: 15 (33%; 95% CI 20-49) of 45 patients had an objective response by investigator assessment, including three complete responses and 12 partial responses (31). Further ongoing studies are evaluating MEK inhibition also in HGG patients. An Open Label, multi-center Roll-over Study is assessing Long-term effect of BRAFV600E and MEK inhibition with dabrafenib and trametinib in a subset of HGG (NCT03975829) (1). A phase I/II Trial is designed to study the combination of Dabrafenib, Trametinib and Hydroxychloroquine for Patients with Recurrent LGG or HGG with a BRAF aberration (NCT04201457). Another phase II trial studies how well the combination of dabrafenib and trametinib after radiation therapy in children and young adults with *BRAF V600* mutated HGG (NCT03919071).

Our case report suggests that BRAF/MEK inhibition is a potential promising strategy also in the treatment of recurrent and refractory HGG, non-stable responsive to surgery, radiotherapy, first and second line chemotherapy. The patient on the third-line combined target therapy achieved even a complete extraordinary response, with disappearance of residual disease.

The patient started a therapy with BRAF and MEK inhibitors on the basis that previous studies on melanoma suggested the possibility of resistance (13, 20), Moreover, Hargrave et al. in a phase II trial in pediatric relapsed/refractory *BRAFV600*–mutant HGG assessed tolerable safety and durable responses of the combined therapy, compared to traditional chemotherapy (32). Hypotheses for mechanisms of acquired resistance to BRAF inhibition include secondary mutations in *BRAF*, MAPK reactivation, and activation of alternative survival pathways (13). Reports in colorectal cancer suggest *BRAF*-mutant tumors may escape inhibition by amplifying receptor tyrosine kinases (20, 33), Additionally, combination of MEK and BRAF inhibitors reduces squamous cell carcinoma risk observed with BRAF inhibitors monotherapy (1). Combined treatment is reported to be well tolerated with mostly moderate and reversible side effects (21). In an open-label study involving patients with metastatic melanoma with *BRAFV600* mutations, dabrafenib and trametinib were safety combined at full monotherapy doses, with significatively improvement of progression-free survival (22). In our case in combined therapy temporary interruption was required in two events: pyrexia and for the occurrence of erythema nodosum, recurred some months later. Dabrafenib was then continued at a reduced dose (25% reduction) and the combined therapy was overall well tolerated.

Data on long-term response are still poor. Our case report describes an extremely great 3-year persistent response on combined target therapy. We must take into account that the combined target therapy was a component of a multimodal approach including neurosurgery and carmustine wafers implantation (CW). Approved to treat newly or recurrent HGG, CW efficacy was reported doubtful: CW may provide a therapeutic coverage during the usual radiotherapy delay of 2 to 6 weeks (34). In our case, the optimal neuro radiological response was observed at almost two years since CW implantation, therefore it was most likely related to the dual target treatment. However, CW was a part of the third line therapy, thus composed of a multimodal approach.

Despite promising preclinical and clinical trials, several issues persist (1). Disease control after MEKi withdrawal was not sustained in a fraction of patients (28). Even on temporary effect, therapeutic goals could include extending survival and improving quality of life in patients with relapsed disease (20). CNS tumors with alternative *BRAF* alterations, such as alternate *V600* mutations or *BRAF* fusions, may differently respond to target therapy (20): for example it is important to note that BRAF inhibitor therapy in patients with *BRAF* gene fusion or duplications activates the MAPK signaling pathway in cells with wild-type *BRAF* at *V600* (27), therefore in this setting MEK inhibitors represent the strategy of choice (35).

Moreover, several studies are investigating the use of targeted therapy as a first-line treatment (26), which could open extraordinary perspectives.

Long term follow up would supply data on disease evolution after treatment discontinuation and further studies are expected to provide standardized treatment duration indications.

In conclusion, our case report suggests that BRAF/MEK inhibition may represent a potential therapeutic strategy also in patients with refractory relapsing HGGs *BRAF* mutated, not responsive to conventional therapies. The achieved complete response in a recurrent disease is an exceptional reached goal. The long-lasting response is also of great importance, giving long-term insights in combined target therapy. However, this is a limited study, reporting our favorable experience only in a single patient. Further studies are ongoing and more data on larger cohorts are needed to clarify present issues. Despite this exciting result, ongoing prospective studies will determine whether dabrafenib and trametinib combination can improve relapsed HGGs *BRAF* mutated outcomes.

Data availability statement

The original contributions presented in the study are included in the article/supplementary material. Further inquiries can be directed to the corresponding author.

Ethics statement

The studies involving humans were approved by Comitato Etico Regione Toscana, Azienda Ospedaliera Universitaria Meyer IRCCS. The studies were conducted in accordance with the local legislation and institutional requirements. Written informed consent for participation was not required from the participants or the participants' legal guardians/next of kin in accordance with the national legislation and institutional requirements. Written informed consent was obtained from the individual(s) for the publication of any potentially identifiable images or data included in this article.

Author contributions

BC: Conceptualization, Data curation, Formal analysis, Methodology, Resources, Validation, Writing – original draft. MT: Writing – original draft. MG: Validation, Visualization, Writing – review & editing. MD: Validation, Visualization, Writing – review & editing. LaG: Resources, Validation, Writing – review & editing. AB: Resources, Validation, Writing – review & editing. MC: Visualization, Writing – review & editing. AI: Resources, Validation, Writing – review & editing. ID: Resources, Validation, Writing – review & editing. LG: Supervision, Validation, Visualization, Writing – review & editing. IS: Conceptualization, Data curation, Supervision, Validation, Visualization, Writing – review & editing. CF: Conceptualization, Data curation, Formal analysis, Methodology, Supervision, Writing – review & editing.

Funding

The author(s) declare financial support was received for the research, authorship, and/or publication of this article. Combined target therapy granted by "Agenzia italiana del farmaco" (AIFA) 5% fund. This work was supported by a grant from Fondazione Anna Meyer, Florence, Italy.

Conflict of interest

CF took part in the Advisory Board financed by Novartis on September 5th 2022 and she took part as principal investigator in CDRB436G2201 NCT02684058 study.

The remaining authors declare that the research was conducted in the absence of any commercial or financial relationships that could be construed as a potential conflict of interest.

The author(s) declared that they were an editorial board member of Frontiers, at the time of submission. This had no impact on the peer review process and the final decision.

Publisher's note

References

1. Rallis KS, George AM, Wozniak AM, Bigogno CM, Chow B, Hanrahan JG, et al. Molecular genetics and targeted therapies for pediatric high-grade glioma. *Cancer Genomics Proteomics*. (2022) 19:390–414. doi: 10.21873/cgp.20328

2. Ostrom QT, Bauchet L, Davis FG, Deltour I, Fisher JL, Langer CE, et al. The epidemiology of glioma in adults: a "state of the science" review. *Neuro-Oncology*. (2014) 16:896–913. doi: 10.1093/neuonc/nou087

3. Aggarwal P, Luo W, Pehlivan KC, Hoang H, Rajappa P, Cripe TP, et al. Pediatric versus adult high grade glioma: Immunotherapeutic and genomic considerations. *Front Immunol*. (2022) 13:1038096. doi: 10.3389/fimmu.2022.1038096

4. Buccoliero AM, Giunti L, Moscardi S, Castiglione F, Provenzano A, Sardi I, et al. Pediatric high grade glioma classification criteria and molecular features of a case series. *Genes*. (2022) 13:624. doi: 10.3390/genes13040624

5. Sturm D, Pfister SM, Jones DTW. Pediatric gliomas: current concepts on diagnosis, biology, and clinical management. *JCO*. (2017) 35:2370–7. doi: 10.1200/JCO.2017.73.0242

6. Zhang ZH, Lin MT, Chen L. Editorial: molecular advances in diagnosis and treatment of CNS tumors. *Front Oncol*. (2020) 10:590293. doi: 10.3389/fonc.2020.590293

7. Cacchione A, Fabozzi F, Carai A, Colafati GS, del Baldo G, Rossi S, et al. Safety and efficacy of mek inhibitors in the treatment of plexiform neurofibromas: A retrospective study. *Cancer Control*. (2023) 30:107327482211449. doi: 10.1177/10732748221144930

8. Grave N, Scheffel TB, Cruz FF, Rockenbach L, Goettert MI, Laufer S, et al. The functional role of p38 MAPK pathway in Malignant brain tumors. *Front Pharmacol*. (2022) 13:975197. doi: 10.3389/fphar.2022.975197

9. Yuan J, Dong X, Yap J, Hu J. The MAPK and AMPK signalings: interplay and implication in targeted cancer therapy. *J Hematol Oncol*. (2020) 13:113. doi: 10.1186/s13045-020-00949-4

10. McCain J, The MAPK. (ERK) pathway: investigational combinations for the treatment of BRAF-mutated metastatic melanoma. *P T*. (2013) 38:96–108.

11. Burotto M, Chiou VL, Lee J, Kohn EC. The MAPK pathway across different Malignancies: A new perspective. *Cancer*. (2014) 120:3446–56. doi: 10.1002/cncr.28864

12. Kyung Myung J, Cho H, Park CK, Kim SK, Lee SH, Park SH. Analysis of the BRAFV600E mutation in central nervous system tumors. *Trans Oncol*. (2012) 5:430–6. doi: 10.1593/tlo.12328

13. Nazarian R, Shi H, Wang Q, Kong X, Koya RC, Lee H, et al. Melanomas acquire resistance to B-RAF(V600E) inhibition by RTK or N-RAS upregulation. *Nature*. (2010) 468:973–7. doi: 10.1038/nature09626

14. Schindler G, Capper D, Meyer J, Janzarik W, Omran H, Herold-Mende C, et al. Analysis of BRAF V600E mutation in 1,320 nervous system tumors reveals high mutation frequencies in pleomorphic xanthoastrocytoma, ganglioglioma and extra-cerebellar pilocytic astrocytoma. *Acta Neuropathol*. (2011) 121:397–405. doi: 10.1007/s00401-011-0802-6

15. Kleinschmidt-DeMasters BK, Aisner DL, Birks DK, Foreman NK. Epithelioid GBMs show a high percentage of BRAF V600E mutation. *Am J Surg Pathol*. (2013) 37:685–98. doi: 10.1097/PAS.0b013e31827f9c5e

16. Proietti I, Skroza N, Michelini S, Mambrin A, Balduzzi V, Bernardini N, et al. BRAF inhibitors: molecular targeting and immunomodulatory actions. *Cancers*. (2020) 12:1823. doi: 10.3390/cancers12071823

17. Subbiah V, Baik C, Kirkwood JM. Clinical development of BRAF plus MEK inhibitor combinations. *Trends Cancer*. (2020) 6:797–810. doi: 10.1016/j.trecan.2020.05.009

18. Kata K, Rodriguez-Quintero JC, Arevalo OD, Zhang JJ, Bhattacharjee MB, Ware C, et al. BRAF/MEK dual inhibitors therapy in progressive and anaplastic pleomorphic xanthoastrocytoma: case series and literature review. *J Natl Compr Cancer Network*. (2022) 20:1193–202. doi: 10.6004/jnccn.2022.7046

19. Rudà R, Capper D, Waldman AD, Pallud J, Minniti G, Kaley TJ, et al. EANO - EURACAN - SNO Guidelines on circumscribed astrocytic gliomas, glioneuronal, and neuronal tumors. *Neuro-Oncology*. (2022) 24:2015–34. doi: 10.1093/neuonc/noac188

20. Robinson GW, Orr BA, Gajjar A. Complete clinical regression of a BRAF V600E-mutant pediatric glioblastoma multiforme after BRAF inhibitor therapy. *BMC Cancer*. (2014) 14:258. doi: 10.1186/1471-2407-14-258

21. Heinzerling L, Eigentler TK, Fluck M, Hassel JC, Heller-Schenck D, Leipe J, et al. Tolerability of BRAF/MEK inhibitor combinations: adverse event evaluation and management. *ESMO Open*. (2019) 4:e000491. doi: 10.1136/esmoopen-2019-000491

22. Flaherty KT, Infante JR, Daud A, Gonzalez R, Kefford RF, Sosman J, et al. Combined BRAF and MEK inhibition in melanoma with BRAF V600 mutations. *N Engl J Med*. (2012) 367:1694–703. doi: 10.1056/NEJMoa1210093

23. Shaikh N, Brahmbhatt N, Kruser TJ, Kam KL, Appin CL, Wadhwani N, et al. Pleomorphic xanthoastrocytoma: a brief review. *CNS Oncol*. (2019) 8:CNS39. doi: 10.2217/cns-2019-0009

24. Rutkowski MJ, Oh T, Niflioglu GG, Safaee M, Tihan T, Parsa AT. Pleomorphic xanthoastrocytoma with anaplastic features: retrospective case series. *World Neurosurg*. (2016) 95:368–74. doi: 10.1016/j.wneu.2016.07.068

25. Choudry UK, Khan SA, Qureshi A, Bari E. Primary anaplastic pleomorphic xanthoastrocytoma in adults. Case report and review of literature. *Int J Surg Case Rep*. (2016) 27:183–8. doi: 10.1016/j.ijscr.2016.08.022

26. Leclair NK, Lambert W, Roche K, Gillan E, Gell JJ, Lau CC, et al. Early experience with targeted therapy as a first-line adjuvant treatment for pediatric low-grade glioma. *Neurosurg Focus*. (2022) 53:E15. doi: 10.3171/2022.9.FOCUS22410

27. Hargrave DR, Bouffet E, Tabori U, Broniscer A, Cohen KJ, Hansford JR, et al. Efficacy and safety of dabrafenib in pediatric patients with *BRAF* V600 mutation–positive relapsed or refractory low-grade glioma: results from a phase I/IIa study. *Clin Cancer Res*. (2019) 25:7303–11. doi: 10.1158/1078-0432.CCR-19-2177

28. Selt F, van Tilburg CM, Bison B, Sievers P, Harting I, Ecker J, et al. Response to trametinib treatment in progressive pediatric low-grade glioma patients. *J Neurooncol*. (2020) 149:499–510. doi: 10.1007/s11060-020-03640-3

29. Barbato MI, Nashed J, Bradford D, Ren Y, Khasar S, Miller CP, et al. FDA approval summary: dabrafenib in combination with trametinib for *BRAF* V600E mutation–positive low-grade glioma. *Clin Cancer Res*. (2024) 30:263–8. doi: 10.1158/1078-0432.CCR-23-1503

30. Arbour G, Ellezam B, Weil AG, Cayrol R, Vanan MI, Coltin H, et al. Upfront BRAF/MEK inhibitors for treatment of high-grade glioma: A case report and review of the literature. *Neuro-Oncol Adv*. (2022) 4:vdac174. doi: 10.1093/noajnl/vdac174

31. Wen PY, Stein A, van den Bent M, De Greve J, Wick A, de Vos FYFL, et al. Dabrafenib plus trametinib in patients with BRAFV600E-mutant low-grade and high-grade glioma (ROAR): a multicenter, open-label, single-arm, phase 2, basket trial. *Lancet Oncol*. (2022) 23:53–64. doi: 10.1016/S1470-2045(21)00578-7

32. Hargrave DR, Terashima K, Hara J, Kordes UR, Upadhyaya SA, Sahm F, et al. Phase II trial of dabrafenib plus trametinib in relapsed/refractory *BRAF* V600–mutant pediatric high-grade glioma. *JCO*. (2023) 41:5174–83. doi: 10.1200/JCO.23.00558

33. Prahallad A, Sun C, Huang S, Di Nicolantonio F, Salazar R, Zecchin D, et al. Unresponsiveness of colon cancer to BRAF(V600E) inhibition through feedback activation of EGFR. *Nature*. (2012) 483:100–3. doi: 10.1038/nature10868

34. Champeaux C, Weller J. Implantation of carmustine wafers (Gliadel®) for high-grade glioma treatment. A 9-year nationwide retrospective study. *J Neurooncol*. (2020) 147:159–69. doi: 10.1007/s11060-020-03410-1

35. Trinder SM, McKay C, Power P, Topp M, Chan B, Valvi S, et al. BRAF-mediated brain tumors in adults and children: A review and the Australian and New Zealand experience. *Front Oncol*. (2023) 13:1154246. doi: 10.3389/fonc.2023.1154246

frontiers | Frontiers in Neurology

TYPE Original Research
PUBLISHED 15 May 2024
DOI 10.3389/fneur.2024.1392691

OPEN ACCESS

EDITED BY
Gerardo Caruso,
University Hospital of Policlinico G. Martino, Italy

REVIEWED BY
Feng Yin,
Aerospace Center Hospital, China
Yuanbo Liu,
Beijing Tiantan Hospital, Capital Medical University, China

*CORRESPONDENCE
Yaming Wang
✉ yamingwang@sohu.com
Yongzhi Shan
✉ shanyongzhi@xwhosp.org
Guoguang Zhao
✉ ggzhao@vip.sina.com

†These authors have contributed equally to this work and share first authorship

RECEIVED 27 February 2024
ACCEPTED 03 May 2024
PUBLISHED 15 May 2024

CITATION
Jin L, Lu D, Yan F, Han J, Wei P, Zhou Y, Wang Y, Shan Y and Zhao G (2024) A disease warranting attention from neurosurgeons: primary central nervous system post-transplant lymphoproliferative disorder. *Front. Neurol.* 15:1392691. doi: 10.3389/fneur.2024.1392691

A disease warranting attention from neurosurgeons: primary central nervous system post-transplant lymphoproliferative disorder

Lei Jin[1,2†], Di Lu[1,2†], Feng Yan[1,2], Jinkun Han[1,2], Penghu Wei[1,2,3], Yiqiang Zhou[1], Yaming Wang[1,2*], Yongzhi Shan[1,2*] and Guoguang Zhao[1,2,3*]

[1]Department of Neurosurgery, Xuanwu Hospital, Capital Medical University, Beijing, China, [2]Clinical Research Center for Epilepsy, Capital Medical University, Beijing, China, [3]Beijing Municipal Geriatric Medical Research Center, Beijing, China

Background: Primary central nervous system post-transplant lymphoproliferative disorder (PCNS-PTLD) is a rare condition, posing diagnostic and treatment challenges, with histological biopsy essential for diagnosis. Standardized treatment protocols are lacking. This disease requires urgent attention due to the increasing number of organ transplant surgeries and the use of immunosuppressive agents.

Methods: From 2020 to 2023, our center diagnosed five patients with PCNS-PTLD. We reviewed their clinical records and conducted a comprehensive analysis of 22 literatures on PCNS-PTLD cases following renal transplantation or allogeneic hematopoietic stem cell transplantation (HSCT).

Results: Four patients had previously received a kidney transplant, one had undergone allogeneic HSCT. The median time from the last transplant surgery to the diagnosis of PCNS-PTLD differs between kidney transplant (21.5 years) and allogeneic HSCT (9 months). Common symptoms included motor weakness (n = 4), headache (n = 2), confusion (n = 2), and nausea (n = 2), with ring-enhancing (n = 5), typically solitary (n = 3) and supratentorial (n = 3) lesions on imaging. Diagnosis involved robot-assisted stereotactic brain biopsy (n = 4) or craniotomy (n = 1), all showing Epstein-Barr virus and CD20 positivity. Most cases (n = 4) were monomorphic diffuse large B-cell lymphoma. Treatment included rituximab (n = 3), surgical resection (n = 2), zanubrutinib (n = 1), whole-brain radiation (n = 1), and methotrexate (n = 1). At the last follow-up, the median duration of follow-up for all patients was 19 months. During this time, 3 patients had died and 2 patients were still alive.

Conclusion: In patients with a history of kidney transplantation or allogeneic HSCT who are on long-term immunosuppressive therapy, any neurological symptoms, particularly the presence of supratentorial ring-enhancing masses in the brain on imaging, whether solitary or multiple, should raise high suspicion for this disease, warranting a timely brain biopsy. Additionally, we found that besides reducing immunosuppressants, zanubrutinib may be a potential, safe,

and effective treatment for this condition. Moreover, post-surgical administration of rituximab in conjunction with whole-brain radiotherapy also appears to be a potentially safe and effective approach.

KEYWORDS

primary central nervous system post-transplant lymphoproliferative disorder, kidney transplant, hematopoietic stem cell transplantation, robot-assisted stereotactic brain biopsy, brain tumor

1 Introduction

Post-transplant lymphoproliferative disorder (PTLD) refers to a group of lymphoproliferative disorders that occur in recipients of solid organ transplantation (SOT) or hematopoietic stem cell transplantation (HSCT) under pharmacologic immunosuppression (1). Although about 7%–15% of all PTLD patients involve the central nervous system (CNS), primary involvement of the nervous system is quite rare (2, 3). Primary CNS post-transplant lymphoproliferative disorder (PCNS-PTLD) is defined as a lymphoproliferative disorder limited to the CNS occurring after SOT or HSCT, with no evidence of systemic PTLD (2, 4). The incidence rate of PCNS-PTLD is approximately 11.5 per 100,000 person-years (3). Due to its extreme rarity, diagnosing and treating PCNS-PTLD pose significant challenges (5). Currently, there are no standard treatment protocols for PCNS-PTLD, and management relies solely on existing case reports and small retrospective case series to guide therapy (6). Additionally, to our knowledge, there have been no independent case series reports of PCNS-PTLD following HSCT to date.

With an increasing number of successful organ transplant surgeries, the growing use of immunosuppressive agents, and the introduction of new immunosuppressive drugs, PCNS-PTLD is expected to occur more frequently (4, 7, 8). Consequently, it is imperative for medical professionals, especially neurosurgeons, to be aware of this condition and maintain a high index of suspicion to initiate appropriate treatment before disease progression (9). Here, we present a single-institution case series of 5 patients, 4 of whom developed PCNS-PTLD after kidney transplantation, and 1 after allogeneic HSCT. Additionally, we reviewed 22 case reports and case series of PCNS-PTLD following kidney transplantation or allogeneic HSCT, focusing on clinical presentations, radiological features, pathological characteristics, treatment modalities, and prognosis to aid in the better diagnosis and management of this disease in the future.

2 Patients and methods

We conducted a thoroughly retrospective review of all clinical records from the Department of Neurosurgery at Xuanwu Hospital, Capital Medical University, from January 2020 to December 2023, and identified a total of 5 patients diagnosed with PCNS-PTLD after kidney or allogeneic HSCT over the past 3 years. Among them, four patients were diagnosed via robot-assisted stereotactic brain biopsy, while pathology findings from tumor resection during craniotomy confirmed the diagnosis in one patient. All patients underwent staging computed tomography (CT) imaging or whole-body postoperative positron emission tomography-computed tomography (PET-CT) to rule out systemic involvement of lymphoma. This study primarily reviewed preoperative clinical symptoms, preoperative magnetic resonance imaging (MRI), or CT scan for each patient. We also examined the immunosuppressive agents used by each patient at the onset of clinical symptoms, treatments administered after diagnosis, and their survival status. Basic information for each patient, including age at onset of clinical symptoms and time interval from last transplantation to onset of clinical symptoms, was collected and is presented in Table 1. The last follow-up date was January 9, 2024.

Furthermore, we conducted a literature review on PCNS-PTLD occurring after kidney or HSCT. Two independent researchers screened titles and abstracts of published manuscripts available on PubMed (https://pubmed.ncbi.nlm.nih.gov/) from the establishment of the database until December 2023. Inclusion criteria required manuscripts to be published in English, meet the definition of PCNS-PTLD (2, 4), involve patients who underwent kidney or HSCT before the onset of clinical symptoms, and qualify as case reports or case series. The search strategy involved combinations of the following terms: "primary central nervous system post-transplant lymphoproliferative disorder", "PCNS-PTLD", "kidney transplant", "HSCT", "renal transplant", and "hematopoietic stem cell transplantation". Ultimately, 22 manuscripts were selected, reporting on a total of 45 patients. Based on the descriptions provided in the literature, we summarized and compiled Table 2.

3 Illustrative cases

3.1 Case 1

A 57-year-old male presented to a local hospital with a two-month history of progressive weakness in the left limbs, characterized by leftward deviation while walking. He underwent a kidney transplant six years prior due to chronic renal failure and has been on a regimen of tacrolimus, mycophenolate mofetil, and prednisone as immunosuppressive therapy since then. There is no personal or family history of malignancies. He denied headaches, dizziness, weight loss, fever, or any prodromal symptoms. A head CT scan revealed a heterogeneous density nodular lesion in the right frontal lobe with finger-like brain edema. Contrast-enhanced MRI of the head exhibited ring-enhancing lesions in the right frontal lobe with surrounding extensive edema (Figure 1). Over the past ten days, weakness in his left upper limb progressively

TABLE 1 Main characteristics of this case series.

No.	Age at diagnosis, median	Sex	Time from the most recent transplantation to diagnosis, median, y	Type of transplantation	Neurological symptoms	Immunosuppressive agents[#]	Lesions	Exact lesion location	Lesion location	Lesion enhancement	Histological subtype	Treatments	Overall survival*	Survival status
1	57	Male	6 y	Kidney	Left motor weakness	Tacrolimus, mycophenolate, prednisone	Solitary	Right frontal lobe	Supra.	Ring enhancement	Polymorphic PTLD	ROI, rituximab, resection	3 y	Die (non-PTLD)
2	13	Female	9 m	Allogeneic HSCT	Left motor weakness, headache, facial droop	Tacrolimus, mycophenolate, prednisone	Multiple	Right basal ganglia, left cerebellum	Supra. & infra.	Ring enhancement	Monomorphic, DLBCL	ROI, rituximab, WBRT, resection	42 m	Alive
3	59	Female	24 y	Kidney	Right motor weakness, confusion, speech difficulties, depression mood	Tacrolimus, mycophenolate, prednisone	Solitary	Left midbrain cerebral peduncle, thalamus, basal ganglia	Supra. & infra.	Ring enhancement	Monomorphic, DLBCL	Rituximab	3 m	Die (non-PTLD)
4	62	Female	19 y	Kidney	Headache, nausea	Cyclosporine, mycophenolate, prednisone	Solitary	Right basal ganglia	Supra.	Ring enhancement	Monomorphic, DLBCL	ROI, zanubrutinib	19 m	Alive
5	52	Female	27 y	Kidney	Confusion, right motor weakness, nausea, right visual field defect	Cyclosporine, mycophenolate, prednisone	Multiple	Bilateral parietal lobe	Supra.	Ring enhancement	Monomorphic, DLBCL	ROI, MTX	18 d	Die (PTLD)

d, days; DLBCL, diffuse large B-cell lymphoma; HSCT, hematopoietic stem cell transplantation; infra, infratentorial; m, months; MTX, methotrexate; NR, not report; PTLD, post-transplant lymphoproliferative disorder; ROI, reduction of immunosuppression; supra, supratentorial; WBRT, whole—brain radiation therapy; y, years.

*Represents the time from date of clinical symptoms appear to date of last follow-up or die.

[#]Represents the immunosuppressive agents at the time of PTLD diagnosis.

10.3389/fneur.2024.1392691

TABLE 2 Main characteristics of 22 reviewed literatures.

References	*N*	Age at diagnosis, median	Time from the most recent trans-plantation to diagnosis, median	Type of trans-plantation	Neurolo-gical symptoms	Immuno-suppressive agents[#]	Lesions	Lesion location (suprate-ntorial or infra-tentorial)	Imaging charact-eristics	Histo-logical subtype	Treatments	Overall survival*, median	Survival status
1. Lake et al. (4)	10	49	4.5 y	7 kidney 3 kidney/ pancreas	Confusion, headache, speech difficulties, facial droop, diplopia, motor weakness, vertigo, ataxia, seizure	Cyclosporine, tacrolimus, mycophenolate, prednisone	3 solitary 7 multiple	8 Supra. 1 infra. 1 supra. & infra.	Ring enhancement, incomplete ring	4 polymorphic, 1 monomorphic, peripheral T cell 5 monomorphic, DLBCL	ROI, dexamethasone, rituximab, MTX, TMZ, WBRT	2.75 y die 1.75 y alive	4 die 6 alive
2. Sola-Valls et al. (7)	5	44	84 m	3 kidney 2 kidney/ pancreas	Headache, seizure, gait disturbance, confusion, hallucinations, dysarthria	Mycophenolate, prednison, tacrolimus, cyclosporine	5 multiple	3 supra. 2 supra. & infra.	Ring enhancement	monomorphic※	ROI, rituximab, WBRT, MTX, TMZ	9 w die 26 m alive	4 die 1 alive
3. Ishihara et al. (10)	6	60	88.3 m	Kidney	NR	Cyclosporine, azathioprine, methylprednisolone, tacrolimus, mycophenolate	NR	NR	NR	1 polymorphic 1 monomorphic, malignant lymphoma 4 monomorphic, DLBCL	ROI, MTX, WBRT, cytarabine-etoposide, R-CHOP, resection	39.25 m alive 3.9 m die	4 alive 2 die
4. Huang et al. (9)	5	35.3	12 y	Kidney	Headache, sleepy, depression mood, consciousness, disturbance, nausea, vomiting, coma, tremor, seizure, left limbs weakness, palsy	Azathioprine, cyclosporine, tacrolimus, mycophen, prednisolone	NR	NR	Ring enhancement	5 monomorphic, DLBCL	ROI, WBRT, resection	36.5 m (alive) **NR (die)	4 alive 1 die

(Continued)

10.3389/fneur.2024.1392691

TABLE 2 (Continued)

References	*N*	Age at diagnosis, median	Time from the most recent trans-plantation to diagnosis, median	Type of trans-plantation	Neurolo-gical symptoms	Immuno-supp-ressive agents[#]	Lesions	Lesion location (suprate-ntorial or infra-tentorial)	Imaging charact-eristics	Histo-logical subtype	Treatments	Overall survival*, median	Survival status
5. Law et al. (11)	2	36	4 y	1 kidney 1 kidney/ pancreas	Seizure, visual field defect	NR	1 solitary 1 multiple	1 supra. 1 NR	NR	2 monomorphic, DLBCL	ROI, rituximab, MTX, ibrutinib, EBV-specific T cells	25.5 m	Alive
6. Yeung et al. (12)	1	41	26 y	Kidney	Seizure, headache	Cyclosporine, mycophenolate, prednisone	Multiple	Supra. & infra.	NR	Monomorphic, DLBCL	ROI, rituximab, MTX, WBRT	12 m	Alive
7. Xu et al. (2)	1	68	5 y	Kidney	NR	Mycophenolate, tacrolimus	Multiple	Supra.	Enhancing	Monomorphic, DLBCL	ROI, rituximab	NR	Alive
8. Brennan et al. (13)	1	6	3 y	Kidney	Headache, nausea, vomiting, seizure	NR	Multiple	Supra.	Ring enhancement	Monomorphic, DLBCL	ROI, acyclovir	26 m	Alive
9. Valencia-Sanchez et al. (8)	1	55	NR	Kidney	Gait instability, vertigo, dysarthria	Mycophenolate, prednison	Multiple	Supra. & infra.	Ring enhancement	Monomorphic, DLBCL	ROI, rituximab, cyclophps-phamide, doxorubicin, vincristine, prednisone, WBRT	17 m	Die
10. Teresa et al. (14)	1	NR	11 y	Kidney	Weakness, memory loss, expressive dysphasia	Mycophenolate, prednison	Solitary	Supra.	Ring enhancement CT	Monomorphic, DLBCL	ROI, WBRT, rituximab	30 m	Alive
11. Imafuku et al. (15)	1	62	4 y	Kidney	Peripheral palsy, bilateral sensorineural hearing loss	Tacrolimus, mycophenolate, prednisone	Multiple	Supra. & infra.	Ring enhancement	Monomorphic, DLBCL	ROI, MTX, cytarabine, WBRT, rituximab	18 m	Alive
12. Reis et al. (16)	1	37	10 y	Kidney	Confusion, hemiparesis	Mycophenolate, prednisone, tacrolimus	Solitary	Supra.	Ring enhancement	Monomorphic※	ROI	NR	Alive
13. Tanaka et al. (17)	1	62	13 y	Kidney	Speech disturbance	Prednisolone, tacrolimus, mycophenolate	Solitary	Supra.	Ring enhancement	Monomorphic, DLBCL	ROI, rituximab	34 m	Alive

(Continued)

10.3389/fneur.2024.1392691

TABLE 2 (Continued)

References	*N*	Age at diagnosis, median	Time from the most recent trans-plantation to diagnosis, median	Type of trans-plantation	Neurolo-gical symptoms	Immuno-supp-ressive agents[#]	Lesions	Lesion location (suprate-ntorial or infra-tentorial)	Imaging charact-eristics	Histo-logical subtype	Treatments	Overall survival*, median	Survival status
14. Azriel et al. (18)	1	49	18 y	Kidney	Headache, nausea, declining visual acuity	Prednisolone, cyclosporine, mycophenolate	Solitary	Supra.	Ring enhancement	Hodgkin lymphoma PTLD	Rituximab, MTX, procarbazine, vincristine, resection	NR	NR
15. Said-Conti et al. (19)	1	11	82 m	Kidney	Seizure, depressed neurological state	Prednisolone, tacrolimus, mycophenolate	Multiple	Supra.	Ring enhancement	Polymorphic	ROI, hydroxyurea, rituximab, WBRT	3 y	Alive
16. Yaginuma et al. (20)	1	36	5 y	Kidney	Consciousness alter	Tacrolimus, mycophenolate, prednisone	Multiple	Supra.	Ring enhancement	Monomorphic, DLBCL	ROI, WBRT	29 m	Alive
17. Kittan et al. (21)	1	49	6 m	Allogeneic HSCT	Confusion, diplopia, ataxia	Prednisolone, mycophenolate	Multiple	Supra. & infra.	Ring enhancement	Monomorphic, B cell lymphoma※	Rituximab, foscarnet, DLI	8 w	Die
18. Aisa et al. (22)	1	58	340 d	Allogeneic HSCT	Headache, consciousness loss	Cyclosporin, MTX, prednisolone, mycophenolate	Multiple	Supra.	-	Monomorphic, DLBCL	-	8 d	Die
19. Toyosaki et al. (23)	1	32	4 m	Allogeneic HSCT	Convulsion	Tacrolimus, prednisolone, cyclophosphamide	Multiple	Supra.	Ring enhancement	Monomorphic, DLBCL	ROI, high does MTX	NR	Die
20. Kassa et al. (5)	1	11	82 d	Allogeneic HSCT	Nausea, vomiting, diplopy	Mycophenolate	Multiple	Supra. & infra.	-	Monomorphic, DLBCL	ROI, nivolumab	1 y	Alive
21. Mayumi et al. (24)	1	51	306 d	Allogeneic HSCT	Hemiplegia	Prednisolone, tacrolimus	Solitary	Supra.	Ring enhancement	Monomorphic, DLBCL	ROI, rituximab, DLI	355 d	Alive
22. Sakamoto et al. (25)	1	17	621 d	Allogeneic HSCT	Seizure	Tacrolimus, prednisolone, mycophenolate	Solitary	Supra.	Ring enhancement	NR	ROI, rituximab, WBRT	397d	Die

d, days; DLBCL, diffuse large B-cell lymphoma; DLI, donor lymphocyte infusion; HSCT, hematopoietic stem cell transplantation; infra, infratentorial; m, months; MTX, methotrexate; NR, not report; PTLD, post-transplant lymphoproliferative disorder; R-CHOP, rituximab, cyclophosphamide, hydroxydaunorubicin, oncovin, prednisone; ROI, reduction of immunosuppression; supra, supratentorial; TMZ, temozolomide; WBRT, whole—brain radiation therapy; y, years.

※Represents the specific type of lymphoma was not specified in the literature, only mentioned as monoclonal.

*Represents the time from date of clinical symptoms appear to date of last follow-up or die.

**Represents the average survival time.

[#]Represents the immunosuppressive agents at the time of PTLD diagnosis.

10.3389/fneur.2024.1392691

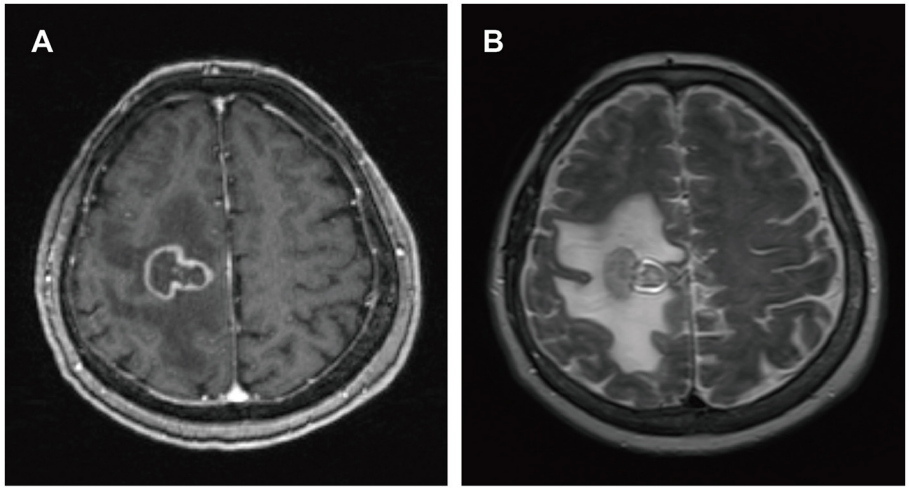

FIGURE 1
MRI findings of patient 1. Irregular ring enhancement lesion in the right frontal lobe on T1-weighted images **(A)**. Extensive perilesional edema in the right frontal lobe on T2-weighted images **(B)**.

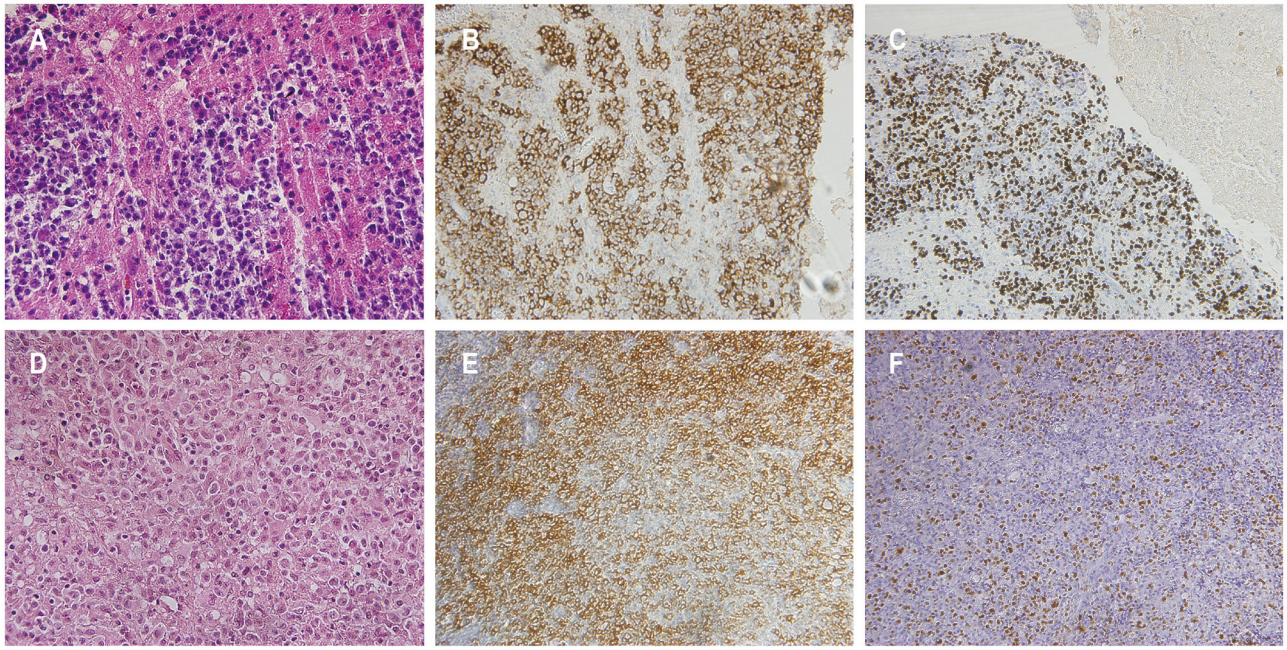

FIGURE 2
Histopathological features of patients 1 and 3. Hematoxylin and eosin staining in patient 1 [**(A)** magnification ×400]. The atypical cells demonstrated positive staining for CD20 in patient 1 **(B)**. Detection of Epstein-Barr virus (EBV) encoded small RNA positive cells was observed in patient 1 **(C)**. Hematoxylin and eosin staining in patient 3 exhibited sheets of atypical cells with prominent nuclear division, visible nucleoli in some cells, and extensive areas of necrosis, indicative of monomorphic PTLD, diffuse large B-cell lymphoma [**(D)** magnification ×400]. The atypical cells in patient 3 stained positive for CD20 **(E)**. Presence of cells positive for EBV-encoded small RNA in patient 3 was confirmed **(F)**.

worsened, resulting in the inability to move his left hand, although he could elevate his left upper limb but couldn't raise it above the shoulder. Consequently, he underwent right frontal lobe lesion resection at our neurosurgery department. Postoperatively, there was improvement in the weakness of the left limbs compared to preoperative status. Histopathological and immunohistochemical studies of the lesion confirmed the diagnosis of PTLD, with a leaning toward polymorphic PTLD (Figure 2). Tumor cells stained positive for CD20 and CD79a. Epstein-Barr virus-encoded RNA (EBER) was positive. CT scans of the neck, chest, abdomen, and pelvis showed no abnormalities. The patient was ultimately diagnosed with PCNS-PTLD. He underwent reduction of immunosuppression combined with rituximab therapy. Follow-up MRI of the head postoperatively revealed no recurrence of

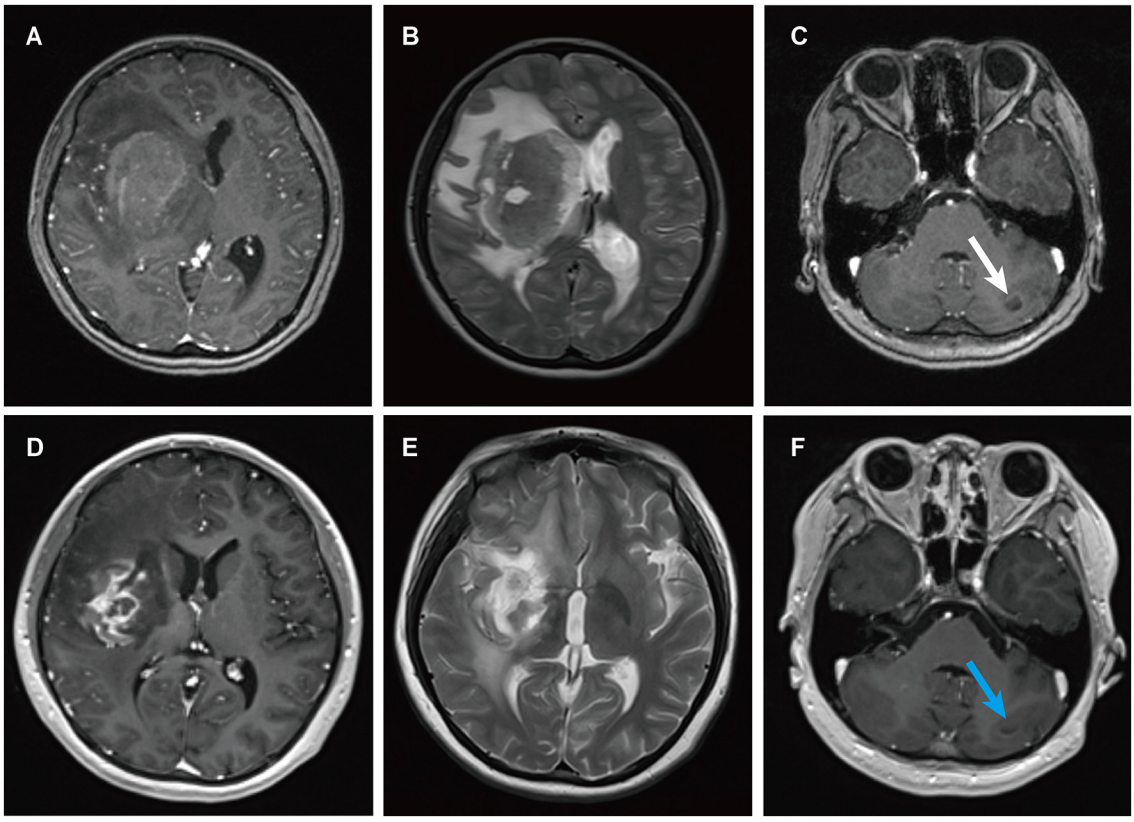

FIGURE 3
MRI findings of patient 2. Preoperative enhanced MRI prior to brain biopsy showed a ring-enhancing lesion in the right basal ganglia area on T1-weighted images **(A)**, with extensive edema surrounding the lesion in the right basal ganglia area on T2-weighted images **(B)**, and abnormal signal intensity in the left cerebellum on T1-weighted images [**(C)** white arrows]. Enhanced MRI scans obtained four months after the diagnosis of PCNS PTLD, persistent ring enhancement lesion in the right basal ganglia on T1-weighted images **(D)**. Continued perilesional edema in the right basal ganglia on T2-weighted images **(E)**. Additionally, the abnormal signal intensity in the left cerebellum persisted on T1-weighted images [**(F)** blue arrows].

the disease. Approximately three years after being diagnosed with PCNS-PTLD, he passed away due to myocardial infarction.

3.2 Case 2

A 13-year-old female presented to a local hospital with a one-month history of facial asymmetry without apparent cause. She underwent allogeneic HSCT for aplastic anemia nine months prior and has been on a regimen of tacrolimus, mycophenolate mofetil, and prednisone as immunosuppressive therapy since then. There is no personal or family history of malignancies. She complained of headaches and left-sided weakness 14 days ago, along with a decrease in mental status and a weight loss of 15 kg over the past nine months. Contrast-enhanced MRI of the head revealed ring-enhancing lesions in the right basal ganglia region and a mass in the left cerebellum (Figure 3). A robot-assisted stereotactic brain biopsy of the right basal ganglia lesion was performed at our department, and histopathological and immunohistochemical studies confirmed the diagnosis of PTLD, consistent with monomorphic diffuse large B-cell lymphoma (DLBCL). Tumor cells stained positive for CD20 and CD79a. EBER *in situ* hybridization was partially positive. CT scans of the neck, chest, abdomen, and pelvis showed no abnormalities. The patient was ultimately diagnosed with PCNS-PTLD. Subsequently, she discontinued all immunosuppressive agents and underwent rituximab therapy. Follow-up MRI of the head four months later showed no significant reduction in the lesion size (Figure 3). Therefore, five months after diagnosis, she underwent tumor resection in the right basal ganglia region at our department. Postoperatively, there was slight improvement in the symptoms of left-sided weakness. Histopathological and immunohistochemical analysis of the brain lesion affirmed the diagnosis of PTLD, exhibiting features characteristic of monomorphic DLBCL, in agreement with earlier brain biopsy results. Tumor cells stained positive for CD20 and CD79a. EBER *in situ* hybridization was positive. She received rituximab and whole-brain radiation therapy (WBRT) after discontinuing all immunosuppressive agents. On the most recent follow-up, there was no recurrence of the disease, and she remained clinically stable.

3.3 Case 3

A 59-year-old female presented with a three-month history of progressive weakness in the right lower limb, characterized

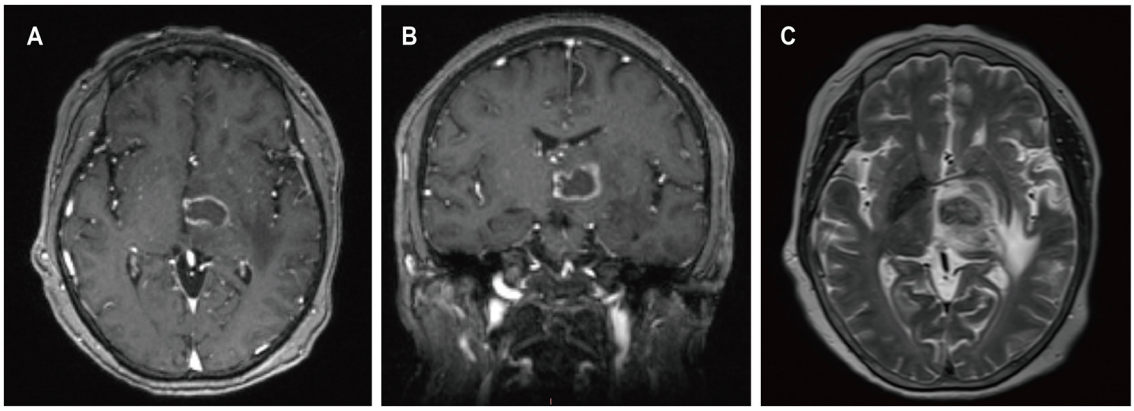

FIGURE 4
MRI findings of patient 3. Preoperative enhanced MRI prior to brain biopsy showed ring-enhancing lesions affecting the left cerebral peduncle, thalamus, and basal ganglia on T1-weighted images **(A, B)**, with surrounding edema around the left cerebral lesion on T2-weighted images **(C)**.

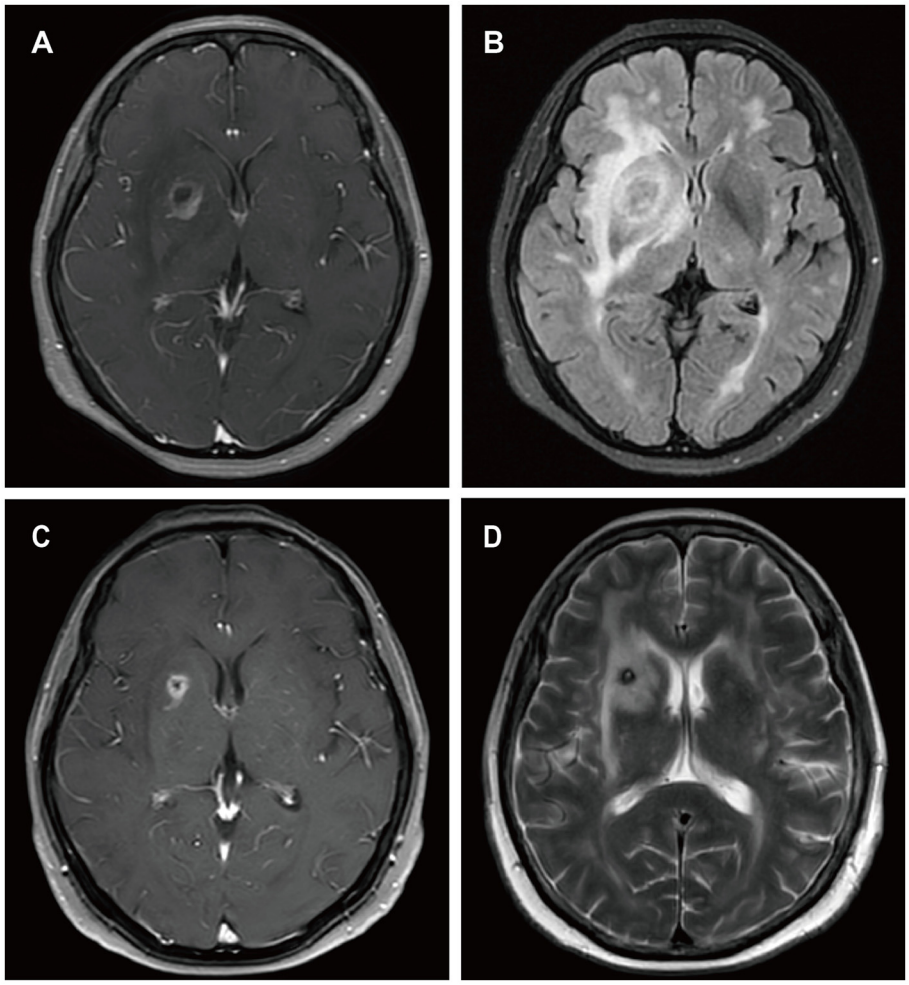

FIGURE 5
MRI findings of patient 4. Preoperative enhanced MRI prior to brain biopsy showed a ring-enhancing lesion in the right basal ganglia area on T1-weighted images **(A)**, with extensive edema surrounding the lesion in the right basal ganglia area on T2-FLAIR images **(B)**. On follow-up enhanced MRI images obtained 3 months after the diagnosis of PCNS PTLD, the ring-enhancing lesion in the right basal ganglia area appeared reduced on T1-weighted images **(C)**, and the edema surrounding the lesion in the right basal ganglia area decreased on T2-weighted images **(D)**.

by difficulty putting on shoes and walking due to weakness and heaviness in the right leg. She attributed these symptoms to lumbar disc herniation and did not seek medical attention. Two months ago, she began experiencing increased sleep (more than ten hours per day), along with declining memory and forgetfulness, primarily involving recent events. One month ago, she developed weakness in the right upper limb, manifesting as difficulty holding chopsticks and writing. The weakness in the right lower limb worsened, and weakness in the left lower limb developed, while strength in the left upper limb remained normal. She also experienced disorganized speech and naming difficulties. She reported recent low mood and a negative attitude toward things, prompting her to seek treatment at our neurology department. Contrast-enhanced MRI of the head revealed a solitary ring-enhancing lesion involving the left midbrain, cerebral peduncle, thalamus, and basal ganglia (Figure 4). Twenty-four years ago, she underwent kidney transplantation for uremia and has been on a regimen of tacrolimus, mycophenolate mofetil, and prednisone as immunosuppressive therapy since then, with no personal or family history of malignancies. She denied experiencing any symptoms of fever, weight loss, or prodromal signs recently. The neurology department initiated thrombolytic therapy, but there was no improvement in symptoms. Subsequently, she underwent robot-assisted stereotactic brain biopsy of the left thalamic lesion at our neurosurgery department. The pathology report confirmed the diagnosis of PTLD, consistent with monomorphic DLBCL (Hans model indicating non-germinal center origin) (Figure 2). Tumor cells stained positive for CD20 and CD79a. EBER *in situ* hybridization was positive. No significant abnormalities were observed on the CT scans of other body parts. The patient was ultimately diagnosed with PCNS-PTLD. She did not undergo reduction of immunosuppressive agents. Despite treatment with rituximab monotherapy, her condition continued to deteriorate. Approximately three months after being diagnosed with PCNS-PTLD, she passed away due to cardiovascular complications.

3.4 Case 4

A 62-year-old female presented to our hospital with occipital pain persisting for three months, occasional mild headaches, and intermittent nausea. Nineteen years ago, she received a kidney transplant for uremia and has been taking mycophenolate mofetil, cyclosporine, and prednisone ever since, without any personal or family history of malignancies. She denied vomiting, fever, weight loss, weakness in the limbs, or any other prodromal symptoms. A week ago, contrast-enhanced MRI of the head revealed a ring-enhancing lesion in the right basal ganglia (Figure 5). Subsequently, she underwent robot-assisted stereotactic brain biopsy of the right basal ganglia lesion at our department. Histopathological and immunohistochemical studies confirmed the diagnosis of PTLD, consistent with monomorphic DLBCL. Tumor cells stained positive for CD20 and CD79a. EBER *in situ* hybridization was positive. CT scans of the neck, chest, abdomen, and pelvis showed no abnormalities. The patient was ultimately diagnosed with PCNS-PTLD. She underwent reduction of immunosuppressive agents combined with treatment with zanubrutinib. Follow-up contrast-enhanced MRI of the head three months later showed a reduction in the lesion size in the right basal ganglia (Figure 5). On the last follow-up, she remained clinically stable.

3.5 Case 5

A 52-year-old female presented with a 23-day history of cognitive decline characterized by transient inability to comprehend normal behavior and recent memory loss lasting 2-3 minutes, with spontaneous recovery. Seven days prior to admission, she developed weakness in the right lower limb, instability while walking, and a right visual field defect, accompanied by occasional nausea and vomiting, prompting evaluation at a local hospital. Twenty-seven years ago, she underwent kidney transplantation for chronic renal failure and has since been on a regimen of cyclosporine, mycophenolate mofetil, and methylprednisolone as immunosuppressive therapy, with no personal or family history of malignancies. She denied fever, night sweats, numbness in the extremities, and joint pain. Her weight had decreased by 1 kg over the past month. Contrast-enhanced MRI of the head revealed a ring-enhancing lesion in the left parietal lobe with surrounding edema and a circular lesion in the right parietal lobe (Figure 6). Robot-assisted stereotactic brain biopsy of the left parietal lobe lesion was performed at our department. Histopathological and immunohistochemical studies confirmed the diagnosis of PTLD, consistent with monomorphic DLBCL. Tumor cells stained positive for CD20 and CD79a. EBER *in situ* hybridization was positive. PET-CT showed a mixed-density mass in the left parietal lobe with increased glucose metabolism, suggestive of an intracranial primary malignant lesion. The patient was ultimately diagnosed with PCNS-PTLD following kidney transplantation. Mycophenolate mofetil was discontinued, cyclosporine dosage was increased, and methotrexate was initiated. Three days after the diagnosis of PCNS-PTLD, she developed coma due to cerebral edema, and considering the poor prognosis, conservative treatment with mannitol was decided upon in consultation with the patient's family. Serial head CT scans showed worsening cerebral edema, and transcranial Doppler (TCD) ultrasonography indicated severe intracranial hypertension with fixed dilated pupils. She passed away 18 days after the diagnosis of PCNS-PTLD due to cerebral herniation.

4 Results

4.1 Demographics and transplantation information

In our institution, a total of five patients were diagnosed with PCNS-PTLD (Table 1). Among them, one patient had previously undergone allogeneic HSCT and was identified with PCNS-PTLD at the age of 13, while four patients had undergone kidney transplantation, with a median age of 58 years at the time of PCNS-PTLD diagnosis. In a review of 22 articles (Table 2), 6 articles reported cases of PCNS-PTLD occurring after allogeneic HSCT, while 16 articles documented cases following kidney transplantation. The median age at diagnosis of PCNS-PTLD for

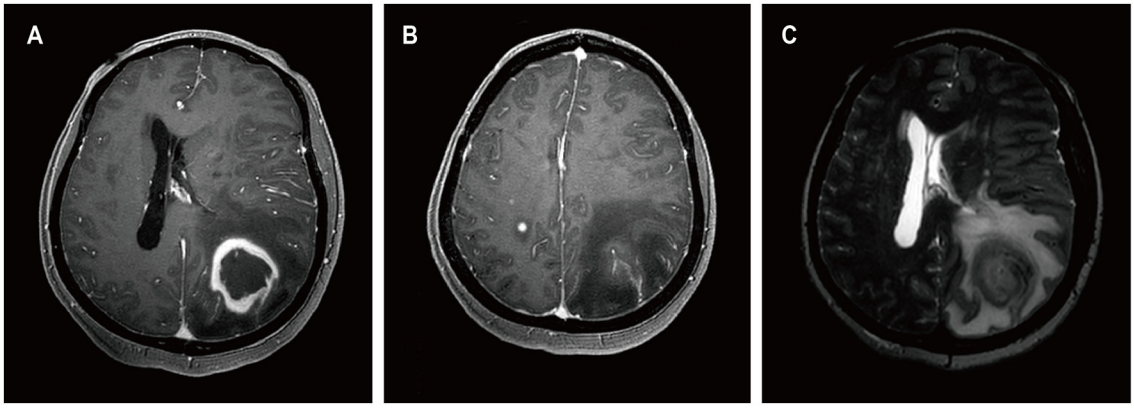

FIGURE 6
MRI findings of patient 5. Preoperative enhanced MRI images showed a ring-enhancing lesion in the left parietal lobe on T1-weighted images **(A)**, a circular lesion in the right parietal lobe **(B)**, and extensive edema surrounding the lesion in the left parietal lobe on T2-weighted images **(C)**.

patients who had undergone allogeneic HSCT was 40.5 years, whereas for those who had kidney transplants, it was 44 years.

In our case series, patients who had undergone kidney transplantation had a median time of 21.5 years from their last transplant surgery to the diagnosis of PCNS-PTLD, whereas for those who had undergone allogeneic HSCT, this period was only 9 months. This trend is also observed in the 22 reviewed articles, where the median time from the last transplant surgery to PCNS-PTLD diagnosis for patients who had kidney transplants was 7 years, compared to just 8 months for those who had undergone allogeneic HSCT.

Immunosuppressive drugs administered to the patients at diagnosis are shown in Tables 1, 2, respectively.

4.2 Presenting symptoms

The clinical symptoms exhibited by the patients were highly variable and included motor weakness (n = 4), headache (n = 2), nausea (n = 2), confusion (n = 2), speech difficulties (n = 1), depressive mood (n = 1), facial droop (n = 1), and visual field defect (n = 1), as shown in Table 1. These symptoms are consistent with those reported in previous literature, which also mentions additional symptoms such as seizures, diplopia, vertigo, ataxia, and palsy (Table 2).

4.3 Imaging findings

All our patients underwent imaging studies preoperatively. Through these imaging examinations, we found that all patients exhibited lesions with ring enhancement (n = 5), with 3 patients presenting with a solitary lesion and 2 with multiple lesions. Specifically, 2 patients had lesions involving both supratentorial and infratentorial regions, while 3 patients had lesions confined to the supratentorial region only, as shown in Table 1. In the review of 22 articles (Table 2), there were 10 patients with solitary lesions and 24 patients with multiple lesions. Among these 22 retrospective articles, 16 mentioned ring-enhancing lesions. Additionally, 24 patients had lesions confined to the supratentorial region, 8 patients had lesions involving both supratentorial and infratentorial regions, and 1 patient had lesions confined to the infratentorial region.

4.4 Brain biopsy findings

The diagnosis of PCNS-PTLD in our patients was confirmed through pathological examination of brain tissue obtained via robot-assisted stereotactic brain biopsies (n = 4) and surgical resection (n = 1). Among these patients, one was diagnosed with polymorphic PTLD, while the remaining four were diagnosed with monomorphic DLBCL (Table 1). In the patients reported in the 22 reviewed articles, 28 were explicitly identified as monomorphic DLBCL, 6 as polymorphic PTLD, with the remaining pathology types detailed in Table 2.

All of our patients exhibited EBV and CD20 positivity in their brain tissue.

4.5 Treatments and survival outcomes

In our patient group, four patients initially had a reduction of immunosuppression. The treatment protocols for three patients included rituximab, two underwent surgical resection, one was treated with WBRT, one with zanubrutinib, and one with methotrexate, as shown in Table 1. In the 22 reviewed articles, 11 reported the use of WBRT in treatment, 3 reported surgical resection, and 1 reported the use of ibrutinib, with the rest of the treatment protocols detailed in Table 2.

As of the most recent follow-up, the median follow-up duration was 19 months (range: 18 days to 42 months). Three patients have passed away: two due to complications related to cardiovascular issues, and one as a result of cerebral herniation, which was a consequence of the progression of PCNS-PTLD. The specific

survival times are detailed in Table 1. The survival outcomes reported in the 22 reviewed articles are presented in Table 2.

Two of our patients are currently alive and in a clinically stable phase. One patient, diagnosed with PCNS-PTLD after allogeneic HSCT, was treated with withdrawal of all immunosuppression, surgical resection, and a combination of rituximab and WBRT. The second patient, who had a history of kidney transplantation, received a reduction in immunosuppression and a combination therapy including zanubrutinib.

5 Discussion

PTLD is a rare complication of SOT or HSCT (13). The etiology of PTLD is multifactorial, involving immunosuppressive drug use, Epstein-Barr virus (EBV) infection, and age (26). For HSCT recipients, factors also include T-cell depletion, HLA mismatch, unrelated donor transplantation, and chronic graft-versus-host disease (GVHD) (26, 27). Typically, a competent host can initiate both humoral immunity through antibody production and cell-mediated immunity through cytotoxic T-cell responses. However, in organ transplant patients, the use of immunosuppressive agents leads to T-cell dysfunction, resulting in loss of T-cell control over B-cell proliferation, leading to uncontrolled proliferation of EBV-transformed B cells (2). Among these drugs, mycophenolate mofetil, tacrolimus, cyclosporine, azathioprine, and corticosteroids are the major medications associated with increased incidence of PTLD (28). In kidney transplant recipients, the incidence of PTLD is approximately 1% (13, 15). In allogeneic HSCT recipients, the incidence is about 1–3% (25), while it is 6.2% in lung transplant recipients, 2% in heart transplant recipients, and 1.4% in liver transplant recipients (29). The variation in incidence rates is related to the specific immunosuppressive regimens for different organs (29). Our study found that the time from the last allogeneic HSCT to the diagnosis of PCNS-PTLD in patients was shorter than that in kidney transplant recipients, a finding that is also confirmed in the reviewed literature. This might be related to the specific immunosuppressive regimen, including the dose of each drug used.

EBV plays a crucial role in the progression of PTLD, with 90% of PCNS-PTLD cases associated with EBV (8). Our reported five patients all tested positive for EBV *in situ* hybridization, confirming this association. During primary infection, EBV immortalizes B lymphocytes, leading to polyclonal activation and proliferation, which is finely balanced by EBV-specific immune control to maintain EBV latency status. However, in immunocompromised hosts, defects in EBV inhibition and cytotoxic function lead to disruption of immune balance, resulting in proliferation of EBV-infected B lymphocytes and ultimately the development of PTLD (30). Currently, there is an increasing trend in the number of EBV-negative PTLD patients, possibly due to new immunosuppressive regimens and increased awareness of EBV-positive risk factors (31). The risk of PTLD is higher in SOT recipients under 10 years old and over 60 years old (26). The incidence of PTLD in children is four times higher than in adults, primarily because children have a higher rate of EBV seronegativity, making EBV-negative children more susceptible to infection from transplanted organs, thereby increasing the likelihood of PTLD development (29). In contrast, the elderly are mainly at risk due to declining immune surveillance capabilities (26).

Diagnosing PCNS-PTLD is often challenging and requires comprehensive physical examination, diagnostic imaging, and histopathological biopsy (2). For EBV-positive PTLD, quantitative polymerase chain reaction (qPCR) testing of EBV DNA is a sensitive early diagnostic tool. Studies suggest that relying on plasma EBV viral load for PTLD diagnosis has a sensitivity of up to 92% (32). Additionally, EBV positivity in cerebrospinal fluid (CSF) also strongly suggests CNS PTLD diagnosis (33). Case reports indicate that in patients with CNS PTLD, CSF EBV can be positive even when blood EBV is negative (34). While blood and CSF EBV DNA testing can support the diagnosis of PCNS-PTLD, final confirmation still relies on histopathological biopsy. Furthermore, there are reports of patients diagnosed with PCNS-PTLD whose EBV is negative in both CSF and blood, highlighting the limitation of relying solely on EBV testing to exclude the disease (35).

Clinical symptoms in PCNS-PTLD patients are highly atypical, usually associated with intracranial lesions, presenting mainly as seizures, neuropsychiatric symptoms, focal neurological deficits, and symptoms of increased intracranial pressure (29). Specifically, patients may experience headaches, nausea, vomiting, limb weakness, hemiparesis, ataxia, gait instability, speech difficulties, confusion, seizures, among other symptoms. Less commonly, facial nerve paralysis can occur (15). Therefore, relying solely on symptomatology for diagnosis or exclusion of PCNS-PTLD is extremely challenging.

Imaging plays a crucial role in the diagnosis of PCNS-PTLD. MRI offers advantages in sensitivity and tissue contrast, making it the preferred imaging modality for evaluating transplant recipients (4). According to the literature review, the imaging characteristics of most PCNS-PTLD lesions are multifocal supratentorial ring-enhancing lesions, although our case series suggests that solitary supratentorial ring-enhancing lesions should also raise suspicion for this disease. Tumors with high cell density are prone to bleeding, cystic changes, necrosis, and surrounding edema (33). Ring enhancement may indicate necrotic lesions in the CNS (25). A study reviewing 221 MRI cases with ring enhancement in CNS found that 40% were gliomas, 30% were brain metastases, 12% were brain abscesses, 6% were multiple sclerosis, and only 2% were lymphomas (36). EBV viral encephalitis can also present as ring-enhancing masses (37). Cases have reported that patients with EBV CNS infection progressed to PCNS-PTLD after 5 months (8). CT scans may show various changes, including high, moderate, and low-density alterations (33). Because PCNS-PTLD patients do not exhibit specific enhancements on CT and MRI scans (17), the presence of supratentorial ring enhancement on MRI, while highly suggestive of PCNS-PTLD, does not exclude other diseases. Definitive diagnosis relies on histopathological biopsy. Recent case reports have indicated that PCNS-PTLD lesions may exhibit high perfusion and elevated levels of choline and lipids, aiding in differentiation from inflammation (16).

Therefore, whether it's the results of plasma and CSF EBV DNA, the clinical presentations of patients, or even imaging findings, they can only assist in the diagnosis of PCNS-PTLD. The final diagnosis requires histopathological biopsy (33). In our cases, 80% of the patients underwent robot-assisted stereotactic brain biopsies

based on the ROSA robotic system (Zimmer Biomet Robotics, Montpellier, France) or the REMEBOT domestic neurosurgical robot (Beijing Baihui Weikang Technology Co., Ltd., Beijing, China).

Stereotactic brain biopsy is a minimally invasive technique aimed at obtaining reliable histological diagnoses (38). Traditionally, there are frameless and frame-based methods, each with its own advantages and disadvantages (38). However, stereotactic brain biopsies guided by the ROSA system integrate the strengths of both methods in terms of technique, time efficiency, and diagnostic accuracy (38). The use of robotic systems in neurosurgery has expanded widely following the advent of MRI-guided stereotaxy (39). Improvements in accuracy, safety, and user-friendly modalities such as frameless surface registration and the ROSA system have facilitated the incorporation of robotics into the biopsy process (40). The ROSA system, an image-guided device with advanced navigation and haptic capabilities, allows neurosurgeons to choose between supervising the robot performing autonomously or directly controlling and moving the surgical instruments during the procedure after offline planning (38). The ROSA system enhances the safety and feasibility of stereotactic brain biopsies, while minimizing surgical risks and time (38, 41). Both ROSA and REMEBOT are active arm robotic systems equipped with six degrees of motion freedom. However, compared to ROSA, the REMEBOT system requires less registration time for the procedures it guides (42). Preoperatively, we utilized thin-slice contrast-enhanced MRI and CT for lesion localization in patients. Patients who were unable to undergo MRI due to various contraindications underwent preoperative localization using contrast-enhanced CT. For surgeries requiring prone or lateral positioning, scalp markers were applied to the patient's head prior to preoperative CT examination. Subsequently, the preoperative MRI and CT imaging data were imported into the operation planning subsystem of robot-assisted stereotactic biopsy systems to set the cranial entry point, puncture tract, and biopsy target. Intraoperatively, facial laser scanning or scalp markers were used for registration. Following this, guided by the pre-set biopsy trajectory, biopsies were performed with negative-pressure aspiration under the assistance of the robot's mechanical arm. The biopsy trajectory should steer clear of significant vessels visible on imaging, extract lesion tissue along its longitudinal axis, and avoid piercing into brain ventricles, among other considerations. Care was taken regarding the magnitude of negative pressure during tissue aspiration. Postoperatively, a cranial CT was conducted to confirm the accuracy of the puncture site and to check for complications such as intracranial hemorrhage. Specimens obtained during surgery were sent for pathological examination, and subsequent treatment measures were determined based on the pathological results.

In 2017, the World Health Organization (WHO) categorized PTLD into six subtypes, with three being non-destructive PTLD, including plasmacytic hyperplasia, infectious mononucleosis-like PTLD, and florid follicular hyperplasia (27). The other three are destructive PTLD, including polymorphic PTLD, monomorphic PTLD, and classic Hodgkin lymphoma-like PTLD (27). Combining our cases with other case reports, monomorphic DLBCL appears to be the most common pathological type of PCNS-PTLD.

Due to the limited number of PCNS-PTLD cases and the lack of systematic studies, there is currently no standardized treatment regimen (43). Existing treatment methods include reducing immunosuppressive drug doses, chemotherapy, rituximab therapy, EBV-specific cytotoxic T lymphocyte therapy, surgical resection, and WBRT. Reducing the dose of immunosuppressive drugs is the primary and initial method for treating PTLD (26). However, reducing immunosuppressive drugs alone is often insufficient (43). A retrospective study showed that its effectiveness rate was only 45% (44).

Previous studies have demonstrated that high-dose methotrexate-based chemotherapy regimens in PCNS-PTLD patients post-SOT are not only effective but also well-tolerated (45). High-dose methotrexate is defined as a dose exceeding 500 mg/m^2 (46). Since 90% of methotrexate relies on renal excretion (46), end-stage renal disease is a contraindication for its use (12).

Although chemotherapy has a high success rate, it carries treatment-related toxicity and mortality rates (43). Additionally, the most common pathological type of PCNS-PTLD is DLBCL derived from B lymphocytes, with CD20 positivity in atypical cells. Rituximab, a monoclonal antibody against CD20 on mature B lymphocytes, induces apoptosis and complement-mediated cytotoxicity against CD20-positive cells (19). Therefore, rituximab is increasingly used (43). Currently, rituximab combined with or without chemotherapy is gradually becoming a first-line treatment option (31).

Recent reports suggest that enhanced high-flux hemodialysis can effectively clear methotrexate from the bodies of end-stage renal disease patients (12, 46). Therefore, in PCNS-PTLD patients with concurrent end-stage renal disease, high-dose methotrexate combined with enhanced high-flux hemodialysis, methotrexate concentration monitoring, and ready-to-use calcium folinate rescue therapy can be attempted (46). However, due to limited related reports, the safety of this method requires further research confirmation.

Furthermore, in our case series, one patient received reduced immunosuppression combined with zanubrutinib treatment, and follow-up MRI revealed a gradual reduction in the tumor mass in the right basal ganglia region (Figure 5). The patient remained clinically stable until the last follow-up visit. Our case suggest that zanubrutinib may also be a potentially safe and effective drug for treating PCNS-PTLD.

Case reports have shown successful treatment of PCNS-PTLD patients using the zanubrutinib induction/maintenance therapy followed by consolidation therapy with third-party specific EBV T lymphocytes for a duration of one year (11). Zanubrutinib is a second-generation Bruton's Tyrosine Kinase inhibitor (BTKi) with superior inhibitory activity, higher bioavailability, and the ability to achieve sustained therapeutic exposure compared to the first-generation BTKi ibrutinib. Moreover, zanubrutinib exhibits significantly improved drug-drug interaction profiles, indicating its potential for concurrent use with a wider range of medications (47). Bruton's Tyrosine Kinase (BTK) plays a crucial role in the intracellular signaling pathway of B lymphocyte receptors, mediating the development, proliferation, and survival of B lymphocytes (47). Aberrant BTK signaling is pivotal in the pathogenesis and progression of various B cell malignancies,

including DLBCL (47). Recent studies have demonstrated that treatment regimens incorporating BTK inhibitors, such as zanubrutinib, can safely and effectively treat both systemic high-risk DLBCL and primary central nervous system lymphoma (PCNSL) (48). Given the safety and efficacy of zanubrutinib in the treatment of various B cell malignancies, it has been approved for use in more than 60 countries and regions (47).

Surgical resection remains controversial in PCNS-PTLD treatment. Traditionally, surgery has been discouraged due to the potential occult spread of lymphoma throughout the brain (39). However, emerging evidence suggests that maximal safe resection may be beneficial for immediate relief of tumor mass effects (49). Furthermore, studies have indicated that patients undergoing subtotal or total resection have significantly improved progression-free survival and overall survival compared to those undergoing biopsy alone (50). In our case series, two patients who underwent surgical resection showed no tumor recurrence on postoperative MRI, with one patient showing no signs of recurrence to date and another succumbing to myocardial infarction three years after surgery rather than PTLD. Therefore, our cases tend to support surgical resection.

Known lymphomas or PTLDs exhibit sensitivity to moderate doses (3,000–4,500 cGy) of radiation (4). Additionally, WBRT offers a high complete remission rate, lacks systemic toxicity, and poses no risk of allograft dysfunction (4). Based on our literature review, it can be observed that WBRT is also a commonly employed method for treating PCNS-PTLD.

Case series have shown that WBRT following complete resection can prolong survival in PCNS-PTLD patients (9). Additionally, case report has confirmed that WBRT in combination with rituximab is an effective treatment for PCNS-PTLD (6). In our case series, there was a patient who developed PCNS-PTLD following allogeneic HSCT. She underwent a combination of the above treatments, which confirmed the safety and efficacy of this combined therapeutic regimen.

The prognosis of PCNS-PTLD is poor and depends primarily on the patient's age, severity of the disease at diagnosis, potential complications, risk of allograft dysfunction, and treatment strategies (4, 23). Studies have shown that lack of response to first-line treatment and elevated lactate dehydrogenase levels are associated with a poor prognosis for PCNS-PTLD (1). Timely diagnosis of this disease is crucial for initiating potentially side-effect-ridden long-term targeted therapies (24). Early brain biopsy is necessary for patients highly suspected of having PCNS-PTLD.

Our study has some limitations. Due to a lack of understanding of the disease at the time, we did not perform EBV tests in blood or CSF preoperatively. Additionally, the number of cases we reported, as well as the quantity of relevant literature, is very limited. Therefore, the potential effectiveness of the treatment protocols we identified requires further validation in future studies.

6 Conclusion

Diagnosing PCNS-PTLD is extremely challenging and can only be confirmed through histopathological biopsy. Clinical presentations in patients are generally associated with intracranial lesions and are not typical. MRI scans in patients may also show various abnormal signals. However, we have found that supratentorial ring-enhancing lesions are the most common feature of this disease. Therefore, for patients who have undergone kidney or allogeneic HSCT and have been on long-term immunosuppressive therapy, any neurological symptoms and MRI evidence of intracranial abnormal signals, especially supratentorial ring-enhancing masses, whether single or multiple lesions, should raise a high suspicion of PCNS-PTLD. Timely brain biopsy should be performed to help choose specific treatments related to this disease as early as possible. The prognosis of PCNS-PTLD is poor, and due to its rarity, there is currently no recommended standard treatment protocol. Here, we report four cases of PCNS-PTLD after kidney transplantation and one case after allogeneic HSCT, contributing to the limited literature available. Based on our case series, apart from reducing the dosage of immunosuppressants, zanubrutinib may be a safe and effective treatment for this disease. A combined treatment approach with rituximab and WBRT after complete tumor resection is also a potential safe and effective strategy.

Data availability statement

The original contributions presented in the study are included in the article/supplementary material, further inquiries can be directed to the corresponding authors.

Ethics statement

The studies involving humans were approved by Xuanwu Hospital Ethics Committee. The studies were conducted in accordance with the local legislation and institutional requirements. Written informed consent for participation in this study was provided by the participants' legal guardians/next of kin. Written informed consent was obtained from the individual(s), and minor(s)' legal guardian/next of kin, for the publication of any potentially identifiable images or data included in this article.

Author contributions

LJ: Data curation, Formal analysis, Investigation, Software, Writing – original draft. DL: Data curation, Formal analysis, Investigation, Methodology, Writing – original draft. FY: Methodology, Resources, Writing – review & editing. JH: Data curation, Investigation, Writing – review & editing. PW: Conceptualization, Writing – review & editing. YZ: Writing – review & editing, Data curation, Investigation. YW: Funding acquisition, Resources, Supervision, Writing – review & editing, Conceptualization, Methodology. YS: Resources, Supervision, Writing – review & editing, Funding acquisition. GZ: Project administration, Resources, Supervision, Writing – review & editing.

Funding

The author(s) declare financial support was received for the research, authorship, and/or publication of this article. This

research was financially supported by Beijing Natural Science Foundation-Haidian Original Innovation Joint Fund Project (L222022).

Acknowledgments

We thank all participants for their time and effort in participating. We also acknowledge the patient and their family. We also extend our gratitude to the Department of Pathology at Xuanwu Hospital for their assistance.

Conflict of interest

The authors declare that the research was conducted in the absence of any commercial or financial relationships that could be construed as a potential conflict of interest.

The reviewer YL declared a shared affiliation with the authors to the handling editor at the time of review.

Publisher's note

All claims expressed in this article are solely those of the authors and do not necessarily represent those of their affiliated organizations, or those of the publisher, the editors and the reviewers. Any product that may be evaluated in this article, or claim that may be made by its manufacturer, is not guaranteed or endorsed by the publisher.

References

1. Batchelor TT, Thye LS, Habermann TM. Current management concepts: primary central nervous system lymphoma, natural killer T-cell lymphoma nasal type, and post-transplant lymphoproliferative disorder. *Am. Soc. Clin. Oncol. Educ. Book.* (2016) 36:e354–66. doi: 10.1200/EDBK_159030

2. Xu H, Rewerska J, Aardsma N, Slavin K, Valyi-Nagy T, Ni H. EBV-positive post-transplant lymphoproliferative disorder presenting as primary diffuse large B-cell lymphoma of the central nervous system. *Folia Neuropathologica*. (2017) 55:221–6. doi: 10.5114/fn.2017.70487

3. Zhu F, Li Q, Liu T, Xiao Y, Pan H, Liu X, et al. Primary central nervous system lymphoma after heart transplantation: a case report and literature review. *Medicine*. (2020) 99:35. doi: 10.1097/MD.0000000000021844

4. Lake W, Chang JE, Kennedy T, Morgan A, Salamat S, Baćskaya MK. A case series of primary central nervous system posttransplantation lymphoproliferative disorder: imaging and clinical characteristics. *Neurosurgery*. (2013) 72:960–70. doi: 10.1227/NEU.0b013e31828cf619

5. Kassa C, Reményi P, Sinkó J, Kállay K, Kertész G, Kriván G. Successful nivolumab therapy in an allogeneic stem cell transplant child with post-transplant lymphoproliferative disorder. *Pediat Transplantat*. (2018) 22:e13302. doi: 10.1111/petr.13302

6. Zimmermann H, Nitsche M, Pott C, Reinke P, Babel N, Hermann RM, et al. Reduction of immunosuppression combined with whole-brain radiotherapy and concurrent systemic rituximab is an effective yet toxic treatment of primary central nervous system post-transplant lymphoproliferative disorder (pCNS-PTLD): 14 cases from the prospective German PTLD registry. *Ann Hematol*. (2021) 100:2043–50. doi: 10.1007/s00277-021-04548-2

7. Sola-Valls N, Rodríguez C NY, Arcal C, Duran C, Oppenheimer F, Ribalta T, et al. Primary brain lymphomas after kidney transplantation: an under-recognized problem? *J Nephrol*. (2014) 27:95–102. doi: 10.1007/s40620-013-0026-z

8. Valencia-Sanchez C, Steenerson KK, Kelemen K, Orenstein R, Kusne S, Grill MF. Post-transplant primary central nervous system lymphoma after Epstein-Barr virus cerebellitis. *J Neurovirol*. (2019) 25:280–3. doi: 10.1007/s13365-018-0711-8

9. Huang YA, Wen MC, Tsai SF, Wu MJ Yu TM, Chuang YW, et al. Outcome of brain lymphoma in a high epstein-barr virus-prevalence country after kidney transplantation. *Transplant Proc*. (2023) 55:858–61. doi: 10.1016/j.transproceed.2023.03.048

10. Ishihara H, Okumi M, Tanabe K, Japan Academic Consortium of Kidney Transplantation (JACK). Primary central nervous system post-transplant lymphoproliferative disorder following kidney transplantation: a multi-institution study in Japan over 30 years. *Ther Apher Dial*. (2017) 21:516–8. doi: 10.1111/1744-9987.12568

11. Law SC, Hoang T, O'Rourke K, Tobin JW, Gunawardana J, Loo-Oey D, et al. Successful treatment of Epstein-Barr virus-associated primary central nervous system lymphoma due to post-transplantation lymphoproliferative disorder, with ibrutinib and third-party Epstein-Barr virus-specific T cells. *Am J Transplantat*. (2021) 21:3465–71. doi: 10.1111/ajt.16628

12. Yeung J, Vaughan E, Chadban S, Saunders J, Thiagarajah N, Brown C. High-dose intravenous methotrexate with high-flux, extended-hours haemodialysis in treatment of primary central nervous system, post-transplant lymphoproliferative disorder and end-stage kidney disease: a case report. *Nephrology*. (2018) 23:1063–4. doi: 10.1111/nep.13254

13. Brennan KC, Lowe LH, Yeaney GA. Pediatric central nervous system posttransplant lymphoproliferative disorder. *Am J Neuroradiol*. (2005) 26:1695–7. Available online at: https://www.ajnr.org/content/26/7/1695

14. Teresa P, Chan AN, Chan TK, Po Y. Post-transplantation primary central nervous system lymphoma in a patient with systemic lupus erythematosus and prolonged use of immunosuppressant. *Hong Kong Med J*. (2014) 20:541–4. doi: 10.12809/hkmj134095

15. Imafuku A, Tanaka K, Marui Y, Ubara Y, Takaichi K, Tomikawa S, et al. Primary central nervous system post-transplant lymphoproliferative disorder diagnosed by peripheral facial nerve palsy. *Intern Med*. (2018) 57:1899–903. doi: 10.2169/internalmedicine.9613-17

16. Reis F, Fukuda A, Bonfitto JFL, Schwingel R, Queiroz LS, Rogerio F, et al. Primary central nervous system post-transplant lymphoproliferative disorder mimicking toxoplasmosis. *Arq Neuropsiquiatr*. (2018) 76:566–7. doi: 10.1590/0004-282x20180049

17. Tanaka H, Matsuda R, Nakamura M, Nakagawa I, Nakase H. Primary central nervous system post-transplant lymphoproliferative disorder misdiagnosed as glioblastoma: a case report. *Anticancer Res*. (2022) 42:3975–9. doi: 10.21873/anticanres.15893

18. Azriel A, Towner JE, Gaillard F, Box G, Rogers T, Morokoff A. Solitary intraventricular Hodgkin lymphoma post-transplant lymphoproliferative disease (HL-PTLD): case report. *J Clini Neurosci*. (2019) 69:269–72. doi: 10.1016/j.jocn.2019.08.053

19. Said-Conti V, Amrolia PJ, Gaze MN, Stoneham S, Sebire N, Shroff R, et al. Successful treatment of central nervous system PTLD with rituximab and cranial radiotherapy. *Pediat Nephrol*. (2013) 28:2053–6. doi: 10.1007/s00467-013-2499-3

20. Yaginuma T, Yamamoto H, Mitome J, Tanno Y, Yamamoto I, Kobayashi A, et al. Successful treatment of monomorphic primary central nervous system post-transplantation lymphoproliferative disorder 5 years after kidney transplantation. *Transplant Infect Dis*. (2012) 14:E102–6. doi: 10.1111/j.1399-3062.2012.00781.x

21. Kittan N, Beier F, Kurz K, Niller H, Egger L, Jilg W, et al. Isolated cerebral manifestation of Epstein-Barr virus-associated post-transplant lymphoproliferative disorder after allogeneic hematopoietic stem cell transplantation: a case of clinical and diagnostic challenges. *Transplant Infect Dis*. (2011) 13:524–30. doi: 10.1111/j.1399-3062.2011.00621.x

22. Aisa Y, Mori T, Nakazato T, Suzuki S, Suzuki N, Ikeda Y, et al. Primary central nervous system post-transplant lymphoproliferative disorder presenting as cerebral hemorrhage after unrelated bone marrow transplantation. *Transplant Infect Dis*. (2009) 11:438–41. doi: 10.1111/j.1399-3062.2009.00409.x

23. Toyosaki M, Onizuka M, Amaki J, Shiraiwa S, Aoyama Y, Machida S, et al. Primary CNS post-transplant lymphoproliferative disorder following haploidentical HSCT using post-transplant high-dose cyclophosphamide. *Blood Cell Therapy*. (2019) 2:1. doi: 10.31547/bct-2018-004

24. Mayumi A, Yamashita T, Matsuda I, Hikosaka K, Fujino S, Norose K, et al. Toxoplasmic encephalitis followed by primary EBV-associated post-transplant lymphoproliferative disorder of the central nervous system in a patient undergoing allogeneic hematopoietic stem cell transplant: a case report. *Transplant Proc*. (2020) 52:2858–60. doi: 10.1016/j.transproceed.2020.08.002

25. Sakamoto H, Itonaga H, Taguchi J, Kato T, Sawayama Y, Hayashi T, et al. Central nervous system post-transplant lymphoproliferative disorder after allogeneic hematopoietic stem cell transplantation: the Nagasaki transplant

group experience. *Leukemia Res Reports*. (2019) 11:27–30. doi: 10.1016/j.lrr.2019.04.003

26. Al-Mansour Z, Nelson BP, Evens AM. Post-transplant lymphoproliferative disease (PTLD): risk factors, diagnosis, and current treatment strategies. *Curr Hematol Malig Rep*. (2013) 8:173–83. doi: 10.1007/s11899-013-0162-5

27. National Organization for Rare Disorders. *Posttransplant Lymphoproliferative Disorders*. (2023). Available online at: https://rarediseases.org/rare-diseases/posttransplant-lymphoproliferative-disorders/#disease-overview-main (accessed December 12, 2023).

28. Cavaliere R, Petroni G, Lopes MB, Schiff D. Primary central nervous system post-transplantation lymphoproliferative disorder: an international primary central nervous system lymphoma collaborative group report. *Cancer*. (2010) 116:863–70. doi: 10.1002/cncr.24834

29. Kempf C, Tinguely M, Rushing EJ. Posttransplant lymphoproliferative disorder of the central nervous system. *Pathobiology*. (2013) 80:310–8. doi: 10.1159/000347225

30. Saha A, Robertson ES. Mechanisms of B-cell oncogenesis induced by Epstein-Barr virus. *J Virol*. (2019) 93:10–1128. doi: 10.1128/JVI.00238-19

31. King RL, Khurana A, Mwangi R, Fama A, Ristow KM, Maurer MJ, et al. Clinicopathologic characteristics, treatment, and outcomes of post-transplant lymphoproliferative disorders: a single-institution experience using 2017 WHO diagnostic criteria. *Hemasphere*. (2021) 5:10. doi: 10.1097/HS9.0000000000000640

32. Tsai D, Douglas L, Andreadis C, Vogl D, Arnoldi S, Kotloff R, et al. EBV PCR in the diagnosis and monitoring of posttransplant lymphoproliferative disorder: results of a two-arm prospective trial. *Am J Transplantat*. (2008) 8:1016–24. doi: 10.1111/j.1600-6143.2008.02183.x

33. White ML, Moore DW, Zhang Y, Mark KD, Greiner TC, Bierman PJ. Primary central nervous system post-transplant lymphoproliferative disorders: the spectrum of imaging appearances and differential. *Insights Imaging*. (2019) 10:1–14. doi: 10.1186/s13244-019-0726-6

34. Liu QF, Ling YW, Fan ZP, Jiang QL, Sun J, Wu XL, et al. E pstein-B arr virus (EBV) load in cerebrospinal fluid and peripheral blood of patients with EBV-associated central nervous system diseases after allogeneic hematopoietic stem cell transplantation. *Transpl Infect Dis*. (2013) 15:379–92. doi: 10.1111/tid.12090

35. Hamadani M, Martin L, Benson D, Copelan E, Devine S, Hofmeister C. Central nervous system post-transplant lymphoproliferative disorder despite negative serum and spinal fluid Epstein-Barr virus DNA PCR. *Bone Marrow Transplant*. (2007) 39:249–51. doi: 10.1038/sj.bmt.1705575

36. Schwartz K, Erickson BJ, Lucchinetti C. Pattern of T2 hypointensity associated with ring-enhancing brain lesions can help to differentiate pathology. *Neuroradiology*. (2006) 48:143–9. doi: 10.1007/s00234-005-0024-5

37. Babik J, Katrak S, Miller S, Shah M, Chin-Hong P. Epstein-Barr virus encephalitis in a renal transplant recipient manifesting as hemorrhagic, ring-enhancing mass lesions. *Transpl Infect Dis*. (2015) 17:744–50. doi: 10.1111/tid.12431

38. De Benedictis A, Trezza A, Carai A, Genovese E, Procaccini E, Messina R, et al. Robot-assisted procedures in pediatric neurosurgery. *Neurosurg Focus*. (2017) 42:E7. doi: 10.3171/2017.2.FOCUS16579

39. Gupta M, Chan TM, Santiago-Dieppa DR, Yekula A, Sanchez CE, Elster JD, et al. Robot-assisted stereotactic biopsy of pediatric brainstem and thalamic lesions. *J Neurosurg: Pediatr*. (2020) 27:317–24. doi: 10.3171/2020.7.PEDS20373

40. Terrier L, Gilard V, Marguet F, Fontanilles M, Derrey S. Stereotactic brain biopsy: evaluation of robot-assisted procedure in 60 patients. *Acta Neurochir*. (2019) 161:545–52. doi: 10.1007/s00701-019-03808-5

41. Nieto-Rios JF, Gómez de los Ríos SM, Serna-Higuita LM, Ocampo-Kohn C, Aristizabal-Alzate A, Gálvez-Cárdenas KM, et al. Treatment of post-transplantation lymphoproliferative disorders after kidney transplant with rituximab and conversion to m-TOR inhibitor. *Colombia Médica*. (2016) 47:196–202. doi: 10.25100/cm.v47i4.1989

42. Feng Y, Yaming W, Yongzhi S, Penghu W, Hong W, Xiaotong F, et al. Novel application of robot-guided stereotactic technique on biopsy diagnosis of intracranial lesions. *Front Neurol*. (2023) 14:1173776. doi: 10.3389/fneur.2023.1173776

43. Reshef R, Vardhanabhuti S, Luskin M, Heitjan D, Hadjiliadis D, Goral S, et al. Reduction of immunosuppression as initial therapy for posttransplantation lymphoproliferative disorder. *Am J Transplantat*. (2011) 11:336–47. doi: 10.1111/j.1600-6143.2010.03387.x

44. Shibamoto Y, Hayabuchi N, Hiratsuka Ji, Tokumaru S, Shirato H, Sougawa M, et al. Is whole-brain irradiation necessary for primary central nervous system lymphoma? Patterns of recurrence after partial-brain irradiation Cancer: Interdisciplinary. *Int J Am Cancer Soc*. (2003) 97:128–33. doi: 10.1002/cncr.11035

45. Nabors L, Palmer C, Julian B, Przekwas A, Kew C. Isolated central nervous system posttransplant lymphoproliferative disorder treated with high-dose intravenous methotrexate. *Am J Transplantat*. (2009) 9:1243–8. doi: 10.1111/j.1600-6143.2009.02598.x

46. Mutsando H, Fahim M, Gill DS, Hawley CM, Johnson DW, Gandhi MK, et al. High dose methotrexate and extended hours high-flux hemodialysis for the treatment of primary central nervous system lymphoma in a patient with end stage renal disease. *Am J Blood Res*. (2012) 2:66.

47. Tam CS, Mu noz JL, Seymour JF, Opat S. Zanubrutinib: past, present, and future. *Blood Cancer J*. (2023) 13:141. doi: 10.1038/s41408-023-00902-x

48. Zhang L, Li C, Yue N, Jiang H, Jin Q, Cao J, et al. Efficacy of BTK inhibitor administered for central high-risk systemic diffuse large B cell lymphoma and primary central nervous system lymphoma: a single-center retrospective study. *Res Square*. (2024). doi: 10.21203/rs.3.rs-3782984/v1

49. Carnevale J, Rubenstein JL. The challenge of primary central nervous system lymphoma. *Hematol/Oncol Clini*. (2016) 30:1293–316. doi: 10.1016/j.hoc.2016.07.013

50. Weller M, Martus P, Roth P, Thiel E, Korfel A. Surgery for primary CNS lymphoma? Challenging a paradigm. *Neuro-oncology*. (2012) 14:1481–4. doi: 10.1093/neuonc/nos159

frontiers | Frontiers in Oncology

TYPE Case Report
PUBLISHED 17 May 2024
DOI 10.3389/fonc.2024.1390542

OPEN ACCESS

EDITED BY
Gerardo Caruso,
University Hospital of Policlinico G. Martino, Italy

REVIEWED BY
Evangelia Liouta,
National and Kapodistrian University of Athens, Greece
Melina Julia Engelhardt,
Charité - Universitätsmedizin Berlin, Germany

*CORRESPONDENCE
Kilian Abellaneda-Pérez
kabellaneda@guttmann.com
Josep María Tormos Muñoz
jm.tormos@ucv.es

†These authors have contributed equally to this work

RECEIVED 26 February 2024
ACCEPTED 26 April 2024
PUBLISHED 17 May 2024

CITATION
Boccuni L, Roca-Ventura A, Buloz-Osorio E, Leno-Colorado D, Martín-Fernández J, Cabello-Toscano M, Perellón-Alfonso R, Pariente Zorrilla JC, Laredo C, Garrido C, Muñoz-Moreno E, Bargalló N, Villalba G, Martínez-Ricarte F, Trompetto C, Marinelli L, Sacchet MD, Bartrés-Faz D, Abellaneda-Pérez K, Pascual-Leone A and Tormos Muñoz JM (2024) Exploring the neural basis of non-invasive prehabilitation in brain tumour patients: An fMRI-based case report of language network plasticity. *Front. Oncol.* 14:1390542. doi: 10.3389/fonc.2024.1390542

Exploring the neural basis of non-invasive prehabilitation in brain tumour patients: An fMRI-based case report of language network plasticity

Leonardo Boccuni[1,2,3], Alba Roca-Ventura[1,4,5], Edgar Buloz-Osorio[1,2,4], David Leno-Colorado[1,2,4], Jesús Martín-Fernández[6,7,8], María Cabello-Toscano[5,9], Ruben Perellón-Alfonso[1,2,4,5,9], Jose Carlos Pariente Zorrilla[9,10], Carlos Laredo[9,10], Cesar Garrido[9,10,11], Emma Muñoz-Moreno[9,10], Nuria Bargalló[5,9,10,11,12], Gloria Villalba[13], Francisco Martínez-Ricarte[14], Carlo Trompetto[15,16], Lucio Marinelli[15,16], Matthew D. Sacchet[17,18], David Bartrés-Faz[1,5,9], Kilian Abellaneda-Pérez[1,2,4*†], Alvaro Pascual-Leone[1,19,20†] and Josep María Tormos Muñoz[1,21*†]

[1]Institut Guttmann, Institut Universitari de Neurorehabilitació adscrit a la UAB, Barcelona, Spain, [2]Universitat Autònoma de Barcelona, Cerdanyola del Vallès, Spain, [3]Department of Conegliano, Scientific Institute IRCCS E. Medea, Treviso, Italy, [4]Fundació Institut d'Investigació en Ciències de la Salut Germans Trias i Pujol, Barcelona, Spain, [5]Departament de Medicina, Facultat de Medicina i Ciències de la Salut, Institut de Neurociències, Universitat de Barcelona, Barcelona, Spain, [6]Department of Neurosurgery, Hôpital Gui de Chauliac, Montpellier, France, [7]Department of Neurosurgery, Hospital Universitario Nuestra Señora de Candelaria, Santa Cruz de Tenerife, Spain, [8]Universidad de La Laguna, San Cristóbal de La Laguna, Spain, [9]Institut d'Investigacions Biomèdiques August Pi i Sunyer (IDIBAPS), Barcelona, Spain, [10]Magnetic Resonance Image Core Facility (IDIBAPS), Barcelona, Spain, [11]Neuroradiology Section, Radiology Department, Diagnostic Image Centre, Hospital Clinic of Barcelona, University of Barcelona, Barcelona, Spain, [12]Centro de Investigación Biomédica en Red de Salud Mental (CIBERSAM), Instituto de Salud Carlos III, Barcelona, Spain, [13]Department of Neurosurgery, Hospital del Mar, Barcelona, Spain, [14]Department of Neurosurgery, Vall d'Hebron Hospital, Universitat Autònoma de Barcelona, Barcelona, Spain, [15]Department of Neuroscience, Rehabilitation, Ophthalmology, Genetics, Maternal and Child Health, University of Genova, Genova, Italy, [16]IRCCS Ospedale Policlinico San Martino, Genova, Italy, [17]Meditation Research Program, Department of Psychiatry, Massachusetts General Hospital, Harvard Medical School, Boston, MA, United States, [18]Athinoula A. Martinos Centre for Biomedical Imaging, Department of Radiology, Massachusetts General Hospital, Harvard Medical School, Boston, MA, United States, [19]Hinda and Arthur Marcus Institute for Aging Research and Deanna and Sidney Wolk Centre for Memory Health, Hebrew Senior Life, Boston, MA, United States, [20]Department of Neurology, Harvard Medical School, Boston, MA, United States, [21]Centro de Investigación Traslacional San Alberto Magno, Universidad Católica de Valencia San Vicente Mártir, Valencia, Spain

Primary brain neoplasms are associated with elevated mortality and morbidity rates. Brain tumour surgery aims to achieve maximal tumour resection while minimizing damage to healthy brain tissue. Research on Neuromodulation Induced Cortical Prehabilitation (NICP) has highlighted the potential, before neurosurgery, of establishing new brain connections and transfer functional activity from one area of the brain to another. Nonetheless, the neural mechanisms underlying these processes, particularly in the context of space-occupying lesions, remain unclear. A patient with a left frontotemporoinsular tumour underwent a prehabilitation protocol providing 20 sessions of inhibitory

non-invasive neuromodulation (rTMS and multichannel tDCS) over a language network coupled with intensive task training. Prehabilitation resulted in an increment of the distance between the tumour and the language network. Furthermore, enhanced functional connectivity within the language circuit was observed. The present innovative case-study exposed that inhibition of the functional network area surrounding the space-occupying lesion promotes a plastic change in the network's spatial organization, presumably through the establishment of novel functional pathways away from the lesion's site. While these outcomes are promising, prudence dictates the need for larger studies to confirm and generalize these findings.

KEYWORDS

brain tumour, prehabilitation, neurorehabilitation, neuromodulation, fMRI, case report

Introduction

Brain tumours are characterized by high mortality rate, severe disability, and burden for the healthcare system. A systematic analysis from the Global Burden of Disease Study outlined that, in 2016 alone, the global incidence of primary brain and central nervous system tumours was 330,000 new cases and 227,000 deaths (1). The overall 5-year survival rate for malignant brain tumours is 36% (2), despite advancements in the field of neurosurgery, radiotherapy, and chemotherapy. Patient's survival is associated with both the extent of tumour resection and postoperative neurological deficits, so that the best outcomes are expected for patients with gross total resection and no worsening of symptoms (3, 4). However, massive resection and preserved functionality are often conflicting goals, posing neurosurgeons in the dilemma of finding a cost-benefit compromise.

One promising approach is Neuromodulation-Induced Cortical Prehabilitation (NICP) (5). NICP aims at leveraging neuroplastic changes before surgery, by performing conditioning sessions over several consecutive days or weeks. This neuroplasticity-based paradigm holds the potential to modulate brain connectivity and activity, facilitating the transfer of functional activity from one brain region to another. The goal of this process is to broaden safe functional margins for excision, to maximize tumour eradication while at the same time preserving neurological status. So far, publications on NICP account for four case reports and one case series, totalling only eight patients (6–10). A common element of all NICP studies is a two-step process, the first step being the 'virtual lesion' of areas considered at risk of being compromised during neurosurgery; and the second step being the promotion of brain activity of alternative brain resources, while the targeted area has been inhibited.

The accomplishment of the first step (i.e., virtual lesion), can be performed invasively, by means of extra-operative continuous high-frequency cortical electrical stimulation (7–9), or non-invasively, for instance, by transcranial magnetic stimulation (TMS) (6, 10). Invasive neuromodulation has been investigated in two case reports (7, 9) and a case series (8), showing consistent patterns of neural reorganization studied through functional magnetic resonance imaging (fMRI). However, invasive techniques required two surgeries and came at the cost of high rate of complications such as infections and seizures (8). Non-invasive neuromodulation was investigated in two case reports by Barcia et al. (6) and Dadario et al. (10). However, task-evoked brain reorganizations were not significant (6) or not reported (10).

The second step (i.e., enhancement of activity for alternative brain areas) is achieved by training the function at risk of being compromised. Such intervention is performed during and/or immediately after inhibition of targeted peritumoural areas, in a condition where the brain is supposedly constrained to recruit alternative pathways within the same functional network. Type and amount of training varied greatly among protocols, from no training (10) up to six hours a day (9).

Given the limited number of studies, the complex nature of the interventions, and the diversity of protocols, the impact of non-invasive NICP interventions at the neuroimaging level, as well as the underlying neurobiological mechanisms responsible for these changes, remains largely unknown. To this end, the present study was designed to capitalize on distinct fMRI modalities (11), utilizing tb-fMRI to investigate the topographical brain changes induced by NICP, while simultaneously using rs-fMRI to explore the connectivity modulations induced in the circuits of interest. During the last decades, tb-fMRI has been a widely used approach for investigating task-related networks implicated in various cognitive and motor processes (12–14). More recently, rs-fMRI has emerged as a valuable tool for investigating brain functioning in the absence of any specific task engagement (15). Particularly, rs-fMRI has been extensively utilized to explore brain functional connectivity, which refers to the temporal correlation between neurophysiological measurements obtained from distinct

brain regions (16, 17). These patterns of temporally correlated oscillations observed during rest underlie the activity of the so-called resting-state networks (18, 19). Notably, Smith et al. demonstrated that these resting-state networks correspond to the same set of regions that form 'networks,' and are activated and/or deactivated during task performance, and provide additional means to explore further features of these neural systems (20). Remarkably, rs-fMRI data has proven valuable in predicting tb-fMRI evoked responses (21), even in pre-surgical patient populations with conditions such as tumour, epilepsy, and vascular lesions (22). Furthermore, pre-operative rs-fMRI BOLD signal is significantly affected by tumours affecting motor and language function, and associated with functionality (23). In particular, for patients with tumour near the inferior frontal gyrus, Liouta et al. found a significantly decreased rs-fMRI BOLD signal in patients with aphasia, as compared with non-aphasics, and a strong positive correlation between rs-fMRI BOLD signal and phonological fluency performance (23).

The present case report was investigated to internally validate the protocol for a subsequent (ongoing) research trial (ClinicalTrials.gov Identifier NCT05844605) (24), to verify (1) whether brain functional patterns at risk, as evidenced by tb-fMRI, could be modified through a non-invasive intensive plasticity-induction protocol; and (2), to explore the potential role of functional connectivity, assessed during rs-fMRI, as a mechanism underlying the observed changes in tb-fMRI brain activity. The main hypothesis is that the proposed neuroplasticity-promoting intervention would facilitate the establishment of new functional connections within the modulated brain system, thus facilitating the emergence of novel brain activity patterns in language network regions more distant from the tumour site. Clinically, such dualistic phenomenon (concurrent inhibition of targeted areas and enhanced recruitment of alternative resources within the same network) would result in unaltered language and cognitive performance.

Methods

Case description

The patient is a right-handed adult in the 40s with past medical history reporting episodic alterations of consciousness, suggestive of epileptic seizures. During such episodes there was no relaxation of sphincters, and the patient recovered ad integrum after each episode; symptomatology presented for approximately three years. By the time of enrolment in the study protocol, no focal neurological symptoms nor clinically relevant sensorimotor or cognitive deficits were evidenced. Brain MRI demonstrated a large infiltrative lesion in the left frontobasal, temporal, and insular regions (See Figure 1A). At this stage, the patient was referred to Institut Guttmann (Guttmann Barcelona, Spain) from the Neurosurgery Department of Vall d'Hebron Hospital (Barcelona, Spain) to be enrolled as a voluntary participant in the PREHABILITA feasibility trial (see individualized prehabilitation description at paragraph 4.3). At the end of NICP protocol, based on clinical and MRI outcomes, a left frontotemporoparietal craniotomy was performed, and a resection of the left frontotemporoinsular space-occupying lesion (transcortical approach) was carried out without complications. Considering the size of the tumour and consequent mass effect, the neurosurgeon (F.M.R.) planned initially a two-step approach: during the first surgery intratumoural debulking was performed with the patient under general anaesthesia. Intraoperative monitoring included continuous recording from a grid of electrodes placed over the motor cortex, and by monopolar stimulation to identify the motor pathway at cortical-subcortical level. Intraoperative neuroimaging comprised neuronavigation, cerebral echography and neuronavigated echography. As planned, subtotal resection was performed, the two most limiting factors being the tumour size and associated mass effect, and the infiltration of basal ganglia at the level of perforating arteries. Based on postsurgical histopathology results (diagnosis of a grade IV frontotemporoinsular glioma with an IDH mutation), the neurosurgeon decided to cancel the second surgery (with patient awake, for further tumour removal), and instead opted for conservative patient's management including radiotherapy and oral chemotherapy.

All procedures from the present study were performed in accordance with the Helsinki declaration. The study was approved by the Research Ethical Committee of Fundació Unió Catalana d'Hospitals (approval number: CEI 21/65, version 1, 13/07/2021).

Assessment protocol

According to the study protocol, the patient received a comprehensive clinical, neurophysiological (i.e., TMS) and neuroimaging assessment. The same assessment was conducted at baseline (TP1, before NICP), at the end of the prehabilitation intervention (TP2, after NICP), and after neurosurgical intervention (TP3, after surgery). The feasibility of the intervention was assessed at TP2 by considering adherence to planned sessions, absence of adverse events attributable to the intervention, and patient's satisfaction of the treatment received (PATSAT questionnaire) (25). The current case report is focused on neuropsychological and neuroimaging procedures.

To ensure transparency and reproducibility of the methods, full protocol description have been previously published (24). Further details of clinical evaluations, neuroimaging acquisition and specific processing for the present case report are available as Supplementary Materials.

Individualized prehabilitation intervention

Figure 1 shows the timeline of interventions (A), neuromodulation targets with respect to tb-fMRI cortical activation clusters (B), and multifocal tDCS pattern (C). Figure 2A illustrates structural MRI of lesion distribution.

The patient performed a total of 20 sessions of NICP within 12 days, primarily organized with a first session in the morning (from

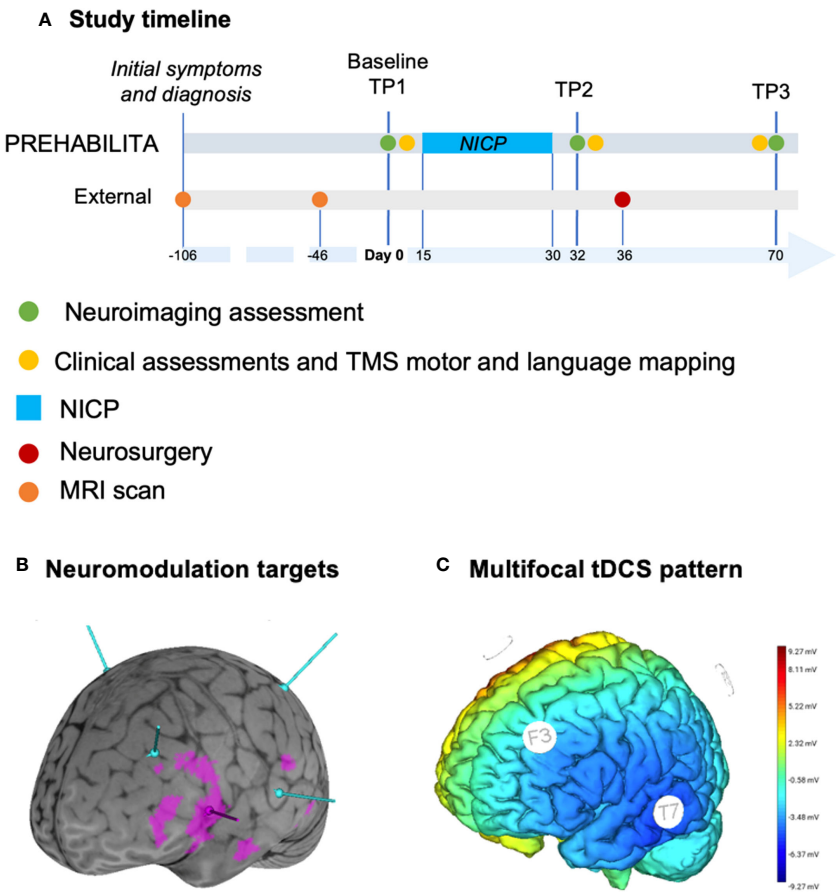

FIGURE 1
Outline of the methodology for the case report. **(A)** Study timeline, where neuroimaging assessments are depicted in green for baseline (TP1: day 0), after NICP (TP2: day 32), and after surgery (TP3: day 70). NICP (azure) consisted of 20 consecutive sessions performed between day 15 and day 30. Clinical assessments and TMS motor and language mapping (yellow) were performed at day 13, 34, and 69. Neurosurgery was performed at day 36. Previous timepoints are initial symptoms, MRI scan and diagnosis at day -106, previous MRI scan at day -46. Referral by neurosurgeon to be included in the NICP protocol was six days before baseline. **(B)** Brainsight curvilinear brain (grey) and activation clusters (derived from tb-fMRI analyses) overlay for semantic decision (violet), with targets for TMS (peak fMRI for semantic decision, in violet) and multichannel tDCS (azure) corresponding to F3, P3, T7, C4 EEG electrodes. **(C)** Map of multichannel tDCS project on Neuroelectrics software.

9:00 to 11:00) and a second session in the afternoon (from 14:00 to 16:00). This schedule was designed to reach the goal of at least 10 and maximum 20 sessions of NICP. Each NICP session consisted of neuromodulation coupled with intensive behavioural training. For this specific case, the function at risk of being compromised was language production. Therefore, the goal of NICP was to inhibit eloquent areas associated with language function (by means of neuromodulation) while at the same time promoting the activation of alternative nodes of the same network (by means of intensive language and cognitive training).

The neuromodulation strategy was designed to induce twofold objectives. The first aim was to achieve a focal disruption of the maximum representativity within the semantic language activation cluster identified by fMRI. The second objective was to achieve widespread inhibition across the entire semantic fMRI circuit in the left hemisphere, using parameters effective in inducing language network changes in healthy subjects and patients with aphasia (26, 27). Each morning session consisted of low frequency rTMS (1800 pulses, 1 Hz, 90% RMT) (28, 29) over the peak fMRI activation (MNI coordinates: -56, 12, 8) of the targeted cluster for semantic decision task, followed by one hour of intensive training of language and high cognitive functions with an experienced neuropsychologist (A.R.V.). The rationale for target selection was that, among the three language-related fMRI tasks, semantic decision showed the largest activation cluster, which was also the closest one to the tumour; hence, peak fMRI activation for this cluster was considered as target because of both its functional relevance and the risk of compromission by neurosurgery. Notably, if only one session per day were performed, this morning protocol was applied. Each afternoon session consisted of multifocal tDCS (30, 31) (F3: -400 μA; T7: -300 μA; P3:-300 μA; C4: 1000 μA). The main goal was to promote a widespread left inhibition over the representation of language related clusters. The total duration of tDCS sessions was 30 minutes. After the first five minutes at rest, for the remaining 25 minutes the patient received tDCS while performing intensive cognitive training by means of a dedicated online platform (Guttmann NeuroPersonalTrainer®, GNPT) (32). At the end of tDCS the patient performed other 30 minutes of cognitive training with GNPT, totalling approximately one hour of training. At the end of the last daily NICP session, the

patient performed a High Intensity Interval Training (HIIT) protocol on a stationary bike, with the following protocol: 5 minutes warm-up, first HIIT bout (30 seconds all-out + 30 seconds rest, 10 times), 5 minutes rest, second HIIT bout (same as the first bout), 5 minutes cool-down. The goal of intensive aerobic training after cognitive training was to foster skill learning encoding and consolidation (33–35).

Results

Neuropsychological results

There were no significant alterations detected in any of the language tasks, which was the cognitive function of interest, at the three distinct time points pre-intervention, post-intervention, and at follow-up (i.e., TP1, TP2 and TP3; Table 1). Notwithstanding, during the comprehensive cognitive evaluation, a decrease in attentional, delayed memory and executive functions performance was observed, yielding clinically significant findings (which were not significant in the baseline NICP assessment). Processing speed, immediate memory and some executive function tasks were below expectation from baseline considering age and education (see Supplementary Table 1).

Language tb-fMRI results

Prehabilitation resulted in an increment of the distance between the tumour (Figure 2A) and the nearest activation cluster during the semantic language fMRI task by 15.9 mm, returning to a similar distance as baseline after surgery (Figures 2B, C). Further, the volume of the closest activation fMRI cluster decreased after prehabilitation in 12.4 mm^3, also showing a subsequent increment to a certain degree following surgery (Figures 2B-D).

Language rs-fMRI network results

There was a noteworthy increase in the resting-state functional connectivity within the language network. This enhancement was particularly prominent between the left inferior frontal gyrus (IFG L, the nearest network node to the target of NICP neuromodulation) and the remaining regions of the language network. Remarkably, this pattern on increased connectivity persisted following the surgical procedure (Figure 3). In addition, an increase of functional connectivity was observed also for the right inferior frontal gyrus (IFG R), though to a lesser extent. Notably, no comparable network reconfigurations were observed within the control visual network (Supplementary Figure 1).

In terms of feasibility, the patient attended all planned sessions and did not report any adverse event during the whole intervention period. Results from questionnaire about patient's satisfaction were excellent.

TABLE 1 Language tasks from neuropsychological assessment.

Language domain	Before NICP	After NICP	After Surgery
Spontaneous language			
Conversation	8	8	8
Narrative speech	6	6	6
Picture description	6	6	6
Informative content of language			
Fluency and grammar	10	10	10
Content of language	10	10	10
Verbal repetition			
Words	10	10	10
Syllables	8	8	8
Pseudowords	8	8	8
Sentences	60	60	60
Verboverbal Naming			
Confrontation naming	6	6	6
Responsive naming	6	6	6
Verbal comprehension			
Commands	16	16	16
Complex ideational sentence	9	9	9
Reading comprehension			
Sentences and text	8	8	8
Word-picture	6	6	6
Words	6	6	6
Pseudowords	6	6	6
Automatic language			
Automatized sequences: Forward series	3	3	3
Mental control: Backward series	3	3	3
Naming visuoverbal			
Naming pictures	14	14	14
Reading - verbalization			
Letters	6	6	6
Numbers	6	6	6
Pseudowords	6	6	6
Text	56	56	56
Writing: Dictate			
Letters	6	6	6
Numbers	6	6	6
Pseudowords	6	6	6
Words	6	6	6
Sentences	13	13	13

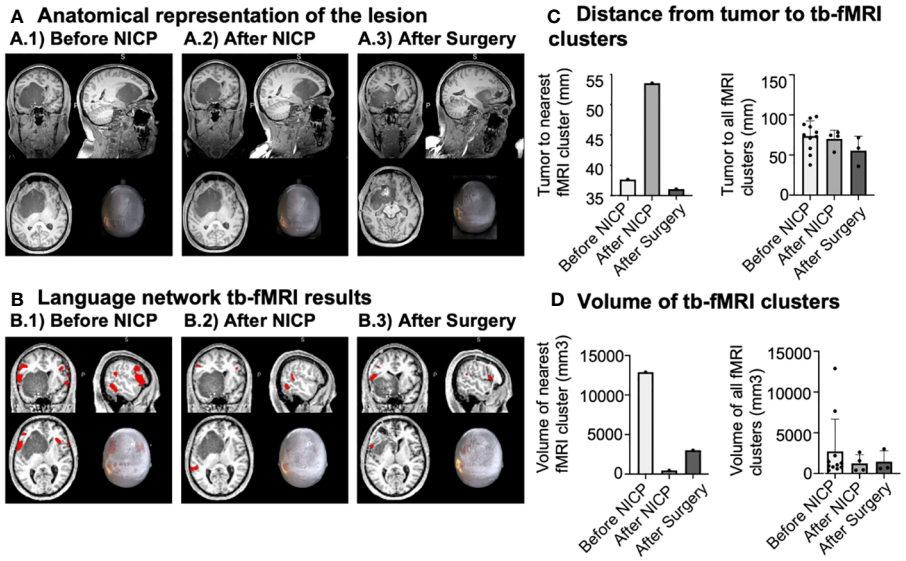

FIGURE 2
Illustration of brain tumour lesion and language network tb-fMRI results. **(A)** Anatomical representation of the tumour lesion at the three different time-points, with the centre of the figure positioned around the centre of masses. **(B)** Language network tb-fMRI results at the three different time-points, with the centre of the figure placed over the stimulation site. **(C)** Distance from the tumour to tb-fMRI clusters, presenting all tb-fMRI clusters and the nearest fMRI cluster. **(D)** Volume of tb-fMRI clusters, displaying the nearest one from the tumour and all of them.

Discussion

The present case report described clinical outcomes and neural correlates of a patient undergoing a non-invasive NICP protocol before neurosurgery for brain tumour. Clinically, the patient exhibited complete functionality at baseline despite the significant tumour mass and did not show clinically relevant changes for language function at the end of NICP nor at follow up after surgery (i.e., he was stable throughout the course of the intervention). On the other hand, when looking at the brain level, the patient presented baseline tb-fMRI activation clusters related to semantic decision in proximity with the tumour, particularly within the IFG L, pars opercularis. These clusters dissipated after prehabilitation with the concomitant enlargement of left temporoparietal fMRI-related clusters (specifically within the posterior divisions of the supramarginal and superior temporal gyri). Finally, after surgery, the activation clusters reappeared at approximately the same location as at baseline. Such brain activity changes were paired by resting-state functional connectivity outcomes, showing increased language network connectivity, particularly in an anteroposterior manner and mostly evident from the IFG L resting-state networks language node (with the centre coordinates over the IFG L, pars triangularis).

Despite full independence in activities of daily living, the patient presented at baseline with scores in cognitive domains such as memory and executive function below what expected based on age and education, which further decreased at the end of the intervention. Being a single case it is only possible to draw causal inferences by considering both the intervention and the tumour itself. In the first hypothesis, it's worth considering that rTMS was applied to peak-fMRI of semantic language network and paired with speech training, while multichannel tDCS was applied to a broad parietofrontal region and paired with cognitive training. Because of the concurrent application of both modalities, it is impossible to discriminate the role of each intervention, though it would be interesting to compare the effectiveness of different approaches (TMS versus tDCS) in future studies. In the second hypothesis, the presence of the lesion determined cognitive scores already below expectations at baseline, with further worsening due to disease progression.

A critical aspect for the whole intervention was the rationale leading to the choice of the target of neuromodulation. Previous cases of non-invasive NICP selected the target based on a combination of clinical symptoms, neuroanatomical considerations, and neural correlates. Barcia et al. applied neuromodulation over a region corresponding to Broca's area because of the proximity with the tumour and symptoms of speech disorders (6). Similarly, Dadario et al. selected targets close to the tumour and in proximity with the planned surgical entry point (10); furthermore, based on rs-fMRI results, areas that were considered hyperconnected or eligible for excision were inhibited, and areas hypoconnected or potential candidates to functionally supply eloquent areas were stimulated (with excitatory paradigms). When looking at invasive NICP case reports (7, 9) and case series (8), a common element was the placement of grids of electrodes for the application of cortical electrical stimulation at the maximum tolerable intensity; grids were placed over extended regions covering eloquent areas, based on clinical and neuroanatomical considerations. For the present study, the patient was completely functional at baseline, hence the starting point was considering the anatomical localization of the tumour, the cortical distribution of language tb-fMRI clusters, and the localization of the peak-fMRI for

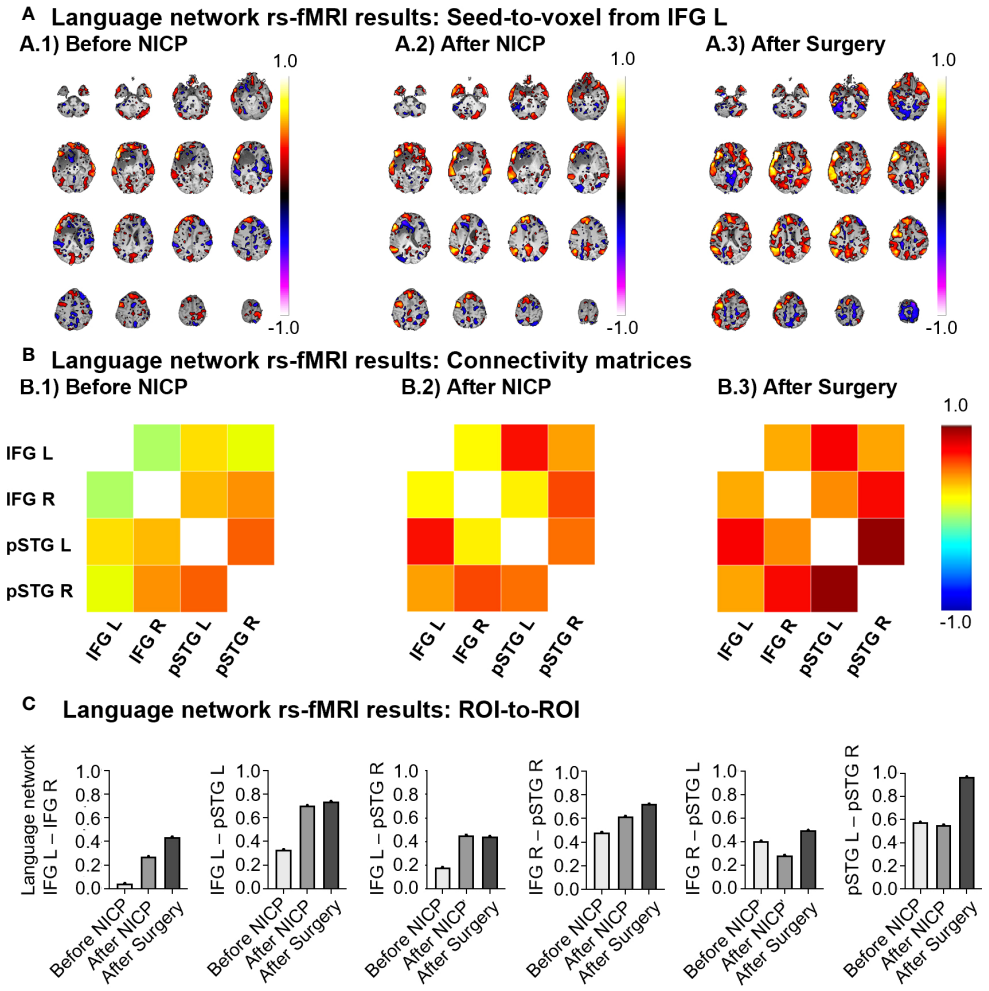

FIGURE 3
Representation of the language network rs-fMRI results. IFG L, left inferior frontal gyrus; IFG R, right inferior frontal gyrus; pSTG L, left posterior superior temporal gyrus; pSTG R, right posterior superior temporal gyrus. **(A)** Seed-to-voxel results displayed from the left inferior frontal gyrus (IFG L) at three different time-points. The colour-map represents the connectivity strength, ranging from 1 to -1. The slices are ordered along the Z-axis, ranging from -46 to 74 in increments of 8 units. **(B)** Connectivity matrices considering the four network ROIs at the three time-points. The color-map also represents the connectivity strength, ranging from 1 to -1. ROI-to-ROI results encompassing all the network couplings at the three time-points. **(C)** Histograms representing the same correlation values reported in the connectivity matrices. Each graph shows the evolution of connectivity for a specific ROI-to-ROI.

each cluster of interest. By delivering a regional neuromodulation, the goal was to elicit widespread neuroplastic reorganization. In this perspective, peak tb-fMRI of the largest cluster close to the tumour was selected as the centre of a relevant node within the semantic language network and targeted with low frequency rTMS to induce a topographical rearrangement of this brain circuit. Furthermore, inhibitory multifocal tDCS was applied with cathodes mainly covering the identified circuit of interest, to boost the inhibition within the targeted cluster in favour of other compensatory network areas.

When looking at functional activation associated to semantic decision task, the minimum distance between the tumour and any activation peak increased by almost 16 mm from TP1 to TP2, indicating an antero-posterior shift of functional activity (i.e., from frontal to the temporoparietal brain regions). From a neurosurgical perspective, a distance between a lesion and eloquent area less than 5 mm is associated with worse outcomes (36, 37). Therefore, the increase in minimum distance obtained may be considered of direct clinical relevance. Furthermore, the minimum distance between the tumour and peak-fMRI returned to approximately baseline levels at TP3, hence suggesting that non-invasive NICP provoked a temporal window of neuroplastic changes beneficial for the preservation of functionality during neurosurgery; in the absence of any specific treatment and likely following spontaneous recovery, the brain reorganized itself by returning to a pattern of functional activity comparable to what was evidenced before the intervention.

When focusing on rs-fMRI, seed-based analysis revealed a notable functional connectivity increase within the language resting-state networks. Specifically, ROI-to-ROI analyses showed an increased connectivity between the IFG L area and all other nodes in the network. Additionally, an anteroposterior connectivity increment between the right hemisphere's IFG and the posterior

superior temporal gyrus (pSTG) was observed. Importantly, these functional connectivity patterns were not present in a control visual network. Therefore, our NICP protocol enhanced the rs-fMRI connectivity of the language network, with a main emphasis on the IFG L, the node roughly aligned with the tb-fMRI peak activation used as the targeted TMS area, and particularly in an anteroposterior fashion. Interestingly, the rs-fMRI functional connectivity results for the language network are spatially consistent with the findings from semantic language tb-fMRI outcomes, wherein there was a subsequent reduction of clusters anteriorly, at the level of the IFG L, and the enlargement of clusters in posterior areas of the network, within the temporoparietal intersection. Consequently, it appears that our NICP protocol was capable of modulating both tb-fMRI brain activity and rs-fMRI functional connectivity. More precisely, this modulation resulted in an amplification of rs-fMRI functional connectivity within the language system, which might presumably underlie the subsequent displacement of brain activation to other regions, farther from the lesion, during task demands.

Some limitations should be addressed. First, the present study is a case report, which heavily limits the interpretation and generalizability of findings, warranting future group-level studies. Another important constraint is that the patient underwent a complex intervention, composed of two different protocols of neuromodulation (low frequency rTMS and multifocal tDCS) coupled with intensive language and cognitive training, followed by intensive aerobic training to promote the consolidation of neuroplastic changes. The overall rationale was to provide a comprehensive intervention based on the best available evidence to achieve the most ambitious clinical outcome, tailored to specific patient's needs. Nonetheless, this prevents us from determining the relative contribution of each ingredient on the outcome of the intervention. Future comparative studies may help elucidating this aspect. Finally, in the absence of a control condition, it is not possible to determine to which extent neuroplastic changes were due to the intervention. Indeed, the presence of the tumour itself may significantly affect the coupling between neural activity and blood flow (neurovascular uncoupling), possibly jeopardizing the interpretation of functional neuroimaging outcomes (38). However, data from the present case indicates a shift of the cortical activation pattern within nodes of the language network, suggesting a true neuroplastic reorganization rather than a random artifact. In conclusion, when putting the present study in perspective with previous literature, it is important to acknowledge that this is the first case showing clinically relevant neuroplastic changes after non-invasive NICP coupled with intensive task training without neurological sequelae. Hence, non-invasive NICP holds significance as an attractive alternative to invasive NICP protocols, warranting further investigation.

Data availability statement

The datasets presented in this article are not readily available because of ethical and privacy restrictions. Requests to access the datasets should be directed to the corresponding authors.

Ethics statement

The studies involving humans were approved by Fundació Unió Catalana d'Hospitals (approval number: CEI 21/65, version 1, 13/07/2021). The studies were conducted in accordance with the local legislation and institutional requirements. The participants provided their written informed consent to participate in this study. Written informed consent was obtained from the individual(s) for the publication of any potentially identifiable images or data included in this article.

Author contributions

LB: Conceptualization, Data curation, Formal analysis, Investigation, Methodology, Project administration, Software, Writing – original draft, Writing – review & editing. AR: Investigation, Validation, Writing – original draft, Writing – review & editing. EB: Investigation, Project administration, Writing – original draft, Writing – review & editing. DL: Investigation, Writing – review & editing. JM: Writing – review & editing. MC: Data curation, Formal analysis, Investigation, Methodology, Software, Writing – original draft, Writing – review & editing. RP: Conceptualization, Software, Writing – review & editing. JP: Data curation, Formal analysis, Writing – review & editing, Validation. CL: Formal Analysis, Writing – review & editing, Validation. CG: Resources, Writing – review & editing. EM: Methodology, Resources, Writing – review & editing. NB: Methodology, Supervision, Writing – review & editing. GV: Investigation, Resources, Writing – review & editing. FM: Resources, Writing – review & editing. CT: Investigation, Writing – review & editing. LM: Investigation, Writing – review & editing. MS: Writing – review & editing. DB: Funding acquisition, Methodology, Project administration, Supervision, Writing – review & editing. KA: Formal analysis, Investigation, Methodology, Project administration, Software, Supervision, Writing – original draft, Writing – review & editing. AP: Conceptualization, Funding acquisition, Project administration, Supervision, Writing – review & editing. JT: Conceptualization, Data curation, Funding acquisition, Investigation, Project administration, Supervision, Writing – review & editing.

Funding

The author(s) declare financial support was received for the research, authorship, and/or publication of this article. This research was principally funded by Joan Ribas Araquistain Foundation (reference project 2020.330). KA-P was financially supported by a Juan de la Cierva research grant (FJC2021-047380-I) of the Spanish Ministry of Science and Innovation. DB-F was supported by an Institut Català de Recerca i Estudis Avançats, ICREA Academia 2019 award from the Catalan government. This work was partially developed at the Centre Esther Koplowitz, IDIBAPS, Barcelona, CERCA Programme/Generalitat de Catalunya and thanks to the Magnetic Resonance Imaging Core Facility IDIBAPS team and the 3T Equipment (project IBPS15-EE-3688 cofounded by MCIU and by ERDF).

Conflict of interest

AP-L is listed as an inventor on several issued and pending patents on the real-time integration of transcranial magnetic stimulation with electroencephalography and magnetic resonance imaging. He is a co-founder of Linus Health and TI Solutions AG and serves on the scientific advisory boards for Starlab Neuroscience, Magstim Inc., Hearts Radiant, MedRhythms, TetraNeuron, and Skin2Neuron.

The remaining authors declare that the research was conducted in the absence of any commercial or financial relationships that could be construed as a potential conflict of interest.

The author(s) declared that they were an editorial board member of Frontiers, at the time of submission. This had no impact on the peer review process and the final decision.

Publisher's note

Supplementary material

The Supplementary Material for this article can be found online at: https://www.frontiersin.org/articles/10.3389/fonc.2024.1390542/full#supplementary-material

References

1. Patel AP, Fisher JL, Nichols E, Abd-Allah F, Abdela J, Abdelalim A, et al. Global, regional, and national burden of brain and other CNS cancer, 1990–2016: a systematic analysis for the Global Burden of Disease Study 2016. *Lancet Neurol.* (2019) 18:376–93. doi: 10.1016/S1474–4422(18)30468-X

2. Miller KD, Ostrom QT, Kruchko C, Patil N, Tihan T, Cioffi G, et al. Brain and other central nervous system tumor statistics, 2021. *CA Cancer J Clin.* (2021) 71:381–406. doi: 10.3322/caac.21693

3. Brown TJ, Brennan MC, Li M, Church EW, Brandmeir NJ, Rakszawski KL, et al. Association of the extent of resection with survival in glioblastoma: A systematic review and meta-analysis. *JAMA Oncol.* (2016) 2:1460–9. doi: 10.1001/jamaoncol.2016.1373

4. Rahman M, Abbatematteo J, Leo EKD, Kubilis PS, Vaziri S, Bova F, et al. The effects of new or worsened postoperative neurological deficits on survival of patients with glioblastoma. *J Neurosurg.* (2016) 127:123–31. doi: 10.3171/2016.7.JNS16396

5. Hamer RP, Yeo TT. Current status of neuromodulation-induced cortical prehabilitation and considerations for treatment pathways in lower-grade glioma surgery. *Life.* (2022) 12:466. doi: 10.3390/life12040466

6. Barcia JA, Sanz A, González-Hidalgo M, de las Heras C, Alonso-Lera P, Díaz P, et al. rTMS stimulation to induce plastic changes at the language motor area in a patient with a left recidivant brain tumor affecting Broca's area. *Neurocase.* (2012) 18:132–8. doi: 10.1080/13554794.2011.568500

7. Barcia JA, Sanz A, Balugo P, Alonso-Lera P, Brin JR, Yus M, et al. High-frequency cortical subdural stimulation enhanced plasticity in surgery of a tumor in Broca's area. *Neuroreport.* (2012) 23:304–9. doi: 10.1097/WNR.0b013e3283513307

8. Rivera-Rivera PA, Rios-Lago M, Sanchez-Casarrubios S, Salazar O, Yus M, González-Hidalgo M, et al. Cortical plasticity catalyzed by prehabilitation enables extensive resection of brain tumors in eloquent areas. *J Neurosurg.* (2017) 126:1323–33. doi: 10.3171/2016.2.JNS152485

9. Serrano-Castro PJ, Ros-López B, Fernández-Sánchez VE, García-Casares N, Muñoz-Becerra L, Cabezudo-Garcia P, et al. Neuroplasticity and epilepsy surgery in brain eloquent areas: case report. *Front Neurol.* (2020) 11:698. doi: 10.3389/fneur.2020.00698

10. Dadario N, Young I, Zhang X, Teo C, Doyen S, Sughrue M. Prehabilitation and rehabilitation using data-driven, parcel-guided transcranial magnetic stimulation treatment for brain tumor surgery: proof of concept case report. *Brain Netw Modulation.* (2022) 1:48–56. doi: 10.4103/2773–2398.340144

11. Buchbinder BR. Functional magnetic resonance imaging. *Handb Clin Neurol.* (2016) 135:61–92. doi: 10.1016/B978–0-444–53485-9.00004–0

12. Logothetis NK, Pauls J, Augath M, Trinath T, Oeltermann A. Neurophysiological investigation of the basis of the fMRI signal. *Nature.* (2001) 412:150–7. doi: 10.1038/35084005

13. Herting MM, Gautam P, Chen Z, Mezher A, Vetter NC. Test-retest reliability of longitudinal task-based fMRI: Implications for developmental studies. *Dev Cogn Neurosci.* (2018) 33:17–26. doi: 10.1016/j.dcn.2017.07.001

14. Sadraee A, Paulus M, Ekhtiari H. fMRI as an outcome measure in clinical trials: A systematic review in clinicaltrials.gov. *Brain Behav.* (2021) 11:e02089. doi: 10.1002/brb3.2089

15. Buckner RL, Andrews-Hanna JR, Schacter DL. The brain's default network: anatomy, function, and relevance to disease. *Ann N Y Acad Sci.* (2008) 1124:1–38. doi: 10.1196/annals.1440.011

16. Friston KJ, Frith CD, Liddle PF, Frackowiak RS. Functional connectivity: the principal-component analysis of large (PET) data sets. *J Cereb Blood Flow Metab.* (1993) 13:5–14. doi: 10.1038/jcbfm.1993.4

17. Ferreira LK, Busatto GF. Resting-state functional connectivity in normal brain aging. *Neurosci Biobehav Rev.* (2013) 37:384–400. doi: 10.1016/j.neubiorev.2013.01.017

18. Damoiseaux JS, Rombouts S a. RB, Barkhof F, Scheltens P, Stam CJ, Smith SM, et al. Consistent resting-state networks across healthy subjects. *Proc Natl Acad Sci U.S.A.* (2006) 103:13848–53. doi: 10.1073/pnas.0601417103

19. Fox MD, Raichle ME. Spontaneous fluctuations in brain activity observed with functional magnetic resonance imaging. *Nat Rev Neurosci.* (2007) 8:700–11. doi: 10.1038/nrn2201

20. Smith SM, Fox PT, Miller KL, Glahn DC, Fox PM, Mackay CE, et al. Correspondence of the brain's functional architecture during activation and rest. *Proc Natl Acad Sci U.S.A.* (2009) 106:13040–5. doi: 10.1073/pnas.0905267106

21. Zheng Y-Q, Farahibozorg S-R, Gong W, Rafipoor H, Jbabdi S, Smith S. Accurate predictions of individual differences in task-evoked brain activity from resting-state fMRI using a sparse ensemble learner. *NeuroImage.* (2022) 259:119418. doi: 10.1016/j.neuroimage.2022.119418

22. Parker Jones O, Voets NL, Adcock JE, Stacey R, Jbabdi S. Resting connectivity predicts task activation in pre-surgical populations. *NeuroImage: Clin.* (2017) 13:378–85. doi: 10.1016/j.nicl.2016.12.028

23. Liouta E, Katsaros VK, Stranjalis G, Leks E, Klose U, Bisdas S. Motor and language deficits correlate with resting state functional magnetic resonance imaging networks in patients with brain tumors. *J Neuroradiol.* (2019) 46:199–206. doi: 10.1016/j.neurad.2018.08.002

24. Boccuni L, Abellaneda-Pérez K, Martín-Fernández J, Leno-Colorado D, Roca-Ventura A, Prats Bisbe A, et al. Neuromodulation-induced prehabilitation to leverage neuroplasticity before brain tumor surgery: a single-cohort feasibility trial protocol. *Front Neurol.* (2023) 14:1243857. doi: 10.3389/fneur.2023.1243857

25. Brédart A, Anota A, Young T, Tomaszewski KA, Arraras JI, Moura De Albuquerque Melo H, et al. Phase III study of the European Organisation for Research and Treatment of Cancer satisfaction with cancer care core questionnaire (EORTC PATSAT-C33) and specific complementary outpatient module (EORTC OUT-PATSAT7). *Eur J Cancer Care (Engl).* (2018) 27. doi: 10.1111/ecc.12786

26. Pascual-Leone A, Walsh V, Rothwell J. Transcranial magnetic stimulation in cognitive neuroscience–virtual lesion, chronometry, and functional connectivity. *Curr Opin Neurobiol.* (2000) 10:232–7. doi: 10.1016/s0959–4388(00)00081–7

27. Devlin JT, Watkins KE. Stimulating language: insights from TMS. *Brain.* (2007) 130:610–22. doi: 10.1093/brain/awl331

28. Maeda F, Keenan JP, Tormos JM, Topka H, Pascual-Leone A. Modulation of corticospinal excitability by repetitive transcranial magnetic stimulation. *Clin Neurophysiol.* (2000) 111:800–5. doi: 10.1016/S1388–2457(99)00323–5

29. Maeda F, Keenan JP, Tormos JM, Topka H, Pascual-Leone A. Interindividual variability of the modulatory effects of repetitive transcranial magnetic stimulation on cortical excitability. *Exp Brain Res.* (2000) 133:425–30. doi: 10.1007/s002210000432

30. Ruffini G, Fox MD, Ripolles O, Miranda PC, Pascual-Leone A. Optimization of multifocal transcranial current stimulation for weighted cortical pattern targeting from realistic modeling of electric fields. *Neuroimage.* (2014) 89:216–25. doi: 10.1016/j.neuroimage.2013.12.002

31. Abellaneda-Pérez K, Vaqué-Alcázar L, Perellón-Alfonso R, Solé-Padullés C, Bargalló N, Salvador R, et al. Multifocal transcranial direct current stimulation modulates resting-state functional connectivity in older adults depending on the induced current density. *Front Aging Neurosci*. (2021) 13:725013. doi: 10.3389/fnagi.2021.725013

32. Solana J, Cáceres C, García-Molina A, Opisso E, Roig T, Tormos JM, et al. Improving brain injury cognitive rehabilitation by personalized telerehabilitation services: guttmann neuropersonal trainer. *IEEE J Biomed Health Inf*. (2015) 19:124–31. doi: 10.1109/JBHI.2014.2354537

33. Roig M, Skriver K, Lundbye-Jensen J, Kiens B, Nielsen JB. A single bout of exercise improves motor memory. *PloS One*. (2012) 7:e44594. doi: 10.1371/journal.pone.0044594

34. Mang CS, Snow NJ, Campbell KL, Ross CJD, Boyd LA. A single bout of high-intensity aerobic exercise facilitates response to paired associative stimulation and promotes sequence-specific implicit motor learning. *J Appl Physiol*. (2014) 117:1325–36. doi: 10.1152/japplphysiol.00498.2014

35. Wanner P, Cheng F-H, Steib S. Effects of acute cardiovascular exercise on motor memory encoding and consolidation: A systematic review with meta-analysis. *Neurosci Biobehav Rev*. (2020) 116:365–81. doi: 10.1016/j.neubiorev.2020.06.018

36. Jiao Y, Lin F, Wu J, Li H, Wang L, Jin Z, et al. A supplementary grading scale combining lesion-to-eloquence distance for predicting surgical outcomes of patients with brain arteriovenous malformations. *J Neurosurg*. (2018) 128:530–40. doi: 10.3171/2016.10.JNS161415

37. Krishnan R, Raabe A, Hattingen E, Szelényi A, Yahya H, Hermann E, et al. Functional magnetic resonance imaging-integrated neuronavigation: correlation between lesion-to-motor cortex distance and outcome. *Neurosurgery*. (2004) 55:904. doi: 10.1227/01.NEU.0000137331.35014.5C

38. Pak RW, Hadjiabadi DH, Senarathna J, Agarwal S, Thakor NV, Pillai JJ, et al. Implications of neurovascular uncoupling in functional magnetic resonance imaging (fMRI) of brain tumors. *J Cereb Blood Flow Metab*. (2017) 37:3475–87. doi: 10.1177/0271678X17707398

frontiers | Frontiers in Oncology

TYPE Case Report
PUBLISHED 24 May 2024
DOI 10.3389/fonc.2024.1399356

OPEN ACCESS

EDITED BY
Bo yuan Huang,
Capital Medical University, China

REVIEWED BY
Sandeep Batra,
Riley Hospital for Children, United States
Shannon Fortin Ensign,
Mayo Clinic Arizona, United States

*CORRESPONDENCE
Magimairajan Issai Vanan
mivanan@cancercare.mb.ca

RECEIVED 11 March 2024
ACCEPTED 07 May 2024
PUBLISHED 24 May 2024

CITATION
Brizini M, Drimes T, Bourne C, Streilein J, Drapeau A, Wrogemann J, Archer LA, Del Bigio M and Vanan MI (2024) Case report: Slipped capital femoral epiphysis: a rare adverse event associated with FGFR tyrosine kinase inhibitor therapy in a child. *Front. Oncol.* 14:1399356. doi: 10.3389/fonc.2024.1399356

Case report: Slipped capital femoral epiphysis: a rare adverse event associated with FGFR tyrosine kinase inhibitor therapy in a child

Meziane Brizini[1,2], Tina Drimes[3], Catherine Bourne[3], Jessica Streilein[4], Annie Drapeau[5], Jens Wrogemann[6], Lori Anne Archer[7], Marc Del Bigio[8] and Magimairajan Issai Vanan[1,2,9]*

[1]Division of Pediatric Hematology-Oncology, Cancer Care Manitoba, Winnipeg, MB, Canada, [2]Department of Pediatrics and Child Health, University of Manitoba, Winnipeg, MB, Canada, [3]Division of Nursing, Cancer Care Manitoba, Winnipeg, MB, Canada, [4]Division of Pharmacy, Cancer Care Manitoba, Winnipeg, MB, Canada, [5]Section of Neuro-Surgery, University of Manitoba, Winnipeg, MB, Canada, [6]Department of Radiology, University of Manitoba, Winnipeg, MB, Canada, [7]Section of Orthopedic Surgery, University of Manitoba, Winnipeg, MB, Canada, [8]Department of Pathology, University of Manitoba, Winnipeg, MB, Canada, [9]Paul Albrechtsen Research Institute, Cancer Care Manitoba, Winnipeg, MB, Canada

We report a case of slipped capital femoral epiphysis (SCFE), an on target skeletal toxicity of a pan-FGFR TKI inhibitor, erdafitinib. A 13-year-old boy was diagnosed to have an optic pathway/hypothalamic glioma with signs of increased intracranial pressure and obstructive hydrocephalus requiring placement of ventriculo-peritoneal (VP) shunt. Sequencing of the tumor showed FGFR1-tyrosine kinase domain internal tandem duplication (FGFR1-KD-ITD). He developed hypothalamic obesity with rapid weight gain and BMI >30. At 12 weeks of treatment with erdafitinib, he developed persistent knee pain. X-ray of the right hip showed SCFE. Erdafitinib was discontinued, and he underwent surgical pinning of the right hip. MRI at discontinuation of erdafitinib showed a 30% decrease in the size of the tumor, which has remained stable at 6 months follow-up. Our experience and literature review suggest that pediatric patients who are treated with pan-FGFR TKIs should be regularly monitored for skeletal side effects.

KEYWORDS

fibroblast growth factor receptor inhibitors, Slipped capital femoral epiphysis, On-target skeletal toxicity, Erdafitinib, hypothalamic obesity

Introduction

The cell surface receptor tyrosine kinases (RTKs) regulate fundamental cellular processes like cellular proliferation, differentiation, and survival through their signaling (1). Fibroblast growth factor receptor (FGFR) tyrosine kinase pathway signaling plays an important role in normal growth and development including metabolism and skeletal homeostasis (2). FGFR1–4 pathway alterations are rare in pediatric cancers (1%–3%) but are enriched in sarcomas and CNS tumors (3) where they account for 10% of pediatric low-grade gliomas and 4% of pediatric high-grade gliomas (4). FGFR tyrosine kinase inhibitors (FGFR-TKIs) are being increasingly used off-label in children with hard-to-treat tumors harboring specific FGFR alterations. This case report illustrates a rare but significant skeletal side effect of erdafitinib—a pan-FGFR inhibitor (2). Our case is an important addition to the recent literature (5) and informs pediatric oncologists to be monitoring for skeletal side effects when treating with FGFR-TKIs.

Case summary

A previously healthy 13-year-old boy presented to the emergency department (ED) with 1 day history of emesis and headaches. His initial neurological exam was unremarkable. He progressively became unresponsive in the ED, showing signs of increased intracranial pressure with bradycardia, non-reactive pupils, and urinary incontinence. An urgent computerized tomography (CT) scan of the head showed a large suprasellar mass with mass effect on foramen of Munro bilaterally with obstructive hydrocephalus. The mass extended into the region of the Sylvian aqueduct resulting in CSF obstruction, which was relieved by placement of bilateral external ventricular drains (EVDs). On further query, the father reported that the patient has been symptomatic with intermittent headaches associated with nausea and vomiting for the past 6 months.

After stabilization, baseline MRI showed rim-enhancing mass arising from the optic chiasm with mass effect on the pituitary infundibulum and perilesional edema involving the splayed cerebral peduncles and bilateral hypothalamus (Figures 1A–C). He was treated with Dexamethasone (1 mg, IV, QID) for increased intracranial pressure over 6 days and subsequently weaned off steroids over a week. Baseline investigations including renal/liver functions and endocrine tests including pituitary and thyroid functions tests were normal except for TSH of 0.3 mU/L (0.7–5.7 mU/L) with normal Free T3 and Free T4 values. The TSH values normalized in the subsequent follow-up visits. A ventriculo-peritoneal shunt was placed in the right lateral ventricle. Biopsy showed a histologically low-grade astrocytoma (WHO, Grade 1). TruSight RNA Pan-Cancer NGS panel showed FGFR1-tyrosine kinase domain internal tandem duplication (FGFR1-KD-ITD) (chromosome 8, exon 18–exon 10). The tumor was negative for BRAF mutation/fusion. Two weeks after biopsy, he presented to the ED with 1-week history of abdominal pain and was diagnosed with abdominal abscess due to VP shunt infection. The shunt was removed. CSF cultures grew *Staphylococcus aureus* (methicillin

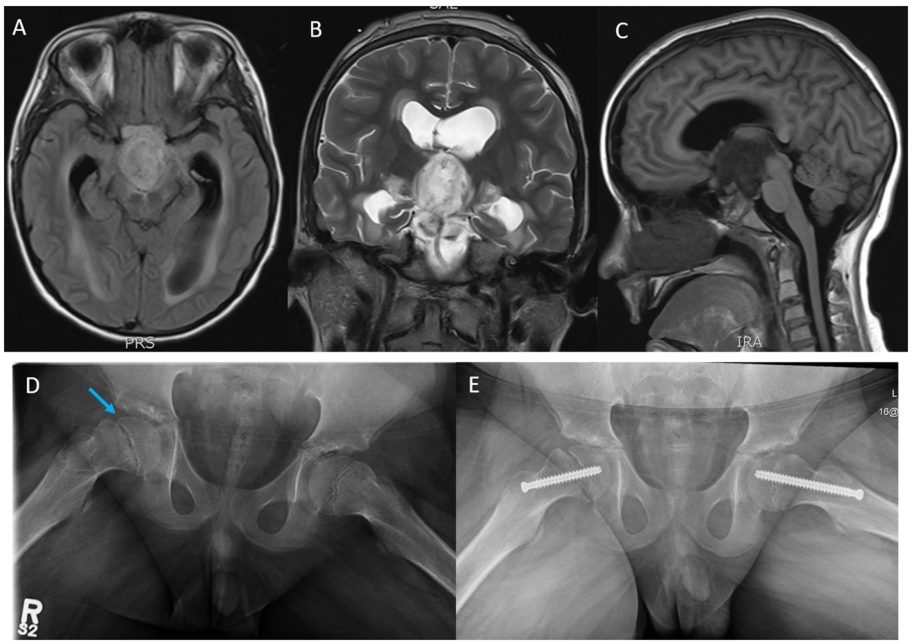

FIGURE 1
Magnetic resonance imaging (MRI); **(A)** axial T1 flair, **(B)** coronal T2, and **(C)** sagittal T1 flair images showing a rim-enhancing tumor mass likely arising from the Optic chiasm and extending into the third ventricle, the prepontine cistern, the interpeduncular cistern intermittent to the optic chiasm measuring 3.0 cm (AP) × 2.7 cm (CC) ×1.8 cm (T). **(D)** Plain X-ray films, open frog leg view showing inferior displacement of the right femoral capital epiphysis (blue arrow) relative to the femoral neck associated with widening of the proximal femoral growth plate and minimal joint effusion. **(E)** Surgical pinning to stabilize the capital epiphysis on the right hip and prophylactic pinning to prevent SCFE on the left hip.

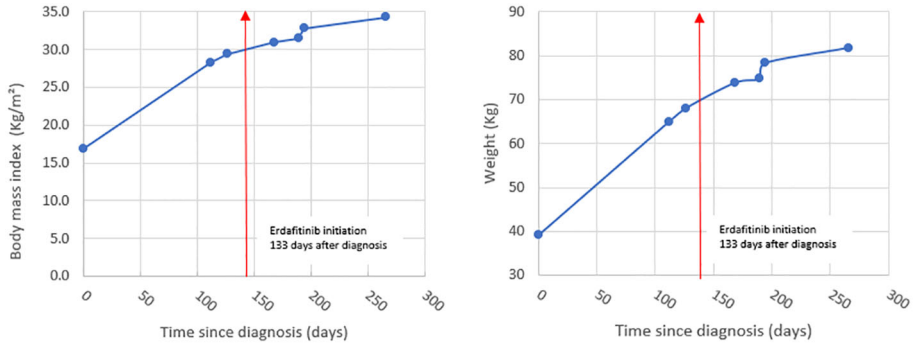

FIGURE 2
Graphs showing BMI and rate of weight gain in our patient.

sensitive, MSSA). He was subsequently treated with IV antibiotics for 6 weeks.

Our patient developed hypothalamic obesity due to the location of the tumor and the perilesional edema involving the hypothalamus at presentation (Figure 1C). This was clinically manifested by a voracious insatiable appetite and accelerated rate of weight gain (82.1 kg->97% percentile for age and sex) (Figure 2). After a 4-month delay from the initial diagnosis, he was started on erdafitinib 4.7mg/m^2/day (Janssen BioAdvance), a pan-FGFR1–4 inhibitor, through a special access program. Four weeks later, he developed nail side effects (discoloration and brittleness) and hyperphosphatemia requiring chelation. Erdafitinib was withheld for a week and restarted as per protocol. At approximately 7 weeks into therapy, he started complaining of intermittent pain in his right leg (knee and ankles), progressing to limping, difficult weight bearing, and complete cessation of ambulation. There was no history of trauma or past history of knee, leg, or hip pain. X-rays of the knee/ankles were reported as normal. At approximately 12 weeks of treatment, the persistent knee pain was suspected to be due to pathology of the hip with referred pain to the knee. X-ray of the hips (Figure 1D) showed slipped capital femoral epiphysis (SCFE) of the right hip. Erdafitinib was discontinued, and he underwent surgery with *in situ* pinning of the right hip and prophylactic pinning of the left hip (to prevent SCFE) (Figure 1E). MRI of the brain at the time of discontinuation of the medication showed a 30% decrease in the size of the tumor, which has remained stable on two subsequent follow-up MRIs.

Discussion

FGFR1–4 inhibitors are being frequently used for hard-to-treat pediatric cancers with FGFR alterations in both ongoing clinical trials (NCI-COG-Pediatric MATCH trial, Phase II, NCT03155620) (6) and off-label (3, 7). FGFR1 and FGFR3 signaling negatively regulates endochondral bone growth by inhibiting growth plate chondrocytes by suppressing mitogenic activity (8, 9). Inhibition of these receptors causes increased linear growth velocity in growing/immature skeleton and predisposes to bone- and joint-related complications (5). These complications are rare in adults, as their growth plates are fused resulting in minimal FGFR signaling in growth plate chondrocytes.

Tyrosine kinase inhibitors are increasingly being used in the treatment of pediatric cancers, and TKI-induced adverse effects have been frequently reported involving multiple organs, most commonly skin, gastrointestinal tract, blood, and cardiac side effects (10). Skeletal side effects of targeted therapies (TKIs, biological therapies) like osteonecrosis and fractures are summarized in a recent review by Konarski et al. (11). SCFE and other skeletal side effects as a complication of FGFR-selective inhibitors was recently reported by Sait et al. (5). In their series, all the three pediatric patients with SCFE had increased growth velocity (Table 1). Two of the three patients were also reported to have obesity. We did not see increased growth velocity in our patient (height between 25th and 50th percentile for age and sex). This could be probably explained by the short duration of erdafitinib treatment in our patient (12 weeks). The unfortunate delay in starting erdafitinib due to MSSA infection resulted in our patient being obese (BMI> 30, >99th percentile for age and sex) at the start of the drug. Obesity has been shown to be a strong and validated risk factor for SCFE (12, 13). Body Mass Index (BMI) >95th percentile for age and sex has a strong correlation with SCFE when compared to children with BMI <85th percentile for age and sex (14). Based on the rate of weight gain and the BMI, we decided to do prophylactic *in situ* pinning for the contralateral (left) hip to prevent SCFE (14).

Pan-FGFR1–4 inhibitors (like erdafitinib) are pharmacologically more potent when compared to FGFR1/2/3 inhibitors (like Debio1347): IC50 values (in nanomolar, nM) for erdafitinib and Debio1347 are as follows: FGFR1 (2.0 nM vs. 9.3 nM), FGFR2 (2.0 nM vs. 7.6 nM), and FGFR3 (4.0 nM vs. 22 nM) (15). The increased potency of erdafitinib in combination with other risk factors like obesity and hyperphosphatemia could probably explain the relatively early onset of SCFE in patients treated with Pan-FGFR1–4 inhibitor erdafitinib when compared to FGFR1/2/3 inhibitor Debio1347 (Table 1). The dose of erdafitinib for both patients in this series was based on the recommendations of the NCI-COG Pediatric MATCH, APEC1621B protocol, which is 4.7 mg/m^2/day (8 mg/1.7 m^2) up to a

TABLE 1 Characteristics of patients with SCFE treated with FGFR TKIs.

Patient number/ age (yrs)/sex	Tumor histology/site	FGFR alteration	Skeletal AEs	Non-skeletal AEs	DOT (months)	FGFRi
1) 8/F	Pilomyxoid astrocytoma/ Optic pathway	FGFR1 mutation (V592M, K687E)	SCFE (b/l hips), AVN of left hip, non-traumatic fractures (finger/hip)	Hyperphosphatemia	9	Debio1347
2) 14/M	Rosette-forming low-grade glioneuronal tumor/cerebellum	FGFR3–TACC3 fusion	SCFE (right hip), osteochondritis dissecans (b/l), coxa valga deformity (b/l)	Hyperphosphatemia	40	Debio1347
3) 12/M	Diffuse brainstem glioma/brainstem	FGFR2–VPS35 fusion	SCFE (right hip), non-traumatic fractures (b/l tibia, vertebral compression fractures)	Hyperphosphatemia	5	Erdafitinib
4) 13/M	Low-grade astrocytoma/ Optic pathway (chiasm)	FGFR1-TKD-ITD (exons 18,10)	SCFE (right hip)	Onycholysis (Grade III), hyperphosphatemia	3	Erdafitinib

AEs, Adverse events; AVN, avascular necrosis; DOT, duration of therapy; F, female; FGFR, fibroblast growth factor receptor; FGFRi, FGFR inhibitor; M, male; SCFE, slipped capital femoral epiphysis; Yrs, years; TACC, transforming acidic coiled coil; b/l, bilateral.
The first three patients are from Ref. 5.

maximum daily dose of 8 mg, orally, once daily (adult recommended phase II dose-RP2D adjusted for BSA).

Hyperphosphatemia, another on-target toxicity specific to FGFR TKIs, was seen in all the patients with SCFE (Table 1). Hyperphosphatemia can potentially contribute to the SCFE, as it can lead to increased bone turnover and bone fragility (16). Our patient did not receive any chemotherapy or radiation prior to starting erdafitinib. Patient 1 in the series was previously treated with chemotherapy (7), and this could have contributed to the SCFE in this patient (17).

Summary

We report a case of SCFE, an on-target skeletal toxicity of a pan-FGFR TKI inhibitor, erdafitinib. Central hypothalamic obesity, secondary to the location of the tumor along with hyperphosphatemia due to drug side effect, contributed to the accelerated onset of SCFE in our patient. Based on our experience and literature review (5) of pediatric patients who are treated with pan-FGFR TKIs, we recommend the following: a) monitor both rate of weight gain/BMI for obesity (especially in suprasellar tumors) and growth velocity while on therapy; b) promptly rule out on-target skeletal toxicities (fractures, SCFE, and osteochondritis) at the onset of clinical symptoms (knee, thigh, or groin pain) with appropriate diagnostic imaging (AP/frog leg lateral views of hip and knee X-rays); c) regular surveillance imaging of the hips to monitor for SCFE especially in pediatric patients with increased weight gain (suprasellar tumors) and/or growth velocity; and d) update the drug toxicity profile of FGFR TKIs to include skeletal toxicities and inform parents/patients of these toxicities at the time of consent for therapy.

Data availability statement

The original contributions presented in the study are included in the article/Supplementary Material. Further inquiries can be directed to the corresponding author.

Ethics statement

Written informed consent was obtained from the individual(s) for the publication of any potentially identifiable images or data included in this article.

Author contributions

MB: Conceptualization, Data curation, Formal analysis, Investigation, Writing – original draft. TD: Investigation, Resources, Writing – review & editing. CB: Investigation, Resources, Writing – review & editing. JS: Investigation, Resources, Writing – review & editing. AD: Conceptualization, Data curation, Investigation, Resources, Validation, Writing – review & editing. JW: Data curation, Resources, Validation, Writing – review & editing. LA: Data curation, Investigation, Resources, Validation, Writing – review & editing. MD: Data curation, Investigation, Resources, Validation, Writing – review & editing. MV: Conceptualization, Data curation,

Investigation, Resources, Supervision, Validation, Writing – original draft, Writing – review & editing.

Funding

The author(s) declare that no financial support was received for the research, authorship, and/or publication of this article.

Acknowledgments

We would like to thank Ms. Jessica Lafreniere form Janssen BioAdvance for helping us to obtain erdafitinib on a compassionate basis for our patient.

Conflict of interest

The authors declare that the research was conducted in the absence of any commercial or financial relationships that could be construed as a potential conflict of interest.

Publisher's note

References

1. Schlessinger J. Cell signaling by receptor tyrosine kinases. *Cell*. (2000) 103:211–25. doi: 10.1016/S0092-8674(00)00114-8

2. Brown LM, Ekert PG, Fleuren EDG. Biological and clinical implications of FGFR aberrations in paediatric and young adult cancers. *Oncogene*. (2023) 42:1875–88. doi: 10.1038/s41388-023-02705-7

3. De La Vega LL, Comeau H, Sallan S, Al-Ibraheemi A, Gupta H, Li YY, et al. Rare FGFR Oncogenic Alterations in sequenced Pediatric solid and brain tumors suggest FGFR is a relevant molecular target in childhood cancer. *JCO Precis Oncol*. (2022) 6: e2200390. doi: 10.1200/PO.22.00390

4. Zhang J, Wu G, Miller CP, Tatevossian RG, Dalton JD. Tang B et al: Whole-genome sequencing identifies genetic alterations in pediatric low-grade gliomas. *Nat Genet*. (2013) 45:602–12. doi: 10.1038/ng.2611

5. Farouk Sait S, Fischer C, Antal Z, Spatz K, Prince DE, Ibanez K, et al. Slipped capital femoral epiphyses: A major on-target adverse event associated with FGFR tyrosine kinase inhibitors in pediatric patients. *Pediatr Blood Cancer*. (2023) 70:e30410. doi: 10.1002/pbc.30410

6. Parsons DW, Janeway KA, Patton DR, Winter CL, Coffey B, Williams PM, et al. Actionable tumor alterations and treatment protocol enrollment of pediatric and young adult patients with refractory cancers in the national cancer institute-children's oncology group pediatric MATCH trial. *J Clin Oncol*. (2022) 40:2224. doi: 10.1200/JCO.21.02838

7. Farouk Sait S, Gilheeney SW, Bale TA, Haque S, Dinkin MJ, Vitolono S, et al. Debio 1347, an oral FGFR inhibitor: results from a single-center study in pediatric patients with current or refractory FGFR-altered Gliomas. *JCO Precis Oncol*. (2021) 5:876–83. doi: 10.1200/PO.20.00444

8. Deng C, Wynshaw-Boris A, Zhou F, Kuo A, Leder P. Fibroblast Growth Factor Receptor 3 is a negative regulator of bone growth. *Cell*. (1996) 84:911–21. doi: 10.1016/S0092-8674(00)81069-7

9. Wang Q, Green RP, Zhao G, Ornitz DM. Differential regulation of endochondral bone growth and joint development by FGFR1 and FGFR3 tyrosine kinase domains. *Development*. (2001) 128:3867–76. doi: 10.1242/dev.128.19.3867

10. Sunder SS, Sharma UC, Pokharel S. Adverse effects of tyrosine kinase inhibitors in cancer therapy: pathophysiology, mechanisms and clinical management. *Signal Transduct Target Ther*. (2023) 8:262. doi: 10.1038/s41392-023-01469-6

11. Konarski W, Pobozy T, Konarska K, Sliwczynski A, Kotela I, Krakowiak J. Exploring the impact of novel anti-cancer therapies on jaw osteonecrosis and other bones: A comprehensive review. *J Clin Med*. (2024) 13:1889. doi: 10.3390/jcm13071889

12. Loder RT. The demographics of slipped capital femoral epiphysis. *Clin Orthop Relat Res*. (1996) 322:8–27. doi: 10.1097/00003086-199601000-00003

13. Restrepo R, Reed MH. Impact of obesity in the diagnosis of SCFE and knee problems in obese children. *Pediatr Radiol*. (2009) 39:S220–225. doi: 10.1007/s00247-008-1123-3

14. Manoff EM, Banfy MB, Winell JJ. Relationship between Body Mass Index and slipped capital femoral epiphysis. *J Pediatr Orthop*. (2005) 25:744–6. doi: 10.1097/01.bpo.0000184651.34475.8e

15. Roskoski R. The role of fibroblast growth factor receptor (FGFR) protein-tyrosine kinase inhibitors in the treatment of cancers including those of the urinary bladder. *Pharmacol Res*. (2020) 151:104567. doi: 10.1016/j.phrs.2019.104567

16. Goyal R, Jialal I. Hyperphosphatemia. In: *StatPearls*. StatPearls Publishing, Treasure Island (FL) (2023).

17. Chung CH, Ko KR, Kim JH, Shim JS. Clinical and radiographic characteristics of atypical slipped capital femoral epiphysis. *J Pediatr Orthop*. (2019) 39:e742–9. doi: 10.1097/BPO.0000000000001339

frontiers | Frontiers in Neurology

TYPE Original Research
PUBLISHED 13 June 2024
DOI 10.3389/fneur.2024.1387743

OPEN ACCESS

EDITED BY
Hongbo Zhang,
Second Affiliated Hospital of Nanchang University, China

REVIEWED BY
Liang Shen,
Changzhou No. 2 People's Hospital, China
Siyi Wanggou,
Central South University, China

*CORRESPONDENCE
Xiaoxing Xiong
✉ xiaoxingxiong@whu.edu.cn
Liang Wei
✉ weiliang05@tkhealthcare.com

†These authors have contributed equally to this work

RECEIVED 18 February 2024
ACCEPTED 20 May 2024
PUBLISHED 13 June 2024

CITATION
Pu B, Feng S, Gu L, Smerin D, Jian Z, Xiong X and Wei L (2024) Exploring MAP2K3 as a prognostic biomarker and potential immunotherapy target in glioma treatment. *Front. Neurol.* 15:1387743. doi: 10.3389/fneur.2024.1387743

Exploring MAP2K3 as a prognostic biomarker and potential immunotherapy target in glioma treatment

Bei Pu[1,2†], Shi Feng[1†], Lijuan Gu[3], Daniel Smerin[4], Zhihong Jian[1], Xiaoxing Xiong[1*] and Liang Wei[2*]

[1]Department of Neurosurgery, Renmin Hospital of Wuhan University, Wuhan, China, [2]Transplantation Health Management Center, Sichuan Taikang Hospital, Chengdu, China, [3]Central Laboratory, Renmin Hospital of Wuhan University, Wuhan, China, [4]Department of Neurosurgery, University of Central Florida College of Medicine, Orlando, FL, United States

Glioma, the most prevalent primary brain tumor in adults, is characterized by significant invasiveness and resistance. Current glioma treatments include surgery, radiation, chemotherapy, and targeted therapy, but these methods often fail to eliminate the tumor completely, leading to recurrence and poor prognosis. Immune checkpoint inhibitors, a class of commonly used immunotherapeutic drugs, have demonstrated excellent efficacy in treating various solid malignancies. Recent research has indicated that unconventional levels of expression of the MAP2K3 gene closely correlates with glioma malignancy, hinting it could be a potential immunotherapy target. Our study unveiled substantial involvement of MAP2K3 in gliomas, indicating the potential of the enzyme to serve as a prognostic biomarker related to immunity. Through the regulation of the infiltration of immune cells, MAP2K3 can affect the prognosis of patients with glioma. These discoveries establish a theoretical foundation for exploring the biological mechanisms underlying MAP2K3 and its potential applications in glioma treatment.

KEYWORDS

glioma, immunotherapy, MAP2K3, tumor immune microenvironment, prognosis

Background

Glioma is the most common primary brain tumor and is a general term for a large group of intracranial primary tumors that occur from glial cells derived from neural ectoderm. Gliomas can be categorized as grade I–IV according to the World Health Organization (WHO) grading standards. Glioblastoma (GBM) is a high-grade glioma, defined as WHO grade IV, and is one of the most lethal gliomas. It makes up 70–75% of all diffuse gliomas, and GBM patients have a median survival time of about 14–17 months. The main treatment options are surgery, radiotherapy, temozolomide (TMZ) chemotherapy and radiotherapy combined with TMZ chemotherapy, but none of the treatment outcomes are satisfactory (1).

The surgical elimination of the tumor, followed by chemotherapy and radiation therapy, is the conventional treatment for glioblastoma. As a result of the extremely aggressive characteristics of glioma cells, complete removal of the tumor is currently difficult to achieve (2). The potential mechanisms of glioma migratory invasion remain to be further investigated (3). Immunotherapy is able to inhibit tumor growth and spread by activating the patient's own

immune system. Common immune cell types in glioma patients include T cells, B cells, dendritic cells, and natural killer cells; which are closely related to tumor immune escape and drug resistance (4). Immunotherapy has been demonstrated to improve patient survival as well as quality of life in glioma patients (5). Additionally, immunotherapy may be used together with more established treatments like radiation and chemotherapy to maximize therapeutic outcomes. Despite the clinical effectiveness of immunotherapy in the management of gliomas, additional investigation is required to address potential issues with immune escape and drug resistance (5).

Mitogen-activated protein kinase 3 (MAP2K3) is a member of the bispecific protein kinase kinases (MKK) group, which is found in the Mitogen-activated protein kinase pathway (MAPK) (6). The MAP2K3 protein was first discovered in 1996, and current research has focused on its role as an activator of the p38-MAPK signaling pathway (7). In the therapeutic studies of esophageal squamous cell carcinoma, MAP2K3 inhibitors have been reported to be effective in inhibiting cell growth. MAP2K3 can mediate cellular responses to external stimuli by phosphorylating and activating the p38-MAPK signaling pathway (8). When cells are subjected to external stimuli, activated MAP3K activates MAP2K3 to phosphorylate and activate the p38-MAPK signaling pathway. The downstream target proteins that are regulated by the active p38-MAPK signaling pathway are also regulating additional biological processes such as cell proliferation, differentiation, and apoptosis. p38-MAPK family proteins play complex and diverse roles in tumors (9, 10). In order to exert an anti-tumor effect, p38-MAPK activation may induce apoptosis and cell cycle arrest in a tumor cell (11). In addition, it has been shown that the p38-MAPK protein can regulate activity of the extracellular signal-regulated kinases 1 and 2 (ERK1/2) and the phosphoinositide 3-kinase/Akt (PI3K/AKT) signaling pathways, which in turn promotes tumor cell proliferation and growth (12). The p38-MAPK signaling pathway may promote tumor growth by regulating inflammatory responses and angiogenesis in the tumor microenvironment (11). Additionally, this pathway contributes to immunomodulation in the tumor microenvironment. The p38-MAPK signaling pathway can support immunological functions like tumor immune surveillance and immune antigen presentation by modulating the activity of immune cells and the production of immune components (13). p38-MAPK signaling pathway activation can promote the production and secretion of cytokines, such as interferon gamma (IFN-γ), interleukin 6 (IL-6), tumor necrosis factor alpha (TNF-α), and interleukin 1 (IL-1), which can promote the activation of immune cells and an immune response (6). In addition, the p38-MAPK signaling pathway can also regulate the activity of antigen-presenting cells, such as macrophages, to enhance the immune response (6). Therefore, a thorough investigation of the function of the MAP2K3 gene, which is closely associated with the p38-MAPK signaling pathway, in the immune microenvironment of glioma tumors may be helpful in understanding the mechanisms underlying glioma development and growth, and result in the development of novel therapeutic methods and targets.

In our study, MAP2K3 expression was discovered to be aberrantly high in a range of tumor tissues, and such high expression was found to be associated with poor clinicopathological characteristics and outcome of gliomas. We found that the genes related to MAP2K3 were primarily enriched in immunomodulatory pathways through functional and pathway enrichment analysis. Finally, we discovered a relationship between MAP2K3 expression and immunological checkpoints, immune-related genes, and immune infiltration in glioma. Taken together, our research highlights the critical function of MAP2K3 in tumor immune modulation and glioma prognosis; indicating the MAP2K3 gene as a potential novel target for the treatment of glioma (see Table 1).

Materials and methods

Collection of data and analysis of MAP2K3 expression

In this study, clinically relevant mRNA expression profile datasets were obtained from the public databases the Gene Expression Omnibus (GEO), the Chinese Glioma Genome Atlas (CGGA), and The Cancer Genome Atlas (TCGA). We utilized the R software for the initial processing of gene expression profiles, which encompassed tasks such as background correction, normalization, and Log 2 transformation. Subsequently, to evaluate the presence of MAP2K3 in gliomas and various other tumors, we used the TIMRE database. This allowed us to investigate MAP2K3 expression levels in tumor samples, juxtaposed with their corresponding healthy tissues. Using the GEPIA (Gene Expression Profiling Interactive Analysis) website, we also investigated the expression of MAP2K3 in low grade glioma (LGG), GBM, and normal tissues. The expression of MAP2K3 in gliomas of different WHO classifications was examined. Using the Human Protein Atlas website, we evaluated the amounts of MAP2K3 protein expression in glioma and normal brain tissues as well as the location of MAP2K3 protein in glioma cells.

Analysis of MAP2K3 protein expression levels in gliomas

We used immunohistochemistry to evaluate the differential expression levels of MAP2K3 protein in glioma tissue compared to normal brain tissue. Images from immunohistochemical staining of normal brain tissue, LGG, and HGG were separately sourced from The Human Protein Atlas database, specifically the cerebral cortex section.

TABLE 1 Summary of the relevant databases.

Name of database	Link
CGGA	http://www.cgga.org.cn/
CancerSEA	http://biocc.hrbmu.edu.cn/CancerSEA/
TIMRE	https://cistrome.shinyapps.io/timer/
GEPIA website	http://gepia.cancer-pku.cn/index.html
Ivy Glioblastoma Atlas Project	https://glioblastoma.alleninstitute.org/
UCSC	https://xenabrowser.net/datapage/
TIGER	http://tiger.canceromics.org/
The Human Protein Atlas	https://www.proteinatlas.org
TCGA	https://cancergenome.nih.gov/
TISCH (14)	http://tisch.comp-genomics.org/home/

The antibody used for immunohistochemistry was anti-MAP2K3 primary antibody (HPA043783).

Evaluation of MAP2K3's prognostic significance in glioma

In this study, both univariate and multivariate Cox regression analyses were performed to determine whether MAP2K3 might be employed as an independent prognostic factor for glioma. WHO categorization, IDH status, gender, 1p/19q code, and age were clinical variables included in the Cox regression analysis (15). The R package "rms" was used to generate column line plots and calibration. To predict overall survival (OS) at 1, 3, and 5 years, we used the "survivor" package. We utilized the "pROC" R tool to generate AUC curves for the ROC study. We additionally investigated the relationship between MAP2K3 and Overall Survival (OS) and Progress Free Survival (PFS) in several clinical cohorts with LGG and GBM.

Gene set variation analysis

In Gene Set Variation Analysis (GSVA), the distribution of genes in a predefined set of genes is used to assess their trends in a table of phenotypically related ordered genes to determine their role in phenotype definition. To investigate the biological significance of MAP2K3, the "GSVA" package in R was used in this study to perform GSVA analysis. Based on their mRNA expression levels, MAP2K3 was split into low and high expression groups to identify the functional and pathway significance differences between the two groups. We downloaded "h.all.v7.2.symbols" and "c2.cp.kegg.v7.2.symbols" from the MsigDB database as reference gene sets for GMT (Hallmarks) and KEGG pathways, respectively. The "Limma" program was used to analyze the differences in GSVA pathways between patients in the high and low MAP2K3 groups, with adjusted criteria of $p < 0.05$ and abs (log2FC) > 0.3. Through heat maps, we displayed the Hallmarks and KEGG differential pathways individually.

Evaluation of immunological microenvironment and tumor immune cell infiltration

In order to figure out immune, stromal, and ESTIMATE scores; our study first examined immune and stromal cell types according to gene expression profiling using the "ESTIMATE" R package. Then, we assessed the correlation between the MAP2K3 gene and various immune cell levels using the CIBERSORT and ssGSEA algorithms, and discovered a link between the level of MAP2K3 expression and the infiltration of various immune cell types.

Evaluation of immunotherapy-related predictors

In this study, we compared the expression of several immunological checkpoints in the groups with high and low levels of MAP2K3 expression. The Wilcoxon rank sum test was used to evaluate the differences in immune checkpoint expression between the high MAP2K3-expressing and low MAP2K3-expressing groups. In order to demonstrate the sensitivity of the relevant subgroups to immune checkpoint inhibitor (ICI) therapy, we calculated the Tumor Immune Dysfunction and Exclusion TIDE (TIDE) scores for the high MAP2K3 expression group and the low MAP2K3 expression group. TIDE scores are used to assess the effectiveness of immunotherapy, with high TIDE scores indicating high tumor tolerance to immune checkpoint inhibitor therapy and low TIDE scores indicating better treatment outcomes. We then calculated the interferon gamma (IFNG) score, T cell receptor abundance (TCR), TCR Shannon score, microsatellite instability (MSI) and single nucleotide variant (SNV) neoantigens from TCGA. These metrics can be used to predict the ability of T cells in the immune microenvironment to exert tumor suppression and calculate levels of tumor neoantigens.

Somatic cell mutation analysis

In this study, somatic mutations and copy number alterations (CNAs) were downloaded from the TCGA database, and VarScan2 software was used to whole-genome sequence data of somatic mutations in the high MAP2K3 expression group and low MAP2K3 expression group. The Fisher's exact test was used to discover various mutation patterns, the CoMEt algorithm was utilized to find both co-occurring and mutated genes, and $p < 0.05$ was established as the threshold for choosing differentially mutated genes. For the purpose of visualizing somatic mutations, "maftools" was a R package.

Single-cell sequencing to assess MAP2K3 expression levels in gliomas

CancerSEA and TISCH, two single-cell sequencing data platforms, were employed to evaluate MAP2K3 expression at the single-cell level in gliomas.

In vitro validation of MAP2K3's function in glioma

U251 glioma cells were cultured in Dulbecco's Modified Eagle Medium supplemented with 10% fetal bovine serum and 1% penicillin-streptomycin, maintained at 37°C with 5% CO_2. For gene silencing, cells underwent transfection with siRNA targeting MAP2K3 and a control siRNA from GenePharma (Shanghai, China), using Lipofectamine 3,000 as per manufacturer's guidelines. MAP2K3 knockdown was verified by qRT-PCR 48 h post-transfection using specific primers (16). The primers used were as follows: for MAP2K3; Forward: GACTCCCGGACCTTCATCAC, Reverse: GGCCCAGTTC TGAGATGGT, and for GAPDH; Forward: TGTGGGCATCAA TGGATTTGG, Reverse: ACACCATGTATTCCGGGTCAAT. The CCK-8 kit was deployed to ascertain the viability of U251 cells, as well as the survival of U251 cells.

Wound healing assay

Cellular migration was assessed using a wound healing assay. Cells seeded in 6-well plates were grown to confluence, and a sterile 200 µL pipette tip was used to scratch a line through the monolayer. After washing away debris with phosphate-buffered saline, the cells were incubated in serum-free medium. Images were captured at 0 and 24 h post-scratch using an inverted microscope, and the rate of migration was quantified by measuring the gap with ImageJ software.

Transwell migration assay

For the Transwell migration assay, cells were suspended in serum-free medium (1×10^5 cells/mL) and 100 µL was placed into the upper chamber of a Transwell insert (Corning, United States). The lower chamber contained 600 µL of medium with 10% fetal bovine serum as a chemoattractant. Following a 24 h incubation at 37°C and 5% CO_2, cells on the upper membrane were removed, while those on the lower surface were fixed, stained with crystal violet, and counted in five fields under a light microscope.

Statistical analysis

The Wilcoxon test was used in this study to compare the differences in MAP2K3 expression between normal tissues and gliomas in the dataset obtained from the GEO database. We compared the variations in MAP2K3 expression in gliomas of various WHO classifications using the data acquired from TCGA and the Kruskal–Wallis test. To examine the association between survival and MAP2K3 expression levels, Kaplan–Meier curves were used.

Results

MAP2K3 is differentially expressed in gliomas and multiple other tumors

To explore the expression pattern of MAP2K3 in gliomas, we first analyzed the expression of MAP2K3 in tumor tissues. We used the TIMER database to explore the expression of MAP2K3 in 33 human cancers and found that MAP2K3 was expressed in multiple tumors (Figure 1A). The HR values of the MAP2K3 gene in LGG and GBM were higher than 1, suggesting that high MAP2K3 expression is associated with an increased risk of LGG and GBM occurrence (Figure 1D). We also used the GEPIA2 website to examine the TCGA database in order to investigate the expression of MAP2K3 in gliomas and healthy brain tissues. The findings demonstrated that GBM had higher levels of MAP2K3 mRNA expression than normal brain (Figure 1B). In addition, the expression level of MAP2K3 in gliomas correlated with the WHO grade of glioma, and the expression level of MAP2K3 in gliomas increased with the grade of glioma (Figure 1C). We found higher levels of MAP2K3 expression in multiple glioma cohorts with WHO grade 3 gliomas than WHO grade 2 (Figures 1G–K). MAP2K3 expression levels were also upregulated in the single-cell EXP0059 glioma cell group (Figures 1E,F).

We then assessed the protein expression level of MAP2K3 in gliomas using The Human Protein Atlas database. According to the results of immunohistochemical staining, glioma tissues generally express more MAP2K3 than healthy brain tissues do, and high-grade gliomas express more of the MAP2K3 protein (Figure 1L). We evaluated the localization of MAP2K3 protein in the glioma cell line SH-SY5Y, and the results showed that MAP2K3 was localized in the cytoplasm (Figure 1M). These results show that MAP2K3 is substantially expressed in both high-grade and low-grade gliomas, and that its expression level rises with increasing WHO grades. This suggests a potential association between MAP2K3 and the malignant behavior of gliomas.

Patient prognosis is correlated with MAP2K3 expression in gliomas

By analyzing multiple GBM cohorts and LGG cohorts, we found that MAP2K3 expression levels differed among glioma patients by age, 1p/19q co-deletion and gender; with higher MAP2K3 expression levels in young and middle-aged (<60 years), 1p/19q non-co-del, and male glioma patients (Figures 2A–K).

To investigate whether high expression of MAP2K3 could be an independent predictor of glioma prognosis, univariate and multivariate Cox regression analyses were conducted. Univariate Cox regression analysis showed that MAP2K3 expression, WHO staging, and age were associated with the prognosis of glioma (Figure 3A). Multivariate Cox regression analysis revealed that MAP2K3 expression, WHO staging, and age were independent prognostic factors affecting glioma prognosis (Figure 3B). Furthermore, by performing Cox regression analysis on multiple GBM cohorts and multiple LGG cohorts, we found that the MAP2K3 gene was a significant risk factor for poor patient prognosis (Figures 3C,D).

We discovered through a multiple cohort survival study that patients with high expression levels of MAP2K3 had shorter overall survival, regardless of whether they had high- (Figures 4A–I) or low-grade gliomas (Figures 4J–N). The Nomogram and calibration curves demonstrate that MAP2K3 is an independent prognostic factor that accurately predict patient prognosis at 1, 3, and 5 years; indicating that MAP2K3 is a good predictor of prognosis for glioma patients in the multiple regression model (Figure 4O). Time-dependent analysis of ROC showed AUC values of 0.89, 0.92, and 0.92 for glioma at 1, 3, and 5 years, respectively, indicating a high predictive power (Figure 4P). As a result, MAP2K3 may be employed as a glioma diagnostic marker. These results all point to MAP2K3's prognostic potential in gliomas.

The potential biological mechanism of MAP2K3 in glioma

To investigate the potential biological mechanisms of MAP2K3 in gliomas, we explored the function of MAP2K3 molecules in multiple cancer-related signaling pathways in the TCGA cohort. To analyze Hallmarker pathway differences between gliomas with two different MAP2K3 expression levels (17), we performed GSVA gene enrichment analysis. "Inflammatory response," "interferon gamma response," "NF-κB/TNFA signaling pathway," "complement," "IL6/JAK/STAT3

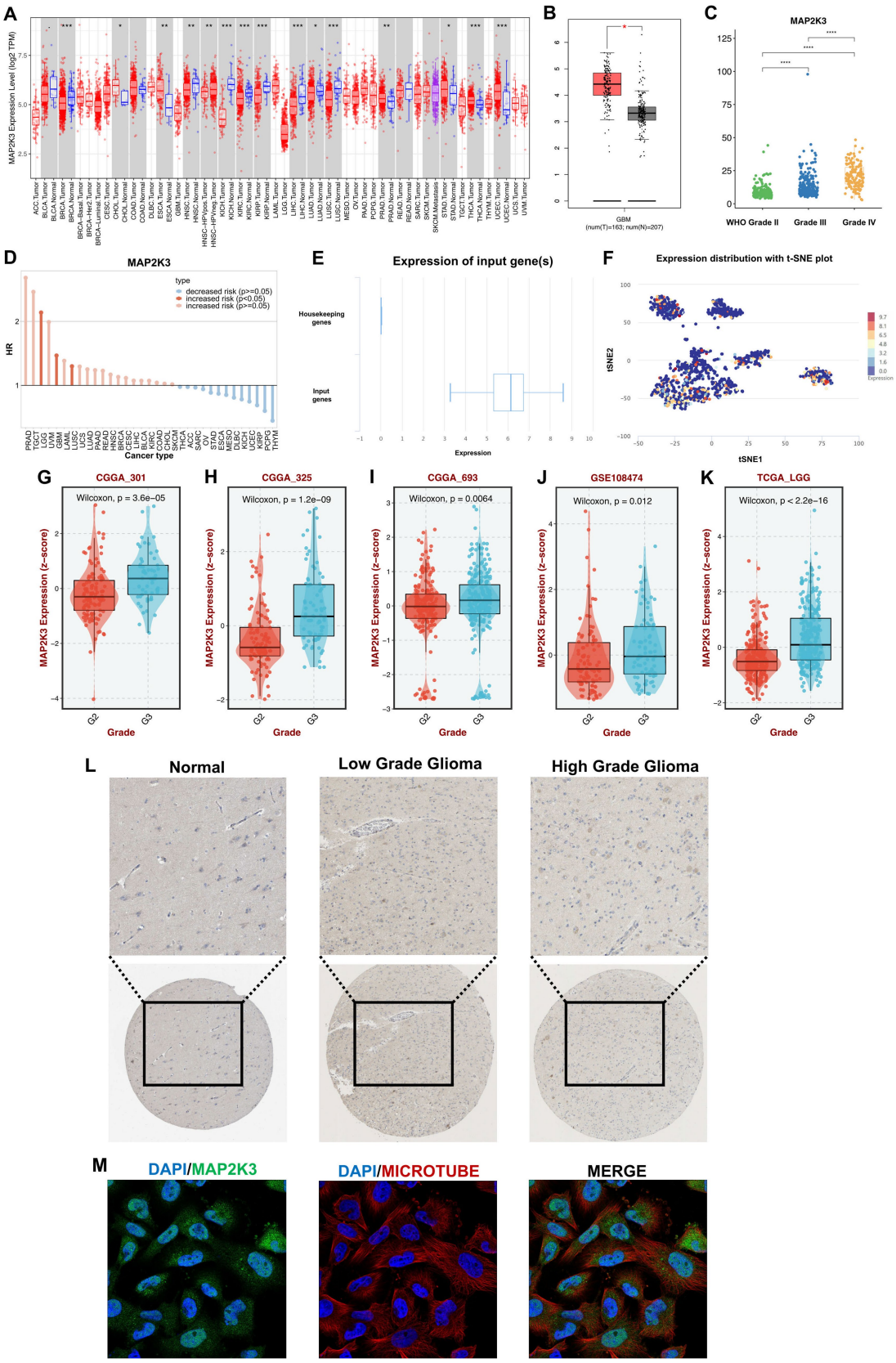

FIGURE 1
MAP2K3 is differentially expressed in gliomas. **(A)** MAP2K3 is differentially expressed in pan-cancer (*$p < 0.05$, **$p < 0.01$, and ***$p < 0.001$, Wilcoxon test). **(B)** MAP2K3 is differentially expressed between GBM and normal patients (*$p < 0.05$, **$p < 0.01$, and ***$p < 0.001$, Wilcoxon test). **(C)** MAP2K3 is differentially expressed among three WHO grades (*$p < 0.05$, **$p < 0.01$, and ***$p < 0.001$, Wilcoxon test). **(D)** Prognostic significance of MAP2K3 in pan-

(Continued)

FIGURE 1 (Continued)

cancer. **(E)** MAP2K3 is highly expressed compared with housekeeping genes. The box plot illustrates the distribution of MAP2K3 gene expression in the glioma EXP0059 dataset. **(F)** The t-SNE plot showed the expression distribution of MAP2K3. T-SNE describes the distribution of cells, every point represents a single cell, and the color of the point represents the expression level of MAP2K3 in the cell. **(G–K)** MAP2K3 is differentially expressed in CGGA301 **(G)**, CGGA325 **(H)**, CGGA693 **(I)**, GSE108474 **(J)**, and TCGA-LGG **(K)** cohorts. **(L)** Representative images of MAP2K3 among different grades in immunohistochemistry. **(M)** Immunofluorescence staining of MAP2K3 in the SH-SY5Y cell line.

signaling pathway," and "interferon α response," which are vital for inflammatory and immunological responses, were significantly elevated. This suggests that high MAP2K3 expression levels are closely related to immune-related signaling pathways (Figure 5A). To further explore the biological pathways of gliomas at both MAP2K3 expression levels, we performed KEGG enrichment analysis on the high MAP2K3-expressing and low MAP2K3-expressing groups of the TCGA cohort. We discovered that the group with high MAP2K3 expression was primarily related to "autoimmune thyroid disease," "IgA-producing intestinal immune network," "systemic lupus erythematosus," and "antigen processing and presentation." The MAP2K3 expression group was mainly associated with "autoimmune thyroid disease," "IgA producing intestinal immune network," "systemic lupus erythematosus," "antigen processing and presentation" and other processes related to immune response (Figure 5B). These findings all point to MAP2K3's potential involvement in immune-related pathways in gliomas.

Based on previous publications, we performed ssGSEA enrichment scoring of 10 classical oncogenic signaling pathways for two MAP2K3 expression levels in TCGA_GBM and LGG cohorts. Scoring signaling pathways including Wnt, TP53, TGF, RAS, PI3K, NRF2, NOTCH, MYC, cell cycle, and Hippo pathways. Based on the enrichment analysis outcomes, groups with higher MAP2K3 expression demonstrated elevated scores in several signaling pathways; namely the Hippo, NRF2, PI3K, and TGF pathways (Figures 5C,D). Each of these pathways are known to be closely intertwined with tumor immune evasion responses (18–22).

MAP2K3-associated somatic mutations in glioma

We analyzed somatic mutations in glioma patients from the TCGA cohort to investigate the mechanisms associated with MAP2K3 expression levels. Non-synonymous mutations are mutations that result in altered amino acid sequences (23). Some nonsynonymous mutations lead to mutations in tumor-associated genes, which may result in enhanced cell proliferation and invasiveness. Synonymous mutations are mutations in which genomic variants do not lead to amino acid sequence alterations (24). Although synonymous mutations do not directly alter the structure and function of proteins, they may affect the expression level and regulation of proteins. These aberrantly expressed proteins or peptides can be recognized by the immune system as allosteric antigens, triggering an immune response. Many tumor somatic mutations can be targets for immunotherapy and thus improve the therapeutic effect. Studying mutations in tumor cells and uncovering mutation-related molecular mechanisms can provide important references and guidance for immunotherapy and prognosis of tumors (25). In comparison to the low MAP2K3 expression group, more mutations were discovered in the high MAP2K3 expression group (Figure 6A), including non-synonymous mutations (Figure 6B) and synonymous mutations (Figure 6C).

We further analyzed the mutation frequencies of the nine most mutated genes (NF1, FUBP1, EGFR, PTEN, TTN, CIC, ATRX, TP53, IDH1) in glioma somatic cells both in the groups with high MAP2K3 expression and those with low MAP2K3 expression. Forest plots showed that IDH1, CIC, ATRX, FUBP1, and TP53 mutation frequencies were significantly higher in the low MAP2K3 expression group; while PTEN, EGFR, NF1, and TTN mutation frequencies were higher in the high MAP2K3 expression group (Figure 6D). Among them, EGFR mutations can inhibit tumor immune response through various mechanisms, such as reducing the number and function of antigen-presenting cells, decreasing T-cell infiltration and activation, and increasing the number of immunosuppressive cells (26). In addition, we observed a large number of co-occurrence of tumor-associated genes in these genes; such as NF1 and TTN, PTEN; FUBP1 and IDH1, CIC; EGFR and TTN, PTEN; PTEN and TTN; CIC and IDH1; ATRX and IDH1, TP53; TP53 and IDH1, which may indicate that these genes are interdependent or synergistic and have important roles in tumorigenesis and development (Figure 6E).

Relationship between glioma immune cell infiltration and MAP2K3 expression level

Since tumor progression and suppression are closely related to immunity, we investigated the differences in the immune microenvironment of tumors at different MAP2K3 expression levels (27, 28). First, we explored the differences in immune checkpoints and immunomodulatory factors at different MAP2K3 expression levels. By analyzing the effect of MAP2K3 expression levels on chemokines in the tumor immune microenvironment, the results showed elevated expression of several chemokines in the MAP2K3 high expression group; such as CXCL10, CCR5, CCR10, CCL5, CCL7, CCR2, and CCL22 (Figure 7A, upper part). Previous studies have shown that these chemokines exert immunosuppressive effects by attracting immunosuppressive cells, such as regulatory T cells (Tregs), macrophages, myeloid-derived suppressor cells (MDSCs) and monocytes, which may play an important role in the immune escape of gliomas. Furthermore, the analysis revealed increased expression of interferon receptors, interleukins, interleukin receptors and some other cytokines in the high MAP2K3 expression group. In contrast, immunomodulatory factor levels were significantly lower in the low MAP2K3-expressing group (Figure 7A, middle and lower part). We further calculated the overall immune cell infiltration abundance using the ssGSEA and CIBERSORT algorithms. By analyzing the gene expression patterns of immune cells, the analysis showed that more immune cells with significant immunosuppressive functions, such as Th2 cells, MDSCs, Treg cells, and M2-type macrophages, were present in the high MAP2K3 expression group, which were closely associated

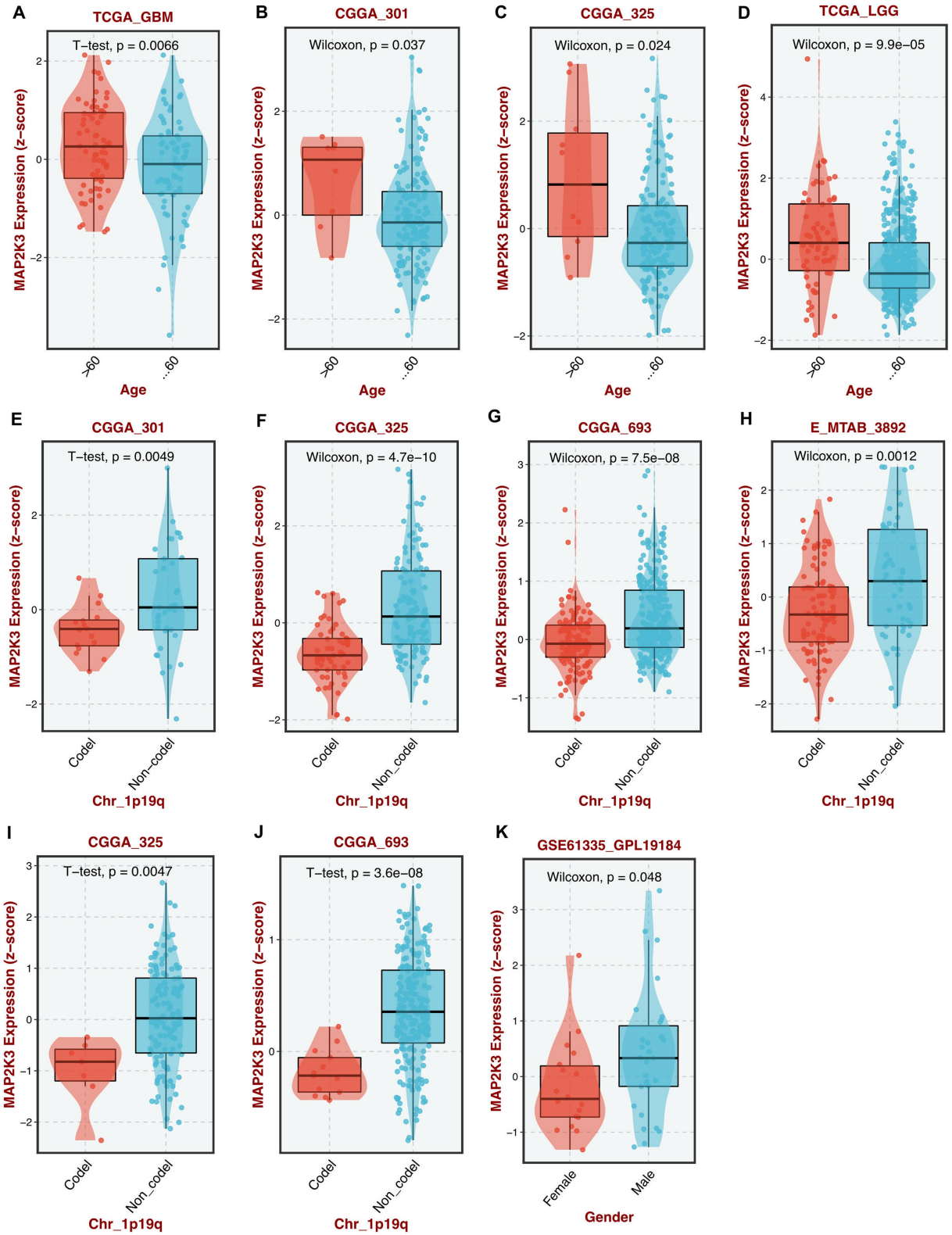

FIGURE 2
Differential expression of MAP2K3 in different clinical features. **(A–D)** MAP2K3 is differentially expressed between different ages in TCGA-GBM **(A)**, CGGA301 **(B)**, CGGA325 **(C)**, and TCGA-LGG **(D)** cohorts. **(E–J)** MAP2K3 is differentially expressed between different 1p19q status in CGGA301 **(E)**, CGGA325 **(F)**, CGGA693 **(G)**, E-MTAB-3892 **(H)**, CGGA325 **(I)**, and CGGA693 **(J)** cohorts. **(K)** MAP2K3 is differentially expressed between different genders in GSE61335 cohort (*$p < 0.05$, **$p < 0.01$, and ***$p < 0.001$, Wilcoxon test).

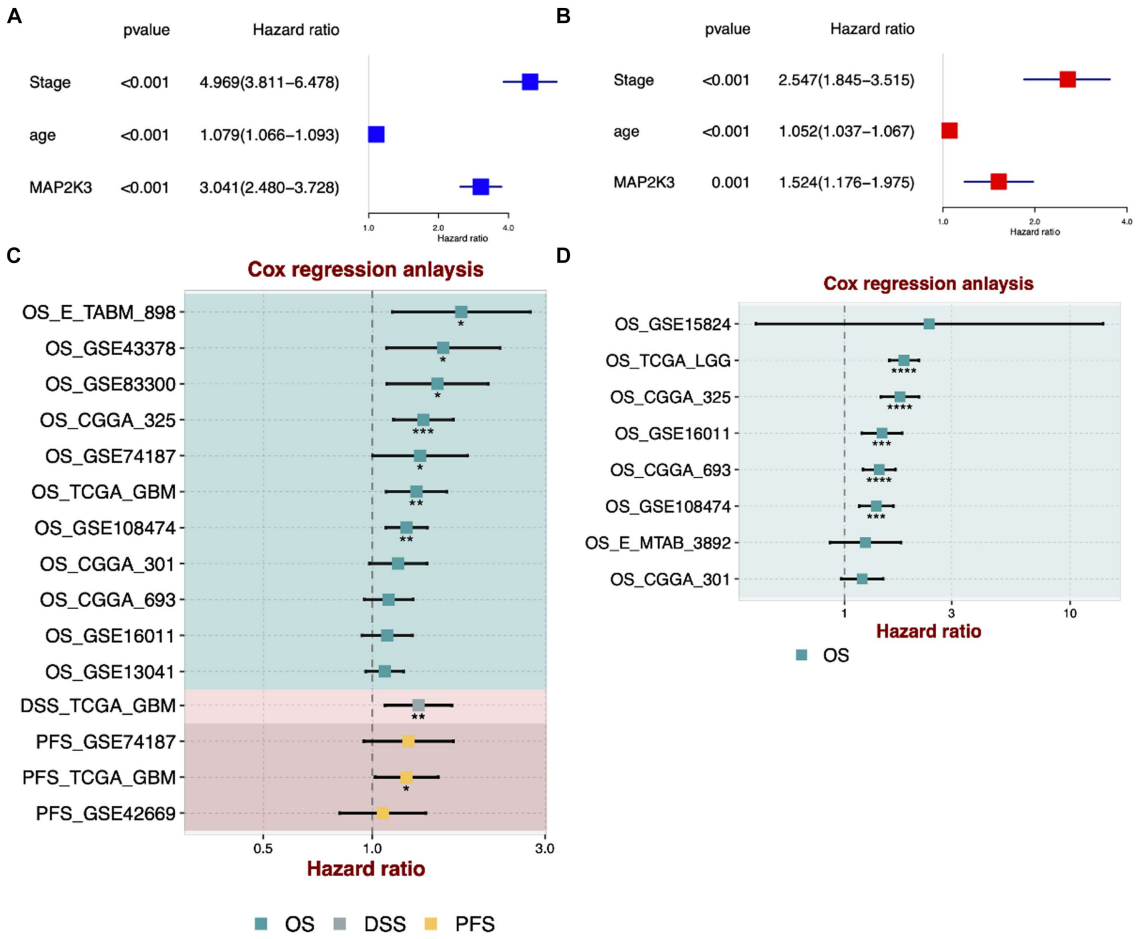

FIGURE 3
Prognostic significance of MAP2K3 in multi-center cohorts. **(A)** Univariate Cox regression analysis of Stage, age, and MAP2K3 expression. **(B)** Multivariate Cox regression analysis of Stage, age, and MAP2K3 expression. **(C)** Univariate Cox regression analysis of MAP2K3 expression in multi-center GBM cohorts. **(D)** Univariate Cox regression analysis of MAP2K3 expression in multi-center LGG cohorts.

with immune escape, drug resistance, and poor prognosis of the tumor. Notably, $CD8^+$ T cells, naive B cells, memory B cells, M1-type macrophages, resting natural killer (NK) cells and neutrophils were also enriched in the high MAP2K3-expressing group; suggesting that the group with high MAP2K3 expression has a significant number of immune cells and immunological-related factors. Therefore, the high MAP2K3-expressing group potentially could respond well to the recognition and attack of the immune system, thereby allowing for better results in immunotherapy may have better results (Figure 7B, middle part; Figure 7O).

Relationship between the glioma's immune microenvironment and MAP2K3 expression levels

Seven immune checkpoint molecules were expressed at higher levels in the high MAP2K3 expression group compared to the low MAP2K3 expression group, including CD274 (PD-L1), CD247, PDCD1, TNFRSF4, PDCD1LG2, TLR9, PDCD1, and CTLA4 (Figure 7B, upper part). This result suggests that the high MAP2K3 expression group expressed higher levels of immune checkpoint molecules to evade an activated anti-tumor immune response. For the antitumor immune response to effectively kill tumor cells, tumor immunotherapy must complete a series of steps and be allowed to iterate and expand, which is referred to as the tumor immune cycle. We calculated scores for the seven tumor immune cycle steps using ssGSEA. The analysis showed that all seven tumor immune cycle steps were scored higher in the high MAP2K3 expression group, which validates the important impact of the MAP2K3 gene on the tumor immune microenvironment (Figure 7B, bottom part).

We also used the TIDE algorithm and ESTIMATE algorithm to compare the relevant differences in the tumor immune microenvironment between the two MAP2K3 expression levels to quantify the association between MAP2K3 expression levels and potential immunotherapeutic effects. As can be seen, the high MAP2K3 expression group had higher stromal scores and immune scores and lower tumor purity, indicating that the high MAP2K3 expression group had a more active immune microenvironment relative to the low MAP2K3 expression group (Figure 7B, top part; Figures 7K,L). Next, using the TIDE algorithm, we found that the high MAP2K3-expressing group showed higher TIDE scores and exclusion scores (Figure 7B, top part; Figures 7I,J), which is consistent with the

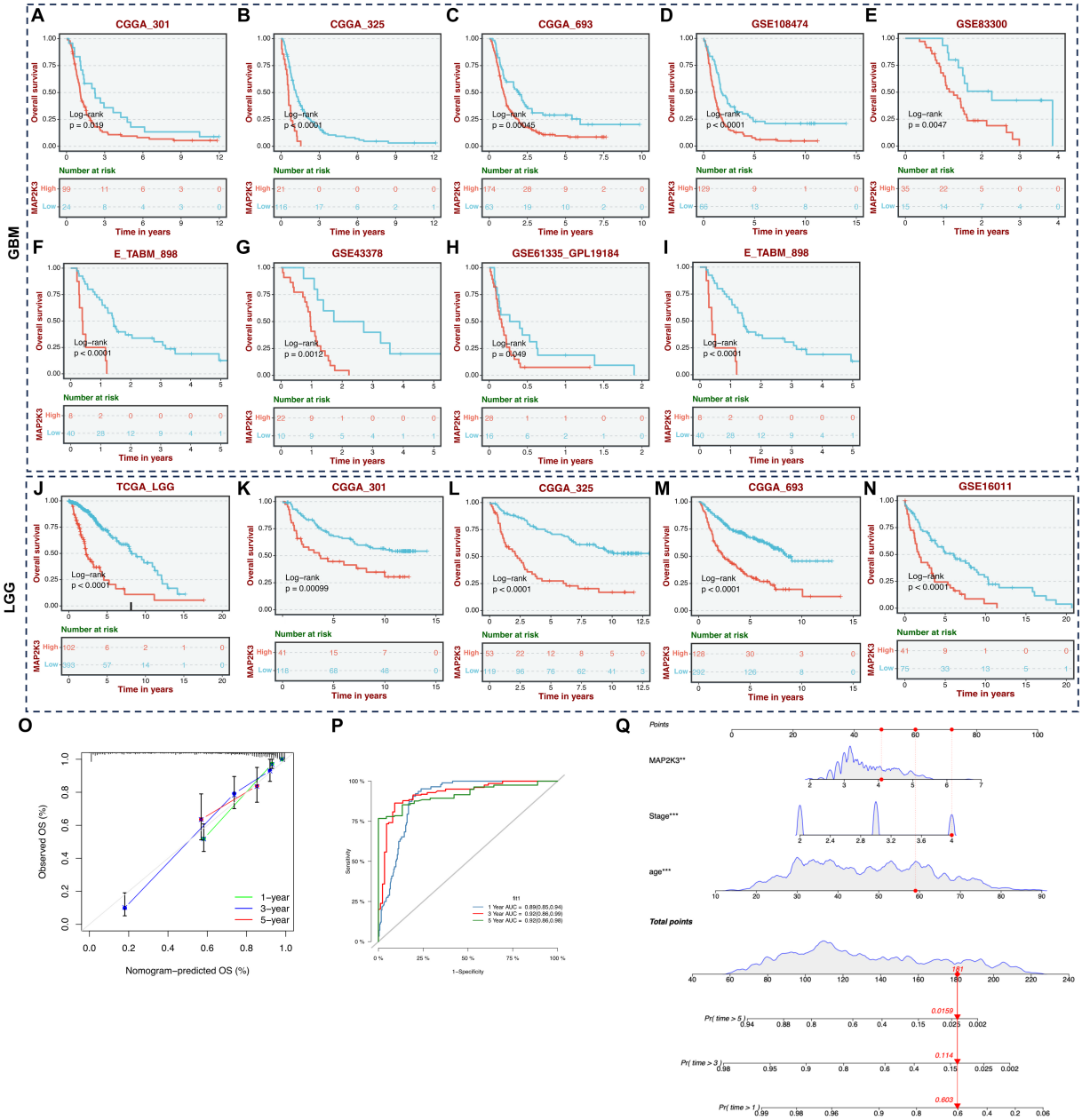

FIGURE 4
Survival analysis of expression level of MAP2K3. **(A–I)** OS Kaplan–Meier survival curves between glioma patients with high and low expression level of MAP2K3 in multi-center GBM cohorts. **(J–N)** OS Kaplan–Meier survival curves between glioma patients with high and low expression level of MAP2K3 in multi-center LGG cohorts. **(O)** Plots depicted the calibration of the nomogram. **(P)** Predictive accuracy at 1, 3, and 5 years of the nomogram in TCGA cohort. **(Q)** The nomogram plot revealed the prognostic prediction model based on MAP2K3, stage, and age in TCGA cohort.

previous analysis, suggesting that higher TIDE scores may be related to immune escape in the high MAP2K3-expressing group.

We scored the tumor immune microenvironment by scoring patients in different MAP2K3 expression groups, and as a result, the high MAP2K3 expression group was found to have a higher exclusion score. In tumor immune microenvironment analysis, the exclusion score is typically used to evaluate whether immune cells are prevented from infiltrating the tumor tissue, thereby indirectly affecting their ability to recognize and eliminate the tumor. This higher exclusion score implies that the group with higher MAP2K3 expression would be more suitable for immunotherapy. By further analysis of the relevant indicators of immunotherapy, we found that IFN-γ, SNV neoantigens expression, the TCR Shannon score and the TCR abundance score were elevated in the high MAP2K3 expression group. All these related expression indicators were elevated suggesting that glioma patients with high MAP2K3 expression levels respond better to immunotherapy (Figures 7C–H).

In addition, we investigated biomarkers of several widely recognized immune pathways. The analysis showed that the immune-related gene sets were scored higher in the high MAP2K3 expression group, including a variety of gene sets including $CD8^+$ T effector cells, DNA damage response, DNA replication, cell cycle regulation, epithelial-mesenchymal

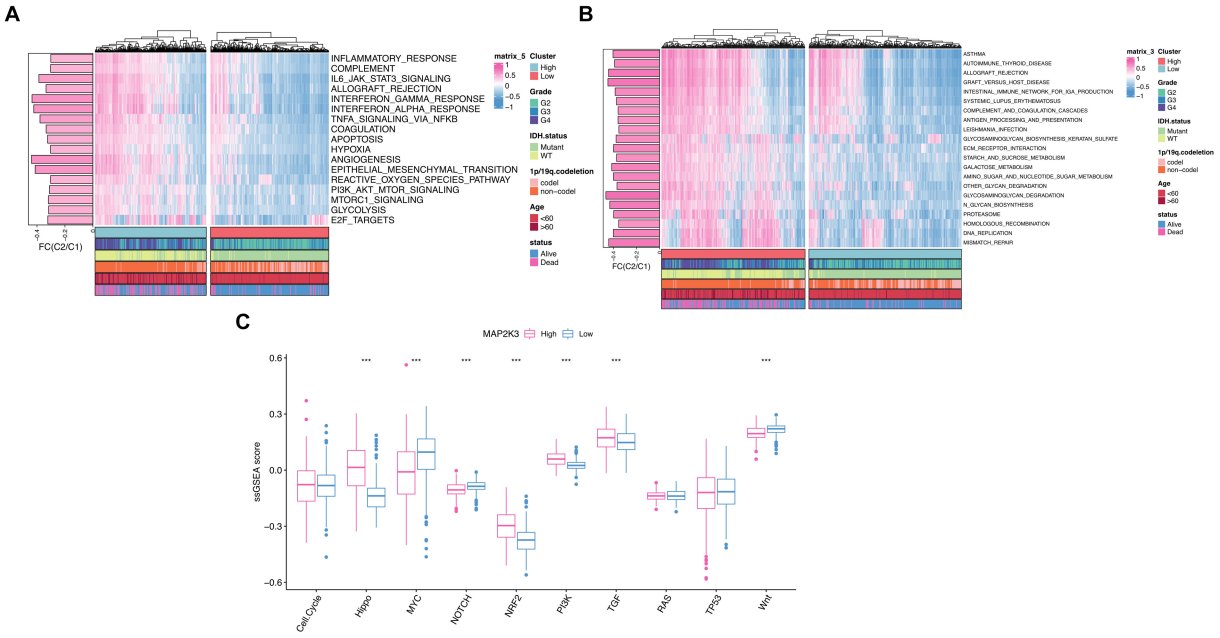

FIGURE 5
Investigations of MAP2K3-related signal pathways. **(A,B)** GSVA enrichment analyses between low and high MAP2K3 expression group illustrated the activation status of Hallmark **(A)** and KEGG **(B)** pathways in TCGA cohort. Pink and blue represent activation and inhibition of the pathway, respectively. **(C)** The Wilcoxon rank-sum test revealed the variances in the normalized scores of ten cancer-related signaling pathways between the low and high MAP2K3 expression group (*$p < 0.05$, **$p < 0.01$, and ***$p < 0.001$).

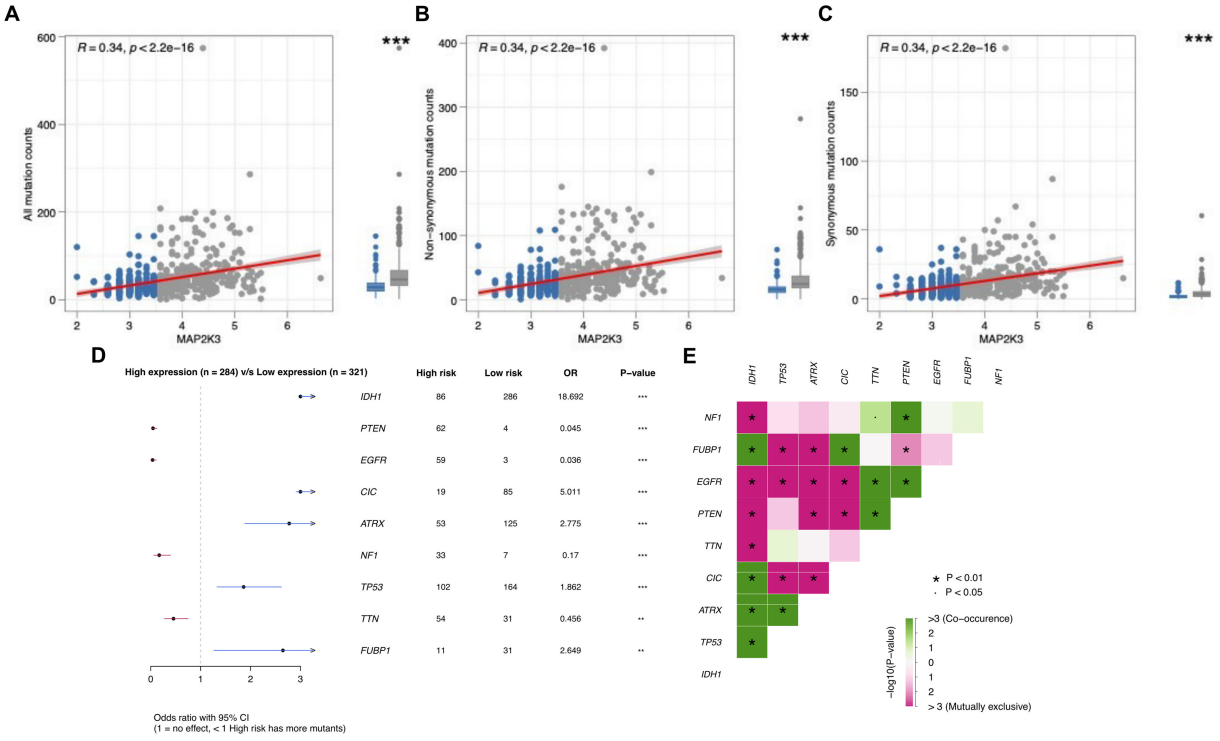

FIGURE 6
The correlation between MAP2K3 expression and tumor mutation status. **(A–C)** The relationship between all mutation **(A)**, non-synonymous **(B)**, and synonymous **(C)** counts and the MAP2K3 expression level, respectively. **(D)** Forest maps show differences of glioma patients in gene mutations in the high and low MAP2K3 expression groups. **(E)** Interaction of differentially mutated genes in glioma patients, including cooccurrence and mutual exclusion.

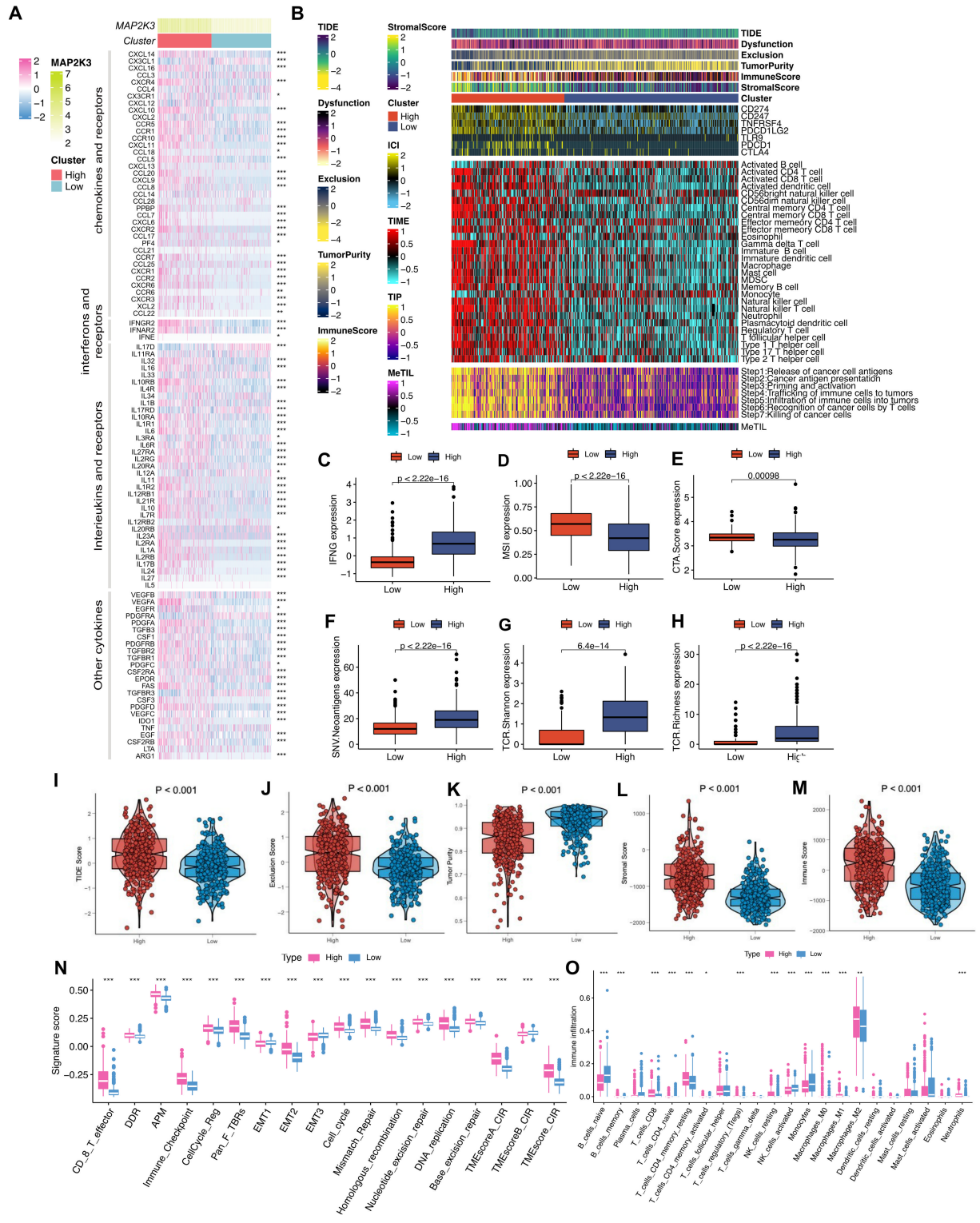

FIGURE 7
Changes in immunomodulators and quantitative types of several tumor immune microenvironments between different MAP2K3 expression groups. **(A)** Heatmap revealed changes in mRNA expression levels of chemokines and their receptors, interleukins and their receptors, interferons and their receptors, and other cytokines between two groups (*$p < 0.05$, **$p < 0.01$, and ***$p < 0.001$, Wilcoxon rank-sum test). **(B)** Heat maps showing the enrichment scores of immune cells between two groups in the TCGA cohort. At the left of the heatmap were annotated the TIDE score, dysfunction score, exclusion score, tumor purity, immune score, and stromal score. **(C–H)** The different level of IFN **(C)**, MSI **(D)**, CTA.Score **(E)**, SNV.Neoantigens **(F)**, TCR.Shannon **(G)**, and TCR.Richness **(H)** between the two groups. **(I–M)** The different level of TIDE score **(I)**, Exclusion score **(J)**, Tumor purity **(K)**, Stromal score **(L)**, and Immune score **(M)** between the two groups. **(N,O)** Two different MAP2K3 expression groups were distinguished by different TME-related signatures **(N)** and immune cells **(O)** (*$p < 0.05$, **$p < 0.01$, and ***$p < 0.001$, Wilcoxon test).

transition markers, immune checkpoints, homologous recombination, mismatch repair, and nucleotide excision repair (Figure 7N).

Relationship between MAP2K3 expression and the TGF signaling pathway in the glioma microenvironment

Previous results demonstrated that TGF-β1, TGF-β2, TGF-β3, and TGF-βR1 were expressed at higher levels in gliomas in the high MAP2K3 expression group, suggesting that high levels of MAP2K3 may convey immunosuppressive effects by activating the TGF-β signaling pathway, thereby promoting immune escape in gliomas with high MAP2K3 expression levels (Figures 8E–H).

According to the Ivy Glioblastoma Atlas Project, MAP2K3, CD68 and CD276 were found to be upregulated in human glioma samples in the Perinecrotic zone (CTpnz) region of expression. In addition, according to the Ivy Glioblastoma Atlas Project database, the distribution of MAP2K3 was consistent with the distribution of macrophage markers CD68 and CD276 (Figures 8I–L). The above analysis further demonstrates that MAP2K3 regulates the immune microenvironment through multiple signaling pathways and promotes immune escape in glioma patients, indicating the potential of MAP2K3 molecules as immunotherapeutic targets.

Validation of MAP2K3 function and expression at the single cell RNA sequencing level

We used the single-cell RNA sequencing database TISCH to further validate MAP2K3 expression in gliomas. The analysis of 17 distinct transcriptome sequencing datasets of glioma single cells from various cell types revealed the presence of MAP2K3 (Figure 8A). MAP2K3 is expressed in various glioma cell lineages and its expression is most abundant in immune and malignant cells, of which we show representative single cell sequencing datasets (GSE102130, GSE163108_10X, and GSE148842) (Figures 8B–D). In the GSE102130 dataset, MAP2K3 was mainly expressed higher in monocytes/macrophages, astrocyte-like malignant cells (AC-like Malignant). In the GSE163108_10X dataset, MAP2K3 was mainly expressed higher in monocytes/macrophages, exhausted $CD8^+$ T Cells (CD8Tex), and mesenchymal-like malignant cells (MES-like Malignant). In the GSE84465 dataset, MAP2K3 was positive in monocytes/macrophages and was positively expressed in monocytes/macrophages and neuronal cells. In addition, the distribution of MAP2K3, TGF-β1, and TGF-βR1 were concentrated in monocytes/macrophages according to the single cell sequencing analysis, which was consistent with our previous analysis. The outcomes of the single cell transcriptome sequencing study

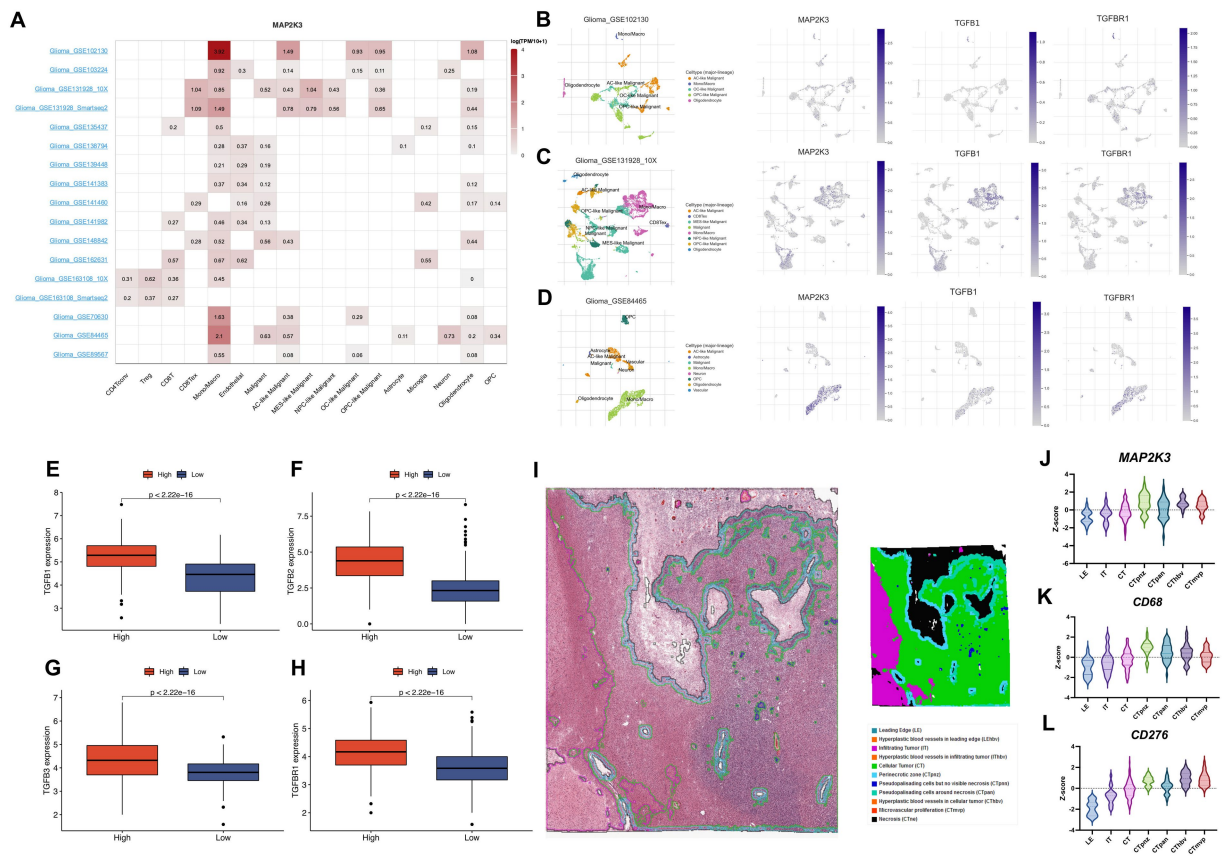

FIGURE 8
The analysis of the function and expression of MAP2K3 in single-cell RNA sequencing datasets. **(A)** The distribution of MAP2K3 expression in 17 single-cell RNA sequencing datasets. **(B–D)** The t-SNE plots showed the distribution of MAP2K3, TGFB1, and TGFBR1 expression in different cell types. **(E–H)** The expression levels of TGF beta signaling pathway between two MAP2K3 groups (Wilcoxon rank-sum test). **(I)** Annotation of tumor characteristics in human glioma samples from the Ivy Glioblastoma Atlas Project. **(J–L)** The expression level of MAP2K3, CD68, CD276 in different parts of the human glioma samples.

completely corroborated our earlier findings and present a macroscopic view of MAP2K3 in glioma.

MAP2K3 facilitates the migration and invasion of glioma cells

We then proceeded with *in vitro* experiments to delve into the role of MAP2K3 in glioma cells. The mRNA expression of MAP2K3 was effectively suppressed in U251 cells through the use of siRNA-MAP2K3 (Figure 9A). As a result, siRNA-MAP2K3 curbed the viability of the glioma cells (Figure 9B). Analysis through wound healing demonstrated that the application of siRNA-MAP2K3 lessened the rate of wound closure compared to the siRNA control group (Figure 9D). The Transwell assay demonstrated that the invasive capacity of U251 glioma cells was reduced by MAP2K3 knockdown (Figure 9C). Taken together, these results provide strong evidence that silencing MAP2K3 notably impedes both migration and invasion of U251 cells.

Evaluation of MAP2K3 in the effectiveness of tumor immunotherapy

Based on the previous assessment of MAP2K3 in the glioma tumor microenvironment, we evaluated the impact of MAP2K3 expression levels on tumor immunotherapy. In the GSE78220, Braun,

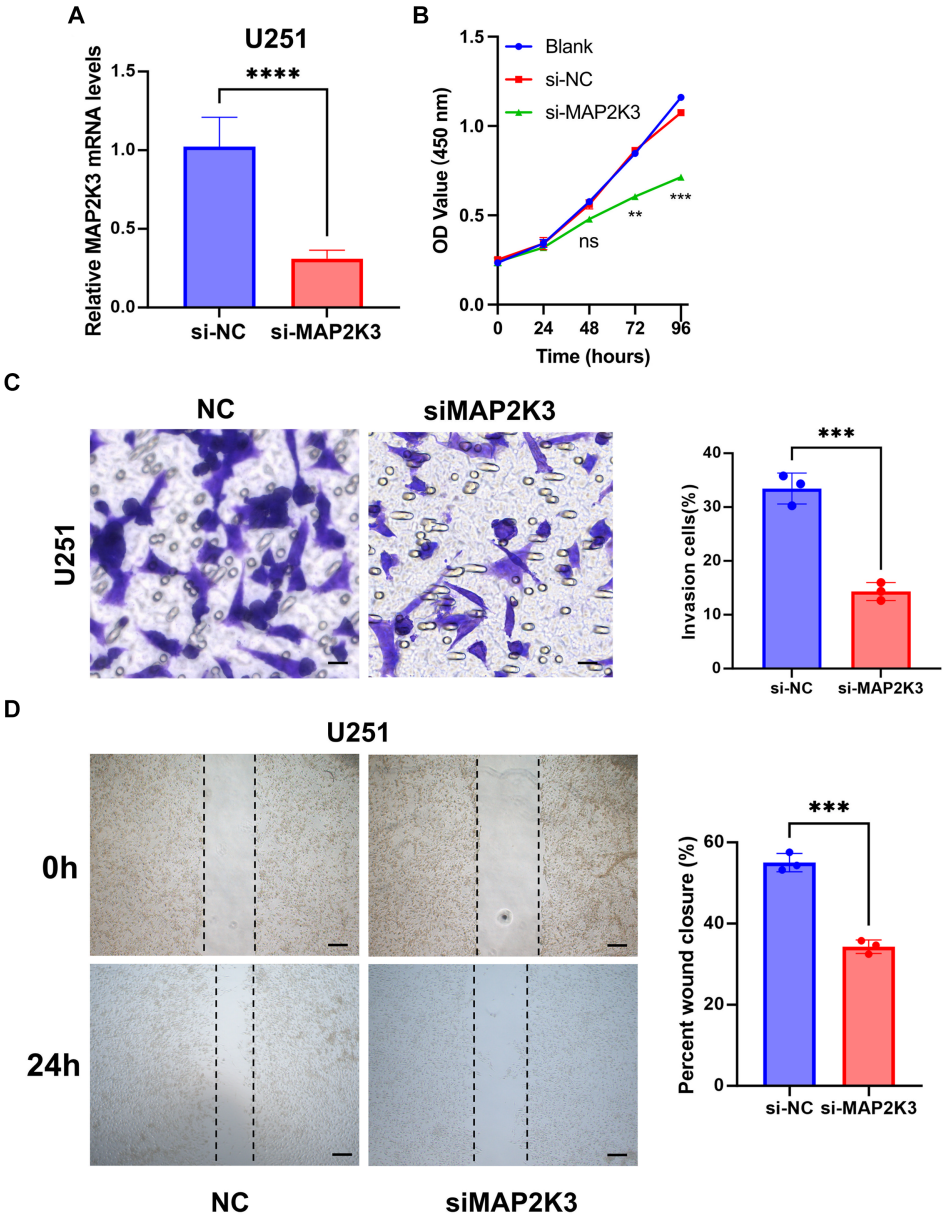

FIGURE 9
Low expression of MAP2K3 inhibited the proliferation and migration of glioma cell *in vitro*. **(A)** The mRNA expression level of MAP2K3 was effectively suppressed in U251 cells by siRNA-MAP2K3 (****$p < 0.0001$, dots represent different sample). **(B)** CCK8 assay detected cell viability after decreased MAP2K3 expression ($n = 3$). **(C)** Transwell assay detected the invasive ability of U251 cells after decreased MAP2K3 expression ($n = 3$, scale bar = 20 μM, ***$p < 0.001$). **(D)** Cell scratch assay detected the proliferation of U251 cells after decreased MAP2K3 expression ($n = 3$, scale bar = 400 μM).

and phs000452 cohorts with treatment by PD-1 inhibitors, survival curve analysis showed that the high MAP2K3 expression group had a significant prognostic advantage with longer prognostic survival after anti-PD-1 immunotherapy (Figures 10A–C). Notably, the same result was found in the PRJNA482620 cohort, an immunotherapy cohort of glioblastoma patients. Small sample sizes may have led to insignificant statistical analysis (Figure 10D). Simultaneously, the high MAP2K3 expression group in the GSE78220, Braun, and phs000452 cohorts indicated more effective anti-PD-L1 immunotherapy (Figure 10E). Additionally, in the Lauss 2017 cohort study exploring predictors and biomarkers in CAR-T therapy, the high MAP2K3-expressing group had a prognostic advantage (Figure 10B). The above results suggest that patients in the high MAP2K3 expression group may derive more benefit from tumor immune checkpoint inhibitor therapy.

Discussion

Glioma is a common primary intracranial malignancy in adults, of which glioblastoma is more malignant and the most aggressive and incurable type with high recurrence rate and high mortality. Traditional treatments such as surgery, radiotherapy and chemotherapy have reached a bottleneck and therefore there is an urgent need to find new treatment methods. The advent of immunotherapy and targeted therapy offers new hope for glioma patients.

In previous studies, MAP2K3 was identified as an oncogene, and reducing MAP2K3 expression could reduce the rate of tumor growth and improve the biological response to chemotherapy. In our study, based on an individual dataset of 33 tumors in the TCGA database, we analyzed the expression of MAP2K3 in different types of cancers. Data analysis showed that MAP2K3 expression differed in a variety of tumors, and the results of applying the Cox Proportional-Hazards model suggested that high MAP2K3 expression was associated with an increased risk of LGG and GBM development. By analyzing the TCGA database, multiple clinical study cohorts and single cell sequencing sets, we found that MAP2K3 mRNA expression was elevated in gliomas and closely correlated with tumor grade. In addition, by analyzing multiple cohorts, we found that MAP2K3 expression levels in gliomas correlated with various clinical characteristics such as age, gender, and 1p/19q mutation status. Among them, MAP2K3 expression levels were higher in male patients, young and middle-aged glioma patients, and glioma patients with 1p/19q present. By performing univariate and multivariate Cox regression analyses, we found that high MAP2K3 expression was an independent predictor of prognosis in glioma patients. It was also established by analysis of survival data from numerous clinical cohorts that glioma patients with high MAP2K3 expression had considerably shorter survival periods

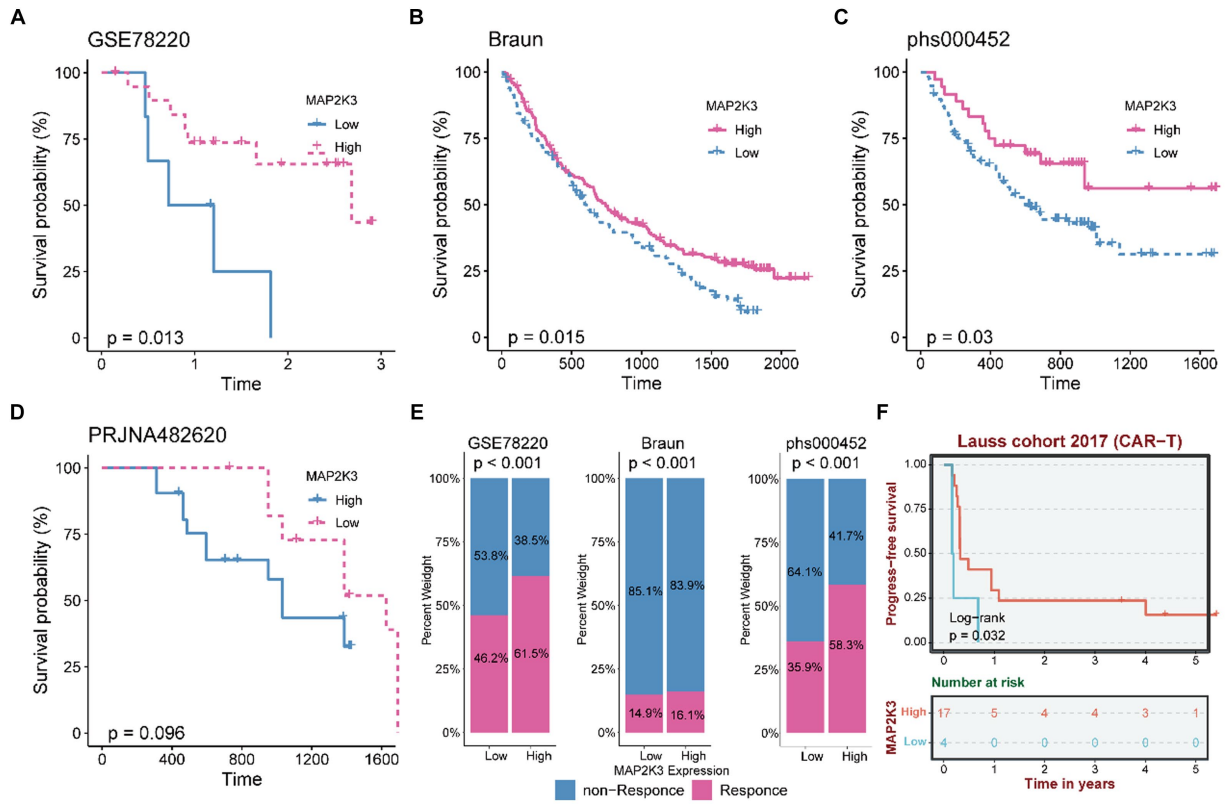

FIGURE 10
MAP2K3 predicts the response of gliomas to immunotherapy. **(A–C)** The Kaplan–Meier curve showed a significant difference in survival rate between the high and low MAP2K3 expression groups in the GSE78220 **(A)**, Braun **(B)**, and phs000452 **(C)** cohorts. **(D)** The Kaplan–Meier curve shows the relationship between survival rate and MAP2K3 expression level in PRJNA482620 cohort. **(E)** The stacked histogram shows the difference in immunotherapy responsiveness between the high and low MAP2K3 expression groups in GSE78220, Braun, and phs000452. **(F)** The Kaplan–Meier curve showed a significant difference in survival rate between the high and low MAP2K3 expression groups in the Lauss cohort.

and shorter progression-free survival than those with low expression. These findings imply that MAP2K3, which may be utilized to predict the prognosis of gliomas by MAP2K3 expression levels, is directly implicated in the biological malignancy of glioma. The mechanism by which MAP2K3 may function biologically in gliomas is not yet known.

Therefore, to investigate the potential biological mechanisms of MAP2K3 in glioma, we explored the functions of MAP2K3 molecules in various cancer-related signaling pathways in the TCGA cohort by GSVA gene enrichment analysis, which showed that several signaling pathways related to immune response and inflammation were significantly activated in gliomas with high MAP2K3 expression levels. We performed KEGG enrichment analysis on the high MAP2K3-expressing and low MAP2K3-expressing groups in the TCGA cohort and found that the high MAP2K3-expressing group was mainly associated with immune response and DNA repair pathways, and all these results suggest that high MAP2K3 expression levels are closely related to immune-related signaling pathways in gliomas. By ssGSEA enrichment scoring of 10 classical oncogenic signaling pathways, we found that the Hippo signaling pathway, NRF2 signaling pathway, PI3K signaling pathway and TGFβ signaling pathway scored higher in the high MAP2K3 expression group.

Given that the TGF signaling pathway is crucial for controlling immune cell activity and tumor immune escape, we specifically focused on the relationship between TGF-β1, TGF-β2, TGF-β3, TGF-βR1, and this MAP2K3 expression level in the TGF signaling pathway. In the tumor microenvironment, activation of the TGF signaling pathway can inhibit the function of immune cells, thus protecting tumors from the immune system (29–31). TGF-β1, TGF-β2, and TGF-β3 are three isoforms of the TGF-β family, which are the most important ligands in the TGF signaling pathway (22). In tumors, ligands of the TGF-β family often lose their normal functions, thus promoting tumor proliferation, metastasis, and invasion. TGF-βR1 is an important signaling molecule in the TGF-β signaling pathway, and it is a subtype of TGF-β receptor type I. TGF-βR1 can activate a variety of downstream signaling pathways through phosphorylation and kinase activation, thereby regulating cell proliferation, apoptosis, cell cycle and many other biological processes (32). In tumors, abnormal expression and uncontrolled function of TGF-βR1 can affect the normal function of the TGF signaling pathway, thus promoting tumor growth and development.

Current studies have shown that MAP2K3 plays an important role in regulating the TGF-β signaling pathway. In the TGF-β signaling pathway, TGF-β, upon binding to its cell membrane receptor, activates Smad proteins and allows them to enter the nucleus, thereby regulating gene transcription (33). In contrast, MAP2K3, a mitogen-activated protein kinase (MAPK) kinase activator, activates JNK and p38 MAPK, members of the MAPK family associated with the regulation of Smad proteins. TGFB1, TGFB2, TGFB3, and TGFBR1 expression in the TGFβ signaling pathway were higher in the high MAP2K3 expression group. This suggests that high levels of MAP2K3 may convey immunosuppressive effects by activating the TGFβ signaling pathway, thus promoting immune escape in gliomas with high MAP2K3 expression levels. Somatic mutations may be an important predictor of tumor response to immunotherapy. By analyzing somatic mutations in glioma patients in the TCGA cohort, we found more somatic mutations in the high MAP2K3-expressing group. These results suggest that there may be strong immune escape in the high MAP2K3-expressing group.

Another important finding of this study was the correlation between MAP2K3 expression and the level of immune infiltration in gliomas. Tumor cells tend to evade cytotoxic T lymphocytes by upregulating immune checkpoint ligands, such as PD-L1. MAP2K3 may regulate immunity in gliomas by interacting with or modulating immune checkpoints. Immunological checkpoint inhibitors can be used to suppress immunological checkpoint expression, stimulate T cells, and alter the tumor microenvironment. However, it is the high tumor heterogeneity, the altered expression of immune checkpoints and the widespread presence of a suppressive tumor immune microenvironment in tumors that make immunotherapy in glioma more challenging. Therefore, it is important to predict the likely therapeutic outcome of patients to immune checkpoint inhibitor therapy. We found elevated expression of multiple immunosuppressive chemokines, increased abundance of multiple immune cell infiltrates with immunosuppressive functions, and higher expression levels of seven immune checkpoint molecules in the high MAP2K3-expressing group; including CD274 (PD-L1), CD247, PDCD1, TNFRSF4, PDCD1LG2, and TLR9. The high expression of these immune checkpoints suggests that glioma patients have a poor prognosis due to the immune escape phenomenon. In addition, multiple tumor immune microenvironment scores were higher in the high MAP2K3 expression group, all suggesting a more active immune microenvironment in glioma patients with high levels of MAP2K3 expression and possibly a better response to immunotherapy. By analyzing multiple clinical cohorts, we evaluated the impact of MAP2K3 expression levels on tumor immunotherapy and found a significant prognostic advantage in the high MAP2K3 expression group after anti-PD-1 immunotherapy, which is consistent with our predicted results. All of these results suggest that patients in the high MAP2K3-expressing group may derive more benefit from tumor immune checkpoint inhibitor therapy.

There are several shortcomings of this study: First, MAP2K3 expression was only validated at the mRNA level, not at the protein level or cellular level, and *ex vivo* experiments are needed to further validate the possible signaling pathways involved in MAP2K3 in glioma. Second, the mechanistic studies in this study were all concomitant phenomena and did not demonstrate a causal association between the two. In addition, this study needs to further expand the sample size and increase the number of study centers to further enhance the significance of the results.

In conclusion, we found that MAP2K3 is expressed at high levels in gliomas and that high MAP2K3 expression predicts poor prognosis in glioma patients. This study also suggests that MAP2K3 may be a novel biomarker for prognosis prediction and immune checkpoint inhibitor therapy in glioma. In addition, patients with high MAP2K3 expression may be considered for immune checkpoint inhibitors treatment.

Conclusion

In summary, we observed a marked overexpression of MAP2K3 in gliomas, correlating with the WHO classification system. Higher levels of MAP2K3 were found to be linked with poor outcomes in low-grade gliomas, gliomas across all WHO grades, as well as recurrent tumors. Additionally, MAP2K3 expression in gliomas displayed associations with a range of immune cells, and showed links with numerous immune checkpoints, implying its potential significance in determining patient responsiveness to immunotherapy. Furthermore, MAP2K3 bore associations with immune-related pathways. These insights point towards the potential of MAP2K3 as a prognostic

indicator for gliomas, and predictive biomarker for immunotherapy responses.

Data availability statement

The raw data supporting the conclusions of this article will be made available by the authors, without undue reservation.

Ethics statement

Ethical approval was not required for the studies on humans in accordance with the local legislation and institutional requirements because only commercially available established cell lines were used.

Author contributions

BP: Writing – review & editing, Writing – original draft. SF: Writing – review & editing, Software, Formal analysis. LG: Writing – review & editing, Supervision. DS: Writing – review & editing, Investigation. ZJ: Writing – review & editing, Conceptualization. XX: Writing – review & editing, Resources, Project administration, Funding acquisition. LW: Writing – review & editing.

Funding

The author(s) declare that financial support was received for the research, authorship, and/or publication of this article. This work was supported by the Fundamental Research Funds for the Central Universities (2042022 kf1216) to XX and Open Project of Sichuan Provincial Key Laboratory for Clinical Immunology Translational Medicine (LCMYZHYX-KFKT202203).

Conflict of interest

The authors declare that the research was conducted in the absence of any commercial or financial relationships that could be construed as a potential conflict of interest.

Publisher's note

References

1. Molinaro AM, Taylor JW, Wiencke JK, Wrensch MR. Genetic and molecular epidemiology of adult diffuse glioma. *Nat Rev Neurol*. (2019) 15:405–17. doi: 10.1038/s41582-019-0220-2

2. Neagu MR, Reardon DA. An update on the role of immunotherapy and vaccine strategies for prim ary brain tumors. *Curr Treat Options Oncol*. (2015) 16:54. doi: 10.1007/s11864-015-0371-3

3. Yabo YA, Niclou SP, Golebiewska A. Cancer cell heterogeneity and plasticity: a paradigm shift in glioblastoma. *Neuro-Oncology*. (2022) 24:669–82. doi: 10.1093/neuonc/noab269

4. Piastra V, Pranteda A, Bossi G. Dissection of the MKK3 functions in human cancer: a double-edged sword? *Cancers*. (2022) 14:483. doi: 10.3390/cancers14030483

5. Roth P, Valavanis A, Weller M. Long-term control and partial remission after initial pseudoprogressio n of glioblastoma by anti-PD-1 treatment with nivolumab. *Neuro-Oncology*. 19:454–6. doi: 10.1093/neuonc/now265

6. Martínez-Limón A, Joaquin M, Caballero M, Posas F, de Nadal E. The p38 pathway: from biology to Cancer therapy. *Int J Mol Sci*. (2020) 21:61913. doi: 10.3390/ijms21061913

7. Raingeaud J, Whitmarsh AJ, Barrett T, Dérijard B, Davis RJ. MKK3- and MKK6-regulated gene expression is mediated by the p38 mitoge n-activated protein kinase signal transduction pathway. *Mol Cell Biol*. (1996) 16:1247–55. doi: 10.1128/MCB.16.3.1247

8. Smiles WJ, Catalano L, Stefan VE, Weber DD, Kofler B. Metabolic protein kinase signalling in neuroblastoma. *Mol Metab*. (2023) 75:101771. doi: 10.1016/j.molmet.2023.101771

9. Beamer E, Corrêa SAL. The p38MAPK-MK2 signaling Axis as a critical link between inflammation and synaptic transmission. *Front Cell Dev Biol*. (2021) 9:635636. doi: 10.3389/fcell.2021.635636

10. Cargnello M, Roux PP. Activation and function of the MAPKs and their substrates, the MAPK-activated protein kinases. *Microbiol Mol Biol Rev*. (2011) 75:50–83. doi: 10.1128/MMBR.00031-10

11. Bonney EA. Mapping out p38MAPK. *Am J Reproduc Immunol*. 77:12652. doi: 10.1111/aji.12652

12. Ventura JJ, Tenbaum S, Perdiguero E, Huth M, Guerra C, Barbacid M, et al. p38alpha MAP kinase is essential in lung stem and progenitor cell prol iferation and differentiation. *Nat Genet*. (2007) 39:750–8. doi: 10.1038/ng2037

13. Urosevic J, Garcia-Albéniz X, Planet E, Real S, Céspedes MV, Guiu M, et al. Colon cancer cells colonize the lung from established liver metastases through p38 MAPK signalling and PTHLH. *Nat Cell Biol*. (2014) 16:685–94. doi: 10.1038/ncb2977

14. Sun D, Wang J, Han Y, Dong X, Ge J, Zheng R, et al. TISCH: a comprehensive web resource enabling interactive single-cell t ranscriptome visualization of tumor microenvironment. *Nucleic Acids Res*. (2021) 49:D1420–30. doi: 10.1093/nar/gkaa1020

15. Louis DN, Perry A, Reifenberger G, von Deimling A, Figarella-Branger D, Cavenee WK, et al. The 2016 World Health Organization classification of tumors of the central nervous system: a summary. *Acta Neuropathol*. (2016) 131:803–20. doi: 10.1007/s00401-016-1545-1

16. Zhu H, Hu X, Ye Y, Jian Z, Zhong Y, Gu L, et al. Pan-Cancer analysis of PIMREG as a biomarker for the prognostic and immunological role. *Front Genet*. (2021) 12:687778. doi: 10.3389/fgene.2021.687778

17. Liberzon A, Birger C, Thorvaldsdóttir H, Ghandi M, Mesirov JP, Tamayo P. The molecular signatures database (MSigDB) hallmark gene set collection. *Cell Syst*. (2015) 1:417–25. doi: 10.1016/j.cels.2015.12.004

18. Fu M, Hu Y, Lan T, Guan KL, Luo T, Luo M. The hippo signalling pathway and its implications in human health and diseases. *Signal Transduct Target Ther*. (2022) 7:1191. doi: 10.1038/s41392-022-01191-9

19. Yang D, Zhang N, Li M, Hong T, Meng W, Ouyang T. The hippo signaling pathway: the trader of tumor microenvironment. *Front Oncol*. (2021) 11:772134. doi: 10.3389/fonc.2021.772134

20. Hayes JD, Dinkova-Kostova AT. The Nrf2 regulatory network provides an interface between redox and intermediary metabolism. *Trends Biochem Sci*. (2014) 39:199–218. doi: 10.1016/j.tibs.2014.02.002

21. Collins NB, al Abosy R, Miller BC, Bi K, Zhao Q, Quigley M, et al. PI3K activation allows immune evasion by promoting an inhibitory myelo id tumor microenvironment. *J Immunother Cancer*. (2022) 10:e003402. doi: 10.1136/jitc-2021-003402

22. Tauriello DVF, Sancho E, Batlle E. Overcoming TGFβ-mediated immune evasion in cancer. *Nat Rev Cancer*. 22:25–44. doi: 10.1038/s41568-021-00413-6

23. Shen X, Song S, Li C, Zhang J. Synonymous mutations in representative yeast genes are mostly strongly non-neutral. *Nature*. (2022) 606:725–31. doi: 10.1038/s41586-022-04823-w

24. Tang X, Zhang T, Cheng N, Wang H, Zheng CH, Xia J, et al. usDSM: a novel method for deleterious synonymous mutation prediction using undersampling scheme. *Brief Bioinform*. (2021) 22:e123. doi: 10.1093/bib/bbab123

25. Anagnostou V, Bardelli A, Chan TA, Turajlic S. The status of tumor mutational burden and immunotherapy. *Nat Cancer*. (2022) 3:652–6. doi: 10.1038/s43018-022-00382-1

26. Hastings K, Yu HA, Wei W, Sanchez-Vega F, DeVeaux M, Choi J, et al. EGFR mutation subtypes and response to immune checkpoint blockade treatment in non-small-cell lung cancer. *Ann Oncol*. (2019) 30:1311–20. doi: 10.1093/annonc/mdz141

27. Romero D. Adding immune-checkpoint inhibitors to chemotherapy extends survival in endometrial cancer. *Nat Rev Clin Oncol*. (2023) 20:353. doi: 10.1038/s41571-023-00763-0

28. Anderson NM, Simon MC. The tumor microenvironment. *Curr Biol*. (2020) 30:R921–5. doi: 10.1016/j.cub.2020.06.081

29. Shi X, Yang J, Deng S, Xu H, Wu D, Zeng Q, et al. TGF-β signaling in the tumor metabolic microenvironment and targeted therapies. *J Hematol Oncol*. (2022) 15:135. doi: 10.1186/s13045-022-01349-6

30. Chan MK, Chung JYF, Tang PCT, Chan ASW, Ho JYY, Lin TPT, et al. TGF-β signaling networks in the tumor microenvironment. *Cancer Lett*. (2022) 550:215925. doi: 10.1016/j.canlet.2022.215925

31. Lainé A, Labiad O, Hernandez-Vargas H, This S, Sanlaville A, Léon S, et al. Regulatory T cells promote cancer immune-escape through integrin αvβ8-mediated TGF-β activation. *Nat Commun*. (2021) 12:6228. doi: 10.1038/s41467-021-26352-2

32. Trelford CB, Dagnino L, Di Guglielmo GM. Transforming growth factor-β in tumour development. *Front Mol Biosci*. (2022) 9:991612. doi: 10.3389/fmolb.2022.991612

33. Ramachandran A, Vizán P, das D, Chakravarty P, Vogt J, Rogers KW, et al. TGF-β uses a novel mode of receptor activation to phosphorylate SMAD1/ 5 and induce epithelial-to-mesenchymal transition. *eLife*. (2018) 7:e31756. doi: 10.7554/eLife.31756

frontiers | Frontiers in Oncology

TYPE Review
PUBLISHED 24 June 2024
DOI 10.3389/fonc.2024.1374249

OPEN ACCESS

EDITED BY
Bo Yuan Huang,
Capital Medical University, China

REVIEWED BY
Dmitry Aleksandrovich Zinovkin,
Gomel State Medical University, Belarus
Hai Xue,
Capital Medical University, China
Jianguang Ji,
Lund University, Sweden
Minglai Zhao,
Fudan University, China, in collaboration with reviewer JJ

*CORRESPONDENCE
Hongwei Zhang
zhanghongwei@ccmu.edu.cn

RECEIVED 21 January 2024
ACCEPTED 11 June 2024
PUBLISHED 24 June 2024

CITATION
Chen Y and Zhang H (2024) Immune microenvironment and immunotherapy for chordoma.
Front. Oncol. 14:1374249.
doi: 10.3389/fonc.2024.1374249

Immune microenvironment and immunotherapy for chordoma

Yujia Chen and Hongwei Zhang*

Department of Neurosurgery, Sanbo Brain Hospital, Capital Medical University, Beijing, China

Chordoma, as a rare, low-grade malignant tumor that tends to occur in the midline of the body, grows slowly but often severely invades surrounding tissues and bones. Due to the severe invasion and damage to the surrounding tissues, chordoma is difficult to be gross totally resected in surgery, and the progression of the residual tumor is often unavoidable. Besides, the tumor is insensitive to conventional radiotherapy and chemotherapy, thus finding effective treatment methods for chordoma is urgent. Nowadays, immunotherapy has made a series of breakthroughs and shown good therapeutic effects in kinds of tumors, which brings new insights into tumors without effective treatment strategies. With the deepening of research on immunotherapy, some studies focused on the immune microenvironment of chordoma have been published, most of them concentrated on the infiltration of immune cells, the expression of tumor-specific antigen or the immune checkpoint expression. On this basis, a series of immunotherapy studies of chordoma are under way, some of which have shown encouraging results. In this review, we reviewed the research about immune microenvironment and immunotherapy for chordoma, combined with the existing clinical trials data, hoping to clarify the frontiers and limitations of chordoma immune research, and provide reference for follow-up immunotherapy research on chordoma.

KEYWORDS

chordoma, immune microenvironment, immunotherapy, immune checkpoint, clinical trial

1 Introduction

Chordoma is a relatively rare, low-grade malignant tumor originating from residual notochord tissue during embryonic development, accounting for 1% to 4% of malignant bone tumors, with an incidence of about 0.08/100,000 people in the population (1–3). It is prone to occur in the midline structures of the human body, with common sites including the skull base (35%), sacrococcygeal region (50%), and the spine (15%) (2). Occasionally, it can be found in metastatic lesions such as ribs, lungs, brain, or spinal cord (4–6).

Although chordoma has a slow proliferation rate, it often causes severe destruction of surrounding soft tissue and bone during tumor progression, which makes it extremely difficult to completely resected and the 5-year progression-free survival (PFS) rate is only 59.2% (3, 7). Besides, chordoma is not sensitive to conventional radiotherapy and chemotherapy, which

requires higher radiation doses (usually greater than 74 Gy) to achieve therapeutic goals, meanwhile also increasing the risk of radiational damage for the surrounding tissues (8, 9). Multiple phase II clinical trials have confirmed that targeted therapy against growth factors could significantly benefit patients overall and also significantly prolong their survival. However, further phase III clinical studies are still lacking to support the clinical application of these targeted treatment strategies (10–12). Such limited treatment options often lead chordoma patients to undergo multiple cycles of "surgery-recurrence" and face a dilemma of "incurable" at last when surgery is no longer possible (13). It's an urgent need to explore new treatments for chordoma.

Previous studies found that Brachyury is a tumor-specific antigen in chordoma, leading to some studies designed tumor vaccines targeting this protein and conducted clinical trials accordingly, which became the beginning of research on immunotherapy of chordoma (14, 15). Since then, more research on the characteristics of the immune microenvironment in chordoma has continued to emerge, which has also provided a theoretical basis for more clinical immunotherapy, especially the immune checkpoint inhibitor (ICI) therapy (16).

In this review, we reviewed the existing evidence on chordoma immune research, clarified the state of the immune microenvironment in chordoma, presented the frontier and focus issues of chordoma immunotherapy clinical research hoping to provide a guideline for follow-up immunotherapy research on chordoma.

2 Immune microenvironment characteristics of chordoma

Due to the low incidence, research on the immune microenvironment of chordoma had been relatively lacking compared to other bone tumors. While the basic research technology developing and the emphasis on tumor immune characteristics increasing, the research on the immune microenvironment of chordoma, especially the infiltration of immune cells, the secretion of cytokines and chemokines in tumor microenvironment (TME), and the expression of immune checkpoints in chordoma had made significant progress nowadays (Figure 1).

2.1 Immune cell in chordoma

2.1.1 The infiltration of immune cell

The infiltration of immune cells are an important part of the immune microenvironment and the cellular basis for immunotherapy. Several studies illustrated the characteristic of immune cells infiltration in chordoma detected by different methods. Shalin performed immunohistochemical (IHC) staining of 24 chordoma specimens and found CD4+ T lymphocyte infiltration in 21 patients and CD8+ T lymphocyte infiltration in only 11 patients (17). Dridi also found that macrophages and CD4+ T cells were the most abundant immune cell groups in chordoma tissues, followed by CD8+ T cells (18). Several studies further analyzed the subgroups of the infiltrated CD4+ T cells and macrophages in chordoma. Wanru conducted single-cell sequencing on 6 chordoma specimens and found that chordoma tissue had abundant regulatory T cells and M2 macrophages (19). Morimoto et al.'s study of 54 skull base chordomas also showed that there were a large number of CD163+ M2 macrophages and Foxp3 + regulatory T cells in skull base chordomas (20). These studies indicated that there was a large infiltration of CD4+ T cells and macrophages in chordoma, especially regulatory T cells and M2 macrophages.

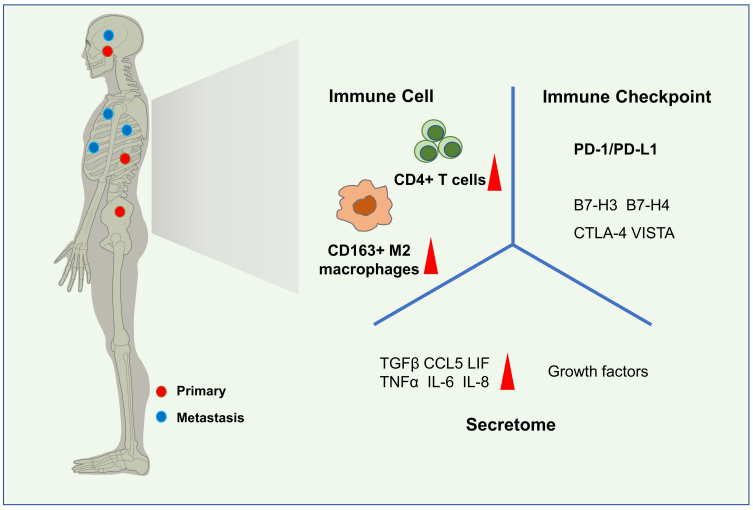

FIGURE 1
Immune microenvironment characteristics of chordoma. Common sites of chordoma include the skull base, sacrum, and spine. Metastatic lesions may be found in the ribs, lungs, brain, or spinal cord(left). In the immune microenvironment of chordoma, CD4+ T cells and CD163+ M2 macrophages are the most abundant immune cells subsets. Kinds of secretome,such as TGFβ, TNFα, CCL5, IL-8, IL-6, LIF are highly expressed in chordomas and some of them play important roles, as well as growth factors. The expression of some immune checkpoints,especially PD-1/PD-L1 has been ddetected in the tumor tissue and peripheral blood.

Although previous studies had been consistent on the degree of infiltration of macrophages, there was inconsistent on the extent of tumor-infiltrated lymphocytes (TIL) in chordoma in the literature. Dancsok detected and calculated the number of infiltrating immune cells per unit area in 28 chordoma cases, they found that macrophages were the highest density infiltrating cell population, with CD163+ M2 macrophages far more than CD86+ M1 macrophages, but both of them were much more than TILs, which differed from the presence of large CD4+ T cell infiltrated in chordomas mentioned in other studies (21). This inconsistence might be due to different experimental assay methods or materials, which need further research to elucidate.

2.1.2 The distribution of immune cell

Previous research also focused on the spatial distribution of immune cells in chordoma. Diana et al. used multiple immunofluorescence (mIF) to observe the distribution of immune cells in 75 chordoma patients. They distinguished the immune cells distribution between tumor parenchyma and the extracellular matrix, observed that macrophage infiltration density was significantly higher in the tumor parenchyma than in the matrix, while helper T cells, cytotoxic T cells and regulatory T cells were more abundant in the tumor matrix than in the tumor. NK cells in chordoma were rare and hardly activated (22). Additionally, since these chordoma tissues came from patients in different locations and stages, the study also found that there was no difference in the distribution of immune cells in chordomas among different locations and stages (22). This research suggested that immune cell infiltration in chordoma was relatively stable, and myeloid cells were more closely distributed to tumor cells than T cells (22).

2.1.3 The correlation between immune cell and prognosis

Several studies had analyzed the correlation between specific immune cell subsets and prognosis in patients with chordoma. Dridi found that the infiltration of CD8+ T cell was a protective factor for chordoma (18). Mingxiang et al. also found that there was a significant positive correlation between CD3+ T lymphocyte infiltration and the degree of tumor invasion, overall survival (OS) and local relapse-free survival (LRFS) in 54 spinal chordomas, and the density of CD4+ T lymphocytes was significantly associated with OS and LRFS, while the density of Foxp3+ regulatory T cells and CD8+ T cells was associated with OS (23, 24). Jinpeng et al.'s study on TIL staining in 93 chordomas found that the content of TIM3+ TILs was associated with the degree of chordoma invasion and was an independent prognostic risk factor for LRFS and OS (25). Furthermore, studies demonstrated that the patient's tumor/stromal ratio and CD8+/Foxp3+ ratio were independent risk factors for prognosis (26, 27).

However, previous studies had mainly observed the correlation between the infiltration of TILs and the prognosis of patients in chordoma, but few of them studied on the correlation between the infiltration of myeloid cells and the prognosis of patients. Only Morimoto's study of 54 skull base chordomas showed that the infiltration of CD163+ M2 macrophages and Foxp3+ regulatory T cells were significantly higher in rapid-progressing chordomas than in slow-progressing chordomas, suggesting that M2 macrophages and regulatory T cells might have a potential role in the progression of chordomas (20).

2.2 Secretome in chordoma

Studies of chordoma immune cells had confirmed the presence of a large number of immune cells infiltrated in chordomas, indicating the presence of complex cell-to-cell interactions. In addition to the direct contact between cells, many cell interactions also require the mediation of cytokines, chemokines, growth factors, and even metabolic products, collectively known as secretome. Although previous studies had not reported on the expression and secretion of growth factors in chordoma, several phase II clinical studies had confirmed that inhibiting growth factors could prolong the survival of patients with chordoma, demonstrating the crucial role of growth factors in chordoma (10–12).

Recently, it had been discovered that kinds of cytokines and chemokines, such as TGFβ, TNFα, CCL5, IL-8, IL-6 and LIF, also as important mediators of cellular interactions, had been found to be highly expressed in chordomas and play important roles in the immune microenvironment.

2.2.1 The TGFβ family in chordoma

Studies on TGFβ in chordoma were relatively abundant, suggesting that the TGFβ pathway played a crucial role in chordoma. Studies showed that the loss of heterozygosity for 1p36 presented in 75%-90% of chordoma samples, which suppressed the expression of RUNX (an inhibitor gene of TGFβ) and in turn led to the activation of the TGFβ pathway in chordoma cells (28–31). Stefan et al. performed RNA-seq on 5 chordoma samples and 3 chordoma cell lines, compared them with notochord tissue and found that TGFβ was highly expressed in chordoma and that inhibition of the TGFβ pathway could attenuate chordoma cell growth (32). Another study performed single-cell sequencing analysis on 6 chordoma cases and revealed that the TGF-β signaling pathway was not only essential on the progression of chordoma, but also induced the malignant progression of tumor cells to extracellular matrix (ECM), maintained the tumor stem cells self-renewal, promoted the change of extracellular matrix (EMT) and the transformation of CD4+T cells to Treg+ cells in chordoma (19). A more detailed study of TGFβ found that the expression level of TGFB1 was an important factor affecting the prognosis of skull base chordoma (33), and the down-regulation of TGFB3—a gene that acted opposite to TGFB1—might be a key factor for chordoma tumorigenesis (34). As for the source of TGFβ, single-cell sequencing studies had shown that TGFβ in chordoma was mainly secreted by fibroblasts and macrophages (19). Overall, the above results suggested that inhibition of TGFβ secretion or activation might be a potential target for chordoma treatment.

2.2.2 The CCL5 in chordoma

The first research on CCL5 in chordoma were just published, demonstrating a critical role for CCL5 in tumor-macrophage

interactions in chordoma. Jiuhui et al. constructed a tumor-macrophage co-culture model to simulate the *in vivo* situation of chordoma, and then screened the expression levels of RNA and protein in MUG-chor1 chordoma cells after co-culture with macrophages. The expression level of CCL5 was significantly increased in chordoma cells, and experiments confirmed that CCL5 could induce the M2 polarization of macrophages and promote the invasion and migration of chordoma cells. It was also confirmed that the expression of CCL5 in recurrent chordoma was significantly higher than that in the original tumor (35). Although there was only this one research on CCL5 in chordoma, the study clearly confirmed the secretory source of CCL5 and verified its role in the chordoma microenvironment.

2.2.3 Other cytokines and chemokines in chordoma

Previous studies suggested that some cytokines and chemokines, including TNFα, LIF, IL-6 and IL-8 played important roles in the immune microenvironment of chordoma, but relatively few studies had been conducted.

Sukru et al. stained some kinds of cytokines in 14 chordoma tissues and found that the expression level of TNFα in chordoma was negatively correlated with the survival time of patients, and positively correlated with higher LIF and PD-L1expression in chordoma (36). And LIF, as a member of the IL-6 cytokine family, was inversely correlated with poorer overall survival and was shown to inhibit tumor inflammatory responses (37). However, the source of their secretion in chordoma and how they played a role in influencing patient outcomes remained unclear.

As for IL-6 and IL-8, studies have shown that the expression levels of IL-6 and IL-8 in the serum of patients with chordoma are significantly higher than those of normal people (38), and their secretion levels in chordoma cells are significantly increased after co-culture with macrophages *in vitro* (35), indicating that their secretion was affected by tumor-immune cell interactions, but the mechanism was still unclear. Based on the finding, a Phase I clinical trial of IL-8 monoclonal antibody for chordoma treatment had been carried out and showed good safety, but the efficacy had yet to be verified (39).

Overall, although we had some understanding of cytokines and chemokines expression, cellular interactions in the immune microenvironment of chordoma, there was still a lack of in-depth research on the source of cytokine secretion, the specific mechanisms by which cytokines mediated cellular interactions, and the expression levels in chordoma. Further addressing these issues was crucial for seeking new potentially effective treatments for chordoma.

2.3 Immune checkpoint in chordoma

2.3.1 PD-1/PD-L1 in chordoma

Due to the excellent therapeutic efficacy of ICI therapy in a wide range of tumors, the expression of immune checkpoints was one of the hotspots in current immune research in chordoma. Among them, PD-1/PD-L1 was the focus of immune checkpoint research in chordoma.

Previous studies on the PD-1/PD-L1 in chordoma mainly focused on the expression levels and sites, but the number of published studies was not substantial. Mathios detected the expression of PD-1 and PD-1 ligands in 10 chordoma specimens and 3 chordoma cell lines by reverse transcription-polymerase chain reaction (RT-PCR) and found that PD-1 expressed on TILs, while PD-L1 expressed on both TILs and tumor-associated macrophages (TAMs) in 3/10 tumor specimens (40). Laura detected two pediatric poorly differentiated chordomas using whole-genome, transcriptome and whole-genome bisulfite sequencing (WGBS) and multiplex immunohistochemistry, revealed the expression of PD-L1in both patient samples (41). Dride stained 81 chordoma specimens and found that PD-L1 was detected on inflammatory cells but not expressed on tumor cells in 26% of patients (18). Interestingly, while other studies have found that PD-L1 is only expressed on immune cells, Chao et al.'s immunofluorescence staining study on 92 chordomas showed that PD-L1 expression could also be found in patient tumor cells, which was inconsistent to other studies, and needed further studies to explain the difference.

Besides, studies had found that the expression of PD-L1 correlated to the prognosis of patients in chordoma. The degree of PD-L1+ immune cells correlated to tumor blood vessel density and lower PD-L1 expression correlated to the better patient prognosis (18, 42). Both PD-1+ cell density and PD-L1+ cell density were significant risk factors for local PFS and OS in chordoma (23, 26, 43).

2.3.2 Other immune checkpoints in chordoma

In addition to the PD-1/PD-L1, research on the others immune checkpoints in chordoma were relatively scarce. He et al.'s study on thirty-two spinal chordomas showed that the expression level of CTLA-4 in chordoma tissues was higher than that in nucleus pulposus tissue, and it was a risk factor for OS (44). Long et al. detected the expression of six kind of cell surface receptors, including PD-L1, B7 -H3, B7-H4 and VISTA which could be targeted by CAR-T in forty-five skull base chordoma samples, the results showed that B7-H3 had the highest positive rate (7/45, 16%) in samples, and the positive rate was ranked as B7-H3 > PD-L1 > VISTA = B7-H4, suggesting that B7-H3 was a good target for CAR-T treatment of chordoma (45). The study also designed a CAR-T targeting B7-H3 and verified its good effectiveness against chordoma *in vitro* experiments.

2.3.3 Soluble immune checkpoints in chordoma

Some studies had attempted to detect the expression of soluble immune checkpoints in peripheral blood of chordoma patients. Kushlinskii et al. conducted ELISA detection for soluble PD-1 (sPD-1), soluble PD-L1 (sPD-L1) and soluble VISTA (sVISTA) in the peripheral blood of chordoma patients and found that there were higher expression of sPD-L1 and lower expression of sVISTA in chordoma patient than in control, no matter the tumor location, stage, tumor type, patient age and gender (46, 47), suggesting that

chordoma could affect the expression of soluble immune checkpoints and might affect the immune status of the whole body.

Overall, studies on immune checkpoints in chordoma had showed that there certainly were kinds of immune checkpoints expressed in chordoma tissues. Although the expression level was general low, the existing preliminary studies still suggested that there were effective targets for ICIs therapy or other immunotherapies targeting these immune checkpoints (such as CAR-T therapy) in chordoma, and related treatments may be effective against chordoma.

3 Research on immunotherapy of chordoma

The tumor immune microenvironment is closely related to tumor immunotherapy. Deeply understanding the immune microenvironment is essential to develop and optimize immunotherapy strategies and find more effective treatment methods. As the understanding of the immune microenvironment of chordoma deepens, research on immunotherapy for chordoma also continues to grow.

Currently, kinds of clinical trials on immunotherapy of chordoma were ongoing, and the published results mainly involved in vaccine therapy and ICI therapy, while other immunotherapy methods such as CAR-T therapy, oncolytic virus therapy, had not been reported in the literature so far. Due to the paucity of published literature, we searched for information on clinical trials in chordoma. As of July 3, 2023, there were 66 registered chordoma clinical trials on the Clinical trial website (https://www.clinicaltrials.gov) and sixteen of them were effective and involved immunotherapy, which was far more than published immune studies, including 9 trials of ICI therapy, 3 trials of vaccine therapy, 2 trials of oncolytic virus therapy and 2 trials of other immunotherapies (Figure 2, Table 1).

3.1 Vaccine therapy

Chordoma cells specifically expressed Brachyury, which was one of the hallmark features of chordoma and constituted a target for chordoma vaccine therapy (48). In 2015, Christopher designed a yeast-derived Brachyury vaccine and conducted a Phase I clinical trial on chordoma. The trial enrolled 34 patients, designed a 3 + 3 dose escalation experiment with three dose gradients, observed the side-effects and Brachyury-specific T cell responses to access the safety and efficacy of the vaccine. The results showed that there were no autoimmune reactions or severe adverse events in all patients, and a transient Brachyury-specific T cell production was observed in most evaluable patients, indicating a good safety profile and potential efficacy (15). Based on this result, Peter et al. conducted a double-blind randomized placebo-controlled Phase II clinical trial of the vaccine on chordoma (NCT02383498). The trial enrolled 24 patients with locally advanced chordomas which were ineligible for surgical resection, and the patients were given a yeast-derived Brachyury vaccine in combination with standard radiotherapy to observe the prognosis. However, the results showed that although Brachyury-specific T cell responses were present in the treatment group, the median survival was unexpectedly shorter than that in the control group (20.6 months vs. 25.9 months), which leading to the termination of this trial (16).

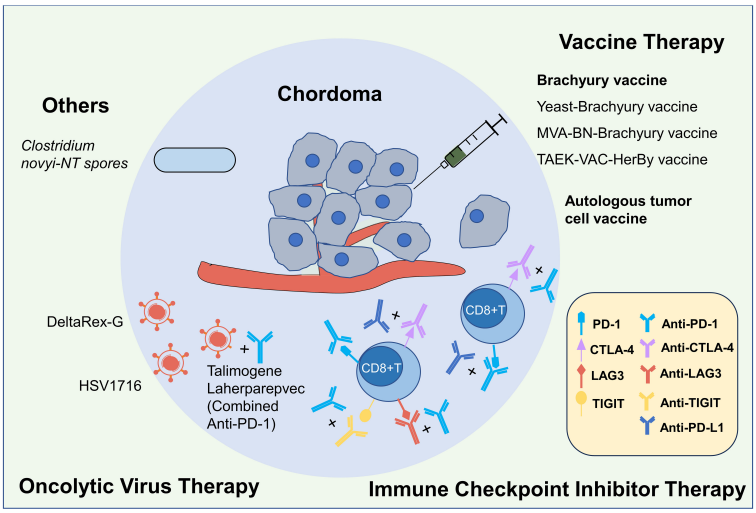

FIGURE 2
Immunotherapies for chordoma. Currently, the immunotherapy research on chordoma mainly includes four categories: vaccine, immune checkpoint inhibitor (ICI), oncolytic virus and others, and previous published studies primarily focused on the first two categories. In terms of the Brachyury vaccine research, the safety of the yeast-derived Brachyury vaccine and the MVA-BN-Brachyury-TRICOM vaccine has been identified, but their efficacy still requires further research. The phase I clinical trial of TAEK-VAC-HerBy vaccine was ongoing (NCT04246671). There have been one case report on autologous tumor cell vaccine. Previous ICIs studies mostly been based on individual cases, lacking large-scale studies, and its afty and efficacy varies. Currently, there are multiple clinical studies underway exploring immune checkpoint inhibitors with different ICI regimens and combination therapies. Research on oncolytic virus and other treatments is relatively limited, but several relevant clinical trials are also underway.

TABLE 1 Immunotherapy Clinical Trials in Chordoma.

Classification	NCT Number	Study Title	Interventions	Age	Phase	Enrollment	Combination with Other Therapy
Immune Checkpoint Inhibitor Therapy	NCT04416568	Study of Nivolumab and Ipilimumab in Children and Young Adults with INI1-Negative Cancers	Nivolumab (Anti-PD-1 antibody), Ipilimumab (Anti-CTLA-4 antibody)	Child, Adult	Phase2	45	/
	NCT03623854	Nivolumab and Relatlimab in Treating Participants with Advanced Chordoma	Nivolumab (Anti-PD-1 antibody), Relatlimab (Anti-LAG-3 antibody)	Child, Adult, Older adult	Phase2	10	/
	NCT03058289	A Phase 1/2 Safety Study of Intratumorally Dosed INT230-6	Anti-PD-1 antibody, Anti-CTLA-4 antibody, INT230-6 (A novel drug)	Adult, Older adult	Phase1, Phase2	110	Combination with a novel, experimental drug, INT230-6.
	NCT02936102	A Study of FAZ053 Single Agent and in Combination with PDR001 in Patients with Advanced Malignancies.	FAZ053 (Anti-PD-L1 antibody), PDR001 (Anti-PD-1 antibody)	Adult, Older adult	Phase1	154	/
	NCT05407441	Tazemetostat +Nivo/Ipi in INI1-Neg/SMARCA4-Def Tumors	Tazemetostat (EZH2 Inhibitor), Nivolumab (Anti-PD-1 antibody), Ipilimumab (Anti-CTLA-4 antibody)	Child, Adult	Phase1, Phase2	49	Combination with EZH2 Inhibitor, Tazemetostat.
	NCT02989636	Nivolumab With or Without Stereotactic Radiosurgery in Treating Patients with Recurrent, Advanced, or Metastatic Chordoma	Nivolumab (Anti-PD-1 antibody), Stereotactic Radiosurgery	Child, Adult, Older adult	Phase1	21	Combination with Stereotactic Radiosurgery
	NCT05286801	Tiragolumab and Atezolizumab for the Treatment of Relapsed or Refractory SMARCB1 or SMARCA4 Deficient Tumors	Tiragolumab (Anti-TIGIT antibody), Atezolizumab (Anti-PD-L1 antibody)	Child, Adult, Older adult	Phase1, Phase2	86	/
	NCT03190174	Nivolumab (Opdivo) Plus ABI-009 (Nab-rapamycin) for Advanced Sarcoma and Certain Cancers	Nab-Rapamycin (mTOR Inhibitor), Nivolumab (Anti-PD-1 antibody)	Child, Adult, Older adult	Phase1, Phase2	34	Combination with mTOR Inhibitor, ABI-009.
	NCT02834013				Phase2	818	/

(Continued)

TABLE 1 Continued

Classification	NCT Number	Study Title	Interventions	Age	Phase	Enrollment	Combination with Other Therapy
		Nivolumab and Ipilimumab in Treating Patients With Rare Tumors	Ipilimumab (Anti-CTLA-4 antibody), Nivolumab (Anti-PD-1 antibody)	Adult, Older adult			
Vaccine	NCT03595228	BN Brachyury and Radiation in Chordoma	BN-Brachyury Radiation	Child, Adult, Older adult	Phase2	29	Combination with radiation.
	NCT02383498	QUILT-3.011 Phase 2 Yeast-Brachyury Vaccine Chordoma	GI-6301 Placebo, GI-6301 Vaccine (Yeast- Brachyury), Radiotherapy	Adult, Older adult	Phase2	55	Combination with radiation.
	NCT04246671	TAEK-VAC-HerBy Vaccine for Brachyury and HER2 Expressing Cancer	TAEK-VAC-HerBy (Expressing Brachyury and HER2)	Adult, Older adult	Phase1	55	/
Oncolytic Virus	NCT00931931	HSV1716 in Patients with Non-Central Nervous System (Non-CNS) Solid Tumors	HSV1716	Child, Adult	Phase1	18	/
	NCT04091295	BLESSED: Expanded Access for DeltaRex-G for Advanced Pancreatic Cancer and Sarcoma	DeltaRex-G	Child, Adult, Older adult	/		
	NCT03886311	Talimogene Laherparepvec, Nivolumab and Trabectedin for Sarcoma	Talimogene Laherparepvec (A novel Oncolytic Virus), Nivolumab (Anti-PD-1 antibody), Trabectedin (A chemotherapy drug)	Adult, Older adult	Phase2	40	Combination with Nivolumab or Trabectedin.
Others	NCT01924689	Safety Study of Intratumoral Injection of Clostridium Novyi-NT Spores to Treat Patients with Solid Tumors That Have Not Responded to Standard Therapies	Clostridium novyi-NT spores (A kind of designed bacterium)	Adult, Older adult	Phase1	24	/

Although this clinical trial failed, it did not dissuade researchers from designing new Brachyury vaccines. Peter et al. conducted another Phase I clinical trial of a recombinant carrier Brachyury vaccine (MVA-BN-Brachyury-TRICOM vaccine) and the results showed good safety and significant Brachyury-specific T cell responses for this carrier Brachyury vaccine (49). At present, the Phase II clinical study of this BN-Brachyury had also been completed (NCT03595228). It enrolled 29 patients with chordoma to evaluate whether BN-Brachyury vaccine combined with radiotherapy could improve the objective radiological response rate (ORR) of patients, and the relevant results had not yet been published. Expect for this study, another Phase I clinical trial of Brachyury vaccine was ongoing (NCT04246671). The experiment used a novel recombinant virus TAEK-VAC-HerBy which expressed both Brachyury and HER2 peptides to stimulate the immune system and activate the anti-tumor immunity. The trial was currently recruiting patients, and the results had not yet been observed.

In addition to Brachyury vaccine therapy, there had been studies using irradiated autologous tumor cells as vaccine to treat chordomas. In 2015, Denis et al. subcutaneously implanted irradiated autologous tumor cells in a 49-year-old male skull base

chondroid chordoma patient (NCT02193503). The patient received a total of five injections over a nine-week period, after which time the patient experienced no systemic toxicity and a delayed-type hypersensitivity reaction to the patient's autologous tumor cells. Two months after vaccination, the tumor showed continuous shrinkage, the mucosal invasive tumor completely disappeared and the skull base and facial tumors showed long-term reduction, showing the good effect of the autologous tumor vaccine (50).

The results mentioned above indicated that the vaccine therapy for chordoma might be effective. However, there were still very few studies at present, and the data obtained were very limited. More clinical trials were needed to screen safe and effective vaccines for chordoma.

3.2 ICI therapy

ICI therapy had shown good results in a variety of tumors. In chordoma, the published literature on ICI therapies were mostly sporadic case reports, and clinical cohort studies were rare. The first ICI study in chordoma was reported in 2017. Denis treated 2 chordoma patients with PD-1 monoclonal antibody, including one conventional chordoma with metastases and one dedifferentiated chordoma with local recurrence. Although IHC staining showed low expression of the PD-1/PD-L1 in both cases before the ICI treatment, both of them received clinical and imaging remission after ICI treatment, and one of them showed a significant increase in PD-L1 expression after (50). Andrew et al. reviewed the cases of 17 patients with recurrent chordomas who received ICI therapy from 2016 to 2020, most of whom received Pembrolizumab (n=9, 53%) treatment. The results showed that the safety of ICI therapy was acceptable, but 2 patients experiencing grade 3/4 immune-related toxicity. In terms of efficacy, most patients had clinical benefits (n=15, 88%), including complete remission (CR, n=1, 6%), partial remission (PR, n=3, 18%) and stable disease (SD, n=11, 65%). Among all responders (n=15), the median response duration was 12 months. The 1-year OS rate was 87%, the 1-year PFS rate was 56% and the median PFS was 14 months (51). Carine et al. reviewed ICI therapies for SMARCB1-deficient sarcomas, including 1 case of atypical chordoma whose tumor shrunk significantly after receiving PD-1 inhibitor treatment (52). The results were encouraging, indicating that ICI therapy had a high clinical benefit rate for patients with recurrent chordomas.

In contrast to the above encouraging results, a Phase II clinical study on PD-L1 monoclonal antibody combined with CTLA-4 monoclonal antibody for advanced or metastatic bone tumors showed that among the 5 chordoma patients included in the study, only 1 patient had obvious tumor shrinkage and achieved CR after receiving a full course of twelve cycles (53). Xiang et al. conducted a systematic review of 22 chordoma cases involving progression from 2015 to 2022 and found that combination therapy with PD-1/PD-L1 antibodies and CTLA-4 monoclonal antibody was no more effective than monotherapy with PD-1/PD-L1 antibodies, but it was more toxic (54). However, due to the small number of cases and inconsistent drug regimens, the reliability of this result needed to be further verified. At present, there were two Phase II clinical trials (NCT04416568, NCT02834013) of PD-1 inhibitors and CTLA-4 inhibitors in the treatment of chordoma ongoing, and the efficacy of them was yet to be reported.

Reviewing the existing clinical data of ICI treatment of chordoma, we thought that ICI therapy might be effective for chordoma, and the choice of treatment plan might have a great impact on the treatment effect. However, it was still difficult to draw conclusions about when chordomas should receive ICI therapy and what treatment plan was optimal because of the limited ICIs therapies cases. Multiple ICI combination regimens, including two-ICI or multi-ICI combination, ICI combined with radiotherapy, ICI combined with chemotherapy were currently in clinical trials, and the relevant results would further deepen our understanding of chordoma immunotherapy.

3.3 Other immunotherapies

Some other immunotherapy options were on the clinical trials, such as CAR-T therapy or oncolytic virus therapy but had not yet been reported in clinical research on chordoma.

For CAR-T therapy, Long et al. had designed a kind of B7-H3 targeted CAR-T and verified its efficacy *in vitro*, but no further clinical trials had been registered (45). And regarding the oncolytic virus, there were three oncolytic virus clinical trials (NCT00931931, NCT00931931, NCT03886311) were in progress and relevant experimental results had not yet been published.

In addition to the above-mentioned common immunotherapy regimens, there was another rare immunotherapy clinical trial ongoing, a Phase I clinical trial (NCT01924689) enrolled 1 case of chordoma patient and studied the safety of the intratumoral injection of *Clostridium novyi-NT spores* in solid tumors which were not sensitive to standard treatment. *Clostridium novyi-NT spores* were an attenuated strain of *C. novyi* that lacked the lethal alpha toxin. When administered intravenously or intratumorally, *C. novyi-NT spores* could colonize and replicate in hypoxic regions of the tumor, triggering strong, precise, and tumor-limited cell lysis and immune-inflammatory responses, resulting in tumor death (55, 56). In this Phase I clinical trial, there were 8 cases of grade 3/4 adverse reactions in all 24 enrolled patients and the chordoma was stable for efficacy assessment after treatment (57). Based on the safety and efficacy of this study, we believed that the safety of this immunotherapy might still need to be further improved, and there was still a long way to go.

Combining the immunotherapy studies results mentioned above, we could see that currently, the only immunotherapy with significant research outcomes for chordoma was vaccine therapy. This was mainly because the presence of the tumor-specific antigen, Brachyury, in chordoma, which provided a clear target for vaccine research. Therefore, it was theoretically feasible to develop a vaccine targeting Brachyury to treat chordoma. The focus of current research on Brachyury vaccine was how to stimulate T cells more effectively to achieve a tumor-killing effect.

In addition, ICI therapy, due to its numerous selectivity options, was part of the widely conducted clinical trials. However, research reports on its safety and drug combinations were controversy and

lacking in large-scale studies. In future research, the safety issue must be addressed first in order to continue further studies. Overall, vaccine therapy and ICI therapy were the main directions for future immunotherapy of chordoma.

4 Conclusion

Through a review of studies on the immune microenvironment and immunotherapy for chordoma, we found that current studies were still relatively limited and narrowly scoped.

For the immune microenvironment of chordoma, CD4+T cells and macrophages were currently believed as the most abundant infiltration subsets of immune cells, a variety of cytokines and chemokines were high secretion and multiple immune checkpoints such as PD-1, PD-L1 and CTLA-4 were high expression there, which had important impact on tumor progression and patient prognosis. However, some existing contradictory research results needed to be further studied, interpreted, and analyzed, and the production mechanism of immune cell infiltration, cytokine secretion, immune checkpoint expression and its interaction mechanism with tumor cells was still blank and needed to be further demonstrated.

For the immunotherapy of chordoma, vaccine therapy and ICI therapy were currently being developed, but no breakthrough progress had been made. Other immunotherapy studies, such as oncolytic virus therapy or CAR-T therapy, were still mainly in the preclinical stage, with only a few clinical trials underway. Overall, there were few published clinical studies on immunotherapy of chordoma and there was a lack of effective pooled analysis. Although clinical trials were underway, there were still insufficient types (e.g., no CAR-T clinical trials) and a small number (only 16 clinical trials), which still needed to be further expanded.

In summary, immunotherapy for chordoma still had a long way to go, and it was necessary to carry out joint research from both basic and clinical aspects to accelerate the pace of immunotherapy research for chordoma.

Author contributions

YC: Writing – review & editing, Writing – original draft. HZ: Writing – review & editing.

Funding

The author(s) declare that no financial support was received for the research, authorship, and/or publication of this article. The authors received no funding for this work.

Conflict of interest

The authors declare that the research was conducted in the absence of any commercial or financial relationships that could be construed as a potential conflict of interest.

The reviewer HX declared a shared parent affiliation with the authors to the handling editor at the time of review.

Publisher's note

References

1. Frezza AM, Botta L, Trama A, Dei Tos AP, Stacchiotti S. Chordoma: update on disease, epidemiology, biology and medical therapies. *Curr Opin Oncol.* (2019) 31:114–20. doi: 10.1097/CCO.0000000000000502

2. Smoll NR, Gautschi OP, Radovanovic I, Schaller K, Weber DC. Incidence and relative survival of chordomas: the standardized mortality ratio and the impact of chordomas on a population. *Cancer.* (2013) 119:2029–37. doi: 10.1002/cncr.28032

3. Kremenevski N, Schlaffer S-M, Coras R, Kinfe TM, Graillon T, Buchfelder M. Skull base chordomas and chondrosarcomas. *Neuroendocrinology.* (2020) 110:836–47. doi: 10.1159/000509386

4. Kaufman D, Farias V, Lipton J, Brichkov I. Lung chordoma: A discussion. *Ann Thorac Surg.* (2022) 114:e33–e4. doi: 10.1016/j.athoracsur.2021.09.018

5. van Akkooi AC, van Geel AN, Bessems JH, den Bakker MA. Extra-axial chordoma. *J Bone Joint Surg Br.* (2006) 88:1232–4. doi: 10.1302/0301-620x.88b9.17873

6. Roberti F, Sekhar LN, Jones RV, Wright DC. Intradural cranial chordoma: A rare presentation of an uncommon tumor. Surgical experience and review of the literature. *J Neurosurg.* (2007) 106:270–4. doi: 10.3171/jns.2007.106.2.270

7. Zhai Y, Bai J, Li M, Wang S, Li C, Wei X, et al. A nomogram to predict the progression-free survival of clival chordoma. *J Neurosurg.* (2019), 1–9. doi: 10.3171/2019.10.JNS192414

8. Strauss SJ, Frezza AM, Abecassis N, Bajpai J, Bauer S, Biagini R, et al. Bone sarcomas: esmo-euracan-genturis-ern paedcan clinical practice guideline for diagnosis, treatment and follow-up. *Ann Oncology: Off J Eur Soc For Med Oncol.* (2021) 32:1520–36. doi: 10.1016/j.annonc.2021.08.1995

9. Ji Z, Long H, Hu Y, Qiu X, Chen X, Li Z, et al. Expression of MDR1, HIF-1α and MRP1 in sacral chordoma and chordoma cell line CM-319. *J Exp Clin Cancer Research: CR.* (2010) 29:158. doi: 10.1186/1756-9966-29-158

10. Stacchiotti S, Tamborini E, Lo Vullo S, Bozzi F, Messina A, Morosi C, et al. Phase II study on lapatinib in advanced EGFR-positive chordoma. *Ann Oncol.* (2013) 24:1931–6. doi: 10.1093/annonc/mdt117

11. Stacchiotti S, Longhi A, Ferraresi V, Grignani G, Comandone A, Stupp R, et al. Phase II study of imatinib in advanced chordoma. *J Clin Oncol.* (2012) 30:914–20. doi: 10.1200/JCO.2011.35.3656

12. Liu C, Jia Q, Wei H, Yang X, Liu T, Zhao J, et al. Apatinib in patients with advanced chordoma: A single-arm, single-centre, phase 2 study. *Lancet Oncol.* (2020) 21:1244–52. doi: 10.1016/s1470-2045(20)30466-6

13. Whelan JS, Davis LE. Osteosarcoma, chondrosarcoma, and chordoma. *J Clin Oncology: Off J Am Soc Clin Oncol.* (2018) 36:188–93. doi: 10.1200/JCO.2017.75.1743

14. Vujovic S, Henderson S, Presneau N, Odell E, Jacques TS, Tirabosco R, et al. Brachyury, a crucial regulator of notochordal development, is a novel biomarker for chordomas. *J Pathol.* (2006) 209:157–65. doi: 10.1002/path.1969

15. Heery CR, Singh BH, Rauckhorst M, Marté JL, Donahue RN, Grenga I, et al. Phase I trial of a yeast-based therapeutic cancer vaccine (Gi-6301) targeting the transcription factor brachyury. *Cancer Immunol Res.* (2015) 3:1248–56. doi: 10.1158/2326-6066.Cir-15-0119

16. DeMaria PJ, Bilusic M, Park DM, Heery CR, Donahue RN, Madan RA, et al. Randomized, double-blind, placebo-controlled phase II study of yeast-brachyury

vaccine (Gi-6301) in combination with standard-of-care radiotherapy in locally advanced, unresectable chordoma. *Oncologist*. (2021) 26:e847–e58. doi: 10.1002/onco.13720

17. Patel SS, Nota SP, Sabbatino F, Nielsen GP, Deshpande V, Wang X, et al. Defective HLA class I expression and patterns of lymphocyte infiltration in chordoma tumors. *Clin Orthop Relat Res*. (2021) 479:1373–82. doi: 10.1097/corr.0000000000001587

18. Dridi M, Krebs-Drouot L, Meyronet D, Dumollard JM, Vassal F, Jouanneau E, et al. The immune microenvironment of chordomas: an immunohistochemical analysis. *Cancers*. (2021) 13. doi: 10.3390/cancers13133335

19. Duan W, Zhang B, Li X, Chen W, Jia S, Xin Z, et al. Single-cell transcriptome profiling reveals intra-tumoral heterogeneity in human chordomas. *Cancer Immunology Immunotherapy: CII*. (2022) 71:2185–95. doi: 10.1007/s00262-022-03152-1

20. Morimoto Y, Tamura R, Ohara K, Kosugi K, Oishi Y, Kuranari Y, et al. Prognostic significance of VEGF receptors expression on the tumor cells in skull base chordoma. *J Neuro-oncology*. (2019) 144:65–77. doi: 10.1007/s11060-019-03221-z

21. Dancsok AR, Gao D, Lee AF, Steigen SE, Blay J-Y, Thomas DM, et al. Tumor-associated macrophages and macrophage-related immune checkpoint expression in sarcomas. *Oncoimmunology*. (2020) 9:1747340. doi: 10.1080/2162402X.2020.1747340

22. Lopez DC, Robbins YL, Kowalczyk JT, Lassoued W, Gulley JL, Miettinen MM, et al. Multi-spectral immunofluorescence evaluation of the myeloid, T cell, and natural killer cell tumor immune microenvironment in chordoma may guide immunotherapeutic strategies. *Front Oncol*. (2022) 12:1012058. doi: 10.3389/fonc.2022.1012058

23. Zou M-X, Lv G-H, Wang X-B, Huang W, Li J, Jiang Y, et al. Clinical impact of the immune microenvironment in spinal chordoma: immunoscore as an independent favorable prognostic factor. *Neurosurgery*. (2019) 84:E318–E33. doi: 10.1093/neuros/nyy274

24. Zou MX, Pan Y, Huang W, Zhang TL, Escobar D, Wang XB, et al. A four-factor immune risk score signature predicts the clinical outcome of patients with spinal chordoma. *Clin Transl Med*. (2020) 10:224–37. doi: 10.1002/ctm2.4

25. Zhou J, Jiang Y, Zhang H, Chen L, Luo P, Li L, et al. Clinicopathological implications of TIM3(+) tumor-infiltrating lymphocytes and the miR-455-5p/Galectin-9 axis in skull base chordoma patients. *Cancer Immunol Immunother*. (2019) 68:1157–69. doi: 10.1007/s00262-019-02349-1

26. Zou MX, Guo KM, Lv GH, Huang W, Li J, Wang XB, et al. Clinicopathologic implications of CD8(+)/Foxp3(+) ratio and miR-574-3p/PD-L1 axis in spinal chordoma patients. *Cancer Immunol Immunother*. (2018) 67:209–24. doi: 10.1007/s00262-017-2080-1

27. Zou MX, Zheng BW, Liu FS, Wang XB, Hu JR, Huang W, et al. The relationship between tumor-stroma ratio, the immune microenvironment, and survival in patients with spinal chordoma. *Neurosurgery*. (2019) 85:E1095–e110. doi: 10.1093/neuros/nyz333

28. Longoni M, Orzan F, Stroppi M, Boari N, Mortini P, Riva P. Evaluation of 1p36 markers and clinical outcome in a skull base chordoma study. *Neuro-oncology*. (2008) 10:52–60. doi: 10.1215/15228517-2007-048

29. Le LP, Nielsen GP, Rosenberg AE, Thomas D, Batten JM, Deshpande V, et al. Recurrent chromosomal copy number alterations in sporadic chordomas. *PloS One*. (2011) 6:e18846. doi: 10.1371/journal.pone.0018846

30. Miozzo M, Dalprà L, Riva P, Volontà M, Macciardi F, Pericotti S, et al. A tumor suppressor locus in familial and sporadic chordoma maps to 1p36. *Int J Cancer*. (2000) 87:68–72.

31. Riva P, Crosti F, Orzan F, Dalprà L, Mortini P, Parafioriti A, et al. Mapping of candidate region for chordoma development to 1p36.13 by LOH analysis. *Int J Cancer*. (2003) 107:493–7. doi: 10.1002/ijc.11421

32. Halvorsen SC, Benita Y, Hopton M, Hoppe B, Gunnlaugsson HO, Korgaonkar P, et al. Transcriptional profiling supports the notochordal origin of chordoma and its dependence on a TGFB1-TBXT network. *Am J Pathol*. (2023) 193:532–47. doi: 10.1016/j.ajpath.2023.01.014

33. Ma J, Tian K, Wang L, Wang K, Du J, Li D, et al. High expression of TGF-B1 predicting tumor progression in skull base chordomas. *World Neurosurg*. (2019) 131:e265–e70. doi: 10.1016/j.wneu.2019.07.128

34. Wang L, Guan X, Hu Q, Wu Z, Chen W, Song L, et al. TGFB3 downregulation causing chordomagenesis and its tumor suppression role maintained by Smad7. *Carcinogenesis*. (2021) 42:913–23. doi: 10.1093/carcin/bgab022

35. Xu J, Shi Q, Lou J, Wang B, Wang W, Niu J, et al. Chordoma recruits and polarizes tumor-associated macrophages *via* secreting CCL5 to promote Malignant progression. *J For Immunotherapy Cancer*. (2023) 11. doi: 10.1136/jitc-2023-006808

36. Gulluoglu S, Tuysuz EC, Sahin M, Yaltirik CK, Kuskucu A, Ozkan F, et al. The role of TNF-A in chordoma progression and inflammatory pathways. *Cell Oncol (Dordrecht)*. (2019) 42:663–77. doi: 10.1007/s13402-019-00454-y

37. Gulluoglu S, Sahin M, Tuysuz EC, Yaltirik CK, Kuskucu A, Ozkan F, et al. Leukemia inhibitory factor promotes aggressiveness of chordoma. *Oncol Res*. (2017) 25:1177–88. doi: 10.3727/096504017x14874349473815

38. Kushlinskii NE, Timofeev YS, Solov'ev YN, Gerstein ES, Lyubimova NV, Bulycheva IV. Components of the RANK/RANKL/OPG system, IL-6, IL-8, IL-16, MMP-2, and calcitonin in the sera of patients with bone tumors. *Bull Exp Biol Med*. (2014) 157:520–3. doi: 10.1007/s10517-014-2605-y

39. Bilusic M, Heery CR, Collins JM, Donahue RN, Palena C, Madan RA, et al. Phase I trial of HuMax-IL8 (BMS-986253), an anti-IL-8 monoclonal antibody, in patients with metastatic or unresectable solid tumors. *J Immunother Cancer*. (2019) 7:240. doi: 10.1186/s40425-019-0706-x

40. Mathios D, Ruzevick J, Jackson CM, Xu H, Shah SR, Taube JM, et al. PD-1, PD-L1, PD-L2 expression in the chordoma microenvironment. *J Neurooncol*. (2015) 121:251–9. doi: 10.1007/s11060-014-1637-5

41. Williamson LM, Rive CM, Di Francesco D, Titmuss E, Chun H-JE, Brown SD, et al. Clinical response to nivolumab in an INI1-deficient pediatric chordoma correlates with immunogenic recognition of brachyury. *NPJ Precis Oncol*. (2021) 5:103. doi: 10.1038/s41698-021-00238-4

42. Karpathiou G, Dridi M, Krebs-Drouot L, Vassal F, Jouanneau E, Jacquesson T, et al. Autophagic markers in chordomas: immunohistochemical analysis and comparison with the immune microenvironment of chordoma tissues. *Cancers (Basel)*. (2021) 13. doi: 10.3390/cancers13092169

43. Xia C, Huang W, Chen YL, Fu HB, Tang M, Zhang TL, et al. Coexpression of HHLA2 and PD-L1 on tumor cells independently predicts the survival of spinal chordoma patients. *Front Immunol*. (2021) 12:797407. doi: 10.3389/fimmu.2021.797407

44. He G, Liu X, Pan X, Ma Y, Liu X. Cytotoxic T lymphocyte antigen-4 (CTLA-4) expression in chordoma and tumor-infiltrating lymphocytes (TILS) predicts prognosis of spinal chordoma. *Clin Transl Oncol*. (2020) 22:2324–32. doi: 10.1007/s12094-020-02387-7

45. Long C, Li G, Zhang C, Jiang T, Li Y, Duan X, et al. B7-H3 as a target for car-T cell therapy in skull base chordoma. *Front In Oncol*. (2021) 11:659662. doi: 10.3389/fonc.2021.659662

46. Kushlinskii NE, Alferov AA, Timofeev YS, Gershtein ES, Bulycheva IV, Bondarev AV, et al. Key immune checkpoint PD-1/PD-L1 signaling pathway components in the blood serum from patients with bone tumors. *Bull Exp Biol Med*. (2020) 170:64–8. doi: 10.1007/s10517-020-05005-2

47. Kushlinskii NE, Kovaleva OV, Kuzmin YB, Korotkova EA, Gershtein ES, Boulytcheva IV, et al. Clinical and prognostic significance of the soluble form of the vista immunity control point in patients with primary bone tumors. *Klin Lab Diagn*. (2021) 66:533–8. doi: 10.51620/0869-2084-2021-66-9-533-538

48. Tarpey PS, Behjati S, Young MD, Martincorena I, Alexandrov LB, Farndon SJ, et al. The driver landscape of sporadic chordoma. *Nat Commun*. (2017) 8:890. doi: 10.1038/s41467-017-01026-0

49. DeMaria PJ, Lee-Wisdom K, Donahue RN, Madan RA, Karzai F, Schwab A, et al. Phase 1 open-label trial of intravenous administration of MVA-BN-brachyury-tricom vaccine in patients with advanced cancer. *J Immunother Cancer*. (2021) 9. doi: 10.1136/jitc-2021-003238

50. Migliorini D, Mach N, Aguiar D, Vernet R, Landis BN, Becker M, et al. First report of clinical responses to immunotherapy in 3 relapsing cases of chordoma after failure of standard therapies. *Oncoimmunology*. (2017) 6:e1338235. doi: 10.1080/2162402x.2017.1338235

51. Bishop AJ, Amini B, Lin H, Raza SM, Patel S, Grosshans DR, et al. Immune checkpoint inhibitors have clinical activity in patients with recurrent chordoma. *J Immunother*. (2022) 45:374–8. doi: 10.1097/cji.0000000000000431

52. Ngo C, Postel-Vinay S. Immunotherapy for SMARCB1-deficient sarcomas: current evidence and future developments. *Biomedicines*. (2022) 10. doi: 10.3390/biomedicines10030650

53. Somaiah N, Conley AP, Parra ER, Lin H, Amini B, Solis Soto L, et al. Durvalumab plus tremelimumab in advanced or metastatic soft tissue and bone sarcomas: A single-centre phase 2 trial. *Lancet Oncol*. (2022) 23:1156–66. doi: 10.1016/s1470-2045(22)00392-8

54. Wang X, Chen Z, Li B, Fan J, Xu W, Xiao J. Immunotherapy as a promising option for the treatment of advanced chordoma: A systemic review. *Cancers (Basel)*. (2022) 15. doi: 10.3390/cancers15010264

55. Dang LH, Bettegowda C, Huso DL, Kinzler KW, Vogelstein B. Combination bacteriolytic therapy for the treatment of experimental tumors. *Proc Natl Acad Sci United States America*. (2001) 98:15155–60. doi: 10.1073/pnas.251543698

56. Roberts NJ, Zhang L, Janku F, Collins A, Bai R-Y, Staedtke V, et al. Intratumoral injection of clostridium novyi-NT spores induces antitumor responses. *Sci Transl Med*. (2014) 6:249ra111. doi: 10.1126/scitranslmed.3008982

57. Janku F, Zhang HH, Pezeshki A, Goel S, Murthy R, Wang-Gillam A, et al. Intratumoral injection of clostridium novyi-NT spores in patients with treatment-refractory advanced solid tumors. *Clin Cancer Research: an Off J Am Assoc For Cancer Res*. (2021) 27. doi: 10.1158/1078-0432.CCR-20-2065

frontiers | Frontiers in Oncology

TYPE Original Research
PUBLISHED 15 July 2024
DOI 10.3389/fonc.2024.1421418

OPEN ACCESS

EDITED BY
Gerardo Caruso,
University Hospital
of Policlinico G. Martino, Italy

REVIEWED BY
Maura Massimino,
Fondazione IRCCS Istituto
Nazionale Tumori, Italy
Apostolos Pourtsidis,
Panagiotis & Aglaia Kyriakou Children's
Hospital, Greece

*CORRESPONDENCE
Cécile Faure-Conter
cecile.conter@ihope.fr

RECEIVED 22 April 2024
ACCEPTED 17 June 2024
PUBLISHED 15 July 2024

CITATION
Palenzuela G, Schiffler C, Frappaz D, Peyrl A, Gerber NU, Kortmann R-D, Philippe M, Zimmermann M, Murray MJ, Nicholson JC, Calaminus G and Faure-Conter C (2024) Acute toxicity of chemotherapy in central nervous system germ cell tumour patients according to age.
Front. Oncol. 14:1421418.
doi: 10.3389/fonc.2024.1421418

Acute toxicity of chemotherapy in central nervous system germ cell tumour patients according to age

Gilles Palenzuela[1], Camille Schiffler[2], Didier Frappaz[3], Andreas Peyrl[4], Nicolas U. Gerber[5], Rolf-Dieter Kortmann[6], Michael Philippe[7], Martin Zimmermann[8], Matthew J. Murray[9,10], James C. Nicholson[9], Gabriele Calaminus[11] and Cécile Faure-Conter[3]*

[1]University Hospital, Department of Paediatric Haematology and Oncology, Montpellier, France, [2]Department of Biostatistics, Centre Léon Bérard, Lyon, France, [3]Department of Pediatric Oncology, Institut d'Hémato-oncologie Pédiatrique, Lyon, France, [4]Department of Paediatrics, Medical University of Vienna, Vienna, Austria, [5]Department of Oncology, University Children's Hospital, Zürich, Switzerland, [6]Department of Radiotherapy, University Hospital, Leipzig, Germany, [7]Department of Clinical Pharmacy and Oncology, Centre Léon Bérard, Lyon, France, [8]Department of Paediatric Hematology and Oncology, Hannover Medical School, Hannover, Germany, [9]Department of Paediatric Haematology and Oncology, Cambridge University Hospitals, Cambridge, United Kingdom, [10]Department of Pathology, University of Cambridge, Cambridge, United Kingdom, [11]Department of Paediatric Haematology and Oncology, University Children's Hospital Bonn, Bonn, Germany

Background: SIOP-CNS-GCT-II European trial was opened for the treatment of patients of any age with central nervous system germ cell tumour (CNS-GCT). Four courses of pre-irradiation chemotherapy were delivered. The influence of patient age on chemotherapy related acute toxicity (CRAT) was assessed.

Methods: CRAT was analysed according to age-groups: children (aged ≤11 years), adolescents (aged 12-17 years), adults (aged ≥18 years) and to chemotherapy type: CarboPEI (alternating etoposide-carboplatin/etoposide-ifosfamide) for non-metastatic germinoma; PEI (cisplatin-etoposide-ifosfamide) for standard-risk non-germinomatous GCT (NGGCT); PEI and high-dose PEI (HD-PEI), for high-risk or poorly responsive NGGCTs.

Results: 296 patients were assessable for CRAT: 105 children, 121 adolescents, 70 adults (max age: 41 years). Median cumulative doses/m^2 of chemotherapy were similar among age-groups. The proportion of germinoma over NGGCT (and accordingly use of CarboPEI chemotherapy) was higher in the adult groups (79%) versus the other two groups (62%). Delay in chemotherapy ≥7 days was noticed in 27%, 38%, and 19% of children, adolescents, and adults, respectively. Grade ≥3 haematological and non-haematological adverse events (AEs) were observed in 94%/31%, 97%/36%, and 77%/21% of children, adolescents, and adults, respectively. No toxic death was reported. Grade ≥3 AEs and delayed chemotherapies were significantly rarer in adults when compared with adolescents, even when adjusted on chemotherapy type: odds ratio: 0.1 [95% CI 0.02-0.4], and 0.2 [95%CI 0.1-0.4] in the group treated with CarboPEI.

Conclusion: Adult patients can be treated safely with a chemotherapy intensive protocol, with even less toxicity than that observed in adolescents. Further work is required to understand age-related differences regarding toxicity.

KEYWORDS

germ cell tumour, chemotherapy, children, adults, adolescents, toxicity, age

Introduction

CNS-GCT are observed in children, adolescents, and young adults (1). In the past, standard treatment was limited to radiotherapy, at least for pure germinoma (2). To avoid the toxicity of radiation on maturing brains, therapeutic strategies including pre-irradiation chemotherapies were developed by paediatric groups (3, 4).

IIn non-metastatic germinoma, the French TC 90 protocol consisted of two cycles of CarboPEI followed by radiotherapy to the primary (40 Gy) and laid the basis of the SIOP-CNS-GCT96 trial (5). Later on, in the SIOP-CNS-GCTII trial, 24 Gy whole ventricular irradiation was added to prevent ventricular relapses (6). In non germinomatous germ cell tumour (NGGCT), the European SIOP-CNS-GCT-96 trial, evaluated a strategy consisting of four courses of PEI (cisplatin-etoposide- ifosfamide), followed by 54 Gy focal radiotherapy in non-metastatic NGGCT (or 30 Gy craniospinal if metastatic) and identified a high-risk (HR) group of patients, namely those aged less than six years or with Alpha-fetoprotein (AFP) level in serum and/or cerebrospinal fluid (CSF) above 1000 ng/ml at diagnosis (7). In the subsequent SIOP-CNS-GCT-II European trial, whose acute toxicity is presented here, chemotherapy for the HR-NGGCT group was intensified with 2 courses of high doses (HD) of etoposide and ifosfamide (HD-PEI) following 2 courses of standard dose PEI. Meanwhile, the upper age limit in the trial was withdrawn.

The potential toxicity, and thus the feasibility of these more intensive chemotherapy protocols in adults, currently remain a matter of debate. Indeed, chemotherapy related acute toxicity (CRAT) might increase with patient age, as already observed in other tumours such as medulloblastoma (8). The objective of this study was therefore to compare the tolerance of chemotherapy across age-groups within the SIOP-CNS-GCT-II trial.

Patients and methods

Population

Records of patients included in the European SIOP-CNS-GCT-II protocol (EudraCT number 2009-018072-33) and treated with chemotherapy were analysed. The inclusion period spanned almost seven years (06/10/2011 to 01/07/2018). Patients were treated either in the pure germinoma or NGGCT group. Information regarding gender, patient age, general status, presence of diabetes insipidus (DI), site of primary tumour and type of tumour were collected at diagnosis.

Treatment

In the germinoma group (Figure 1A), only patients with localised tumours (no spinal nor intracranial metastasis and negative CSF cytology, including bifocal presentation in suprasellar and pineal areas) received chemotherapy: two cycles of CarboPEI (etoposide 100 mg/m² on days 1-3 and days 22-24, carboplatin 600 mg/m² on day 1, ifosfamide 1800 mg/m² on days 22-26), followed by 24 Gy whole ventricular radiotherapy and, in case of post chemotherapy residual disease, a 16 Gy boost on residual disease. Cumulative doses of chemotherapy in this group were as follows: etoposide 1200 mg/m², carboplatin 1200 mg/m², ifosfamide 18000 mg/m². Patients with either metastatic or incompletely staged germinoma received craniospinal radiotherapy alone and were not analysed in this series.

In the NGGCT group (Figure 1B), all patients, regardless of stage, received four courses of pre-irradiation chemotherapy. Patients with standard-risk (SR)-NGGCT [serum and CSF AFP ≤1000 ng/ml and age ≥6 years at diagnosis] received three courses of PEI (cisplatin 20 mg/m² on days 1-5, etoposide 100 mg/m² on days 1-3, ifosfamide 1500 mg/m² on days 1-5) every 21 days, followed by tumour imaging reassessment. In case of complete remission, a fourth course of PEI was administrated; otherwise, resection of any residual was recommended. If no viable malignant tumour was identified on pathological review of the resection specimen, a fourth course of PEI was administrated. Cumulative doses in this group were as follows: cisplatin 400 mg/m², etoposide 1200 mg/m², ifosfamide 30000 mg/m². If malignant viable tumour cells were present on pathology of the resection specimen, the fourth course consisted of HD-PEI (cisplatin 20 mg/m² on days 1-5, etoposide 300 mg/m² on days 1-5, ifosfamide 2000 mg/m² on days 1-5) with haematopoietic stem cell support on day 7. Cumulative doses of chemotherapy in this group were as follows: cisplatin 400 mg/m², etoposide 2400 mg/m², ifosfamide 32500 mg/m². Patients with HR-NGGCT (serum or CSF AFP >1000 ng/ml or age <6 years at diagnosis) received two PEI with harvest of hematopoietic stem cells and two HD-PEI before surgery of any resectable residual disease. Cumulative doses of chemotherapy in this group were as follows: cisplatin 400 mg/m², etoposide 3600 mg/m², ifosfamide

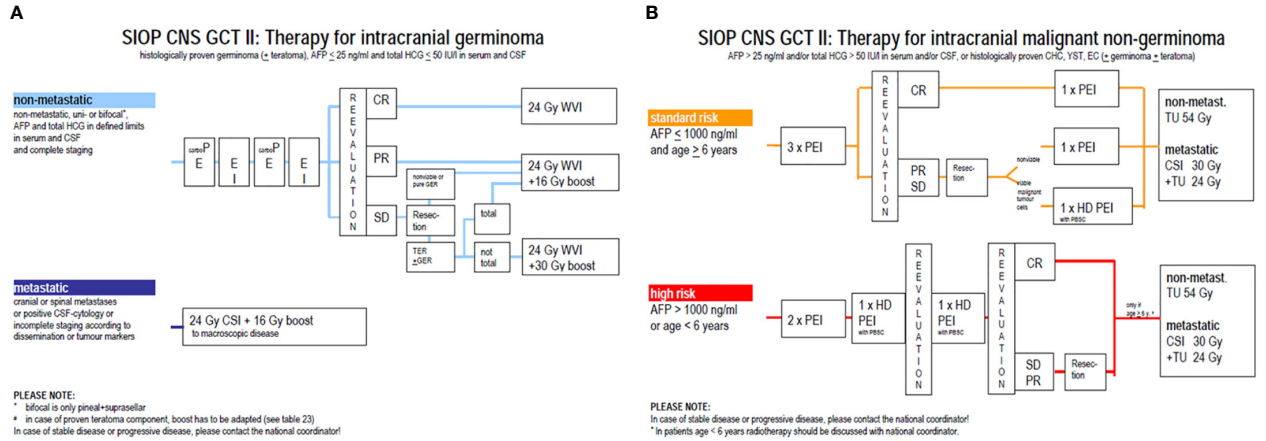

FIGURE 1
Overview of treatment for germinoma **(A)** and non germinomatous germ cell tumours **(B)**.

55000 mg/m². Then, all patients aged 6 years or more with SR and HR-NGGCT received 54 Gy focal irradiation to the initial tumour volume, with 30 Gy to the craniospinal axis for metastatic cases.

Data were analysed by therapeutic groups according to the three chemotherapy schemes: 'CarboPEI', 'PEI', and 'PEI/HD-PEI'. Patients who received non-protocol chemotherapy or a combination of protocol chemotherapies not described above were excluded from the analysis.

Chemotherapy-related acute toxicity

CRAT was assessed through two indicators: grade ≥3 adverse events (AE) and delayed chemotherapy. AE were recorded and graded prospectively in the database according to the common terminology criteria for adverse events (CTCAE) v4.0 scale. Grade ≥3 AE were analysed and split into haematological and non-haematological (peripheral neurotoxicity, infection/fever, gastrointestinal, renal, and auditory) AE.

Delayed chemotherapy was defined as an interval ≥28 days between two courses.

Statistical analysis

Statistical analyses were performed using SAS (Statistical Analysis System) version 9.4 (SAS Institute). Categorical data were summarised by frequencies and percentages and presented by age-group. Logistic regression analyses were performed to assess whether patient age or therapeutic group was correlated with delayed chemotherapy and/or occurrence of grade ≥3 AE. The odds ratio (OR) was assessed with a confidence interval (CI) of 95%. P-values of <0.05 were considered statistically significant.

Written informed consent was obtained from all patients/guardians at diagnosis, and national ethics review boards approved the trial.

Results

Population and treatment

Among the 306 patients included in the SIOP-CNS-GCT-II trial, 10 were excluded: two patients did not receive chemotherapy, five received non-protocol chemotherapy, and three received a combination of CarboPEI and PEI. Among the 296 remaining patients (Table 1), 105 (35%) were children, 121 (41%) were adolescents, and 70 (24%) were adults. Patients were predominantly male (80%). Median age at diagnosis was 14 years (range 0 to 41 years). The primary tumour was pineal site in 52% of patients, suprasellar in 25%, bifocal (pineal and suprasellar) in 20%.

The majority (66%) of patients had germinoma, and this proportion was higher in adults (79%) than in children and adolescents (61 and 62%, respectively). All 194 patients with germinoma received CarboPEI. Among the 102 patients with NGGCT, 77 (76%) received PEI, and 24 (24%) received PEI/HD-PEI (eight received one HD-PEI and 16 received two). One child (1%) with a localised pineal tumour had a CSF HCG level (52 UI/L) just above the trial threshold but received CarboPEI and was analysed in germinoma group. Upon local physician's choice, ten patients out of 296 (3%) had their chemotherapy doses reduced for all courses: for three adult patients, the body surface area (BSA) was capped at 2 m², leading to a 10% dose reduction for all the drugs (two patients in the CarboPEI group and one in the PEI group). For six adults and one adolescent (all in the CarboPEI group), carboplatin doses were capped at 1000 mg. In the PEI/HD-PEI therapeutic group, the mean doses of etoposide were 25% lower in the adult patients (2700 mg/m²) than in children and adolescents (3600 mg/m² and 3500 mg/m², respectively). Reasons for lowering the etoposide dosing in adults was not captured in the database; nevertheless, this represents the smallest therapeutic group with only four adult patients included. Despite those modifications, and with the exception of etoposide in the PEI/HD-PEI therapeutic group, cumulative doses of chemotherapy ultimately received by the

10.3389/fonc.2024.1421418

TABLE 1 Characteristics of patients and tumours at diagnostic by age groups.

	Children (0-11 y) n=105		Adolescents (12-17 y) n=121		Adults (≥18 y) n=70		All n=296	
Sex								
Male (%)	63	60%	108	89%	67	96%	238	80%
Female (%)	42	40%	13	11%	3	4%	58	20%
Age (years)								
N (missing)	105	0	121	0	70	0	296	0
Mean (std)	9	1,9	15	2	23	4,6	15	6
Median (min; max)	10	0;12	15	12; 18	22	18; 41	14	0; 41
General condition (Lansky/Karnofsky index)								
10-50 (%)	6	6%	8	7%	3	4%	17	6%
60-70 (%)	12	11%	12	10%	10	14%	34	12%
80-100 (%)	53	50%	77	64%	33	47%	163	55%
Not available (%)	34	32%	24	20%	24	34%	82	28%
Diabetes insipidus								
No (%)	52	50%	77	64%	48	69%	177	60%
Yes (%)	43	41%	42	35%	19	27%	104	35%
Not available (%)	10	10%	2	2%	3	4%	15	5%
Site of primary tumour								
Pineal (%)	47	45%	70	58%	38	54%	155	52%
Suprasellar (%)	42	40%	24	20%	9	13%	75	25%
Bifocal (pineal + suprasellar) (%)	15	14%	25	21%	19	27%	59	20%
Other site (%)	1	1%	2	2%	4	6%	7	2%
Diagnosis								
NGGCT (%)	41	39%	46	38%	15	21%	102	35%
Germinoma (%)	64	61%	75	62%	55	79%	194	66%

NGGCT, non-germinomatous germ cell tumour.

patients (Table 2) corresponded to the recommended doses and were similar within a therapeutic group across age-groups.

The vast majority of patients (n=289; 98%) received the four planned courses of treatment. Five patients (all with NGGCT) received only one (n=1 patient), two (n=2) or three (n=2) courses of chemotherapy (reason unknown). Conversely, two patients received five courses: one with HR-NGGCT received three PEI and two HD-PEI, and one patient with germinoma received a reduced dose course of etoposide-carboplatin and then two standard dose CarboPEI (reason unknown).

Adverse events

The numbers of patients with at least one grade ≥3 haematological and/or non-haematological AE are presented by age-group (Table 3). In the whole population, haematological grade ≥3 toxicity was observed in a vast majority of patients (91%). Haematological grade ≥3 toxicity was less frequent in the adult group (77%) than in the child and adolescent groups (94 and 97%, respectively). Non-haematological grade ≥3 AE were rarer and mainly gastrointestinal or infectious, being observed in approximately one-third (31%) of patients. Again, the frequency was lower in the adult group (21%) than in the child and adolescent groups (31 and 36% respectively). When considering the occurrence of AE by therapeutic group, all patients with the PEI/HD-PEI strategy had at least one grade ≥3 AE. The rate of patients with at least one haematological grade ≥3 AE was slightly greater in patients receiving PEI/HD-PEI than in patients with PEI or CarboPEI strategies (100% vs. 92% and 90%, respectively). Non-haematological grade ≥3 AE were more frequent in PEI/HD-PEI and PEI strategies than in the CarboPEI strategy (79% and 42% vs. 21%, respectively) and were mainly gastrointestinal and infection/fever. In the PEI/HD-PEI group, three of 24 patients (12%) had grade ≥3 peripheral neurotoxicity, and two patients had grade ≥3 renal toxicity.

10.3389/fonc.2024.1421418

TABLE 2 Median cumulative doses by therapeutic and age groups.

	Children (0-11 y) n=105		Adolescents (12-17 y) n=121		Adults (≥18 y) n=70		All n=296	
CarboPEI	65	62%	75	62%	55	79%	195	66%
Carboplatin mg/m² (min; max)	1200 (1000; 1200)		1200 (600; 2400)		1200 (600; 2400)		1200 (600; 2400)	
Ifosfamide mg/m² (min; max)	18000 (9000; 19000)		18000 (8500; 18300)		18000 (8500; 18000)		18000 (8500; 19000)	
Etoposide/Etoposide phosphate mg/m² (min; max)	1200 (1100; 1300)		1200 (300; 1600)		1200 (600; 1300)		1200 (300; 1600)	
PEI	32	31%	34	28%	11	16%	77	26%
Cisplatin mg/m² (min; max)	400 (100; 400)		400 (300; 420)		400 (320; 400)		400 (100; 420)	
Ifosfamide mg/m² (min; max)	30000 (460; 30500)		30000 (15000; 30500)		30000 (24000; 31000)		30000 (460; 31000)	
Etoposide/Etoposide phosphate mg/m² (min; max)	1200 (340; 1400)		1200 (900; 1300)		1200 (1100; 1300)		1200 (400; 1400)	
PEI/HD-PEI	8 (a)	8%	12 (b)	10%	4 (c)	6%	24	8%
Cisplatin mg/m² (min; max)	400 (300; 400)		400 (280; 400)		400 (330; 400)		400 (280; 400)	
Ifosfamide mg/m² (min; max)	33700 (17000; 38000)		34600 (24100; 35300)		32500 (28700; 34900)		33500 (17000; 38000)	
Etoposide/ Etoposide phosphate mg/m² (min; max)	3600 (2400; 3800)		3500 (2000; 4100)		2700 (2400; 3600)		3600 (2000; 4100)	

(a) 5 patients had 2 PEI + 2 HD-PEI, 2 patients had 3 PEI + 1 HD-PEI, 1 patient had 3 PEI + 2 HD-PEI; (b) 8 patients had 2 PEI + 2 HD-PEI, 4 patients had 3 PEI + 1 HD-PEI; (c) 2 patients had 2 PEI + 2 HD-PEI, 2 patients had 3 PEI + 1 HD-PEI. HD-PEI: haute dose PEI.

Multivariable analyses (Table 4) revealed that the occurrence of grade ≥3 haematological and non-haematological AE was neither statistically related to therapeutic group (p=0.9636), nor to sex (p=0.1617) but instead to age-group (p= 0.0011), with a lower risk for adults [OR=0.1 (0.03-0.4), when compared with adolescents. This was confirmed when considering only the subgroup of patients treated with CarboPEI (main group): adults treated with CarboPEI were less likely (p=0.0002) to experience a grade ≥3 AE [OR=0.1 (0.02-0.4)] when compared with adolescents treated similarly.

Delayed chemotherapy

The interval between two courses of chemotherapy was similar in the three age-groups, with a median interval of 22 days (range 15-79 days). Twenty-nine percent of patients experienced delayed chemotherapy. This rate was higher in adolescents than in the paediatric or adult population (38% vs. 27% and 19%, respectively) (Table 5).

Logistic regression analyses (Table 6) revealed that the occurrence of delayed chemotherapy was not statistically related to sex (p=0.1591) but statistically related to therapeutic group (p=0.0164), with a greater risk for the PEI strategy [OR: 3.4 (1.4-8.5)] and was statistically related to patient age (p=0.0001), with a lower risk for adults [OR: 0.2 (0.1-0.4)] when compared with adolescents. This was confirmed when considering only the subgroup of patients treated with CarboPEI (main group), again adults were less statistically (p=0.0002) likely to experience a delay in chemotherapy [OR: 0.2 (0.1-0.4)] when compared with adolescents. Qualitative analysis of missing data demonstrated a

TABLE 3 Patients with at least one ≥ grade 3 adverse event according to age groups.

	Children (0-11 y) n=105		Adolescents (12-17 y) n=121		Adults (≥18 y) n=70		All n=296	
Hematological toxicities (%)	99	94%	118	98%	54	77%	271	92%
Non-hematological toxicities (%)	33	31%	44	36%	15	21%	92	31%
Digestive toxicity (%)	17	16%	29	24%	5	7%	51	17%
Infection/Fever (%)	17	16%	20	17%	7	10%	44	15%
Peripheral neurotoxicity (%)	6	6%	3	3%	2	3%	11	4%
Renal toxicity (%)	4	4%	3	3%	2	3%	9	3%
Auditory toxicity (%)	1	1%	2	2%	1	1%	4	1%

10.3389/fonc.2024.1421418

TABLE 4 Impact of age, sex and therapeutic group on the occurrence of grade ≥3 adverse event in the whole population and in the CarboPEI group.

	Occurrence of grade ≥3 adverse event				All; n=296		Odd ratio [95% confidence interval]	p-value
	No; n=24		Yes; n=272					
Age group								
Children (0-11 y)	6	25%	99	36%	105	35%	0.3 [0.1-1.4]	p:0.0011
Adolescent (12-17 y)	3	12%	118	43%	121	41%	Ref	
Adults (≥18 y)	15	63%	55	20%	70	24%	0.1 [0.03-0.4]	
Therapeutic group								
PEI	6	25%	71	26%	77	26%	0.9 [0.3-2.4]	p:0.9636
PEI/HD-PEI	0	0%	24	9%	24	8%	∞ [∞-∞]	
CarboPEI	18	75%	177	65%	195	66%	Ref	
Sex								
Male	23	96%	215	79%	238	80%	Ref	p:0.1617
Female	1	4%	57	21%	58	20%	4.5 [0.5-37.3]	
	Occurrence of grade ≥3 adverse event				Carbo PEI; n=195		Odd ratio [95% confidence interval]	p-value
	No; n=18		Yes; n=177					
Age group								
Children (0-11 y)	2	11%	63	36%	65	33%	0.9 [0.1-6.3]	p:0.0002
Adolescent (12-17 y)	2	11%	73	41%	75	39%	Ref	
Adults (≥18 y)	14	78%	41	23%	55	28%	0.1 [0.02-0.4]	

similar percentage of missing data per cure across age-group (date not shown).

Discussion

The current study investigated the impact of age on the occurrence of (CRAT). It unexpectedly did not reveal higher levels of CRAT in adults, but reported higher CRAT in the adolescent group. Apart from lower cumulative doses of etoposide in the small adult HR-NGGCT group, similar doses of chemotherapy were otherwise applied. These results seem not explained by under-reporting of AEs, although we cannot rule out the possibility that a longer interval between treatment and completion of the clinical formulary (CRF) in the adult department may have underestimated toxicity. This observation may rather reflect either an age-specific susceptibility to the drug but other explanations such as differences in the management of supportive care or at-risk behaviours could be considered.

The relationship between age and CRAT has been widely reported, but sometimes with conflicting data. Whereas in sarcoma it has been suggested that the toxicity was equivalent or

TABLE 5 Patients with at least one delayed course of chemotherapy according to age group.

	Children (0-11 y) n=105		Adolescents (12-17 y) n=121		Adults (≥18 y) n=70		All n=296	
Chemotherapy delayed 7 days or more	28	27%	46	38%	13	19%	87	29%
Reason for delayed chemotherapy								
Prolonged aplasia (%)	15	14%	27	22%	5	7%	47	16%
Renal toxicity (%)	0	0%	2	2%	0	0%	2	1%
Clinical status (%)	5	5%	5	4%	0	0%	10	3%
Other (%)	12	11%	15	12%	10	14%	37	13%

10.3389/fonc.2024.1421418

TABLE 6 Impact of age, sex and therapeutic group on delayed chemotherapy on the whole population and in the CarboPEI group.

	Delayed chemotherapy				All; n=296		Odd ratio [95% confidence interval]	p-value
	No; n=209		Yes; n=87					
Age group								
Children (0-11 y)	77	37%	28	32%	105	35%	0.5 [0.2-1.1]	0.0003
Adolescent (12-17 y)	75	36%	46	53%	121	41%	Ref	
Adults (≥18 y)	57	27%	13	15%	70	24%	0.2 [0.1-0.4]	
Therapeutic group								
PEI	57	27%	20	23%	77	26%	3.4 [1.4-8.5]	0.0164
PEI/HD-PEI	10	5%	14	16%	24	8%	3.0 [0.6-13.5]	
CarboPEI	142	68%	53	61%	195	66%	Ref	
Sex								
Male	165	79%	73	84%	238	80%	Ref	0.1591
Female	44	21%	14	16%	58	20%	2.0 [0.8-5.5]	
	Delayed chemotheraphy				Carbo PEI, n=195		Odd ratio [95% confidence interval]	p-value
	No; n=142		Yes; n=53					
Age group								
Children (0-11 y)	52	36%	13	24%	65	33%	0.6 [0.2-1.5]	0.0002
Adolescent (12-17 y)	45	32%	30	57%	75	39%	Ref	
Adults (≥18 y)	45	32%	10	19%	55	28%	0.2 [0.1-0.4]	

inferior in the adult population (9–11) it seems the opposite for acute leukemia (12, 13). However, data regarding CRAT in the specific adolescent population is limited and underlines the heterogeneity of drug metabolism in this unique population (14). For example, it has been reported in medulloblastoma that alder patient (10-20 years old) may experience more CRAT than children aged 5-10 years when treated with identical chemotherapy (8). It is important to consider the adolescents as a separate age-group because of the specific physiology at this time: rapid growth and development. These changes may affect drug distribution, clearance, and the cytochrome P450 system (14, 15). Metabolism and clearance of most chemotherapy drugs are related to cytochrome P450 (CYP) isoenzymes, which play an important role in the biotransformation of anticancer agents. Activity of CYP enzymes has a wide inter-patient variation, but is also influenced by puberty, showing a decreased expression of CYP1A2, CYP2B6, and CYP2C19 as oestrogen and androgen levels rise (15, 16). Ifosfamide is an anticancer pro-drug metabolised and activated in the liver by the P450 cytochrome. In a series of 16 children aged 1 to 16 years, the estimated pharmacokinetic parameters (clearance, volume of distribution, and half-life) were dependent on body size and age but not any other patient variable (17). Clearance of ifosfamide thus appeared to be higher in paediatric patients compared with adolescents treated with the same dosing and mode of administration (17).

Several series have reported etoposide pharmacokinetics, but few have reported data regarding the relationship between etoposide disposition and age, and none were designed to specifically evaluate differences in clearance between young children and adolescents leading to conflicting data: some series describing an inverse correlation between clearance and age, whereas others didn't (14). Clearance of cisplatin is influenced by renal function but also perfusion duration. A circadian variability of tubular uptake of cisplatin related to testosterone levels has also been reported (18). Whether this could explain heterogeneity within the adolescent population according to pubertal stage warrants further study.

In addition to physiological differences, adolescents may display more at-risk behaviours such as alcohol, tobacco, and/or drug use, unadvised dietary intake, or non-compliance with e.g., neutropenic hygiene rules. Compliance with supportive treatment (antibiotic, mucositis prophylaxis, etc.) might be less effective for adolescents, thus potentially leading to higher toxicity. Thus, adolescents have unique medical and psychosocial needs that warrant appropriate consideration and potential interventions (19).

Moreover, differences in CRAT incidence may represent different clinical approaches between paediatric and adult oncologists. Some studies reported that wider use of Granulocyte-Colony-Stimulating Factor (G-CSF) resulted in a lower incidence of neutropenic fever in adult patients (9, 10). Unfortunately, no data about the institution delivering treatment were available in the database and thus it is not possible to ascertain whether adolescents were treated in paediatric or adult units. We cannot exclude that a different use of G-CSF between paediatric and adult oncologists could have had some impact on the occurrence of haematological toxicity.

CNS-GCT are rarer in adults than in children/adolescents. In these situations of orphan disease, physicians responsible for such patients are encouraged either to share discussions in multidisciplinary boards (20) and/or to use existing paediatric protocols. Currently, international endeavours such as the European reference network EURACAN (https://euracan.eu/) encourage paediatric and adult neuro-oncology collaboration on orphan brain diseases. However, transposing a paediatric strategy to adult practice may be challenging. The SIOP-CNS-GCT-II European trial was opened without age limitation, offering the opportunity to include older patients than in the preceding SIOP-CNS-GCT-96 protocol. The current study encourages further trials without age limitations which has also recently become a reality for other brain tumours such as medulloblastoma (21). Such an approach will ensure the most equitable and representative trial enrollment and ensure improvements to patient outcomes will benefit all, regardless of age.

Data availability statement

The raw data supporting the conclusions of this article will be made available by the authors, without undue reservation.

Ethics statement

The studies involving humans were approved by the Comité de Protection des Personnes SUD-EST IV centre leon berard. The studies were conducted in accordance with the European legislation. Written informed consent for participation in the SIOP-CNS-GCTII trial was provided by the participants or participants' legal guardians.

Author contributions

GP: Writing – review & editing, Writing – original draft, Conceptualization. CS: Writing – review & editing, Writing – original draft, Methodology, Investigation, Formal analysis. DF: Writing – review & editing, Writing – original draft, Visualization, Methodology, Conceptualization. AP: Writing – review & editing, Writing – original draft, Data curation. NG: Writing – review & editing, Writing – original draft, Data curation. R-DK: Writing – review & editing, Writing – original draft, Data curation. MP: Writing – review & editing, Writing – original draft, Visualization, Resources, Investigation. MZ: Writing – review & editing, Writing – original draft, Methodology, Data curation. MM: Writing – review & editing, Writing – original draft, Visualization, Validation, Data curation. JN: Writing – review & editing, Writing – original draft, Visualization, Validation, Data curation. GC: Writing – review & editing, Writing – original draft, Visualization, Validation, Investigation, Data curation, Conceptualization. CF-C: Writing – review & editing, Writing – original draft, Validation, Supervision, Project administration, Methodology, Investigation, Data curation, Conceptualization.

Funding

The author(s) declare that no financial support was received for the research, authorship, and/or publication of this article.

Conflict of interest

The authors declare that the research was conducted in the absence of any commercial or financial relationships that could be construed as a potential conflict of interest.

Publisher's note

References

1. Gittleman H, Cioffi G, Vecchione-Koval T, Ostrom QT, Kruchko C, Osorio DS, et al. Descriptive epidemiology of germ cell tumors of the central nervous system diagnosed in the United States from 2006 to 2015. *J Neurooncol.* (2019) 143:251–60. doi: 10.1007/s11060-019-03173-4

2. Allen JC, Kim JH, Packer RJ. Neoadjuvant chemotherapy for newly diagnosed germ-cell tumors of the central nervous system. *J Neurosurg.* (1987) 67:65–70. doi: 10.3171/jns.1987.67.1.0065

3. Calaminus G, Bamberg M, Harms D, Jürgens H, Kortmann RD, Sörensen N, et al. AFP/beta-HCG secreting CNS germ cell tumors: long-term outcome with respect to initial symptoms and primary tumor resection. Results of the cooperative trial MAKEI 89. *Neuropediatrics.* (2005) 36:71–7. doi: 10.1055/s-2005-837582

4. Baranzelli MC, Patte C, Bouffet E, Couanet D, Habrand JL, Portas M, et al. Nonmetastatic intracranial germinoma: the experience of the French Society of Pediatric Oncology. *Cancer.* (1997) 80:1792–7. doi: 10.1002/(ISSN)1097-0142

5. Calaminus G, Kortmann R, Worch J, Nicholson JC, Alapetite C, Garrè ML, et al. SIOP CNS GCT 96: final report of outcome of a prospective, multinational nonrandomized trial for children and adults with intracranial germinoma, comparing craniospinal irradiation alone with chemotherapy followed by focal primary site irradiation for patients with localized disease. *Neuro Oncol.* (2013) 15:788–96. doi: 10.1093/neuonc/not019

6. Alapetite C, Brisse H, Patte C, Raquin MA, Gaboriaud G, Carrie C, et al. Pattern of relapse and outcome of non-metastatic germinoma patients treated with chemotherapy and limited field radiation: the SFOP experience. *Neuro Oncol.* (2010) 12:1318–25. doi: 10.1093/neuonc/noq093

7. Calaminus G, Frappaz D, Kortmann RD, Krefeld B, Saran F, Pietsch T, et al. Outcome of patients with intracranial non-germinomatous germ cell tumors-lessons from the SIOP-CNS-GCT-96 trial. *Neuro Oncol.* (2017) 19:1661–72. doi: 10.1093/neuonc/nox122

8. Tabori U, Sung L, Hukin J, Laperriere N, Crooks B, Carret AS, et al. Medulloblastoma in the second decade of life: a specific group with respect to toxicity and management: a Canadian Pediatric Brain Tumor Consortium Study. *Cancer*. (2005) 103:1874–80. doi: 10.1002/cncr.21003

9. Paioli A, Luksch R, Fagioli F, Tamburini A, Cesari M, Palmerini E, et al. Chemotherapy-related toxicity in patients with non-metastatic Ewing sarcoma: influence of sex and age. *J Chemother*. (2014) 26:49–56. doi: 10.1179/1973947813Y.0000000103

10. Ferrari S, Palmerini E, Staals E, Abate ME, Longhi A, Cesari M, et al. Sex- and age-related chemotherapy toxicity in patients with non-metastatic osteosarcoma. *J Chemother*. (2009) 21:205–10. doi: 10.1179/joc.2009.21.2.205

11. Juergens C, Weston C, Lewis I, Whelan J, Paulussen M, Oberlin O, et al. Safety assessment of intensive induction with vincristine, ifosfamide, doxorubicin, and etoposide (VIDE) in the treatment of Ewing tumors in the EURO-E.W.I.N.G. 99 clinical trial. *Pediatr Blood Cancer*. (2006) 47:22–9. doi: 10.1002/pbc.20820

12. Gupta A, Damania RC, Talati R, O'Riordan MA, Matloub YH, Ahuja SP. Increased toxicity among adolescents and young adults compared with children hospitalized with acute lymphoblastic leukemia at children's hospitals in the United States. *J Adolesc Young Adult Oncol*. (2021) 10:645–53. doi: 10.1089/jayao.2020.0154

13. Burke MJ, Devidas M, Chen Z, Salzer WL, Raetz EA, Rabin KR, et al. Outcomes in adolescent and young adult patients (16 to 30 years) compared to younger patients treated for high-risk B-lymphoblastic leukemia: report from Children's Oncology Group Study AALL0232. *Leukemia*. (2022) 36:648–55. doi: 10.1038/s41375-021-01460-6

14. Veal GJ, Hartford CM, Stewart CF. Clinical pharmacology in the adolescent oncology patient. *J Clin Oncol*. (2010) 28:4790–9. doi: 10.1200/JCO.2010.28.3473

15. Cotreau MM, von Moltke LL, Greenblatt DJ. The influence of age and sex on the clearance of cytochrome P450 3A substrates. *Clin Pharmacokinet*. (2005) 44:33–60. doi: 10.2165/00003088-200544010-00002

16. Bukowinski AJ, Burns KC, Parsons K, Perentesis JP, O'Brien MM. Toxicity of cancer therapy in adolescents and young adults (AYAs). *Semin Oncol Nurs*. (2015) 31:216–26. doi: 10.1016/j.soncn.2015.05.003

17. Boddy AV, Yule SM, Wyllie R, Price L, Pearson AD, Idle JR. Pharmacokinetics and metabolism of ifosfamide administered as a continuous infusion in children. *Cancer Res*. (1993) 53:3758–64.

18. Chen R, Li J, Hu WW, Wang ML, Zou SL, Miao LY. Circadian variability of pharmacokinetics of cisplatin in patients with non-small-cell lung carcinoma: analysis with the NONMEM program. *Cancer Chemother Pharmacol*. (2013) 72:1111–23. doi: 10.1007/s00280-013-2288-5

19. Coccia PF, Pappo AS, Beaupin L, Borges VF, Borinstein SC, Chugh R, et al. Adolescent and young adult oncology, version 2.2018, NCCN clinical practice guidelines in oncology. *J Natl Compr Canc Netw*. (2018) 16:66–97. doi: 10.6004/jnccn.2018.0001

20. Frappaz D, Sunyach MP, Le Rhun E, Blonski M, Laurence V, Bonneville Levard A, et al. La neuro-oncologie des adolescents et adultes jeunes (AJAS): place d'une RCP nationale. Au nom de l'ANOCEF, GO-AJA et de la SFCE [Adolescent and Young Adults (AYAS) brain tumor national Web conference. On behalf of ANOCEF, GO-AJA and SFCE societies]. *Bull Cancer*. (2016) 103:1050–6. doi: 10.1016/j.bulcan.2016.10.010

21. Bailey S, André N, Gandola L, Massimino M, Wheatley K, Gates S, et al. Clinical Trials in High-Risk Medulloblastoma: Evolution of the SIOP-Europe HR-MB Trial. *Cancers (Basel)*. (2022) 14(6):1084. doi: 10.3390/cancers16061084

frontiers | Frontiers in Oncology

TYPE Mini Review
PUBLISHED 19 July 2024
DOI 10.3389/fonc.2024.1438905

OPEN ACCESS

EDITED BY
Bo Yuan Huang,
Capital Medical University, China

REVIEWED BY
Xiancheng Chen,
Fudan University, China
Tao Zeng,
Tongji University, China
Bernd Kaina,
Johannes Gutenberg University Mainz, Germany

*CORRESPONDENCE
Shepeng Wei
dr_weishepeng@126.com

RECEIVED 26 May 2024
ACCEPTED 08 July 2024
PUBLISHED 19 July 2024

CITATION
Bao J, Sun R, Pan Z and Wei S (2024) Current chemotherapy strategies for adults with IDH-wildtype glioblastoma.
Front. Oncol. 14:1438905.
doi: 10.3389/fonc.2024.1438905

Current chemotherapy strategies for adults with IDH-wildtype glioblastoma

Jing Bao, Rui Sun, Zhenjiang Pan and Shepeng Wei*

Shidong Hospital, University of Shanghai for Science and Technology, Shanghai, China

Introduction: Glioblastoma, despite advancements in molecular evolution, remains incurable and has low survival rates. Currently, two of the most commonly used chemotherapy regimens are temozolomide and CCNU. This review aims to provide a comprehensive analysis of the current status of chemotherapy strategies for GBM.

Methods: We reviewed the published literature describing the chemotherapy regimen differences in system treatment of GBM reported in the last ten years and summarised the available information that may reveal the latest changes in chemotherapy.

Results: In patients with adequate functioning, temozolomide and radiation are the primary treatments for newly diagnosed GBM. We recommend postoperative radiation therapy with concurrent and adjuvant temozolomide for patients with MGMT-methylated GBM who are less than 70 years old. Combining temozolomide and lomustine with radiation therapy may be an option for younger, fit patients, but efficacy data is inconclusive. For patients with unknown MGMT methylation status, radiation therapy combined with temozolomide remains the standard of care. We recommend hypofractionated radiation and concurrent temozolomide treatment for elderly patients over 70 years old who have satisfactory performance and no significant underlying health conditions. We should tailor treatment choices to each patient's personal preferences, previous treatments, function, quality of life, and overall care objectives.

Conclusion: Radiation therapy, along with temozolomide, is still the standard of care for most people with MGMT-unmethylated GBMs because there aren't any better options, and it's generally safe and well-tolerated. These patients have a lower overall survival rate and less benefit from temozolomide, but there are no better alternatives. Clinical trial participation is encouraged.

KEYWORDS

glioblastoma, chemotherapy, temozolomide, lomustine, MGMT

1 Introduction

Glioblastoma (GBM) is a type of brain tumour that is believed to originate from neuroglial stem cells or their progenitors in the subventricular zone. It is classified as a subtype of adult diffuse glioma and is located in the primary central nervous system (CNS) (1–3). The incidence of GBM increases after the age of 40 and peaks in adults aged 75 to 84 years (4, 5).

Actually, GBM is the most prevalent malignant primary brain tumour, with a median survival rate of under 2 years. The median overall survival for IDH-wild-type GBM patients is between 12 and 21 months, with only approximately 7% of patients surviving for 5 years (6, 7).

Histopathologically, GBMs are characterised by pleomorphism, high cellularity, diffuse infiltration, mitotic activity, and either microvascular necrosis, proliferation, or both. At the molecular level, GBMs are characterised by the absence of mutations in IDH1/2, H3 K27M, and H3 G34, as per their definition. In diffuse gliomas that do not have mutations in the IDH and H3 genes, the presence of either microvascular proliferation or necrosis is enough to diagnose GBM as grade 4. Tumours that have epidermal growth factor receptor (EGFR) amplification, telomerase reverse transcriptase (TERT) promoter mutation, or concurrent chromosome 7 gain/chromosome 10 loss exhibit a clinical course similar to that of GBM (8, 9). These tumours are now classified as IDH-wildtype GBM according to the 2021 WHO revision (3). The diagnosis of GBM in adults is shown in Figure 1.

Consequently, GBM now specifically denotes the most severe type of isocitrate dehydrogenase (IDH)-wild-type diffuse adult-type astrocytoma. The prognosis of this condition is determined by the methylation status of the MGM promoter.

Although there has been progress in comprehending the molecular evolution of GBM, the disease remains incurable and is associated with low survival rates. The conventional multimodal treatments of surgically removing as much of the tumour as possible and using radiation therapy (RT), along with the simultaneous and subsequent use of temozolomide (TMZ), continue to be the mainstay of treatment. Clinical trials are ongoing to further explore innovative strategies, such as targeted agents and immunotherapy. This review aims to provide a comprehensive analysis of the current status of chemotherapy strategies for GBM.

2 Temozolomide: a classic old medicine

Temozolomide, an oral alkylating agent, is dosed according to body surface area (BSA). During radiation treatment, 75 mg/m^2 of temozolomide is administered daily (seven days per week). Temozolomide is taken on an empty stomach, at least two hours after the previous meal.

Some clinicians recommend timing weekday doses of temozolomide one hour before radiation therapy to maximise synergy. Other clinicians have patients take their medication at the same time every day, either first thing in the morning before breakfast or at bedtime, two or more hours after dinner.

Complete blood counts (CBCs) must be done every week during the concurrent phase for monitoring. Platelets should not be given if they drop below 100,000/microL, or ANC should not be given if it drops below 1500/microL, because counts can drop quickly. After that, monitoring may need to happen more often until nadirs are found.

Temozolomide is usually given at a dose of 150 mg/m^2 every day for five days out of a 28-day cycle. The first post-radiation cycle starts four weeks after the last day of radiation therapy. After the first six cycles, the dose is 200 mg/m^2 if the blood counts are good. On days 22 and 29 of each cycle, a CBC should be done, along with a basic metabolic panel and liver function tests once a month. This is to check for toxicity and help with dose adjustments if needed. Clinicians should look at the temozolomide product label to see how to change the dose to avoid hematologic toxicity.

It is recommended to treat patients who have received standard concurrent and adjuvant temozolomide with six cycles of monthly adjuvant temozolomide instead of a longer treatment course.

Alternative temozolomide schedules have not demonstrated superior efficacy compared to the conventional postradiation schedule of 5 days every 28 days in the adjuvant setting (10–12).

During radiation with concurrent temozolomide, patients with additional risk factors for opportunistic infections (such as lymphopenia or the use of glucocorticoids) should be given antimicrobial prophylaxis to prevent pneumocystis pneumonia. Given the low risk of pneumocystis, the risks of prophylaxis may be greater than the benefits for other patients.

3 GBMs, age ≤70 years

3.1 MGMT-methylated GBMs

A European Organisation for Research and Treatment of Cancer/National Cancer Institute of Canada (EORTC/NCIC) open-label trial in 573 adults with GBM randomised them to receive involved-field radiation therapy alone or radiation plus concurrent daily temozolomide followed by up to six monthly cycles of adjuvant temozolomide (6). After five years, temozolomide improved median overall survival compared to radiation alone (14.6 versus 12.1 months, HR 0.63, 95% CI 0.53-0.75) (6). Temozolomide improved survival at two years (27 versus 11%) and five years (10 versus 2%) (13). Temozolomide caused more grade 3 or 4 hematologic toxicity, mostly thrombocytopenia (12%) and lymphopenia (7%) but maintained health-related quality of life (6, 14). All patient subsets, including those over 60 and those with poor prognostic factors, benefited from adjuvant temozolomide (6, 13). A smaller phase II trial in GBM patients yielded similar results (15).

In a retrospective analysis of 206 EORTC/NCIC trial patients, MGMT promoter methylation was a major prognostic factor for improved survival and chemotherapy benefit (16). People with MGMT methylation (45% of cases) had twice as much two-year overall survival with temozolomide as with radiation alone (46% vs.

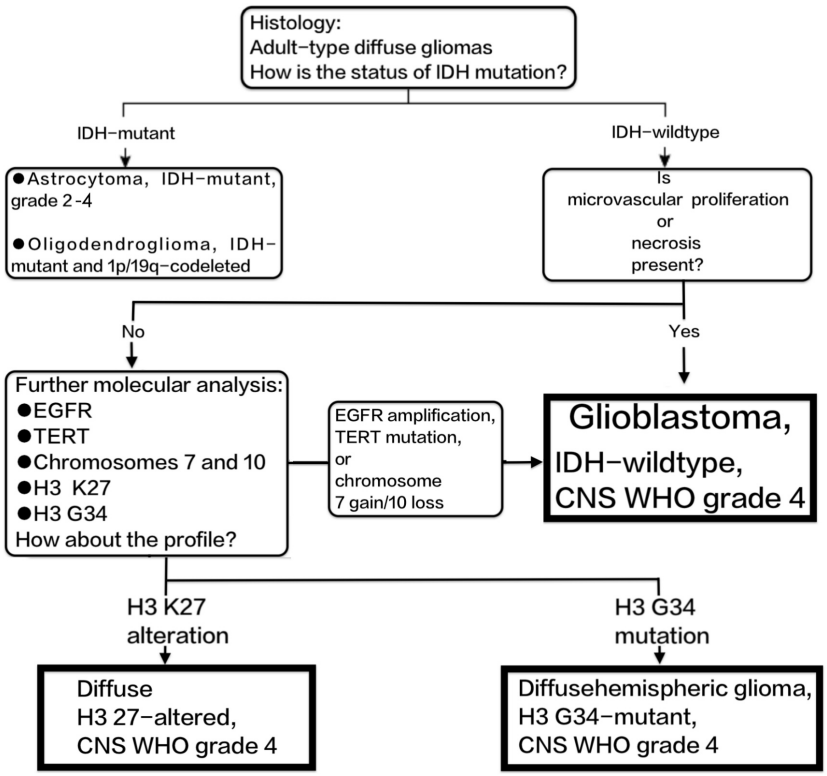

FIGURE 1
Shows the diagnostic process of GBM according to the 2021 revision of the WHO classification of CNS tumours.

23%); their median overall survival was 21.7 months vs. 15.3 months, with an HR of 0.45 and a 95% confidence interval of 0.32-0.61 (16). Those without MGMT methylation showed a non-significant survival difference (two-year survival: 14% vs. <2%; median overall survival: 12.7 vs. 11.8 months, HR 0.69, 95% CI 0.47-1.02).

Later trials in MGMT-methylated GBM have tried to improve radiation plus temozolomide. CeTeG/NOA-09 screened >650 patients to enrol 141 patients aged 18 to 70 with MGMT-methylated GBM and randomly assigned them to a combined lomustine/temozolomide regimen during and after radiation therapy (up to six 42-day cycles of lomustine 100 mg/m^2 on day 1 and temozolomide 100 mg/m^2 on days 2 to 6) or standard therapy (17). Centre-stratified randomization, A modified intent-to-treat (mITT) analysis included 129 patients after 12 randomised patients (six in each arm) dropped out before therapy. Sex distribution and other baseline prognostic factors differed statistically and numerically between treatment groups. Lomustine/temozolomide and standard temozolomide had similar median overall survival in mITT patients (37.9 vs. 31.4 months, HR 0.90, 95% CI 0.58–1.41). Using inverse probability weights, an adjusted mITT analysis of these 129 patients found a nonsignificant trend towards improved survival in the lomustine/temozolomide arm (HR 0.74, 95% CI 0.47–1.17) but no difference in progression-free survival. This matched analysis (n = 109), which excluded 32 randomised patients, showed that the combination arm had better overall survival (48.1 versus 31.4 months, HR 0.60, 95% CI 0.35–1.03) and similar progression-free survival (16.7 months in both groups). Grade 3 or 4 hematologic toxicity (36 vs. 29%) and nausea (30 vs. 19%) were more common with combination therapy. Lomustine/temozolomide completed 39 percent of six chemotherapy cycles, while standard temozolomide completed 60 percent.

These findings suggest that lomustine/temozolomide combination therapy may improve survival in younger, fit MGMT-methylated GBM patients compared to standard temozolomide. The trial's small size and the exclusion of a large number of randomised patients in the prespecified analyses reduce confidence in combination therapy's superior efficacy. Combination therapy has higher nausea and hematologic toxicity risks, so some patients and clinicians may prefer standard temozolomide until more is known.

So, we suggest that people younger than 70 who have been newly diagnosed with MGMT-methylated GBM get temozolomide and radiation therapy at the same time, followed by temozolomide every month. Younger, fit patients with MGMT-methylated tumours may benefit from temozolomide and lomustine combined with radiation therapy, but efficacy is inconclusive and toxicity may be higher.

3.2 MGMT-unmethylated GBMs

Patients with MGMT-unmethylated tumours may benefit from clinical trials due to their poor prognosis and response to standard treatments. To treat MGMT-unmethylated GBM, we recommend

temozolomide and radiation outside of clinical trials, based on the EORTC/NCIC trial, where MGMT status was not known (6, 13).

Patients with MGMT-unmethylated tumours have lower overall survival and less benefit from temozolomide compared to those with methylated tumours. In a retrospective analysis of 206 EORTC/NCIC trial patients with MGMT-unmethylated tumours (n = 114), adding temozolomide to radiation therapy resulted in a non-significant survival advantage (two-year survival 15 versus 2%; median overall survival 12.7 versus 11.8 months, HR 0.69, 95% CI 0.47-1.02) (16).

Investigations are underway for alternatives to temozolomide in MGMT-unmethylated tumour patients. For example, a phase II study of 182 people who had just been diagnosed with MGMT-unmethylated GBM looked at the effects of bevacizumab during radiation, bevacizumab plus irinotecan, and radiation with temozolomide given at the same time or afterward (18). Similar to unselected GBM trials, bevacizumab improved six-month progression-free survival (79 versus 43 percent) but not median overall survival (16.6 versus 17.5 months) or quality-of-life. Bevacizumab was given to two-thirds of temozolomide patients at progression. In a trial comparing radiation and nivolumab to radiation and temozolomide, the nivolumab arm had lower survival rates (median overall survival 13.4 vs. 14.9 months, HR 1.31, 95% CI 1.09–1.58) (19).

3.3 MGMT status unknown

Due to insufficient tissue, MGMT methylation assays may fail in a significant minority of patients, especially those who undergo stereotactic biopsy. We recommend using temozolomide with radiation therapy for patients who are candidates for standard therapy (age ≤70 years, good functional status) and whose MGMT status is unknown at the time of decision-making. The rationale for temozolomide is the expected clinically significant survival improvement for 30–40% of patients with MGMT-methylated tumours, the lack of better alternatives for unmethylated tumours, and its relative safety and tolerability.

4 GBMs, age >70 years

4.1 Radiation with concurrent and adjuvant temozolomide

For individuals over 70 years old who exhibit good performance status (e.g., Karnofsky Performance Status [KPS] ≥70), hypofractionated radiation (e.g., 40 Gy in 15 fractions) in conjunction with adjuvant and concurrent temozolomide is recommended. However, in older patients compared to younger patients, the potential for improved survival with the addition of chemotherapy is more closely balanced with the risks of toxicity. Individuals with specific concerns regarding side effects may logically opt for monotherapy.

The results of a randomised trial of hypofractionated radiation (40 Gy in 15 fractions) with or without concurrent and adjuvant temozolomide provide support for combined-modality therapy in older patients with newly diagnosed GBM (20). Patients with an Eastern Cooperative Oncology Group (ECOG) score of 0 to 2 who were 65 years of age or older were eligible. 562 patients with a median age of 73 years (range 65 to 90) were included in the trial. Results include the following:

- When temozolomide was added to radiation, the survival rate was higher than when radiation was used alone (9.3 versus 7.6 months, hazard ratio [HR] 0.67, 95% CI 0.56-0.80). Additionally, progression-free survival increased (5.3 versus 3.9 months).
- MGMT was examined in 354 patients. In 165 patients with MGMT-methylated tumours, adding temozolomide increased overall survival by nearly six months (13.5 vs. 7.7 months, HR 0.53, 95% CI.38–0.73). Despite a smaller effect (10 versus 7.9 months, HR 0.75, 95% CI 0.56–1.01), temozolomide improved survival in patients with MGMT unmethylated tumours (n = 189).
- Functional domain quality-of-life outcomes were similar. More nausea, vomiting, constipation, and hematologic toxicity (grade 3 or 4)—thrombocytopenia (11 versus 0.4 percent), neutropenia (8 versus 1 percent), and lymphopenia (27 versus 10 percent)—were seen in the combined therapy.

Extra supporting information comes from observational studies involving older adults, which might have bias related to selection (21, 22). The median overall survival was 13 months in a pooled analysis of four phase II trials, including older patients (>65 years old) with newly diagnosed GBM treated with concurrent and adjuvant temozolomide plus standard or short-course radiation therapy. This result compared favourably with outcomes in younger patients (21). The prevalence of grade 3 or 4 toxicity ranged from 8 to 46%.

Although the patient population for the seminal European Organisation for Research and Treatment of Cancer/National Cancer Institute of Canada Clinical Trials Group (EORTC/NCIC) trial was restricted to individuals aged 18 to 70, a breakdown of outcomes by age was incorporated into the five-year analysis of results (13). Thirty percent (170) of the 573 patients in that study were between the ages of 61 and 70. The combined-modality approach's median overall survival for this older patient subset was comparable to that of radiation therapy alone (median 10.9 versus 11.8 months).

Adjuvant temozolomide significantly increased overall survival compared to radiation therapy alone, resulting in more long-term survivors (22% versus 6% at two years and 7% versus 0% at five years, HR 0.7, 95% CI 0.5-0.97).

In older patients, at least one retrospective study found that combined therapy had worse outcomes than radiation alone (23), and other studies found that the benefit of adding temozolomide

decreased with age (24), particularly in those with MGMT unmethylated tumours (25).

4.2 Temozolomide alone

Emerging data suggests that temozolomide chemotherapy may be a viable alternative to radiation therapy for older patients with MGMT-methylated tumours who cannot benefit from a combined-modality approach due to poor functional status or significant comorbidity.

Two randomised trials in older patients provide partially overlapping data on the best approach for this population, specifically the role of temozolomide alone as an alternative to radiation. Both the Methusalem (NOA-08) trial (26) and the Nordic Clinical Brain Tumour Study Group trial (27) compared initial chemotherapy as monotherapy to initial radiation alone. Neither trial had a combined temozolomide-radiation arm.

These trials indicate that both hypofractionated radiation and temozolomide are viable treatment options for older patients. However, temozolomide is more effective in patients with MGMT-methylated tumours than in those with unmethylated tumours.

Table 1 summarises the initial chemotherapy drug regimen for GBM. In Figure 2, the clinical approach for the initial selection of chemotherapy drugs for GBM is illustrated.

5 Recurrent GBM

The systemic agents most frequently employed in the treatment of recurrent GBM include bevacizumab, nitrosoureas, and temozolomide rechallenge (as the majority of patients would have already received temozolomide as part of their initial therapy). Whenever feasible, it is preferable for patients with a satisfactory performance status to engage in a research clinical study.

Prospective studies in patients with recurrent GBM have shown that using only lomustine as a treatment results in a response rate of 9 to 14 percent and a median progression-free survival of 1.5 to 2.7 months (28–30). The typical initial dosage for monotherapy is 110 mg/m^2, with a maximum limit of 200 mg. Approximately 50 percent of individuals experience grade 3 or higher hematologic toxicity.

The largest study, known as RESCUE, examined the effects of continuous daily administration of temozolomide at a dosage of 50 mg/m^2/day for a maximum duration of one year in a group of 120 patients (31). The six-month progression-free survival rate for patients with GBM varied between 15 and 29 percent, depending on whether progression occurred during or after the initial adjuvant temozolomide treatment. The patients who underwent a rechallenge after completing an adjuvant regimen exhibited the highest likelihood of responding.

A randomised phase II trial was conducted to compare the efficacy of two different dosing regimens of temozolomide (150 mg/m^2/day one week on, one week off, or 100 mg/m^2/day three weeks on, one week off) in patients with recurrent GBM. However, the trial had to be stopped prematurely due to a lack of funding. Despite the early termination, both dosing regimens showed similar performance (32). MGMT status was the primary determinant of effectiveness. The six-month progression-free survival was significantly higher in patients with MGMT-methylated tumours compared to those with unmethylated tumours, regardless of the dosing regimen. The survival rate was 40 percent for patients with MGMT methylated tumours, while it was only 7 percent for patients with unmethylated tumours.

Similar to other medications, the administration of high-dose temozolomide in patients who have not responded well to bevacizumab-containing treatment plans is linked to a low rate of positive response and overall survival (33–35).

TABLE 1 Initial chemotherapy strategies for adults with IDH-wildtype glioblastoma.

KPS≥70	
Age ≤70 years	
MGMT -methylated	•Daily TMZ with standard Rt followed by ≤ 6 cycles of monthly TMZ •TMZ + CCNU in combination with Rt
MGMT -unmethylated	•Encouraged to participate in clinical trials. •Daily TMZ with standard Rt followed by ≤ 6 cycles of monthly TMZ
MGMT status unknown	•Daily TMZ with standard Rt followed by ≤ 6 cycles of monthly TMZ
Age >70 years	
no matter what MGMT status	•Daily TMZ with short-course Rt followed by ≤ 6 cycles of monthly TMZ
KPS<70	
•Rt alone •TMZ chemotherapy alone, particularly in patients with MGMT methylated tumors. •Best surpportive care	

TMZ, temozolomide; CCNU, lomustine; Rt, radiation therapy.

6 Treatment duration

Based on the design of the original study that led to the acceptance of temozolomide as the standard of care, up to six cycles of postradiation temozolomide are recommended (6).

The results of a phase II randomised trial, in which 159 glioblastoma patients who had not progressed after six cycles of adjuvant temozolomide were randomly assigned to stop temozolomide (control) or continue temozolomide for up to 12 cycles overall, provide evidence in favour of this approach (36). The groups' progression-free survival was comparable after a median follow-up of 33 months, and the extended temozolomide group's overall survival was not significantly worse (hazard ratio [HR] 1.3, 95% CI 0.90-1.88).

Comparable findings have been drawn from observational studies (37, 38). A retrospective study of 624 patients in four randomised trials found that receiving more than six cycles of

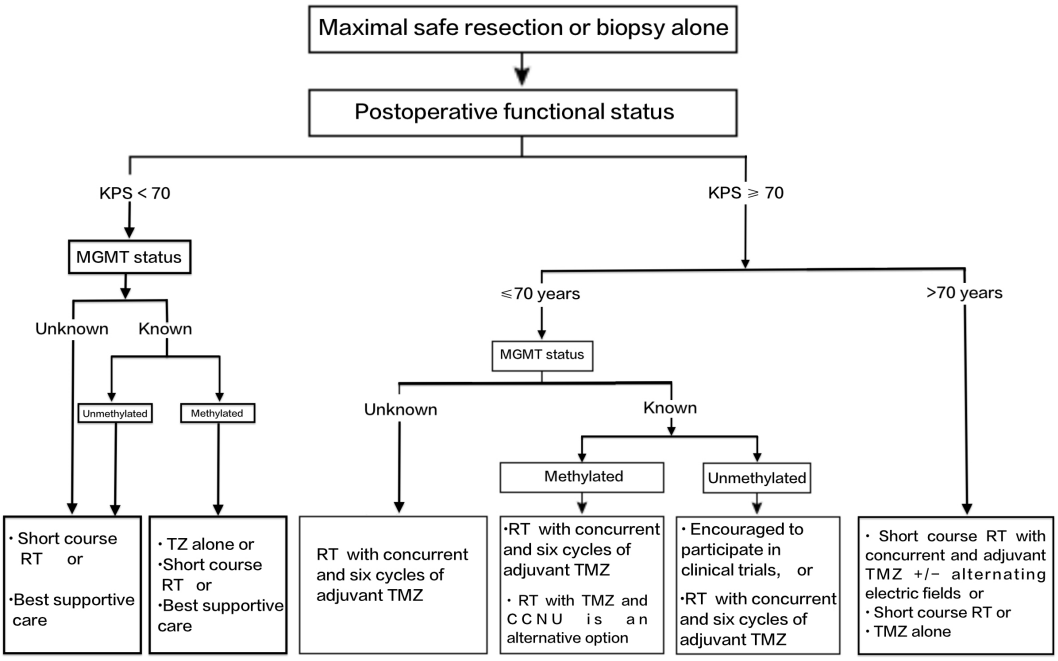

FIGURE 2
Initial approach to chemotherapy in GBM patients. TMZ, temozolomide; CCNU, lomustine; Rt, radiation therapy.

adjuvant temozolomide was associated with improved progression-free survival, particularly in patients with MGMT-methylated tumours (HR 0.65, 95% CI 0.50-0.85). However, there was no difference in overall survival (HR 0.92, 95% CI 0.71-1.19), even in the MGMT-methylated subgroup (HR 0.89, 95% CI 0.63-1.26) (38).

7 Conclusion

Looking at the chemotherapy regimens for GBM, only two drugs, TMZ and CCNU, are currently in use (Table 1). Temozolomide and radiation are the primary components of the initial treatment for newly diagnosed GBM in patients who have a sufficient level of functioning. For patients with MGMT-methylated GBM ≤70 years old, postoperative radiation therapy with concurrent and adjuvant temozolomide is recommended. Combining temozolomide and lomustine with radiation therapy may be an option for younger, fit patients, but efficacy data is inconclusive and toxicity may be higher.

For patients with MGMT-unmethylated GBM ≤70 years old, postoperative radiation therapy with concurrent and adjuvant temozolomide is recommended. These patients have lower overall survival and less benefit from temozolomide, but there are no better alternatives. Clinical trial participation is encouraged.

For patients with unknown MGMT methylation status (≤70 years), based on the clinically meaningful improvement in survival that is anticipated from temozolomide for the 30 to 40 percent of patients who are predicted to have an MGMT-methylated tumour, the absence of better alternatives for MGMT-unmethylated tumours, and the relative safety and tolerability of temozolomide, radiation therapy combined with temozolomide continues to be the standard of care.

In the case of elderly patients (>70 years old) who have a satisfactory performance status and no significant underlying health conditions, it is recommended to use hypofractionated radiation (such as 40 Gy delivered in 15 fractions) along with concurrent and adjuvant temozolomide treatment (administered in six monthly cycles) instead of a single treatment modality. With advancing age, the potential for improved survival more closely balances the risks of toxicity associated with combination therapy. However, patients who have significant concerns about side effects may justifiably opt for single-modality therapy.

In the case of elderly patients (>70 years old) who are not candidates for a combined-modality approach because of poor functional status or significant comorbidity, the MGMT methylation status of the tumour is useful for decision-making. In cases where patients have tumours with MGMT methylated, temozolomide rather than radiation is recommended.

Although a combined-modality approach is employed, the majority of patients ultimately experience a relapse. Managing patients with recurrent or progressive high-grade gliomas is challenging, and there is no evidence that active reintervention extends survival. At this point, treatment choices should be tailored to each patient, considering their personal preferences, previous treatments, ability to function, quality of life, and overall care objectives.

Patients who have experienced a relapse a few months after the completion of adjuvant temozolomide treatment and whose

tumours contain a methylated MGMT promoter may be the most suitable candidates for rechallenge with temozolomide.

Author contributions

JB: Writing – original draft, Writing – review & editing. RS: Writing – original draft, Writing – review & editing, Investigation, Methodology. ZP: Writing – original draft, Writing – review & editing. SW: Writing – original draft, Writing – review & editing, Conceptualization, Methodology, Resources.

Funding

The author(s) declare that no financial support was received for the research, authorship, and/or publication of this article.

Conflict of interest

The authors declare that the research was conducted in the absence of any commercial or financial relationships that could be construed as a potential conflict of interest.

Publisher's note

Author disclaimer

All claims expressed in this article are solely those of the authors and do not necessarily represent those of their affiliated organizations, or those of the publisher, the editors and the reviewers. Any product that may be evaluated in this article, or claim that may be made by its manufacturer, is not guaranteed or endorsed by the publisher.

The opinions stated in this article are exclusively those of the authors and may not necessarily reflect the views of their associated organisations, or those of the publisher, the editors, and the reviewers. The publisher does not guarantee or endorse any product mentioned in this article or any claims made by its manufacturer.

References

1. Canoll P, Goldman JE. The interface between glial progenitors and gliomas. *Acta Neuropathol.* (2008) 116(5):465–77. doi: 10.1007/s00401-008-0432-9

2. Lee JH, Lee JE, Kahng JY, Kim SH, Park JS, Yoon SJ, et al. Human glioblastoma arises from subventricular zone cells with low-level driver mutations. *Nature.* (2018) 560:243–7. doi: 10.1038/s41586-018-0389-3

3. Louis DN, Perry A, Wesseling P, Brat DJ, Cree IA, Figarella-Branger D, et al. The 2021 WHO classification of tumors of the central nervous system: a summary. *Neuro Oncol.* (2021) 23(8):1231–51. doi: 10.1093/neuonc/noab106

4. Ostrom QT, Cioffi G, Waite K, Kruchko C, Barnholtz-Sloan JS. CBTRUS statistical report:primary brain and other central nervous system tumors diagnosed in the United States in 2014-2018. *Neuro Oncol.* (2021) 23:iii1–iii105. doi: 10.1093/neuonc/noab200

5. Wen PY, Weller M, Lee EQ, Alexander BM, Barnholtz-Sloan JS, Barthel FP, et al. Glioblastoma inadults: a Society for Neuro-Oncology (SNO) andEuropean Society of Neuro-Oncology (EANO) consensus review on current management and future directions. *Neuro Oncol.* (2020) 22(8):1073–113. doi: 10.1093/neuonc/noaa106

6. Stupp R, Mason WP, van den Bent MJ, Weller M, Fisher B, Taphoorn MJB, et al. European Organisation for Research and Treatment of Cancer Brain Tumor and Radiotherapy Groups; National Cancer Institute of Canada Clinical Trials Group. Radiotherapy plus concomitant and adjuvant temozolomide for glioblastoma. *N Engl J Med.* (2005) 352(10):987–96. doi: 10.1056/NEJMoa043330

7. Stupp R, Taillibert S, Kanner A, Read W, Steinberg D, Lhermitte B, et al. Effect oftumor-treating fields plus maintenancetemozolomide vs maintenance temozolomide alone on survival in patients with glioblastoma: a randomized clinical trial. *JAMA.* (2017) 318(23):2306–16. doi: 10.1001/jama.2017.18718

8. Brat DJ, Aldape K, Colman H, Holland EC, Louis DN, Jenkins RB, et al. cIMPACT-NOW update 3: recommended diagnostic criteria for "diffuse astrocytic glioma, IDH-wildtype, with molecular features of glioblastoma, WHO grade IV. *" Acta Neuropathol.* (2018) 136:805. doi: 10.1007/s00401-018-1913-0

9. Bale TA, Jordan JT, Rapalino O, Ramamurthy N, Jessop N, DeWitt JC, et al. Financially effective test algorithm to identify an aggressive, EGFR-amplified variant of IDH-wildtype, lower-grade diffuse glioma. *Neuro Oncol.* (2019) 21:596. doi: 10.1093/neuonc/noy201

10. Gilbert MR, Wang M, Aldape KD, Stupp R, Hegi ME, Jaeckle KA, et al. Dose-dense temozolomide for newly diagnosed glioblastoma: a randomised phase III clinical trial. *J Clin Oncol.* (2013) 31:4085. doi: 10.1200/JCO.2013.49.6968

11. Armstrong TS, Wefel JS, Wang M, Gilbert MR, Won M, Bottomley A, et al. Net clinical benefit analysis of radiation therapy oncology group 0525: a phase III trial comparing conventional adjuvant temozolomide with dose-intensive temozolomide in patients with newly diagnosed glioblastoma. *J Clin Oncol.* (2013) 31:4076. doi: 10.1200/JCO.2013.49.6067

12. Brada M, Stenning S, Gabe R, Thompson LC, Levy D, Rampling R, et al. Temozolomide versus procarbazine, lomustine, and vincristine in recurrent high-grade gliomas. *J Clin Oncol.* (2010) 28:4601. doi: 10.1200/JCO.2009.27.1932

13. Stupp R, Hegi ME, Mason WP, van den Bent MJ, Taphoorn MJB, Janzer RC, et al. Effects of radiotherapy with concomitant and adjuvant temozolomide versus radiotherapy alone on survival in glioblastoma in a randomised phase III study: a 5-year analysis of the EORTC-NCIC trial. *Lancet Oncol.* (2009) 10:459. doi: 10.1016/S1470-2045(09)70025-7

14. Taphoorn MJ, Stupp R, Coens C, Osoba D, Kortmann R, van den Bent MJ. Health-related quality of life in patients with glioblastoma: a randomised controlled trial. *Lancet Oncol.* (2005) 6:937. doi: 10.1016/S1470-2045(05)70432-0

15. Athanassiou H, Synodinou M, Maragoudakis E, Paraskevaidis M, Verigos C, Misailidou D, et al. A randomised phase II study of temozolomide and radiotherapy compared with radiotherapy alone in newly diagnosed glioblastoma multiforme. *J Clin Oncol.* (2005) 23:2372. doi: 10.1200/JCO.2005.00.331

16. Hegi ME, Diserens AC, Gorlia T, Hamou M-F, de Tribolet N, Weller M, et al. MGMT gene silencing and benefit from temozolomide in glioblastoma. *N Engl J Med.* (2005) 352:997. doi: 10.1056/NEJMoa043331

17. Herrlinger U, Tzaridis T, Mack F, Steinbach JP, Schlegel U. Lomustine-temozolomide combination therapy versus standard temozolomide therapy in patients with newly diagnosed glioblastoma with methylated MGMT promoter (CeTeG/NOA-09): a randomised, open-label, phase 3 trial. *Lancet.* (2019) 393:678. doi: 10.1016/S0140-6736(18)31791-4

18. Herrlinger U, Schäfer N, Steinbach JP, Weyerbrock A, Hau P, Goldbrunner R, et al. Bevacizumab plus irinotecan versus temozolomide in newly diagnosed O6-methylguanine-DNA methyltransferase nonmethylated glioblastoma: the randomised GLARIUS trial. *J Clin Oncol.* (2016) 34:1611. doi: 10.1200/JCO.2015.63.4691

19. Omuro A, Brandes AA, Carpentier AF, Idbaih A, Reardon DA, Cloughesy T, et al. Radiotherapy combined with nivolumab or temozolomide for newly diagnosed glioblastoma with unmethylated MGMT promoter: An international randomised phase III trial. *Neuro Oncol.* (2023) 25:123. doi: 10.1093/neuonc/noac099

20. Perry JR, Laperriere N, O'Callaghan CJ, Brandes AA, Menten J, Phillips C, et al. Short-course radiation plus temozolomide in elderly patients with glioblastoma. *N Engl J Med*. (2017) 376:1027. doi: 10.1056/NEJMoa1611977

21. Fiorentino A, Balducci M, De Bonis P, Chiesa S, De Filippo L, Mangiola A, et al. Can elderly patients with newly diagnosed glioblastoma be enrolled in radiochemotherapy trials? *Am J Clin Oncol*. (2015) 38:23. doi: 10.1097/COC.0b013e3182868ea2

22. Rusthoven CG, Koshy M, Sher DJ, Ney DE, Gaspar LE, Jones BL, et al. Combined-modality therapy with radiation and chemotherapy for elderly patients with glioblastoma in the temozolomide era: A national cancer database analysis. *JAMA Neurol*. (2016) 73:821. doi: 10.1001/jamaneurol.2016.0839

23. Cao JQ, Fisher BJ, Bauman GS, Megyesi JF, Watling QJ, Macdonald DR, et al. Hypofractionated radiotherapy with or without concurrent temozolomide in elderly patients with glioblastoma multiforme: a review of ten-year single institutional experience. *J Neurooncol*. (2012) 107:395. doi: 10.1007/s11060-011-0766-3

24. Laperriere N, Weller M, Stupp R, Perry JR, Brandes AA, Wick W, et al. Optimal management of elderly patients with glioblastoma. *Cancer Treat Rev*. (2013) 39:350. doi: 10.1016/j.ctrv.2012.05.008

25. Franceschi E, Depenni R, Paccapelo A, Ermani M, Faedi M, Sturiale C, et al. Which elderly, newly diagnosed glioblastoma patients can benefit from radiotherapy and temozolomide? PERNO prospective study. *J Neurooncol*. (2016) 128:157. doi: 10.1007/s11060-016-2093-1

26. Wick W, Platten M, Meisner C, Felsberg J, Tabatabai G, Simon M, et al. Temozolomide chemotherapy alone versus radiotherapy alone for Malignant astrocytoma in the elderly: the NOA-08 randomised, phase 3 trial. *Lancet Oncol*. (2012) 13:707. doi: 10.1016/S1470-2045(12)70164-X

27. Malmstrom A, Gronberg BH, Stupp R. Glioblastoma (GBM) in Elderly Patients: A Randomised Phase III Trial Comparing Survival in Patients Treated with 6-Week Radiotherapy (RT) versus Hypofractionated RT over 2 Weeks versus Temozolomide Single Agent Chemotherapy (TMZ) for Glioblastoma (GBM) in the Elderly. *J Clin Oncol*. (2010) 28:949s. doi: 10.1200/jco.2010.28.18_suppl.lba2002

28. Wick W, Gorlia T, Bendszus M, Taphoorn M, Sahm F, Harting I, et al. Lomustine and bevacizumab in progressive glioblastoma. *N Engl J Med*. (2017) 377:1954. doi: 10.1056/NEJMoa1707358

29. Wick W, Puduvalli VK, Chamberlain MC, van den Bent MJ, Carpentier AF, Cher LM, et al. Phase III study of enzastaurin compared with lomustine in the treatment of recurrent intracranial glioblastoma. *J Clin Oncol*. (2010) 28:1168. doi: 10.1200/JCO.2009.23.2595

30. Batchelor TT, Mulholland P, Neyns B, Nabors LB, Campone M, Wick A, et al. conducted a Phase III randomised trial comparing the efficacy of cediranib as monotherapy and in combination with lomustine versus lomustine alone in patients with recurrent glioblastoma. *J Clin Oncol*. (2013) 31:3212. doi: 10.1200/JCO.2012.47.2464

31. Perry JR, Bélanger K, Mason WP, Fulton D, Kavan P, Easaw J, et al. Phase II trial of continuous dose-intense temozolomide in recurrent Malignant glioma: RESCUE study. *J Clin Oncol*. (2010) 28:2051. doi: 10.1200/JCO.2009.26.5520

32. Weller M, Tabatabai G, Kästner B, Felsberg J, Steinbach JP, Wick A, et al. MGMT promoter methylation is a strong prognostic biomarker for benefit from dose-intensified temozolomide rechallenge in progressive glioblastoma: the DIRECTOR trial. *Clin Cancer Res*. (2015) 21:2057. doi: 10.1158/1078-0432.CCR-14-2737

33. Omuro A, Chan TA, Abrey LE, Khasraw M, Reiner AS, Kaley TJ, et al. Phase II trial of continuous low-dose temozolomide for patients with recurrent Malignant glioma. *Neuro Oncol*. (2013) 15:242. doi: 10.1093/neuonc/nos295

34. Desjardins A, Reardon DA, Coan A, Marcello J, Herndon JE 2nd, Bailey L, et al. Bevacizumab and daily temozolomide for recurrent glioblastoma. *Cancer*. (2012) 118:1302. doi: 10.1002/cncr.26381

35. Verhoeff JJ, Lavini C, van Linde ME, Stalpers LJA, Majoie CBLM, Reijneveld JC, et al. Bevacizumab and dose-intense temozolomide in recurrent high-grade glioma. *Ann Oncol*. (2010) 21:1723. doi: 10.1093/annonc/mdp591

36. Balana C, Vaz MA, Manuel Sepúlveda J, Mesia C, Del Barco S, Pineda E, et al. A phase II randomized, multicenter, open-label trial of continuing adjuvant temozolomide beyond 6 cycles in patients with glioblastoma (GEINO 14-01). *Neuro Oncol*. (2020) 22:1851. doi: 10.1093/neuonc/noaa107

37. Gramatzki D, Kickingereder P, Hentschel B. Limited role for extended maintenance temozolomide for newly diagnosed glioblastoma. *Neurology*. (2017) 88:1422. doi: 10.1212/WNL.0000000000003809

38. Blumenthal DT, Gorlia T, Gilbert MR, Dayani M, Abdi A. Is more better? The impact of extended adjuvant temozolomide in newly diagnosed glioblastoma: a secondary analysis of EORTC and NRG Oncology/RTOG. *Neuro Oncol*. (2017) 19:1119. doi: 10.1093/neuonc/nox025

frontiers | Frontiers in Oncology

TYPE Review
PUBLISHED 09 August 2024
DOI 10.3389/fonc.2024.1397863

OPEN ACCESS

EDITED BY
Gerardo Caruso,
University Hospital of Policlinico G. Martino, Italy

REVIEWED BY
Prakashbabu Phanithi,
University of Hyderabad, India
Suyasha Roy,
National Institutes of Health (NIH), United States

*CORRESPONDENCE
Wei Xiang
scxiangwei23@163.com
Jie Zhou
zhoujie@swmu.edu.cn

†These authors have contributed equally to this work

RECEIVED 08 March 2024
ACCEPTED 22 July 2024
PUBLISHED 09 August 2024

CITATION
Luo M, Luan X, Yang C, Chen X, Yuan S, Cao Y, Zhang J, Xie J, Luo Q, Chen L, Li S, Xiang W and Zhou J (2024) Revisiting the potential of regulated cell death in glioma treatment: a focus on autophagy-dependent cell death, anoikis, ferroptosis, cuproptosis, pyroptosis, immunogenic cell death, and the crosstalk between them.
Front. Oncol. 14:1397863.
doi: 10.3389/fonc.2024.1397863

Revisiting the potential of regulated cell death in glioma treatment: a focus on autophagy-dependent cell death, anoikis, ferroptosis, cuproptosis, pyroptosis, immunogenic cell death, and the crosstalk between them

Maowen Luo[1,2†], Xingzhao Luan[3,4†], Chaoge Yang[1,2,5†], Xiaofan Chen[1,2], Suxin Yuan[4], Youlin Cao[3,4], Jing Zhang[4], Jiaying Xie[1,2], Qinglian Luo[1,2,5], Ligang Chen[1,2,5], Shenjie Li[1,2,5], Wei Xiang[1,2,5*] and Jie Zhou[1,2,5*]

[1]Department of Neurosurgery, the Affiliated Hospital, Southwest Medical University, Luzhou, Sichuan, China, [2]School of Clinical Medicine, Southwest Medical University, Luzhou, Sichuan, China, [3]Department of Neurosurgery, the Affiliated Hospital of Panzhihua University, Panzhihua, Sichuan, China, [4]School of Clinical Medicine, the Affiliated Hospital of Panzhihua University, Panzhihua, Sichuan, China, [5]School of Clinical Medicine, Sichuan Clinical Research Center for Neurosurgery, Luzhou, Sichuan, China

Gliomas are primary tumors that originate in the central nervous system. The conventional treatment options for gliomas typically encompass surgical resection and temozolomide (TMZ) chemotherapy. However, despite aggressive interventions, the median survival for glioma patients is merely about 14.6 months. Consequently, there is an urgent necessity to explore innovative therapeutic strategies for treating glioma. The foundational study of regulated cell death (RCD) can be traced back to Karl Vogt's seminal observations of cellular demise in toads, which were documented in 1842. In the past decade, the Nomenclature Committee on Cell Death (NCCD) has systematically classified and delineated various forms and mechanisms of cell death, synthesizing morphological, biochemical, and functional characteristics. Cell death primarily

Abbreviations: RCD, regulated cell death; PCD, programmed cell death; NCCD, Nomenclature Committee on Cell Death; ACD, accidental cell death; MPT, mitochondrial permeability transition; CLL, chronic lymphocytic leukemia; SLL, small lymphocytic lymphoma; AML, acute myeloid leukemia; NASH, non-alcoholic steatohepatitis; WHO, World Health Organization; TMZ, temozolomide; NCOA4, nuclear receptor coactivator 4; LA, lipoic acid; CBD, cannabidiol; RTK, receptor tyrosine kinase; EGFR, epidermal growth factor receptor; ARG, anoikis-related gene; Lnc RNA, long non-coding RNA; ROS, reactive oxygen species; ER, endoplasmic reticulum; PTE, Pterostilbene; CQ, chloroquine; HCQ, hydroxychloroquine; mTOR, mammalian targets of rapamycin; AF, amentoflavone; LA, lipoic acid; EGF, epidermal growth factor; MTD, maximum tolerated dose; ATG, Autophagy-related gene; DAMP, damage-associated molecular pattern; DHA, dihydroartemisinin; RSV, resveratrol; HP, Haloperidol Tablets.

manifests in two forms: accidental cell death (ACD), which is caused by external factors such as physical, chemical, or mechanical disruptions; and RCD, a gene-directed intrinsic process that coordinates an orderly cellular demise in response to both physiological and pathological cues. Advancements in our understanding of RCD have shed light on the manipulation of cell death modulation - either through induction or suppression - as a potentially groundbreaking approach in oncology, holding significant promise. However, obstacles persist at the interface of research and clinical application, with significant impediments encountered in translating to therapeutic modalities. It is increasingly apparent that an integrative examination of the molecular underpinnings of cell death is imperative for advancing the field, particularly within the framework of inter-pathway functional synergy. In this review, we provide an overview of various forms of RCD, including autophagy-dependent cell death, anoikis, ferroptosis, cuproptosis, pyroptosis and immunogenic cell death. We summarize the latest advancements in understanding the molecular mechanisms that regulate RCD in glioma and explore the interconnections between different cell death processes. By comprehending these connections and developing targeted strategies, we have the potential to enhance glioma therapy through manipulation of RCD.

KEYWORDS

glioma, autophagy-dependent cell death, anoikis, ferroptosis, cuproptosis, pyroptosis, immunogenic cell death, regulated cell death

1 Introduction

Glioma is a highly heterogeneous, aggressive primary brain tumor. The current standard of care for patients diagnosed with glioma includes performing a maximum safe extent resection of the tumor, undergoing radiotherapy over a 6-week period, and receiving concomitant systemic therapy with the alkylating agent TMZ (1). In addition to this, treatments such as immunotherapy, targeted precision therapy, electric field therapy, and supportive care have resulted in some improvement in the survival duration of glioma patients. However, these patients typically experience a poor prognosis and low quality of life, with only a 4-5% 5-year survival rate (2). Furthermore, cognitive and focal neurological deficits can significantly impact long-term survivors of brain tumors, regardless of tumor histology and grading (3).

The genesis of the scientific inquiry into RCD is often attributed to Karl Vogt's discernment of cellular demise in toads in 1842. A significant leap in the conceptual framework occurred in 1972 when Kerr, Wyllie, and Currie introduced the term "apoptosis" to the research lexicon, propelling the study of RCD to the scientific forefront (4). The discovery by Sulston and Horvitz in 1976, utilizing the model organism C. elegans, was instrumental in unearthing the genetic underpinnings of apoptosis and revealing a predetermined fate for approximately 13% of somatic cells during embryogenesis (5). Over the past decade, NCCD has meticulously curated a taxonomy of cell death modalities, based on distinguishing cellular morphology, biochemistry, and functional outcomes. The dichotomy between cell death pathways lies within two realms: accidental pathways triggered by external factors such as mechanical, chemical, and physical stressors that lead to cellular demise when they surpass the cell's compensatory capacities; and RCD, which represents an inherent and orchestrated cessation of cellular function mediated precisely by genetic regulation to maintain internal homeostasis. This gene-directed cessation in a physiological context is also known as programmed cell death (PCD) (6). Diverging from the unregulated nature of accidental cell death (ACD), RCD involves a meticulous network of signaling cascades and molecular machinery. The exploration of RCD has revealed numerous novel mechanisms with profound connections to human pathologies, expanding beyond apoptosis to encompass diverse processes such as autophagy-dependent cell death, ferroptosis, lysosome-dependent cell death, mitochondrial permeability transition (MPT)-driven necrosis, necroptosis, pyroptosis, anoikis, NETosis, among others (7). Each mechanism reflects a unique aspect of the cell's ability to maintain physiological integrity and their ongoing elucidation holds significant promise in enlightening the pathogenesis of various diseases and refining therapeutic strategies.

RCD, a significant pathway in the cell death process, exhibits dual effects in central nervous system tumors, particularly glioma. On one hand, dysregulated apoptotic pathways in gliomas can contribute to the anti-apoptotic properties of tumor cells, thereby facilitating tumor growth and resistance to treatment (8, 9). Over-expression of anti-apoptotic proteins, such as members of the Bcl-2 family, by glioma cells potentially inhibits the activation of RCD

(10, 11). Moreover, the abnormal regulation of RCD pathways can make glioma cells resistant to conventional therapies such as RT and chemotherapy (12). However, in certain scenarios, RCD can have an inhibitory impact on glioma. Studies have indicated that by enhancing RCD in glioma cells, tumor volume can be reduced and treatment efficacy can be improved (13, 14).

Despite the progress made in the realm of RCD, the journey toward its clinical application remains challenging. To date, therapeutic strategies harnessing apoptosis have only yielded a limited number of approved pharmacological agents for human disease management. No agents that intentionally inhibit apoptosis have been established for clinical use. An example of an approved therapy is Venetoclax, a BCL2 inhibitor which has demonstrated efficacy as a monotherapy or in combination regimens for treating chronic lymphocytic leukemia (CLL), small lymphocytic lymphoma (SLL), and acute myeloid leukemia (AML) (15–17). Furthermore, the caspase inhibitor Emricasan garnered accelerated attention from the U.S. FDA in 2016 for its focus on non-alcoholic steatohepatitis (NASH); nevertheless, the clinical outcomes have exhibited variability, underscoring the unpredictable nature of current interventions (18, 19). Looking ahead, a comprehensive investigation into the molecular intricacies of cell death, particularly within the context of the interconnected networks among various RCD pathways, is expected to stimulate innovative breakthroughs. It is through such a thorough understanding of the interplay between these pathways that novel therapeutic strategies can be developed, paving the way for their translation from laboratory research to practical application in medical treatment. The emphasis on these mechanistic insights holds great promise for unveiling new opportunities for clinical intervention and represents a significant advancement in harnessing RCD for disease management.

Overall, the regulation of RCD in glioma involves intricate signaling pathways and regulatory factors. Its influence on glioma depends on the complex interplay of multiple factors, including tumor cell characteristics, the tumor microenvironment, and treatment modalities (20, 21). Thus, this review provides a concise overview of the role of RCD in the onset, treatment, and prognosis of glioma. It focuses on several significant apoptotic pathways including autophagy-dependent cell death (22, 23), anoikis (24), ferroptosis (25, 26), cuproptosis (27), pyroptosis and immunogenic cell death (Figures 1, 2; Table 1). We propose strategies to optimize and coordinate traditional or novel approaches for glioma treatment based on these pathways. This comprehensive understanding of RCD in glioma will not only enhance readers' comprehension of its underlying mechanisms but also serve as a theoretical foundation for developing more effective treatment strategies.

2 Glioma and glioma immunotherapy

Gliomas represent 40-60% of primary central nervous system tumors in adults and are the most prevalent primary intracranial tumors in this population. According to the World Health Organization (WHO), gliomas are classified into four grades: grades 1 and 2 are low-grade, whereas grades 3 and 4 are high-grade (32). Despite advancements in glioma treatment over the past decades, challenges persist due to their unique location and the characteristics of "cold" tumors, which contribute to high recurrence rates, poor prognoses, and short median survival times (33).

The immune system fulfills three critical roles: immune surveillance, immune defense, and immune homeostasis, all of which are integral to tumor initiation, progression, metastasis, and response to treatment. Immune checkpoint inhibitors (ICIs) have revolutionized cancer therapy in recent years. However, gliomas, characterized as "cold" tumors, often exhibit poor or non-responsive behavior to ICIs, limiting the success of immunotherapy. Enhancing the immune microenvironment to convert "cold" tumors into "hot" ones may provide a new avenue for improving treatment responses (34, 35).

Bevacizumab, an FDA-approved monoclonal antibody targeting vascular endothelial growth factor (VEGF), inhibits tumor vascularization rather than directly targeting T cells (36). PD-1 inhibitors such as Pembrolizumab and Nivolumab have shown promise in clinical trials. PD-1, a receptor on T cells, interacts with PD-L1 to suppress T cell activity, aiding tumor immune evasion. Pembrolizumab disrupts this interaction, reactivating T cells to recognize and attack tumor cells (37, 38). Similarly, Nivolumab restores T cell functions by blocking the PD-1 receptor. Although a phase III clinical trial comparing Nivolumab plus RT to TMZ plus RT in newly diagnosed patients with non-methylated MGMT promoter gliomas did not achieve the primary endpoint of extending overall survival, it marked a significant step towards using Nivolumab with RT in glioma treatment, without identifying major safety concerns (39). Other immunotherapy strategies are also being explored. Oncolytic viruses (OVs) selectively replicate within and induce apoptosis in cancer cells while sparing normal tissues. A multicenter study using the oncolytic virus DNX-2401 in combination with an anti-PD-1 monoclonal antibody demonstrated safety and survival benefits (40). Dendritic cell (DC) vaccines like DCVax-L hold promise in clinical trials; these vaccines involve extracting and loading dendritic cells with tumor antigens *in vitro* before re-injecting them into the patient to stimulate an immune response (41).

The Nobel Prize in Medicine was awarded to James Allison and Tasuku Honjo six years ago for their groundbreaking work in immunotherapy (42). Current standard treatment for glioblastoma includes surgical resection combined with TMZ chemotherapy but remains insufficient. Recent studies indicate that RCD can play a synergistic role in anti-tumor immunotherapy, including for ICI-resistant tumors. Existing research highlights significant distinctions in RCD processes between low-grade and high-grade gliomas. In low-grade gliomas, apoptosis levels are relatively low, and the role of autophagy remains controversial, though these tumors generally exhibit better cellular survival activity. By contrast, high-grade gliomas demonstrate a higher resistance to apoptosis and possess a more intricate autophagy function, often accompanied by more extensive necrotic areas. These malignant tumors feature markedly

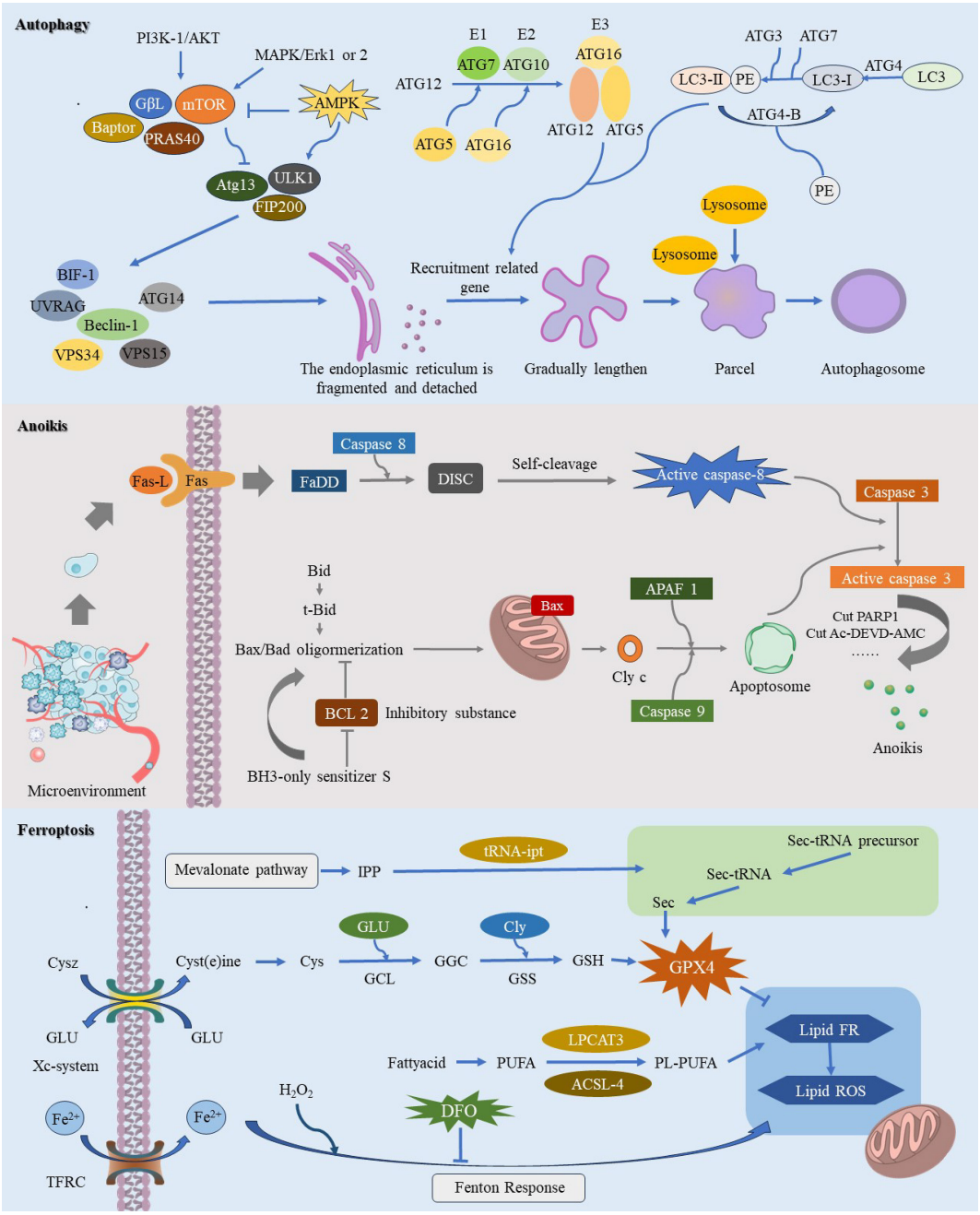

FIGURE 1
This image provides a comprehensive illustration of the molecular mechanisms underlying three pathways of regulated cell death (RCD): autophagy-dependent cell death, anoikis, and ferroptosis. Autophagy-dependent cell death is characterized by the crucial role of autophagy in degrading essential cellular components, ultimately leading to cell demise. During autophagy-dependent cell death, continuous autophagic activity undermines cellular structure and function, resulting in eventual cell death. Anoikis is primarily initiated when cells dissociate from the extracellular matrix, causing them to lose vital survival signals. This detachment disrupts integrin and other adhesion molecule signaling pathways, leading to the downregulation of survival pathways such as PI3K/Akt and Ras/MAPK, while upregulating pro-apoptotic factors like Bim and Bid. The resulting alterations in mitochondrial membrane potential facilitate the insertion of pro-apoptotic proteins Bax and Bak into the mitochondrial membrane, which then releases cytochrome c and activates downstream apoptotic caspases, ultimately driving cell apoptosis. The process of ferroptosis is initiated by elevated intracellular iron levels, which amplify the Fenton reaction and enhance ROS production. This process triggers lipid peroxidation of polyunsaturated fatty acids in the cell membrane, leading to oxidative stress and compromising membrane integrity, ultimately resulting in cell death.

different gene expression profiles, which in turn lead to varied treatment responses. Low-grade gliomas tend to be more responsive to radiation and chemotherapy, while high-grade gliomas exhibit a stronger resistance to these treatments (43). As immunotherapy advances, it becomes crucial to investigate the different pathways that either inhibit or activate various RCD processes, as well as their synergistic effects. Such exploration could pave the way for more effective targeted treatments for gliomas.

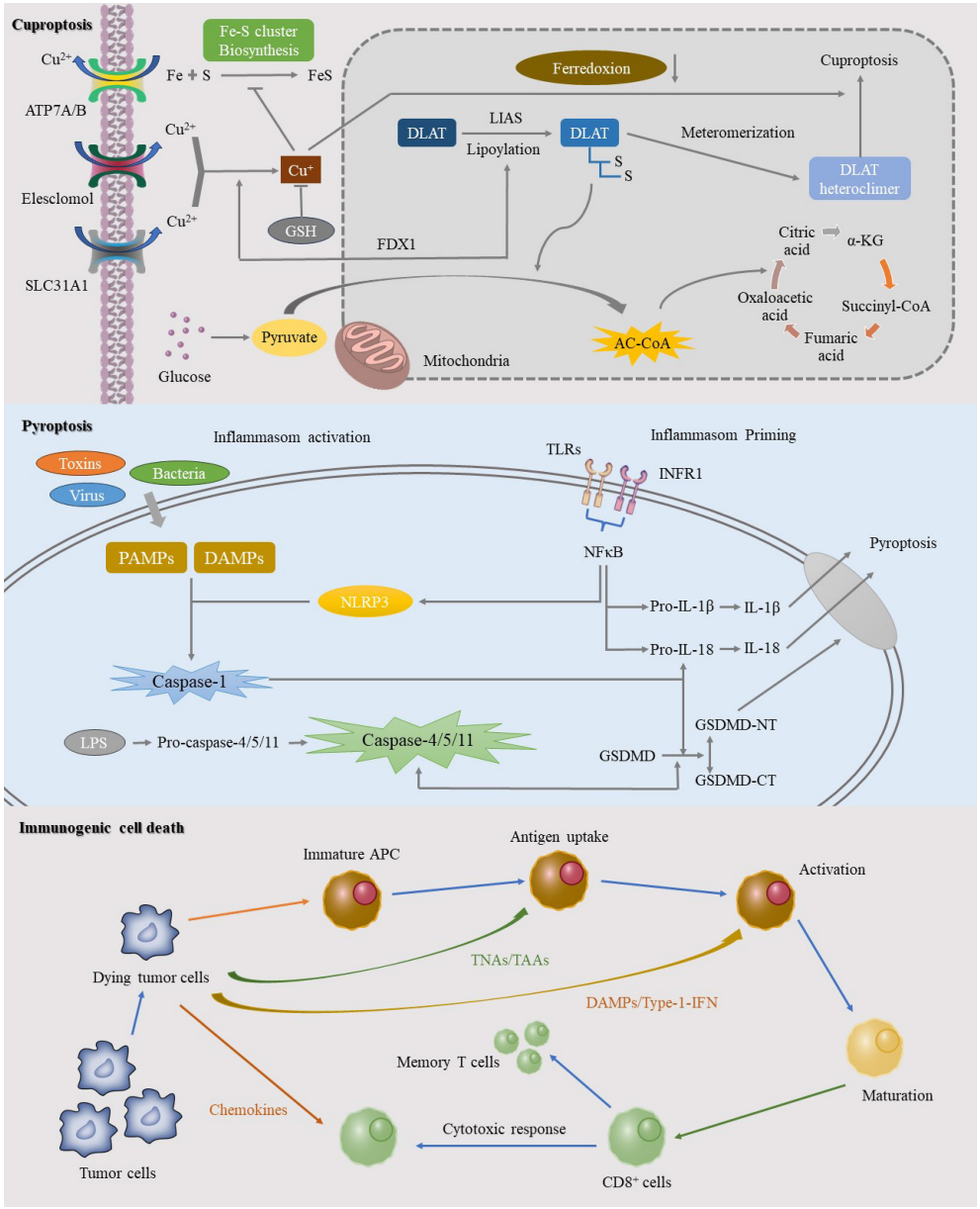

FIGURE 2
This image elucidates the specific mechanisms of three significant RCD pathways: cuproptosis, pyroptosis, and ICD. Cuproptosis, a copper-dependent form of cell death, is initiated by the intracellular accumulation of copper ions. The mechanism involves the binding of copper ions to thioredoxin cluster proteins, leading to protein aggregation and mitochondrial dysfunction. Pyroptosis, another RCD process, is mediated by inflammasome activation in response to pathogens or intracellular danger signals, resulting in a robust inflammatory response. ICD represents an RCD pathway that triggers a potent anti-tumor immune response. This process involves the release of specific death signals and DAMPs that activate the immune system.

2 Regulated cell death and glioma

2.1 Autophagy-dependent cell death

Coined by Christian de Duve and colleagues in 1963, the term "autophagy" describes the process by which cellular components, whether originating from within or outside the cell, are transported to lysosomes for degradation (44). Since the 1990s, research on autophagy has been greatly expanded due to its use as a model organism in yeast studies. Initial findings showed an accumulation of autophagosomes and lysosomes in dying cells, leading to the naming of "autophagic cell death" (45, 46). Autophagy plays multifaceted roles throughout disease progression, particularly in tumor. In the early stages of oncogenesis, autophagy acts as a guardian of genomic integrity and internal stability by regulating quality control and responding to oxidative stress. This helps

TABLE 1 Comparison of distinct aspects of RCD pathways.

RCD pathway	Morphological characteristics		Occurrence mechanism	Common inspection methods and indicators	Major associated disease
Autophagy-dependent cell death (22, 23, 28)	Cytomembrane	The autophagosome is formed, which wraps around and encloses the organelles to be degraded.	The autophagy pathway primarily occurs in two ways (1): non-selective autophagy, involving the extensive degradation of encapsulated organelles and intracellular proteins; and (2) selective autophagy, targeting the degradation of specific entities such as diseased cells or viruses.	The localization of the transcription factor TFEB, determination of ATG expression (such as Atg5, Atg7, and Atg8/LC3), and observation of autophagosomes (including their membrane structure and proteins) are necessary.	Tumors, neurodegenerative diseases, cardiovascular diseases, etc.
	Cytoplasm	The number of autophagosomes gradually increased, and the fusion of lysosomes led to the formation of autolysosomes.			
	Nucleus	No special change.			
	Organelle	The shape and number of mitochondria are significantly altered, and the number of autophagosomes increases, while the structure of the endoplasmic reticulum also appears to be expanded or fragmented.			
Anoikis (24, 29)	Cytomembrane	The cytomembrane displays folds and bulbous expansions, leading to the formation of flower-like ring protrusions.	The loss of cell-matrix force or the weakening of cell-cell adhesion leads to the activation of signaling proteins and apoptosis pathways.	Apoptosis-related markers, such as Annexin V, and nuclear and chromosomal histochemical staining were detected.	It is closely related to the metastasis of tumor
	Cytoplasm	The organelles gradually compact, resulting in cell shrinkage and clumping.			
	Nucleus	Chromatin aggregation, nuclear membrane rupture, and nucleus fragmentation occur.			
	Organelle	The cytoskeleton is reorganized, mitochondrial function is impaired, and ultimately, the system collapses completely.			
Ferroptosis (25, 26)	Cytomembrane	Lipid per, leading to the rupture of cell membranes.	The main cause is the excessive presence of free iron ions in the cell, which leads to oxidative stress and increased lipid peroxidation of the cell membrane. This triggers the signaling pathway for cell death.	The degree of lipid peroxidation, the content of endogenous iron ions, and the expression levels of related genes and proteins were assessed.	It is mainly associated with neurodegenerative diseases and tumors.
	Cytoplasm	Mineralized clusters appear.			
	Nucleus	No special change.			
	Organelle	Mitochondrial structural changes, increased oxidative stress, and endoplasmic reticulum stress.			
Cuproptosis (27)	Cytomembrane	Multiple villous bulges are formed on the cytomembrane	Intracellular overload of copper ions leads to oxidative stress, disrupts the intracellular REDOX balance, and ultimately results in cell death.	The concentration of copper ions, oxidative stress and cell death were measured.	Neurodegenerative diseases and metabolic related diseases.
	Cytoplasm	The organelles become smaller and tightly packed.			
	Nucleus	Nuclear morphology is irregular and nuclear fragments appear.			

(Continued)

10.3389/fonc.2024.1397863

TABLE 1 Continued

RCD pathway	Morphological characteristics		Occurrence mechanism	Common inspection methods and indicators	Major associated disease
	Organelle	Mitochondrial structural changes, increased oxidative stress, and endoplasmic reticulum stress.			
Pyroptosis (30)	Cytomembrane	The cell membrane forms numerous holes, leading to an ion imbalance that causes the cell to swell and dissolve, ultimately leading to the rupture of the cell membrane.	The main way to activate Caspase-1 or Caspase-4/5/11 by inflammasome complexes (such as NLRP3, AIM2), these Caspases then cleave Gasdermin D (GSDMD), causing its N-terminal fragment to insert into the cell membrane and form pores, leading to cell membrane rupture and release of cellular contents, including pro-inflammatory cytokines such as IL-1β and IL-18, thereby triggering a severe inflammatory response and cell death.	Lactate dehydrogenase (LDH) release assay, enzyme-linked immunosorbent assay (ELISA) etc.	Inflammatory diseases, cardiovascular diseases, and tumors.
	Cytoplasm	The cells rapidly swell, and cellular contents leak out, releasing inflammatory factors such as IL-1β and IL-18 into the cytoplasm.			
	Nucleus	The nuclear DNA fragments, but not in a structured way like apoptosis; chromatin is partially condensed.			
	Organelle	Mitochondrial depolarization, loss of integrity of lysosomal membrane.			
ICD (31)	Cytomembrane	The surface exposes high mobility group box protein B1 (HMGB1), calreticulin (CRT), and heat shock proteins (HSPs).	This mainly involves the translocation and release of specific signaling molecules, such as endoplasmic reticulum stress-induced calreticulin (CRT) on the surface and high-mobility group box 1 (HMGB1) released extracellularly, as well as ATP released, which are recognized and taken up by dendritic cells and other antigen-presenting cells.	Flow cytometry, immunofluorescence staining, ATP release detection, etc.	Tumors, autoimmune diseases, and infections.
	Cytoplasm	Releases multiple immune stimulating substances.			
	Nucleus	DNA breaks and chromatin condensation resemble apoptosis, but also involve the release of immune-related molecules.			
	Organelle	The mitochondrial membrane potential is lost, and there is a significant endoplasmic reticulum stress response.			

The divergence in the mechanisms underlying different RCD pathways can be attributed to the regulation of both internal and external signals. These signals encompass DNA damage, perturbation of cell cycle control, cytokine signaling, nutrient deprivation, as well as extracellular matrix cues. Upon sensing these signals, specific pathways are triggered, ultimately leading to cell death. In this table, we compare various RCD pathways in terms of cell morphological characteristics, pathogenesis, commonly employed examination methods and indicators, as well as key associated diseases. By doing so, we aim to provide a comprehensive summary of the commonalities and distinctions among different pathways, which could facilitate future practical applications.

10.3389/fonc.2024.1397863

prevent tissue damage, inflammation, and ultimately inhibits tumorigenesis and metastasis. However, during advanced stages of tumor, autophagy can serve as a source of nutrients that facilitate neoplastic growth, enhance immune evasion, and promote tumor advancement (47). Historically, reliance on morphological delineation has been the cornerstone of autophagy research, resulting in a gap in establishing causal relationships between autophagy and cell death. The present consensus among scientists categorizes autophagy's involvement in cell death into three primary types: autophagy-related, autophagy-dependent, and autophagy-mediated cell death (48). Autophagy-dependent cell death is considered as a regulated form of cell death that relies on the autophagic apparatus and generally adheres to the following criteria (1): elevated autophagy flux occurring simultaneously with cell death (2), reversibility of cell death when autophagy is inhibited through pharmacological or genetic means (3), dependence on at least two components of the autophagic process, and (4) absence of concurrent alternative forms of cell death (6).

The notion of autophagy-dependent ferroptosis emerged amidst deepening investigations into ferroptosis, a form of cell death described in 2012 as iron-dependent and distinct from apoptosis, autophagy, and necrosis (49). However, the specificity of this classification has come under scrutiny. Because Minghui Gao et al. found that under the action of ferroptosis activator, autophagosomes gradually accumulated, and cells died because of some components of the autophagy mechanism, they named this death mode as autophagy dependent ferroptosis (50–52). This reevaluation highlights the dynamic and interconnected nature of autophagic processes and cell fate, keeping autophagy at the forefront of contemporary biomedical research.

As far as the current research on glioma is concerned, most of the research still stays on the acceleration or delay of the autophagy process. Celastrol, a triterpenoid compound derived from Tripterygium wilfordii, a traditional Chinese medicine, demonstrates potential anti-glioma effects. It activates the ROS/JNK signaling pathway while inhibiting the Akt/mTOR pathway, leading to G2/M phase arrest and triggering autophagy (53). Thiolidazine enhances P62-mediated autophagy by upregulating AMPK activity and the Wnt/β-catenin signaling pathway, thereby inhibiting glioma cell proliferation and migration (54).

In this case, there are still a few studies to explore the relationship between autophagy dependent cell death and the occurrence and development of glioma. Investigator Svenja Zielke established a rigorous criterion for autophagy-dependent cell death and carefully identified three effective agents - loperamide, pimozide, and STF-62247 - from a wide range of over 70 compounds that induce autophagy. These agents were observed to promote LC3B lipidation and puncta formation, which are hallmarks of autophagic activity. This promotes autophagic flux through interactions with essential autophagy proteins ATG5 and ATG3. Ultrastructural analysis revealed an abundance of autophagosomes and autolysosomes in cells treated with loperamide and pimozide. Additionally, these compounds induced a noticeable dephosphorylation trend in complex 1 of the mammalian targets of rapamycin (mTOR), indicating activation of autophagy. Consequently, these findings suggest that loperamide, pimozide, and STF-62247 could potentially trigger autophagy-dependent cell death in glioma cells, providing a novel paradigm for therapeutic intervention in glioblastomas (55). Separately, amentoflavone (AF), a polyphenolic compound endemic to the Selaginella species, exhibits a broad spectrum of biological activities including anti-inflammatory, anti-neoplastic, radioprotective, antioxidative, and neuroprotective properties. Experimental observations have documented conspicuous depletion in intracellular glutathione levels and mitochondrial membrane potential following AF exposure, concomitant with a surge in cellular iron concentrations, malondialdehyde, and lipid peroxidation. Subsequent inquiry has substantiated the capability of AF to inhibit neoplastic proliferation by instigating autophagy-dependent ferroptosis *in vivo* potentially attributable to the modulation of the AMP-activated protein kinase (AMPK)/mTOR signaling cascade (56). These insights could delineate unrecognized molecular conduits for curtailing tumor growth and reinforce the therapeutic potential of autophagy-centric interventions in tumor management.

2.2 Anoikis

When a cell loses its normal connection to the stroma, it senses signaling abnormalities that trigger anoikis, leading to disruption of intracellular signaling and cell death. Ultimately, this results in the effective removal of displaced cells (29). Because of this characteristic, this RCD pathway has been named amnesiotic apoptosis. NCCD defines lost-nest apoptosis as a specific variant of intrinsic apoptosis induced by integrin-dependent anchoring loss (6).

In the case of tumors, the absence of anoikis can promote tumor cell survival and proliferation, thereby facilitating tumor development and drug resistance (57–59).

With advancements in bioinformatics, several researchers have developed predictive models based on genes associated with anoikis. Zhongzheng Sun et al. utilized nine genes related to anoikis to predict the survival rate and prognosis of glioma patients. They constructed a risk score and employed this model to forecast patient outcomes. Based on these findings, the possibility of exploring immunotherapy for glioma using genes and mechanisms correlated with anoikis was investigated (60). Dongdong Zhang analyzed the expression and survival of genes related to five types of anoikis, including ETV4, HMOX1, MYC, NFE2L2, and UBE2C. Additionally, a clinical prediction model was constructed (61). This work laid the foundation for subsequent progress in basic experimental research. The lncRNA ANRIL exhibited a positive correlation with glioma grade in glioma tissues regarding the induction of anoikis, and it was found to indirectly induce anoikis by inhibiting the anti-apoptosis gene Bcl-2 (62). In terms of the tumor microenvironment, MNX1 was found to be ectopically

expressed in glioma cells and associated with glioma grade. This substance was observed to contribute to cell adhesion and potentially enhance the ability of glioma cells to evade anoikis by regulating the expression of its downstream molecule TrkB (63).

2.3 Ferroptosis

Ferroptosis is a recently discovered novel form of RCD that is dependent on reactive oxygen species (ROS). The process of cell death is typically accompanied by significant accumulation of iron and lipid peroxidation (64). With the deepening of the understanding of ferroptosis, many studies believe that ferroptosis should be attributed to autophagy dependent ferroptosis, but due to the uniqueness of its cause and process, it is still discussed as a separate concept here.

Ferroptosis is intricately linked to various diseases and pathological processes, encompassing neurological conditions (e.g., Parkinson's disease, Alzheimer's disease) (65, 66), cardiovascular diseases (67), and liver diseases (68). The orchestrated process of ferroptosis in gliomas is primarily regulated by four pathways, including metabolism, the GPX4 pathway, the FSP1 pathway, and lipid metabolism (69). In the process of iron metabolism, cells absorb ferric ions (Fe3+) via the transferrin receptor TfR1, and subsequently reduce them to ferrous ions (Fe2+). The GPX4 pathway represents the classical pathway of ferroptosis. At the heart of this pathway is the lipid repair enzyme glutathione peroxidase 4 (GPX4), which plays a crucial role in inhibiting intracellular lipid peroxidation by degrading small molecule peroxides and some lipid peroxides using GSH as a substrate (70).

Current studies have provided evidence that various factors and pathways can either induce or inhibit ferroptosis in glioma. Strychnine, a weakly basic indole alkaloid derived from strychnine seeds, has demonstrated potent antitumor activity against multiple tumor types, including glioma (71). Recent investigations have revealed its ability to induce ferroptosis in glioma cells (72). TRIM7, which utilizes a K4-linked chain, directly binds to and ubiquitinates nuclear receptor coactivator 4 (NCOA4), thereby reducing NCOA4-mediated ferritin phagocytosis and subsequent ferroptosis in human glioblastoma cells (73). Ferroptosis exhibits both beneficial and adverse effects in the development and progression of glioma. Some studies have suggested that increased ferroptosis may compromise the efficacy of PD-L1 immunotherapy, while inhibiting ferroptosis remodels the immunosuppressive microenvironment and enhances the effectiveness of immunotherapy (74). Conversely, plumbagin has exhibited tumor growth inhibition by targeting the NQO1/GPX4 pathway-mediated ferroptosis, suggesting therapeutic implications for inducing ferroptosis (75). In summary, ferroptosis exhibits dual effects on glioma, influencing the efficacy of immunotherapy and potential therapeutic strategies. However, a comprehensive understanding of ferroptosis in gliomas remains elusive, necessitating further research to identify key molecular targets and mechanisms.

2.4 Cuproptosis

Similar to ferroptosis, cuproptosis is a copper-dependent and unique cell death (76). A recent study suggests that cuproptosis is an independent form of RCD and is highly associated with mitochondrial respiration and the lipoic acid (LA) pathway (77), and plays a key role in tumor cell proliferation, metastasis, and drug resistance.

Studies on cuproptosis in glioma have mainly relied on bioinformatics and gene sequencing techniques for which there are limited experimental validations available. Due to the restricted predictive value of individual biomarkers, researchers have incorporated multiple biomarkers into models to predict the behavior and progression of glioma accurately. For example, Bo Chen et al., identified a signaling pathway along with 13 ligand-receptor pairs such as ICAM8, ITGAX, ITGB1 ANXA2-FRR1 etc., constructing an activity score based on genes associated with cuproptosis while ensuring its stability through machine learning technology (78). Similarly, Lin Wang et al. identified 10 lncRNAs associated with cuproptosis that target 7 resistance genes (FDX1, LIAS, LIPT1, DLD, DLAT, PDHA1, and PDHB) and 3 sensitization genes (MTF1, GLS, and CDKN2A). They developed a prognostic risk model based on these cuproptosis-related lncRNAs which accurately predicts the tumor microenvironment status (79). Notably, FDX1 has been found to be highly expressed in gliomas and is primarily involved in lipid acylation of tumor proteins and cuproptosis, which significantly affects the prognosis of low-grade gliomas (80). Methylation of FDX1 is believed to promote malignant behavior in glioma. Functional experiments further revealed that the target gene C-MYC enhances the proliferation and invasion of glioma cells through YTHDF1 and FDX1 methylation, possibly due to aberrant copper ion behavior in mitochondria (81). Although existing studies are insufficient to establish the clinical value of cuproptosis-related mechanisms in glioma development and progression, multiple potential factors indicate that cuproptosis, like other RCD modalities, warrants further investigation and can profoundly impact glioma research.

2.5 Pyroptosis

Pyroptosis, a newly identified form of RCD, plays a pivotal role in the body's defense against pathogens. This mechanism is distinguished by specific morphological changes, including cell swelling, vesicle formation, membrane perforation, and eventual cell lysis. Unlike ferroptosis and autophagy, cell pyroptosis is mediated by proteins of the gasdermin (GSDM) family, which cause progressive cell swelling until membrane rupture. This process is tightly linked to inflammatory cascades and immune responses and can be categorized into classical and non-classical types based on the activation of caspase-1 (82).

To date, most investigations into pyroptosis in glioma have been conducted at the bioinformatics level, with limited experimental and clinical validation. Guilong Tanzhu and colleagues developed a prognostic model leveraging lncRNAs associated with pyroptosis to predict glioma patient outcomes.

They further analyzed molecular alterations and immune infiltration across different risk groups, constructing a lncRNA-miRNA-mRNA regulatory network grounded in prognostic gene risk scores (83). Hanzhang Liu et al. identified nine key differential genes by examining 523 low-grade glioma (LGG) and 1,152 normal tissue samples. Their findings indicate that these genes are instrumental in LGG progression and tumor immunity, potentially benefiting prognosis and immunotherapy (84). Caspase-6 (CASP6), a critical protein in the pyroptosis pathway, presents fluctuating relevance in glioma prognosis. Kai Guo et al. conducted an extensive analysis of four bioinformatics data routes, extracting pyroptosis-related differentially expressed genes (PRDEGs) from 81 data sets within the GeneCards database. Their research revealed CASP6 overexpression in glioma, primarily implicating it in immune responses and antigen processing. CASP6 expression was inversely correlated with overall survival and disease progression in glioma patients (85).

In summary, bioinformatics analyses suggest a significant link between pyroptosis and glioma pathogenesis. Future studies encompassing basic experimental validation and clinical research are crucial to elucidate the precise mechanisms and impacts of pyroptosis in glioma.

2.6 Immunogenic cell death

Prior to the identification of ICD, apoptosis was typically regarded as a non-immunogenic process. The recent definitions by the Committee on Cell Death Nomenclature (NCCA) describe ICD as a regulated form of cell death that can activate host immune responses within an adaptive immune context. Unlike other forms of cell death, ICD is triggered by a narrow range of stimuli, including chemotherapy agents, viral infections, and various physical or chemical factors. These stimuli induce a cascade of damage-associated molecular patterns (DAMPs), subsequently eliciting an immune response (6).

Curcumin, a bioactive phenolic compound, exhibits antioxidant, anti-inflammatory, and antibacterial properties, and has been documented to modulate several cell death pathways. Research conducted by Zenghe Xiu et al. demonstrated that curcumin can potentiate ionizing radiation-induced death of glioma cells via activation of the endoplasmic reticulum (ER) stress PERK-eIF2α and IRE1α-XBP1 signaling pathways—a finding corroborated in murine models (86). Carbonic anhydrase IX (CAIX) is a tumor-associated cell surface glycoprotein that moderates tumor cell survival by influencing pH homeostasis. S4, a highly selective CAIX inhibitor, has shown substantial efficacy in breast and colorectal cancer models. Investigations by Jing Cui et al. revealed that S4 markedly diminishes glioma cell viability and induces both apoptosis and autophagy. Further analysis indicated that S4 promotes calreticulin exposure and the release of HMGB1 and HSP70/90, thereby activating the PERK-eIF2α and IRE1α-XBP1 pathways and facilitating DAMP release linked to ICD in glioma cells through the ER stress pathway (87). Recent studies assessed the potential of TNFAIP2 knockout in enhancing the therapeutic outcomes of PD-1 inhibitors. Both *in vitro* and *in vivo* experiments demonstrated that TNFAIP2 knockout increases surface expression of calreticulin (CALR), heat shock protein 70 (HSP70), and heat shock protein 90 (HSP90) in glioblastoma (GBM) cell lines, thereby inducing ICD. Consequently, TNFAIP2 knockout during PD-1 therapy could significantly bolster survival rates in glioma patients (88).

While molecular mechanisms underlying ICD have been extensively studied, the clinical implications of ICD in disease classification, treatment, and prognosis remain underexplored. Bioinformatics offers a robust platform to address these challenges. Jiayang Cai et al. identified 34 ICD-related genes, ultimately focusing on 12 key genes including IL17RA, IL1R1, EIF2AK3, CD4, PRF1, CXCR3, CD8A, BAX, PDIA3, CASP8, MYD88, and CASP1. They established associations with non-codeletion of 1p19q, higher WHO grades, wild-type IDH, and immunosuppressive tumor microenvironments (89). Additionally, Sun et al. analyzed 1,896 glioma samples across five databases, devising a risk score model based on 14 ICD-associated genes that independently predicts survival and response to immunotherapy in glioma patients (90).

2.7 Crosstalk between multiple RCDs

Different modes of RCD, including apoptosis and necroptosis, have been extensively studied and elucidated. Apoptosis, characterized by its orderly and systematic nature, is vital for maintaining tissue homeostasis and eliminating damaged cells, thereby influencing numerous diseases and pathophysiological states. Under physiological conditions, apoptosis ensures the timely demise of cells through the meticulous regulation of both intrinsic and extrinsic signaling pathways (91). Glioma cells frequently demonstrate overexpression of anti-apoptotic proteins (e.g., Bcl-2, Bcl-xL) and deactivation of pro-apoptotic proteins (e.g., Bax, Caspase family). This apoptosis evasion mechanism not only enhances the survivability of tumor cells but also increases their resistance to conventional chemoradiotherapy and chemotherapy (92). Hence, restoring the normal apoptotic pathway is a pivotal research direction in anti-glioma therapies, with the reactivation of apoptosis presenting a promising strategy for effective tumor cell eradication. Necroptosis, a form of RCD that intersects characteristics of both apoptosis and necrosis, is primarily regulated by the receptor-interacting serine/threonine-protein kinases 1 and 3 (RIPK1 and RIPK3). In contrast to apoptosis, necroptosis resembles necrosis through the rupture of the cell membrane and the release of pro-inflammatory factors (93). Glioma cells often manipulate the necroptosis pathway to avert cell death, including the inhibition of RIPK1/RIPK3 activity and the prevention of downstream mixed lineage kinase domain-like protein (MLKL) translocation (94). The induction of necroptosis via exogenous signals such as tumor necrosis factor (TNF) or chemotherapeutic agents can lead to irreversible cell death in glioma cells, coupled with a potent inflammatory response that augments the immune system's ability to target tumor cells. However, the excessive activation of necroptosis can also precipitate unnecessary tissue damage and inflammation,

underscoring the necessity of precise regulation and the establishment of an optimal therapeutic window. Overall, a deeper understanding of necroptosis in glioma could pave the way for the development of innovative targeted therapies, thereby enhancing patient outcomes.

Tumors exhibit intricate crosstalk among various RCD pathways. Despite mechanistic and regulatory differences, these pathways can interact and influence one another under certain conditions, highlighting the importance of intercellular communication, especially as tumor cells develop mechanisms to evade drug-induced apoptosis in the context of targeted therapies.

Pyroptosis and apoptosis are primarily interconnected through the caspase family. The caspase-3/GSDME axis acts as a switch between these two forms of cell death, significantly impacting conditions like lung cancer and melanoma (95, 96). In infectious disease contexts, ZBP1 functions as a sensor for NLRP3 inflammasome activation triggered by influenza virus, paralleling the role of caspase-11 or caspase-4/5 in the non-classical LPS-induced pathway, intertwining with both pyroptosis and apoptosis. Additionally, ZBP1 is crucial in initiating PANoptosis in response to IAV (97).

The tumor suppressor gene TP53 mediates apoptosis and ferroptosis. TP53 upregulates numerous pro-apoptotic genes including BAX, PUMA, and NOXA, promoting mitochondrial-mediated apoptosis by inducing mitochondrial outer membrane permeabilization, releasing cytochrome c, and activating downstream caspases. TP53 also suppresses the SLC7A11 gene, which encodes a component of the system Xc^- transmembrane amino acid transporter responsible for importing glutathione precursor cysteine. Consequently, inhibition of SLC7A11 by TP53 reduces glutathione synthesis, leading to lipid peroxide accumulation and inducing ferroptosis (98). Ferroptosis is characterized by ROS generation and lipid peroxidation, processes that intersect with endoplasmic reticulum (ER) stress. Under ER stress, transcription factors such as IRE1, PERK, and ATF6 are activated, regulating apoptosis-related proteins like Bcl-2 and cytochrome c, thereby influencing the apoptosis pathway. Thus, modulating ferroptosis can also impact apoptosis (99).

Autophagy, particularly lipid autophagy and Beclin-1-mediated xCT degradation, can precipitate ferroptosis. Recent research has revealed that autophagy can induce ferroptosis through the regulation of intracellular ROS, LIP, and lipid peroxide levels, defined as autophagy-dependent ferroptosis (52). Studies by Eunhee Park et al. demonstrated that autophagy could be induced by ROS generated by erastin, an inducer of ferroptosis, with ferritin degradation and increased transferrin receptor 1 (TfR1) expression leading to ferroptosis. NRF2 plays a pivotal role in both ferroptosis and necroptosis; it can activate NLRP3 and AIM to induce necroptosis and exhibits specific functions in ferroptosis. Contrarily, NRF2 can also inhibit NLRP3 activation by reducing ROS levels, thereby blocking necroptosis (100, 101).

ICD is distinctive for its capacity to elicit an immune response. Although distinct from apoptosis, programmed necrosis, autophagy, and ferroptosis, these pathways can transition into ICD under specific conditions. Research on processes such as copper-induced cell death and aneuploid apoptosis in gliomas remains limited, with insufficient evidence to confirm their interaction with other RCD pathways. Collectively, the interrelationships among various RCD pathways are complex and tightly knit, forming an interactive network that regulates cell death and immune responses. Understanding these relationships is paramount for advancing treatments for tumors, autoimmune diseases, and infectious diseases.

3 The promise of RCD in targeted glioma therapy

3.1 Potential application of autophagy-dependent cell death in glioma targeted therapy

Autophagy-dependent cell death is a type of RCD that relies on autophagy mechanisms or components and plays a significant role in the central nervous system (28). Despite extensive research, there is still no definitive causal link between autophagy and cellular demise. The interplay between autophagy and various forms of cell death makes it challenging to distinguish them based solely on morphological observations throughout the cellular lifecycle. Therefore, here we mainly discuss the therapeutic concepts and methods based on inhibiting or accelerating the autophagy process to hinder tumor development.

The underlying mechanisms of autophagy that contribute to cellular death are notably distinct from those that promote cellular survival. These differences are primarily characterized by variations in the rate of autophagic flux, the duration and intensity of the involved pathways, as well as the nature and turnover rates of the substrates undergoing autophagic recycling and degradation. Such nuances play a crucial role in determining the balance between cell viability and death, thus representing potential focal points for innovative tumor therapies. A wealth of preclinical research has meticulously examined the function of autophagy in tumor treatment, employing two prevalent methodologies. The first method involves triggering autophagy through the administration of broad-spectrum anticancer agents, such as rapamycin, which antagonizes mTORC1 (102). The second strategy involves indirectly activating autophagy by selectively inhibiting specific drug targets, such as the inhibition of ERK in PDAC cell lines (103). Although the precise mechanism underlying modulation of autophagy remains elusive, the current understanding leans towards the notion that upregulation of autophagy confers a protective effect on tumor cells.

With the increasing understanding of autophagy, novel therapeutic agents targeting glioma cell autophagy have entered clinical trials. Chloroquine (CQ) and hydroxychloroquine (HCQ), known for their anti-malarial properties, have shown potential in inhibiting autophagy and enhancing the efficacy of DNA damage therapy. Previous studies investigated combination therapy with hydroxychloroquine for glioma by conducting phase I/II clinical trials to determine its efficacy and maximum tolerated dose (MTD). Despite effectively inhibiting autophagy, the clinical application of hydroxychloroquine is limited due to its toxicity at higher dosages

(104). After that, while HCQ has been widely used in the treatment of malaria (105), primary progressive multiple sclerosis (106), IgA nephropathy (107), and even COVID-19 (108), it has rarely been utilized for glioma. However, in 2020, due to the COVID-19 pandemic and the urgent need for new glioma treatments, HCQ and CQ have regained attention, leading to the emergence of corresponding clinical trial studies. In a recent study by Inge Compter et al., the investigators examined the safety, pharmacokinetics, and MTD of a combination therapy consisting of chloroquine, RT, and daily TMZ administration in newly diagnosed glioblastoma patients. This novel therapeutic approach holds promise for the treatment of gliomas (109).

Furthermore, due to the gradual advancement of autophagy research and the rapid progress in bioinformatics in recent years, numerous studies have progressed to the stage of clinical trials. Mutations in the epidermal growth factor (EGF) have been implicated in gliomas' resistance to conventional chemotherapy (110). Chloroquine, a potent autophagy inhibitor, impairs this survival mechanism by blocking the lysosomal degradation pathways activated by mutated epidermal growth factor receptor (EGFRvIII). This recently registered clinical study marks a new frontier in efforts to overcome therapeutic resistance within gliomas. A pioneering Phase I/II clinical trial, initiated in 2020, is investigating the combined efficacy of dabrafenib, trametinib, and hydroxychloroquine in the treatment of recurrent gliomas characterized by BRAF mutations. This trial specifically focuses on determining the extent of autophagy inhibition and its correlation with resistance profiles of gliomas, as well as the specific involvement of autophagic processes in the context of BRAF anomalies. Building on preclinical findings, delta-9-tetrahydrocannabinol and cannabidiol (CBD) have demonstrated their potential in tempering glioma proliferation and metastasis. These phytocannabinoids engage type 1 and type 2 cannabinoid receptors, triggering the endoplasmic reticulum stress response and subsequently inducing autophagy (111). Last year witnessed the initiation of a Phase I multicentric clinical trial in Spain dedicated to assessing the therapeutic safety of this novel combined modality. Phase I/II clinical trials are currently underway to investigate sphingoid modulators and the glioma autophagy inducer idroxioleic acid. These studies aim to determine the MTD of these drugs, evaluate their safety and initial efficacy, and shed light on their potential for anti-tumor treatment of glioma (112).

Unfortunately, numerous autophagy-related molecules possess a wide range of vital physiological roles beyond their established functions within the autophagic pathway. Autophagy-related genes (ATGs) exert their influence on various processes, both in healthy and pathological states, that go beyond their canonical duties as autophagy facilitators. For example, the ATG5-ATG12/ATG16L1 protein complex has demonstrated antiviral capabilities mediated by interferon-gamma—actions that differ from its involvement in autophagy (113, 114). Additionally, ATG7 is one of the core proteins of autophagy, but the ATG7 dependent non-autophagy pathway plays a key role in the regulation of neovascularization (115). While the classical autophagy pathway remains an essential aspect of ATG function, the non-autophagic capabilities demonstrated by these molecules cannot be disregarded. The multifaceted nature of autophagy-related molecules often complicates the understanding of their complex physiological interactions, presenting a significant challenge in unraveling their roles in clinical trials, which may contribute to suboptimal outcomes observed. Future research endeavors must adopt a broader perspective that is not confined to the solitary functions attributed to autophagy-related molecules. Enhancing our understanding of their versatile involvement in cell death regulation and the distinct disease-modulating processes mediated through autophagy-dependent death pathways in various neoplastic contexts will be crucial for advancing therapeutics.

3.2 Potential application of anoikis in glioma targeted therapy

Anoikis, a distinct form of RCD triggered by cell detachment, holds significant importance in maintaining cellular homeostasis and microenvironmental stability. Mechanisms that activate resistance to anoikis hinder the induction of apoptosis in cells upon tumor initiation, impeding their ability to undergo cell death when detached. This phenomenon promotes the proliferation and migration of tumor cells. Consequently, inhibiting resistance to anoikis and restoring normal anoikis processes emerge as promising avenues for exploration in tumor research (Figure 3).

Despite the inherent radiation resistance of gliomas, RT remains a standard treatment in the context of tumor drug resistance (116). In a study of prostate cancer, Erk and PIK-AKT signaling enabled isolated tumor cells to acquire resistance related to anoikis, leading to drug resistance (117). In glioma, the commonly used alkylating agent TMZ is an essential component of adjuvant chemotherapy. However, recent research has demonstrated that astrocytes resistant to anoikis exhibit robust resistance to TMZ, resulting in minimal reduction in cell viability and unaffected colony formation (118). These findings suggest a potential association between induction of anoikis and drug resistance in glioma.

Considering the potential correlation between anoikis and the development of drug resistance in RT and chemotherapy, targeted therapy against anoikis demonstrates promise as an ideal adjunctive strategy in glioma treatment. Exploring the molecular regulation of anoikis may provide novel insights into prognostic assessment in glioma. For instance, a recent study developed a prognostic model for low-grade glioma (LGG) based on the ANRG and LGG subtypes (119). Another investigation employed differentially expressed anoikis-related genes (ARG) derived from GeneCards to construct a prognostic ARG model for glioma, revealing that patients in the high-risk group exhibit a worse prognosis (61). These findings collectively underscore the clinical significance of anoikis in glioma treatment and prognosis, despite the need for further mechanistic investigations. Continued research in this area will undoubtedly contribute to advancements in glioma therapeutics.

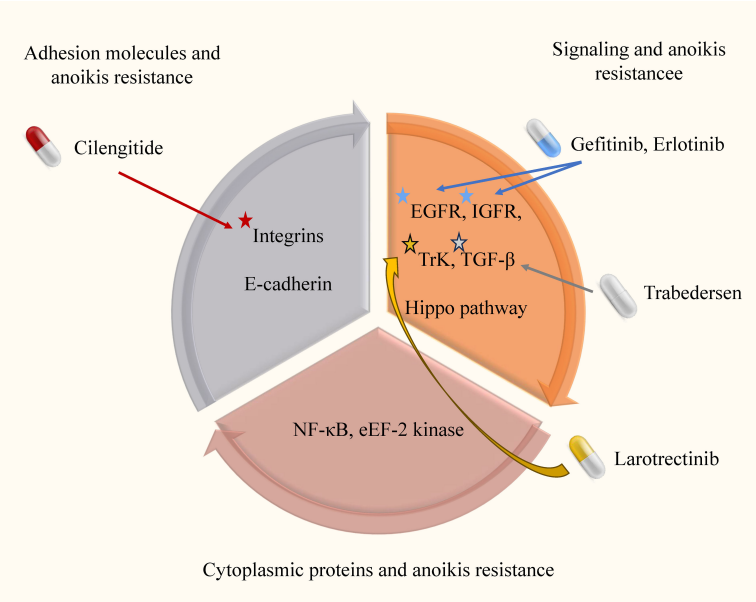

FIGURE 3
Anoikis resistance mechanism and targeted drugs in glioma. In this image, we elucidate the intricate anoikis-resistance pathways operative in glioma, along with their consequential clinical implications. Anoikis, which is inherently designed to eliminate impaired cells, is crucial for maintaining cellular equilibrium within the microenvironment. However, in gliomas, a disrupted resistance to anoikis emerges, enabling cancerous cells to evade this regulatory process and disrupting the natural course of malignant cell clearance.

3.3 Potential application of ferroptosis in glioma targeted therapy

With the increasing understanding of ferroptosis, researchers have initiated investigations into its potential in tumor therapy. Multiple studies have demonstrated that specific anti-tumor drugs can induce ferroptosis, highlighting its potential in glioma treatment.

Recent findings suggest a close association between ferroptosis and treatment resistance in targeting tumor cells. Viswanathan et al. demonstrated that the lipid peroxidase pathway, mediated by GPX4 which can partially suppress ferroptosis, regulates the development of highly resistant mesenchymal cells (120). Another study revealed that depleting immunosuppressive cells in the tumor microenvironment can reverse drug resistance through ferroptosis (121). These findings underscore the potential of ferroptosis as an effective adjunct therapy against glioma resistance.

Extensive research has been sparked into the potential induction of ferroptosis in tumor treatment, with several clinically approved drugs (e.g., sorafenib and artesunate) demonstrated to effectively induce ferroptosis (122). The integration of nanomaterials with targeted ferroptosis has garnered significant attention in the field of tumor treatment research. Nano-based drug delivery systems offer advantages such as enhanced stability, improved availability, minimal side effects, and robust targeting capabilities. Chen et al. developed trehalose-loaded nanoparticles that combined GSH consumption-induced ferroptosis with trehalose-induced autophagy, demonstrating the potential of nanaterial design in developing ferroptosis-induced nanomedicine (123). While most nanoscale research on ferroptosis has focused on breast and liver cancer, this approach is expected to become a future treatment strategy for glioma. It also demonstrates the importance of interconnection between different RCD pathways.

The increasing recognition of the significance of ferroptosis in the tumor microenvironment and its potential as a prognostic predictor has led to studies investigating its clinical relevance. Zhuo et al. conducted a study examining genetic markers associated with ferroptosis and found that these markers could potentially serve as prognostic indicators for glioma patients (124). Similarly, Wan RJ et al. identified differential expression of ferroptosis-related genes between glioma patients and non-patients, suggesting the possibility of using these genes as a new standard for prognostic evaluation in the future (125). These findings highlight the significance of comprehending the role of ferroptosis in the tumor microenvironment and its potential as a prognostic marker for glioma patients. Further research is necessary to validate and expand upon these findings, ultimately advancing prognostic prediction in glioma.

3.4 Potential application of cuproptosis in glioma targeted therapy

Perturbations in serum and tumor tissue copper levels have been observed in patients with malignant tumors such as lung cancer (126) and breast cancer (127), suggesting alterations in copper homeostasis that may contribute to tumor progression, invasiveness, or drug resistance. Although experimental research on cuproptosis is still in its early stages, it is undeniable that cuproptosis holds promising potential as a therapeutic target for tumor treatment.

TABLE 2 Comparative analysis of metal-mediated RCD pathways.

Metal-mediated cell death pathway	occurrence mechanism	Induction pathway	suppressor pathway	clinical application value
Ferroptosis (25)	It mediates cell death by participating in intracellular REDOX reactions and generating ROS.	Iron overload, oxidative stress, and abnormal glutathione metabolism.	Inhibition of iron ionophores and enhancement of antioxidant system.	Could be a potential treatment for tumors.
Cupoptosis (27)	It participates in a series of REDOX reactions within the cell, leading to intracellular oxidative stress that promotes cellular death.	Imbalance and oxidative stress in copper ion tray system.	Not clear.	Could be a potential treatment for tumors.
Cadmium-induced cell death (128)	Cell death is mediated through various mechanisms, such as interfering with the REDOX balance, activating the apoptosis pathway, inducing mitochondrial dysfunction, and causing DNA damage.	Accumulation of cadmium ions, mitochondrial dysfunction.	Reduce the accumulation of cadmium ion and enhance mitochondrial function.	It may influence cell apoptosis, promoting or inhibiting the development of certain tumors.
Chromium-induced cell death (129)	Cell death is mediated by interfering with DNA repair, activating apoptotic pathways, and inducing oxidative stress.	Chromium ion excess, oxidative stress.	Not clear.	Could be a new way to treat tumor.
Bismuth-induced cell death (130)	It mediates cell death by inducing oxidative stress, interfering with mitochondrial function, and triggering apoptosis.	Accumulation of bismuth ions.	Not clear.	Could be a new way to treat tumor.

Metal-induced RCD plays a significant role in cellular demise. In this phenomenon, metal ions exert regulatory control over the apoptotic signaling pathway by interacting with crucial intracellular proteins, ultimately leading to cell death. In the present study, we provide a comprehensive comparison of disparate metal-mediated RCD pathways, focusing on the pathogenesis, induction, and inhibition of these pathways in tumor cells. Furthermore, we discuss the potential clinical applications associated with these metal-induced RCD pathways.

Pertinent findings from several studies have established a correlation between cuproptosis markers and the prognosis of glioma. In research conducted by Li Wang and colleagues, notably elevated expression levels of cuproptosis-related genes were observed in the high-risk group of glioma patients as compared to the low-risk group. Moreover, the researchers developed a risk model grounded on long non-coding RNA (lncRNA) associated with cuproptosis, which partially reflects its prognostic significance in glioma (79). However, additional experimental validation is necessary to corroborate the prognostic implications of cuproptosis-related genes in this disorder.

In our review of tumors, we have discovered that certain metal ions, namely cadmium (128), chromium (129), and bismuth (130), possess carcinogenic properties to some extent (Table 2). Recent research suggests that their mechanism of action may be closely linked to ferroptosis, cuproptosis, and autophagy. Ashish Tyagi et al. conducted mouse experiments and found that chronic exposure to cadmium consistently activates the NOX1 complex, leading to the generation of ROS and endoplasmic reticulum (ER) stress in cells. This activation subsequently results in defective autophagy (131). In a separate study conducted by Caijun Zhao et al., it was discovered that cadmium-induced ER stress mediates the activation of autophagy, which leads to ferroptosis in renal tubular epithelial cells (128). The potential therapeutic application of these metal ions in disease treatment is a topic of discussion, for instance, bismuth has been widely used for the eradication of H. pylori infection (132). It is important to note that the therapeutic and side effects of metal ions are often dose-dependent and influenced by the method of administration. Currently, metal ions have not been utilized in tumor therapy, and further research is necessary to explore their potential in this field.

3.5 Potential application of pyroptosis in glioma targeted therapy

The relationship between pyroptosis and tumor dynamics, particularly in glioma, is intricate and multifaceted. On one hand, as a significant form of RCD, pyroptosis can effectively inhibit tumor initiation and progression. Conversely, the inflammation and immune responses triggered by pyroptosis release various inflammatory mediators and cytokines, such as interleukin-1β and interleukin-8, which might promote tumor growth, modify the tumor microenvironment, and contribute to drug resistance (133).

Current research endeavors aim to harness pyroptosis to enhance glioma treatment. For instance, Li-Wen Ren utilized weighted gene co-expression network analysis (WGCNA) on data from The Cancer Genome Atlas (TCGA) to identify key genes in glioblastoma (GBM). Using the connectivity map (CMAP) platform, three substances—flubendazole, mebendazole, and fenbendazole—were identified as potential anti-glioma agents. These compounds were shown to induce pyroptosis in GBM cells via the NF-κB/NLRP3/GSDMD pathway and also trigger mitochondria-dependent apoptosis in nude mice models (134). In another study, Wenpeng Zhao and colleagues conducted high-throughput screening of 2,718 compounds from approved drug and clinical compound libraries. They discovered that the second-generation small molecule polyCDK inhibitor AT7519 holds

promise as a GBM therapy. AT7519 notably inhibited glioma cell viability and proliferation in a dose-dependent manner and induced pyroptosis through caspase-3-mediated cleavage of gasdermin E (GSDME) (135). Meanwhile, Chinese researchers have explored traditional Chinese medicine formulations, identifying Xihuang Pill as a noteworthy candidate. This traditional preparation promotes the pyroptosis of glioma cells via the POU4F1/STAT3 axis and effectively halts glioma proliferation, although its precise mechanisms and clinical applicability warrant further investigation (136). Despite these promising approaches, translating them into effective clinical treatments faces substantial challenges. The glioma microenvironment is exceptionally complex and exhibits significant heterogeneity in treatment response. Furthermore, researchers must address issues of selectivity, drug delivery, side effects, and resistance associated with pyroptosis-inducing agents.

In summary, while pyroptosis offers potential therapeutic avenues for glioma, extensive research is necessary to overcome the inherent challenges and fully realize its clinical benefits.

3.6 Potential application of ICD in glioma targeted therapy

In 1893, American orthopedic surgeon William Coley made a serendipitous discovery that postoperative pyogenic streptococcal infections could induce tumor regression in sarcoma patients, thus marking the dawn of tumor immunotherapy. Over the past decade, ICD has emerged as a crucial link between oncological treatment and the immune system, paving the way for numerous advancements in cancer therapy. Several factors can induce ICD, including chemotherapeutic agents, oncolytic viruses, high hydrostatic pressure, and cytotoxic heat shock (31). ICD inducers can be categorized based on their immune induction mechanisms: Type I inducers primarily comprise genotoxic agents that lead to abnormal protein activation and DNA damage, while Type II inducers are generally more potent, inducing endoplasmic reticulum oxidative stress, perturbing ER homeostasis, raising intracellular Ca2+ levels, and rapidly activating danger signal pathways to expose and release DAMPs (137–139). Consequently, modulating these factors in cancer therapy might offer new targeted treatment strategies.

Sonodynamic therapy (SDT) is a novel treatment modality that integrates low-intensity ultrasound with chemotherapeutic drugs, boasting high tissue penetration and non-invasive characteristics. Yan Zhou et al. first identified that TMZ, a standard treatment for glioma, generates significant reactive oxygen species (ROS) when exposed to ultrasound. Therefore, employing TMZ as an SDT sensitizer could enhance glioma treatment efficacy (140). Subsequent studies have shown that TMZ-based SDT causes ER expansion, mitochondrial swelling, and initiates the ER stress response (ERSR), nuclear DNA damage, and mitochondrial permeability transition pore (mPTP) opening. This process also induces “danger signals” from glioma cells, promoting the maturation and activation of bone marrow-derived dendritic cells (BMDCs), ultimately reshaping the glioma immune microenvironment and eliciting robust anti-tumor responses. Anti-tumor vaccines have recently gained attention in immunotherapy. These vaccines are created by exposing autologous dendritic cells to glioma tissue-induced ICD, wherein the dead glioma cells produced by ICDs activate astrocytoma cells and DAMPs. Upon administration to patients, the DC-presented tumor antigens trigger a specific T cell response, targeting residual astrocytoma cells, thereby reducing tumor recurrence and extending patient survival (141). Furthermore, genetically engineered virus technologies are being developed to leverage ICD, using viral vectors to deliver cytotoxic agents specifically to tumor tissues, thus inducing ICD and circumventing the blood-brain barrier’s interference with therapeutic efficacy (142).

Recently, two drugs, lurbinectedin and belantamab mafodotin, have been validated to drive ICD-mediated tumor treatment and have received FDA approval for cancer therapy (143–145). Despite the current fragmented, uncertain, and indirect nature of research on ICD-based cancer treatments, the promising potential of ICD underpins its prospective role as a pivotal component in future cancer therapies, necessitating further investigation.

4 Probing the synergistic impact of variegated RCD pathways for oncological treatment strategies

RCD orchestrates a range of physiological and pathological phenomena, including developmental dynamics, homeostatic integrity, and immune responses (7). It fundamentally interfaces with disease pathogenesis and healthcare outcomes. RCD plays a pivotal role in terminal cellular demise and is intricately linked to critical pathological episodes such as myocardial infarctions and neurodegenerative disorders (146–148). Furthermore, aberrations in RCD signaling cascades are implicated in uncontrolled cellular proliferation and excessive mass accumulation characteristic of neoplastic transformation (149). From an interventional standpoint, ACD is triggered by acute environmental insult, a phenomenon considered spontaneous and inevitable according to prevailing research paradigms. Conversely, the processes of RCDs are regarded as modifiable and potentially therapeutically manipulable due to their more gradual and controlled nature (150).

In recent decades, with the deepening of research on RCD, people have gradually explored the potential of various RCD pathways in treating diseases, especially tumors, using different therapeutic approaches such as targeted drug therapy, gene therapy, adjuvant RT, and immunotherapy (151, 152). Despite extensive clinical scrutiny, the translation of these insights into effective treatments has been limited due to various obstacles including challenges related to pharmacokinetics and dynamics, suboptimal trial outcomes, and safety concerns. A significant obstacle is the profound interconnectivity and complexity within mammalian RCD signaling networks; blocking one pathway pharmacologically often requires simultaneous inhibition of multiple molecular entities and cascades, thus hindering specificity. Furthermore, despite extensive research on RCD, the field remains in its early stages, with many

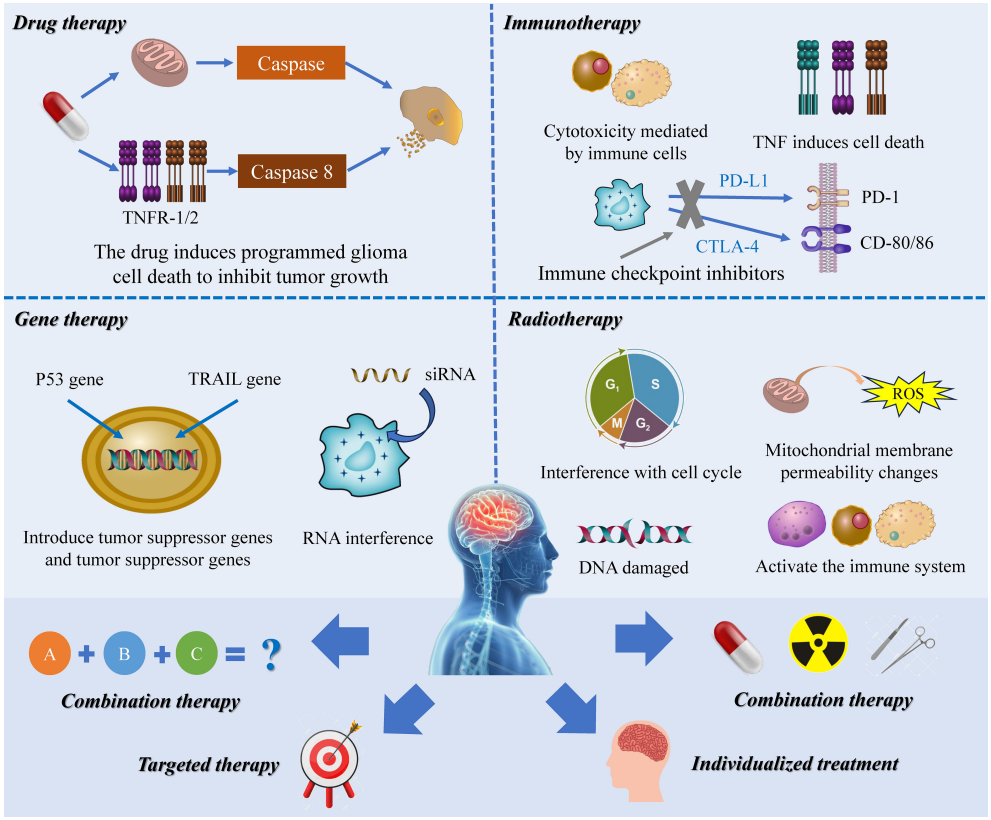

FIGURE 4
The therapeutic prospect of RCD in glioma. This image delineates the multifaceted role of RCD as a dynamic player in oncological treatments, encompassing gene therapies, precision pharmacotherapy, immune-modulatory strategies, and radiological interventions. Research highlights the intricate involvement of RCD mechanisms in mediating therapeutic efficacy. Advancing this domain, a synergistic approach that harnesses the collective force of RCD pathways and seamlessly integrates various treatment modalities holds promise as a novel paradigm in tumor management.

molecular mechanisms and signaling conduits yet to be elucidated. Hasty intervention risks disrupting other physiological processes, raising doubts about the feasibility and prudence of applying RCD inhibitors in therapeutic contexts. With the emergence of one difficulty after another, researchers have gradually shifted their focus to the combination treatment and mutual tandem of RCD, which has brought new hope for tumor treatment (Figure 4).

RT functions primarily by inducing double-strand DNA breaks, which subsequently increase the permeability of the mitochondrial outer membrane (153). This elevation in permeability facilitates the release of pro-apoptotic proteins, thereby triggering downstream apoptotic signaling cascades. Accumulating evidence from RT research has revealed instances of anti-tumor responses in non-irradiated regions, a phenomenon known as the bystander effect. Subsequent investigations suggest that this effect may stem from the activation of anti-tumor T cells and the initiation of specific RCD mechanisms. These processes facilitate tumor eradication and, on occasion, may induce systemic bystander effects (154). Occasionally, radiation may also evoke autophagy-dependent cell death, serving as a damage control mechanism to eliminate compromised cells (155). Conversely, TMZ, an alkylating agent, inflicts DNA damage through alkyl group addition to DNA strands, culminating in cell death. The DNA damage response (DDR), particularly involving the p53 pathway, is activated during this process and leads to apoptosis. Notably, reports indicate that TMZ may also induce various forms of RCD, including necrosis, ferroptosis, and autophagy-dependent cell death (156). By leveraging these insights into radiation and TMZ-induced cell death pathways, there is potential to optimize glioblastoma treatment paradigms, thereby advancing therapeutic efficacy.

Future research endeavors may benefit from unraveling the collective dynamics among different RCD modalities. Concurrently, exploring the propagation of secondary RCD after initial cellular demise and the signal transduction of damage-associated molecular patterns (DAMPs) could provide fertile ground for pharmacological targeting.

In this immediate discourse, we focus on the interplay between autophagy and ferroptosis, particularly how autophagic mechanisms modulate the latter in response to external ferroptotic stimuli. Several studies have proposed the term “iron-dependent autophagy” to describe ferroptosis as a subset within the spectrum of autophagy. However, their distinct pathways require separate consideration; thus, this discourse will analyze their interrelation separately. Autophagy initiates ferroptosis by regulating intracellular levels of ROS, LIP, and lipid peroxides (52). Findings from these studies have primarily revolved around the xc, GPX4, and FTH systems. The phosphorylation of Beclin-1 by AMPK generates a complex with SLC7A11, thereby inhibiting its

function as a Cys transporter and stimulating lipid peroxidation and iron metabolism (157). PNO1-induced autophagy enhances the synthesis and accumulation of intracellular glutamate, augmenting system Xc activity and preventing ferroptosis. Moreover, by preserving redox homeostasis, PNO1-autophagy metabolism activates system Xc responsible for cysteine synthesis and cell protection against ferroptosis (158). Owing to its interaction with distinct autophagy receptors, GPX4 has been demonstrated to be degraded following treatment with inducers of ferritin deposition or excessive copper, thereby instigating ferroptosis (159).

Within the contemporary oncological therapeutic landscape, the strategic coordination of two or more RCD pathways to combat tumor progression is increasingly evident. Lu01-m, identified as a natural compound, demonstrates a potential in stymieing prostate cancer proliferation and dissemination by propelling cells into G2/M phase arrest accompanied by DNA damage, thereby eliciting RCD pathways including necroptosis and autophagy (160). Cisplatin, a stalwart in lung cancer chemotherapy, has been documented to invoke caspase-3/GSDME-dependent pyroptosis in neoplastic cells, alongside the induction of ferroptosis through reduced glutathione levels and compromised glutathione peroxidase activity (95). Dihydroartemisinin (DHA), an artemisinin derivative, exerts its anti-tumorigenic effects by inducing cell cycle standstill and impairing angiogenesis, which culminates in the ferroptosis and apoptosis of malignant cells (161). Research by Farhan Basit and colleagues has underscored the role of BAY 87-2243, an inhibitor of mitochondrial respiratory chain complex I, in unleashing mitochondrial dysregulation, augmented ROS accumulation, lipid peroxidation, and reduced glutathione stores to foster autophagosome formation and propel ferroptotic cell death in melanoma cells (162). In the context of ovarian cancer, an investigation by Rongjun Zhang et al. unveiled the DNA-damaging capabilities of a citrus-derived substance through upregulation of poly (ADP-ribose) polymerase in a dose-dependent manner, which subsequently instigates autophagy and apoptosis. This substance also precipitates mitochondrial membrane potential diminution and ROS generation, facilitating pyroptotic cell demise (163).

The combined RCD effect has demonstrated utility in overcoming tumor resistance. Clinically, the concomitant use of resveratrol (RSV) with docetaxel (DTX) has been observed to suppress Bcl-2, amplify apoptosis, and necroptosis, thereby mitigating the drug resistance often associated with DTX monotherapy and elevating therapeutic efficacy (164). In the realm of triple-negative breast cancer, the combination of cetuximab with miR-155-5p antagonists can induce an increase in EGFR levels, promoting apoptosis and pyroptosis in breast cancer cells through the upregulation of GSDME-N and cleaved caspase-1, opening new possibilities for treatment (165).

While these insights predominantly derive from non-glioma malignancies potentially confined by the blood-brain barrier, similar therapeutic principles have been identified in glioma (Table 3). Yucheng Liu and colleagues have detailed an apoptotic regulatory cascade that starts with autophagy inhibition leading to mitochondrial turnover disruption, ROS amplification, DNA injury, p53 trans-activation, and culminating in apoptosis. Such suppression of autophagy propelled by TRPML1 modulation significantly hinders glioma cell proliferation. An ongoing clinical trial is investigating the synergistic impact of Haloperidol Tablets (HP) in conjunction with TMZ. TMZ has been reported to increase dopamine D2 receptor (DRD2) expression, which can cause chemotherapy resistance. As a DRD2 antagonist, Haloperidol mitigates this mechanism and enhances GBM's susceptibility to TMZ by inducing pathways of autophagy and ferroptosis (166).

In summary, the mechanisms and functions of individual RCD pathways have been relatively well studied and understood, and inhibitors for these pathways have been discovered and applied (Table 4). However, the common mechanisms and interactions among all RCD pathways have not yet been fully elucidated. This is mainly because research in these areas is still in its early stages and is constantly evolving, encompassing a range of processes from unique molecular signals to biological processes. Despite these

TABLE 3 List the RCD pathway inhibitors or inducers that have been approved/are undergoing clinical trials.

Targeted Drug	The main regulatory mechanism	Progress	Clinical Trial ID
Venetoclax	Inhibit BCL-2 and promote cell apoptosis.	It has been approved by the FDA and Venetoclax is primarily used for blood system malignant tumors, but its evaluation in gliomas is also underway.	/
Navitoclax	Inhibiting both BCL-2 and BCL-XL enhances cell apoptosis response.	Inhibiting both BCL-2 and BCL-XL enhances apoptotic response.	NCT03181126
Erastin	Inhibiting ferroptosis pathway	The potential therapeutic effects of ferroptosis inhibitors for GBM, which are resistant to traditional treatments, are being studied.	Not provide
Chloroquine	Inhibiting the autophagy process causes cells to accumulate toxic substances, leading to autophagy-dependent cell death.	The efficacy of chloroquine combined with TMZ and/or other therapeutic drugs for glioblastoma is being evaluated.	NCT02378532
Caspase Activators	Activate the calreticulin-dependent cytosolic pathway of necroptosis.	These drugs are designed to increase the death of tumor cells by inducing pyroptosis.	NCT02103335
Fluphenazine and TMZ Combined Therapy	Induces autophagy-dependent cell death and ferroptosis.	The DRD2 antagonist haloperidol can weaken the function of DRD2 and increase the sensitivity of GBM to TMZ by inducing lethal autophagy and ferroptosis.	NCT06218524

TABLE 4 A summary of small molecule inhibitors targeting key components of RCD.

Inhibitor	Process of inhibition	Illustrate
Bcl-2 family inhibitors	Apoptosis	ABT-199(Venetoclax)
Caspase inhibitor	Apoptosis	Z-VAD-FMK
RIPK1 inhibitor	Necroptosis	Necrostatin-1(Nec-1)
RIPK3 inhibitor	Necroptosis	GSK'872
Caspase-1 inhibitor	Pyroptosis	VX-765
Gasdermin D inhibitor	Pyroptosis	Under research
PI3K/mTOR inhibitor	Autophagy	Rapamycin
VPS34 inhibitor	Autophagy	3-Methyladenine (3-MA)
Iron chelating agent	Ferroptosis	Deferoxamine (DFO)
Copper chelating agent	Cuproptosis	D-Penicillamine
HSP90 inhibitor	Anoikis	NVP-AUY922
PARP inhibitor	ICD	Olaparib

challenges, our discussion has revealed potential commonalities among these RCD pathways, suggesting promising directions for future research. Our hope is that these exploratory pathways will bring about key advancements in the field of tumor targeted drug therapy (Figure 5).

5 Conclusion and future perspectives

Currently, in glioma investigations, there is a primary emphasis on either enhancing or impeding the autophagy cascade for autophagy-dependent cell death. While ferroptosis studies have not gained as much prominence as in other tumor types, a subset has advanced to clinical evaluation. However, research into the modalities of cuproptosis and anoikis remains relatively scarce, with the majority confined to preliminary bioinformatics analyses.

Although different forms of RCD pathways may appear distinct, there is a close connection among them. Therefore, comprehensively studying and applying multiple mechanisms could potentially become a means of targeted therapy for glioma in the future.

By regulating autophagic processes, there is potential to improve therapeutic outcomes for glioma. Current studies mainly focus on related genes, pathways, and adhesion molecules; however,

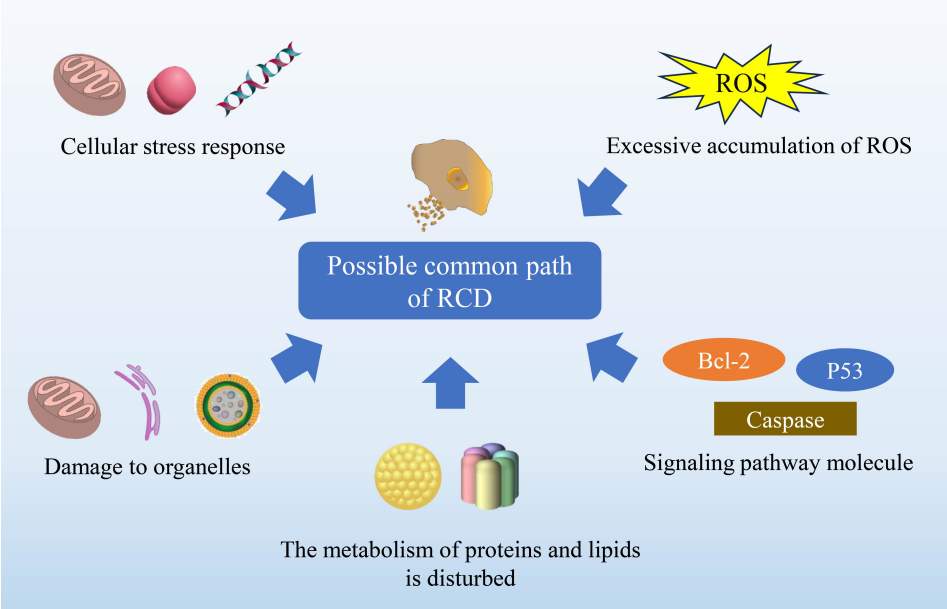

FIGURE 5
Explores potential commonalities among diverse RCD pathways. The intricate nature of RCD mechanisms remains an active area of investigation, with each pathway governed by distinct molecular signals and biological processes. As such, the full scope of autophagy-dependent cell death, ferroptosis, cuproptosis, anoikis, pyroptosis and immunogenic cell death remains to be elucidated. Nevertheless, certain fundamental characteristics might be common across these mechanisms, which include: Cellular stress response, encompassing the adaptation of proteins, lipids, DNA, and organellar structures to various forms of injury. ROS generation, where an excess can impair lipids, proteins, and DNA, hence functioning as a ubiquitous harbinger of cellular demise. Organelle dynamics involving mitochondria, lysosomes, and the endoplasmic reticulum that may engage in a coordinated response. Convergence of key molecular pathways, such as those involving tumor suppressor P53, the Bcl-2 protein family, and caspases. Perturbations in protein and lipid metabolism, which are increasingly recognized as contributors to RCD.

there are evident limitations due to the specific nature and location of glioma. In the future, drawing upon research strategies from other tumors and proposing relevant studies on anoikis and glioma could provide valuable insights for analyzing and modulating the tumor microenvironment of gliomas. Considering the accumulation and abnormal distribution of metal ions in glioma therapy, understanding the mechanisms of ferroptosis and cuproptosis holds significant therapeutic potential. Future studies could investigate the underlying mechanisms behind the abnormal accumulation of iron and copper ions in glioma cells, which would involve developing novel therapeutic strategies targeting these metal ions to regulate apoptosis, as well as evaluating their clinical efficacy and safety.

The continuous advancement of artificial intelligence has led to the increasing utilization of deep learning in the diagnosis, grading, typing, and prognosis prediction of gliomas. Lei Jin et al. employed deep learning techniques on slide images and molecular markers stained with hematoxylin and eosin to classify gliomas, achieving an accuracy rate of 86.5% at the slide level and 87.5% at the patient level (167). In a separate investigation, Chenhua Luo et al. extracted 512 histopathological features from HE stained slides and constructed a deep learning model based on histological images to forecast glioma recurrence and patients' survival (168). Currently, there are four commonly used methods for detecting RCD: histopathological examination, immunohistochemical staining, Terminal deoxynucleotidyl transferase dUTP Nick End Labeling (TUNEL), and Annexin V/PI staining. Among these methods, one of the most prevalent approaches is to stain and microscopically observe biopsy or surgical excision tissue specimens in order to detect changes in cell morphology (169). In the future, the utilization of machine learning and deep learning algorithms to analyze vast medical image datasets, combined with artificial intelligence's capability to identify and extract features associated with RCD, may present a viable method for predicting glioma cell apoptosis. Integrating such a method into the diagnosis and prognosis of gliomas holds the potential to significantly improve treatment outcomes for glioma patients.

Over the years, the concept of RCD has been proposed and extensively studied. However, current research primarily focuses on analyzing and constructing clinical prediction models through bioinformatics, which has its limitations. Relying solely on large-scale data analysis and statistical methods for research may lead to data overfitting where the model becomes overly complex and fails to accurately fit new data. Furthermore, these models are constructed based on predetermined assumptions as well as patterns derived from existing data, which may potentially overlook other essential factors and underlying mechanisms. Moreover, observations and reasoning that solely rely on population statistics often disregard individual differences and heterogeneity, thereby impeding the adoption of precision therapy. Although bioinformatics tools along with predictive models offer great potential in medical research and clinical practice, it is vital to recognize their limitations. It is necessary to make efforts towards addressing these limitations while optimizing the utilization of such models. In future advancements within this field, emphasis should be placed on conducting large-scale clinical trials as well as practical applications to assess and refine both the validity and reliability of said predictive models.

Author contributions

ML: Conceptualization, Funding acquisition, Project administration, Writing – original draft, Writing – review & editing. XL: Writing – review & editing. CY: Writing – review & editing. XC: Writing – original draft, Writing – review & editing. SY: Writing – review & editing. YC: Writing – review & editing. JZ (7th Author): Writing – review & editing. JX: Writing – original draft, Writing – review & editing. QL: Funding acquisition, Writing – review & editing. LC: Funding acquisition, Writing – review & editing. SL: Funding acquisition, Resources, Writing – review & editing. WX: Funding acquisition, Resources, Writing – review & editing. JZ (13th Author): Writing – review & editing.

Funding

The author(s) declare financial support was received for the research, authorship, and/or publication of this article. This research was supported by National Natural Science Foundation of China (Grant No. 82072780), Sichuan Science and Technology Program (Grant No. 2022YFS0630), Sichuan medical youth innovation research project (Grant No. Q22044) Luzhou Science and Technology Program (2022-ZRK-184), Southwest Medical University Innovation and Entrepreneurship Training Program (Grant No.202210632054, S202210632192), and Panzhihua Medical Research Center Project (Grant No. PYYZ- 2023-02 and PYYZ-2023-04).

Conflict of interest

The authors declare that the research was conducted in the absence of any commercial or financial relationships that could be construed as a potential conflict of interest.

Publisher's note

References

1. Stupp R, Mason WP, van den Bent MJ, Weller M, Fisher B, Taphoorn MJ, et al. Radiotherapy plus concomitant and adjuvant temozolomide for glioblastoma. *N Engl J Med*. (2005) 352:987–96. doi: 10.1056/NEJMoa043330

2. Alexander BM, Cloughesy TF. Adult glioblastoma. *J Clin Oncol*. (2017) 35:2402–9. doi: 10.1200/JCO.2017.73.0119

3. Brandes AA, Tosoni A, Franceschi E, Reni M, Gatta G, Vecht C. Glioblastoma in adults. *Crit Rev Oncol Hematol*. (2008) 67:139–52. doi: 10.1016/j.critrevonc.2008.02.005

4. Kerr JF, Wyllie AH, Currie AR. Apoptosis: a basic biological phenomenon with wide-ranging implications in tissue kinetics. *Br J Cancer*. (1972) 26:239–57. doi: 10.1038/bjc.1972.33

5. Hengartner MO, Ellis RE, Horvitz HR. Caenorhabditis elegans gene ced-9 protects cells from programmed cell death. *Nature*. (1992) 356:494–9. doi: 10.1038/356494a0

6. Galluzzi L, Vitale I, Aaronson SA, Abrams JM, Adam D, Agostinis P, et al. Molecular mechanisms of cell death: recommendations of the Nomenclature Committee on Cell Death 2018. *Cell Death Differ*. (2018) 25:486–541. doi: 10.1038/s41418-017-0012-4

7. Tang D, Kang R, Berghe TV, Vandenabeele P, Kroemer G. The molecular machinery of regulated cell death. *Cell Res*. (2019) 29:347–64. doi: 10.1038/s41422-019-0164-5

8. Han L, Zhou J, Li L, Wu X, Shi Y, Cui W, et al. SLC1A5 enhances Malignant phenotypes through modulating ferroptosis status and immune microenvironment in glioma. *Cell Death Dis*. (2022) 13:1071. doi: 10.1038/s41419-022-05526-w

9. Tong S, Hong Y, Xu Y, Sun Q, Ye L, Cai J, et al. TFR2 regulates ferroptosis and enhances temozolomide chemo-sensitization in gliomas. *Exp Cell Res*. (2023) 424:113474. doi: 10.1016/j.yexcr.2023.113474

10. Tian YH, Jia LW, Liu ZF, Chen YH. LINC01087 inhibits glioma cell proliferation and migration, and increases cell apoptosis via miR-384/Bcl-2 axis. *Aging (Albany NY)*. (2021) 13:20808–19. doi: 10.18632/aging.v13i16

11. Feng J, Yao Z, Yang H, Ma J, Zhong X, Qin Y, et al. Bone marrow-derived mesenchymal stem cells expressing BMP2 suppress glioma stem cell growth and stemness through Bcl-2/Bax signaling. *J Cancer Res Ther*. (2022) 18:2033–40. doi: 10.4103/jcrt.jcrt_1983_21

12. Tang JH, Yang L, Chen JX, Li QR, Zhu LR, Xu QF, et al. Bortezomib inhibits growth and sensitizes glioma to temozolomide (TMZ) via down-regulating the FOXM1-Survivin axis. *Cancer Commun (Lond)*. (2019) 39:81. doi: 10.1186/s40880-019-0424-2

13. Gao H, Liu Z, Xu W, Wang Q, Zhang C, Ding Y, et al. Pterostilbene promotes mitochondrial apoptosis and inhibits proliferation in glioma cells. *Sci Rep*. (2021) 11:6381. doi: 10.1038/s41598-021-85908-w

14. Liu Y, Yaozu Z, Zhao H, Peng P, Tingbao Z, Jincao C. Inhibition of glioma cell growth and apoptosis induction through targeting wnt10B expression by pyrazolo[4,3-c]pyridine-4-one. *Med Sci Monit*. (2020) 26:e923912. doi: 10.12659/MSM.923912

15. Roberts AW, Davids MS, Pagel JM, Kahl BS, Puvvada SD, Gerecitano JF, et al. Targeting BCL2 with venetoclax in relapsed chronic lymphocytic leukemia. *N Engl J Med*. (2016) 374:311–22. doi: 10.1056/NEJMoa1513257

16. DiNardo CD, Jonas BA, Pullarkat V, Thirman MJ, Garcia JS, Wei AH, et al. Azacitidine and venetoclax in previously untreated acute myeloid leukemia. *N Engl J Med*. (2020) 383:617–29. doi: 10.1056/NEJMoa2012971

17. Fischer K, Al-Sawaf O, Bahlo J, Fink AM, Tandon M, Dixon M, et al. Venetoclax and obinutuzumab in patients with CLL and coexisting conditions. *N Engl J Med*. (2019) 380:2225–36. doi: 10.1056/NEJMoa1815281

18. Harrison SA, Goodman Z, Jabbar A, Vemulapalli R, Younes ZH, Freilich B, et al. A randomized, placebo-controlled trial of emricasan in patients with NASH and F1-F3 fibrosis. *J Hepatol*. (2020) 72:816–27. doi: 10.1016/j.jhep.2019.11.024

19. Garcia-Tsao G, Bosch J, Kayali Z, Harrison SA, Abdelmalek MF, Lawitz E, et al. Randomized placebo-controlled trial of emricasan for non-alcoholic steatohepatitis-related cirrhosis with severe portal hypertension. *J Hepatol*. (2020) 72:885–95. doi: 10.1016/j.jhep.2019.12.010

20. He J, Huang Z, He M, Liao J, Zhang Q, Wang S, et al. Circular RNA MAPK4 (circ-MAPK4) inhibits cell apoptosis via MAPK signaling pathway by sponging miR-125a-3p in gliomas. *Mol Cancer*. (2020) 19:17. doi: 10.1186/s12943-019-1120-1

21. Wan S, Zhang G, Liu R, Abbas MN, Cui H. Pyroptosis, ferroptosis, and autophagy cross-talk in glioblastoma opens up new avenues for glioblastoma treatment. *Cell Commun Signal*. (2023) 21:115. doi: 10.1186/s12964-023-01108-1

22. Levine B, Kroemer G. Biological functions of autophagy genes: A disease perspective. *Cell*. (2019) 176:11–42. doi: 10.1016/j.cell.2018.09.048

23. Klionsky DJ, Petroni G, Amaravadi RK, Baehrecke EH, Ballabio A, Boya P, et al. Autophagy in major human diseases. *EMBO J*. (2021) 40:e108863. doi: 10.15252/embj.2021108863

24. Raeisi M, Zehtabi M, Velaei K, Fayyazpour P, Aghaei N, Mehdizadeh A. Anoikis in cancer: The role of lipid signaling. *Cell Biol Int*. (2022) 46:1717–28. doi: 10.1002/cbin.11896

25. Tang D, Chen X, Kang R, Kroemer G. Ferroptosis: molecular mechanisms and health implications. *Cell Res*. (2021) 31:107–25. doi: 10.1038/s41422-020-00441-1

26. Chen X, Kang R, Kroemer G, Tang D. Broadening horizons: the role of ferroptosis in cancer. *Nat Rev Clin Oncol*. (2021) 18:280–96. doi: 10.1038/s41571-020-00462-0

27. Chen L, Min J, Wang F. Copper homeostasis and cuproptosis in health and disease. *Signal Transduct Target Ther*. (2022) 7:378. doi: 10.1038/s41392-022-01229-y

28. Denton D, Kumar S. Autophagy-dependent cell death. *Cell Death Differ*. (2019) 26:605–16. doi: 10.1038/s41418-018-0252-y

29. Taddei ML, Giannoni E, Fiaschi T, Chiarugi P. Anoikis: an emerging hallmark in health and diseases. *J Pathol*. (2012) 226:380–93. doi: 10.1002/path.3000

30. Dubyak GR, Miller BA, Pearlman E. Pyroptosis in neutrophils: Multimodal integration of inflammasome and regulated cell death signaling pathways. *Immunol Rev*. (2023) 314:229–49. doi: 10.1111/imr.13186

31. Kroemer G, Galassi C, Zitvogel L, Galluzzi L. Immunogenic cell stress and death. *Nat Immunol*. (2022) 23:487–500. doi: 10.1038/s41590-022-01132-2

32. Louis DN, Perry A, Wesseling P, Brat DJ, Cree IA, Figarella-Branger D, et al. The 2021 WHO classification of tumors of the central nervous system: a summary. *Neuro Oncol*. (2021) 23:1231–51. doi: 10.1093/neuonc/noab106

33. Xu S, Tang L, Li X, Fan F, Liu Z. Immunotherapy for glioma: Current management and future application. *Cancer Lett*. (2020) 476:1–12. doi: 10.1016/j.canlet.2020.02.002

34. Zou W. Immunosuppressive networks in the tumour environment and their therapeutic relevance. *Nat Rev Cancer*. (2005) 5:263–74. doi: 10.1038/nrc1586

35. Mohme M, Riethdorf S, Pantel K. Circulating and disseminated tumour cells - mechanisms of immune surveillance and escape. *Nat Rev Clin Oncol*. (2017) 14:155–67. doi: 10.1038/nrclinonc.2016.144

36. Curry RC, Dahiya S, Alva Venur V, Raizer JJ, Ahluwalia MS. Bevacizumab in high-grade gliomas: past, present, and future. *Expert Rev Anticancer Ther*. (2015) 15:387–97. doi: 10.1586/14737140.2015.1028376

37. Cloughesy TF, Mochizuki AY, Orpilla JR, Hugo W, Lee AH, Davidson TB, et al. Neoadjuvant anti-PD-1 immunotherapy promotes a survival benefit with intratumoral and systemic immune responses in recurrent glioblastoma. *Nat Med*. (2019) 25:477–86. doi: 10.1038/s41591-018-0337-7

38. Zhao J, Chen AX, Gartrell RD, Silverman AM, Aparicio L, Chu T, et al. Immune and genomic correlates of response to anti-PD-1 immunotherapy in glioblastoma. *Nat Med*. (2019) 25:462–9. doi: 10.1038/s41591-019-0349-y

39. Omuro A, Brandes AA, Carpentier AF, Idbaih A, Reardon DA, Cloughesy T, et al. Radiotherapy combined with nivolumab or temozolomide for newly diagnosed glioblastoma with unmethylated MGMT promoter: An international randomized phase III trial. *Neuro Oncol*. (2023) 25:123–34. doi: 10.1093/neuonc/noac099

40. Lang FF, Conrad C, Gomez-Manzano C, Yung WKA, Sawaya R, Weinberg JS, et al. Phase I study of DNX-2401 (Delta-24-RGD) oncolytic adenovirus: replication and immunotherapeutic effects in recurrent Malignant glioma. *J Clin Oncol*. (2018) 36:1419–27. doi: 10.1200/JCO.2017.75.8219

41. Liau LM, Ashkan K, Brem S, Campian JL, Trusheim JE, Iwamoto FM, et al. Association of autologous tumor lysate-loaded dendritic cell vaccination with extension of survival among patients with newly diagnosed and recurrent glioblastoma: A phase 3 prospective externally controlled cohort trial. *JAMA Oncol*. (2023) 9:112–21. doi: 10.1001/jamaoncol.2022.5370

42. Fridman WH, Teillaud JL. [From the time in the wilderness to the Nobel Prize in Physiology or Medicine awarded to James Allison and Tasuku Honjo: the Long March of cancer immunotherapy]. *Med Sci (Paris)*. (2019) 35:367–73. doi: 10.1051/medsci/2019074

43. Peng F, Liao M, Qin R, Zhu S, Peng C, Fu L, et al. Regulated cell death (RCD) in cancer: key pathways and targeted therapies. *Signal Transduct Target Ther*. (2022) 7:286. doi: 10.1038/s41392-022-01110-y

44. Klionsky DJ, Emr SD. Autophagy as a regulated pathway of cellular degradation. *Science*. (2000) 290:1717–21. doi: 10.1126/science.290.5497.1717

45. Tsukada M, Ohsumi Y. Isolation and characterization of autophagy-defective mutants of Saccharomyces cerevisiae. *FEBS Lett*. (1993) 333:169–74. doi: 10.1016/0014-5793(93)80398-E

46. Thumm M, Egner R, Koch B, Schlumpberger M, Straub M, Veenhuis M, et al. Isolation of autophagocytosis mutants of Saccharomyces cerevisiae. *FEBS Lett*. (1994) 349:275–80. doi: 10.1016/0014-5793(94)00672-5

47. Li X, He S, Ma B. Autophagy and autophagy-related proteins in cancer. *Mol Cancer*. (2020) 19:12. doi: 10.1186/s12943-020-1138-4

48. Klionsky DJ, Abdelmohsen K, Abe A, Abedin MJ, Abeliovich H, Acevedo Arozena A, et al. Guidelines for the use and interpretation of assays for monitoring autophagy (3rd edition). *Autophagy*. (2016) 12:1–222. doi: 10.1080/15548627.2015.1100356

49. Yang Z, Klionsky DJ. Eaten alive: a history of macroautophagy. *Nat Cell Biol*. (2010) 12:814–22. doi: 10.1038/ncb0910-814

50. Kang R, Tang D. Autophagy and ferroptosis - what's the connection? *Curr Pathobiol Rep*. (2017) 5:153–9. doi: 10.1007/s40139-017-0139-5

51. Hou W, Xie Y, Song X, Sun X, Lotze MT, Zeh HJ 3rd, et al. Autophagy promotes ferroptosis by degradation of ferritin. *Autophagy*. (2016) 12:1425–8. doi: 10.1080/15548627.2016.1187366

52. Gao M, Monian P, Pan Q, Zhang W, Xiang J, Jiang X. Ferroptosis is an autophagic cell death process. *Cell Res*. (2016) 26:1021–32. doi: 10.1038/cr.2016.95

53. Liu X, Zhao P, Wang X, Wang L, Zhu Y, Song Y, et al. Celastrol mediates autophagy and apoptosis via the ROS/JNK and Akt/mTOR signaling pathways in glioma cells. *J Exp Clin Cancer Res*. (2019) 38:184. doi: 10.1186/s13046-019-1173-4

54. Chu CW, Ko HJ, Chou CH, Cheng TS, Cheng HW, Liang YH, et al. Thioridazine enhances P62-mediated autophagy and apoptosis through wnt/β-catenin signaling pathway in glioma cells. *Int J Mol Sci*. (2019) 20:473. doi: 10.3390/ijms20030473

55. Zielke S, Meyer N, Mari M, Abou-El-Ardat K, Reggiori F, van Wijk SJL, et al. Loperamide, pimozide, and STF-62247 trigger autophagy-dependent cell death in glioblastoma cells. *Cell Death Dis*. (2018) 9:994. doi: 10.1038/s41419-018-1003-1

56. Chen Y, Li N, Wang H, Wang N, Peng H, Wang J, et al. Amentoflavone suppresses cell proliferation and induces cell death through triggering autophagy-dependent ferroptosis in human glioma. *Life Sci*. (2020) 247:117425. doi: 10.1016/j.lfs.2020.117425

57. Yu Y, Song Y, Cheng L, Chen L, Liu B, Lu D, et al. CircCEMIP promotes anoikis-resistance by enhancing protective autophagy in prostate cancer cells. *J Exp Clin Cancer Res*. (2022) 41:188. doi: 10.1186/s13046-022-02381-7

58. Wang YN, Zeng ZL, Lu J, Wang Y, Liu ZX, He MM, et al. CPT1A-mediated fatty acid oxidation promotes colorectal cancer cell metastasis by inhibiting anoikis. *Oncogene*. (2018) 37:6025–40. doi: 10.1038/s41388-018-0384-z

59. Ashrafizadeh M, Mohammadinejad R, Tavakol S, Ahmadi Z, Roomiani S, Katebi M. Autophagy, anoikis, ferroptosis, necroptosis, and endoplasmic reticulum stress: Potential applications in melanoma therapy. *J Cell Physiol*. (2019) 234:19471–9. doi: 10.1002/jcp.28740

60. Sun Z, Zhao Y, Wei Y, Ding X, Tan C, Wang C. Identification and validation of an anoikis-associated gene signature to predict clinical character, stemness, IDH mutation, and immune filtration in glioblastoma. *Front Immunol*. (2022) 13:939523. doi: 10.3389/fimmu.2022.939523

61. Zhang D, Wang Y, Zhou H, Han X, Hou L, Lv Z, et al. The study of an anoikis-related signature to predict glioma prognosis and immune infiltration. *J Cancer Res Clin Oncol*. (2023) 149:12659–76. doi: 10.1007/s00432-023-05138-7

62. Dai W, Tian C, Jin S. Effect of lncRNA ANRIL silencing on anoikis and cell cycle in human glioma via microRNA-203a. *Onco Targets Ther*. (2018) 11:5103–9. doi: 10.2147/OTT

63. Jiang L, Chen S, Zhao D, Yan J, Chen J, Yang C, et al. MNX1 reduces sensitivity to anoikis by activating TrkB in human glioma cells. *Mol Med Rep*. (2018) 18:3271–9. doi: 10.3892/mmr

64. Dixon SJ, Lemberg KM, Lamprecht MR, Skouta R, Zaitsev EM, Gleason CE, et al. Ferroptosis: an iron-dependent form of nonapoptotic cell death. *Cell*. (2012) 149:1060–72. doi: 10.1016/j.cell.2012.03.042

65. Mahoney-Sánchez L, Bouchaoui H, Ayton S, Devos D, Duce JA, Devedjian JC. Ferroptosis and its potential role in the physiopathology of Parkinson's Disease. *Prog Neurobiol*. (2021) 196:101890. doi: 10.1038/s41418-021-00785-0

66. Ma H, Dong Y, Chu Y, Guo Y, Li L. The mechanisms of ferroptosis and its role in alzheimer's disease. *Front Mol Biosci*. (2022) 9:965064. doi: 10.3389/fmolb.2022.965064

67. Fang X, Ardehali H, Min J, Wang F. The molecular and metabolic landscape of iron and ferroptosis in cardiovascular disease. *Nat Rev Cardiol*. (2023) 20:7–23. doi: 10.1038/s41569-022-00735-4

68. Yu Y, Jiang L, Wang H, Shen Z, Cheng Q, Zhang P, et al. Hepatic transferrin plays a role in systemic iron homeostasis and liver ferroptosis. *Blood*. (2020) 136:726–39. doi: 10.1182/blood.2019002907

69. Lu M, Zhou Y, Sun L, Shafi S, Ahmad N, Sun M, et al. The molecular mechanisms of ferroptosis and its role in glioma progression and treatment. *Front Oncol*. (2022) 12:917537. doi: 10.3389/fonc.2022.917537

70. Luo Y, Tian G, Fang X, Bai S, Yuan G, Pan Y. Ferroptosis and its potential role in glioma: from molecular mechanisms to therapeutic opportunities. *Antioxidants (Basel)*. (2022) 11:2123. doi: 10.3390/antiox11112123

71. Zlotos DP, Mandour YM, Jensen AA. Strychnine and its mono- and dimeric analogues: a pharmaco-chemical perspective. *Nat Prod Rep*. (2022) 39:1910–37. doi: 10.1039/D1NP00079A

72. Lu S, Wang XZ, He C, Wang L, Liang SP, Wang CC, et al. ATF3 contributes to brucine-triggered glioma cell ferroptosis via promotion of hydrogen peroxide and iron. *Acta Pharmacol Sin*. (2021) 42:1690–702. doi: 10.1038/s41401-021-00700-w

73. Li K, Chen B, Xu A, Shen J, Li K, Hao K, et al. TRIM7 modulates NCOA4-mediated ferritinophagy and ferroptosis in glioblastoma cells. *Redox Biol*. (2022) 56:102451. doi: 10.1016/j.redox.2022.102451

74. Liu T, Zhu C, Chen X, Guan G, Zou C, Shen S, et al. Ferroptosis, as the most enriched programmed cell death process in glioma, induces immunosuppression and immunotherapy resistance. *Neuro Oncol*. (2022) 24:1113–25. doi: 10.1093/neuonc/noac033

75. Zhan S, Lu L, Pan SS, Wei XQ, Miao RR, Liu XH, et al. Targeting NQO1/GPX4-mediated ferroptosis by plumbagin suppresses in *vitro* and in *vivo* glioma growth. *Br J Cancer*. (2022) 127:364–76. doi: 10.1038/s41416-022-01800-y

76. Wang Y, Zhang L, Zhou F. Cuproptosis: a new form of programmed cell death. *Cell Mol Immunol*. (2022) 19:867–8. doi: 10.1038/s41423-022-00866-1

77. Tsvetkov P, Coy S, Petrova B, Dreishpoon M, Verma A, Abdusamad M, et al. Copper induces cell death by targeting lipoylated TCA cycle proteins. *Science*. (2022) 375:1254–61. doi: 10.1126/science.abf0529

78. Chen B, Zhou X, Yang L, Zhou H, Meng M, Zhang L, et al. A Cuproptosis Activation Scoring model predicts neoplasm-immunity interactions and personalized treatments in glioma. *Comput Biol Med*. (2022) 148:105924. doi: 10.1016/j.compbiomed.2022.105924

79. Wang L, Li Y, Wang Y, Li J, Sun Y, Chen J, et al. Identification of cuproptosis-related lncRNAs for prognosis and immunotherapy in glioma. *J Cell Mol Med*. (2022) 26:5820–31. doi: 10.1111/jcmm.17603

80. Lu H, Zhou L, Zhang B, Xie Y, Yang H, Wang Z. Cuproptosis key gene FDX1 is a prognostic biomarker and associated with immune infiltration in glioma. *Front Med (Lausanne)*. (2022) 9:939776. doi: 10.3389/fmed.2022.939776

81. Guowei L, Xiufang L, Qianqian X, Yanping J. The FDX1 methylation regulatory mechanism in the Malignant phenotype of glioma. *Genomics*. (2023) 115:110601. doi: 10.1016/j.ygeno.2023.110601

82. Al Mamun A, Mimi AA, Aziz MA, Zaeem M, Ahmed T, Munir F, et al. Role of pyroptosis in cancer and its therapeutic regulation. *Eur J Pharmacol*. (2021) 910:174444. doi: 10.1016/j.ejphar.2021.174444

83. Tanzhu G, Li N, Li Z, Zhou R, Shen L. Molecular subtypes and prognostic signature of pyroptosis-related lncRNAs in glioma patients. *Front Oncol*. (2022) 12:779168. doi: 10.3389/fonc.2022.779168

84. Liu H, Tao T. Prognosis and immune features of pyroptosis-related RNA patterns in low-grade glioma. *Front Oncol*. (2022) 12:1015850. doi: 10.3389/fonc.2022.1015850

85. Guo K, Zhao J, Jin Q, Yan H, Shi Y, Zhao Z. CASP6 predicts poor prognosis in glioma and correlates with tumor immune microenvironment. *Front Oncol*. (2022) 12:818283. doi: 10.3389/fonc.2022.818283

86. Xiu Z, Sun T, Yang Y, He Y, Yang S, Xue X, et al. Curcumin enhanced ionizing radiation-induced immunogenic cell death in glioma cells through endoplasmic reticulum stress signaling pathways. *Oxid Med Cell Longev*. (2022) 2022:5424411. doi: 10.1155/2022/5424411

87. Cui J, Xu H, Shi J, Fang K, Liu J, Liu F, et al. Carbonic anhydrase IX inhibitor S4 triggers release of DAMPs related to immunogenic cell death in glioma cells via endoplasmic reticulum stress pathway. *Cell Commun Signal*. (2023) 21:167. doi: 10.1186/s12964-023-01180-7

88. Hou C, Shi S, Gao M, Ji J, Ma C, Wang T, et al. Targeting TNFAIP2 induces immunogenic cell death and sensitizes glioblastoma multiforme to anti-PD-1 therapy. *J Neurooncol*. (2023) 165:79–90. doi: 10.1007/s11060-023-04449-6

89. Cai J, Hu Y, Ye Z, Ye L, Gao L, Wang Y, et al. Immunogenic cell death-related risk signature predicts prognosis and characterizes the tumour microenvironment in lower-grade glioma. *Front Immunol*. (2022) 13:1011757. doi: 10.3389/fimmu.2022.1011757

90. Sun Z, Jiang H, Yan T, Deng G, Chen Q. Identification of immunogenic cell death-related signature for glioma to predict survival and response to immunotherapy. *Cancers (Basel)*. (2022) 14:5665. doi: 10.3390/cancers14225665

91. Kashyap D, Garg VK, Goel N. Intrinsic and extrinsic pathways of apoptosis: Role in cancer development and prognosis. *Adv Protein Chem Struct Biol*. (2021) 125:73–120. doi: 10.1016/bs.apcsb.2021.01.003

92. Panada J, Klopava V, Kulahava T, Koran S, Faletrov Y, Frolova N, et al. Differential induction of C6 glioma apoptosis and autophagy by 3β-hydroxysteroid-indolamine conjugates. *Steroids*. (2023) 200:109326. doi: 10.1016/j.steroids.2023.109326

93. Martens S, Bridelance J, Roelandt R, Vandenabeele P, Takahashi N. MLKL in cancer: more than a necroptosis regulator. *Cell Death Differ*. (2021) 28:1757–72. doi: 10.1038/s41418-021-00785-0

94. Sun L, Wang H, Wang Z, He S, Chen S, Liao D, et al. Mixed lineage kinase domain-like protein mediates necrosis signaling downstream of RIP3 kinase. *Cell*. (2012) 148:213–27. doi: 10.1016/j.cell.2011.11.031

95. Zhang CC, Li CG, Wang YF, Xu LH, He XH, Zeng QZ, et al. Chemotherapeutic paclitaxel and cisplatin differentially induce pyroptosis in A549 lung cancer cells via caspase-3/GSDME activation. *Apoptosis*. (2019) 24:312–25. doi: 10.1007/s10495-019-01515-1

96. Erkes DA, Cai W, Sanchez IM, Purwin TJ, Rogers C, Field CO, et al. Mutant BRAF and MEK inhibitors regulate the tumor immune microenvironment via pyroptosis. *Cancer Discovery*. (2020) 10:254–69. doi: 10.1158/2159-8290.CD-19-0672

97. Zheng M, Kanneganti TD. The regulation of the ZBP1-NLRP3 inflammasome and its implications in pyroptosis, apoptosis, and necroptosis (PANoptosis). *Immunol Rev*. (2020) 297:26–38. doi: 10.1111/imr.12909

98. Wang H, Guo M, Wei H, Chen Y. Targeting p53 pathways: mechanisms, structures, and advances in therapy. *Signal Transduct Target Ther*. (2023) 8:92. doi: 10.1038/s41392-023-01347-1

99. Rochette L, Dogon G, Rigal E, Zeller M, Cottin Y, Vergely C. Lipid peroxidation and iron metabolism: two corner stones in the homeostasis control of ferroptosis. *Int J Mol Sci*. (2022) 24:449. doi: 10.3390/ijms24010449

100. Yan Z, Qi W, Zhan J, Lin Z, Lin J, Xue X, et al. Activating Nrf2 signalling alleviates osteoarthritis development by inhibiting inflammasome activation. *J Cell Mol Med*. (2020) 24:13046–57. doi: 10.1111/jcmm.15905

101. Ahmed SM, Luo L, Namani A, Wang XJ, Tang X. Nrf2 signaling pathway: Pivotal roles in inflammation. *Biochim Biophys Acta Mol Basis Dis*. (2017) 1863:585–97. doi: 10.1016/j.bbadis.2016.11.005

102. Laplante M, Sabatini DM. mTOR signaling in growth control and disease. *Cell*. (2012) 149:274–93. doi: 10.1016/j.cell.2012.03.017

103. Bryant KL, Stalnecker CA, Zeitouni D, Klomp JE, Peng S, Tikunov AP, et al. Combination of ERK and autophagy inhibition as a treatment approach for pancreatic cancer. *Nat Med*. (2019) 25:628–40. doi: 10.1038/s41591-019-0368-8

104. Rosenfeld MR, Ye X, Supko JG, Desideri S, Grossman SA, Brem S, et al. A phase I/II trial of hydroxychloroquine in conjunction with radiation therapy and concurrent and adjuvant temozolomide in patients with newly diagnosed glioblastoma multiforme. *Autophagy*. (2014) 10:1359–68. doi: 10.4161/auto.28984

105. Zhou W, Wang H, Yang Y, Chen ZS, Zou C, Zhang J. Chloroquine against malaria, cancers and viral diseases. *Drug Discovery Today*. (2020) 25:2012–22. doi: 10.1016/j.drudis.2020.09.010

106. Koch MW, Kaur S, Sage K, Kim J, Levesque-Roy M, Cerchiaro G, et al. Hydroxychloroquine for primary progressive multiple sclerosis. *Ann Neurol*. (2021) 90:940–8. doi: 10.1002/ana.26239

107. Zhang J, Lu X, Feng J, Li H, Wang S. Effects of hydroxychloroquine on proteinuria in igA nephropathy: A systematic review and meta-analysis. *BioMed Res Int*. (2021) 2021:9171715. doi: 10.1155/2021/9171715

108. Gautret P, Lagier JC, Parola P, Hoang VT, Meddeb L, Mailhe M, et al. Hydroxychloroquine and azithromycin as a treatment of COVID-19: results of an open-label non-randomized clinical trial. *Int J Antimicrob Agents*. (2020) 56:105949. doi: 10.1016/j.ijantimicag.2020.105949

109. Compter I, Eekers DBP, Hoeben A, Rouschop KMA, Reymen B, Ackermans L, et al. Chloroquine combined with concurrent radiotherapy and temozolomide for newly diagnosed glioblastoma: a phase IB trial. *Autophagy*. (2021) 17:2604–12. doi: 10.1080/15548627.2020.1816343

110. Xu B, Huo Z, Huang H, Ji W, Bian Z, Jiao J, et al. The expression and prognostic value of the epidermal growth factor receptor family in glioma. *BMC Cancer*. (2021) 21:451. doi: 10.1186/s12885-021-08150-7

111. Scott KA, Dalgleish AG, Liu WM. The combination of cannabidiol and Δ9-tetrahydrocannabinol enhances the anticancer effects of radiation in an orthotopic murine glioma model. *Mol Cancer Ther*. (2014) 13:2955–67. doi: 10.1158/1535-7163.MCT-14-0402

112. Lopez J, Lai-Kwon J, Molife R, Welsh L, Tunariu N, Roda D, et al. A Phase 1/2A trial of idroxioleic acid: first-in-class sphingolipid regulator and glioma cell autophagy inducer with antitumor activity in refractory glioma. *Br J Cancer*. (2023) 129:811–8. doi: 10.1038/s41416-023-02356-1

113. Hwang S, Maloney NS, Bruinsma MW, Goel G, Duan E, Zhang L, et al. Nondegradative role of Atg5-Atg12/Atg16L1 autophagy protein complex in antiviral activity of interferon gamma. *Cell Host Microbe*. (2012) 11:397–409. doi: 10.1016/j.chom.2012.03.002

114. Hamaoui D, Subtil A. ATG16L1 functions in cell homeostasis beyond autophagy. *FEBS J*. (2022) 289:1779–800. doi: 10.1111/febs.15833

115. Chen J, Liang Y, Hu S, Jiang J, Zeng M, Luo M. Role of ATG7-dependent non-autophagic pathway in angiogenesis. *Front Pharmacol*. (2023) 14:1266311. doi: 10.3389/fphar.2023.1266311

116. Fleischmann DF, Schön R, Corradini S, Bodensohn R, Hadi I, Hofmaier J, et al. Multifocal high-grade glioma radiotherapy safety and efficacy. *Radiat Oncol*. (2021) 16:165. doi: 10.1186/s13014-021-01886-3

117. Kyjacova L, Hubackova S, Krejcikova K, Strauss R, Hanzlikova H, Dzijak R, et al. Radiotherapy-induced plasticity of prostate cancer mobilizes stem-like non-adherent, Erk signaling-dependent cells. *Cell Death Differ*. (2015) 22:898–911. doi: 10.1038/cdd.2014.97

118. da SSR, de SLT, da Silva CT, Gonçalves JD, Lerario AM, Marie SKN, et al. Cellular model of Malignant transformation of primary human astrocytes induced by deadhesion/readhesion cycles. *Int J Mol Sci*. (2022) 23:4471. doi: 10.3390/ijms23094471

119. Zhao S, Chi H, Ji W, He Q, Lai G, Peng G, et al. A bioinformatics-based analysis of an anoikis-related gene signature predicts the prognosis of patients with low-grade gliomas. *Brain Sci*. (2022) 12:1349. doi: 10.3390/brainsci12101349

120. Viswanathan VS, Ryan MJ, Dhruv HD, Gill S, Eichhoff OM, Seashore-Ludlow B, et al. Dependency of a therapy-resistant state of cancer cells on a lipid peroxidase pathway. *Nature*. (2017) 547:453–7. doi: 10.1038/nature23007

121. Zhang C, Liu X, Jin S, Chen Y, Guo R. Ferroptosis in cancer therapy: a novel approach to reversing drug resistance. *Mol Cancer*. (2022) 21:47. doi: 10.1186/s12943-022-01530-y

122. Su Y, Zhao B, Zhou L, Zhang Z, Shen Y, Lv H, et al. Ferroptosis, a novel pharmacological mechanism of anti-cancer drugs. *Cancer Lett*. (2020) 483:127–36. doi: 10.1016/j.canlet.2020.02.015

123. Yang Y, Tian Q, Wu S, Li Y, Yang K, Yan Y, et al. Blue light-triggered Fe(2+)-release from monodispersed ferrihydrite nanoparticles for cancer iron therapy. *Biomaterials*. (2021) 271:120739. doi: 10.1016/j.biomaterials.2021.120739

124. Zhuo S, Chen Z, Yang Y, Zhang J, Tang J, Yang K. Clinical and biological significances of a ferroptosis-related gene signature in glioma. *Front Oncol*. (2020) 10:590861. doi: 10.3389/fonc.2020.590861

125. Wan RJ, Peng W, Xia QX, Zhou HH, Mao XY. Ferroptosis-related gene signature predicts prognosis and immunotherapy in glioma. *CNS Neurosci Ther*. (2021) 27:973–86. doi: 10.1111/cns.13654

126. Wang F, Lin H, Su Q, Li C. Cuproptosis-related lncRNA predict prognosis and immune response of lung adenocarcinoma. *World J Surg Oncol*. (2022) 20:275. doi: 10.1186/s12957-022-02727-7

127. Zou Y, Xie J, Zheng S, Liu W, Tang Y, Tian W, et al. Leveraging diverse cell-death patterns to predict the prognosis and drug sensitivity of triple-negative breast cancer patients after surgery. *Int J Surg*. (2022) 107:106936. doi: 10.1016/j.ijsu.2022.106936

128. Zhao C, Yu D, He Z, Bao L, Feng L, Chen L, et al. Endoplasmic reticulum stress-mediated autophagy activation is involved in cadmium-induced ferroptosis of renal tubular epithelial cells. *Free Radic Biol Med*. (2021) 175:236–48. doi: 10.1016/j.freeradbiomed.2021.09.008

129. Li X, Abdel-Moneim AE, Yang B. Signaling pathways and genes associated with hexavalent chromium-induced hepatotoxicity. *Biol Trace Elem Res*. (2023) 201:1888–904. doi: 10.1007/s12011-022-03291-7

130. Leussink BT, Nagelkerke JF, van de Water B, Slikkerveer A, van der Voet GB, Srinivasan A, et al. Pathways of proximal tubular cell death in bismuth nephrotoxicity. *Toxicol Appl Pharmacol*. (2002) 180:100–9. doi: 10.1006/taap.2002.9379

131. Tyagi A, Chandrasekaran B, Navin AK, Shukla V, Baby BV, Ankem MK, et al. Molecular interplay between NOX1 and autophagy in cadmium-induced prostate carcinogenesis. *Free Radic Biol Med*. (2023) 199:44–55. doi: 10.1016/j.freeradbiomed.2023.02.007

132. Gravina AG, Priadko K, Granata L, Facchiano A, Scidà G, Cerbone R, et al. Single capsule bismuth quadruple therapy for eradication of H. pylori infection: A real-life study. *Front Pharmacol*. (2021) 12:667584. doi: 10.3389/fphar.2021.667584

133. Rao Z, Zhu Y, Yang P, Chen Z, Xia Y, Qiao C, et al. Pyroptosis in inflammatory diseases and cancer. *Theranostics*. (2022) 12:4310–29. doi: 10.7150/thno.71086

134. Ren LW, Li W, Zheng XJ, Liu JY, Yang YH, Li S, et al. Benzimidazoles induce concurrent apoptosis and pyroptosis of human glioblastoma cells via arresting cell cycle. *Acta Pharmacol Sin*. (2022) 43:194–208. doi: 10.1038/s41401-021-00752-y

135. Zhao W, Zhang L, Zhang Y, Jiang Z, Lu H, Xie Y, et al. The CDK inhibitor AT7519 inhibits human glioblastoma cell growth by inducing apoptosis, pyroptosis and cell cycle arrest. *Cell Death Dis*. (2023) 14:11. doi: 10.1038/s41419-022-05528-8

136. Tang N, Zhu Y, Yu J. Xihuang pill facilitates glioma cell pyroptosis via the POU4F1/STAT3 axis. *Funct Integr Genomics*. (2023) 23:334. doi: 10.1007/s10142-023-01263-1

137. Moserova I, Truxova I, Garg AD, Tomala J, Agostinis P, Cartron PF, et al. Caspase-2 and oxidative stress underlie the immunogenic potential of high hydrostatic pressure-induced cancer cell death. *Oncoimmunology*. (2017) 6:e1258505. doi: 10.1080/2162402X.2016.1258505

138. Buytaert E, Callewaert G, Hendrickx N, Scorrano L, Hartmann D, Missiaen L, et al. Role of endoplasmic reticulum depletion and multidomain proapoptotic BAX and BAK proteins in shaping cell death after hypericin-mediated photodynamic therapy. *FASEB J*. (2006) 20:756–8. doi: 10.1096/fj.05-4305fje

139. Dewaele M, Martinet W, Rubio N, Verfaillie T, de Witte PA, Piette J, et al. Autophagy pathways activated in response to PDT contribute to cell resistance against ROS damage. *J Cell Mol Med*. (2011) 15:1402–14. doi: 10.1111/j.1582-4934.2010.01118.x

140. Wang F, Xu L, Wen B, Song S, Zhou Y, Wu H, et al. Ultrasound-excited temozolomide sonosensitization induces necroptosis in glioblastoma. *Cancer Lett*. (2023) 554:216033. doi: 10.1016/j.canlet.2022.216033

141. Zhou Y, Jiao J, Yang R, Wen B, Wu Q, Xu L, et al. Temozolomide-based sonodynamic therapy induces immunogenic cell death in glioma. *Clin Immunol*. (2023) 256:109772. doi: 10.1016/j.clim.2023.109772

142. Koks CA, Garg AD, Ehrhardt M, Riva M, Vandenberk L, Boon L, et al. Newcastle disease virotherapy induces long-term survival and tumor-specific immune memory in orthotopic glioma through the induction of immunogenic cell death. *Int J Cancer*. (2015) 136:E313–25. doi: 10.1002/ijc.29202

143. Kepp O, Zitvogel L, Kroemer G. Lurbinectedin: an FDA-approved inducer of immunogenic cell death for the treatment of small-cell lung cancer. *Oncoimmunology*. (2020) 9:1795995. doi: 10.1080/2162402X.2020.1795995

144. Xie W, Forveille S, Iribarren K, Sauvat A, Senovilla L, Wang Y, et al. Lurbinectedin synergizes with immune checkpoint blockade to generate anticancer immunity. *Oncoimmunology*. (2019) 8:e1656502. doi: 10.1080/2162402X.2019.1656502

145. Montes de Oca R, Alavi AS, Vitali N, Bhattacharya S, Blackwell C, Patel K, et al. Belantamab mafodotin (GSK2857916) drives immunogenic cell death and immune-mediated antitumor responses in vivo. *Mol Cancer Ther*. (2021) 20:1941–55. doi: 10.1158/1535-7163.MCT-21-0035

146. Galluzzi L, Blomgren K, Kroemer G. Mitochondrial membrane permeabilization in neuronal injury. *Nat Rev Neurosci*. (2009) 10:481–94. doi: 10.1038/nrn2665

147. Lee Y, Karuppagounder SS, Shin JH, Lee YI, Ko HS, Swing D, et al. Parthanatos mediates AIMP2-activated age-dependent dopaminergic neuronal loss. *Nat Neurosci*. (2013) 16:1392–400. doi: 10.1038/nn.3500

148. Liu Y, Shoji-Kawata S, Sumpter RM Jr., Wei Y, Ginet V, Zhang L, et al. Autosis is a Na+,K+-ATPase-regulated form of cell death triggered by autophagy-inducing peptides, starvation, and hypoxia-ischemia. *Proc Natl Acad Sci U.S.A*. (2013) 110:20364–71. doi: 10.1073/pnas.1319661110

149. Koren E, Fuchs Y. Modes of regulated cell death in cancer. *Cancer Discovery*. (2021) 11:245–65. doi: 10.1158/2159-8290.CD-20-0789

150. Galluzzi L, Bravo-San Pedro JM, Kepp O, Kroemer G. Regulated cell death and adaptive stress responses. *Cell Mol Life Sci*. (2016) 73:2405–10. doi: 10.1007/s00018-016-2209-y

151. Meyer N, Henkel L, Linder B, Zielke S, Tascher G, Trautmann S, et al. Autophagy activation, lipotoxicity and lysosomal membrane permeabilization synergize to promote pimozide- and loperamide-induced glioma cell death. *Autophagy*. (2021) 17:3424–43. doi: 10.1080/15548627.2021.1874208

152. Battaglia AM, Chirillo R, Aversa I, Sacco A, Costanzo F, Biamonte F. Ferroptosis and cancer: mitochondria meet the "Iron maiden" Cell death. *Cells*. (2020) 9:1505. doi: 10.3390/cells9061505

153. Baskar R, Lee KA, Yeo R, Yeoh KW. Cancer and radiation therapy: current advances and future directions. *Int J Med Sci*. (2012) 9:193–9. doi: 10.7150/ijms.3635

154. Rodríguez-Ruiz ME, Vanpouille-Box C, Melero I, Formenti SC, Demaria S. Immunological mechanisms responsible for radiation-induced abscopal effect. *Trends Immunol*. (2018) 39:644–55. doi: 10.1016/j.it.2018.06.001

155. Kuwahara Y, Tomita K, Urushihara Y, Sato T, Kurimasa A, Fukumoto M. Association between radiation-induced cell death and clinically relevant radioresistance. *Histochem Cell Biol*. (2018) 150:649–59. doi: 10.1007/s00418-018-1728-z

156. Chiang IT, Liu YC, Liu HS, Ali AAA, Chou SY, Hsu TI, et al. Regorafenib reverses temozolomide-induced CXCL12/CXCR4 signaling and triggers apoptosis mechanism in glioblastoma. *Neurotherapeutics*. (2022) 19:616–34. doi: 10.1007/s13311-022-01194-y

157. Song X, Zhu S, Chen P, Hou W, Wen Q, Liu J, et al. AMPK-mediated BECN1 phosphorylation promotes ferroptosis by directly blocking system X(c)(-) activity. *Curr Biol*. (2018) 28:2388–2399.e5. doi: 10.1016/j.cub.2018.05.094

158. Hu X, He Y, Han Z, Liu W, Liu D, Zhang X, et al. PNO1 inhibits autophagy-mediated ferroptosis by GSH metabolic reprogramming in hepatocellular carcinoma. *Cell Death Dis*. (2022) 13:1010. doi: 10.1038/s41419-022-05448-7

159. Xue Q, Yan D, Chen X, Li X, Kang R, Klionsky DJ, et al. Copper-dependent autophagic degradation of GPX4 drives ferroptosis. *Autophagy*. (2023) 19:1982–96. doi: 10.1080/15548627.2023.2165323

160. Lin HY, Lin YS, Shih SP, Lee SB, El-Shazly M, Chang KM, et al. The Anti-Proliferative Activity of Secondary Metabolite from the Marine Streptomyces sp. against Prostate Cancer Cells. *Life (Basel)*. (2021) 11:1414. doi: 10.3390/life11121414

161. Lin R, Zhang Z, Chen L, Zhou Y, Zou P, Feng C, et al. Dihydroartemisinin (DHA) induces ferroptosis and causes cell cycle arrest in head and neck carcinoma cells. *Cancer Lett*. (2016) 381:165–75. doi: 10.1016/j.canlet.2016.07.033

162. Basit F, van Oppen LM, Schöckel L, Bossenbroek HM, van Emst-de Vries SE, Hermeling JC, et al. Mitochondrial complex I inhibition triggers a mitophagy-dependent ROS increase leading to necroptosis and ferroptosis in melanoma cells. *Cell Death Dis*. (2017) 8:e2716. doi: 10.1038/cddis.2017.133

163. Zhang R, Chen J, Mao L, Guo Y, Hao Y, Deng Y, et al. Nobiletin triggers reactive oxygen species-mediated pyroptosis through regulating autophagy in ovarian cancer cells. *J Agric Food Chem*. (2020) 68:1326–36. doi: 10.1021/acs.jafc.9b07908

164. Lee SH, Lee YJ. Synergistic anticancer activity of resveratrol in combination with docetaxel in prostate carcinoma cells. *Nutr Res Pract*. (2021) 15:12–25. doi: 10.4162/nrp.2021.15.1.12

165. Liu JH, Yang Y, Song Q, Li JB. MicroRNA-155regulates the proliferation and metastasis of human breast cancers by targeting MAPK7. *J buon*. (2019) 24:1075–80.

166. Liu Y, Wang X, Zhu W, Sui Z, Wei X, Zhang Y, et al. TRPML1-induced autophagy inhibition triggers mitochondrial mediated apoptosis. *Cancer Lett*. (2022) 541:215752. doi: 10.1016/j.canlet.2022.215752

167. Jin L, Shi F, Chun Q, Chen H, Ma Y, Wu S, et al. Artificial intelligence neuropathologist for glioma classification using deep learning on hematoxylin and eosin stained slide images and molecular markers. *Neuro Oncol*. (2021) 23:44–52. doi: 10.1093/neuonc/noaa163

168. Luo C, Yang J, Liu Z, Jing D. Predicting the recurrence and overall survival of patients with glioma based on histopathological images using deep learning. *Front Neurol*. (2023) 14:1100933. doi: 10.3389/fneur.2023.1100933

169. Obeng E. Apoptosis (programmed cell death) and its signals - A review. *Braz J Biol*. (2021) 81:1133–43. doi: 10.1590/1519-6984.228437

frontiers | Frontiers in Oncology

TYPE Case Report
PUBLISHED 19 September 2024
DOI 10.3389/fonc.2024.1444172

OPEN ACCESS

EDITED BY
Jun Yang,
Capital Medical University, China

REVIEWED BY
Valeria Nele,
University of Naples Federico II, Italy
Yu Hao,
First Hospital, Peking University, China
Weihai Ning,
Capital Medical University, China
Rajen Dey,
Swami Vivekananda University, India

*CORRESPONDENCE
Wenjing Zong
caoyeying.student@sina.com
Zhongdong Li
zhdl009@126.com

†These authors have contributed equally to this work

RECEIVED 05 June 2024
ACCEPTED 03 September 2024
PUBLISHED 19 September 2024

CITATION
Yuan M, Zong M, Ren C, Zong W and Li Z (2024) Ceftazidime/avibactam combined with colistimethate sodium successfully cures carbapenem-resistant *Pseudomonas aeruginosa*-induced brain abscess in a child post-craniotomy: a case report.
Front. Oncol. 14:1444172.
doi: 10.3389/fonc.2024.1444172

Ceftazidime/avibactam combined with colistimethate sodium successfully cures carbapenem-resistant *Pseudomonas aeruginosa*-induced brain abscess in a child post-craniotomy: a case report

Minglu Yuan[1], Miao Zong[2], Cong Ren[2], Wenjing Zong[3*†] and Zhongdong Li[1*†]

[1]Department of Pharmacy, Beijing Electric Power Hospital of State Grid Co. of China, Capital Medical University Electric Teaching Hospital, Beijing, China, [2]Department of Neurosurgery, Beijing Electric Power Hospital of State Grid Co. of China, Capital Medical University Electric Teaching Hospital, Beijing, China, [3]Institute of Chinese Materia Medica, China Academy of Chinese Medical Sciences, Beijing, China

The treatment of brain abscess induced by carbapenem-resistant *Pseudomonas aeruginosa* (CRPA) is a clinical challenge around the world. Apart from novel β-lactam/β-lactamase inhibitors and polymyxins, there are few sufficiently powerful antibiotics that are effective against CRPA-induced infections. Considering the blood-brain barrier factor, there are even fewer drugs that can be used to treat intracranial CRPA-induced infections. In this article, we reported a case of CRPA-induced brain abscess that was successfully treated with intravenous ceftazidime/avibactam and intrathecal colistimethate sodium in a child after intracranial tumor resection.

KEYWORDS

brain abscess, central nervous system infections, carbapenem-resistant pseudomonas aeruginosa, ceftazidime/avibactam, colistimethate sodium

1 Introduction

Brain abscess is a serious postoperative complication after neurosurgical craniectomy, which usually leads to prolonged hospitalization and higher mortality rates. Although the incidence is only 0.17% (1), once a brain abscess has formed, more than 60% of patients need secondary craniectomy due to the limited availability of effective antibiotics (2). Brain abscesses are mainly caused by Gram-positive cocci, but 20% are due to Gram-negative

bacilli (2, 3). *Pseudomonas aeruginosa* (PA), which is highly virulent and invasive, is one such Gram-negative bacillus. The risk factors for PA-induced central nervous system infections (CNSI) include craniocerebral trauma, otorhinolaryngology-head and neck surgery, cerebrospinal fluid (CSF) leakage or ventricular drainage, implantation of invasive catheter, spreading of ear or sinus infections, immune deficiency, and chemotherapy. If CNSI is caused by CRPA, clinical treatment is extremely difficult.

Traditional antibiotics with anti-PA activity include piperacillin/tazobactam, cefoperazone/sulbactam, ceftazidime, aztreonam, quinolones (ciprofloxacin, levofloxacin), aminoglycosides (gentamicin, amikacin), and carbapenems (meropenem, imipenem). If CRPA is susceptible to these conventional antibiotics, it should be treated with them in the first instance. However, if these drugs do not effectively control the CRPA-induced infection or the infection is severe, a novel β-lactam/β-lactamase inhibitor can be used, such as ceftolozane/tazobactam, ceftazidime/avibactam, imipenem-cilastatin/relebactam, meropenem/vaborbactam, or polymyxins combined with other conventional sensitive drugs (4). In addition, some studies reported that a combination of antibiotics with glucocorticoids or vitamin C could effectively reduce the brain abscess area by modulating glucocorticoid receptor and toll-like receptor-2 expression, glucocorticoids or vitamin C can be considered as an adjuvant therapy (5–7). Because polymyxins such as colistimethate sodium (CMS) barely penetrate the blood-brain barrier (BBB), CMS has been approved for ventricular/intrathecal administration to treat CRPA-induced intracranial infections. In addition, among these novel β-lactam/β-lactamase inhibitors, only ceftazidime/avibactam, an excellent antimicrobial drug against most carbapenem-resistant Enterobacteriaceae (CRE), including CRPA (8), has been approved for clinical application in China. Some studies have reported that ceftazidime/avibactam is able to penetrate the BBB to treat intracranial infections, but the degree of penetration into the brain abscess is still unknown. Currently, intravenous ceftazidime/avibactam combined with intrathecal CMS, or intravenous or intrathecal amikacin, or intravenous fosfomycin have been reported to successfully treat CRPA-induced meningitis or ventriculitis (8–13), but the use of these drugs for treatment of CRPA-induced brain abscess has not yet been reported. In this article, we presented the first case of a child with CRPA-induced brain abscess after intracranial tumor resection that has been successfully cured by intravenous ceftazidime/avibactam combined with intrathecal CMS. We have also reviewed the literature to provide new ideas and experience to inform clinical pharmacological therapy of CRPA-induced brain abscess.

2 Case report

The male patient was 14-years-old, 168 cm tall, and weighed 55 kg. He had complained of intermittent headaches and vomiting since September 2023. A ventricular tumor was identified by enhanced magnetic resonance imaging (MRI) and the patient underwent ventricular tumor resection by ventriculoscope at another tertiary care hospital on October 4th 2023. The pathological type of the tumor was subventricular giant cell astrocytoma. The patient developed positive cervical resistance immediately after surgery, with a maximum body temperature of 39°C. He was treated by intermittent lumbar puncture and a combined regimen of linezolid and meropenem for 20 days. Unfortunately, the treatment had little success. Therefore, the patient was transferred to our hospital for further treatment.

On day 1, he had a body temperature of 39°C with nuchal rigidity. He underwent lumbar cistern drainage, which drained-out turbid orange CSF. Routine and biochemical examination of the CSF showed a positive Pandy test with a leukocyte count of 192/mm^3 (normal range: 0-8/mm^3), microprotein 273 mg/dL (normal range: 0-40 mg/dL), chloride 118.6 mmol/L (normal range: 120-132 mmol/L), and glucose 2.64 mmol/L (normal range: 2.5-4.4 mmol/L). A computed tomography (CT) scan of the head showed slight hyperdensity along the surgical path. Vancomycin (20 mg, qd, intrathecal) combined with meropenem (2 g, q8h, intravenous) was used empirically. On day 4, the child remained intermittently febrile with a maximum body temperature of 40°C. Accordingly, the CSF was sampled for bacterial culture and drug susceptibility testing.

On day 5, the patient had a sudden convulsion of the limbs with loss of consciousness and an upward gaze, which was diagnosed as an epileptic seizure. The seizure was not alleviated by intravenous phenobarbital and valproate, but was eventually controlled by continuous intravenous pumping of midazolam. An urgent routine blood examination found a leukocyte count of 13.9 × 10^9/L and the neutrophil ratio was 85.4%. Routine CSF and biochemical examination showed a positive Pandy test, leukocyte count increased to 510/mm^3, microprotein increased to 282 mg/dL, glucose increased to 5.8 mmol/L, and normal chloride (121.8 mmol/L). A head CT scan showed a round cystic-solid lesion in the operative area, with the interior of the lesion being hypointense and the surrounding solid cystic wall being hyperintense. The brain tissue around the lesion was evidently edematous (Figure 1). Enhanced MRI of the head showed significant enhancement of all brain parenchyma along the surgical path, and the lesion localized in the surgical area formed a complete cystic wall, which exhibited significant central enhancement (Figure 2). Consequently, the child was diagnosed with a brain abscess according to the CT and MRI data. Metagenomic next generation sequencing identified PA. On day 6, analysis of CSF cultures indicated that the pathogen was CRPA (the antimicrobial susceptibility data, which was determined by agar dilution, are shown in Table 1). A clinical pharmacist participated in the treatment and suggested adjusting the regimen to intravenous ceftazidime/avibactam (2.5 g, q8h) combined with intrathecal CMS (125,000 U, qd).

On day 9, after treatment with the new regimen for 3 days, the child's body temperature and routine blood results returned to normal, but cervical resistance remained positive. The CSF was pale yellow and the Pandy test was weakly positive. The CSF leukocyte count was reduced to 284/mm^3, microprotein was reduced to 143 mg/dL, glucose to 2.58 mmol/L, while chloride remained normal at 124.4 mmol/L. The head CT showed that the lesion was smaller and there was reduced edema in the surrounding brain tissue. All of these results suggested that the regimen exerted therapeutic effectiveness.

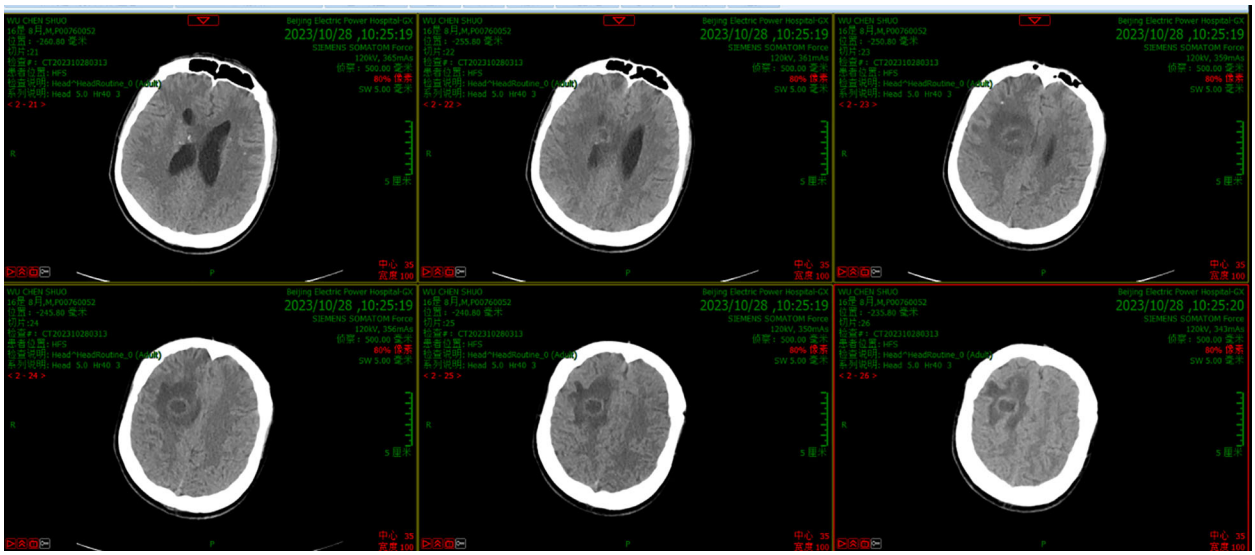

FIGURE 1
CT scanning before the new therapeutic regimen showed a round cystic-solid lesion in the operative area, with the interior of the lesion being hypointense and the surrounding solid cystic wall being hyperintense. The brain tissue around the lesion was evidently edematous.

On day 20, after treatment with the new regimen for 14 days, the patient's body temperature and routine blood results remained normal, with negative cervical resistance. The CSF was colorless and clear, and the Pandy test was negative. The CSF leukocyte count decreased to 54/mm^3, microprotein reduced to 56 mg/dL, while chloride (125.6 mmol/L) and glucose (2.61 mmol/L) were unchanged. A head CT and enhanced MRI showed that the abscess cavity had disappeared (Figures 3, 4). According to these results, the therapeutic regimen was terminated and the lumbar drainage tube was removed. Two days later, the child underwent lumbar puncture again and the CSF examination showed a further reduction of leukocyte count to 28/mm^3, microprotein was 57 mg/dL, while chloride (126.6 mmol/L) and glucose (3.16 mmol/L) remained normal. Ultimately the child was successfully cured and discharged from the hospital. A summary of the clinical treatment process is shown in Figure 5.

3 Discussion

Brain abscess is a focal suppurative inflammation of brain tissue with a distinct wall that is associated with a high rate of lethality and disability. Because of the high risk of death in patients with intracranial CRPA-induced infections, the World Health Organization has classified CRPA as a strain that urgently needs new antibiotic treatment as well as innovative and effective therapies (14).

Because there are few reports on CRPA-induced CNSI, the optimal antimicrobial regimen remains unclear. In the present case, the results of antimicrobial sensitivity screening showed that the pathogen was not only resistant to conventional β-lactam/β-lactamase inhibitors (piperacillin/tazobactam, cefoperazone/sulbactam), quinolones and aminoglycosides, but also resistant to imipenem and meropenem (Table 1). The carbapenem-resistance mechanisms of PA are complex, but one is its ability to produce multifarious β-lactamases,

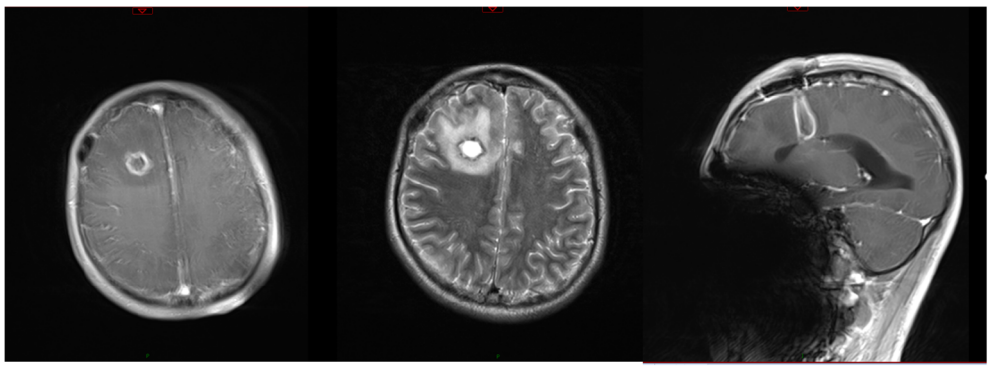

FIGURE 2
Results of MRI before the new therapeutic regimen. T2 scanning showed that the T2 signal from the interior of the lesion was long, while that from the surrounding cystic wall was short. Enhanced MRI scanning showed significant enhancement along the surgical path. The lesion localized in the surgical area formed a complete cystic wall and was significantly enhanced.

TABLE 1 Antimicrobial susceptibility data.

Antibiotics	MIC (mg/L)	Susceptibility
Amikacin	≥64	resistant
Piperacillin/Tazobactam	≥128	resistant
Imipenem	≥8	resistant
Levofloxacin	≥8	resistant
Ceftazidime	32	resistant
Tobramycin	8	resistant
Ciprofloxacin	2	resistant
Cefepime	≥32	resistant
Meropenem	≥8	resistant
Cefoperazone/Sulbactam	≥64	resistant

including extended-spectrum β-lactamases (ESBLs), AmpC β-lactamases, carbapenemases such as Klebsiella pneumoniae carbapenemase (KPC), and oxacillinase-48-like (OXA-48) carbapenemases (15). Avibactam, a novel semisynthetic β-lactamase inhibitor, inhibits the above enzymes to restore the efficacy of ceftazidime against CRE (16). Globally, the susceptibility of CRPA to ceftazidime/avibactam is above 60% (17). Currently, ceftazidime/avibactam has been approved by the US Food and Drug Administration for the treatment of hospital-acquired pneumonia, complicated abdominal infections, complicated urinary tract infections, and associated bacteremia caused by CRE, including CRPA. There are, however, limited clinical data available on the treatment of CRPA-induced CNSI with ceftazidime/avibactam.

To investigate the clinical therapeutic effects of ceftazidime/avibactam against PA-induced CNSI, we conducted a comprehensive review of literature in the PubMed, Medline, and Web of Science databases from their inception to January 2024 for all case reports and series reports on CNSI caused by PA. The search keywords were: *Pseudomonas aeruginosa*, brain abscess, meningitis, ventriculitis, central nervous system infection, and ceftazidime/avibactam. Only seven reports were found that covered the use of ceftazidime/avibactam to treat PA-associated CNSI, among which the pathogens in six cases were CRPA. In one case, drug resistance of the pathogen was not described (Table 2).

We found from the seven reports that: (1) the medication regimens were ceftazidime/avibactam combined with another drug, including intrathecal CMS, intravenous or intrathecal aminoglycosides, and intravenous fosfomycin; and (2) the ceftazidime/avibactam concentration in CSF from one case suggested that a standard dose (2.5 g, q8h) could achieve effective therapeutic concentrations (ceftazidime: 21-29 μg/mL, avibactam: 1.42-2.44 μg/mL) (8). Previous studies have demonstrated that ceftazidime effectively penetrated into inflammatory CSF (18), whereas the ability of avibactam to cross the BBB requires further investigation. Yasmin M (8) used astandard dose of ceftazidime/avibactam to treat a patient with CRPA-induced ventriculitis and found that the steady-state concentration ratio of avibactam in CSF compared to serum was in the range of 20% to 38%, which is consistent with that observed in a rabbit meningitis model (19). The percentage of the dosing interval during which ceftazidime/avibactam free drug concentration was above the MIC (% fT > MIC) reached 50% (12). Gatti M reported that if the dose of ceftazidime/avibactam was increased to 2.5 g q6h, the % fT > MIC increased to 100% (9). These results indicate that ceftazidime/avibactam can reach an effective therapeutic concentration for treating CRPA-induced infections in CSF. As drug concentration in brain abscesses is difficult to measure in clinical practice, the drug concentration in CSF is used as a

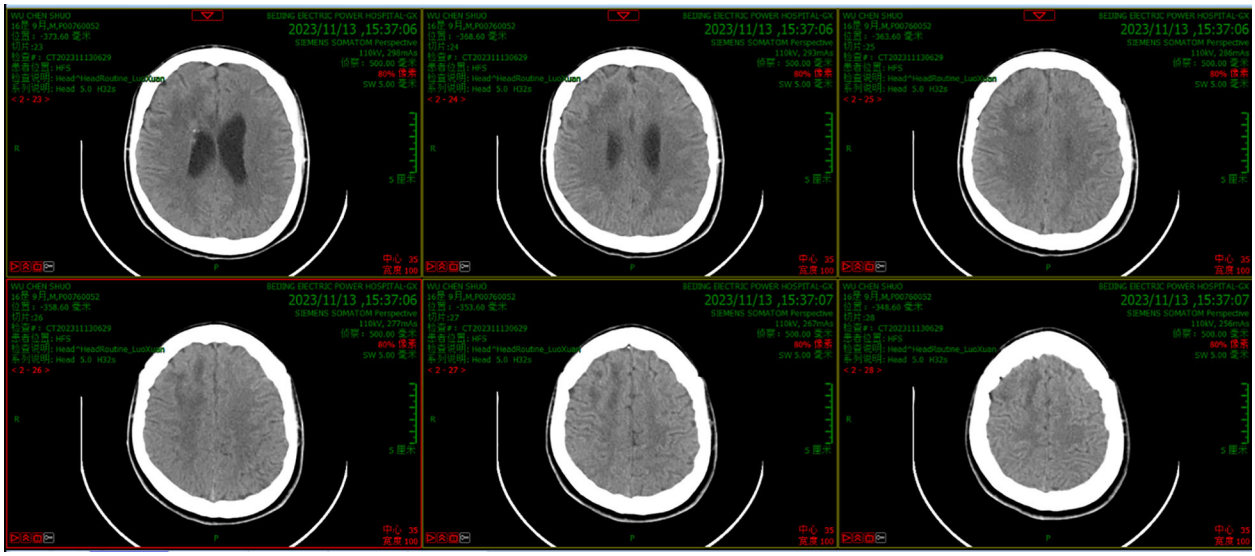

FIGURE 3
CT scanning results after treatment with the new regimen for 14 days showed that the abscess had disappeared and that there was little edema in the surrounding brain tissue.

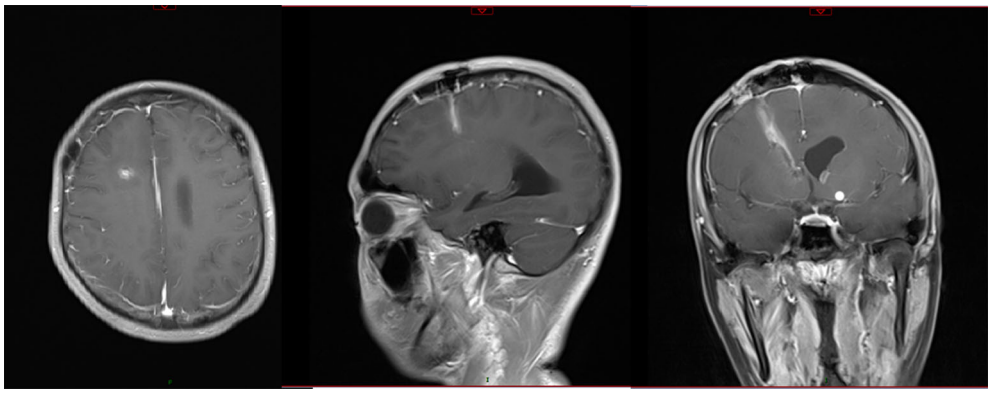

FIGURE 4
Enhanced MRI scanning after treatment with the new regimen for 14 days showed that the abscess had disappeared, with little enhancement along the surgical path.

surrogate in the clinic based on the assumption that drugs in CSF can permeate through the brain abscess by continuous exchange with interstitial fluid. However, this exchange between CSF and interstitial fluid barely reaches an equilibrium state (20). Unfortunately, there are no studies on whether an effective therapeutic concentration of ceftazidime/avibactam can be achieved in brain abscesses. Considering that the location of the infected lesion in this patient was deep within the brain parenchyma, we selected ceftazidime/avibactam combined with polymyxins such as CMS to achieve an optimal therapeutic effect.

Polymyxins are antibiotics having cationic cyclic peptide structures that have strong affinity for lipid A of the bacterial extracellular membrane. They are able to competitively replace magnesium and calcium ions of lipopolysaccharide to increase permeability of the bacterial extracellular membrane, resulting in leakage of the cellular contents, and thus exert bactericidal effects (21). Accordingly, polymyxins have excellent antimicrobial activity against most carbapenem-resistant gram-negative bacilli, including CRPA. However, the low penetration of intravenous polymyxins into CSF does not provide an effective bactericidal concentration at conventional doses, and high intravenous doses of polymyxins carry a risk of renal damage (22). The Infectious Disease Society of America recommended ventricular/intrathecal administration of polymyxins to treat intracranial infection, so that polymyxins in the CSF can diffuse and penetrate into the brain abscess and exert their antibacterial effect (20, 23). Currently, polymyxins used in the clinic include CMS, polymyxin B and polymyxin E. Only CMS has been approved for ventricular/intrathecal administration. Because the child patient in this case only underwent lumbar puncture drainage, we adopted intrathecal injection of CMS to treat CRPA-induced intracranial infection.

CMS can remove lipopolysaccharide from the bacterial outer membrane, which facilitates binding of ceftazidime/avibactam to penicillin-binding proteins to inhibit synthesis of bacterial cell wall, thus exerting a synergistic antibacterial effect. Based on the above analysis, we adopted a therapeutic regimen of intravenous ceftazidime/avibactam combined with intrathecal CMS. After 14 days of this combined regimen, the patient's brain abscess had disappeared and the results of routine CSF and biochemical tests were essentially normal. Ultimately, he was discharged from the hospital successfully without any adverse drug reactions. The difference between our case and other reported cases was that the brain abscess in our case had formed after severe CNSI. Enhanced head MRI showed that the abscess was completely encapsulated. Generally, under these circumstances, surgical abscess resection is

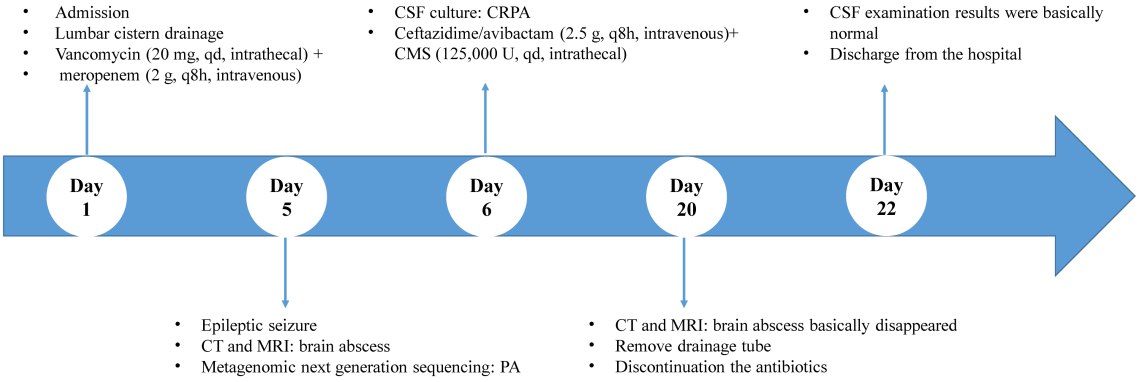

FIGURE 5
A summary of the clinical treatment process.

TABLE 2 Summary of cases of ceftazidime/avibactam in the treatment of *Pseudomonas aeruginosa*-induced CNSI.

Author/ Published Time	Patient Age	Diagnosis	Potential Risk Factors	Strain Characterization	Drug Sensitivity Results of C/A	Treatment Program before C/A	Dosage and course of C/A	Combined Medicine	Prognosis
Yasmin M,2023 (8)	69	meningitis	lung transplantation, ventricular leakage	DTR-PA	Unknow	Ceftazidime + Amikacin	2.5 g, q8h, intravenous, 21 days	CMS 125,000 U, qd, intrathecal injection + CMS 4.5 MU, q12h, intravenous,21 days	clinical cured
Gatti M,2022 (9)	52	meningitis	craniotomy	CRPA	C/A 4 mg/L	Cefepime + Compound Sulfamethoxazole	2.5 g, q6h, intravenous, 23 days	fosfomycin 16g/d (Continuous intravenous pumping),23 days	CSF test turned negative
Gofman N,2018 (10)	32	ventriculitis	cranial removal surgery	PA+CRKP	Ceftazidime 2 mg/L, Avibactam 1 mg/L	Vancomycin, linezolid, ceftriaxone, cefepime, meropenem	2.5 g, q8h, intravenous,42 days	Amikacin 30 mg, qd, intrathecal injection,28 days	CSF test turned negative 3 days later
Zhou Q,2021 (11)	21	acute purulent meningitis	cranial removal surgery	MDR-PA	ceftazidime 8 mg/L	①meropenem 1.5 g, q6h, intravenous +linezolid 0.6 g, q12h, intravenous,10 days. ② CMS 500,000 U, q8h, intravenous +CMS 50,000 U, qd, intracerebroventricular injection, 3 days. ③ CMS 500,000 U, q8h, intravenous + CMS 50,000 U, qd(intracerebroventricular injection)+amikacin 400 mg, q12h, intravenous, 24 days	2.5 g, q8h, intravenous, 14 days	Amikacin 600 mg, q12h, intravenous, 14 days	CSF test turned negative 6 days later
Xipell M,2017 (12)	56	meningitis	renal transplant, sinus debridement	XDR-PA	Unknow	Meropenem 2 g, q8h, intravenous + CMS 2 MU, q8h, intravenous	2.5 g, q8h, intravenous, 30 days	CMS 2 MU, q8h, intravenous	clinical cured
Rodríguez-Núñez O, 2018 (13)	58	suppurative meningitis	renal transplant, maxillofacial surgery	XDR-PA	Unknow	Meropenem + ciprofloxacin, CMS	Undescribe dosage, 38 days	CMS (undescribe dosage intravenous),7 days	survived for 90 days
Almangour TA, 2022 (26)	2	CNSI	ventriculoperitonealshunt	MDR-PA	Ceftazidime 2 mg/L, Avibactam 4 mg/L	vancomycin, ceftazidime, meropenem, amikacin, gentamicin, colistin	450 mg, q8h, intravenous, 21 days	colistin 125,000 U, intraventricular, 14 days	clinical cured

XDR, extensively drug resistant; MDR, multidrug resistant; DTR, difficult-to-treat resistant; CRKP, carbapenem-resistant Klebsiella pneumoniae; C/A, ceftazidime/avibactam; CSF, cerebrospinal fluid.

10.3389/fonc.2024.1444172

required. However, our protocol of intravenous ceftazidime/avibactam combined with intrathecal CMS effectively cured the brain abscess, which avoided the pain of a second craniotomy for the child patient. Therefore, the therapeutic regimen in our case provided a novel therapeutic approach for the treatment of CRPA-induced brain abscess. Recent findings suggested that attenuating cytokine-induced microglial activation, for instance, Th1 and Th17 cytokines in Gram-positive cocci-induced and Th2 cytokine in Gram-negative bacilli-induced CNSI, may contribute to a reduction of the brain abscess and promote the restoration of neurological function (24, 25). The major limitation of this case was that our present study was predominantly focused on the pharmacological rationale behind the bactericidal effectiveness of antibiotics at the lesion site, with no investigation into the possible efficacy in neuroendocrine-immune interaction, which can be undertaken in future research.

In conclusion, according to the experience from our present case, we believe that intravenous ceftazidime/avibactam combined with intrathecal CMS may be an effective therapeutic regimen to treat CRPA-induced CNSI, which is worthy of clinical reference.

Data availability statement

The original contributions presented in the study are included in the article/supplementary material. Further inquiries can be directed to the corresponding authors.

Ethics statement

The studies involving humans were approved by IRB of Beijing Electric Power Hospital, State Grid Corporation of China. The studies were conducted in accordance with the local legislation and institutional requirements. Written informed consent for participation in this study was provided by the participants' legal guardians/next of kin. Written informed consent was obtained from the individual(s) for the publication of any potentially identifiable images or data included in this article.

Author contributions

MY: Conceptualization, Data curation, Formal Analysis, Writing – original draft, Writing – review & editing. MZ: Writing – review & editing. CR: Writing – review & editing. WZ: Conceptualization, Resources, Supervision, Writing – review & editing. ZL: Conceptualization, Resources, Supervision, Writing – review & editing.

Funding

The author(s) declare that no financial support was received for the research, authorship, and/or publication of this article.

Conflict of interest

The authors declare that the research was conducted in the absence of any commercial or financial relationships that could be construed as a potential conflict of interest.

Publisher's note

References

1. Yang KY, Chang WN, Ho JT, Wang HC, Lu CH. Postneurosurgical nosocomial bacterial brain abscess in adults. *Infection*. (2006) 34:247–51. doi: 10.1007/s15010-006-5607-5

2. Brouwer MC, Coutinho JM, van de Beek D. Clinical characteristics and outcome of brain abscess: systematic review and meta-analysis. *Neurology*. (2014) 82:806–13. doi: 10.1212/WNL.0000000000000172

3. Corsini Campioli C, Castillo Almeida NE, O'Horo JC, Wilson WR, Cano E, DeSimone DC, et al. Diagnosis, management, and outcomes of brain abscess due to gram-negative versus gram-positive bacteria. *Int J Infect Dis*. (2022) 115:189–94. doi: 10.1016/j.ijid.2021.12.322

4. Tamma PD, Aitken SL, van Duin D, Clancy CJ. Infectious Diseases Society of America 2022 Guidance on the Treatment of Extended-Spectrum β-lactamase Producing Enterobacterales (ESBL-E), Carbapenem-Resistant Enterobacterales (CRE), and *Pseudomonas aeruginosa* with Difficult-to-Treat Resistance (DTR-P. aeruginosa). *Clin Infect Dis*. (2022) 75:187–212. doi: 10.1093/cid/ciac268

5. Dey R, Bishayi B. Ciprofloxacin and dexamethasone in combination attenuate S. aureus induced brain abscess via neuroendocrine-immune interaction of TLR-2 and glucocorticoid receptor leading to behavioral improvement. *Int Immunopharmacol*. (2021) 97:107695. doi: 10.1016/j.intimp.2021.107695

6. Dey R, Bishayi B. Ascorbic acid along with ciprofloxacin regulates S. aureus induced microglial inflammatory responses and oxidative stress through TLR-2 and glucocorticoid receptor modulation. *Inflammopharmacology*. (2022) 30:1303–22. doi: 10.1007/s10787-022-01012-z

7. Dey R, Bishayi B. Dexamethasone exhibits its anti-inflammatory effects in S. aureus induced microglial inflammation via modulating TLR-2 and glucocorticoid receptor expression. *Int Immunopharmacol*. (2019) 75:105806. doi: 10.1016/j.intimp.2019.105806

8. Yasmin M, Nutman A, Wang L, Marshall S, Chen K, Wang J, et al. Utilizing ceftazidime/avibactam therapeutic drug monitoring in the treatment of neurosurgical meningitis caused by difficult-to-treat resistant Pseudomonas aeruginosa and KPC-producing enterobacterales. *Open Forum Infect Dis*. (2023) 10:ofad507. doi: 10.1093/ofid/ofad507

9. Gatti M, Virgili G, Cojutti PG, Gaibani P, Conti M, Sturiale C, et al. Real-Time Optimization of Pharmacodynamic Target Attainment at Infection Site during Treatment of Post-Neurosurgical Ventriculitis Caused by Carbapenem-Resistant Gram Negatives with Ceftazidime-Avibactam-Based Regimens: A Report of Two Cases. *Microorganisms*. (2022) 10:154. doi: 10.3390/microorganisms10010154

10. Gofman N, To K, Whitman M, Garcia-Morales E. Successful treatment of ventriculitis caused by *Pseudomonas aeruginosa* and carbapenem-resistant *Klebsiella pneumoniae* with i.v. ceftazidime-avibactam and intrathecal amikacin. *Am J Health Syst Pharm*. (2018) 75:953–7. doi: 10.2146/ajhp170632

11. Zhou Q, Wang H, Zhan T, Yang X, Wen L. Successful treatment of Ventriculitis caused by MDR/XDR gram-negative bacillus using ceftazidime/avibactam: case series and literature review. *Infect Drug Resist*. (2021) 14:1691–701. doi: 10.2147/IDR.S306222

12. Xipell M, Bodro M, Marco F, Losno RA, Cardozo C, Soriano A. Clinical experience with ceftazidime/avibactam in patients with severe infections, including meningitis and lung abscesses, caused by extensively drug-resistant *Pseudomonas aeruginosa*. *Int J Antimicrob Agents*. (2017) 49:266–8. doi: 10.1016/j.ijantimicag.2016.11.005

13. Rodríguez-Núñez O, Ripa M, Morata L, de la Calle C, Cardozo C, Fehér C, et al. Evaluation of ceftazidime/avibactam for serious infections due to multidrug-resistant and extensively drug-resistant *Pseudomonas aeruginosa*. *J Glob Antimicrob Resist*. (2018) 15:136–9. doi: 10.1016/j.jgar.2018.07.010

14. acconelli E, Carrara E, Savoldi A, Harbarth S, Mendelson M, Monnet DL, et al. Discovery, research, and development of new antibiotics: the WHO priority list of antibiotic-resistant bacteria and tuberculosis. *Lancet Infect Dis*. (2018) 18:318–27. doi: 10.1016/S1473-3099(17)30753-3

15. Giovagnorio F, De Vito A, Madeddu G, Parisi SG, Geremia N. Resistance in *Pseudomonas aeruginosa*: A narrative review of antibiogram interpretation and emerging treatments. *Antibiotics (Basel)*. (2023) 12:1621. doi: 10.3390/antibiotics12111621

16. Zhen S, Wang H, Feng S. Update of clinical application in ceftazidime-avibactam for multidrug-resistant Gram-negative bacteria infections. *Infection*. (2022) 50:1409–23. doi: 10.1007/s15010-022-01876-x

17. Kiratisin P, Kempf M, Stone G, Utt E. Ceftazidime-avibactam and comparators against *Pseudomonas aeruginosa* isolates collected globally and in each geographical region between 2017-2020. *J Glob Antimicrob Resist*. (2023) 34:113–8. doi: 10.1016/j.jgar.2023.06.005

18. Tunkel AR, Hasbun R, Bhimraj A, Byers K, Kaplan SL, Scheld WM, et al. 2017 Infectious diseases society of America's clinical practice guidelines for healthcare-Associated ventriculitis and meningitis. *Clin Infect Dis*. (2017) 64:e34–65. doi: 10.1093/cid/ciw861

19. Falcone M, Paterson D. Spotlight on ceftazidime/avibactam: a new option for MDR Gram-negative infections. *J Antimicrob Chemother*. (2016) 71:2713–22. doi: 10.1093/jac/dkw239

20. Pardridge WM. CSF, blood-brain barrier, and brain drug delivery. *Expert Opin Drug Deliv*. (2016) 13:963–75. doi: 10.1517/17425247.2016.1171315

21. Poirel L, Jayol A, Nordmann P. Polymyxins: antibacterial activity, susceptibility testing, and resistance mechanisms encoded by plasmids or chromosomes. *Clin Microbiol Rev*. (2017) 30:557–96. doi: 10.1128/CMR.00064-16

22. Nation RL, Rigatto MHP, Falci DR, Zavascki AP. Polymyxin acute kidney injury: dosing and other strategies to reduce toxicity. *Antibiotics (Basel)*. (2019) 8:24. doi: 10.3390/antibiotics8010024

23. Nance E, Pun SH, Saigal R, Sellers DL. Drug delivery to the central nervous system. *Nat Rev Mater*. (2022) 7:314–31. doi: 10.1038/s41578-021-00394-w

24. Konsman JP. Cytokines in the brain and neuroinflammation: we didn't starve the fire! *Pharm (Basel)*. (2022) 15:140. doi: 10.3390/ph15020140

25. Bajpai A, Prasad KN, Mishra P, Singh AK, Gupta RK, Ojha BK. Distinct cytokine pattern in response to different bacterial pathogens in human brain abscess. *J Neuroimmunol*. (2014) 273:96–102. doi: 10.1016/j.jneuroim.2014.05.009

26. Almangour TA, Alsubaie S, Ghonem L, Almohaini HA, Mohammed Bakheet H, Altweijri I. Ceftazidime-avibactam for the treatment of multidrug-resistant Pseudomonas aeruginosa central nervous system infection in pediatric patient: A case report. *Pediatr Infect Dis J*. (2022) 41:436–8. doi: 10.1097/INF.0000000000003439

frontiers | Frontiers in Oncology

TYPE Case Report
PUBLISHED 27 September 2024
DOI 10.3389/fonc.2024.1438011

OPEN ACCESS

EDITED BY
Gerardo Caruso,
University Hospital of Policlinico G. Martino, Italy

REVIEWED BY
Felix Mircea Brehar,
Carol Davila University of Medicine and Pharmacy, Romania
Girish Vajramani,
University Hospital Southampton NHS Foundation Trust, United Kingdom

*CORRESPONDENCE
Zhaomu Zeng
zzmhemisphere@163.com
Shuhong Mei
mshsjwk@163.com

RECEIVED 24 May 2024
ACCEPTED 12 September 2024
PUBLISHED 27 September 2024

CITATION
Gui Y, Zhou F, Li B, Wu B, Huang X, Zeng Z and Mei S (2024) Case report: A rare case of neurocytoma of the Vth cranial nerve. *Front. Oncol.* 14:1438011. doi: 10.3389/fonc.2024.1438011

Case report: A rare case of neurocytoma of the Vth cranial nerve

Yongping Gui[1], Fanghua Zhou[2], Bin Li[3], Bin Wu[3], Xingen Huang[3], Zhaomu Zeng[1]* and Shuhong Mei[3]*

[1]Department of Neurosurgery, Jiangxi Provincial People's Hospital, The First Affiliated Hospital of Nanchang Medical College, Nanchang, China, [2]Department of Anesthesiology, Ji'an Central People's Hospital, Ji'an, China, [3]Department of Neurosurgery, Ji'an Central People's Hospital, Ji'an, China

We report a case of neurocytoma originating from cranial nerve V. A 53-year-old female patient presented with a 20-day history of right frontotemporal facial paresthesia and pain. Magnetic resonance imaging (MRI) showed a 2.5-cm × 1.4-cm "dumbbell" enhancing lesion located in the cisternal segment of cranial nerve V with extension into Meckel's cave, and the signal characteristics were suggestive of trigeminal neurinoma. The lesion was resected through a subtemporal middle cranial fossa approach. Intraoperative findings revealed that the tumor originated from the cisternal segment of cranial nerve V and extended into Meckel's cave through the trigeminal foramen. No dural attachment was found. The tumor was debulked using sharp dissection and bipolar cautery under the microscope. Extraventricular neurocytomas (EVNs) are extremely rare tumors of the central nervous system. To date, only two cases of neurocytomas arising from cranial nerve VIII have been described. This paper summarizes the clinicopathological features of a case of neurocytoma originating from the cisternal segment of cranial nerve V with extension into Meckel's cave and expounds the relevant diagnoses and treatments, which may provide a practical clinical basis and experience for the diagnosis and treatment of EVN in the future.

KEYWORDS

extraventricular neurocytoma, trigeminal nerve, immunohistochemistry, origin and pathological basis, case report

1 Introduction

Neurocytoma is a rare neoplasm of the central nervous system (CNS) and shows a propensity to occur within the lateral ventricles, known as central neurocytoma (CN). In contrast, neurocytoma arising outside the ventricles, known as extraventricular neurocytoma (EVN), is an extremely rare neuronal neoplasm that has not been well-characterized (1). In 1989, Ferrol et al. (2) reported a case of extraventricular tumor. Gangaspero et al. (3) frist proposed the concept of EVN in 1997. The incidence rate of EVN is about 0.13%, and only more than 100 cases have been described to date. As reported, EVNs occur in heterogeneous

locations, most commonly in the cerebral hemisphere (particularly the frontal and temporal lobes), but also in the thalamus, sellar region, cerebellar hemispheres, brainstem, and rarely in an extracranial locations of the spinal cord and cranial nerves (4). So far, only two cases of EVNs arising from the VIII cranial nerve have been described (5, 6). The present study is the first to report a case of trigeminal neurocytoma due to the rare involvement of cranial nerves by EVNs.

2 Case report

A 53-year-old female patient presented to our neurosurgery department in June 2022 due to due to a 20-day history of right frontotemporal facial paresthesia and knifelike pain, accompanied by right facial twitching. The hearing test showed no abnormality. Magnetic resonance imaging (MRI) showed a 2.5 × 1.4-cm "dumbbell" enhancing lesion located in the cisternal segment of cranial nerve V and protruding into Meckel's cave; the signal characteristics were suggestive of a trigeminal neurinoma (Figure 1). The Gd-DTPA-enhanced MRI revealed clear margins and substantial enhancement of the mass. The lesion was excised through the subtemporal middle cranial fossa approach, and the tumor can be completely exposed in the surgical field after grinding off the tip of the petrous bone. During the operation, the tumor was found to be cystic and solid, with soft texture and clear boundary with the Meckel's cave, and it grew through the trigeminal foramen and extended into the Meckel's cave. After opening the cerebellar tentorium, it could be seen that the tumor originated from the trigeminal nerve cistern segment. After cutting open the tumor capsule, it was found that the tumor tissue presented grayish white and lacked abundant blood supply. A portion of tumor was debulked using sharp dissection and bipolar cautery under the microscope, thereby exposing the trigeminal nerve and stripping the tumor along the nerve root, and completely removing the tumor tissue in Meckel's cave (Figure 2).

Pathological Findings. Histological examination revealed that the tumor cells were diffusely distributed in the form of sheets. The size of tumor cells was relatively uniform. The nuclei were oval to round and the cytoplasm was lightly stained, with rare mitotic Figures. The cells exhibited positive immunostaining for synaptophysin and NeuN (Figure 3). Additionally, the cells were strongly positive for CD56

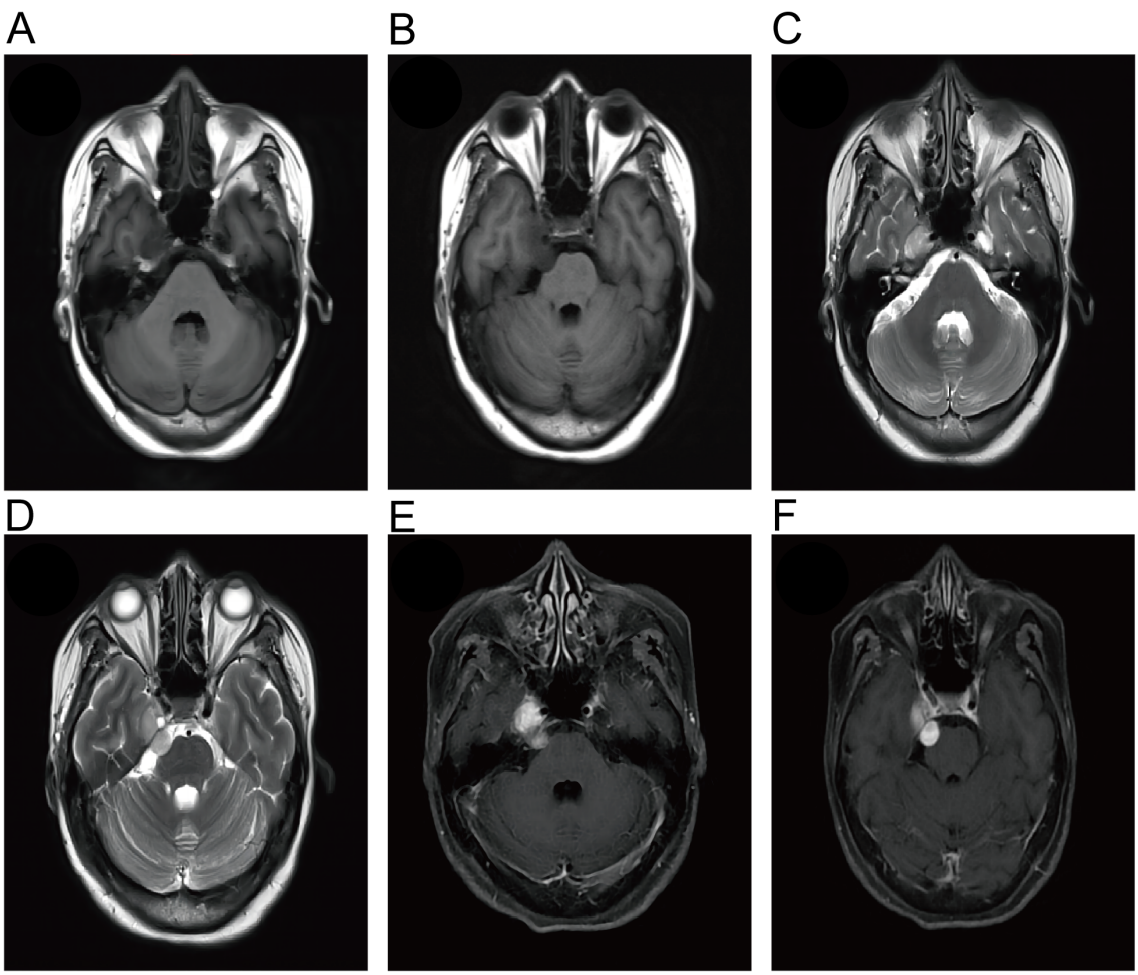

FIGURE 1
Magnetic resonance imaging (MRI) of the patient showed an enhancing lesion in the cisternal segment of the trigeminal nerve that protruded into Meckel's cavity. The lesions showed hypointense on T1-WI **(A, B)** and hyperintense on T2-WI **(C, D)**. **(E, F)** Gd-enhanced MRI showed a well-circumscribed dumbbell-like mass.

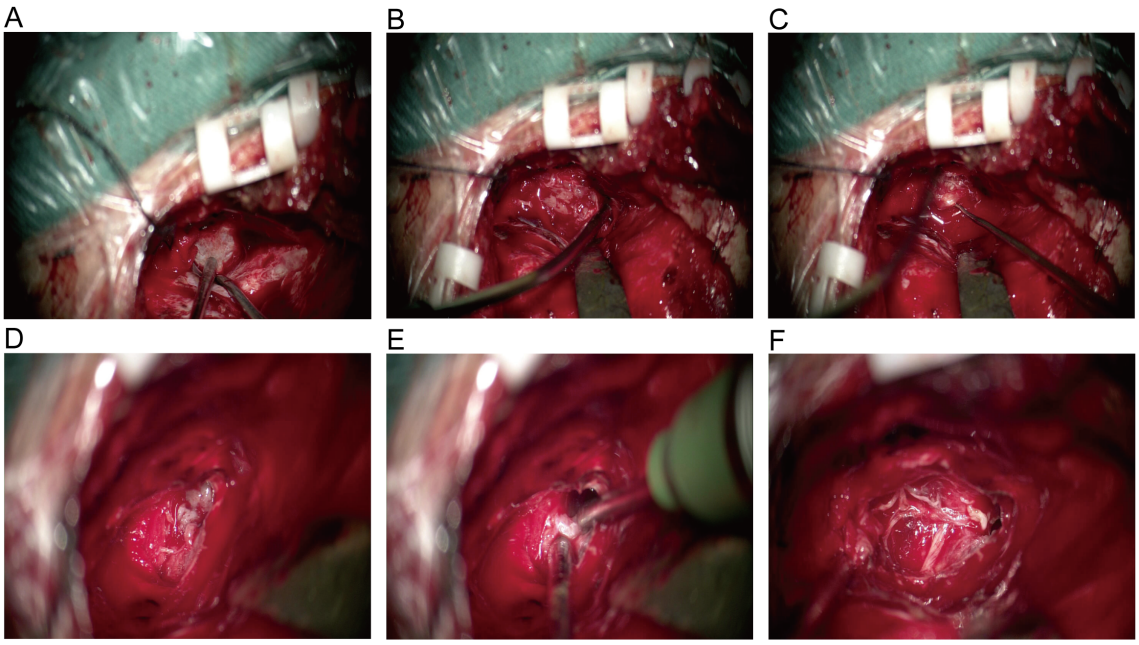

FIGURE 2
(A) Intraoperative exploration revealed intact tumor capsule and no adhesion to the dura mater. **(B)** Cut open the tumor capsule, the tumor texture is soft and gray white in color. **(C)** After removing a portion of the tumor tissue, expose the trigeminal nerve and strip the remaining tumor tissue along the nerve root. **(D)** The tumor grows through the trigeminal foramen and extends into Meckel's cave. **(E)** Clear boundary between tumor and surrounding brain tissue, complete resection of tumors within Meckel's cave. **(F)** After tumor resection, nerve protection was intact, and intraoperative exploration confirmed the origin of the EVN in the V cranial nerve.

and INI-1, and partially positive for CD99 and vimentin, while negative for EMA, S-100 protein, GFAP, SOX10, LCA, NSE, CgA, olig-2, and Brachyury. The Ki-67 index was high (> 5%).

Treatment and Follow-up. Postoperative MRI showed that the tumor was resected. The patient recovered well postoperatively and did not require adjuvant therapy. One month postoperatively, facial knifelike pain and hemifacial spasm were improved significantly and there were no signs of tumor recurrence. One year after surgery, the patient underwent a follow-up examination and found improvement in facial sensation. MRI did not reveal any signs of tumor recurrence (Figure 4).

3 Discussion

CNs usually involve the lateral ventricles and septum pellucidum near the foramina of Monro. EVNs that occur in the brain parenchyma outside the ventricular system are rare (1), affecting almost 0.022 per 100,000 people (7). As reported, EVNs may appear in heterogeneous locations, including the cerebral lobes, sellar region, cerebellum, pons, brainstem, thalamus, hypothalamus, amygdala, basal ganglia, spinal cord, cauda equina, retina, pelvis, and ovaries (8). To date, merely two cases of EVNs arising from the cranial nerves have been reported, both originated

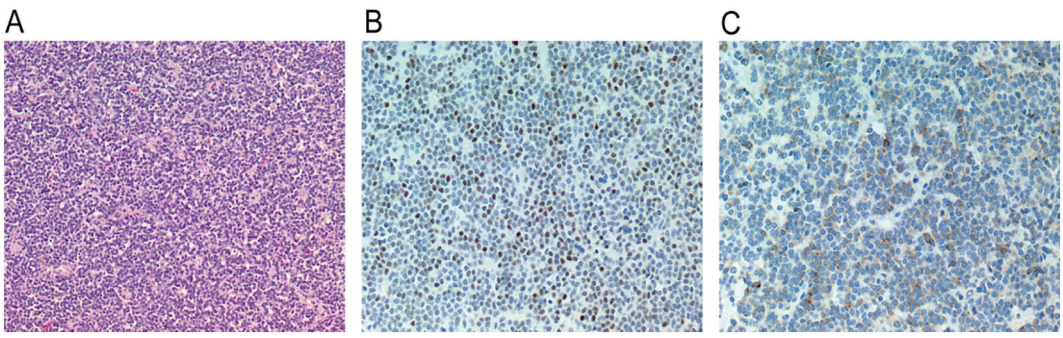

FIGURE 3
(A) Tumor cells were diffusely distributed in sheets, the size of the tumor cells was relatively uniform, the nuclei were oval to round, the cytoplasm was lightly stained, and mitotic figures were rare (hematoxylin and eosin, ×100). **(B)** Tumor cells express NEUN positive (original magnification, ×200). **(C)** Immunohistochemical stain for synaptophysin showing diffuse, strong reactivity in tumor cells (original magnification, ×200).

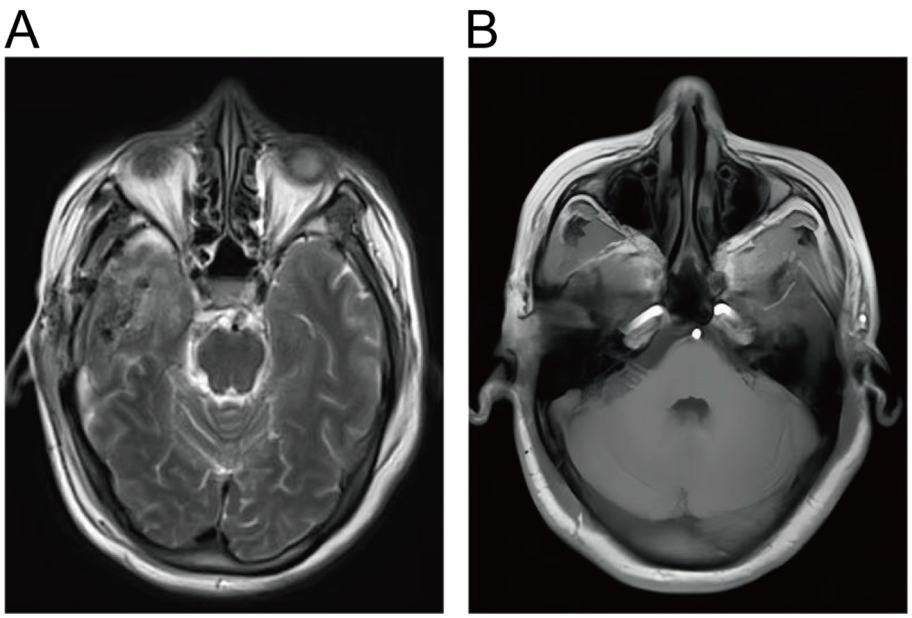

FIGURE 4
(A, B) Postoperative cranial MRI showed complete resection of EVN without residual lesions.

from cranial nerve VIII (5, 6). In our patient, the tumor originated from the cisternal segment of cranial nerve V and extended through the trigeminal foramen into Meckel's cave. To our knowledge, this is the first reported case of EVN originating from the trigeminal nerve.

Since EVNs occur in heterogeneous locations and their symptoms depend on the mass effect of lesions on surrounding tissues. Due to the absence of characteristic imaging features, EVNs are difficult to be differentiated from other intracranial tumors on imaging (4, 9). Our patient presented with right frontotemporal paresthesia and pain. Her MRI showed a dumbbell-enhancing lesion located in the cisternal segment of cranial nerve V and projecting into Meckel's cave, similar to the findings of trigeminal neuroma. Histologically, CNs and EVNs typically show uniform, small, and round cells with clear cytoplasm in a background of nerve fibers (8), which is consistent with the microscopic observations in our case. Synaptophysin is the most reliable immunohistochemical marker of CNs and EVNs because of its strong immunoreactivity in nerve cells (10). Moreover, CNs and EVNs also frequently exhibit immunoreactivity to NeuN and neuron-specific enolase (11). In our case, the tumor was positive for synaptophysin and NeuN. Additionally, the tumor cells were strongly positive for CD56 and INI-1, and partially positive for CD99 and vimentin. At present, surgical resection remains the mainstay treatment of CNs and EVNs. Although gross total resection (GTR) is the preferred surgical option, subtotal resection and radiotherapy are sometimes necessary considering the proximity of the tumors to functionally important areas (12). In our case, the intraoperative findings revealed that the tumor was covered by capsules with sharp margins. The tumor was excised during the surgery. Although the Ki67 index was greater than 5%, we did not administer radiotherapy. The patient is on regular follow-up.

The origin of CNs and EVNs has not been clarified yet. Previously, CNs were considered to be purely neuronal tumors; however, emerging evidence suggests that CNs arise from undifferentiated precursor cells with neuronal and glial differentiation potential (13). Since EVNs are rarer and more diverse than CNs, the origin of EVNs from the peripheral nervous system (PNS) remains highly debated. Some experts have proposed that EVNs originate from bipotent progenitor cells in the periventricular interstitium, because of the potential of EVNs to differentiate into mature neurons or astrocytes (14). By contrast, some experts have also pointed out that EVNs are a component of the displaced CNS. Stephan et al. (15) reported a case of neurocytoma involving the cauda equina nerve roots, suggesting that the tumor may arise from the central stump of the nerve root or from the displaced CNS tissue in the peripheral segments of the nerve root. Finally, some studies have proposed that EVNs originate from the transitionnl zone between the CNS and PNS. Onguru et al. (5) reported a case of EVN that originated from the cochlear and vestibular portions of cranial nerve VIII, presumably from its CNS-PNS transitional zone. Similarly, we assumed that the tumor in our patient originated from the trigeminal root entry zone, the transitional zone of central and peripheral tissue compartments in the trigeminal nerve (16). In our patient, the tumor was located in the cisternal portion and extended into the Meckel cave near the trigeminal root entry zone. The initial segment of the nerve (root entry zone) contains glial cells, which are gradually replaced by peripheral Schwann cells in the transitional zone. The longest glial

segments are located in the root entry zone of cranial nerve VIII (almost 10 mm), followed by the sensory part of cranial nerve V (almost 3 mm) and cranial nerve III (almost 1 mm) (17–19). Arnautovic et al. (20) found that the length of glial segments of these cranial nerves corresponded to the number of cases of extra-axial primary glial tumors (CN VIII, 8 cases; CN V, 3 cases; CN III, 1 case). Accordingly, it was speculated that oligodendrogliomas originated from the root entry zones of cranial nerves VIII and V. In line with this, Breshears et al. (21) first reported a case of glioblastoma involving the trigeminal nerve root entry zone in 2014 and revealed that glial tumors can occur in the root entry zones of cranial nerves VIII, V, and III. Moreover, two cases of neurocytoma arsing from cranial nerve VIII have also been reported. In our patient, the tumor originated from cranial nerve V. These findings support the hypothesis that neurocytomas of the cranial nerve originate from the CNS-PNS transitional zone. We speculate that neurocytomas may also arise from cranial nerve III, albeit very rarely.

4 Conclusion

In conclusion, EVNs originating from cranial nerves are extremely rare. At present, relatively little is known about the origin and pathobiological basis of the lesion location. Our case report of neurocytoma originating from cranial nerve V may provide new clinical information on the origin and pathological basis of lesion location in neurocytomas originating from cranial nerves.

Data availability statement

The original contributions presented in the study are included in the article/supplementary material. Further inquiries can be directed to the corresponding authors.

Ethics statement

Written informed consent was obtained from the individual(s) for the publication of any potentially identifiable images or data included in this article.

Author contributions

YG: Writing – original draft, Writing – review & editing. FZ: Investigation, Writing – original draft. BL: Data curation, Writing – original draft. BW: Software, Writing – original draft. XH: Software, Writing – original draft. ZZ: Writing – original draft, Writing – review & editing. SM: Writing – original draft.

Funding

The author(s) declare that financial support was received for the research, authorship, and/or publication of this article. Medicine and Health Science and Technology Plan of Zhejiang Provincial Health Commission (No.2023RC306).

Conflict of interest

The authors declare that the research was conducted in the absence of any commercial or financial relationships that could be construed as a potential conflict of interest.

Publisher's note

References

1. Louis DN, Perry A, Wesseling P, Brat DJ, Cree IA, Figarella-Branger D, et al. The 2021 who classification of tumors of the central nervous system: A summary. *Neuro-oncology*. (2021) 23:1231–51. doi: 10.1093/neuonc/noab106

2. Ferreol E, Sawaya R, de Courten-Myers GM. Primary cerebral neuroblastoma (Neurocytoma) in adults. *J neuro-oncology*. (1989) 7:121–8. doi: 10.1007/bf00165096

3. Giangaspero F, Cenacchi G, Losi L, Cerasoli S, Bisceglia M, Burger PC. Extraventricular neoplasms with neurocytoma features. A clinicopathological study of 11 cases. *Am J Surg Pathol*. (1997) 21:206–12. doi: 10.1097/00000478-199702000-00011

4. Sweiss FB, Lee M, Sherman JH. Extraventricular neurocytomas. *Neurosurg Clinics North America*. (2015) 26:99–104. doi: 10.1016/j.nec.2014.09.004

5. Onguru O, Kurtkaya-Yapicier O, Scheithauer BW, Luetmer P, Burger PC, Mann SJ, et al. Neurocytoma of the viiith cranial nerve: case report. *Neurosurgery*. (2005) 57: E1065. doi: 10.1227/01.neu.0000179981

6. Sugita Y, Furuta T, Komaki S, Ohshima K, Sakata K, Morioka M. Malignant progression of an extraventricular neurocytoma arising from the viiith cranial nerve: A case report and literature review. *Neuropathology: Off J Japanese Soc Neuropathology*. (2019) 39:120–6. doi: 10.1111/neup.12533

7. Tish S, Habboub G, Jones J, Ostrom QT, Kruchko C, Barnholtz-Sloan JS, et al. The epidemiology of central and extraventricular neurocytoma in the United States between 2006 and 2014. *J neuro-oncology*. (2019) 143:123–7. doi: 10.1007/s11060-019-03144-9

8. Swinson BM, Friedman WA, Yachnis AT. Pontine atypical neurocytoma: case report. *Neurosurgery*. (2006) 58:E990. doi: 10.1227/01.Neu.0000210213.12847.1e

9. Romano N, Federici M, Castaldi A. Imaging of extraventricular neurocytoma: A systematic literature review. *La Radiologia Med*. (2020) 125:961–70. doi: 10.1007/s11547-020-01198-8

10. Buccoliero AM, Caldarella A, Ammannati F, Mennonna P, Taddei A, Taddei GL. Extraventricular neurocytoma: morphological and immunohistochemical considerations on differential diagnosis. *Pathology Res Pract*. (2002) 198:627–33. doi: 10.1078/0344-0338-00312

11. Englund C, Alvord EC Jr., RD F, Silbergeld D, DE B, Small R, et al. Neun expression correlates with reduced mitotic index of neoplastic cells in central neurocytomas. *Neuropathology Appl Neurobiol*. (2005) 31:429–38. doi: 10.1111/j.1365-2990.2005.00665.x

12. Kane AJ, Sughrue ME, Rutkowski MJ, Aranda D, Mills SA, Lehil M, et al. Atypia predicting prognosis for intracranial extraventricular neurocytomas. *J Neurosurg*. (2012) 116:349–54. doi: 10.3171/2011.9.Jns10783

13. von Deimling A, Kleihues P, Saremaslani P, Yasargil MG, Spoerri O, Südhof TC, et al. Histogenesis and differentiation potential of central neurocytomas. *Lab investigation; J Tech Methods Pathol.* (1991) 64:585–91.

14. Brat DJ, Scheithauer BW, Eberhart CG, Burger PC. Extraventricular neurocytomas: pathologic features and clinical outcome. *Am J Surg Pathol.* (2001) 25:1252–60. doi: 10.1097/00000478-200110000-00005

15. Stephan CL, Kepes JJ, Arnold P, Green KD, Chamberlin F. Neurocytoma of the cauda equina. *Case Rep J Neurosurg.* (1999) 90:247–51. doi: 10.3171/spi.1999.90.2.0247

16. Lin R, Luo L, Gong Y, Zheng J, Wang S, Du J, et al. Immunohistochemical analysis of histone H3 acetylation in the trigeminal root entry zone in an animal model of trigeminal neuralgia. *J Neurosurg.* (2018) 131:828–38. doi: 10.3171/2018.5.Jns172948

17. Edwards B, Wang JM, Iwanaga J, Loukas M, Tubbs RS. Cranial nerve foramina: part ii - a review of the anatomy and pathology of cranial nerve foramina of the posterior cranial fossa. *Cureus.* (2018) 10:e2500. doi: 10.7759/cureus.2500

18. Koekelkoren E. Histological, anatomo-pathological features of the cranial nerves. *Acta oto-rhino-laryngologica Belgica.* (1986) 40:51–78.

19. Bridger MW, Farkashidy J. The distribution of neuroglia and schwann cells in the 8th nerve of man. *J laryngology otology.* (1980) 94:1353–62. doi: 10.1017/s0022215100090186

20. Arnautovic KI, Husain MM, Linskey ME. Cranial nerve root entry zone primary cerebellopontine angle Gliomas: A rare and poorly recognized subset of extraparenchymal tumors. *J neuro-oncology.* (2000) 49:205–12. doi: 10.1023/a:1006488905526

21. Breshears JD, Ivan ME, Cotter JA, Bollen AW, Theodosopoulos PV, Berger MS. Primary glioblastoma of the trigeminal nerve root entry zone: case report. *J Neurosurg.* (2015) 122:78–81. doi: 10.3171/2014.10.Jns14449

frontiers | Frontiers in Neurology

TYPE Original Research
PUBLISHED 08 October 2024
DOI 10.3389/fneur.2024.1429826

OPEN ACCESS

EDITED BY
Bo Yuan Huang,
Electric Power Teaching Hospital, Capital Medical University, China

REVIEWED BY
Peng-Bo Zhou,
Shengjing Hospital of China Medical University, China
Min Bao,
China Medical University, China
Liang Zhang,
Chinese Academy of Medical Sciences and Peking Union Medical College, China
Theodora Katsila,
National Hellenic Research Foundation, Greece
Jinn-Rung Kuo,
Chi Mei Medical Center, Taiwan
Gang Lin,
Peking University, China

*CORRESPONDENCE
Jiachun Liu
✉ jiachunliu2005@163.com
Aihua Liu
✉ 15901398688@163.com

†These authors have contributed equally to this work

RECEIVED 08 May 2024
ACCEPTED 19 September 2024
PUBLISHED 08 October 2024

CITATION
Shen H, Mei Q, Chai X, Jiang Y, Liu A and Liu J (2024) The prognostic significance of synchronous metastasis in glioblastoma multiforme patients: a propensity score-matched analysis using SEER data. *Front. Neurol.* 15:1429826. doi: 10.3389/fneur.2024.1429826

The prognostic significance of synchronous metastasis in glioblastoma multiforme patients: a propensity score-matched analysis using SEER data

Hui Shen[1,2†], Qing Mei[3†], Xubin Chai[2,4†], Yuanfeng Jiang[1], Aihua Liu[2*] and Jiachun Liu[1,5*]

[1]Department of Interventional Neuroradiology, Sanbo Brain Hospital, Capital Medical University, Beijing, China, [2]Department of Interventional Neuroradiology, Beijing Tiantan Hospital, Beijing Neurosurgical Institute, Capital Medical University, Beijing, China, [3]Department of Neurology, Beijing Pinggu Hospital, Beijing, China, [4]State Key Laboratory of Brain and Cognitive Science, Institute of Biophysics, Chinese Academy of Sciences, Beijing, China, [5]Department of Neurosurgery, Beijing Hospital, Beijing, China

Background: Glioblastoma multiforme (GBM) with synchronous metastasis(SM) is a rare occurrence. We extracted the data of GBM patients from the SEER database to look into the incidence of SM in GBM, determine the prognostic significance of SM in GBM, and assess therapeutic options for patients presenting with SM.

Methods: From 2004 to 2015, information on GBM patients was obtained from the Surveillance, Epidemiology, and End Results (SEER) database. The propensity score matching (PSM) method was employed to mitigate confounding factors between SM and non-SM groups, subsequently investigating the prognostic significance of SM in patients with GBM. Multivariate Cox proportional hazards regression analyses were employed to identify independent prognostic variables for GBM patients with SM. A forest plot was used to visualize the results.

Results: A cohort of 19,708 patients was obtained from the database, among which 272 (1.4%) had SM at the time of diagnosis. Following PSM at a 3:1 ratio, in both univariate and multivariate cox regression analysis, SM (HR = 1.27, 95% CI: 1.09–1.46) was found to be an independent predictive predictor for GBM patients. Furthermore, the Cox proportional hazard forest plot demonstrated that independent risk variables for GBM patients with SM included age (Old vs. Young, HR = 1.44, 95% CI: 1.11–1.88), surgery (biopsy vs. no surgery, HR = 0.67, 95% CI: 0.46–0.96;Subtotal resection vs. no surgery, HR = 0.47, 95% CI: 0.32–0.68;Gross total resection vs. no surgery, HR = 0.44, 95% CI: 0.31–0.62), radiotherapy (HR = 0.58, 95% CI: 0.41–0.83), and chemotherapy (HR = 0.51, 95% CI: 0.36–0.72).

Conclusion: The predictive value of SM in GBM was determined by this propensity-matched analysis using data from the SEER database. Radiotherapy, chemotherapy, and surgery constitute an effective treatment regimen for patients with SM. A more positive approach toward the use of aggressive treatment for GBM patients with SM may be warranted.

KEYWORDS

glioblastoma multiforme, synchronous metastasis, propensity score matching, cancer-specific survival, SEER

Introduction

Glioblastoma multiforme (GBM) is the most common type of primary malignant brain tumor in adults, distinguished by a dismal prognosis and poor quality of life. Intracranial and extracranial metastases have been documented in 1–2% (1) and 0.4–0.5% (2, 3) of cases, occurring late in the course of the disease, respectively. The prevalence rates might be underestimated since metastatic screening is not a standard practice. Synchronous metastasis(SM) of GBM is even more uncommon, with only a few case reports in the literature (4). The precise incidence of SM in GBM remains elusive.

Metastasis holds critical importance for the prognosis of GBM, as evidenced by a comprehensive literature review (5). Several studies have shown the intensive treatment can prolong survival time for certain individuals with metastases (6–8). However, these researches are confined to tiny sample size, and susceptible to selection bias. Therefore, it is essential to uncover additional information regarding prognostic factors and treatment strategies for these patients.

The present study aimed to use large, population-based cancer registry data to investigate both the incidence and risk factors of SM in patients with GBM. Additionally, it seeks to identify prognostic factors and formulate treatment strategies for patients with SM.

Patients and methods

Patients

The patient cases were enrolled in the study based on the latest version of the publicly available SEER17 database (published in November 2022) by using SEER*Stat 8.4.2.[1]

Patients diagnosed with primary GBM, both with and without SM, between the years 2004 and 2015, were retrospectively identified in this study. The inclusion criteria were as follows: (1) histology diagnosis with GBM (SEER Brain and CNS Recode 1.1.2 GB); (2) year of diagnosis (range: 2004–2015). While the exclusion criteria included: (1) information on SM (CS mets dx) unknown; (2) not only primary tumor; (3) patient with unknown survival time; (4) incomplete or unconfirmed diagnoses, and (5) tumor size unknown. The patient selection flowchart from the SEER database is delineated in Figure 1.

The following variables were incorporated in the current study: demographic characteristics (year, age, sex, race, marital status, household income, rural–urban area); clinicopathological information (primary site, laterality, tumor size, SM, surgery, radiotherapy and chemotherapy), and follow-up data (cause-specific death and survival time).

Age at diagnosis as a continuous variable was separated into young group (<60 years) and old group (≥60 years). Median household income inflation-adjusted to 2021 was used to classify individuals into the low-income ($60,000 or less) and high-income ($60,001 or more) groups. Tumor size was characterized by the dimensions of the primary tumor. The surgical interventions, which pertain to the resection of the primary tumor, were systematically documented using a specific coding schema.: gross total resection (GTR) was designated with codes 30 or 55; subtotal resection (STR) was represented by codes 22, 21, or 40; biopsy was assigned codes 10, 20, or 90; and instances where no surgery was performed were denoted with code 0. SM: Defined as intracranial and/or extracranial metastatic lesions resulting from the spread of a primary GBM at the initial diagnosis. In the SEER database, SM, which includes both extracranial and intracranial metastasis, is denoted by the term "CS mets dx." Extracranial metastasis is denoted by codes 30 or 50, whereas intracranial metastasis by codes 10 or 20. Cancer-specific survival (CSS) is defined as the duration between the primary diagnosis and the date of death associated with GBM.

Statistical analysis

A Propensity Score Matching (PSM) analysis was utilized to adjust for all other variables between patients with and without SM. The "Matchit" package in R was employed to match the propensity scores between the two groups, employing the nearest neighbor algorithm with a matching ratio of 1:3. Then, Pearson's Chi-squared test ("gtsummary" package) was used to compare baseline characteristics between groups. Categorical variables are presented as proportions and percentages of the total. Cox proportional hazards regression analysis was performed to evaluate the prognostic effect of SM in GBM ("survival" package). The effect of these confounders was quantified by calculating the changes in the effect size of SM for GBM when each variable is added to the model sequentially in a step-wise fashion ("chest" package) (9). Based on the observed effects, a multivariable Cox proportional hazards regression analysis was conducted. Furthermore, the Kaplan–Meier method and log-rank analysis were utilized to depict the CSS curves before and after PSM in both groups ("survminer" package).

Cox proportional hazards regression models, both univariable and multivariable, were used to identify the prognostic factors for GBM patients with SM. Moreover, a forest plot ("forestmodel" package) was constructed to visualize the findings.

In our study, statistical significance was defined as a two-tailed p value<0.05. The statistical analysis was performed with R program (version 4.3.2).

1 https://seer.cancer.gov/

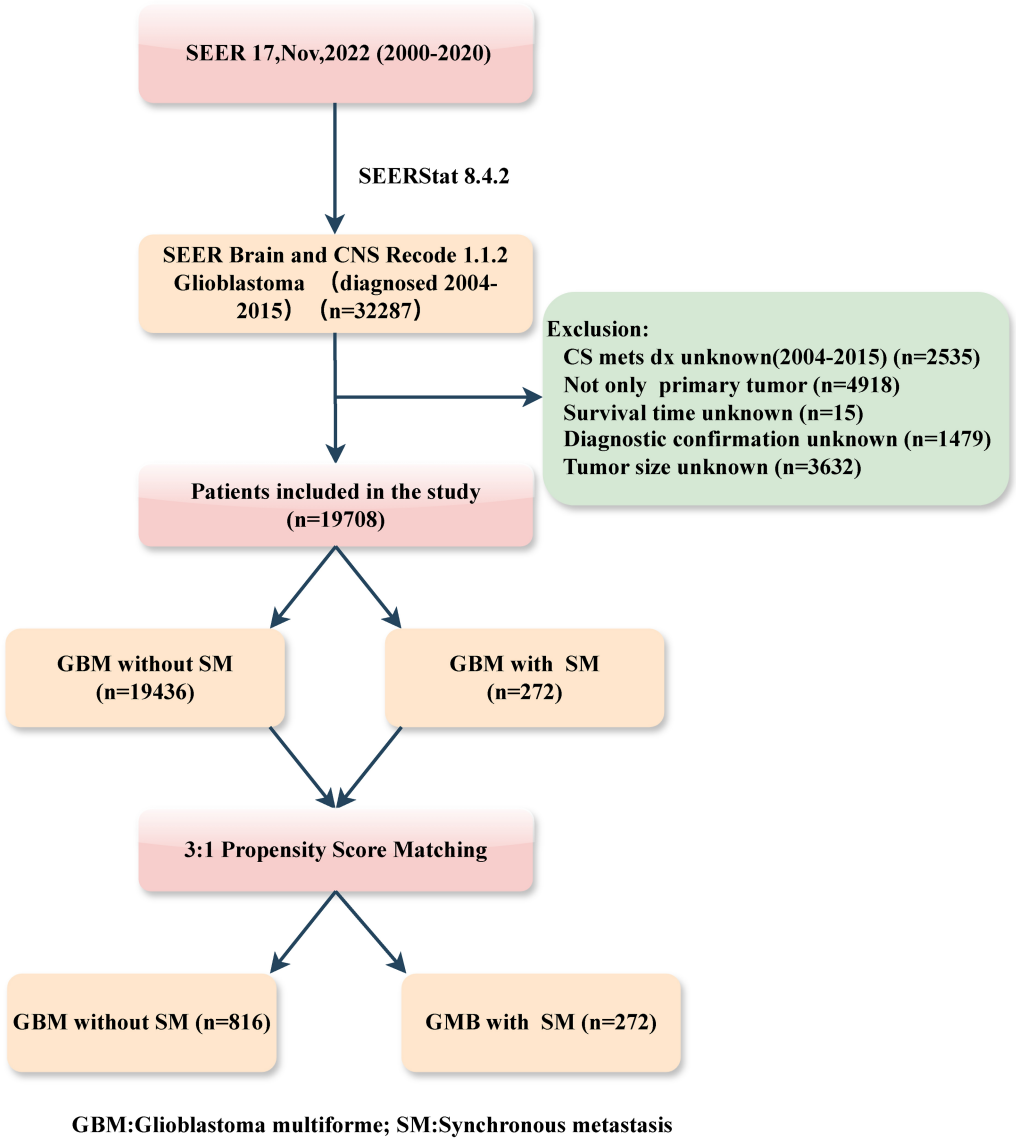

FIGURE 1
Flowchart illustrating patient selection of this study.

Results

Baseline characteristics before and after PSM

Based on inclusion and exclusion criteria, a total of 19,708 GBM patients were selected from the SEER database. Demographical and clinical characteristics for GBM with or without SM were shown in Table 1. Patients diagnosed with SM tended to be non-white, infratentorial, and not to have a paired site ($p < 0.05$); additionally, they were less likely to have undergone radiotherapy, chemotherapy, or surgery ($p < 0.001$).

After 1:3 PSM, 1088 patients were matched, which included 272 patients with SM and 816 patients without SM. All demographic and clinical characteristics were well-matched, suggesting that the PSM effectively minimized potential selection bias ($p > 0.05$).

The prognostic effect of SM in patients after PSM

The univariate Cox proportional hazards model demonstrated a significant increment in mortality risk for GBM patients with SM after PSM (HR: 1.27, 95% CI:1.10–1.46, $p < 0.00$; Table 2). Moreover, Kaplan–Meier analysis curves comparing CSS for SM and non-SM groups before and after PSM are depicted in Figure 2.

The confounding effect of each remaining variable on the association of SM on the CSS of GBM patients was quantified and is presented in Figure 3. The results remain stable with each variable being added to multivariable Cox proportional hazards model sequentially in a step-wise fashion. Based on the effects and clinical experience, multivariable Cox proportional hazards model was established. After adjusting for potential confounding variables including age, primary site, tumor size, surgery, chemotherapy and

TABLE 1 Characteristics of glioblastoma multiforme patients before and after propensity score matching.

Characteristic	Before matching			After matching[3]		
	Non-SM	SM		Non-SM	SM	
	N = 19,436[1]	*N* = 272	*p*-value[2]	*N* = 816	*N* = 272	*p*-value[2]
Year, *n* (%)			0.10			0.7
2004–2007	5,559 (29%)	71 (26%)		205 (25%)	71 (26%)	
2008–2011	6,453 (33%)	80 (29%)		262 (32%)	80 (29%)	
2012–2015	7,424 (38%)	121 (44%)		349 (43%)	121 (44%)	
Age, *n* (%)			0.5			0.8
Young	8,386 (43%)	112 (41%)		344 (42%)	112 (41%)	
Old	11,050 (57%)	160 (59%)		472 (58%)	160 (59%)	
Sex, *n* (%)			0.3			0.4
Female	8,022 (41%)	120 (44%)		338 (41%)	120 (44%)	
Male	11,414 (59%)	152 (56%)		478 (59%)	152 (56%)	
Race, *n* (%)			<0.001			0.6
Others	2,049 (11%)	47 (17%)		129 (16%)	47 (17%)	
White	17,387 (89%)	225 (83%)		687 (84%)	225 (83%)	
Marital status, *n* (%)			0.6			0.4
Divorced	6,964 (36%)	102 (38%)		285 (35%)	102 (38%)	
Married	12,472 (64%)	170 (63%)		531 (65%)	170 (63%)	
Household income, *n* (%)			0.8			0.3
<60,000	5,766 (30%)	79 (29%)		209 (26%)	79 (29%)	
60,000+	13,670 (70%)	193 (71%)		607 (74%)	193 (71%)	
Rural urban, *n* (%)			0.6			0.8
Metropolitan	17,017 (88%)	241 (89%)		728 (89%)	241 (89%)	
Nonmetropolitan	2,419 (12%)	31 (11%)		88 (11%)	31 (11%)	
Tumor size, *n* (%)			0.4			0.8
<4.5 cm	9,443 (49%)	139 (51%)		409 (50%)	139 (51%)	
4.5 cm+	9,993 (51%)	133 (49%)		407 (50%)	133 (49%)	
Primary site, *n* (%)			<0.001			0.7
Frontal lobe	5,574 (29%)	79 (29%)		211 (26%)	79 (29%)	

(Continued)

10.3389/fneur.2024.1429826

TABLE 1 (Continued)

Characteristic	Before matching			After matching[3]		
	Non-SM	SM		Non-SM	SM	
	N = 19,436[1]	*N* = 272	*p*-value[2]	*N* = 816	*N* = 272	*p*-value[2]
Parietal lobe	3,160 (16%)	52 (19%)		172 (21%)	52 (19%)	
Temporal lobe	5,007 (26%)	41 (15%)		136 (17%)	41 (15%)	
Others	5,695 (29%)	100 (37%)		297 (36%)	100 (37%)	
Laterality, *n* (%)			0.010			0.9
Left	8,376 (43%)	113 (42%)		336 (41%)	113 (42%)	
Not a paired site	2,580 (13%)	53 (19%)		171 (21%)	53 (19%)	
Right	8,480 (44%)	106 (39%)		309 (38%)	106 (39%)	
Surgery, *n* (%)			<0.001			0.7
NS	3,240 (17%)	81 (30%)		262 (32%)	81 (30%)	
Biopsy	3,657 (19%)	56 (21%)		152 (19%)	56 (21%)	
STR	3,015 (16%)	57 (21%)		188 (23%)	57 (21%)	
GTR	9,524 (49%)	78 (29%)		214 (26%)	78 (29%)	
Radiotherapy, *n* (%)	15,128 (78%)	179 (66%)	<0.001	553 (68%)	179 (66%)	0.6
Chemotherapy, *n* (%)	13,822 (71%)	152 (56%)	<0.001	481 (59%)	152 (56%)	0.4

[1]*n* (%), [2]Pearson's Chi-squared test; [3]Nearest Neighbor Matching with a ratio 1:3. NS, No surgery; STR, Subtotal resection; GTR, Gross total resection; SM, Synchronous metastasis.

10.3389/fneur.2024.1429826

TABLE 2 Univariate and multivariate analyses of cancer-specific survival (CSS) in the cohort after propensity score matching.

Characteristic	Univariate			Multivariate		
	HR[1]	95% CI[1]	*p*- value	HR[1]	95% CI[1]	*p*- value
Year						
2004–2007	—	—				
2008–2011	0.81	0.69, 0.96	0.012			
2012–2015	0.80	0.69, 0.93	0.005			
Age						
Young	—	—		—	—	
Old	1.93	1.70, 2.18	<0.001	1.77	1.54, 2.03	<0.001
Sex						
Female	—	—				
Male	0.94	0.83, 1.06	0.33			
Race						
Others	—	—				
White	1.06	0.89, 1.25	0.53			
Marital status						
Divorced	—	—				
Married	1.00	0.88, 1.13	>0.99			
Household income						
<60,000	—	—				
60,000+	1.01	0.88, 1.16	0.91			
Rural urban						
Metropolitan	—	—				
Nonmetropolitan	1.09	0.90, 1.32	0.40			
Primary site						
Frontal lobe	—	—		—	—	
Parietal lobe	0.95	0.80, 1.14	0.60	0.90	0.75, 1.08	0.3
Temporal lobe	1.02	0.84, 1.23	0.88	1.00	0.82, 1.22	>0.9
Others	1.22	1.04, 1.42	0.012	1.16	0.99, 1.37	0.067
Laterality						
Left	—	—				
Not a paired site	1.29	1.10, 1.52	0.002			
Right	1.01	0.88, 1.16	0.85			
Tumor size(cm)						
<4.5 cm	—	—		—	—	
4.5 cm+	1.07	0.95, 1.21	0.27	1.15	1.02, 1.31	0.028
SM						
No	—	—		—	—	
Yes	1.27	1.10, 1.46	<0.001	1.27	1.09, 1.46	0.001
Surgery						
NS	—	—		—	—	
Biopsy	0.57	0.48, 0.68	<0.001	0.61	0.50, 0.73	<0.001
STR	0.47	0.39, 0.55	<0.001	0.54	0.45, 0.65	<0.001
GTR	0.42	0.35, 0.49	<0.001	0.43	0.36, 0.51	<0.001
Radiotherapy						
No	—	—		—	—	
Yes	0.41	0.36, 0.47	<0.001	0.58	0.48, 0.71	<0.001

(Continued)

TABLE 2 (Continued)

Characteristic	Univariate			Multivariate		
	HR[1]	95% CI[1]	*p*- value	HR[1]	95% CI[1]	*p*- value
Chemotherapy						
No	—	—		—	—	
Yes	0.43	0.38, 0.48	<0.001	0.59	0.49, 0.71	<0.001

[1]HR, Hazard Ratio; CI, Confidence Interval; NS, No surgery; SM, Synchronous metastasis; STR; Subtotal resection; GTR, Gross total resection.

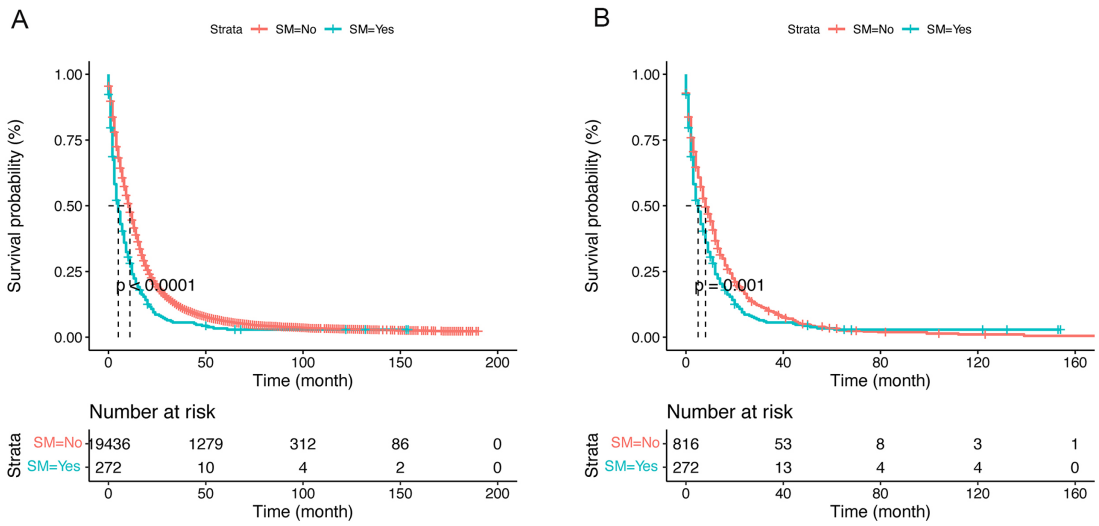

FIGURE 2
Kaplan–Meier curves of cause-specific survival (CSS) by synchronous metastasis (SM) before **(A)** and after **(B)** propensity score matching (PSM).

radiotherapy, SM was still found to be an independent risk factor (HR:1.28, 95% CI:1.11–1.48, $p < 0.001$) in GBM patients (Table 2).

Prognostic factors for GBM patients with SM

In the present research, a cohort of 272 patients diagnosed with GBM exhibiting SM were analyzed to identify and evaluate potential prognostic factors. As delineated in Table 1, the majority were male (56%), white (83%), and diagnosed between 2012 and 2015 (44%). And a total of 191 (70%) patients underwent surgical intervention, 179 (66%) received radiotherapy, and 152 (56%) were administered chemotherapy. Prognostic factors were identified using multivariate Cox regression analyses, revealing that for GBM patients with SM, age ($p = 0.007$), surgery ($p < 0.001$), chemotherapy ($p < 0.001$), and radiotherapy ($p = 0.003$) were independent prognostic factors (Figure 4). The Kaplan–Meier curves of the age, surgery, radiotherapy and chemotherapy subgroups are displayed in Figure 5.

The prognostic effect of different types of SM in patients

Of these, 272 (1.4%) had SM, with 29 (0.1%) presenting extracranial metastasis and 243 (1.3%) presenting intracranial metastasis. Compared to those with extracranial metastasis, patients with intracranial metastasis were more likely to undergo GTR (30% vs. 14%) (Supplementary Table S1). The Kaplan–Meier curve and forest plot generated using the chest package (Supplementary Figure S1) revealed no statistically significant differences between the two groups.

Discussion

GBM represents the most prevalent form of malignant primary brain tumors in adults (10), with a 5-year overall relative survival of 6.9% (11). GBM patient with SM is uncommon (12), and the prognostic factors and optimal therapeutic approaches for these patients have not yet been fully elucidated. In this population-based study, we employed the SEER database to conduct a comprehensive analysis of patients diagnosed with GBM, both with and without SM, between the years 2004 and 2015. SM is extremely rare, affecting 1.4% of all patients with GBM in our cohort. We found that SM was an independent prognostic factor for CSS in patients with GBM before and after PSM. Additionally, the analysis also revealed age, surgery, chemotherapy, and radiation therapy as significant prognostic indicators for patients with SM. Notably, the statistical analysis did not discern a significant difference between intracranial and extracranial metastasis, potentially due to the constrained sample size of patients with SM.

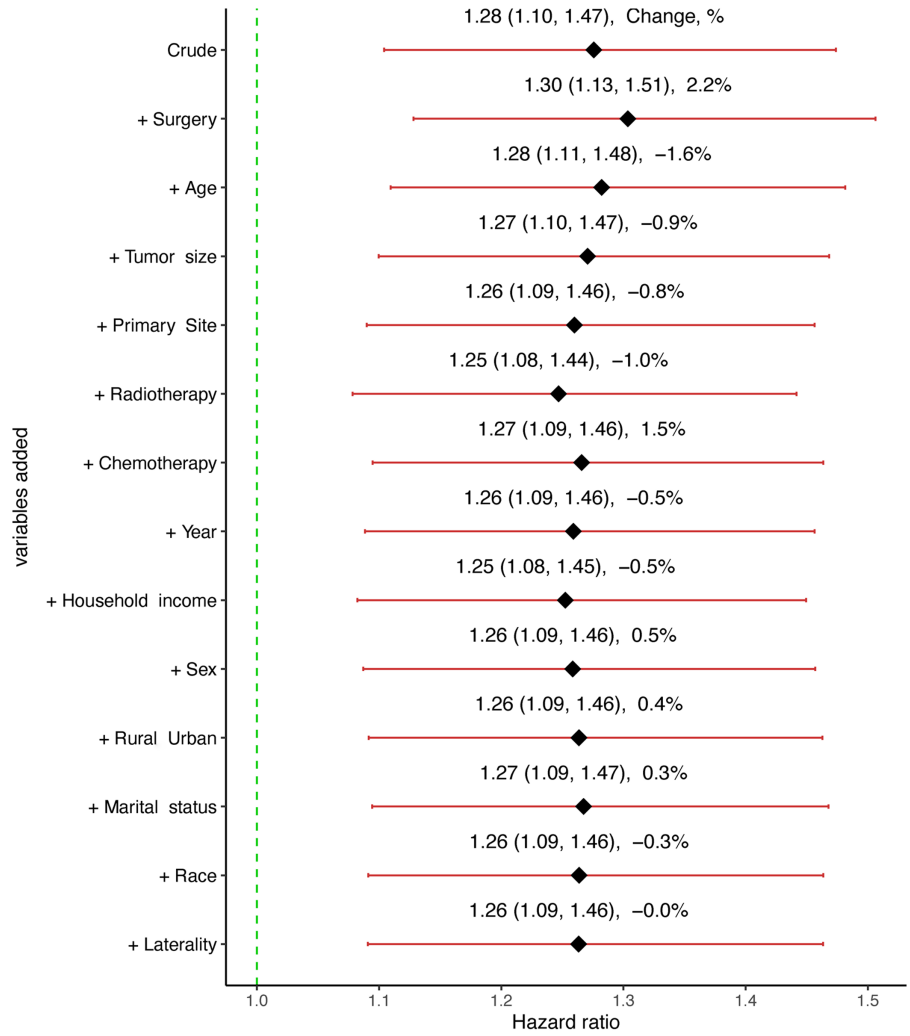

FIGURE 3
Graphical representation of the change in the estimate of the effect of synchronous metastasis (SM) on cause-specific survival (CSS) with each variable added to the multivariable Cox regression model.

Previous studies (12–14) have demonstrated SM is a significant prognostic factor for GBM, yet the exact value of this prognosis remains unknown. Amelot et al. (15) conducted a retrospective analysis of GBM patients with spinal cord metastasis in a French database between January 2004 and 2016, accompanied by a review of the pertinent literature. They found that spinal cord metastasis is associated with a poor prognosis. In our study, to balance baseline confounding factors, we employed PSM analysis to ascertain the exact value of SM for patients with GBM. After adjusting for various covariates, SM consistently emerged as an independent risk factor in GBM patients. This finding underscores the importance of conducting a comprehensive assessment of synchronous metastasis status at the time of initial diagnosis.

The underlying mechanism accounting for SM remains elusive (16). The majority of GBM metastases occur within the central nervous system, which is believed to be attributed to white matter tract infiltration and cerebrospinal fluid seeding (17–19). Extracranial metastases are documented in approximately 0.4–0.5% of all patients (2, 3, 20), suggesting that such interventions may facilitate the dissemination of tumor cells beyond the central nervous system. The presence of extracranial metastasis may be indicative of the existence of circulating tumor cells (CTCs) within the bloodstream. These cells exhibit advanced characteristics, such as epithelial-to-mesenchymal transition and dormancy (21, 22), which are crucial to survive in the bloodstream. And the detection of glioblastoma CTCs holds significant clinical promise for the early diagnosis and prognosis (23, 24).

The standard treatment of primary GBM is maximal safe resection followed by concomitant radiotherapy and temozolomide chemotherapy and then adjuvant temozolomide (25). However, due to the scarcity of case reports, the optimal treatment strategy for patients with SM has yet to be fully established. A meta-analysis of individual patient data, encompassing 115 younger patients from 1928 to 2013, indicated that while a survival benefit could not be statistically validated, an aggressive treatment approach may be ethically justified whenever

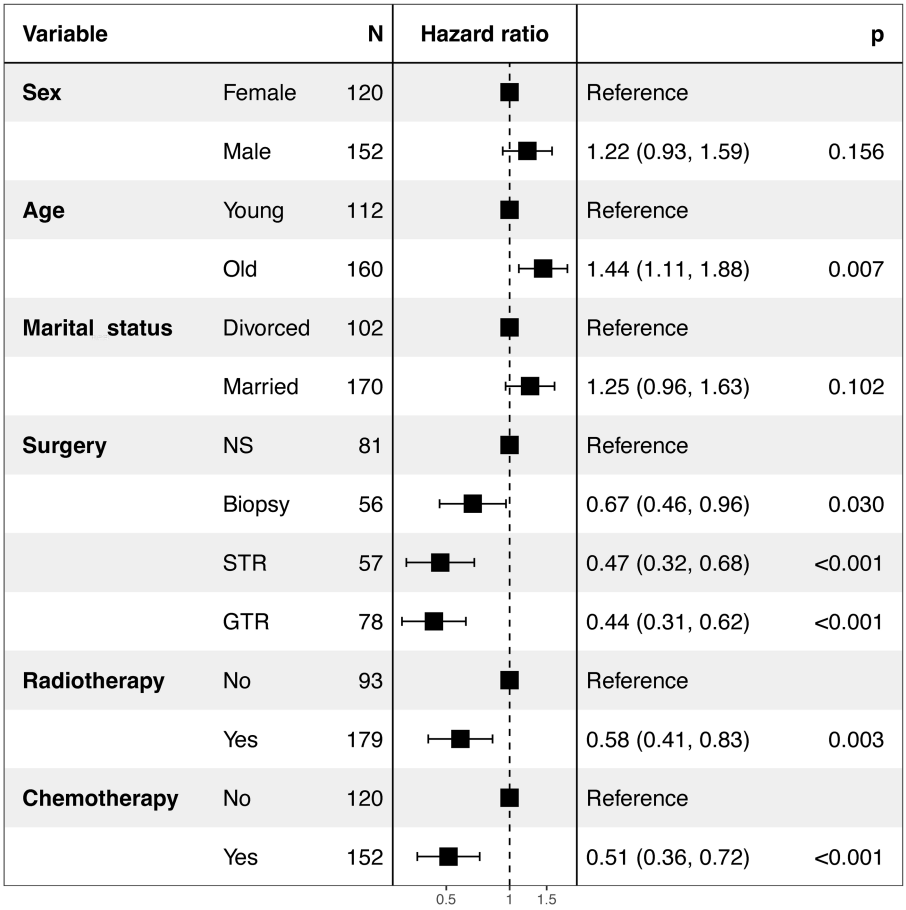

FIGURE 4
Forest plot of the multivariate Cox analysis of CSS in GBM patients with SM. NS, No surgery; STR, Subtotal resection; GTR, Gross total resection; SM, Synchronous metastasis.

feasible (6). Furthermore, another meta-analysis revealed that surgical intervention, chemotherapy, and radiotherapy significantly prolongs survival in GBM patients with metastasis (7). In our study, we discovered that surgical intervention exerted a significant impact on the management of patients with SM. Gross total resection, subtotal resection, and biopsy can significantly enhance the cancer-specific survival of patients compared to those no surgical intervention. This indicated that surgical resection can effectively decrease the tumor mass, consequently restoring neurological functions. Additionally, we identified both radiation therapy and chemotherapy as significant prognostic factors. Consistent with a previous study, patients who underwent an aggressive treatment, including surgery, radiation, chemotherapy, and cerebrospinal fluid shunting, demonstrated favorable prognosis (26). Overall, our results suggested that a combination of surgical intervention, chemotherapy, and radiation constitutes an effective therapeutic strategy for patients with SM. Therefore, GBM patients with SM may experience enhanced benefits from more aggressive therapeutic regimens. Nonetheless, additional studies are required to validate these preliminary findings.

Several limitations of our study need to be recognized. Firstly, in the retrospective study, the restricted sample size of patients with SM ($N = 272$) might have a risk of selection bias. Therefore, prospective registry studies with larger sample sizes are necessary to validate our findings. Secondly, as our study included patients from 2004 to 2015 and utilized diagnostic criteria established prior to 2016, these were solely based on pathological diagnosis without integrating molecular diagnosis. Thirdly, information was gathered when the diagnosis was initially made from the SEER database, excluding any metastasis that developed subsequently. Fourthly, the SEER database lacks comprehensive details regarding specific chemotherapeutic agents used, including dosages, treatment duration, and patient responses. Details pertaining to radiation therapy and surgical procedures for metastasis are also missing. These limitations may hinder a thorough evaluation of the efficacy of various treatment modalities.

Conclusion

In conclusion, the propensity-matched analysis has identified the prognostic value of SM in patients with GBM based on the SEER database. Our findings suggest that surgery, chemotherapy, and radiotherapy constitute an effective therapeutic strategy for GBM patients with SM. However, further research is necessary to confirm

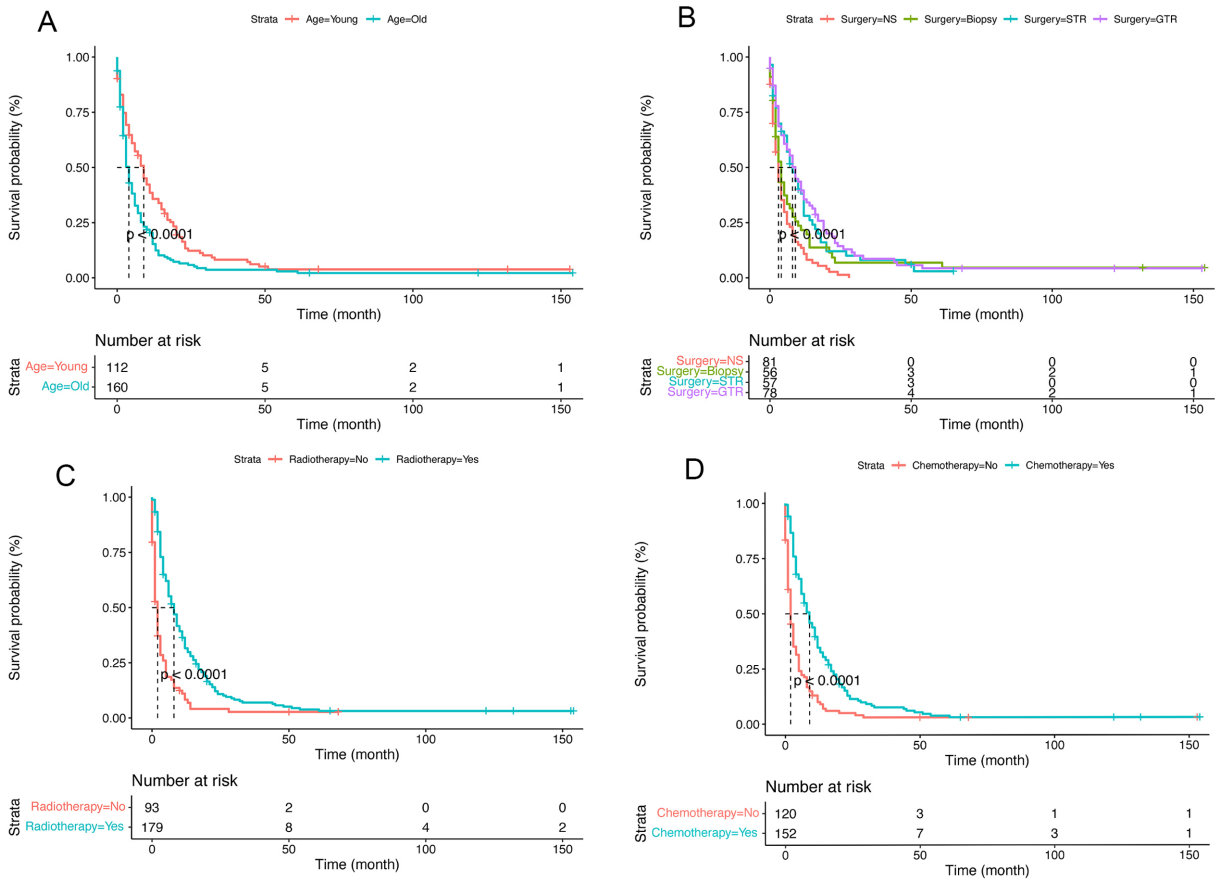

FIGURE 5
Kaplan–Meier survival curves comparing the cancer-specific survival (CSS) of glioblastoma multiforme (GBM) patients with synchronous metastasis (SM). **(A)**, Age; **(B)**, Surgery; **(C)**, Radiotherapy; **(D)**, Chemotherapy; NS, No surgery; STR, Subtotal resection; GTR, Gross total resection.

these findings through prospective registry studies with larger sample size.

Data availability statement

The original contributions presented in the study are included in the article/Supplementary material, further inquiries can be directed to the corresponding authors.

Ethics statement

Ethical approval was not required for the study involving humans in accordance with the local legislation and institutional requirements. Written informed consent to participate in this study was not required from the participants or the participants' legal guardians/next of kin in accordance with the national legislation and the institutional requirements.

Author contributions

HS: Conceptualization, Data curation, Formal analysis, Software, Visualization, Writing – original draft, Writing – review & editing. QM: Conceptualization, Data curation, Formal analysis, Visualization, Writing – original draft, Writing – review & editing. XC: Conceptualization, Visualization, Writing – original draft, Writing – review & editing. YJ: Data curation, Funding acquisition, Writing – original draft, Writing – review & editing. AL: Conceptualization, Project administration, Supervision, Writing – original draft, Writing – review & editing. JL: Conceptualization, Project administration, Supervision, Writing – original draft, Writing – review & editing.

Funding

The author(s) declare that financial support was received for the research, authorship, and/or publication of this article. This work was supported by the Natural Science Foundation of Beijing Municipality (grant no. 7222053), National Natural Science Foundation of China (grant no. 82003134) and Beijing Science and Technology Commission (Project no. Z171100000417046).

Conflict of interest

The authors declare that the research was conducted in the absence of any commercial or financial relationships that could be construed as a potential conflict of interest.

The handling editor BH declared a shared parent affiliation with the authors JL, HS, XC, YJ, and AL at the time of review.

Publisher's note

All claims expressed in this article are solely those of the authors and do not necessarily represent those of their affiliated organizations, or those of the publisher, the editors and the reviewers. Any product that may be evaluated in this article, or claim that may be made by its manufacturer, is not guaranteed or endorsed by the publisher.

Supplementary material

The Supplementary material for this article can be found online at: https://www.frontiersin.org/articles/10.3389/fneur.2024.1429826/full#supplementary-material

References

1. Choi PP, Shapera S. What's your call? Drop metastases. *CMAJ Can Med Assoc J*. (2006) 175:475, 477. doi: 10.1503/cmaj.060308

2. Smith DR, Hardman JM, Earle KM. Metastasizing neuroectodermal tumors of the central nervous system. *J Neurosurg*. (1969) 31:50–8. doi: 10.3171/jns.1969.31.1.0050

3. Pasquier B, Pasquier D, N'Golet A, Panh MH, Couderc P. Extraneural metastases of astrocytomas and glioblastomas clinicopathological study of two cases and review of literature. *Cancer*. (1980) 45:112–25. doi: 10.1002/1097-0142(19800101)45:1<112::AID-CNCR2820450121>3.0.CO;2-9

4. Witoonpanich P, Bamrungrak K, Jinawath A, Wongwaisayawan S, Phudhichareonrat S, Witoonpanich R. Glioblastoma multiforme at the corpus callosum with spinal leptomeningeal metastasis. *Clin Neurol Neurosurg*. (2011) 113:407–10. doi: 10.1016/j.clineuro.2010.12.001

5. Yang R, Isaacs AM, Cadieux M, Hirmer TJ, Creve Coeur TS, Lapointe AP, et al. Primary and metastatic glioblastoma of the spine in the pediatric population: a systematic review. *Childs Nerv Syst*. (2021) 37:1849–58. doi: 10.1007/s00381-021-05098-8

6. Pietschmann S, Von Bueren AO, Kerber MJ, Baumert BG, Kortmann RD, Müller K. An individual patient data meta-analysis on characteristics, treatments and outcomes of glioblastoma/gliosarcoma patients with metastases outside of the central nervous system. *PLoS One*. (2015) 10:e0121592. doi: 10.1371/journal.pone.0121592

7. da Cunha MLV, Maldaun MVC. Metastasis from glioblastoma multiforme: a meta-analysis. *Rev Assoc Med Bras*. (2019) 65:424–33. doi: 10.1590/1806-9282.65.3.424

8. Ray A, Manjila S, Hdeib AM, Radhakrishnan A, Nock CJ, Cohen ML, et al. Extracranial metastasis of gliobastoma: three illustrative cases and current review of the molecular pathology and management strategies. *Mol Clin Oncol*. (2015) 3:479–86. doi: 10.3892/mco.2015.494

9. Wang Z. Two postestimation commands for assessing confounding effects in epidemiological studies. *Stata J*. (2007) 7:183–96. doi: 10.1177/1536867X0700700203

10. Wen PY, Weller M, Lee EQ, Alexander BM, Barnholtz-Sloan JS, Barthel FP, et al. Glioblastoma in adults: a Society for Neuro-Oncology (SNO) and European Society of Neuro-Oncology (EANO) consensus review on current management and future directions. *Neuro-Oncology*. (2020) 22:1073–113. doi: 10.1093/neuonc/noaa106

11. Ostrom QT, Price M, Neff C, Cioffi G, Waite KA, Kruchko C, et al. CBTRUS statistical report: primary brain and other central nervous system tumors diagnosed in the United States in 2016-2020. *Neuro-Oncology*. (2023) 25:iv1–iv99. doi: 10.1093/neuonc/noad149

12. Sibanda Z, Farahani N, Ogbonnaya E, Albanese E. Glioblastoma Multiforme: a rare case of spinal drop metastasis. *World Neurosurg*. (2020) 144:24–7. doi: 10.1016/j.wneu.2020.08.086

13. Shibahara I, Saito R, Osada Y, Kanamori M, Sonoda Y, Kumabe T, et al. Incidence of initial spinal metastasis in glioblastoma patients and the importance of spinal screening using MRI. *J Neuro-Oncol*. (2019) 141:337–45. doi: 10.1007/s11060-018-03036-4

14. Dardis C, Milton K, Ashby L, Shapiro W. Leptomeningeal metastases in high-grade adult glioma: development, diagnosis, management and outcomes in a series of 34 patients. *Front Neurol*. (2014) 5 JUN:) 5:220. doi: 10.3389/fneur.2014.00220

15. Amelot A, Terrier LM, Cognacq G, Jecko V, Marlier B, Seizeur R, et al. Natural history of spinal cord metastasis from brain glioblastomas. *J Neuro-Oncol*. (2023) 162:373–82. doi: 10.1007/s11060-023-04298-3

16. Georgescu MM, Olar A. Genetic and histologic spatiotemporal evolution of recurrent, multifocal, multicentric and metastatic glioblastoma. *Acta Neuropathol Commun*. (2020) 8:10. doi: 10.1186/s40478-020-0889-x

17. Hu Y, Yin W, Ma J, Liu J, Huang S, Chen H. Glioblastoma multiforme of the conus medullaris with leptomeningeal dissemination that presented as intracranial hypertension: a case report and literature review. *Glioma*. (2021) 4:57–61. doi: 10.4103/glioma.glioma_15_21

18. Zhang K, Yang Y, Zhuang J, Guo G, Chao X, Zhang Z. Intracranial dissemination of glioblastoma multiforme: a case report and literature review. *J Int Med Res*. (2022) 50:030006052211120. doi: 10.1177/03000605221112047

19. Wright CH, Wright J, Onyewadume L, Raghavan A, Lapite I, Casco-Zuleta A, et al. Diagnosis, treatment, and survival in spinal dissemination of primary intracranial glioblastoma: systematic literature review. *J Neurosurg Spine*. (2019) 31:723–32. doi: 10.3171/2019.5.SPINE19164

20. Hamilton JD, Rapp M, Schneiderhan TM, Sabel M, Hayman A, Scherer A, et al. Glioblastoma multiforme metastasis outside the CNS: three case reports and possible mechanisms of escape. *J Clin Oncol*. (2014) 32:e80–4. doi: 10.1200/JCO.2013.48.7546

21. Chistiakov DA, Chekhonin VP. Circulating tumor cells and their advances to promote cancer metastasis and relapse, with focus on glioblastoma multiforme. *Exp Mol Pathol*. (2018) 105:166–74. doi: 10.1016/j.yexmp.2018.07.007

22. Lombard A, Goffart N, Rogister B. Glioblastoma circulating cells: reality, trap or illusion? *Stem Cells Int*. (2015) 2015:1–11. doi: 10.1155/2015/182985

23. Senhaji N, Houssaini AS, Lamrabet S, Louati S, Bennis S. Molecular and circulating biomarkers in patients with glioblastoma. *Int J Mol Sci*. (2022) 23:474. doi: 10.3390/ijms23137474

24. Müller Bark J, Kulasinghe A, Chua B, Day BW, Punyadeera C. Circulating biomarkers in patients with glioblastoma. *Br J Cancer*. (2020) 122:295–305. doi: 10.1038/s41416-019-0603-6

25. McKinnon C, Nandhabalan M, Murray SA, Plaha P. Glioblastoma: Clinical presentation, diagnosis, and management. *The BMJ*. (2021) 374:15060. doi: 10.1136/bmj.n1560

26. Lun M, Lok E, Gautam S, Wu E, Wong ET. The natural history of extracranial metastasis from glioblastoma multiforme. *J Neuro-Oncol*. (2011) 105:261–73. doi: 10.1007/s11060-011-0575-8

frontiers | Frontiers in Neurology

TYPE Original Research
PUBLISHED 20 November 2024
DOI 10.3389/fneur.2024.1454056

OPEN ACCESS

EDITED BY
Jun Yang,
Capital Medical University, China

REVIEWED BY
Faisal Alotaibi,
King Faisal Specialist Hospital and Research Centre, Saudi Arabia
Matteo Martinoni,
IRCCS Institute of Neurological Sciences of Bologna, Italy

*CORRESPONDENCE
Qiang Guo
✉ eqiangguo@163.com
Yanwu Guo
✉ eguoyanwu@163.com

RECEIVED 24 June 2024
ACCEPTED 28 October 2024
PUBLISHED 20 November 2024

CITATION
He G, Tan H, Li S, Zhang L, Li Q, Li H, Guo Y and Guo Q (2024) Polymorphic low-grade neuroepithelial tumors of the young: disease characteristics and treatment decisions from the epilepsy surgery perspective.
Front. Neurol. 15:1454056.
doi: 10.3389/fneur.2024.1454056

Polymorphic low-grade neuroepithelial tumors of the young: disease characteristics and treatment decisions from the epilepsy surgery perspective

Guilu He[1,2], Hongping Tan[2], Shaochun Li[2], Limin Zhang[2], Qiao Li[2], Hainan Li[3], Yanwu Guo[1]* and Qiang Guo[2]*

[1]Department of Neurosurgery, Zhujiang Hospital, Southern Medical University, Guangzhou, China, [2]Department of Neurosurgery, Guangdong Sanjiu Brain Hospital, Guangzhou, China, [3]Department of Pathology, Guangdong Sanjiu Brain Hospital, Guangzhou, China

Background: The Polymorphic Low-Grade Neuroepithelial Tumor of the Young (PLNTY) is a rare, epilepsy-associated brain tumor that has been increasingly recognized but is not well understood due to the scarcity of clinical reports. Our study reviews the clinical characteristics and treatment outcomes of 14 patients with PLNTY to enhance the understanding of this condition from an epilepsy surgery perspective.

Methods: We performed a retrospective analysis of 14 PLNTY cases at our hospital. A literature review on prior studies was also conducted.

Results: Our study included 8 males and 6 females, all presenting with epilepsy. Despite anti-seizure medication, 92.3% of patients continued to have seizures, with 58.3% diagnosed as having drug-resistant epilepsy. Neuroimaging revealed that 64.3% of the lesions were in the temporal lobe, with 75.0% showing calcification on CT, 71.4% exhibiting mixed signals on T2-weighted images, and 92.7% showing tumor enhancement. The transmantle sign was noted in 57.1% of T2 FLAIR sequences. EEGs indicated abnormal activity in 69.2% of patients, with 30.7% showing bilateral discharges. SEEG in two patients confirmed the tumor's epileptogenicity. A 78.6% total resection rate was achieved, with a 90.0% postoperative seizure-free rate and an 85.7% excellent Engel grade 1 rate. No instances co-occurring with focal cortical dysplasia (FCD) were observed.

Conclusion: PLNTY is characterized by unique neuroimaging features and a strong association with epilepsy. SEEG is pivotal for cases with unclear lateralization, aiding in identifying the link between the tumor and seizures. Following established epilepsy surgery protocols for brain tumor management, early intervention and extended resection can improve the rate of postoperative seizure freedom.

KEYWORDS

PLNTY, stereoelectroencephalography, epilepsy, neuroepithelial tumors, treatment

1 Introduction

PLNTY is a novel entity recently incorporated into the 2021 World Health Organization classification of central nervous system (CNS) tumors (1). It is distinguished by a significant association with epileptic seizures in adolescent individuals. Pathologically, PLNTY exhibits a diffuse growth pattern, scattered calcifications, and frequent oligodendroglioma-like components. Furthermore, immunohistochemistry reveals CD34 positivity and abnormal gene activation of the MAPK pathway. However, recent analyses suggest a considerable variability in its radiological and clinical presentation (1, 2). Given the limited number of reported clinical cases, a comprehensive understanding of the electro-clinical characteristics and treatment outcomes of this tumor is imperative. This study provides a detailed analysis of the clinical profiles and treatment courses of 14 pathologically confirmed PLNTY cases from our institution. We elucidate the unique features and therapeutic responses, supported by a relevant literature review.

2 Materials and methods

The medical records of all patients who underwent surgical treatment at our hospital from January 2021 to January 2024 were reviewed. In accordance with the Declaration of Helsinki, the Ethics Committee of Guangdong Sanjiu Brain Hospital does not require informed consent for the use of anonymous clinical data for retrospective analysis.

Data collection included demographic details, clinical presentations, diagnostic findings, extent of surgical resection, and therapeutic efficacy. The follow-up period begins after the individual's surgery date, with a duration ranging from 3 months to 3 years to evaluate the outcomes of epilepsy treatment. The dataset was meticulously analyzed and interpreted by experienced epilepsy specialists. Due to the limited patient cohort, advanced statistical software was not necessary for the analysis.

A personalized surgical strategy was developed for each patient. The correlation between tumors and epileptic seizures was initially assessed using video-EEG monitoring. In cases where the localization of epilepsy was inconclusive or precise tumor resection was necessary, combined stereoelectroencephalography (SEEG) may be considered. Our institution utilizes a stereotactic planning system and MRI imaging to create a three-dimensional cerebral model, aiding in the precise delineation of the tumor and its adjacent anatomical structures. Intraoperatively, neuronavigation and electrocorticography (ECoG) are employed to guide the surgical resection. Postoperative MRI scans are performed to confirm the completeness of the resection.

Postoperative tissue samples were fixed in 10% neutral buffered formalin for subsequent immunohistochemistry (IHC) and molecular diagnostics. The IHC protocol targeted a panel of markers, including glial fibrillary acidic protein (GFAP), Oligodendrocyte transcription factor 2 (Olig2), B-type Raf kinase (BRAF), Cluster of Differentiation 34 (CD34), and Isocitrate Dehydrogenase 1 (IDH1). Samples with positive BRAF immunoreactivity underwent polymerase chain reaction (PCR) analysis to detect the BRAFV600E mutation.

3 Results

In this study, a total of 8 males (57.1%) and 6 females (42.9%) were included. The median age of onset was 19.3 years, ranging from 2.7 to 41 years. Three patients experienced disease onset after the age of 30, all of whom presented with temporal lobe lesions. Seizure was the initial symptom in all patients, with two cases also reporting auras. The duration of the disease ranged from 2 months to 18 years, with an average of 59.3 months. Prior to surgery, all patients had received varying degrees of anti-seizure drug therapy. Importantly, 92.3% (12 out of 13) of the patients had poorly controlled seizures, and among them, 58.3% (7 out of 12) met the criteria for refractory epilepsy. Detailed information regarding patient demographics and medication history can be found in Table 1.

3.1 Imaging features

Temporal lobe lesions were found in 46.3% (9/14) of cases, with 3 cases involving the medial temporal lobe and 6 cases involving the lateral temporal lobe. Frontal lobe lesions were present in 14% (2/14) of cases, occipital lobe lesions in 14% (2/14), and parietal lobe lesions in 7% (1/14). The average tumor diameter was approximately 21.6 ± 8.8 mm (mean ± SD), with the largest tumor measuring 38 mm in diameter. On MRI, 71.4% (10/14) of tumors showed a mixed cystic-solid composition. Enhancement was observed on T1-weighted post-contrast sequences in 92.7% (11/12) of patients. Calcifications were detected on CT scans in 75.0% (9/12) of cases. Detailed information can be found in Table 2.

3.2 Electroencephalogram findings

The preoperative 24-hour EEG data were analyzed for 13 patients, revealing a 69.2% (9/13) concordance between EEG abnormalities and tumor locations. The remaining 4 patients showed bilateral abnormal discharges. Two patients underwent SEEG implantation. In Case 2, a pediatric patient with temporal lobe lesions opted for this invasive procedure to precisely define the resection margins at the parents' request. Ictal SEEG recordings indicated significant intrinsic epileptogenicity within the tumor, with epileptic discharges rapidly spreading to the surrounding tissues, particularly affecting the lateral neocortex (Figures 1, 2). In Case 4, SEEG implantation was performed due to inconclusive lateralizing information from clinical symptoms, EEG, and PET scans (Figures 3, 4). During the ictal SEEG period, the tumor exhibited pronounced intrinsic epileptogenicity, with the epileptogenic zone strictly confined to the tumor's interior. There were no signs of seizure involvement outside the tumor, including in the surrounding peripheral tissues.

3.3 Pathological results

In this cohort, all tumors exhibited positive expression for CD34 and GFAP (14/14, 100%), and were negative for IDH1. Regarding Olig-2 immunohistochemistry, one case initially considered weakly positive was ultimately classified as negative, resulting in a final

TABLE 1 Basic data and clinical information of patients with PLNTY.

case	Sex	onset (years)	First neurological event/ Duration (months)	Frequency	ASM tried	Response to ASM
1	F	6.8	Seizures/2	Daily	NA	No
2	F	15.3	Seizures/32	Monthly	VPA,CLN	No
3	M	20.6	Seizures/17	Weekly	VPA	No
4	M	22.3	Seizures/33	Daily	VPA,LEV,OXC	No
5	M	6.0	Seizures/36	Daily	OXC	No
6	F	25.0	Seizures/24	Monthly	LTG	No
7	M	2.7	Seizures/4	Weekly	OXC	Yes
8	M	37.2	Seizures/10	NA	NA	NA
9	F	18.0	Seizures/168	Monthly	VPA,CBZ	No
10	M	17.0	Seizures/216	Monthly	VPA,CBZ	No
11	F	30.0	Seizures/120	Daily	VPA,LTG	No
12	M	41.0	Seizures/60	Daily	VPA,OXC	No
13	F	28.0	Seizures/60	Monthly	OXC	No
14	M	10.0	Seizures/48	Daily	OXC, LTG, LEV, Lacosamide	No

NA, not available; VPA, Valproic Acid; CLN,Clonazepam; LEV, Levetiracetam; OXC, Oxcarbazepine; LTG, Lamotrigine; CBZ, Carbamazepine.

positive expression rate of 92.9% (13/14) for Olig-2. In the BRAF assay, 57.2% of cases (8/14) showed positive expression. Among these, one case could not undergo further PCR analysis due to financial constraints. The remaining cases demonstrated a 100% (7/7) BRAFv600E mutation rate. No instances of these tumors co-occurring with focal cortical dysplasia (FCD) were observed In our cases. Detailed results can be found in Table 2.

3.4 Treatment outcome

Following postoperative MRI, complete tumor resection was successfully achieved in 78.6% of the cases. Three patients underwent partial resection due to the proximity of their lesions to eloquent brain regions, such as the lingual gyrus and corona radiata, necessitating a conservative surgical approach. During postoperative follow-up, "transmantle-like" signals were still evident on MRI in two patients, with one patient experiencing ongoing epileptic seizures. After surgery, complete seizure resolution was observed in 90.0% (9/10) of cases, and 85.7% (6/7) of patients attained Engel Class I status. Detailed outcomes are summarized in Table 2.

4 Discussion

PLNTY, a neuroepithelial tumor associated with epilepsy, was classified and categorized in the 2021 WHO classification of central nervous system neoplasms (1, 2). In this review, the age of onset ranged from 2.7 to 41 years, with an average of 20 years. The longest documented disease duration was 18 years, consistent with historical data (3). Unlike previous reports where 82.2% of patients presented with epileptic seizures as the initial symptom (3), all patients in our cohort presented with seizures. Table 1 provides detailed information on anti-seizure medication regimens and therapeutic responses. The high rate of drug resistance observed in our series highlights the importance of early surgical intervention in managing these tumors.

In our case series, PLNTY exhibited three notable imaging characteristics: cystic changes, calcification, and contrast enhancement, corresponding to proportions of 71.4% (10/14), 75.0% (9/12), and 92.7% (11/12), respectively. These tumors were most commonly located in the temporal lobe, particularly the lateral temporal region, and appeared as solid or mixed solid-cystic lesions. Cystic components varied in size, ranging from subtle punctate signal changes to more substantial eccentric cystic expansions. The cystic areas were typically well-demarcated compared to the solid portions, and the tumors rarely caused mass effect or peritumoral edema. After contrast administration, the tumors often showed mild, indistinct patchy or mottled enhancement patterns. This observed rate of enhancement is significantly higher than the previously reported 33% (4), which may be attributed to subjective differences in imaging assessments among various researchers. Calcifications were observed as central dense opacities or sparse lamellar calcifications at the tumor's edge. Besides, it appears as hypometabolism during the interictal phase on PET-CT.

There is limited reporting on EEG characteristics related to PLNTY. Our study shows that the discharge patterns exhibited by PLNTY are similar to those of most brain tumor-related epilepsy. Scalp EEG indicates that the tumor-related discharge sites are consistent with the lobe of the brain where the tumor is located, but there is a certain proportion of cases with discharges involving both cerebral hemispheres. Additionally, we observed significant intrinsic epileptogenicity of the tumor in 2 patients who underwent SEEG. However, the presence of early rapid spread of electroencephalographic activity was observed to be different. This observation differs from previous descriptions, which noted epileptic discharge areas around PLNTY deviating from the tumor's center (5).

TABLE 2 Test data and related treatment results of PLNTY patients.

Case	Tumor location	EEG finding	T2Fsignals	Cystic component	Calculation	Contrast enhancement	transmantle singal	CD34	BRAF mutation	Treatment	Seizure outcome
1	L Parietal	Left posterior cortical	mixed	Yes	Yes	Yes	Yes	+	-	GTR	Seizure free
2	R Lateral temporal	Right temporal region	mixed	Yes	Yes	Yes	Yes	+	+	ER	Seizure free
3	L Occipital	Bilateral hemispheric discharge	mixed	No	Yes	NA	No	+	+	ER	Seizure free
4	R Frontal	Bilateral hemispheric discharge	mixed	No	Yes	Yes	No	+	-	GTR	NA
5	R Lateral temporal	Right frontal-temporal region	mixed	Yes	Yes	Yes	No	+	+	ER	Seizure free
6	R Lateral temporal	Right temporal region	iso	No	No	Yes	Yes	+	+	ER	NA
7	R Occipital	Right central-parietal–temporal region	mixed	Yes	Yes	Yes	Yes	+	-	PTR	Seizure free
8	L Lateral temporal	Bilateral hemispheric discharge	mixed	Yes	No	Yes	No	+	+	GTR	Seizure free
9	L Lateral temporal	Left temporal region	mixed	Yes	Yes	Yes	Yes	+	+	PTR	Uncontrolled
10	R Medial temporal	Bilateral hemispheric discharge	iso	Yes	No	none	Yes	+	+	ER	Seizure free
11	L Medial temporal	NA	hyper	Yes	NA	Yes	No	+	-	PTR	Seizure free
12	R Medial temporal	Right temporal region	hyper	No	NA	NA	Yes	+	-	GTR	NA
13	L Lateral temporal	Left temporal region	mixed	Yes	Yes	Yes	No	+	+	ER	NA
14	R Frontal	Right posterior cortical	hyper	Yes	Yes	Yes	Yes	+	-	ER	Seizure free

NA, not available; ER, enlarged resection; GTR, gross total resection; PTR, partial resection.

10.3389/fneur.2024.1454056

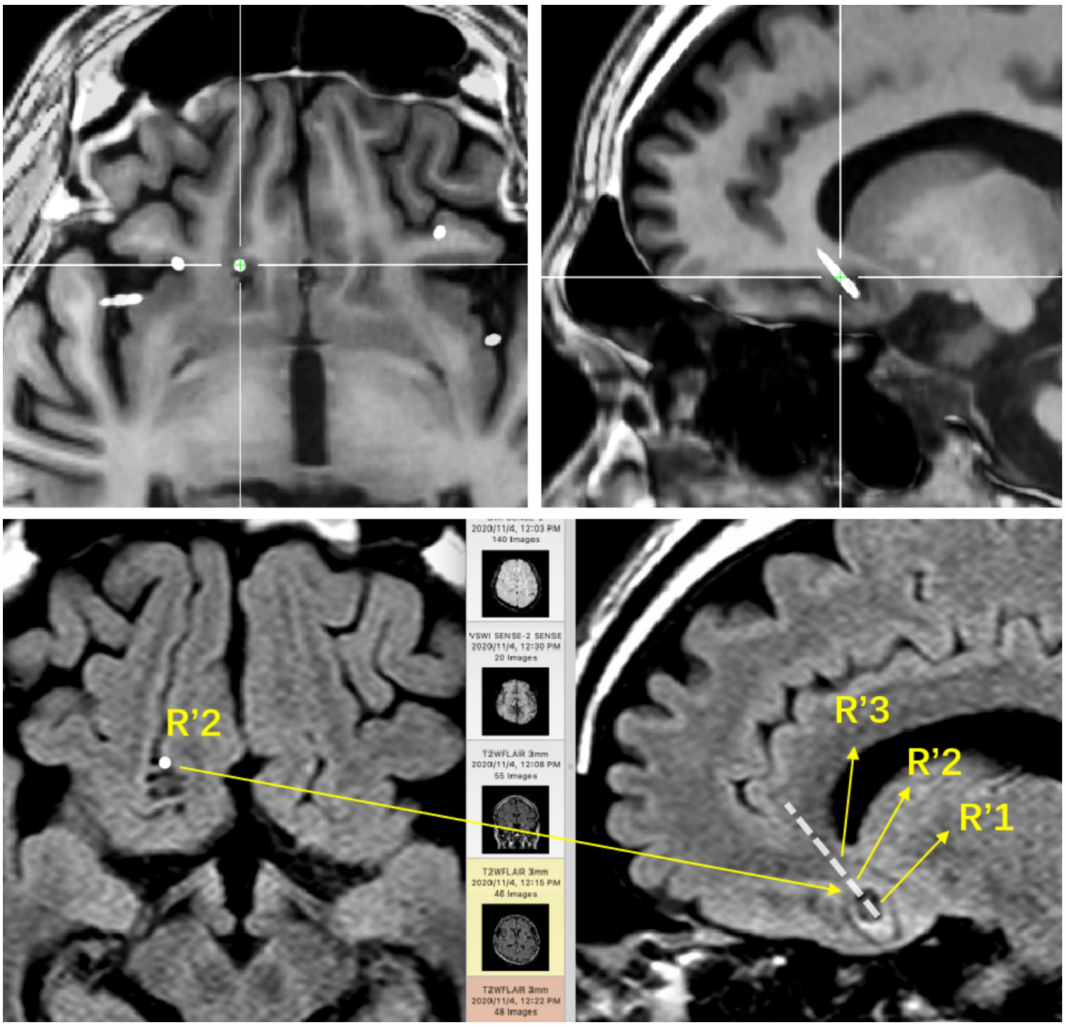

FIGURE 1
The base of the right frontal lobe. The positional relationship between the electrode contacts and the lesion entity: R'1 is located in the calcification of the lesion; R'2 is located in the parenchyma of the lesion; R'3 is located around the lesion.

It suggests that for PLNTY with strong epileptogenicity, expanding the resection scope to relatively safe areas may be advantageous for epilepsy control.

Similar to the management of other epilepsy-related brain tumors, surgical resection is the primary therapeutic approach for PLNTY, involving the removal of both the tumor and associated epileptogenic foci. A comprehensive preoperative evaluation, including clinical symptoms, EEG data, and understanding of epileptogenic network pathways, is crucial for establishing the link between the tumor and epilepsy and defining surgical margins. In cases where there is a discrepancy between the epileptogenic zone identified by non-invasive methods and the tumor boundaries delineated by MRI, invasive intracranial electroencephalography with depth electrodes may be employed to determine their correlation (3, 5).

In our series of cases, patients who underwent complete or extended resections were seizure-free postoperatively. It is noteworthy that PLNTY often presents with "Transmantle-like" peritumoral signal changes on MRI, and the persistence of these signal abnormalities post-resection is significantly correlated with unfavorable epilepsy control outcomes (3). Achieving total tumor resection is paramount for optimizing the prognosis of patients with epilepsy. "Transmantle-like" changes were observed in 57.1% (8/14) of our cases. Due to the proximity of these changes to critical functional areas, only partial resections were performed in two patients, and one of them, with a medical history of 168 months, experienced early postoperative seizures.

A literature review by Armocida et al., which examined 51 cases, identified a significant association between tumor contrast enhancement on MRI and adverse postoperative epilepsy outcomes (2). In our series, 92.7% (11/12) of patients exhibited contrast enhancement on T1-weighted imaging, with a 90.0% (9/10) rate of complete seizure resolution postoperatively, and 85.7% (6/7) achieving Engel Class I status. Our follow-up data suggest that surgical tumor resection has a definitive impact on improving drug-resistant epilepsy in patients. However, the correlation between MRI contrast enhancement and postoperative epilepsy control outcomes necessitates further validation with a larger sample size.

PLNTY is characterized by its unique pathological features, with CD34 positive expression and BRAF V600E mutation being its most distinctive alterations (2). Research indicates that CD34-positive tumor

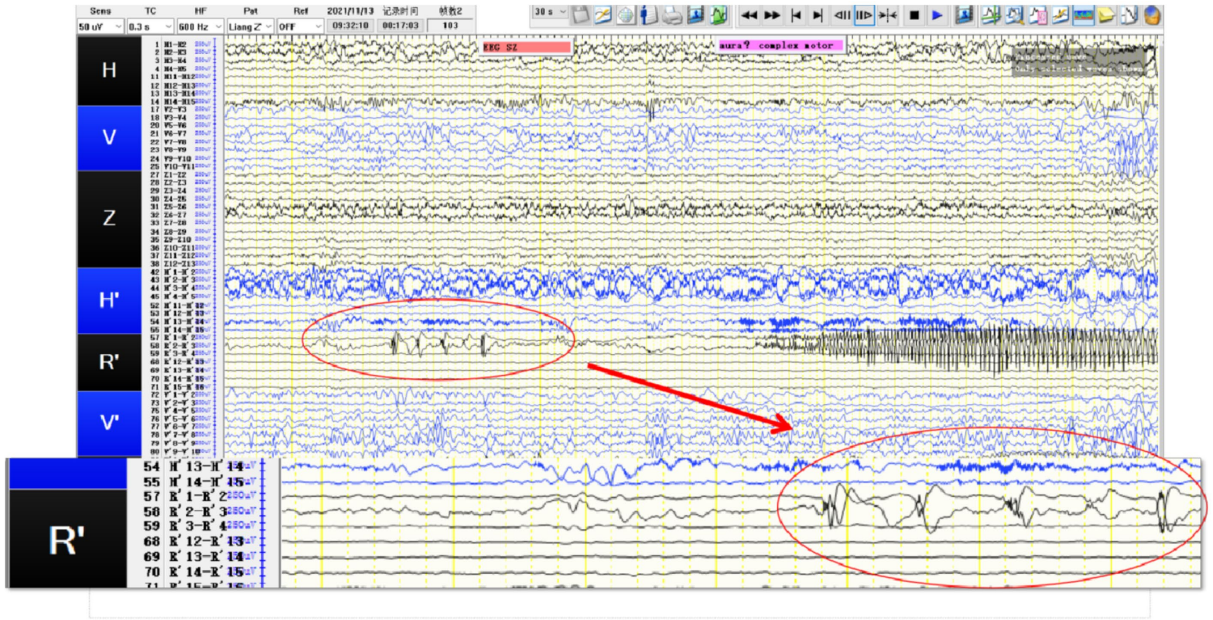

FIGURE 2
SEEG recording results: R'1 and R'2 are the seizure onset areas, while R'3 has not changed significantly. The tumor in this patient showed obvious intrinsic epileptogenicity, and the epileptogenic zone was only located within the tumor, while the surrounding tissues of the tumor showed no signs of seizure involvement.

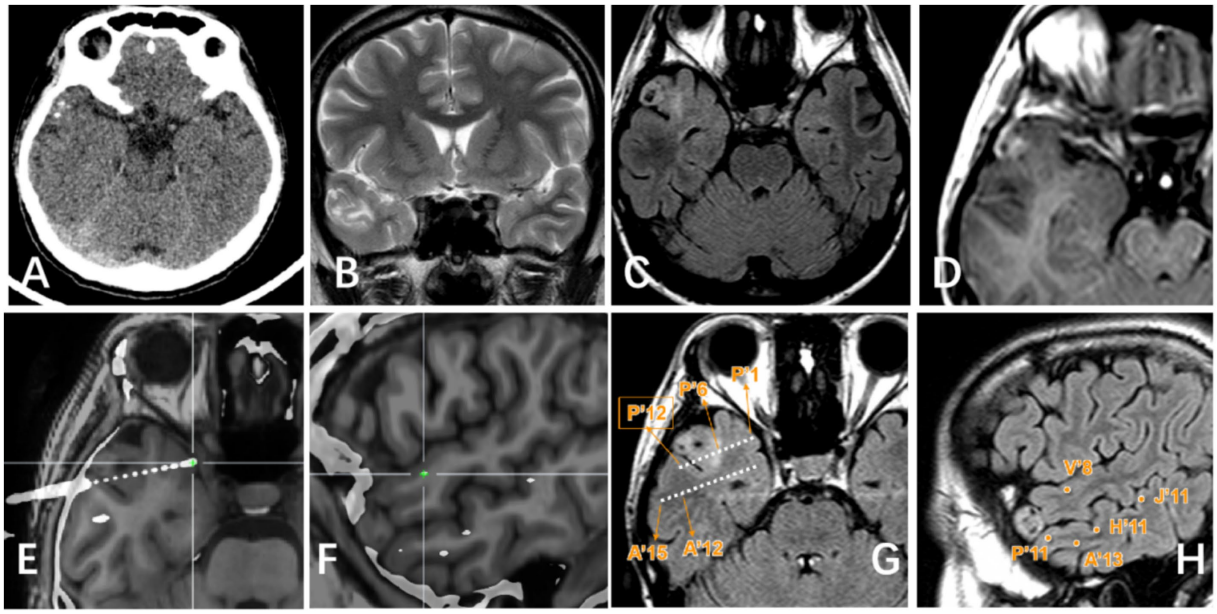

FIGURE 3
Right lateral temporal lobe lesion. (A) Scattered calcification in CT image; (B) Mixed signal in the lateral temporal lobe in T2WI image; (C) Transmantle sign changes can be seen in T2Flair; (D) Mild enhancement of tumor can be seen in T1 enhanced image; (E–H) Display the positional relationship between the electrode contact point and the tumor entity: P'6–12 is located in the tumor parenchyma and shows high signal on T2 Flair. Electrode contacts such as P'1–5/A'/H'/V'/J' are located around the tumor and T2 Flair shows relatively normal signals.

cells can trigger an inflammatory response, leading to inflammation and damage to surrounding brain tissue, thereby increasing the risk of epileptic seizures, which clinically manifests as a significant association with a longer history of epilepsy (6). In this series， no instances co-occurring with focal cortical dysplasia (FCD) were observed. Nearly all patients appearance of structural disorder in the center of the tumor and the adjacent cortex, and there is also a dendritic positive pattern of immunohistochemical CD34. We believe this represents the tumor's involvement of the surrounding cortex rather than type FCDIIIb. Our findings may imply the tumor's invasion of the surrounding brain

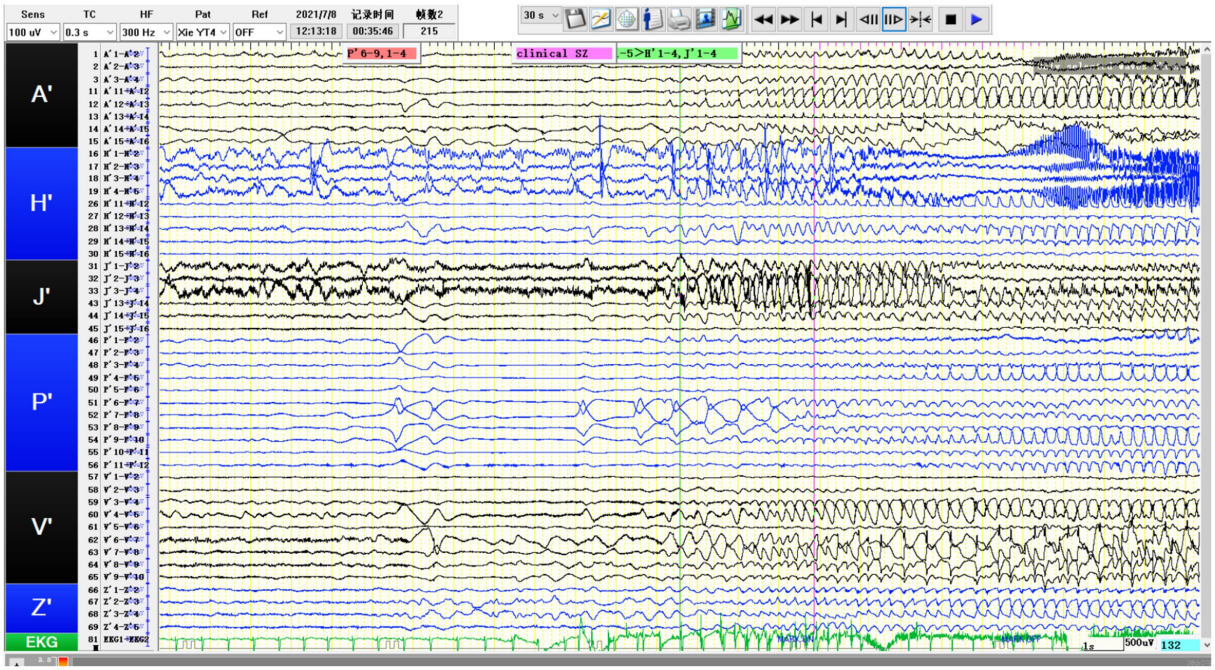

FIGURE 4
SEEG recording results: P'6–12 is the onset area of the seizure, while P'1-5/A'12-15/H'8-12/V'5-8/J'6–14 are rapidly affected in the early stage of the attack. The patient's tumor showed obvious intrinsic epileptogenicity, and epileptic discharges rapidly spread to the surrounding tissues of the tumor at an early stage, especially the lateral neocortex and the medial hippocampus (H'1-3/J'1–3) not affected (still showing intermittent discharges).

tissue, explaining the necessity of early intervention and extensive tumor resection from a pathological standpoint.

The BRAF mutation is associated with various types of epilepsy (7). The expression of mutated BRAF protein may impact neural networks, causing abnormal discharges in different neuronal populations in different locations, potentially resulting in various epileptic patterns. BRAF V600E is the most prevalent type of activating BRAF mutation and is linked to the development of epileptic activity mediated by alterations in ion transport and synaptic activity regulation. There is a perspective that tumors with positive BRAF V600E expression may represent a distinct subset of PLNTY tumors, exhibiting a more indolent course, later age of onset, and a delay in clinical symptom presentation (2). In our case series, 57.2% of patients tested positive for BRAF V600E. The average age of onset for BRAF V600E-positive patients is 20.6 years, with 87.5% (7 out of 8) of these tumors located in the temporal lobe. This proportion closely aligns with Baumgartner's reported 87.1% of BRAF V600E-positive tumors involving the temporal lobe (2). This observation may suggest a specific association between the BRAF V600E mutation and the occurrence of temporal lobe tumors, warranting further attention in future mechanistic research.

5 Limitations

This article reports on a retrospective study. The lack of detailed records of intraoperative monitoring results limits our ability to extensively discuss this aspect. Additionally, the small number of cases, single-center sampling, and short follow-up periods for some patients may restrict our capacity to fully assess the treatment effects, which in turn limits the scope and depth of our study. Future research should aim to expand the sample size, prolong the follow-up period, and focus on intraoperative monitoring to better understand the neuroelectric relationships between tumors and surrounding tissues.

6 Conclusion

PLNTY is known for its high epileptogenicity and distinctive imaging features. SEEG implantation may be suitable for elucidating the relationship between non-lateralized tumors and epileptic seizures. Early intervention and extended resection appear to increase the rate of postoperative seizure freedom.

Data availability statement

The original contributions presented in the study are included in the article/supplementary material, further inquiries can be directed to the corresponding author.

Ethics statement

The studies involving humans were approved by the Ethics Committee of Guangdong Sanjiu Brain Hospital. The studies were conducted in accordance with the local legislation and institutional requirements. Written informed consent for participation in this study was provided by the participants' legal guardians/next of kin. Written informed consent was obtained from the individual(s) and/or minor(s)' legal guardian/next of kin for the publication of any potentially identifiable images or data included in this article.

Author contributions

GH: Conceptualization, Formal analysis, Methodology, Writing – original draft, Writing – review & editing. HT: Data curation, Writing – review & editing. SL: Data curation, Writing – review & editing. LZ: Data curation, Writing – review & editing. QL: Data curation, Writing – review & editing. HL: Data curation, Writing – review & editing. YG: Conceptualization, Supervision, Writing – original draft. QG: Conceptualization, Supervision, Writing – original draft.

Funding

The author(s) declare that no financial support was received for the research, authorship, and/or publication of this article.

Conflict of interest

The authors declare that the research was conducted in the absence of any commercial or financial relationships that could be construed as a potential conflict of interest.

Publisher's note

References

1. Bale TA, Rosenblum MK. The 2021 WHO classification of tumors of the central nervous system: an update on pediatric low-grade gliomas and glioneuronal tumors. *Brain Pathol.* (2022) 32:e13060. doi: 10.1111/bpa.13060

2. Baumgartner ME, Lang SS, Tucker AM, Madsen PJ, Storm PB, Kennedy BC, et al. Systematic review and cumulative analysis of clinical properties of BRAF V600E mutations in PLNTY histological samples. *Childs Nerv Syst.* (2023) 40:1361–6. doi: 10.1007/s00381-023-06256-w

3. Fei X, Zhao J, Wei W, Wang W, Kong X, Qian R, et al. Clinical, radiological, pathological features and seizure outcome with surgical management of polymorphous low-grade neuroepithelial tumor of the young associated with epilepsy. *Front Oncol.* (2022) 12:863373. doi: 10.3389/fonc.2022.863373

4. Armocida D, Berra LV, Frati A, Santoro A. Radiological and surgical aspects of polymorphous low-grade neuroepithelial tumor of the young (PLNTY). *Acta Neurol Belg.* (2023) 123:327–40. doi: 10.1007/s13760-023-02231-z

5. Hagiwara K, Kamada T, Suzuki SO, Miyoshi A, Tanaka H, Shigeto H, et al. Stereo-electroencephalography evidence of an eccentrically located seizure-onset zone around a polymorphous low-grade neuroepithelial tumor of the young: illustrative case. *J Neurosurg Case Less.* (2022) 3:106. doi: 10.3171/CASE22106

6. Vornetti G, Marucci G, Zenesini C, de Biase D, Michelucci R, Tinuper P, et al. Relationship among clinical, pathological and bio-molecular features in low-grade epilepsy-associated neuroepithelial tumors. *J Clin Neurosci.* (2017) 44:158–63. doi: 10.1016/j.jocn.2017.06.022

7. Bitar M, Danish SF, Rosenblum MK. A newly diagnosed case of polymorphous low-grade neuroepithelial tumor of the young. *Clin Neuropathol.* (2018) 37:178–81. doi: 10.5414/NP301081

Frontiers in Neurology

Explores neurological illness to improve patient care

The third most-cited clinical neurology journal explores the diagnosis, causes, treatment, and public health aspects of neurological illnesses. Its ultimate aim is to inform improvements in patient care.

Discover the latest Research Topics

See more →

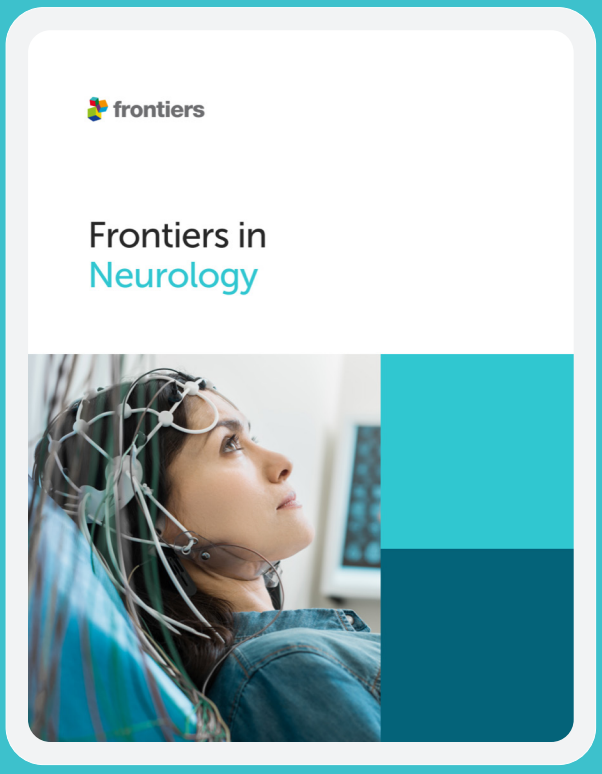

Frontiers

Avenue du Tribunal-Fédéral 34
1005 Lausanne, Switzerland
frontiersin.org

Contact us

+41 (0)21 510 17 00
frontiersin.org/about/contact